

**МІНІСТЕРСТВО ОСВІТИ І НАУКИ, МОЛОДІ ТА СПОРТУ УКРАЇНИ  
ПРИКАРПАТСЬКИЙ НАЦІОНАЛЬНИЙ УНІВЕРСИТЕТ  
ІМЕНІ ВАСИЛЯ СТЕФАНІКА**

**Фізико-хімічний інститут  
Бердянський державний педагогічний університет  
Івано-Франківський національний технічний університет нафти і газу**

**ДЕРЖАВНЕ АГЕНТСТВО З ПИТАНЬ НАУКИ, ІННОВАЦІЇ ТА  
ІНФОРМАЦІЇ УКРАЇНИ**

**Державний фонд фундаментальних досліджень**

**НАЦІОНАЛЬНА АКАДЕМІЯ НАУК УКРАЇНИ  
Інститут фізики напівпровідників ім. В.Є. Лашкарьова  
Інститут металофізики ім. Г.В. Курдюмова  
Інститут загальної і неорганічної хімії ім. В.І. Вернадського  
Інститут хімії поверхні ім. О.О.Чуйка**

**УКРАЇНСЬКЕ ФІЗИЧНЕ ТОВАРИСТВО  
АСОЦІАЦІЯ "ВЧЕНІ ПРИКАРПАТТЯ"  
ЛЮБЛІНСЬКИЙ ТЕХНІЧНИЙ УНІВЕРСИТЕТ (ПОЛЬЩА)  
УНІВЕРСИТЕТ ГАЗІ (ТУРЕЧЧИНА)**

# **ФІЗИКА І ТЕХНОЛОГІЯ ТОНКИХ ПЛІВОК ТА НАНОСИСТЕМ**

**Матеріали XIII Міжнародної конференції**

**МКФТТПН-XIII**

**Т О М 1**

*16-21 травня 2011 р.*

**Івано-Франківськ  
Україна**

УДК 539.2  
ББК 22.373.1  
Ф 83

**Фізика і технологія тонких плівок та наносистем. Матеріали XIII Міжнародної конференції: У 2 т. – Т. 1.** / За заг. ред. заслуженого діяча науки і техніки України, д.х.н., проф. **Фреїка Д.М.** – Івано-Франківськ: Видавництво Прикарпатського національного університету імені Василя Стефаника, 2011. – 312 с.

Представлено результати теоретичних і експериментальних досліджень з питань: технологія тонких плівок (метали, напівпровідники, діелектрики, провідні полімери) і методи їх дослідження; фізико-хімічні властивості плівок; нанотехнології і наноматеріали, квантово-розмірні структури; тонкоплівкові елементи електронних пристроїв.

Матеріали підготовлено до друку Організаційним комітетом та Редакційною колегією конференції і подано в авторській редакції.

Для наукових та інженерних працівників з проблем тонкоплівкового матеріалознавства та мікроелектроніки.

Рекомендовано до друку науково-технічною радою Фізико-хімічного інституту Прикарпатського національного університету імені Василя Стефаника.

**Рецензенти:**

**Литовченко В.Г.**

*чл.-кор. НАН України, Інститут фізики напівпровідників  
ім. В.Є. Лашкарьова НАН України*

**Уваров В.М.**

*чл.-кор. НАН України, Інститут металофізики  
ім. Г.В. Курдюмова НАН України*

**Харченко М.Ф.**

*академік НАН України, Фізико-технічний інститут низьких температур  
ім. Б.І. Веркіна НАН України*

**УДК 539.2  
ББК 22.373.1**

© Прикарпатський  
національний університет  
імені Василя Стефаника  
вул. Шевченка, 57,  
м. Івано-Франківськ,  
76025, Україна  
Тел. (0342) 596082  
Факс (03422) 31574  
E-mail: [freik@pu.if.ua](mailto:freik@pu.if.ua)

**MINISTRY OF EDUCATION AND SCIENCE, YOUTH AND SPORT OF UKRAINE  
'VASYL STEFANYK' PRECARPATHIAN NATIONAL UNIVERSITY**

Physico-Chemical Institute

Berdyansk State Pedagogical University

Ivano-Frankivsk National Technical University of Oil and Gas

STATE AGENCY OF SCIENCE, INNOVATION AND INFORMATION OF UKRAINE

STATE FUND OF FUNDAMENTAL RESEARCH

**NATIONAL ACADEMY OF SCIENCE OF UKRAINE**

'V.E. Lashkarev' Institute of Semiconductor Physics

Institute of Surface Chemistry

'G.V. Kurdyumov' Institute of the Physics of Metals

'V.I. Vernadsky' Institute of General and Inorganic Chemistry

Chuiko Institute of Surface Chemistry

UKRAINE PHYSICS SOCIETY

"SCIENTISTS OF THE PRECARPATHIAN" ASSOCIATION

LUBLIN TECHNICAL UNIVERSITY (POLAND)

GAZY UNIVERSITY (TURKEY)

**PHYSICS AND TECHNOLOGY OF THIN FILMS  
AND NANOSYSTEMS**

***XIII INTERNATIONAL CONFERENCE***

**Materials**

*16-21, May, 2011*

Ivano-Frankivsk, Ukraine

---

---

**МИНИСТЕРСТВО ПРОСВЕЩЕНИЯ И НАУКИ, МОЛОДИ И СПОРТА УКРАИНЫ  
ПРИКАРПАТСКИЙ НАЦИОНАЛЬНЫЙ УНИВЕРСИТЕТ ИМЕНИ ВАСИЛИЯ СТЕФАНИКА**

Физико-химический институт

Бердянский государственный педагогический университет

Ивано-Франковский национальный технический университет нефти и газа

**ГОСУДАРСТВЕННОЕ АГЕНТСТВО ПО ВОПРОСАМ НАУКИ, ИННОВАЦИИ И  
ИНФОРМАЦИИ УКРАИНЫ**

Государственный фонд фундаментальных исследований

**НАЦИОНАЛЬНАЯ АКАДЕМИЯ НАУК УКРАИНЫ**

Институт физики полупроводников имени В.Е. Лашкарева

Институт химии поверхности

Институт металлофизики имени Г.В. Курдюмова

Институт общей и неорганической химии имени В.И. Вернадского

Институт химии поверхности им. О.О.Чуйка

УКРАИНСКОЕ ФИЗИЧЕСКОЕ ОБЩЕСТВО

АССОЦИАЦИЯ "УЧЕНЫЕ ПРИКАРПАТЬЯ"

ЛЮБЛИНСКИЙ ТЕХНИЧЕСКИЙ УНИВЕРСИТЕТ (ПОЛЬША)

**УНИВЕРСИТЕТ ГАЗИ (ТУРЕЧЧИНА)**

**ФИЗИКА И ТЕХНОЛОГИЯ ТОНКИХ  
ПЛЁНОК И НАНОСИСТЕМ  
XII МЕЖДУНАРОДНАЯ КОНФЕРЕНЦИЯ**

**Материалы**

16-21 мая 2011 года

Ивано-Франковск, Украина

**Physics and Technology of Thin Films and Nanosystems. Materials of XIII International Conference: On 2 V. – V. 1. / Ed by Honored engineer and techniques of Ukraine, Dr.Chem.Sci., Prof. Freik D.M. – Ivano-Frankivsk: A publishn-designing department of ‘Vasyl Stefanyk’ Precarpathian National University, 2011. – 312 c.**

The results of theoretical and experimental researches in directions are submitted: technology of thin films (metals, semiconductors, dielectrics, and carrying out polymers) and methods of their investigation; physic-chemical properties of thin films; nanotechnology and nanomaterials, quantum-size structures; thin-film devices of electronics.

The materials preformed for printing by Organizational Committee and Editorial Board of Conference, are conveyed in authoring edition.

For the scientific and engineering workers on thin-film material sciences and microelectronics.

It is recommended for printing by Scientific and Technical Advice of Physico-Chemical Institute at the ‘Vasyl Stefanyk’ Precarpathian National University.

---

---

**Физика и технология тонких пленок и наносистем. Материалы XIII Международной конференции: В 2 т. – Т. 1. / Под общ. ред. заслуженного деятеля науки и техники Украины, д.х.н., проф. Фрейка Д.М. – Ивано-Франковск: Издательство Прикарпатского национального университета имени Василия Стефаника, 2011. – 312 с.**

Предоставлены результаты теоретических и экспериментальных исследований в направлениях: технология тонких пленок (металлы, полупроводники, диэлектрики, проводящие полимеры) и методы их исследования; физико-химические свойства пленок; нанотехнологии и наноматериалы, квантово-размерные структуры; тонкопленочные элементы электронных приборов.

Материалы подготовлены к печати Организационным комитетом и редакционной коллегией конференции, поданы в авторской редакции.

Для научных и инженерных работников по вопросам тонкопленочного материаловедения и микроэлектроники.

Рекомендовано к печати научно-техническим советом Физико-химического института Прикарпатского национального университета имени Василия Стефаника.

## ОРГАНІЗАЦІЙНИЙ КОМІТЕТ

### Бюро

Литовченко В.Г., Миронюк І.Ф., Остафійчук Б.К., Сукач Г.О., Фреїк Д.М.

### Міжнародний

Анатичук Л. (Україна), Ахиска Р. (Туреччина), Бабанли М. (Азербайджан), Беляєв О. (Україна), Блонський І. (Україна), Бродин М. (Україна), Булавін Л. (Україна), Власенко О. (Україна), Волков С. (Україна), Вуйцік В. (Польща), Галушак М. (Україна), Горбик П. (Україна), Готра З. (Україна), Грігоніс А. (Литва), Гриньов Б. (Україна), Гуревич Ю. (Мексика), Гончаренко М. (Україна), Жуковські П. (Польща) Зломанов В. (Росія), Івасишин О. (Україна), Калінкін І. (Росія), Картель М. (Україна), Кияк Б. (Україна), Кікінеші О. (Угорщина), Комаров Ф. (Білорусь), Кумар М. (Індія), Кучмій С. (Україна), Мазуренко Є. (Україна), Малашкевич Г. (Білорусь), Мачулін В. (Україна), Мітгова І. (Росія), Младенов Г. (Болгарія), Мовчан Б. (Україна), Наумовець А. (Україна), Находкін М. (Україна), Нікіфоров К. (Росія), Новиков М. (Україна), Панасюк В. (Україна), Птушинський Ю. (Україна), Раренко І. (Україна), Свечніков С. (Україна), Сидоренко С. (Україна), Сизов Ф. (Україна), Скатков Л. (Ізраїль), Солонін Ю. (Україна), Стасюк І. (Україна), Стріха М. (Україна), Харченко М. (Україна) Челідзе Т. (Грузія), Чобанюк В. (Україна), Тигиняну І. (Молдова), Тодоран Р. (Румунія), Томчук П. (Україна), Уваров В. (Україна), Фірстов С. (Україна), Фістуль В. (Росія), Шпак А. (Україна), Шпілевський Е. (Білорусь), Шпотюк О. (Україна)

### Національний

Бойчук В. (Дрогобич), Буджак Я. (Львів), Гасюк І. (Івано-Франківськ), **Гладких М.** (Харків), Давидюк Г. (Луцьк), Дзундза Б. (Івано-Франківськ), Дмитрук М. (Київ), Дружинін А. (Львів), Запухляк Р. (Івано-Франківськ), Зауличний Я. (Київ), Зінченко В. (Одеса), Зиман З. (Харків), Ігнатенко П. (Донецьк), Кідалов В. (Бердянськ), Кланічка В. (Івано-Франківськ), Коваленко О. (Дніпропетровськ), Корбутяк Д. (Київ), Куницький Ю. (Київ), Лашкарьов Г. (Київ), Лепіх Я. (Одеса), Ліщинський І. (Івано-Франківськ), Лоп'янко М. (Івано-Франківськ), Матвеева Л. (Київ), Мельничук О. (Ніжин), Миколайчук О. (Львів), Никируй Л. (Івано-Франківськ), Похмурський В. (Львів), Прокопів В. (Івано-Франківськ), Проценко І. (Суми), Прокопенко І. (Київ), Птащенко О. (Одеса), Рогачова О. (Харків), Рубіш В. (Ужгород), Рувінський М. (Івано-Франківськ), Середа Б. (Запоріжжя), Смертенко П. (Київ), Стасюк З. (Львів), Стронський О. (Київ), Студеняк І. (Ужгород), Ткач М. (Чернівці), Томашик В. (Київ), Чуйко Г. (Херсон)

### Секретаріат

Межиловська Л.Й. – вчений секретар конференції  
Борик В.В., Гургула Г.Я., Дзумедзей Р.О.,  
Соколов О.Л., Потяк В.Ю. – секретарі

## ORGANIZING COMMITTEE

### Bureau

**D. Freik, V. Lytovchenko, I. Myronyuk, B. Ostafiychuk, G. Sukach**

### International

**R. Ahiska** (Turkey), **L. Anatychyk** (Ukraine), **M. Babanly** (Azerbaijan), **O. Belyaev** (Ukraine), **I. Blonskiy** (Ukraine), **M. Brodyn** (Ukraine), **L. Bulavin** (Ukraine), **V. Chobanyuk** (Ukraine), **S. Firstov** (Ukraine), **V. Fistulj** (Russia), **M. Galushchak** (Ukraine), **M. Goncharenko** (Ukraine), **P. Gorbyk** (Ukraine), **Z. Gotra** (Ukraine), **A. Grigonis** (Lithuania), **B. Grynyov** (Ukraine), **Yu. Gurevich** (Mexico), **O. Ivasyshyn** (Ukraine), **I. Kalinkin** (Russia), **M. Kartel** (Ukraine), **M. Kharchenko** (Ukraine), **O. Kikineshi** (Hungary), **F. Komarov** (Belarus), **S. Kuchmij** (Ukraine), **B. Kyyak** (Ukraine), **M. Kumar** (India), **V. Machulin** (Ukraine), **G. Malashkevich** (Belarus), **Ye. Mazurenko** (Ukraine), **I. Mittova** (Russia), **G. Mladenov** (Bulgaria), **B. Movchan** (Ukraine), **A. Naumovetsj** (Ukraine), **M. Nahodkin** (Ukraine), **K. Nikiforov** (Russia), **M. Novykov** (Ukraine), **V. Panasjuk** (Ukraine), **Yu. Ptushynskiy** (Ukraine), **I. Rarenko** (Ukraine), **A. Shpak** (Ukraine), **E. Shpilevsky** (Belarus), **O. Shpotyuk** (Ukraine), **F. Sizov** (Ukraine), **L. Skatkov** (Israel), **Yu. Solonin** (Ukraine), **I. Stasjuk** (Ukraine), **M. Striha** (Ukraine), **S. Svechnikov** (Ukraine), **S. Sydorenko** (Ukraine), **T. Tchelidze** (Georgia), **R. Todoran** (Romania), **P. Tomchuk** (Ukraine), **I. Tiginyanu** (Moldova), **V. Uvarov** (Ukraine), **O. Vlasenko** (Ukraine), **S. Volkov** (Ukraine), **V. Wojcik** (Poland), **V. Zlomanov** (Russia), **P. Zukowski** (Poland)

### National

**V. Boychuk** (Drogobych), **Ya. Budzhak** (Lviv), **G. Chuyko** (Kherson), **G. Davydyuk** (Lutsk), **B. Dzungza** (Ivano-Frankivsk), **M. Dmytruk** (Kyiv), **A. Druzhynin** (Lviv), **I. Gasyuk** (Ivano-Frankivsk), **M. Gladkykh** (Kharkiv), **P. Ignatenko** (Donetsk), **V. Kidalov** (Berdyansk), **V. Klanichka** (Ivano-Frankivsk), **D. Korbutyak** (Kyiv), **O. Kovalenko** (Dnipropetrovsk), **Yu. Kunitskiy** (Kyiv), **G. Lashkaryov** (Kyiv), **I. Lepikh** (Odesa), **I. Lishchynskyy** (Ivano-Frankivsk), **M. Lopyanko** (Ivano-Frankivsk), **L. Matveeva** (Kyiv), **Yu. Melnychuk** (Nizhyn), **O. Mykolaychuk** (Lviv), **L. Nykyruy** (Ivano-Frankivsk), **V. Pohmursjkyy** (Lviv), **V. Prokopiv** (Ivano-Frankivsk), **I. Protsenko** (Sumy), **I. Prokopenko** (Kyiv), **O. Ptashchenko** (Odesa), **O. Rogachova** (Kharkiv), **V. Rubish** (Uzhgorod), **M. Ruvinskyy** (Ivano-Frankivsk), **B. Sereda** (Zaporizzhya), **P. Smertenko** (Kyiv), **Z. Stasyuk** (Lviv), **O. Stronsjkyy** (Kyiv), **I. Studenyak** (Uzhgorod), **M. Tkach** (Chernivtsi), **V. Tomashyk** (Kyiv), **R. Zapykhlyak** (Ivano-Frankivsk), **I. Zaulychnyy** (Kyiv), **Z. Zyman** (Kharkiv), **V. Zinchenko** (Odesa)

### Secretariate

Scientific Secretary – **L. Mezhylovska**

Secretaries – **V. Boryk, G. Gurgula, R. Dzumedzey, O. Sokolov, V. Potyak**

**Вельмишановні пані та  
панове! Друзі! Колеги!  
Учасники  
XIII МКФТТПН – 2011!**

Історія розвитку подій часто повторюється! Це не обійшло стороною і нашу міжнародну конференцію! Маю на увазі місце її проведення у серці Гуцульщини – смт. Верховині! Постійним учасникам, нашим друзям, буде приємно згадати минулі роки, коли ми були молодими. Отож юнацького запалу всім Вам у науковому пошуку, спілкуванні!

Сподіваюся, що наша зустріч сприятиме насамперед консолідації діяльності провідних науковців і молоді України та інших держав, зміцнить наукові дослідження у нових стратегічних напрямках.

***Оптимізму і успіхів Вам!***

**З великою повагою,  
голова Оргкомітету  
МКФТТПН-ХІІІ**

**Дмитро Фреїк**



*с.м.т. Верховина, Івано-  
Франківська обл., Україна  
16 травня 2011 р.*



**Ladies and Gentlemen, Friends!  
Colleagues  
Participants  
XIII ICPTTFN – 2011!**

History of events often repeats! This is not spared our international conference! I mean the venue in the heart Hutsulshchyna – town Verkhovyna! Regular members, our friends, be nice to remember the years when we were young. So youthful enthusiasm to all of You in scientific research, communication!

I hope that our meeting will first consolidate the work of scholars and youth of Ukraine and other countries, strengthen scientific research in new strategic directions.

***Optimism and good luck to You!***

**With great respect,  
Chairman of the Organizing Committee  
ICPTTFN-XIII**

**Dmytro Freik**



*Town Verkhovyna, Ivano-Frankivsk  
region, Ukraine  
May, 16, 2011.*

**ПЛЕНАРНІ ДОПОВІДІ**

17-20 травня 2011 р.

**PLENARY REPORT**

May, 17-20, 2011



## TEPAS Computer Controlled System for Measuring Parameters of Semiconductors in Real Thermoelectric Modules

Ahıska Rasit<sup>1</sup>, Ahıska Günay<sup>2</sup>

<sup>1</sup>Gazi University, Ankara, Turkey

<sup>2</sup>Ankara University, Ankara, Turkey

In this study, a computer controlled test system composed of hardware and software, Thermoelectric Performance Analysis System (TEPAS) based on a new method [1] taking inputs of easily measurable parameters like temperature, current and voltage, is employed in calculation of thermal conductivity,  $\kappa$ , Seebeck coefficient,  $\alpha$ , specific resistivity,  $\rho$ , and quality parameter,  $z$ , of semiconductor in standard TE modules of MELCOR Inc. CP 1.0-127-05L, CP 1.4-127-10L and CP 1.4-71-06L (TEC1-07106) [2].

Computer controlled TEPAS, with its hardware and software, has been designed and realized for performance analysis and acquisition of parameters of operating TE modules and systems. In figure 1 below, internal and external views of TEPAS are demonstrated. According on CP modules direct measurements with TEPAS have  $I_{max}$  - 0.6%;  $V_{max}$  - 3.3%;  $\Delta T_{max}$  - 1.9% average precision, and calculations have  $z$  - 4.6% error percentages.



Fig. 1. General view of TEPAS.

Error percentages in  $\rho$ ,  $k$  and  $z$  measured with TEPAS and the new method are found to be very little compared to other methods and apparatuses. It is demonstrated that  $\rho$ ,  $k$  and  $z$  parameters linearly depends on  $E$  and thermoemf is the key parameter, and with TEPAS based on the new method all parameters can be directly measured. In conclusion thanks to new TE performance analysis system,  $\rho$ ,  $k$  and  $z$  parameters of semiconductors in TE module can be measured fast, with high reliability and practically. TEPAS can be employed not in testing of TE modules or semiconductors but also in mass production of these as a quality controller.

1. Ahıska R, and Ahıska, K., 2010 New method for investigation of parameters of real thermoelectric modules *Energy Conversion and Management* **51**, 338–345.
2. <http://www.melcor.com> homepage of Melcor.

## Polymer-magnet nanosystems

Aksimentyeva O.<sup>1</sup>, Opaynych I.<sup>1</sup>, Dyakonov V.<sup>2</sup>, Piechota S.<sup>2</sup>,  
Gorbenko Yu.<sup>1</sup>, Szymczak H.<sup>2</sup>

<sup>1</sup>*Ivan Franko National University of Lviv, Lviv, Ukraine*

<sup>2</sup>*Institute of Physics, Polish Academy of Science, Warsaw, Poland*

Polymer magnet materials arise to a great scientific attention due to their practical application in novel technologies and researchers. Flexibility, small losses at demagnetization, ability to film formation and low specific weigh determine an important part of these materials in different fields, such as molecular electronics, recording of information, sensor engineering, catalysis and new diagnostic methods in medicine. Together with intensive investigation of molecular polymer magnets there is a special interesting to study the hybrid polymer-magnet materials [1, 2].

Polymerization of aromatic monomers in the magnetite colloidal dispersion stabilized by surfactants leading to capsulation of the magnetite particles by polymer shell with formation of self – assembled molecular aggregates provide a stability of the system. Obtaining by developed method polymer-magnetite composites were characterized by X-ray diffraction, Raman spectroscopy, atom-force and electron microscopy, thermo gravimetric and thermo-mechanical measurements.

Conducting polymer-magnetite composites are found to exhibit both electrical and magnet functions. By investigation of mechanical, thermal and thermo-mechanical properties of hybrid composites we determined the optimal interval of magnetite content provided a compacting of composites and increasing of their mechanical hardness, glass transition and flow temperature.

**Acknowledgement.** This work was partially supported by the Ministry of Science and Higher Education (PL), Grant N 507 492438.

1. Vasyukov V.N., Dyakonov V.P., Shapovalov V.A., Aksimentyeva O.I., Szymczak H., Piehota S. Temperature-induced change in the ESR spectrum of the Fe<sup>3+</sup> ion in polyaniline // Low Temperature Physics. – 2002. – Vol.26, N4. – P. 265-269.
2. Opainych I. Ye., Aksimentyeva O.I., Szymczak H., Dyakonov V.P. // 5-th Int. Work-shop on Functional and Nanostructured Materials. – Lviv, Ukraine, 2008. – P. 122-124.

## New ternary compounds $Tl_9LnTe_6$ type and variable composition phases on their base

Babanly M.B., Imamaliyeva S.Z., Yusibov Yu.A., Sadiqov F.M.

*Baku State University, Baku*

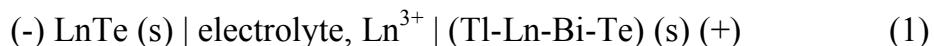
Narrow bang gap semiconductors based on heavy metals and rare-earth tellurides and also multicomponent phases on their base are promising compounds for obtaining thermoelectric materials. Thallium subtelluride  $Tl_5Te_3$  (I4/mcm) which possesses thermoelectric characteristics owing to features of the crystal structure has a number of ternary analogs. One of them -  $Tl_9BiTe_6$  has record thermoelectric parameters and can serve as a base compound for the development of new similar materials with the improved properties [1].

The new ternary compounds  $Tl_9LnTe_6$  also crystallising in structural type  $Tl_5Te_3$  and having following parameters  $a = 8.890$ ,  $c = 13.015 \text{ \AA}$ ,  $z = 2$  ( $Tl_9CeTe_6$ );  $a = 8.888$ ,  $c = 13.014 \text{ \AA}$ ,  $z = 2$  ( $Tl_9NdTe_6$ );  $a = 8.888$ ,  $c = 13.013 \text{ \AA}$ ,  $z = 2$  ( $Tl_9SmTe_6$ );  $a = 8.887$ ,  $c = 13.012 \text{ \AA}$ ,  $z = 2$  ( $Tl_9GdTe_6$ ) and  $a = 8.887$ ,  $c = 13.011 \text{ \AA}$ ,  $z = 2$  ( $Tl_9TmTe_6$ ) are revealed in [2, 3].

In given work the phase equilibriums in systems  $Tl_5Te_3$ - $Tl_9LnTe_6$ - $Tl_9BiTe_6$  (Ln-Ce, Nd, Sm, Gd, Tm) for obtaining of solid solutions with  $Tl_5Te_3$  structure are investigated.

The alloys were synthesized from preliminary synthesized compounds in quartz ampoules under vacuum ( $\sim 10^{-2}$  Pa) and exposed for a long thermal annealing (500-1000 h.) at 600 K.

We have used the differential thermal, X-ray phase and microstructural analyses, as well as measurements of microhardness and EMF of concentration chains of type



at 300 – 430 K temperature interval.

On the base of data of DTA a number of vertical sections and isothermal sections at 600 and 700 K of phase diagrams as well as projections of liquidus and solidus surfaces of the above-stated systems were constructed. In was shown, that all investigated systems are characterised by unlimited mutual solubility of components in liquid and solid states and form phase diagrams of I type on Rozebom.

According to data X-ray phase analyses solid solutions have tetragonal structure of  $Tl_5Te_3$  type, and concentration dependences of their lattice parameters are almost linear.

From the results of EMF measurements the partial molar thermodynamic functions ( $\Delta\bar{G}, \Delta\bar{H}, \Delta\bar{S}$ ) of LnTe in alloys at 298 K are calculated. Characters of concentration dependences of these functions, and also microhardness have confirmed the formation of continuous solid solutions in the above-stated systems.

The constructed phase diagrams are used for development of techniques and for a choice of conditions of obtaining mono-crystals of the phases with given structure by the directed crystallization from non-stoichiometrical melts.

1. Wolfing B., Kloc C., Teubner J., Bucher E. // Phys. Rev. Lett. – 2001. - V.36, №19. - PP.4350-4353.
2. S.Z.Imamaliyeva, F.M.Sadygov, M.B.Babanly // Inorgan. Materials. – 2008. - V.44, №9. - PP.935-938.
3. M.B. Babanly, S.Z. Imamaliyeva, D.M. Babanly, F.M. Sadygov. // Azerb. Chem. J. – 2009. - №2. - P.122-125.

## **Evolution of the predictable applications of nanoobjects in the field of thermoelectricity**

Baranskii P. I.<sup>1</sup>, Gaidar G. P.<sup>2</sup>

<sup>1</sup>*V. E. Lashkaryov Institute of Semiconductor Physics NAS of Ukraine, Kyiv, Ukraine*

<sup>2</sup>*Institute for Nuclear Research of NAS of Ukraine, Kyiv, Ukraine*

The most important and probably the most hard-to-eliminable features of nanoobjects (NO) are typical for them spatial irregularities in the distribution of dopants and, in more general case, of chemical composition.

Another essential feature of NO is their structural heterogeneity: the matrix with enclosed nanoinclusions or repetitive ultra-thin layers, which differ in their chemical nature, and the presence of interfaces between them.

From the presence of spatial irregularities in the distribution of atoms it is inevitably follows the fact of coexistence of the interatomic forces, typical both for the atoms in the volume of crystal and for the atoms at the surface (with all possible intermediate states). This fact ensures the absence of a single interatomic distance (the lattice constant) within the NO, and, in general, the lack of the translational symmetry with all the ensuing consequences.

With the above mentioned circumstances it is connected that the internal potential in NO can noticeably vary at the distances comparable with the interatomic. And in this case the using of the effective mass method becomes problematic.

Third, and perhaps the most important, feature of NO is the presence of large internal mechanical stresses arising from differences of the interatomic interactions in the separate elements of the NO [1].

The above mentioned features of the NO leads to the fact, that the opportunities to increase the  $Z = \frac{\alpha^2 \sigma}{\chi}$  due to the utilization of NO for this purpose, which at the beginning seem stupendous, quickly disappeared. The vast experience has shown that the significantly increase of the value of this parameter due to the use of NO (for example, in the form of superlattices) at the present state of science and technology is practically impossible.

1. Baranskii P. I., Fedosov A. V., Gaidar G. P. Heterogeneities of semiconductors and urgent problems of the interdefect interaction in the radiation physics and nanotechnology // Kyiv-Lutsk: Editorial and Publishing Department of the Lutsk State Technical University.– 2007. – 316 p.

## **Diffusion barriers in ohmic contacts to semiconductor device structures**

Belyaev A.E.<sup>1</sup>, Boltovets N.S.<sup>2</sup>, Konakova R.V.<sup>1</sup>, Kudryk Ya.Ya.<sup>1</sup>,  
Milenin V.V.<sup>1</sup>

<sup>1</sup> *V. Lashkaryov Institute of Semiconductor Physics, NAS of Ukraine, Kyiv, Ukraine*

<sup>2</sup> *State Enterprise Research Institute "Orion", Kyiv, Ukraine*

The problem of development of solid-state microelectronic devices of increased reliability and resistance to active actions involves search for and use of such materials for contact metallization that exclude or reduce considerably the action of factors stemming from migration processes.

The attempts to solve the problem of stabilization and reliability of the parameters of contact systems as well as reduction of the area and depth of such systems by using conventional thermodynamic and kinetic approaches did not succeed. Another way turned out to be more promising. It involves formation in the contact structure of stabilizing layers, namely, diffusion barriers that are not products of interactions between phases of the contacting layers. Just that approach makes it possible to make radically new versions of contact structures for semiconductor devices that are resistant to various extreme actions and have smaller sizes.

The requirements placed upon contact metallization are as follows: the materials for diffusion barriers must have high conductivity and low coefficient of thermal expansion as well as demonstrate high thermal and chemical stability. The manufacturing technology for such materials should be rather simple.

It was found that nitrides and borides of the metals belonging to groups IV, V and VI meet the above requirements. The crystalline structure of these compounds is close-packed; their composition and structure can be varied over wide ranges.

We present the results of our investigations of contact systems (with diffusion barriers made as amorphous  $TiB_x$  films) to the device structures that are based on Si, GaAs, GaP, InP, SiC and GaN epitaxial films and are used when making microwave diodes and transistors. The stress is laid on the features of the physico-chemical processes proceeding at formation of ohmic contacts as well as factors that limit their thermal stability.

## Strain-resistance effect in the thin-films of cadmium and germanium tellurides

Berceshchuk M., Bojko M., Kryskov A., Kryskov Ts., Lyuba T.,  
Rachkovsky O., Turnickyj V.

*Ivan Ohienko Kamianets-Podilskiy national university, Kamianets-Podilsky, Ukraine*

A change of resistance in the thin-films of chalcogenide semiconductors, conditioned by their deformation, was researched. Films besieged from the preliminary synthesized ground up materials (CdTe, GeTe) by the method of vacuum thermal deposition on the thin plates of mica by the sizes (4,5x1, 5) cm and in thick a 0,2 mm with the beforehand formed copper electric contacts on their edges. In the undeformed state of resistance of thin-films folded: 660 and 340  $\kappa\Omega$  for tellurides of cadmium and germanium accordingly. All measuring is executed at a room temperature.

The deformations of wricked, bend and twisting are carried on samples. The change of resistance of thin-films in dependence on the size of relative deformation was measured. The coefficient of tensosensibility  $k$  determined as division of relative change of resistance of thin-films toward their relative deformation. Results of researches are shown in the table.

Changing of the resistance of thin films at the deformation

Compounds	Type of deformation	R/R, %	k
CdTe	wricked	4,55	79,6
	bend	6,06	79,8
	twisting	6,2	80,2
GeTe	wricked	5,47	80,4
	bend	6,12	80,8
	twisting	10,9	91,6

Small values of the coefficient of tensosensibility can be caused by insufficient structural perfection of films and by the lack of deep local levels in the restricted area.

1. Маматкаримов О.О., Хамидов Р.Х. Тензорезистивный эффект в кремнии с примесью олова при статических и динамических давлениях. // Письма в ЖТФ. – 2003. – Т.29, вып. 3. – С. 24-28.
2. Федосов А.В., Луньов С.В., Захарчук Д.А., Федосов С.А., Панасюк Л.І. Вплив глибоких енергетичних рівнів на тензоефекти в кристалах n-Ge:Аu // Вісник Луцького національного технічного університету. – 2009. – вип. 8. – С. 301-303.

## **Non-Standard Dispersion Law for Charge Carriers in Highly Anisotropic and Layered Semi-Conductors and Related Effects**

Bercha D.M.<sup>1</sup>, Bondar V.M.<sup>3</sup>, Solonchuk L.S.<sup>2</sup>, Kharkhalis L.Yu.<sup>1</sup>,  
Shenderovskij V.A.<sup>3</sup>

<sup>1</sup>*Uzhhorod National University, Uzhhorod, Ukraine*

<sup>2</sup>*The Yu.Fedkovych Chernivci National University, Chernivci, Ukraine*

<sup>3</sup>*The Institute of Physics of NAS of Ukraine, Kyiv, Ukraine*

The paper contains consequent theoretical and experimental studies of transfer phenomena in highly anisotropic and layered semi-conductors with accounting for the real gap structure and peculiarity of charge carriers scattering nature. We have carried out detailed analysis of elastic and inelastic scattering influence on field and temperature dependencies of kinetic coefficients.

We have established that charge carriers dispersion law peculiarities show themselves well in high electric (heating carriers) fields. One can expect such peculiarities in low-symmetry semi-conductors with certain numbers of atoms within elementary cell. Layered crystals of In<sub>4</sub>Se<sub>3</sub>, crystal Te and two-dimensional crystal structures are the particular examples.

We have considered in detail plasma-electric effect that occurs in a semi-conductor within external electric field and essentially depends on parameters characterizing charge carriers dispersion law deviation from its standard parabolic form. When compared with Te crystal, this effect is more clear in the case of layered In<sub>4</sub>Se<sub>3</sub> crystals.

Moreover, we have established that electric field, heating carrier and carrier energy dispersion law deviation from its parabolic form produces new effects in combination light scattering, namely, can generate scattering coefficients' anisotropy and, for some electric field orientations, wave scattering effects can have anomalously high values that can be put into the origin of solid state lasers with regulated emission frequency.

We have discovered some distinctions of free carrier emission polarization dependencies in low-symmetry crystals from those of multi-valley semi-conductors related to peculiarities of carrier energy gap spectrum and charge carriers scattering nature.

1. V. A. Shenderovskij, Solid State Physics and Chemistry. – 2005. – V.6. №3. – P. 262-265.
2. M. Snajder, L.Yu. Kharkhalis, V. A. Shenderovskij, D.M. Bercha. Acta Physica Polonica A. – 2009. – V.116, №5. – P.952-953.
3. P. M. Tomchuk, V. A. Shenderovskij. JETP, – 1972, – V.62, №3. – P. 1131-1143.
4. V. M. Bondar, N. F. Chornomorec'. UJPh. – 2003. – V. 48, №1. – P. 51-55.

## **A<sup>I</sup>-Bi-C<sup>VI</sup> thin films as gas sensors: structural, optical and electrical investigations.**

Bilozertseva V.I.<sup>1</sup>, Khlyap H.M.<sup>2</sup>, Mamalui A.O.<sup>1</sup>, Dyakonenko N.L.<sup>1</sup>,  
Gaman D.O.<sup>1</sup>, Petrenko L.G.<sup>1</sup>

<sup>1</sup> *National Technical University "Kharkov Polytechnical Institute", Kharkiv, Ukraine*

<sup>2</sup> *University of Technology, Kaiserslautern, Germany*

Ternary compounds A<sup>I</sup>-Bi-C<sup>VI</sup> (A<sup>I</sup>-Li,Na,K and C<sup>VI</sup>-S, Se, Te) are very interesting semiconductor materials and almost unknown in the field of the materials science. Thin films obtained from these compounds are non-equilibrium thermodynamic systems with various characteristics. Their structural, optical and electric properties are seemed to be of special importance for nanotechnology and nanoelectronic applications, while the simplicity of growth technology gives wide possibilities in preparing structures with in-advance defined sensitive and electric properties.

Earlier [1] we have showed that the optical transmission coefficients of these films increase under interaction with aggressive atmospheric impurities in spectral range 400 – 1200 nm. It was demonstrated that interaction between Bi-contained thin films and nitrogen oxide NO leads first of all to the sufficient changes of optical properties and morphology of the film surface. NO concentration in the experimental chamber was maximally closed to the value of 1 mg/m<sup>3</sup> while this value is the most interesting as a danger limit for a man safety. This result gives a good possibility to prepare a large area gas sensor suitable for operation in dangerous atmospheric conditions. The transmission spectra of KBi<sub>3</sub>S<sub>5</sub> films obtained under the room temperature before and after 1 hour NO exposition are examined.

Investigations of electric characteristics are to give additional possibilities and freedom under creating an active element of the device. Nevertheless, these characteristics were not studied previously.

The paper reports for the first time experimental data on gas sensitivity of investigated films and room-temperature electric field-induced characteristics of the corresponding metal-semiconductor structures based on LiBiSe<sub>2</sub> and NaBiTe<sub>2</sub> films.

Thin films were deposited onto glass substrates at different substrate temperatures from Knudsen cell under vacuum level  $P = 10^{-3}$  Pa. The controllable shutter mechanism made it possible to obtain the films with different thicknesses (60 – 200 nm) during one deposition cycle. The average rate of deposition was governed by change of the evaporator temperature and estimated to be 0.1 - 0.5 nm/s.

The microstructure and phase composition of thin films were investigated by transmission electron microscopy (TEM) and electron diffraction methods. The morphological peculiarities of the film relief had been studied by atomic force microscopy (AFM). Typical TEM images and microdiffraction patterns show



amorphous  $\text{LiBiSe}_2$  and polycrystalline  $\text{LiBi}_3\text{Se}_5$  structures of the films manufactured by this technology [2].

Electric measurements of the  $\text{LiBiSe}_2$  films were carried out at the room temperature in open air under normal atmospheric conditions. *In* was used as material for contacts.

Two sets of  $\text{NaBiTe}_2$  samples were prepared: with Cr-contacts for electric studies and without them for gas sensitivity investigations.

The room-temperature current-voltage characteristics of  $\text{In/LiBiSe}_2$  and  $\text{Cr/NaBiTe}_2$  structures are also investigated and possible mechanisms of charge carrier's transport are discussed.

Studies of the electric field-induced properties of  $\text{Cr/NaBiTe}_2$  structures were carried out in vacuum (in the growth chamber *in situ*) as well as in open air under normal atmospheric conditions and the applied electric field up to  $10^5$  V/m.

In order to examine gas sensitivity the as-grown  $\text{NaBiTe}_2$  films were placed in the closed chamber with  $\text{NO}$  concentration up to  $1 \text{ mg/m}^3$  at the room temperature.

Experimental optical transmission spectra of initial samples and after interaction with nitrogen monoxides of various concentration are presented. It is shown that films demonstrate significant changes of their optical characteristics even at low concentrations of the aggressive gas. As the nitrogen monoxide concentration increases, the transmission of the examined layers is also increasing.

AFM investigations of as-grown samples and after  $\text{NO}$  exposition were carried out. The standard numerical processing of the image enabled to estimate the parameters of the surface roughness. After  $\text{NO}$  exposition the film relief changes: the roughness of the layer surface is decreasing.

The electrical conductivity of  $\text{NaBiTe}_2$  films changes under exposure of different aggressive environments: the time profile of the dc current flowing through the sensor in response to adsorption and desorption of different gases as a very important characteristic of the device had been investigated. Current response curves measured after undergoing the examined samples to  $\text{H}_2\text{S}$  and  $\text{NH}_3$  gas exposure at the room temperature are discussed. These data point out the following: (i) a relatively high sensitivity; (ii) a fast response of the films to  $\text{NH}_3$  exposure; (iii) a good but slower response of the layers to  $\text{H}_2\text{S}$  exposure.

1. V. Bilozertseva, A. Ryabchun, N. Dyakonenko, L. Petrenko, S. Gapochenko.  $\text{A}^{\text{I}}\text{Bi}_3\text{C}_5^{\text{VI}}$  thin films application for  $\text{NO}$  sensors // Photoelectronics. – 2003. – V. **12**. - PP. 20-24.
2. V.I. Bilozertseva, H.M. Khlyap, P.S. Shkumbatyuk, N.L. Dyakonenko, A.O. Mamaluy, D.O. Gaman. Li-Bi-Se semiconductor thin films: technology, structure and electrophysical properties // Semiconductor Physics, Quantum Electronics & Optoelectronics. – 2010. – V. **13**(1). - PP. 61 - 64.

**Induced anisotropy of surface plasmon optical response  
in spherical noble metal nanoparticles  
in the field of powerful femtosecond pulses**

Blonskyi I.V.<sup>1</sup>, Dmitruk I.M.<sup>1,2</sup>, Dmytruk A.M.<sup>1</sup>, Zubrilin N.G.<sup>1</sup>,  
Yeshchenko O.A.<sup>2</sup>, Kadan V.M.<sup>1</sup>, Korenyuk P.I.<sup>1</sup>, Pavlov I.A.<sup>1</sup>,  
Alexeenko A.A.<sup>3</sup>

<sup>1</sup>*Institute of Physics, NAS of Ukraine, Kyiv, Ukraine*

<sup>2</sup>*Taras Shevchenko National University of Kyiv, Kyiv, Ukraine*

<sup>3</sup>*Pavel Sukhoi State Technical University of Gomel, Gomel, Republic of Belarus*

High intensity of electromagnetic field (up to the ionization threshold) is one of the features of femtosecond laser radiation. It promotes a pronounced manifestation of nonlinear effects in transparent media, strong heating of electron gas in absorbing materials, dynamic and irreversible modifications of properties of actual optical construction materials, etc. Here we report our results of investigations of propagation of powerful ( $\sim 10^{12}$  W/cm<sup>2</sup>) femtosecond pulses in transparent SiO<sub>2</sub> matrix, and interaction of the femtosecond pulses with noble metal nanoparticles, which are incorporated in a transparent matrix. Our studies were carried out using the facilities of the Center for collective use of equipment of NAS of Ukraine - "Femtosecond Laser Complex".

The main result of the research is the new phenomenon of dynamic polarization splitting of surface plasmons in noble metal spherical nanoparticles, which are incorporated in transparent dielectric matrices, and instability of the eigenfrequency of such collective excitations in the field of powerful femtosecond pulses. The theoretical model that explains the nature of the observed anomalies has been suggested. The model is based on induction of optical anisotropy in SiO<sub>2</sub> matrix by femtosecond pulses. The induced anisotropy has complex time evolution that is determined by the total contribution from the high-frequency Kerr effect and plasma effects. The experimentally determined parameters, which quantitatively characterize the mentioned nonlinear processes, match the calculation parameters used in the theoretical model.

1. Dmitruk I., Blonskyi I., Pavlov I., Yeshchenko O., Alexeenko A., Dmytruk A., Korenyuk P., Kadan V., Zubrilin N. Optically induced anisotropy of surface plasmons in spherical nanoparticles. // Phys. Rev. B. – 2010. – V. 82. – P. 033401-1033401.

## **Modification of absorption spectra of organic semiconductor thin films doped with plasmonic nanoparticles**

Bogach V.N., Dynich R.A., Zamkovets A.D., Ponyavina A.N.

*Institute of Physics, National Academy of Sciences of Belarus, Minsk, Belarus*

Last year hybrid plasmonic nanostructures contained of both non-organic and organic components are of a growing interest for their promising applications in nanophotonics and nanoelectronics. These nanomaterial considerable promises are essentially connected with a fast and tunable optical response of metal plasmonic nanoparticles as well as with a strong enhancement of electromagnetic fields near their surface at the spectral range of a surface plasmon resonance (SPR) in the visible [1]. However spectral features of nanostructures consisted of plasmonic nanoparticles imbedded into an absorbing matrix (including organic films) are still studied slowly.

In order to establish an influence of plasmonic nanoparticles on absorption of the matrix where they are placed we studied spectra of the Ag/CuPc nanocomposites and their components. Samples were fabricated by thermal evaporation in vacuum and constituted the Ag island layers into the organic semiconductor (CuPc) thin-film matrix. A sample structure was characterized with the atomic-force microscope. Numerical calculations were made with the use of the noncoherent and coherent single scattering approximation modified for the absorbing matrix.

We found a strong modification of the Ag/CuPc nanocomposite spectra in comparison with the spectra of the Ag island layer and the CuPc thin film. The degree of a spectra change was found to be dependent on silver nanoparticle sizes and their surface concentration, as well as on a CuPc film thickness. The most common feature is that the SPR of silver nanoparticles grows weaker into the absorbing matrix. Besides, a matrix filling by plasmonic nanoparticle leads to matrix absorption enhancement especially in the long-wavelength (relative to the SPR) spectral range. This enhancement may reach 65 % at a special choice of silver nanoparticle sizes and a CuPc film thickness.

Comparison of theoretical and experimental data shown also that in order to describe the spectra of the Ag / CuPc nanocomposites one needs to take into account the near-field effects which results in strong absorbency increase of the CuPc matrix.

1. Dynich R.A., Ponyavina A.N., and Filippov V.V. Local field enhancement around spherical nanoparticles in the absorbing medium // *J. Appl. Spectr.* – 2009. – V.76 (5). - P.746 – 751.

## **Exciton and impurity states in quantum dot heterosystems**

Boichuk V.I., Bilyns'kyi I.V., Leshko R.Ya.

*Ivan Franko Drohobych State Pedagogical University, Drohobych, Ukraine*

Intensive progress of semiconductor physics of low-dimensional structures observed in the past decades is caused by unique physical properties of these systems. New physical phenomena of nanoscale heterosystems made it possible to fabricate a number of modern micro- and optoelectronic devices: high electron mobility transistors, resonant tunnel diodes, quantum well lasers. Tendencies of novel micro- and nanoelectronics development are determined by miniaturization of elements and high-speed performance. These requirements are satisfied best with the use of devices based on quantum-sized effects.

Now physicists face the problem of fabrication of light emitting devices based on nanocrystals with radiative wavelength which can be tuned due to crystal size change, choice of the environment, etc.

In the paper the review of theoretical studies on exciton, impurity absorption and luminescence spectra of nanocrystals of various nature and symmetry is performed. The effects of matrix polarization properties, fine structure of the conduction and the valence bands, nanocrystal shape on exciton and impurity states.

## Metal nano-particles in the applications for photovoltaic, light emission and microelectronic: experiments and theory

Boltaev A.P.<sup>1,2</sup>, Bothe K.<sup>3</sup>, Kazaryan S.A.<sup>1</sup>, Krotova K.E.<sup>2</sup>, Pors A.<sup>4</sup>,  
Protsenko I.E.<sup>1,2</sup>, Pudonin F.A.<sup>1,2</sup>, Sherstnev I.A.<sup>1,2</sup>, Starodubtsev N.F.<sup>1</sup>,  
 A. V. Uskov<sup>1,2,4</sup>, Willatzen M.<sup>4</sup>

<sup>1</sup>*P. N. Lebedev Physical Institute (FIAN), Moscow, Russia*

<sup>2</sup>*Plasmonics LTD, Moscow, Russia*

<sup>3</sup>*Institut für Solarenergieforschung Hameln (ISFH), Emmental, Germany*

<sup>4</sup>*Mads Clausen Institute (MCI), University of Southern Denmark, Sønderborg, Denmark*

Results of our recent research concerning applications of optical (“plasmonic”) and electro-physical properties of metal nano-particles used for performance improvement of various devices (solar cells, for instance) and development of new devices (likely to “dipole” nano-lasers), are presented.

First, we present preliminary results of experiments carried out on crystalline Si solar cells (SC) coated by metal (Au, Ag and Al) nanoparticles [1] (NP-coating) (Russia, Germany), compare our results with theoretical predictions [2] (Russia, Denmark), show new perspectives, and discuss the most relevant technological aspects of deposition of Al nanoparticles. Increase of SC efficiency in near IR region is observed due to Au or Ag nanoparticles on SC surface – Fig., - in good agreement with modeling results. Plasmonic theory predicts that NP-coating may act as an anti-reflection coating. In contrast to standard anti-reflection coatings (such as Si<sub>3</sub>N<sub>4</sub>) the effective index of refraction

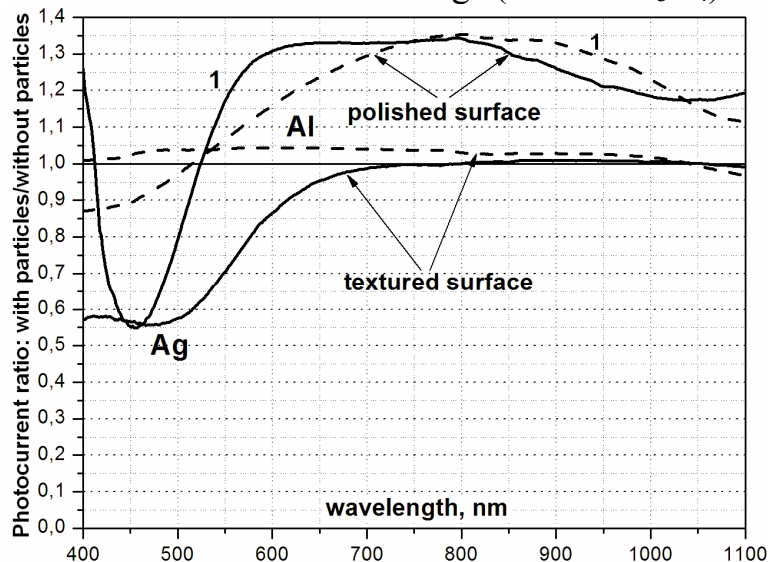


Fig. Relative photocurrent for solar cell samples with Ag (solid curves) and Al (dashed curves) nanoparticles. Samples are from Pavlovsk, Russia (curves 1) and ISFH, Germany (other curves).

can be continuously varied by changing the volume concentration of nano-particles. In principle, the NP-coating allows for an optimized transparency for a wide (solar) spectral range. Decrease in solar cell efficiency with NP coating in the visible region (Fig.1) is due to absorption by nanoparticles at the Localized Plasmon Resonance (LPR), however the overall impact of the NP-coating on SC efficiency is positive. Moreover, the theory predicts a shift of the absorption to

blue side, i.e. out of the solar spectrum. This prediction is experimentally confirmed in the case of Al nanoparticles. Thus, Al nano-particles are promising candidates for SC NP-coating and can easily be deposited by electron-beam evaporation even in the matrix of Al<sub>2</sub>O<sub>3</sub>.

Second, dipole nano-lasers (DNL) and optical nano-modulators are proposed and described theoretically [3]. DNL consist of metal nano-particles electromagnetically coupled to a resonant radiative medium (semiconductor, dye solution etc) or to single quantum dots. Nano-particles act as optical emitting antenna. Bosonic properties of resonant oscillations of dipole momentum of nano-particle (“plasmons”) ensures coherent generation of dipole momenta or “dipole lasing”. Theoretical model of DNL shows importance of spontaneous emission; DNL can be “thresholdless”. Experiments show an increase in the luminescence intensity from GaAs layers due to metal nano-particles by more than two times. Metal nano-antennas can provide broad band modulation of light, optical bistability, increase the brightness of LEDs and result in a more transversal profile of the emitted light beam. Light absorption stimulated by nano-antennas may also increase the efficiency of quantum dot solar cells.

Third, we present experimental and theoretical studies of applications of metal island films with nonlinear conductance in weak (<50 V/cm) electric fields as anti-faked labels for documents and items [4]. Nonlinear conductance arises due to carrier tunneling between metal islands in the film. Such films cannot be prepared without knowledge of technology, however industrial manufacturing of films has low cost and detection nonlinear conductance of films is simple. It may allow use of such films as labels for identification of authenticity of tickets, credit cards, precision items etc. Metal island films with nonlinear conductance is an interesting example of nonlinear dynamics in dissipative system.

1. O.V. Dementeva, S.A. Kazaryan, I.E. Protsenko, et al. Increase of efficiency of Si-based solar cells by nano-particles and micro-structures // *II Nanotechnology International Forum*, Moscow, October 6-9, 2009.
2. A. Pors, A.V. Uskov, M. Willatzen, I.E. Protsenko. Control of the input efficiency of photons into solar cells with plasmonic nanoparticles // *Opt. Comm.* in press, 2011.
3. I.E. Protsenko, A.V. Uskov, O.A. Zaimidoroga, et al. Dipole nanolaser // *Phys. Rev. A.* – 2005. – V. 71. – P. 063812.
4. A.P. Boltaev, I.E. Protsenko, F.A. Pudonin. Security element for verifying a security object and method for verifying same // EP 2246824 (A2) 2010.

## Nonlinear optical response and its dynamics of island gold films under femtosecond laser pulses excitation

Brodyn M., Volkov V., Lyakhovetsky V.

*Institute of Physics of NAS of Ukraine, Kiev, Ukraine*

Nonlinear optical response and its dynamics have been studied in gold island films on glass substrates under femtosecond laser pulse excitation at 496 and 800 nm light wavelength ( $\tau=150$  fs). Well known Z-scan technique (nonlinear length method) has been used to measure value and sign of the real part of the third order optical nonlinear susceptibility responsible for the nonlinear refraction. It was shown that in the case of far distance from the plasmon resonance ( $\lambda=560$ nm) for both  $\lambda=496$ nm and  $\lambda=800$ nm the sign of the susceptibility is positive and its value is about  $10^{-7}$ esu. At the same time in our previous work [1] it has been shown that the nonlinearity is positive near plasmon resonance and its value is two orders of magnitude higher ( $-10^{-5}$ ).

Studies of nonlinear optical response by means of Pump&Probe technique showed very short times. The leading edge of the response is less than 1ps and is connected with the heating of the free electrons [2]. The back edge (relaxation of the induced nonlinearity) has two time components ( $\tau_1 = 3$  ps та  $\tau_2 = 300$  ps) (Рис.1). The fast component  $\tau_1$  might be attributed to thermalization of hot electrons in Au as in Cu [3]. The slow component  $\tau_2$  is probably responsible for the energy transfer from metal nanoparticles to the substrate.

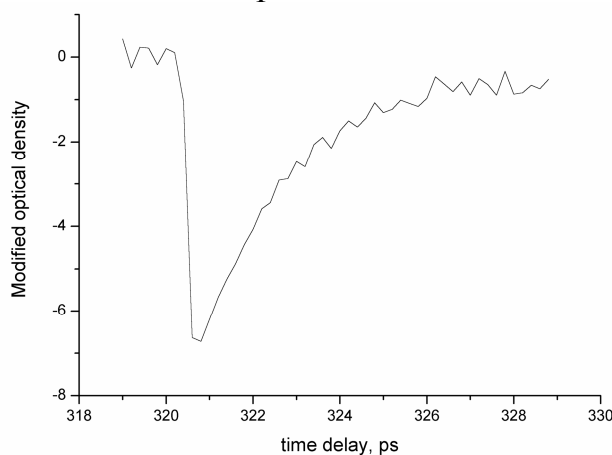


Fig. 1. Optical density of the island Au films kinetics near surface plasmon resonance under femto second laser excitation at  $\lambda = 800$ nm.

1. A.A.Borshch, M.S.Brodyn, V.R.Lyakhovetsky, V.I.Volkov and R.D.Fedorovich. Giant nonlinear refraction in gold island films. JETP Letters, vol. 84, No. 4, pp.214-216 (2006).
2. E. D. Belotskii and P. M. Tomchuk, Int. J. Electron. **69**, 173 (1990).
3. I. V. Blonskii, I. N. Dmitruk, O. A. Eshchenko, I. A. Pavlov, V. N. Kadan, P. I. Korenyuk, A. A. Alekseenko, and A. N. Dmitruk, JETP Lett. **88**, 41 (2008).

## Effect of Seebeck in thin crystalline films of Ge p-type conductivity

Budzhak Ya.S., Zub O.V.

Lviv Polytechnic National University, Lviv, Ukraine

It is known from the quantum mechanics that spatial quantization of energy spectrum of current carriers is observed in thin conductor crystalline films. In this work, using the results [1], where was shown that in thin film crystals of Ge p-type conductivity with such parameters as:  $N_D = 2.123 \cdot 10^{18} \text{ cm}^{-3}$ ,  $N_A = 3.47 \cdot 10^{18} \text{ cm}^{-3}$ ,  $E_D = 0.022$  and thickness  $d$ , coefficient of Seebeck effect and reduced chemical potential of current carriers dependence on their thickness (Fig.1.- 4.).

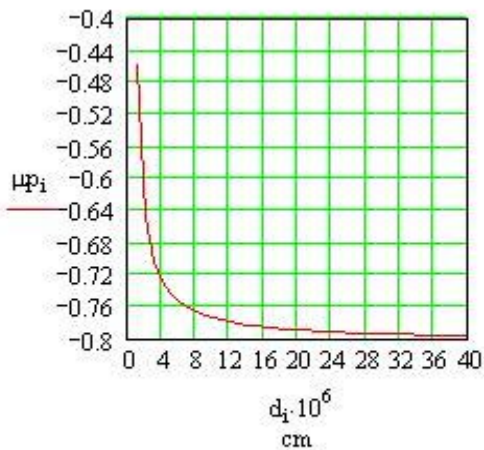


Fig.1.

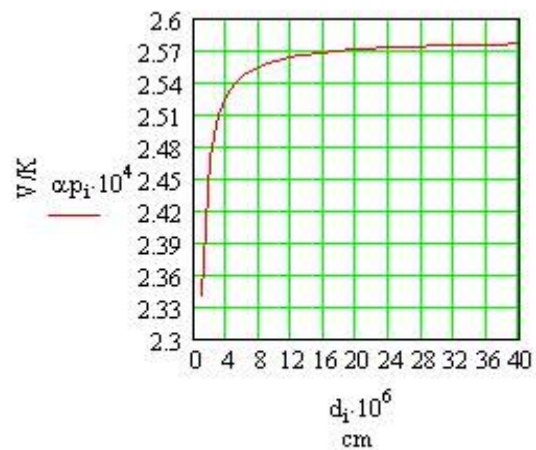


Fig.2.

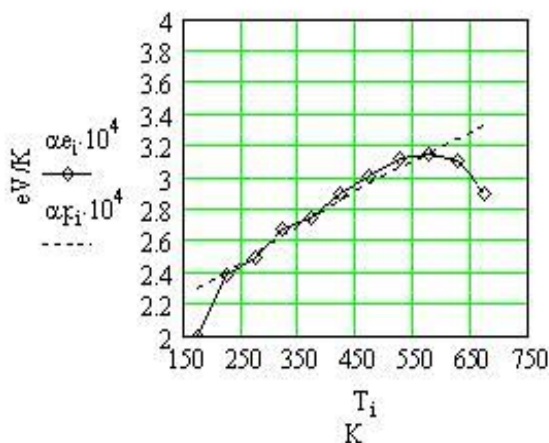


Fig.3.

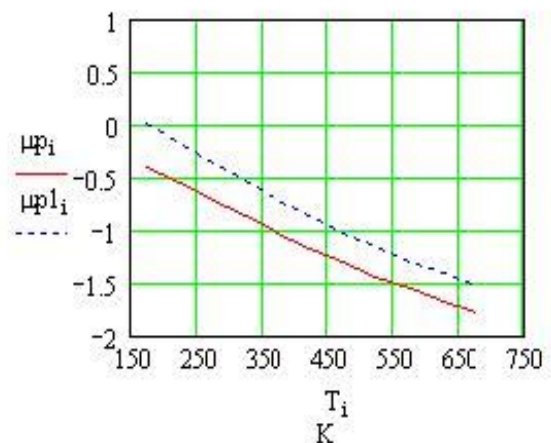


Fig.4.

- Budzhak Ya.S., Zub O.V. The thin crystalline films as a quantum size structure // Eastern-European journal of Enterprise Technologies.–2010.– V. 2/5 , №44. – P. 7-9.



## **Accompanying Thermoelectric Phenomena at Operation of Micro-and Nanoelectronic Elements**

Bulat L.P., Asach A.V., Nefedova I.A., Kozavkin D.O.

*St. Petersburg State University of Refrigeration and Food Engineering, St. Petersburg, Russia*

The modern microelectronics is characterized by the enormous increase of the volume density of active elements (diodes, transistors, etc.) in electronic microcircuits (chips). The size of transistors in electronic chips already reaches tens nanometers. Accordingly the heat density which is allocated in microcircuits owing to the Joule heating increases dramatically. It is enough to remind, that in some cases it is required to remove the heat flow density more than  $1\text{kW}/\text{cm}^2$  for thermostabilization of micro- and photoelectronic elements.

It means that the local Joule heating originates in nanometers areas inside of electronic microcircuits. And the temperature appears essentially various in different spots of a microcircuit; we should take into consideration that diverse materials (substrates, p- and n-types of semiconductors, switching materials, etc.) are structurally concentrated in the microcircuit. Hence, the conditions for realization of the Seebeck effect are created in the microcircuit. On the other hand the operation of the microcircuit assumes with the passing of the electric currents in the chip; it is a functional destination of any microcircuit. Therefore the Peltier effect is realized in the microcircuit: heating or cooling of contacts of diverse conductors (or semiconductors) when a DC electric current passes through the contacts. Nobody was considered earlier the role of the Seebeck and the Peltier effects in conditions of a microcircuit operation. We had fulfilled a computer simulation of the accompanying thermoelectric phenomena in an elementary model of an electronic microcircuit by the finite-element method. An estimation of the value of the thermoelectric effects in the electronic microcircuits and influences of these effects on the microcircuit operation are completed.

## **Particularities of the formation and annealing of nano-size defect clusters in CdS single crystals irradiated with 1 MeV neutrons**

Davydyuk G.Y., Myronchuk G.L., Bozhko V.V.

*Lesia Ukrainka Volyn National University, Lutsk, Ukraine*

Cadmium sulfide is popular with many researchers as a model material for the study of optical processes in binary chalcogenide compounds  $A^{II}B^{VI}$ . The structure defects in such crystals often have an important role in the phenomena that define the possible application of the crystals in modern electronics. A particular interest is attracted to the single crystals that were irradiated with fast neutrons ( $E = 1 \text{ MeV}$ ). Such material represents a mainly undamaged matrix embedded into which are nano-size defect clusters created by neutron radiation.

It was shown that the vacancy clusters with the excessive concentration of cadmium vacancies in the cluster nucleus ( $V_{Cd}$ ) dominate the electric and optical properties of the irradiated samples. A physical model that explains the particularities of the formation of defect clusters in neutron-irradiated samples is suggested. According to this model, a part of the kinetic energy of a fast neutron upon its collision with the crystal lattice atom is transferred to the inner electron shells of Cd atoms (most probably, to K-shell). Due to the relaxation processes of the electron transitions in K-shell, atom ionization follows. Thus formed in a small volume, like Cd ions are expelled from the lattice sites increasing the concentration of  $V_{Cd}$  in the cluster nucleus. Defect clusters in neutron-irradiated crystals are stable defect formations that are not repaired at room temperature for several years. The annealing of neutron-induced defects is strongly accelerated after additional X-ray irradiation of the sample; this is explained by the realignment of the distribution of the screening point defects that form along with the defect clusters during the neutron irradiation.

## **Plasmonic thin-film solar cells with enhanced efficiency**

Dmitruk N.L., Korovin A.V., Malynych S.Z., Mamontova I.B.

*Institute for Physics of Semiconductors, National Academy of Sciences of Ukraine,  
Kyiv, Ukraine*

The main problem of modern photovoltaics, as a conversion of solar energy into electricity, is enhancement of efficiency of this conversion and significant reduction of materials and processing costs.

Because at present most of the solar-cell market is based on silicon wafers with thickness about  $300 \mu\text{m}$ , in conventional Si solar cells (SC) the efficiency enhancement is typically achieved with surface texturing which causes multiscattering of light (randomization), i.e. increasing the effective path length of photons in SC and light trapping inside. Second-generation of SCs provided an essential reduction of SC production costs by using thin film materials (Si,

GaAs, CdTe, CuInSe<sub>2</sub>, organic semiconductors etc.). However, the light trapping in thin film SC by means of large-scale texturing is not suitable for thin film SCs. Therefore, in SCs of 3<sup>rd</sup> generation a new method for light trapping in thin film SCs is used, namely, the use of non-direct interaction of light with solid by excitation of localized quasiparticles, surface plasmons (SP) or evanescent waves - surface plasmon polaritons (SPP).

There are several ways to enhance the SC efficiency by using of plasmonics principles which have been considered in this report:

1) The process of excitation of SPPs in periodically corrugated metal or heavily doped semiconductor film (emitter) in heterostructure SC has been investigated theoretically. This process leads to the essential increase of light transmission into the photoactive semiconductor base, especially in the case of anticorrelated relief. As a result, the efficiency enhancement of a surface barrier heterostructure of metal–semiconductor type,  $\eta \propto J_{SC} \cdot V_{OC}$ , has been predicted. Besides, the internal quantum efficiency  $Q_i(\lambda)$  has been calculated in the 1D model and the influence of both surface recombination velocity and the rate of major carriers emission into the emitter has been analyzed.

2) The photocurrent enhancement by metal nanoparticles incorporated into transition layer on semiconductor substrate, due to light-trapping by scattering from sub-wavelength particles, have been calculated in dependence on spherical particles size and their interdistances. The theoretical calculations are based on the modified differential formalism for the system of Maxwell's equations, when the boundary conditions are simplified by the introduction of a curvilinear non-orthogonal coordinates system. The obtained light transmittance spectra demonstrate the essential transmittance increasing in the case of the gold nanoparticles ensembles embedded into high refractive index dielectric (SiO<sub>2</sub> was used in calculation) for two semiconductor substrates (GaAs and Si) in contrast to flat semiconductor substrates without metallic nanoparticles ensembles.

3) So far as a new method for light-trapping in thin film SC caused by scattering from metal nanoparticles, we present the results of calculations of the optical radiation efficiency of Ag and Au nanoparticles, defined by the ratio of the scattering cross-section to the extinction one. The calculations were performed using Mie theory formalism for surrounding medium of various refractive indexes. It has been shown that silver nanoparticles exhibit substantially larger optical efficiency in a broad spectral range in compare to gold nanoparticles. Optical efficiency for silver nanoparticles with diameter over 90 nm exceeds 90 %. This is important for design of the broad band SC.

4) Later on calculations have been performed for rectangular metal nanowires at increasing of metal filling factor,  $f$  from 1/8 to 6/8 and results are compared with flat continuous film with the same mass thickness. The transformation of SPs into SPPs with  $f$ -factor increase at the increase of wire width is considered. The averaged photocurrent of solar cell with nanowire periodic system increases in comparison with a flat gold film on GaAs or Si

substrate, for example, by 40 - 60% for Si into surrounding medium with  $n = 1.45$  and gold wire height 50 nm, period 550 nm. Photocurrent generation in both far-field (wave) and near-field zones peculiarities in transmittance/reflectance spectra of emitter thin layer is discussed.

5) SPs or SPPs excitation on metal nanoparticles or nanowires, with penetration of plasmon-concentrated near-field into base and following generation of non-equilibrium electron-hole pairs has been considered too. This allows us to calculate spatial dependencies of generation rates at normal incidence taking into account the Baraff law for impact ionization by hot electrons (holes). It has been shown that the z-coordinate dependence (normal to interface) of generation rate has two components including near-field component at  $z < 50$  nm. Introducing in the phenomenological theory the additional surface generation of minority carriers in space charge region by near-field as some term in the boundary conditions, we calculated the external quantum efficiency,  $Q_e$ . The enhancement of  $Q_e$  and non-usual influence of surface recombination velocity are predicted.

All the above mentioned methods for SC efficiency enhancement have been used in this report which review our recent papers [1 - 6].

1. A.A. Akopyan, Kh.N. Bachronov, O.Yu. Borkovskaya, N.L. Dmitruk et. al. Photoconverters based on Gallium Arsenide diffused  $p$ - $n$  junctions formed on a microprofile GaAs Surface. // *Semiconductors*. - 2009.- V.43, No.3. - P.385-390.
2. N.L. Dmitruk, O.Yu. Borkovskaya, A.V. Korovin, I.B. Mamontova, A.V. Sukach. Optimal nano/micro-relief of surface barrier structures for solar cells application. *Proc. of 22<sup>nd</sup> European Photovoltaic Solar Energy Conference and Exhibition*, 3–7 September 2007, Milan, Italy, p.345-348.
3. N.L. Dmitruk, A.V. Korovin, I.B. Mamontova. Efficiency enhancement of surface barrier solar cells due to excitation of surface plasmon polaritons. // *Semicond. Sci. Technol.* - 2009. - V.24. - P.125011 (7p).
4. N.L. Dmitruk, A.V. Korovin. Plasmonic photovoltaics: photocurrent enhancement by metal nanoparticles on solar cells interface. *Proc. of the 24<sup>th</sup> European Photovoltaic Solar Energy Conference and Exhibition*. - 21-25 September 2009. Hamburg, Germany. - P.566-569.
5. N.L. Dmitruk, A.V. Korovin. Plasmonic photovoltaics: metal nanowires on solar cell interface. *Proc. of 25<sup>th</sup> European Photovoltaic Solar Energy Conference and Exhibition and 5<sup>th</sup> World Conference on Photovoltaic Energy Conversion/* - 6 – 10 September 2010, Valencia, Spain, P.385-388.
6. A.V. Korovin. Improved method for computing of light-matter interaction in multilayer corrugated structures, *JOSA A*. – 2008/ - V.25, №2. - P.394-399.

## **Silicon whiskers for sensor electronics**

Druzhinin A.A., Maryamova I., Kutrakov A., Liakh-Kaguy N.

*Lviv Politechnic National University, Lviv, Ukraine*

Silicon whiskers, grown by chemical transport reactions from the vapour phase, due to their structure perfection, morphology, mechanical properties and strain sensitivity were successfully used as sensitive elements of piezoresistive mechanical sensors for different applications.

To extend the functional possibilities of mechanical sensors based on these crystals complex studies of strain induced effects in silicon whiskers in the wide temperature range 4.2 – 300 K at high magnetic fields and under electronic irradiation were carried out in the Laboratory of sensor electronics of Lviv Politechnic National University. The p-type Si whiskers, heavily boron doped (degenerate) with resistivity  $\rho_{300K} = 0.005 - 0.006 \text{ } \Omega \cdot \text{cm}$  and with boron concentration in the vicinity of metal-insulator transition (MIT) were studied.

In our studies in silicon whiskers with boron concentration in the vicinity of MIT from the insulating side of transition at low temperatures near liquid helium temperature the giant non-classical piezoresistance was found: the gauge factor of these crystals at uniaxial compressive strain achieves  $GF = - (10^5 - 10^6)$  at 4.2 K [1]. On the basis of such crystals different high-sensitive mechanical sensors operating at low temperatures were developed, particularly, strain sensors, sensors to measure pressure and level of cryogenic liquids.

Studies of silicon whiskers at high magnetic fields up to 14 T at low temperatures showed that degenerate crystals have a small magnetoresistance and therefore could be used as sensitive elements of mechanical sensors operating at low temperatures and high magnetic fields.

Influence of electron irradiation with energy 10 MeV and different fluencies on the low temperature conductivity, magnetoresistance and piezoresistance of doped silicon whiskers were studied also. It was shown that Si whiskers with boron concentration in the vicinity of MIT could be used as sensitive elements of mechanical sensors operating under electron irradiation with energy 10 MeV and fluence  $\Phi \leq 1 \times 10^{17} \text{ el/cm}^2$ . On the basis of degenerate p-type silicon whiskers the piezoresistive sensors with stability to electron irradiation with energy 10 MeV and fluence  $\Phi \leq 1 \times 10^{18} \text{ el/cm}^2$ , operating at high magnetic fields could be created.

1. Druzhinin A.A., Maryamova I.I., Pavlovsky I.V., Palewski T. Piezoresistive properties of boron-doped silicon whiskers at cryogenic temperatures // *Functional Materials*. – 2004. – Vol.11, No.2. – P. 268-272.

## Quantum-size effects in nanostructures condensed matter

Freik D.M.

*Vasyl Stefanyk Precarpathian National University, Ivano-Frankivsk, Ukraine*

Recently, in the process of creating highly effective thermoelectric materials it had place an intensification of research activity in low-dimensional structures [1,2].

Reduction the dimension of the material creates the conditions for observing the phenomenon of quantum-size effect, what leads to increase the density of states near the Fermi energy. This helps to preserve high conductivity at relatively low Fermi energy, where the high values of the Seebeck coefficient  $S$  have place. Significant influence of quantum effects on thermoelectric properties is probable only if the size of the structure in restricting direction is comparable with carriers de Broglie wavelength. This condition holds for structures in the form of quantum wells, quantum wires and quantum dots, where it have place a dimensional restriction in one, two and three directions, respectively. Thus, the electronic density of states shows marked deviation from the usual parabolic law in bulk materials.

Thermoelectric parameters behavior (electrical and thermal conductivity, Seebeck coefficient) in bulk materials is usually described in terms of electronic and phonon properties, which vary greatly with decreasing sample size below the micrometer range, where quantum effects become more significant. Spatial confinement of acoustic phonons and the corresponding modification of the group velocity leads to an increase of the phonon relaxation rate, resulting in reducing of lattice thermal conductivity [3]. In addition, nature of interaction between particles changes much. Taking into account the multiple energy layers in like-well structure can lead to nonmonotonic change in the various transport coefficients such as mobility, Seebeck and Hall coefficients.

The paper presents an analysis of new approaches to improve the thermoelectric parameters of nanostructures on the basis of compounds IV-VI. The optimal parameters of quantum dots, wires and wells superlattices for maximum value of thermoelectric figure of merit  $ZT$  is determined.

The relative simplicity of creating a quantum wells superlattice explains that in this direction as the research object is used quite a lot of compounds and their combinations in heterostructures. Determination of  $ZT$  experimental values for such structures is difficult due to the complexity of measuring their thermal conductivity. Therefore, in experiments to evaluate the QW parameters it's usually used the thermoelectric power  $S^2\sigma$ .

Thus, in [4 for QW (100) KCl/PbSe/EuS  $S^2\sigma \approx 90 \mu\text{W}/\text{K}^2\text{cm}$ . In theoretical paper [5] it has been shown that power factor reaches value of  $110 \mu\text{W}/\text{K}^2\text{cm}$  in quantum wells structure PbTe/Pb<sub>1-x</sub>Eu<sub>x</sub>Te at 300 K. In addition, the experimental data for thickness dependencies of thermoelectric

parameters in lead chalcogenides nanostructures indicate their oscillatory character. It is naturally to assume that such behavior is due to size effects in quantum well formed by potential barriers at the borders of the sandwich structure.

For quantum wells with high walls electrons are confined in the  $z$ -direction and in  $x$ - and  $y$ -directions their motion is free. In this case thermoelectric transport coefficients may be obtained from Boltzmann equations, which can be written under the assumption that electron distribution function in stationary state remains constant and can be changed only by external forces and fields. Then, electrons system go back to equilibrium state due to different relaxation processes with characteristic relaxation times. So, we get theoretical thickness dependences of thermoelectric parameters, which have oscillatory character with some oscillation period and it give the possibility to find out structure energy characteristic – Fermi energy. This values are shown in table 1 for lead chalcogenides nanostructures.

*Table 1*

The values of oscillation period ( $\Delta d_{exp}$ ), effective mass ( $m_z^*$ ) and calculated on their base Fermi energy ( $\epsilon_F$ ) for lead chalcogenides nanostructures.

Structures	$\Delta d_{exp}$ , nm	$m_z^*$	Fermi energy $\epsilon_F$ , eV
KCl(001)/n-PbS/EuS	30	0.08 $m_e$	$5,17 \cdot 10^{-3}$
KCl(001)/n-PbSe/EuS	35	0.04 $m_e$	$7,75 \cdot 10^{-3}$
KCl(001)/n-PbTe/EuS	100	0.024 $m_e$	$1,55 \cdot 10^{-3}$

1. Davies J.H. The physics of low-dimensional semiconductors. An introduction. – Cambridge university press. – 1998. – 451 p.
2. Dresselhaus M.S., Ghen G., Rang M.I., Yang R., Lee H., Wang D., Ren Z., Fleurial J-P., Gogna P. New Directions for Low-Dimensional Thermoelectric Materials // Adv. Mater. – 2007. – № 19. – P. 1043-1053.
3. Baladin A., Wang K.A. Effect of phonon confinement on the thermoelectric figure of merit of quantum wells // J. Appl. Phys. – 1998. – Vol. 84. – P. 6149.
4. Rogacheva E.I., Tavrina T.V., Nashchekina O.N., Grigorov S.N., Nasedkin K.A., Quantum size effects in PbSe quantum wells // Applied Physics Letters. – 2002 – V80 – №15. - P. 2690-2692.
5. Casian A., Sur I., Scherrer H., Dashevsky Z. Thermoelectric properties of n-type PbTe/Pb<sub>1-x</sub>Eu<sub>x</sub>Te quantum wells // Phys. Rev. B. – 2000. – Vol. 61, No. 23. – P. 15965-15974.

## Photosensitive MBE structures $\text{Cd}_x\text{Hg}_{1-x}\text{Te}/\text{CdTe}/\text{GaAs}$ : determination of the parameters, finding of the unusual acceptor states

Gasanzade S.G., Staryj S.V., Strikha M.V., Tetiorkin V.V., Shepelskii G.A.

*V.E. Lashkariov Institute of Semiconductor Physics of NAS of Ukraine, Kyiv, Ukraine*

The epitaxial layers of  $\text{Cd}_x\text{Hg}_{1-x}\text{Te}$  compounds, grown up by MBE method (with 7-15  $\mu\text{m}$  width) as the structures of  $\text{Cd}_x\text{Hg}_{1-x}\text{Te}/\text{CdTe}/\text{GaAs}$ , with both  $n$ -, and  $p$ -type conductivity ( $x = 0.2-0.22$ , this corresponds the small gap width  $E_g$  of 100 meV order) were studied. We have determined the carriers concentrations and mobility out of the Hall coefficient and conductivity temperature and field dependence:  $n=5\cdot 10^{14}-4\cdot 10^{15} \text{ cm}^{-3}$ ,  $\mu_n=(2-4)\cdot 10^5 \text{ cm}^2/\text{V}\cdot\text{s}$  for the  $n$ -type and  $p=5\cdot 10^{15}-3\cdot 10^{16} \text{ cm}^{-3}$ ,  $\mu_p=750-1100 \text{ cm}^2/\text{V}\cdot\text{s}$  for the  $p$ -type material respectively.

The spectral dependence of the photoconductivity (PC), the photoelectromagnetic effect (PME) and the optical transmission were obtained, and the characteristics of non-equilibrium carriers in the epitaxial layers were determined.

The anomalous PME behavior with the change of its signal sign with increasing magnetic field was observed in the  $p$ - $\text{Cd}_x\text{Hg}_{1-x}\text{Te}$  films at  $T=4.2-10 \text{ K}$ . The anomaly of PME is determined by the surface charge, which causes the minority carriers drift towards the illuminated surface. This charge is caused by the special, before unknown acceptor states with a rather small ionization energy (approximately 1 meV), that can be recharged by the photons with the energy  $h\nu > E_g$ . This acceptor states belong not to the surface only, but to the whole bulk of  $\text{Cd}_x\text{Hg}_{1-x}\text{Te}$  - layers. The similar anomalies of PME were observed previously in the undoped bulk  $\text{Cd}_x\text{Hg}_{1-x}\text{Te}$  crystals of  $p$ -type [1].

We have obtained the evidence for the relation between these states and the third (the most shallow) level of mercury vacancy  $\text{V}_{\text{Hg}}^+$ , which was not observed experimentally up to now, to the best of our knowledge.

It was demonstrated, that the simultaneous measurement of PME and PC can be an effective method for the determination of the parameters of  $\text{Cd}_x\text{Hg}_{1-x}\text{Te}$  and InSb thin films.

1. S.G. Gasanzade, M.V. Strikha and G.A. Shepelsky. Low-temperature anomalies of the photoelectromagnetic effect in  $p$ - $\text{Cd}_x\text{Hg}_{1-x}\text{Te}$  due to recharging of surface states // Semiconductors. – 2008. – V. 42, №.4. – P. 422-428.



## Effect of oxidation and porosity on nonlinear optical response of mesoporous silicon films

Gayvoronsky V.Ya.<sup>1</sup>, Brodyn M.S.<sup>1</sup>, Kopylovsky M.A.<sup>1</sup>, Rostotskiy A.I.<sup>1</sup>,  
Yatsyna V.O.<sup>1</sup>, Golovan L.A.<sup>2</sup>, Tselikov G.I.<sup>2</sup>, Timoshenko V.Yu.<sup>2</sup>

<sup>1</sup>*Institute of Physics NASU, Kiev, Ukraine;*

<sup>2</sup>*Physics Department, Moscow State University, Moscow, Russia*

Semiconductor materials possessing efficient nonlinear optical (NLO) response seem to be a good choice for ultra-high bandwidth switching applications in modern telecommunication. Formation of semiconductor-based nanocomposites resulting in rise of the field inside them as well as generation of new and increase of intrinsic energy state is able to bring about new very efficient devices for the optical control. The mesoporous silicon (mesopor-Si) consisted of the pores of 5 – 100 nm and crystalline silicon (c-Si) remainders of the same sizes is a very promising material for formation of the devices based on all-optical switching. Apart from its high NLO susceptibility responsible for the light self-action, it is low-cost and easy to produce [1].

The samples of mesopor-Si were formed by means of electrochemical treatment of (100) c-Si (specific resistance 1 - 3 mOhm·cm) in HF (49 %):ethanol solution (1:1). The current densities for different samples varied from 20 to 100 mA/cm<sup>2</sup>. We employed mesopor-Si films detached from the substrate by a short pulse of high current density. Thicknesses of the films were about 10 μm. Some pieces of the films were thermally oxidized in air at temperatures from 300 to 1000 C. The IR spectroscopy of the films demonstrated both their chemical composition (absorption by chemical bonds) and a good optical quality (e.g., well-expressed interference fringes).

The thermal oxidation at temperatures below 400C leads to the incorporation of oxygen atoms in near-surface layer of Si nanocrystals and then to the formation of as-called back-bonded oxygen (O-Si-H surface groups). The annealing at temperatures above 600C can lead to complete removal of hydrogen and formation of O-Si-O bonds and surface defects like P<sub>b</sub>-centers. The centers density depends on the annealing temperature, duration and atmosphere.

We have studied self-action effects of CW and picosecond range pulsed laser beam at 1064 nm in free-standing mesopor-Si films with different porosity. A pronounced NLO response in oxidized mesopor-Si due to the resonance excitation of the interface defect states within picosecond laser pulses was observed [2]. The CW laser excitation resulted in a strong modification of the ratio between the real and imaginary parts of the cubic NLO susceptibilities for the films annealed at high temperatures. Thus the self-action effects monitoring is a promising diagnostics technique for surface states at the developed surface of silicon nanostructures.

1. L.A. Golovan, V.Yu.Timoshenko, P.K.Kashkarov UFN. – 2007. - № 177. – P.619.
2. V.Ya. Gayvoronsky, M.A.Kopylovsky et al. Laser Phys. Lett. – 2008. - № 5. – P. 894.

## Elements and optoelectronic devices based on organic material

Gotra Z.Yu.

*Lviv Polytechnic National University, Lviv, Ukraine*

At present, organic materials are among the promising to create integrated circuits, LEDs, displays, photodetectors, solar cells, organic lasers, and others. They are an integral part of modern electronics - organic electronics. It is known that for a thin film of organic semiconductor materials and form the basis for new electro-luminescent photosensitive structures and uses chemical and electrochemical deposition methods, but they do not always meet the requirements of electro-physical parameters of films, which significantly limits their use to create organic electro elements.

We have developed and investigated new organic light-emitting and photovoltaic devices, developed technologies and the formation of new anodic electrodes for making organic light emitting devices, organic passivation technology development of semiconductor devices optically transparent inorganic semiconductors, conducted a study of optical, structural and electro-physical properties of organic thin films and structures. First formed and studied organic photosensitive structures based on nickel phthalocyanine ITO/NiPc/Al on flexible substrate and conducted complex investigations of electro-physical parameters.

Options developed LED structures

Electroluminescent structure	Voltage inclusion, V	Maximum glow brightness, Kd/m <sup>2</sup>	Maximum current efficiency, Kd/m <sup>2</sup>
ITO/Alq3/PEDOT/Al	8.3	2900	2.1
ITO/CuI/Alq3/PEDOT/Al	5.6	4000	2.6
ZnO/CuI/Alq3/PEDOT/Al	7.8	3500	3.1

The new technology solutions for the predicted formation hetero-barriers based on organic (Alq3) and inorganic (CuI) semiconductors, proposed new light-emitting structures based on them.

Investigation of nematic liquid crystal mixtures with dye showed the possibility of obtaining fluorescence at wavelengths corresponding to blue, green and red. Introduction of chiral impurities in such mixtures provides a cholesteric supramolecular structure, thus obtaining laser generation within the fluorescence spectra.

1. Hotra Z., Cherpak V., Stakhira P., Aksimentyeva O., Tsizh B., Volynyuk D., Bordun I. Vacuum-deposited poly(o-methoxyaniline) thin films: Structure and electronic properties // *Journal of Non-Crystalline Solids*. – 2008. – 354. – P. 4282-4286.
2. Hotra Z., Stakhira P., Cherpak V., Volynyuk D., Ivastchyshyn F., Tataryn V., Luka G. Characteristics of Organic Light Emitting Diodes with Copper Iodide as Injection Layer // *Thin Solid Films*. – 2010. – 518. P. 7016-7018.

## Optoacoustical Effects in the Dielectric Media with a Metallic Nano-inclusions

Grigorchuk N.I.<sup>1</sup>, Tomchuk P.M.<sup>2</sup>

<sup>1</sup>*Bogolyubov Institute for Theoretical Physics, Kyiv, Ukraine*

<sup>2</sup>*Institute for Physics, Kyiv, Ukraine*

The theory of the photo-acoustical effect caused by a laser action on metal nanoclusters embedded in a dielectric matrix is build. The energy absorbed by clusters propagates through the dielectric matrix and generates the sound waves in it via the thermo-deformation mechanism. The formulae for an acoustical signal are derived, and the high sensitivity of the sound wave amplitude to the shape of metal clusters, as well to such parameters of a laser irradiation as the frequency, polarization, and intensity, is revealed. The behavior of the sound vibrations amplitude in a region of the surface plasmons absorption is studied in detail. It is found that this amplitude at light absorption by a discrete metal film (a system of clusters in the matrix) can exceed the corresponding amplitude for the absorption by a continuous metal film in the region of plasmon resonances by several orders of magnitude.

Both the case of clusters irradiation by quasi-stationary laser ray modulated in intensity by low acoustical frequency and the case of ultrashort laser ray action are considered rather thoroughly. Two mechanisms of sound generation were studied. The first one is described above, and the second one is caused by the surface vibrations of metal clusters as a result of the hot electron pressure which is changed in time. The intensity of sound generation was calculated for separates cluster as well as for system of clusters.

The starting points for this presentation are based on our works [1-3].

1. Grigorchuk N. I., Tomchuk P.M. // *Phys. Rev.*–2009.– V.14.–P.741-755.
2. Bilotsky Y., Grigorchuk N.I., and Tomchuk P.M. // *Surf. Sci.*–2009.– V.14.–P.741-755.
3. Grigorchuk N.I. and Tomchuk P.M. // *Europ. Phys. J. B*, to be published 2011.

## Templates as instrument of nanotechnology

Grin'ko D.O.<sup>1</sup>, Barabash M. Yu<sup>2</sup>, Kunitsky Yu. A<sup>2</sup>., Vlaykov G. G<sup>2</sup>.

<sup>1</sup>*Institute of Semiconductor Physics NAS of Ukraine, Kyiv, Ukraine*

<sup>2</sup>*Technical Centre, NAS of Ukraine, Kyiv, Ukraine*

The problem of material structuring in nanoscale, moreover an organization of processes about nanoobjects ordering with the help of templates is one of main ways of nanotechnologies development. Template is an instrument for an organization in space and time of physical and chemical processes of nanoobjects structuring on material surface in different nature at the expense of near-field nanoobjects interaction with template structure.

The purpose of given work is development of methods of templates producing on basis of photosensitive nanocomposite polymeric materials in electrophotographic process for order-placed clusters formation of different physical nature.

The possibility of Au nanoclusters ordering on the surface of photoconductive carbazole-content organic molecular nanocomposites is researched. A photoconductive sphere was being received by general condensation on glass backing with a sphere of conductive stannum oxide of molecular fascicles CdSe, 2,4,7- trinitro-9-fluorene and products of N-vinylcarbazole monomer. Example with nanocomposite film was placed near by anode of main device in air atmosphere. In result of ions deposition at film surface monotonously distributed surfaced charge was formed.

Formation of localized charge in nanocomposite film was done by electrophotographic method at example exposition by hologram after three-rayed scheme. Automatic registration of holograms at nanocomposite film included three stages. At exposition by nanocomposite film with light in electric field  $E$  of flat condensator a carrier photogeneration is happened and a photoconductivity is appeared, which current density is a moduled intensity of light field. After exposition ending at film surface a non-uniform distribution of surfaced charge was formed. On the surface of electret formed template aurum was sputtered by thermal method, what is condensed by in view of nanoclusters exclusively in areas of maximum tension of local field at received charge in photoconductive film [1]. The mechanism of self-ordering Au during thermal sputtering on surface of electric template is motion of atoms of molecular fascicle in local electric field  $E=150$  MV/m. In template electric filed gradient area in atoms of Au an occasional moment appears, what causes their transmitting to film surfaces area, where a charge is localized. Directed transmitting of polarized particles Au is happened in direction of gradient of electric field. Sizes and volume of deposited nanoclusters Au are defined by intensity and time of condensed molecular fascicle at surface of electret template. The most little period of formed structure of nanoclusters Au by holographic method calculates a quarter of length wave at opposite distribution of laser rays. In case of laser using, which radiate in short-wave area, one can form nanoclusters structures with period of 80 – 120 nm. Distribution and symmetry of deposited nanoclusters can be changed by the way of verifying topology of hologram light field, what is used for electret template formation. On surface of such templates there is possible a deposition not only of metals, but a wide sphere of organic and non-organic compounds by the way of sputtering in vacuum, or an deposition from gas and liquid phases.

1. Grin'ko D.O., Barabash Yu.M., and etc. Template as instrument of nanotechnology group // Nanosystems, nanomaterials, nanotechnology. – 2008. – V5, № 4. – P. 521-530.

## Transport and recombination, new boundary conditions and perspectives

Gurevich Yu.G.

*CINVESTAV, México D.F., México*

This paper reports on some unsolved basic problems, namely: a model of the recombination processes that does not contradict Maxwell's equations; the role played by space charges in the transport phenomena, and the formation of quasi-neutral regions under the presence of nonequilibrium carriers. In this work, a new formulation of the theory that explains the underlying physical phenomena is presented. Additionally, boundary conditions to be employed when solving the transport set of equations are presented and discussed.

In both limiting cases of the strong and absence of bulk recombination the Shockley model of Current-Voltage Characteristic (CVC) of the p-n junction leads to unphysical results. The model needs to be properly modified and corrected. Some of the modifications are addressed in this paper. It is shown, in particular, that the Peltier effect strongly affects the CVC of p-n diodes weakly biased.

1. Yu.G. Gurevich, I.N. Volovichev. Forgotten Mechanism of Nonlinearity in the Theory of Hot Electrons // *Phys. Rev. B*, 60, pp. 7715-7717 (1999).
2. I.N. Volovichev, G.N. Logvinov, O.Yu. Titov, Yu.G. Gurevich. Recombination and Lifetimes of Charge Carriers in Semiconductors (Communications) // *J. Appl. Phys.*, 95, pp. 4494-4496 (2004).
3. Yu.G. Gurevich, J.E. Velazquez-Perez, G. Espejo-Lopez, I.N. Volovichev, O. Yu. Titov. Transport of Nonequilibrium Carriers in Bipolar Semiconductors // *J. Appl. Phys.*, 101, 023705 (2007).
4. I.N. Volovichev, J.E. Velazquez-Perez, Yu.G. Gurevich. Transport Boundary Condition for Semiconductor Structures // *Solid State Electronics*, 52, pp. 1703-1709 (2008).
5. O.Yu. Titov, J. Giraldo, Yu.G. Gurevich. Boundary Conditions in an Electric Current Contact // *Appl. Phys. Lett.*, 80, pp. 3108-3110 (2002).
6. Yu.G. Gurevich, G.N. Logvinov, J.E. Velazquez, O.Yu. Titov. Transport and Recombination in Solar Cells: New Perspectives // *Solar Energy Materials and Solar Cells*, 91, pp. 1408-1411, (2007).
7. G.N. Logvinov, J.E. Velazquez, I.M. Lashkevych, Yu.G. Gurevich. Heating and Cooling in Semiconductor Structures by an Electric Current // *Appl. Phys. Lett.*, 89, 092118 (2006).
8. Yu.G. Gurevich, G. N. Logvinov. Physics of thermoelectric cooling (Review) // *Semicond. Sci. Technol.*, 20, pp. R57-R.64 (2005).
9. I.Lashkevych, C. Cortes, Yu.G. Gurevich, Physics of thermoelectric cooling: Alternative approach // *J. Appl. Phys.*, 105, 053706 (2009).

## **Lacks of radial distribution functions method in electron diffraction of amorphous films and nanosystems**

Ivanitsky V.P., Sabov V.I.

*Uzhgorod national university, Uzhgorod, Ukraine*

Electronic diffraction – actually unique direct method of research of structure of atomic networks for amorphous thin films and disordered nanosystems. Radial distribution functions (RDF) methods are based on use of Fourier integrated transformation. This method was used in x-ray researches and transferred in electron diffraction formally. Many essential features of electronic diffraction on amorphous nanosize samples haven't been considered. Therefore a number of lacks of method RDF application for nanosize systems, is analysed in detail.

1. In physical aspect the discreteness of a structure of substance within a near and intermediate order is ignored. In method RDF this discrete structure is described by continuous functions of atomic density which not always accordingly describe real atomic networks.

2. In methodological aspect aren't taken into consideration nano sizes of samples and of elements of their microstructure and diffractograms registration features. One of conditions of method RDF applicability is enough big size of a site of the investigated sample which is exposed to an irradiation. Besides, Fourier transformation demands, that intensity diffractogram has been given in infinite limits of electron scattering vectors. Actually, this area is limited by a range 5-200 nanometers<sup>-1</sup>.

3. In experimental aspect not always the appropriate attention is given to insufficient accuracy of diffraction pattern registration and to background from not elastic scattering. Modern devices of electronic research are equipped by filters for not elastic electrons and by systems of registration on the basis of imaging plates. But even such newest decisions provide accuracy of registration of coherent scattering intensity on peripheral sites of diffraction patterns only at level of 8-10 %. Besides, they not completely delete not coherent background from diffraction pattern. That is the problem of an exception of the given background remains unresolved and today.

4. In mathematical aspect it is specificity of mathematical procedure of Fourier transformation. It can be precisely spent only for the continuous differentiated functions. Radial distribution functions often don't satisfy to this condition, especially in the field of the first coordination peak.

5. Received RDF demands the corresponding analysis and calculation of shot order parameters of atomic network: coordination spheres radiuses, coordination numbers and dispersions of interatomic distances distribution. Procedure of definition of all these sizes from RDF remains ambiguous and brings additional errors in the received results.

## **Electro-optical effects in 2D macroporous silicon structures with surface nanocrystals**

Karachevtseva L.<sup>1</sup>, Kuchmii S.<sup>2</sup>, Lytvynenko O.<sup>1</sup>, Sizov F.<sup>1</sup>,  
 Stronska O.<sup>1</sup>, Stroyuk A.<sup>2</sup>

<sup>1</sup>*V. Lashkaryov Institute of Semiconductor Physics of NASU, Kyiv, Ukraine*

<sup>2</sup>*L.V. Pisarzhevskii Institute of Physical Chemistry of NASU, Kyiv, Ukraine*

One of the perspective materials for the development of 2D photonic structures is macroporous silicon that can be obtained by the method of photoanodic etching. In view of the potential barrier on a macropore surface or heterojunction on «macropore-nanocoating» boundary, one should take into account processes on the local surface centres at energies below that of the indirect interband transition.

Optical absorption in 2D photonic macroporous silicon structures was investigated taking into account the linear electro-optical effect. The spectral dependence of optical absorption in the near-IR area (impurity absorption) has oscillating structure and varies under the “3/2” law at long wavelengths. This correlates with frequency dependence of the imaginary part of permittivity for optical transitions between impurity levels and the allowed bands of a crystal in an electric field (the impurity Franz-Keldysh effect). The experimental absorption spectra of macroporous silicon agree well with the corresponding spectral dependences of the electro-optical energy and the imaginary part of permittivity in the weak electric field approximation, thus confirming realization of the impurity Franz-Keldysh effect. The electric field of the reflected electromagnetic wave at the grazing angle of light incidence onto macropore surface changes effectively a local surface electric field.

The near-IR light absorption oscillations for 2D macroporous silicon structures with microporous silicon and as well as CdTe, ZnO surface nanocrystals were investigated taking into account electro-optical effect within the strong electric field approximation. Well-separated oscillations with one order amplitude at spectral ranges of the surface bonds were observed. An analysis of the experimental absorption spectra is carried out within the model of the resonant electron scattering on impurity states in the strong electric field with difference between two resonant energies equaled to Wannier-Stark ladder. The model of the resonant electron scattering on impurity states in an electric field of heterojunction «silicon-nanocoating» on macropores surface and the realization of Wannier-Stark effect on the randomly distributed surface bonds were considered. The Wannier-Stark ladders are not destroyed by impurities due to the longer scattering lifetime relatively the oscillation period of an electron in an external electric field at all investigated spectral region for macroporous silicon structures with CdTe and ZnO surface nanocrystals.

## Obtain and application of porous $A^3B^5$ compounds

Kidalov V.V.<sup>1</sup>, Suchikova J.A.<sup>1</sup>, Konovalenko A.A.<sup>1</sup>, Sukach G.A.<sup>2</sup>

<sup>1</sup> *Berdyansk state pedagogical university, Berdyansk, Ukraine*

<sup>2</sup> *National University of Life and Environmental Sciences of Ukraine*

Recently the attention of researchers involve particular  $A^3B^5$  compounds alongside with porous Si and other porous semiconductors. The scope of porous compounds  $A^3B^5$  constantly extends.

Porous substrates on the basis of compounds  $A^3B^5$  are perspective material for homo- and hetero-epitaxial layers of high structural quality obtain. Properties of the high-quality cubic GaN films, obtained by a method nitridization on porous substrates GaAs, are presented in our work [1]. The photoluminescence of porous GaP films was investigated in [2] by using CdSe particles ( $d = 2.8\text{nm}$ ). Properties of the porous InP are highlighted in [3].

Obtain of high-quality porous structures is the important physical and technological problem that became an object of research of many scientists.

Report represents the properties of porous  $A^3B^5$  compounds and properties of GaN films obtained on porous GaAs substrates and the properties of InN films obtained on porous InP substrates.

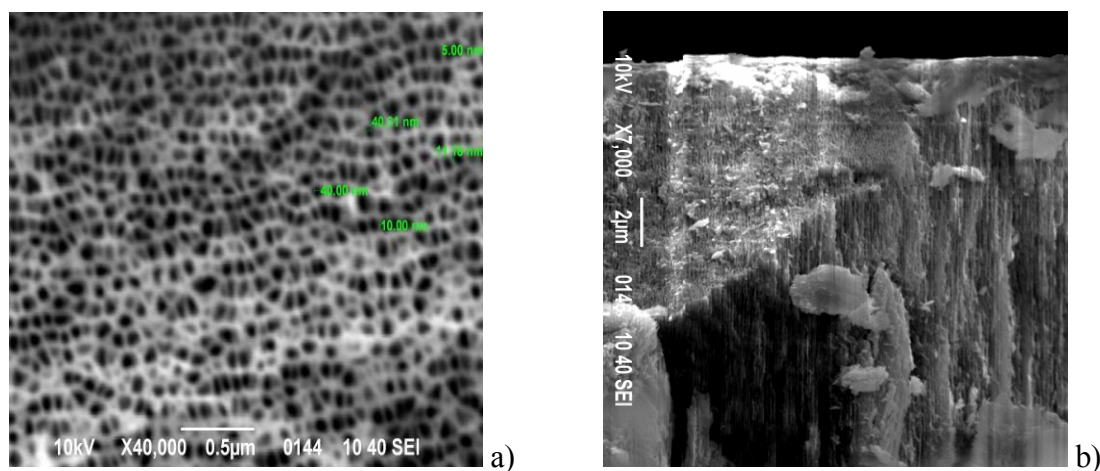


Fig. 1. REM image of the morphology of the porous n-InP (100), obtained by electrochemical etching in 5% HCl,  $t = 5$  min; a) surface, and b) cleavage.

1. V.V. Kidalov, G.A. Sukach, *Journal of Luminescence*, 102–103, 712 (2003).
2. Yu.Yu. Bachericov, O.V. Okhrimenko, V.V. Kidalov. *Semiconductors*, 43, 1473(2009).
3. V.V. Kidalov, G.A. Sukach, // *Semiconductors*, 45, Number 1, 121(2011).



## IR Fourier-transform spectrohologoellipsometry the light's scattering by twodimensional crystals

Kiryanov A.P.<sup>1,2</sup>, Ali M.<sup>1</sup>

<sup>1</sup>National Research University «MSTU named N.E.Bauman»; Moscow, Russia

<sup>2</sup>Scientific&Technological Center for Unique Instrumentation of RAS; Moscow, Russia

Nanotechnologies are needed the monitoring of a nanofilms [1]. It's able to ensure the coupling of the light's scattering [2] with a holoellipsometry [3]. Our approach is explained by fig.1. The flat beam 1 of wide-band IR waves passes through a linear polarizer 2 to a beam-splitter 3 splitting its beam on two parts: one is main (m) and other is reference (r). A main beam lights up a nanofilm 4 and its share scatters along the film's normal to a lens 5 collimates the scattered light on a beam-splitter 6. Mirrors 7&8 send the reference beam from a beam-splitter 3 to a beam-splitter 6. Here beams (m)&(r) were interfered. A linear wire-grid polarizer 10 detaches the interference beams with linear p-&s-polarizations. Its beams were detected by photodetectors 11,12. The angled reflector 9 of the mirror 8 changes the components of the signals' phases regularly, moreover one is a linear function and other is sinus function of a time. Data are received yet for an etalon (e) when a main nanofilm (m) is placed by an ordinary flat mirror; its data permit to exclude the instrumental function's share. The received signal  $I_{(p,s)(m,e)}(t)$  from the main nanofilm (m) or the etalon (e) with p- or s-polarization fixes be correspondent electronic devices tuned a modulation frequency and then they are processing by a computer. Ins signals are given as:

$$I_{(p,s)(m,e)}(t) = 2I_{o(p,s)}A_{(p,s)}S_{(p,s)(m,e)}\sin[\omega_F t + \delta\sin(\Omega_M t) + \varphi_{A(p,s)} + \varphi_{S(p,s)(m,e)}] \quad (1)$$

Here  $I_{o(p,s)}$  – the power of beams with p- or s-polarization;  $A_{(p,s)}$  and  $\varphi_{A(p,s)}$ ,  $S_{(p,s)(m,e)}$  and  $\varphi_{S(p,s)(m,e)}$  – modules and phases of polarizer instrumental device's functions and of the complex amplitude vectors Johns for scattering light on the main nanofilm (m) or etalon film (e) at a case of beams with p- or s-polarization;  $\omega_F$  and  $\Omega_M$  – the cycle frequency of a Fourier-coding and a phase modulation.

The reverse complex Fourier transformation  $F^{*-1}[I_{(p,s)(m,e)}(t)]$  gives vector Johns  $S_{p,s}^* = S_{p,s}\exp[j\varphi_{Sp,s}]$  describing IR light's scattering's by a nanofilm.

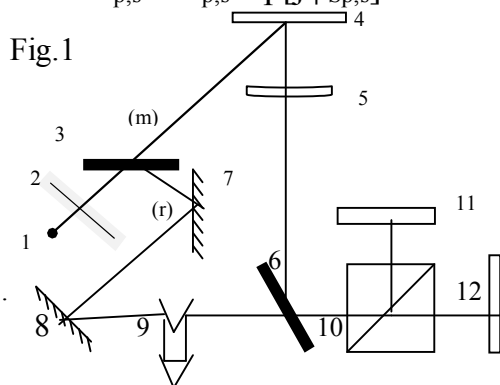


Fig.1

1. Langereis E., Heil S.B.S., Knoop H.C.M., Keuning W., van de Sanden M.C.M., Kessels W.M.M. In situ spectroscopic ellipsometry as a versatile tools for studying atomic layer deposition // J.Phys.D. Appl.Phys. –2009.– V.42, № 073001.– P.19.
2. Pemble M.P. NESSPIOM – Network for enhanced semi-conductor surface processing through in situ optical moniring // Surf. Interface Anal.– 2001.– V.31. – P.1012-1016.
3. Kiryanov A.P. In situ holoellipsometry: principles and applica-tions // M.– 2003. – P.221.

## Oscillations in radiation spectrum of system of electrons moving in spiral in transparent medium

Konstantinovich A. V.<sup>1</sup>, Konstantinovich I. A.<sup>1,2</sup>

<sup>1</sup>Chernivtsi National University, Chernivtsi, Ukraine

<sup>2</sup>Institute of Thermoelectrics, National Academy of Sciences and Ministry of Education and Science of Ukraine, Chernivtsi, Ukraine

The law of motion and the velocity of the  $l^{th}$  electron in magnetic field are given by the expressions

$$\vec{r}_l(t) = r_0 \cos\{\omega_0(t + \Delta t_l)\}\vec{i} + r_0 \sin\{\omega_0(t + \Delta t_l)\}\vec{j} + V_{\parallel}(t + \Delta t_l)\vec{k}, \quad \vec{V}_l(t) = \frac{d\vec{r}_l(t)}{dt}.$$

Here  $r_0 = V_{\perp}\omega_0^{-1}$ ,  $\omega_0 = ec^2 B^{ext} \tilde{E}^{-1}$ ,  $\tilde{E} = c\sqrt{p^2 + m_0^2 c^2}$ , the magnetic induction vector  $\vec{B}^{ext} \parallel OZ$ ,  $V_{\perp}$  and  $V_{\parallel}$  are the components of the velocity,  $\vec{p}$  and  $\tilde{E}$  are the momentum and energy of the electron,  $e$  and  $m_0$  are its charge and rest mass, respectively.

In this case, the time-averaged radiation power of system of electrons  $\bar{P}^{rad}$  can be calculated by the instrumentality of spectral distribution  $W(\omega)$

$$\bar{P}^{rad} = \int_0^{\infty} W(\omega) d\omega,$$

$$W(\omega) = \frac{2e^2}{\pi c^2} \int_0^{\infty} dx \mu(\omega) S_N(\omega) \omega \frac{\sin\left\{\frac{n(\omega)}{c} \omega \eta(x)\right\}}{\eta(x)} \cos \omega x \left[ V_{\perp}^2 \cos(\omega_0 x) + V_{\parallel}^2 - \frac{c^2}{n^2(\omega)} \right],$$

where  $\eta(x) = \sqrt{V_{\parallel}^2 x^2 + 4 \frac{V_{\perp}^2}{\omega_0^2} \sin^2\left(\frac{\omega_0}{2} x\right)}$ ,  $\omega$  is the cyclic frequency,  $c$  is the velocity of light in vacuum.

In the case of electrons moving one by one along a spiral the coherence factor  $S_N(\omega)$  takes the form:

$$S_N(\omega) = \sum_{l,j=1}^N \cos\{\omega(\Delta t_l - \Delta t_j)\}.$$

The peculiarities in synchrotron and synchrotron-Cherenkov radiation spectrum of the one, two, three, and four electrons moving in the spiral in transparent medium are investigated combining analytical and numerical methods. The overlapping between neighbour harmonics as well as oscillations in the spectral distribution of radiation power of the one, two, three, and four electrons are studied for the case when the transversal component of velocity (perpendicular to the magnetic induction vector) is bigger than the light phase velocity ( $V_{\perp} > c/n(\omega)$ ) in transparent medium.

## Influence of back contact on CdTe thin film solar cells efficiency

Kopach G., Khrypunov G., Meriuts A., Deyneko N.

*National Technical University «Kharkiv Polytechnical Institute», Kharkiv, Ukraine*

CdTe/CdS thin film solar cells (SC) are perspective for large-scale terrestrial application. One of the direction development terrestrial photovoltaic is created tandem device structure with superstrate CdTe/CdS SC. Presently for tandem structures was tested a new construction of the CdS/CdTe SC with transparent back thin film electrode made up indium and tin oxides (ITO). The peculiarities of photo-electric processes in CdS/CdTe SC with different thin film back contact have been studied. With this purpose we carried out comparative investigation glass/SnO<sub>x</sub>:F/CdS/CdTe/ITO, glass/SnO<sub>x</sub>:F/CdS/CdTe/Cu/ITO and glass/SnO<sub>x</sub>:F/CdS/CdTe/Cu/Au SC.

The CdS/CdTe/ITO film heterosystems were prepared thermal vacuum evaporation method on the glass substrates covered with a layer of SnO<sub>x</sub>:F. The “chloride” treatment is applied by evaporation CdCl<sub>2</sub> thin film on to the CdTe surface and then annealing the stack in air at 430°C. Prior to the formation of back electrodes, the surface of the CdTe base layer was etched in a bromine–methanol solution. Then the ITO layers 300-350 nm thick were deposited on the etched surface by nonreactive high-frequency magnetron sputtering at 250°C. To form the back electrode of the CdS/CdTe/Cu/Au solar cell, the Cu films 11 nm thick and Au films 50 nm thick were sequentially deposited on the surface of the etched base layer by thermal vacuum evaporation method. Then the solar cells were annealed in the air at 250°C for 25 min. To form the back electrode of the CdS/CdTe/Cu/ITO solar cell, the Cu films 1 nm thick were deposited by thermal vacuum evaporation method on the surface of the etched base layer. Then the ITO layers 300-350 nm thick were deposited by nonreactive high-frequency magnetron sputtering at 250°C.

The dark I-V characteristics of SC at various temperatures and voltage-capacitance C-V characteristics were measured. For calculation of coefficient of quantum efficiency  $Q(\lambda)$  measurements of density of a short-circuit current  $J_{sh}(\lambda)$  were carried out. For a comparative analysis of CdS/CdTe/ITO and CdS/CdTe/Cu/Au SC, the absolute values of  $Q(\lambda)$  were normalized by the maximal value of the quantum efficiency coefficient measured for the CdS/CdTe/Cu/Au SC at  $V = 0$ .

The studies dark I-V characteristics of CdS/CdTe/Cu/Au solar show that the density of the current flowing across the solar cell starts to be limited by the density of the saturation current of the back contact. The activation energy of the saturation current of the rear contact is 0.16 eV and ideality coefficient  $A = 1.9$ . The potential-barrier height is 0.30 eV. It was show, that the thermal emission mechanism of the charge transport exist in the device structure in the mentioned voltage range. The studies of CdS/CdTe/ITO show, that the tunnel-

recombination mechanism of the charge transport exist in such device structure. The research of (C-V) characteristics show, that for the CdS/CdTe/Cu/Au structures height of the back potential barrier CdTe-Cu/Au is 0.25 eV, which corresponds to the value of this parameter found by us from the analysis of the dark I-V characteristic. For the CdS/CdTe/ITO solar cells height of potential barrier is 2.20 eV. Concentration charge carriers  $N_b = 9.5 \cdot 10^{-20} \text{ m}^{-3}$  for the CdS/CdTe/Cu/Au structures, and  $N_b = 2 \cdot 10^{-21} \text{ m}^{-3}$  for the CdS/CdTe/ITO structures. A high carrier concentration near the back contact and a high potential barrier of the back contact gave rise to the tunnel- recombination, concentration charge carriers  $N_b = 9.5 \cdot 10^{-20} \text{ m}^{-3}$  for the CdS/CdTe/Cu/Au structures, and  $N_b = 2 \cdot 10^{-21} \text{ m}^{-3}$  for the CdS/CdTe/ITO structures. A high carrier concentration near the back contact and a high potential barrier of the back contact gave rise to the tunnel- recombination mechanism of the charge transport in the CdS/CdTe/ITO solar cells under the forward-bias voltage above 1 V, which follows from the analysis of the dark I-V characteristics.

Comparative studies of the  $Q(\lambda)$  dependences, obtained for CdS/CdTe/Cu/Au and CdS/CdTe/ITO solar were carried out. The measurements of  $Q(\lambda)$  have been made on front side (across glass substrate) of the SC ITO back contact and the behaviour has been compared with the one of the standard Cu/Au back contact. This last one has a very similar response in the red part near the absorption edge, but has a better response in the 400-550 nm region most probably due to the presence of copper in the bulk of CdTe for Cu/Au back contact SC which might passivity the grain boundaries and increase the quantum efficiency. If the CdS/CdTe/ITO system is illuminated from the frontal side (across glass substrate) hand the applied electrical bias is positive, the electrical voltage growth results in reduction of the spectral response. An increase of the direct bias results in a reduction of the electrical field of the front heterojunction CdS/CdTe and an increase of the electrical field of the back heterojunction ITO/CdTe. At  $V > 0.8 \text{ V}$  the change of photocurrent polarity from positive to negative is registered. The change of photocurrent polarity is caused by the existence of two heterojunctions (nCdS-pCdTe, pCdTe-nITO) in the device which are in opposite connection.

The SC CdS/CdTe/Cu/Au have efficiency 10.4% with  $V_{oc} = 790 \text{ mV}$ ,  $J_{sc} = 20.1 \text{ mA/cm}^2$ ,  $FF = 0.66$ . By illumination on the front side the efficiency SC CdS/CdTe/ITO was 7.7% with  $V_{oc} = 690 \text{ mV}$ ,  $J_{sc} = 18.5 \text{ mA/cm}^2$ ,  $FF = 0.60$ . The efficiency SC CdS/CdTe/Cu/ITO was 9.9% with  $V_{oc} = 740 \text{ mV}$ ,  $J_{sc} = 19.5 \text{ mA/cm}^2$ ,  $FF = 0.68$ . By analytical processing light BAX is established, that use of thin layers copper in a design of transparent contact results in decrease of reverse current saturation density. It was shown, that as against SC with Cu/Au back contact the SC with back ITO/Cu contact would have the same high stability as well as SC with ITO back contact.

## Light-emitting properties of $A_2B_6$ nanocrystals in colloidal solution and solid-state matrices

Korbutyak D.V.<sup>1</sup>, Kovalenko O.V.<sup>2</sup>

<sup>1</sup>*V. Lashkaryov Institute of Semiconductor Physics, National Academy of Sciences of Ukraine,  
Kyiv, Ukraine*

<sup>2</sup>*Oles Honchar Dnipropetrovsk National University, Dnipropetrovsk, Ukraine*

Unique properties of quantum structures, in particular of nanocrystals (NCs), resulted not only in the discovery of new physical phenomena, but also in the development and application of new high-tech devices, which in many parameters like high stability, low energy consumption, extreme miniaturization, etc. are substantially superior to their three-dimensional analogs. Among a great variety of devices, where NCs based on II-VI semiconductor materials are employed, a worthy place belongs to light-emitting devices: light-emitting diodes with a preset wavelength of emission (from near IR to near UV range), sources of white light, low-threshold lasers, etc.

In our report, we present a review of some works aimed at synthesizing II-VI NCs in colloidal solutions and techniques of NCs transferring into solid polymeric matrices. The photoluminescent properties of II-VI NCs (CdTe, CdS, CdSe) are considered in dependence on their growth technology and post growth treatments.

The results are presented on the investigations of the photoluminescence (PL) spectra for II-VI NCs in dependence on the temperature and laser excitation intensity. This allows us to establish the nature of the corresponding PL bands. The Stokes shift in II-VI NCs dependence on NC sizes, their dispersion, energy of phonons participating in the absorption and emission processes and the values of potential barriers for charge carriers at the NC/matrix heterointerface.

A substantial attention in the report is attracted to a review of works aimed at developing light-emitting devices of new generation of low-threshold lasers based on II-VI quantum structures. Mainly, lasers pumped by an electron beam are considered. In this case, it is important to optimize the design of laser diodes to obtain light generation at extremely low values of acting energy of the electron beam and low values of the threshold current density. The dependence of the threshold current density on the electron beam energy has been analyzed; light generation spectra at various energies of the electron beam as well as the dependence of emission efficiency on the current value and electron beam energy are presented. An outlook for the application of wide-band compounds (ZnSe, ZnS, ZnO) in laser systems is shown.

## Using of single quantum well structures and superlattices based on the $A_2B_6$ compounds in a modern laser systems

Kovalenko A.V.<sup>1</sup>, Korbutyak D.V.<sup>2</sup>, Tishchenko V.V.<sup>3</sup>

<sup>1</sup>*Dnipropetrovsk National University of name Olesya Gonchara, Dnipropetrovsk, Ukraine,*

<sup>2</sup>*V. Lashkaryov Institute of Semiconductor Physics of the National Academy of Sciences of Ukraine, Kyiv, Ukraine,*

<sup>3</sup>*Institute of Physics of the National Academy of Sciences of Ukraine, Kyiv*

Despite on the significant progress in creating of emitting structures (such as LED and laser) based on nitrides, compounds  $A_4B_4$ ,  $A_3B_5$ , compounds  $A_2B_6$  remain the most promising materials for the development of the emitting structures in view of the fact that these compounds can create lasers from UV to IR the spectrum of radiation. So for the UV, violet and blue spectral range are very promising compounds as well as ZnO, ZnS, ZnSe; for IR and red spectral range - CdTe, HgSe, HgTe, and such compounds as ZnTe, CdS, CdSe, together with the already listed compounds successfully overlap the orange-yellow-green band emission spectrum. It should be stressed that the boundaries of spectral bands emitting structures rather conventionally tied to a particular kind of compounds  $A_2B_6$ . It is well known that only crystals ZnS, having a band gap  $\sim 3,7$  eV, at the expense of impurity's emitting recombination centers (Mn, Cu, Ag, Al, Cr, Fe) of photoluminescence can create structures emitting from UV to IR radiation. It should be further emphasized that the laser material based on  $A_2B_6$  compounds can be created on the basis of volumetric material or the classic p-n heterojunctions, hybrid systems such as  $A_3B_5/A_2B_6$  or  $A_4B_4/A_2B_6$ , and in recent times and on the basis of quantum-well structures (QWS).

In this case, where we used QWS in the form of short-period superlattices (SL) it can be applied as a component of the bulk p-n junction, replacing the emitter, or they can be used to create wave structures. Similar SL prevents the penetration of various defects in the active region, effectively stopping them at the barrier of emitter-wave structure, in addition, providing a simultaneous improvement in optical and electron restriction. Furthermore SL significantly compensate strain, arising from the mismatch of the crystal lattice of the substrate and epitaxial layers. The use of SL in such lasers affect the thermal mode, reducing thermal resistance, as well as to significantly increase the degradation stability of the structure. Different kind of SL laser structure will be the subject of this report.

In the second part of report we inform about our results in this field. As well known that semiconductors ZnS and ZnSe is a suitable materials for various optoelectronic devices, laser systems and so on. Using the PAVPE (photo-assisted VPE) technology (radiation source He-Cd laser  $h\nu = 2,807$  eV,  $P = 0,8$  mW/cm<sup>2</sup>, substrate temperature  $T = 170$  °C – 350 °C), single QWS of ZnS-ZnSe-ZnS/GaAs(100) and ZnS/ZnSe/GaAs(100) SL have

been grown and reflection and photoluminescence spectra of the QWS and SL have been studied (Fig. 1a, 1c).

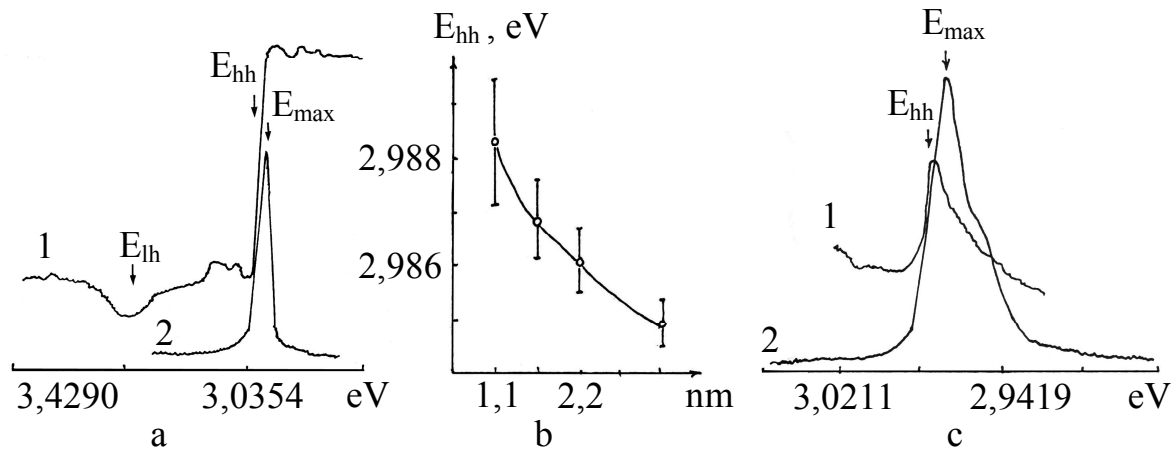


Fig. 1. Reflection (1) and photoluminescence (2) spectra of ZnS(4,3 nm)-ZnSe(1,1 nm)-ZnSe(4,3 nm)/GaAs(100) QWS (a), the dependence of energy of  $E_{hh}$  exciton on the ZnSe well thickness in ZnS-(4,3 nm)-ZnSe-ZnS(4,3 nm)/GaAs(100) QWS(b), reflection (1) and photoluminescence (2) spectra 80 (ZnS(4,3 nm)-ZnSe(2,3 nm))/ZnS<sub>0,06</sub>Se<sub>0,94</sub>/GaAs(100) SL (c);  $T = 4.5\text{K}$ .

The paper will report on our investigations on the growth mechanism for  $A_2B_6$  on GaAs(100) by PAVPE, influence of lattice mismatch on optical properties, dependence of energy of  $E_{hh}$  exciton on the ZnSe well thickness in the ZnS-(4,3 nm)-ZnSe-ZnS(4,3 nm)/GaAs(100) single QWS.

At the reflection spectra of QWS we can see two excitons: light exciton ( $E_{lh}$ ) at 3,1788 eV and heavy exciton ( $E_{hh}$ ) at 2,9907 eV. The value of maxima of photoluminescence spectra in QWS has been shown good coincidence with value of energy of  $E_{hh}$ . Fig. 1b plots the emission peak energy against the ZnSe well width. The half width value is shown by a vertical bar. The width of barrier in QWS was constantly 43 Å (8 layers of ZnS) and width of wall was from 11 Å to 33 Å (2-6 layers of ZnSe). The solid curve shows the dependence of the calculated emission energy on the well thickness based on a simple square well potential model.

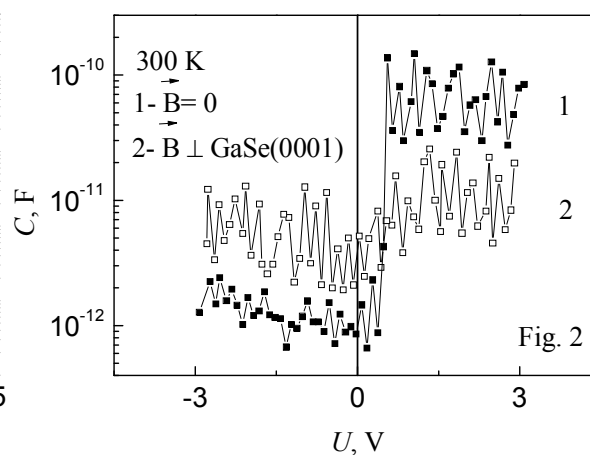
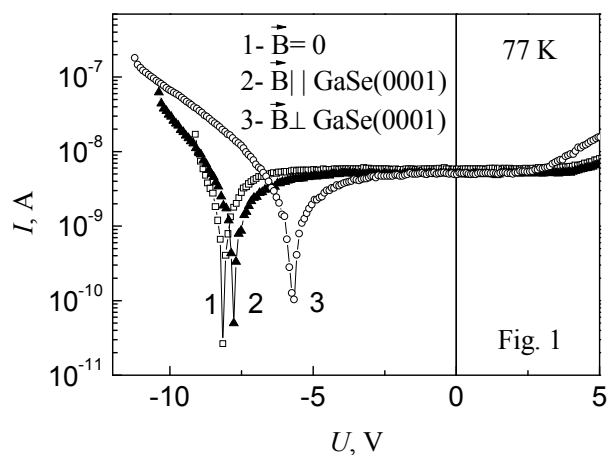
The reflection and photoluminescence spectra SL of ZnS/ZnSe/GaAs(100) is presented in Fig. 1c. A 1000 Å thick ZnS<sub>0,06</sub>Se<sub>0,94</sub> layer was grown on GaAs(100) substrate before than SL of ZnS/ZnSe. For this case was found a special correlation between the two main carrier gas flow with ZnS and ZnSe sources. ZnS<sub>0,06</sub>Se<sub>0,94</sub> layer have had just the same lattice parameter as GaAs, so that give us possibility to decrease of elastic strain in SL of ZnS/ZnSe. The small of half width values of photoluminescence spectra QWS of ZnS-ZnSe-ZnS/GaAs (100) and SL of ZnS/ZnSe/GaAs (100) shown good crystal quality of this structures.

## Spin-dependent tunneling in hybrid “ferromagnetic – layered semiconductor” AuNi - Ga<sub>2</sub>O<sub>3</sub> - p- GaSe heterostructures with carbon encapsulated Ni nanoparticles embedded in Ga<sub>2</sub>O<sub>3</sub>.

Kovalyuk Z.D., Bakhtinov A.P., Vodop'yanov V.N., Netyaga V.V.

Frantsevich Institute of Material Science Problems, National Academy of Sciences of Ukraine, Chernivtsy, Ukraine

Multilayered nanostructures Au(5nm)Ni(60nm)/  $\delta$ -doped  $n^+$ -Ga<sub>2</sub>O<sub>3</sub>/  $n$ -Ga<sub>2</sub>O<sub>3</sub> (10 nm) were grown on a layered substrate  $p$ -GaSe (0001). Carbon coated magnetic Ni nanoparticles with size range below 4-8 nm were fabricated on an atomic-smooth oxidized surface GaSe (0001). The device was operated with the bias applied between the Ni and GaSe. The negative differential conductance effect and a clear staircase (Coulomb blockade effect) were observed in the I-V characteristics of nanostructures at T= (77-300) K. Peculiarities observed in the I-V (Fig.1) and C-V(ac-frequency  $f=1$ kHz) (Fig.2) characteristics of hybrid structures for different geometry a low applied magnetic field (B=60 mT) may be caused by the phenomena of the magnetic anisotropic in the small particles, spin accumulation and spin-dependent tunneling between magnetic nanoparticles and a ferromagnetic Ni layer [1,2].



1. Tran M., Jaffres H., Deranlot C., George J. –M., Fert A., Miard A., Lemaître A. Enhancement of the spin accumulation at the interface between a spin – polarized tunnel junction and a semiconductor // Phys Rev Lett – 2009. – V.102, №3 – P. 036001(1)-036001(4).
2. Bakhtinov A.P., Vodop'yanov V.N., Kovalyuk Z.D., Netyaga V.V., Lytvyn OS. Electric properties of hybrid (ferromagnetic metal - layered semiconductor) Ni/  $p$ -GaSe structures // Semiconductors. – 2010. – V.44, №2. – P. 171-183.



## Films and Nanostructures for Optoelectronics based on ZnO

Lashkarev G.V., Karpyna V.A., Lazorenko V.I., Ievtushenko A.I.,  
 Khranovskyy V.D., Shteplyuk I.I., Demydyuk P.V., Myroniuk D.V.,  
 Yaremko A.M.<sup>1</sup> and Yakimova R.<sup>2</sup>

*I.M.Frantsevich Institute for Problems of Material Science, National Academy of Sciences of  
 Ukraine, Kyiv, Ukraine*

<sup>1</sup>*V.E.Lashkarev Institute of Semiconductor Physics, National Academy of Sciences of Ukraine,  
 Kyiv, Ukraine*

<sup>2</sup>*Linkoping Universitet, Linkoping, Sweden*

Zinc oxide is the most investigated direct wide-gap semiconductor in the world because of its physical, ecological and economic benefits which make it promising one for optoelectronic applications. The properties of ZnO films strongly depend on the concentration of various defects appearing at the film growth and further technological processes. Therefore it is of importance to control the properties of this semiconductor (perfectness of crystal structure, the magnitude of band gap, ultraviolet (UV) and defect luminescence, photosensitivity to UV radiation) by technological procedures of deposition, annealing and doping. ZnO-based radiation-robust devices are also important.

The application of multistage magnetron sputtering proposed by us allows depositing textured ZnO films of high perfectness and intensive UV luminescence. Such layer-by-layer growth mode was realized by several stages of deposition at which next ZnO layer grown on the previously grown one. As a result, ZnO films of improved quality are formed. Following LO phonon modes were observed experimentally by Raman scattering measurements: 580, 1160, 1742, 2321, 2912, 3485, 4075, 4649 cm<sup>-1</sup>. They all correspond to longitudinal optical mode A<sub>1</sub>. The analysis of these spectra was carried out in the frames of second order perturbation theory. Developed theory describes very well the peaks positions of LO phonon replicas of the experimental Raman spectrum. Comparing our Raman spectrum with one for ZnO single crystal allow us to state that ZnO films, obtained by our technology approach, possess the perfect crystal structure close to bulk crystals.

The nitrogen in ZnO is an acceptor impurity which is widely used in attempts to obtain stable p-type conductivity in ZnO. However, based on our studies, we suppose that nitrogen doping leads to the passivation of oxygen vacancies of ZnO and therefore increase the photosensitivity, response speed and stability of photodetectors on their basis. The effect of increasing the concentration of nitrogen in ZnO films on physical properties was studied.

On the basis of ZnO films doped by nitrogen Ni/n-ZnO:N/p-Si/Al phototransistor structures were developed. Bending of the bands at the Ni/n-ZnO contact occurs what results in effective injection of current carriers to n-ZnO. In these phototransistors internal current gain is realized and high photosensitivity

about 210 A/Wt at  $\lambda=390$  nm as well as response speed with time constant  $\sim 100$  ns were achieved.

The effect of Ag and Cu impurities on the properties of ZnO films was explored. For this purpose the close space sublimation method was firstly used for doping ZnO films with Ag and Cu. This doping method is based on the diffusion of the dopant under heating in water vapour. The PL spectra revealed strong enhancement of UV emission in ZnO:Ag films, especially in ZnO:Ag/r-Al<sub>2</sub>O<sub>3</sub>, as compared with the samples deposited on the other substrates. Opposite to the undoped and Ag doped films for the samples ZnO:Cu the green intensive three fold structured band with central peak at 514 nm and less intensive bands at  $\sim 460$  nm and  $\sim 590$  nm were observed. The mechanism of UV enhancement for ZnO:Ag as well as the features of the emission centers in ZnO:Cu are discussed.

A control of the energy gap  $E_g$  of the zinc oxide is one of the biggest challenges in designing of various heterostructures for optoelectronic devices. Decreasing of  $E_g$  can be achieved through partial substitution of zinc by cadmium ions. We report the effect of deposition technology (the ratio of working gases, the substrate properties and annealing conditions) on the microstructure and optical properties of the films Zn<sub>1-x</sub>Cd<sub>x</sub>O grown by magnetron sputtering. The researchers of X-ray diffraction, optical transmission and luminescence spectra of Zn<sub>1-x</sub>Cd<sub>x</sub>O films deposited on the m, R,  $\alpha$  and c-sapphire substrates and different technological parameters are discussed in the aspect of their further applications in development of blue-green light emission diodes (LEDs).

The ZnO Nanorods (NRs) and Nanowires (NWs), prepared via catalyst (Au) assisted growth on Si substrates, were studied by cathodoluminescence (CL) analysis. By comparison of an SEM image and a respective CL images one can reveal a local correlation between structural and light emitting properties. The room temperature CL spectra of both NRs and NWs possess narrow peak of near band edge (NBE) emission in the UV region ( $\lambda_{\max} \approx 390$  nm) and four overlapped peaks of deep level emission DLE (at 480, 503, 540, 583 nm respectively) in the visible range of spectra. The relative NBE/DLE intensity of the NWs is larger than for the NRs, evidencing the better optical quality. The low temperature PL spectrum of ZnO NWs contains well-resolved peaks of ionized and neutral donor bound excitons ( $D^+X$  at 3.3669 eV  $D^0X$  at 3.3642 eV) followed by two-electron satellites (TES) and the first and second longitudinal phonon replicas of  $D^+X$ , separated between each other by 72 meV. The  $D^0X$  emission was attributed to H impurity as a contaminant in ZnO. Defects in NRs are distributed nonuniformly: inside the rods ZnO is stoichiometric and demonstrates UV NBE. Their envelope is nonstoichiometric, contains defects and displays DLE. All PL peaks of NBE and DLE are shifted to short wavelength what testifies to manifestation of quantum confinement at the transition from NRs to lower dimensional NWs.

## **Silicon Nanowires, Nanostructured and Nanoporous Silicon as Materials for New Generation Sensors**

Lepikh Ya.<sup>1</sup>, Gordienko Yu.<sup>2</sup>, Druzhinin A.<sup>3</sup>, Evtukh A.<sup>4</sup>, Lenkov S.<sup>5</sup>

<sup>1</sup>*I. Mechnikov Odessa National University, Odessa, Ukraine*

<sup>2</sup>*Kharkov National University of Radioelektronics, Kharkov, Ukraine*

<sup>3</sup>*Lviv National Technical University 'Lviv Polytechnica', Lviv, Ukraine*

<sup>4</sup>*V. Lashkaryov Institute of Semiconductor Physics, Kiev, Ukraine*

<sup>5</sup>*T. Shevchenko Kiev National University, Kiev, Ukraine*

Modern sensors have to obtain and develop much information. Sensors and intelligent sensors systems are vital to people awareness of their surrounding and provide safety, security, and surveillance, as well as enabling monitoring of people health and environmental. Silicon based sensors and systems are widely used and are very promising for future development first of all due to compatibility with highly developed silicon CMOS technology. Nanotechnology proposes new nanomaterials with unique properties for development of various sensors and sensors intelligent systems with improved parameters.

In this work the Si based nanomaterials, namely: Si nanowires, nanostructured and nanoporous silicon are considered and analyzed as the promising materials for new generation sensors. The physical properties of Si based nanomaterials and their application for various sensors are demonstrated.

The new technologies for obtaining of nanostructured silicon have been realized during formation of sensitive elements. Under investigation of Si nanowires properties the many interesting and useful results aimed on sensor application have been obtained. Some new types of sensors have been created based on Si nanowires. Among them (i) the sensor deformation and pressure of cryogenic liquid for different temperature range, piezoresistive sensors of pressure and liquid nitrogen level etc. It was also demonstrated that Si<sub>1-x</sub>Ge<sub>x</sub> nanowires allow to create sensors with unique parameters.

The parameters of developed sensors based on Si and Si<sub>1-x</sub>Ge<sub>x</sub> nanowires have been demonstrated and analyzed.

The results of research and development of MS and MIS gas sensors based on porous silicon are presented. The important peculiarities of developed sensors are the using of (i) nanoporous silicon, (ii) various catalytically active and usually non-active electrodes, and (iii) compatibility with microelectronics CMOS technology. During creation of gas sensors the such important properties of nanoporous silicon have been exploited: (i) unique combination of the crystal structure and the huge internal surface area (200-500 m<sup>2</sup>cm<sup>-2</sup>) that is able to enhance the adsorption processes; (ii) high surface chemical reactivity, significant change of porous silicon surface as a result of different kinds of treatment (thermal and optical annealing, etc.); (iii) possibility to use the novel effects in quantum limited systems (the increase of the energy bandgap, optical properties modulation through the layer depth, photoluminescence); (iv) simplicity and cheapness of the technology that could be compatible with silicon IC technology; (v) possibility to make 3D device structures and multisensors; (vi) opportunity to modify the morphology by the control of the pores dimensions from nano- to microscale. The parameters of developed prototypes of H<sub>2</sub> and H<sub>2</sub>S gas sensors based on MIS structure with porous silicon have been demonstrated.

## The modified graphene – new type of semiconductor films

Litovchenko V. G., Strikha M.O.

*V. Lashkarev Institute of Semiconductor Physics NAS of Ukraine, Kiev, Ukraine*

Carbon has some more once represented a surprise for the mankind - the Nobel Price in physics for 2010 year.

Chemical element carbon has many faces or, in physical terms, it is polimorphous. It can be in form of the hardest material in the world, which is diamond as well as in form of superfluid solid matter. Recently, a new superstrengthened carbon material was introduced, the graphene.

Theoretically such material was predicted long ago as monoatomic layers of graphite-like hexagonal structure, for which planar chemical bonds are formed of 3 orbitals (s, s, p) and after hybridisation create super strong chemical bonds. Paradox was that some of the outstanding physicists (Landau et al.) predicted in 30-th years the nonstability of such monolayer structure (in insulating states).

Nevertheless, an experimental study of real graphite-like films were carried out in many laboratories, including Kiev Institute of Semiconductor Physics. Here, the group of scientists [1, 2] obtained important new results, which precorcord more than 20 years of the discovery and broad study of the new state of carbon, later named graphene.

That state of graphite-like carbon film becomes stable after deposition on the solid substrate. Two-layer graphene (or even with several monolayers) becomes a stable structure. Namely, such structures were theoretically analysed in the mentioned publications [1, 2]. A set of important results was obtained:

- 1) Such monolayer samples become stable under local deformation.
- 2) Even more unexpected was the conclusion that semimetal graphene layer transforms in semiconductor state already at relatively small deformations or by incorporation of defects or doping, see Fig. 1.
- 3) The origin of this transformation is the phase-structural transition, distortion of the pure  $sp^2$  bonds and creation of the hybrid mixed bonds  $xSp^2 - ySp^3$ , which are possibly dominating for carbon. This is the reason for the carbon to be the basis of all organic substances.
- 4) Hence, the important discovery, namely the phase transition from metal to semiconductor state was realised. This means the opening of the new branch of semiconductor material engineering.

This result was proven experimentally on the carbon films obtained by different technologies. It could be possible to vary the energy gap of carbon films from milivolts up to several volts.

## Constitutional diagrams with kinematical & minimal surfaces for heterogeneous design

Lutsyk V.V.

*Buryat Scientific Centre of RAS (Siberian Branch), Physical Problems Department,  
Republic Buryatia, Russian Federation*

Computer model of phase diagram (PD) is a tool for the data storage in compact form [1-2]. It produces any PD projection and section with decoding of intersected surfaces and phase regions. It helps to discover the errors and incorrectly interpreted experimental data in the PD graphics, e.g. the unclosed contours of solvus surfaces in T-x-y diagrams of A.Prince with the immiscibility [3]. It shows the mass balances, distinguishing the crystals of different prehistory for any alloy and images a history of solidification. It has been used as an instrument to design the microstructures of heterogeneous materials.

Computer model of PD and mass balances for arbitrary chosen melts make it possible to perform the most comprehensive investigation of the crystallization processes occurring in the system with the transition from the eutectic equilibrium ( $L \leftrightarrow \alpha + \beta$ ) to the peritectic one ( $L + \beta \leftrightarrow \alpha$  or  $L + \alpha \leftrightarrow \beta$ ). Concurrency of the primary crystals  $A^1$  and the eutectical ones  $A^e$  was investigated for the quasiperitectic reaction  $L + A = B + R$  with the binary incongruently melting compound of fixed composition.

First results of ceramics and alloys microstructures design were received by the PD computer models with the so-called kinematical surfaces. The prospect is promised to use the surfaces with the minimal areas, when experimental data within the surface's contour isn't required [4]. A task is reduced to a problem of Plato with the definition of a surface  $Z = Z(x,y)$  by its borders. The smooth surface of property within the whole concentration triangle, like the liquidus of continuous rows of solid solutions, is considered in the A-B-C system. As a character of a surface isn't known, it is possible to assume that its average curvature  $H = 0$ , and to receive a surface with the minimal area among a set of surfaces with the same borders.

1. V.I. Lutsyk, A.M. Zyryanov, A.E. Zelenaya. Computer model of a T-x-y diagram for a ternary system with monotectic monovariant equilibrium // *Russian. J. of Inorg. Chem.* – 2008. – V. **53**(5). - PP. 794 - 799.
2. V.I. Lutsyk, V.P. Vorob'eva. Computer models of eutectic type T-x-y diagrams with allotropy. Two inner liquidus fields of two low-temperature modifications of the same component // *J Therm. Analysis and Calorimetry*. – 2010. – V. **101**(1). - PP. 25 – 31.
3. [http://www.msiport.com/fileadmin/content/research/freetools/a\\_prince/book\\_files/FIGURES/fig\\_216.htm](http://www.msiport.com/fileadmin/content/research/freetools/a_prince/book_files/FIGURES/fig_216.htm)
4. V.I. Lutsyk. *Analysis of liquidus surfaces in the ternary systems*, Nauka Publ. Comp, Moscow (in Russian). – 1987.- PP. 98 – 100.

## Specific features of isovalent-substituted zinc oxide layers

Makhniy V.P.<sup>1</sup>, Khusnutdinov S.V.<sup>2</sup>

<sup>1</sup>*Yu.Fedkovych Chernivtsi National University, Chernivtsi, Ukraine*

<sup>2</sup>*Institute of Physics, Polish Academy of Sciences, Warsaw, Poland*

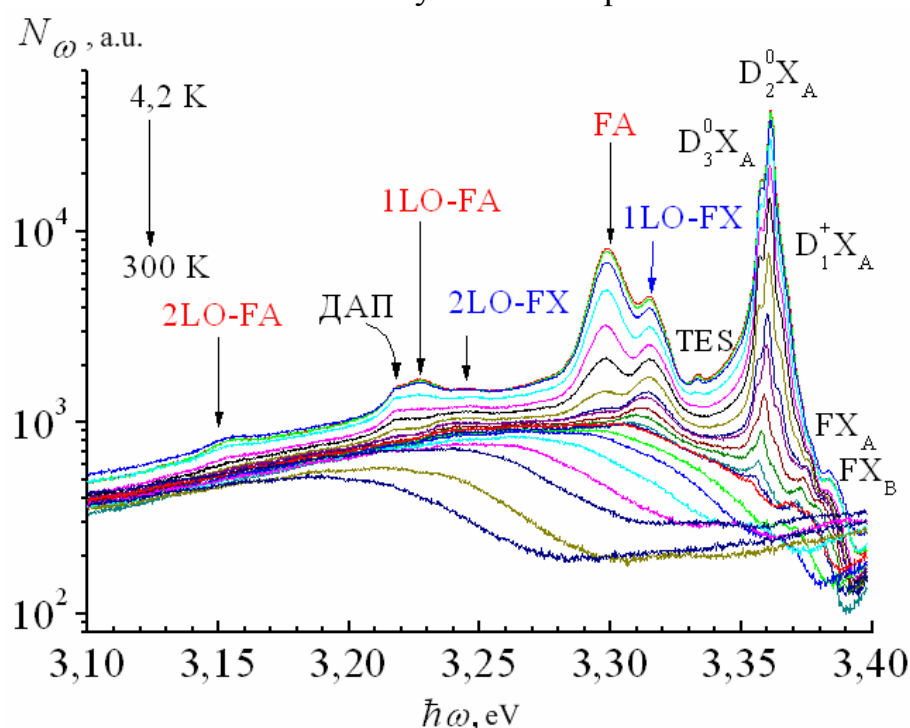
Among the wide-gap II-VI compounds, noted for their excellent luminescent and photoelectric properties, particular place is occupied by zinc oxide [1]. It is also characterized by considerable electrooptical and piezoelectric effects, and with regard to a direct gap and a wide energy gap ( $E_g \approx 3,2-3,4$  eV at 300 K), it can be the basic material for creation of efficient optoelectronic elements in the short-wave range. Besides, calculations show that ZnO with magnetic impurities has one of the highest values of Curie temperature ( $T_c \geq 300$  K), which is important for its use in spintronics. Since the active areas of the overwhelming majority of electronic and spintronic devices are thin layers, along with development of techniques for bulk crystal growing, considerable attention is also focused on the synthesis of ZnO thin layers and films. Instead, the widespread technologies demand for complicated and costly equipment and in some cases the application of highly toxic metal organometallic compounds. These shortcomings can be eliminated with the use of isovalent substitution method offering a series of undeniable advantages over the traditional methods of synthesis of thin layers of II-VI compounds [2].

Heterolayers were created by annealing in the air of single-crystal substrates of zinc chalcogenides (ZnTe, ZnSe and ZnS), each compound having its own range of annealing temperatures. It was established that isovalent substitution process is of diffusion type, and concentration of residual atoms of chalcogen (Te, Se and S) is about  $10^{19}$  cm<sup>-3</sup>. They serve as isovalent impurities and determine high radiation efficiency and temperature stability of luminescent characteristics and parameters.

It was established that ZnO heterolayers, irrespective of the type of basic substrate, are composed of heavily deformed nanocrystallites with the average dimensions  $\sim 300$  nm. Crystal lattice constants found from X-ray diffraction analysis, correlate with known parameters for hexagonal zinc oxide. Wurzite structure of ZnO heterolayers is also confirmed by Raman scattering spectra, and the energies of optical and acoustic phonons found on their basis are in agreement with those reported in the literature.

From the optical reflection spectra in the exciton area there were found cleavage values due to spin-orbital interaction and crystal field. It was shown that the luminescence efficiency and its spectral composition depend on the type of basic substrate, the surface microstructure of a heterolayer, the temperature and duration of synthesis. Technological conditions were experimentally determined, whereby the efficiency of ultraviolet radiation band in the region of room temperatures reaches 30%.

It is shown that the boundary radiation is caused by several recombination channels: annihilation of free and bound excitons, transitions with participation of shallow levels and donor-acceptor pairs. It is illustrated by a drawing that represents boundary luminescence spectra for ZnO/ZnSe heterostructure in the temperature range of 4.2-300 K. A similar shape and behaviour of spectra in the specified area of photon energy is also observed for isovalent-substituted layers synthesized on ZnTe and ZnS substrates. Calculated were the binding energies of excitons and the depth of centres taking part in formation of the boundary luminescence. From the temperature dependences of parameters of free excitons there were found characteristic Debye and Einstein temperatures. The established abnormally large temperature coefficient of ZnO energy gap compared to that reported thus far is explained by a strong lattice deformation of nanocrystallites of which the heterolayers are composed.



It is established that low-energy radiation bands of isovalent-substituted ZnO heterolayers are determined by transitions through deep levels formed by the intrinsic point defects. The shape of observed bands and the energy parameters of recombination centres are adequately described in the framework of Kopylov-Pikhtin model.

1. U. Ozgur, Ya.I. Alivov, C. Liu et al. // J. Appl. Phys. – 2005 – V.98 – P. 2-103
2. V.P. Makhniy, V.Ye. Baranyk, M.V. Demich at al. // Proc. SPIE. – 2000 – V.4425 – P. 272-276.

## **CeO<sub>2</sub>:Ln-containing nanostructures in oxide matrixes: spectroscopy, photophysics and technology**

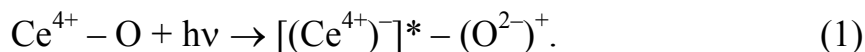
Malashkevich G.E.<sup>1</sup>, Khottchenkova T.G.<sup>1</sup>, Kouhar V.V.<sup>1</sup>,  
Sigaev V.N.<sup>2</sup> and Pestryakov E.V.<sup>3</sup>

<sup>1</sup>*B.I. Stepanov Institute of Physics of the NAS of Belarus, Minsk, Belarus*

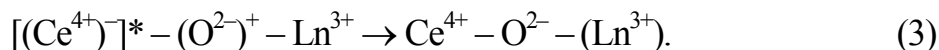
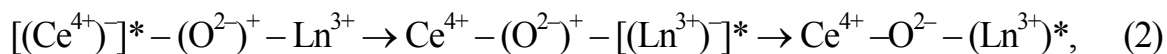
<sup>2</sup>*Mendeleev University of Chemical Technology of Russia, Moscow, Russia*

<sup>3</sup>*Institute of Laser Physics of the SB RAS, Novosibirsk, Russia*

This work arises from discovered effect consisting in significant excessing of luminescence quantum yield of Ce<sup>3+</sup> ions over the fraction of photons absorbed by ones in silica glasses synthesized by the sol-gel methods and including of triply and quadruply charged cerium [1, 2]. Afterward, it was shown that similar effect takes place at formation in the glasses of CeO<sub>2</sub> nanoparticles whose Ce<sup>4+</sup> ions are partially substituted by Ce<sup>3+</sup> ions or by other Ln<sup>3+</sup> ions [3]. It could be explained by transfer of excitations to the stable Ce<sup>3+</sup> ions from the charge transfer state of Ce(IV) oxocomplexes and/or from photoreduced central ions (Ce<sup>4+</sup>)<sup>-</sup> of these oxocomplexes in conditions of the superexchange interaction. This latter can be realized upon bonding of Ce<sup>4+</sup> and Ln<sup>3+</sup> ions by a bridge oxygen with the formation of configuration close to a collinear one. The formation of such photocharge-exchanged ions is the result of Ce<sup>4+</sup> ions capturing electron from excited sublevels of the charge transfer complex, which exist in resonance with the corresponding energy states of the (Ce<sup>4+</sup>)<sup>-</sup>, and is described as follows:



For one's turn, the transfer of excitations from the [(\text{Ce}^{4+})<sup>-</sup>]<sup>\*</sup> ions may occurs by means of electron transfer to Ln<sup>3+</sup> (for ions possessing with polycharged properties) or by transfer of energy which are described correspondingly by the following schemes:



The formation of CeO<sub>2</sub>:Ln nanoparticles in the glasses investigated was confirmed with the help of X-ray analyses, small-angle neutron scattering and spectral-luminescent investigation. As shown by the indicated methods, these nanoparticles have a cubic lattice with space group of symmetry  $O_h^5 - Fm\bar{3}m$ , in which the coordination number of the cations is 8, and their predominant 'diameter' consist about 10 nm.

By now, we have created by the colloid-chemical method an extensive set of silica glasses, oxide powders and ceramics activated with different CeO<sub>2</sub>:Ln<sup>3+</sup> nanoparticles which display a number of attractive spectral-luminescent properties. For example, luminescence spectra of Ln<sup>3+</sup> ions incorporated in the



nanoparticles generated in silica glasses are characterized by a significantly higher relative intensity of their magnetic dipole transitions (see Fig.) that permits to realize new laser transitions for the ions. At co-existence in the matrix of similar nanoparticles and isolated simple  $\text{Ln}^{3+}$  and complicated  $\text{Ce}^{4+}\text{-Ln}^{3+}$  centers the materials possess by a strong dependence of their luminescence spectrum on excitation wavelength due to extremely weak transfer of excitations between the isolated ions and nanoparticles. It should be noted that a reduction of quadruply charged cerium to triply charged state in the nanoparticles by saturation of the matrixes with hydrogen permits to reach an efficiency of sensitization of their  $\text{Ln}^{3+}$  ions luminescence by the stable  $\text{Ce}^{3+}$  ions close to 100 %. However, the luminescence spectrum of  $\text{Ln}^{3+}$  ions into the  $[\text{Ce}^{3+}\text{O}_8\text{H}]_n\text{:Ln}^{3+}$  nanoparticles can significantly differ from their spectrum in the initial  $[\text{Ce}^{4+}\text{O}_8]_n\text{:Ln}^{3+}$  nanoparticles.

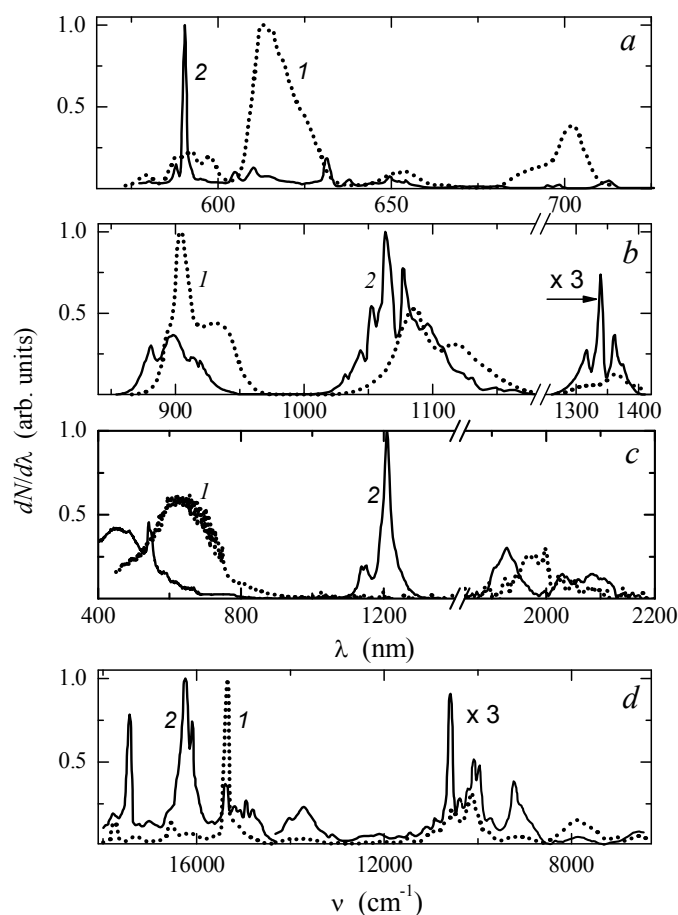


Fig. Luminescence spectra of (1) isolated  $\text{Ln}^{3+}$  ions and (2)  $\text{CeO}_2\text{:Ln}^{3+}$  nanoparticles in silica glasses. Ln = (a) Eu, (b) Nd, (c) Ho and (d) Sm.

1. G.E. Malashkevich, E.N. Poddenezhny, I.V. Melnichenko, A.A. Boiko. // J. Non-Cryst. Solids, – 1995. – V.188. – P. 107-117.
2. G.E. Malashkevich, E.N. Poddenezhny, I.V. Velnichenko, A.A. Boiko, and L.G. Brazhnik. // Optics and Spectroscopy. – 1995. –V.78, No. 1. – P. 74–77.
3. G.E.Malashkevich, V.N.Sigaev, G.I.Semkova, and B.Shampagnon. // Physics of the Solid State. – 2004. –V.46, No. 3.– P. 552-556.

## Technology and physical properties of the heterosystems with C<sub>60</sub> fullerenes

Matveeva L.A., Neluba P.L., Venger E.F.

*Institute of Semiconductor Physics of NAS Ukraine, Kyiv, Ukraine*

The discovery of new carbon cage molecules C<sub>n</sub> called fullerenes has led to a new class of carbon-based solids and heterosystems. At ambient conditions, C<sub>60</sub> forms nearly ideal molecular crystals with the molecules bound together by Van der Waals interaction. Besides, these materials show different electrical, optical, electron and mechanical behaviors, according to their structure, depending on several parameters in each production method. These properties are unique and very interesting. The heterosystems with C<sub>60</sub> are new promising materials for electronic, sensor and biomedical application.

We review results obtained from our Institute regarding the production, composition, morphology, structure, optical, electron and mechanical properties of the heterosystems with C<sub>60</sub> films. The films were deposited onto various unheated substrates (Si, GaAs, Ti, NaCl, KBr and glass) from microcrystalline C<sub>60</sub> powder by vacuum sublimation methods. For modification of the structure and properties of obtained films have been used the active treatments.

The heterosystems were characterized by room temperature Raman scattering, Fourier transform (FTIR), transmission and reflectance of light, electroreflectance spectroscopy and atom-force microscopy (AMF). The method profilography were used to determine of inner mechanical strains in films. Signs and level inner strains were calculated by the Stoney formula using the bending radius of heterosystems. To determine of inner mechanical strains in substrate on interface were used electroreflectance method.

The method of electroreflectance modulation spectroscopy were applied to control of electron parameters of the heterosystems. Measurements were made in quartz electrolytic cells with 0,1 water solution of KCl. There were determined energy of junction E<sub>g</sub>, the value of the phenomenological broadening parameter  $\Gamma$  (it describe the scattering of light excited charge carrier in material and depend on the type electron junction) and relaxation energy time of charge carriers  $\tau$ . Calculation of the electron parameters was realized using energy location of the dominant peaks in the spectra, its intensity or half-width of line.

Raman spectra C<sub>60</sub> films display lines peaked at 1426, 1470 and 1578 cm<sup>-1</sup>, FTIR spectra display lines peaked at 527, 576, 1180 and 1427 cm<sup>-1</sup>. The substrates with fullerene films C<sub>60</sub> (100 nm thick) were mounted on a cathode in a plasma treatment setup. The discharge voltage was 460 V. The plasma treatment duration was varied from 1 to 30 min. After 10-min treatment, a broad background band appears in the spectrum in the region from 1300 to 1700 cm<sup>-1</sup>. The appearance of this band in our samples reflects the initial stage of fullerene degradation and the formation of an isotropic amorphous carbon structure. As

the plasma treatment duration is increased, the broad background band disappears but a weak band centered at  $1560\text{ cm}^{-1}$  appears instead (graphitic G-band). The plasma-treated films contain two phases: fullerene and graphitelike clusters. After a 30-min exposure to the plasma, no Raman scattering signal was detected from the samples. It explained by the fact that the film was completely removed from substrate as a result of the ion sputtering. When treated of the fullerene films are not only subject to the ion bombardment but exposed to the UV radiation on the gas discharge as well. In order to determine which of these factors is responsible for the degradation of fullerenes, we studied the Raman spectra of  $C_{60}$  films exposed to the UV radiation from a quartz-mercury lamp with the most intense line corresponding to a wavelength of 365 nm. It was found that a 6-h exposure did not significantly affect the Raman spectra of  $C_{60}$  films. This result gives us ground to assert that the decomposition of fullerene molecules during the treatment is mostly related to the ion bombardment.

Fullerene coating was made by thermal evaporation of the fullerene powder in vacuum on unheated polished Ti 6Al 4V substrate from effusion tantalum cells at  $470^{\circ}\text{C}$ . The thickness of coating was 1–1.5  $\mu\text{m}$ . The wear at the friction pair - Ti 6Al 4V alloy coated by fullerene was approximately tenfold less than the one for the same pair, but without  $C_{60}$  and was comparable to the wear in the pair polyethylene –  $\text{Al}_2\text{O}_3$  based ceramics. After friction during 20 hours the surface roughness of polyethylene and the  $C_{60}$  coated Ti 6Al 4V disk were preserved almost the same as before friction. There were also no surface scratches, alteration of color or diminishing of the thickness of Ti 6Al 4V. Thus after clinical testes the titanium alloys with fullerene  $C_{60}$  coating can be successfully used in friction pairs of endoprosthesis of different joints: hip, knee, shoulder joints, etc.

Inclusion of the fullerenes in polymer matrix represents scientific and practical interest for nanotechnology and semiconductor industry. Combination of the low-temperature polymer technologies and semiconductor properties of the  $C_{60}$  fullerenes is used for photosensitive and solar cells production. For modification of the films and interfaces properties and too improvement of the devices quality have been used the microwave radiation. There was prepared of the heterostructures with polymer composite films ( $C_{60}$  are part of this films) on substrate silicon. For creation lower contact of the solar cell the titanic layer was deposited by thermal evaporation in vacuum on unheated plate. The Au and Ti high contacts were sputtering on polymer composite films. Resistance Au-polymer contact is appreciable bigger than Ti-polymer one. Metal-polymer contact resistance after microwave treatment is found to decrease (owing to interdiffusion). Interdiffusion was explained by intrinsic mechanical stresses. More considerable decrease occurred for structures with titanium metallization. There were determined the changes of the parameters  $E_g$ ,  $\Gamma$  and  $\tau$ . It be found that the microwave treatment reduce to appearance of the surface dimensional quantization effect on interface and improve their electronic parameters.

It was discussed the radiation stability of  $C_{60}$  films to  $\gamma$ -irradiation.

## **Some Properties of PbTe and Bi<sub>2</sub>Te<sub>3</sub> Crystals and Converters on Their Basis**

Meglei D.

*Institute of Electronic Engineering and Nanotechnology "D. Gitsu",  
Chisinau, Republic of Moldova*

In this work, we describe a technology for the preparation of glass-insulated microwires based on PbTe and Bi<sub>2</sub>Te<sub>3</sub> of the n- and p-type conduction. A process for the preparation of a bifilar microwire in which one core exhibits the n-type and the other p-type conductivity is developed.

The temperature dependences of electric conductivity and thermopower in a temperature range of 77-400 K are studied. The thermal efficiency of resulting wires is calculated.

On the basis of the derived wire crystals, we prepared laboratory samples of the following microconverters: a Bi<sub>2</sub>Te<sub>3</sub>-based microelectrode for measuring biopotentials, a highly sensitive microthermocouple; a PbTe-based photovoltaic receiver and an infrared laser operating at the liquid nitrogen temperature.

The article is dedicated to the Scientific and Research Cooperation JOINT Moldovan-Ukrainian Project 10.820.05.09UA "Technology and physicochemical properties of thin films and wires on the basis of lead telluride for thermoelectric energy convectors".

## Atomic structure of fumed silica nanoparticles

Myronyuk I.F.<sup>1</sup>, Gergel T.V.<sup>1</sup>, Danylenko M.I.<sup>2</sup>, Chelyadyn V.L.<sup>1</sup>

<sup>1</sup>Preคาร์pathion National University named after Vasyl Stefanyk, Ivano-Frankivsk, Ukraine

<sup>2</sup>Frantsevich Institute for Problems of Materials Science of NASU, Kyiv, Ukraine

In addition to the crystalline modifications of silica - quartz, cristobalite, varieties of amorphous SiO<sub>2</sub> are quite common in nature. These include primarily natural opals, quartz glass, silica of biogenic origin, synthetic form of silicon dioxide with extended surface - silica gel, sylohromy, aerosils, poruvate glass based on SiO<sub>2</sub>, white black and other.

Characteristic expression of an amorphous structure of silica is the lack of long range order in the arrangement of oxygen and silicon atoms, isotropy of physical and chemical properties, the different from zero entropy of the said materials at 0 K.

The basis of modern ideas about the structure of amorphous silica species is microcrystalline model. It implies the existence of ordered domains in the material - size of microcrystallites ≤ 0.8-1.0 nm separated unordered plots. According to investigators crystallites contain several tens of SiO<sub>4</sub> tetrahedrons.

In this paper we aim to investigate the atomic structure of fumed SiO<sub>2</sub> nanoparticles using transmission electron microscopy, infrared spectroscopy and low-temperature adsorption-desorption of nitrogen molecules.

The research allowed to find out that structural motifs of X-ray amorphous silica are short open-branched chain clusters with the length of 0.6-2.4 nm. In one repetitive fragment of the linear part of the chained cluster, there are two SiO<sub>4</sub> the vertexes of which go up and down in turn and which are connected with each other through the common oxygen atom (fig. 1). The intertetrahedral angle

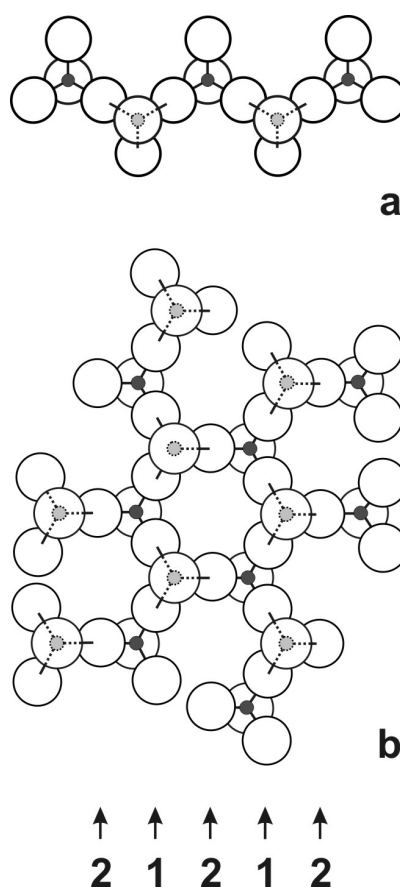


Fig. 1. Chain motif in structure of amorphous SiO<sub>2</sub> creates linear condensation of SiO<sub>4</sub> tetrahedrons (a) and fragment of silica structure (b). Numerals show rows of oxygen atoms with big (large) (1) and small (2) their density on length unit.

SiOSi along the chain is about  $180^\circ$ . Valence angles in the bridge Si-O-Si, which connect each chain clusters are  $\sim 137-147^\circ$ .

The presence in the IR spectra of small nanoparticles  $\text{SiO}_2$  with weak intensity bands at  $968-939\text{ cm}^{-1}$  confirms the presence of globules in the volume of a small number of isolated chains in which the  $\text{SiO}_4$  tetrahedron are connected by common edges.

Small length and spatial disorientation of chain clusters create structural disorder and make silica nanoparticles amorphous X-ray.

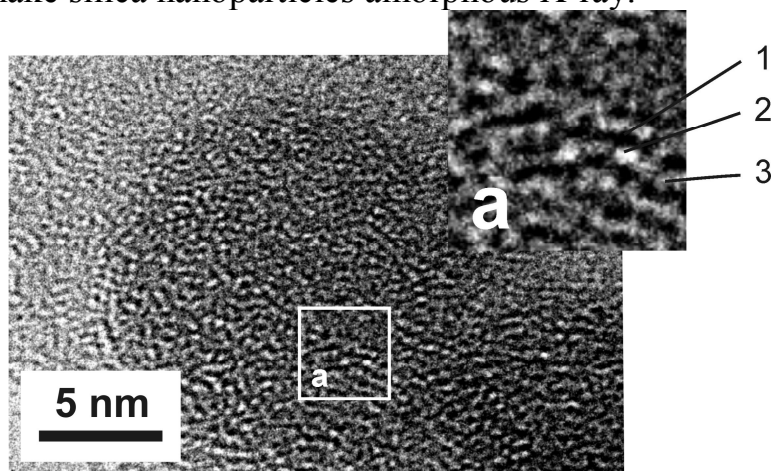


Fig. 2. Images of protoparticle of fumed silica. Numerals show black (1) and white (3) domens, and also structural defects of material (2).

Porosity fumed silica is connected with aggregation of initial nanoparticles. The volume of mesopores in pyrogenic material is  $0.26 \div 0.6\text{ cm}^3 \cdot \text{g}^{-1}$ . It is found out that the mean radius of mesopores decreases from 34 nm to 10 nm if dispersion of initial nanoparticles increases. The contribution of micropores to the total volume of material pores is small and is only  $0.003 \div 0.029\text{ cm}^3 \cdot \text{g}^{-1}$ .

The photos globules  $\text{SiO}_2$ , obtained at the maximum distinction microscope revealed micropores with an average size of 0.3 nm, which proportionate with  $\text{SiO}_4$  tetrahedrons and are structural defects of amorphous X-ray material (Fig. 2).

Note that reveal a linear increase in the total volume of pores with increasing specific surface of pyrogenic silica nanoparticles.

## **Kinetics of dispergation and coagulation during annealing on air of silver nanofilms which were deposited onto oxide materials**

Naidich Y.V.<sup>1</sup>, Gab I.I.<sup>1</sup>, Kostyuk B.D.<sup>1</sup>, Stetsyuk T.V.<sup>1</sup>, Dukarov S.V.<sup>2</sup>,  
Kryshtal A.P.<sup>2</sup>, Lytvin O.S.<sup>3</sup>

<sup>1</sup>*Frantsevich Institute for Materials Science Problems of NASU, Kyiv, Ukraine*

<sup>2</sup>*Karazin Kharkov National University, Kharkov, Ukraine*

<sup>3</sup>*Lashkariov Institute physics of semiconductors of NASU, Kiev, Ukraine*

Kinetics of dispergation and the subsequent coagulation during annealing of silver nanofilms 50 – 150 nm thickness which were deposited onto alumina ceramics, sapphire and quartz glass was investigated. The silver films were deposited onto well polished samples of oxide materials (the roughness of samples surface did not exceed 0,05 microns) by electron beam sputtering method. The annealing samples were covered by films was carried out on air inside muffle furnace at temperatures 400 – 900 °C during different time – from 15 s up to 4 h. The annealed samples were investigated by methods of optical, scanning electronic and atomic-power microscopy. As a research result was established that during long annealing (~4 h) silver film of 100 nm thickness was noticeably dispersed already at rather low temperatures (300 – 400 °C). With annealing temperature rising this process was accelerated very much and at 600 °C first indications a film dispergation were occurred already after 15 s, after 2 min the film was disintegrated completely into great number of small solid drops 100 – 200 nm in diameter which at the further annealing started coagulate with forming of bigger drops and, thus, there is a redistribution of quantity of small and bigger drops up to big drops number increasing. Already after 20-minute annealing at 600 °C this redistribution was finished by formation of enough big drops up to 1 mcm in diameter. At temperatures 700 – 900 °C distribution speed considerably raises. Speed of these processes proceedings essentially depends on the film thickness: so the film of 50 nm thickness on sapphire during 5-minute annealing at 600 °C has completely turned into separate round drops, and the film of 150 nm thickness after annealing at the same conditions almost was not changed. Character of processes dispergation-coagulation proceeding of film onto all three oxides was practically identical. Explanations of processes which occur during annealing of silver nanofilms from the point of view of physical and chemical interaction of surfaces of metal film and oxide substrate are given, and also the assumption is stated, that process of coagulation of metal film during annealing can be similar to process of particles sintering in a theory of powder metallurgy and can be described by the same equations.

## **Nanomaterials in the generation and energy storage devices**

Ostafiychuk B.K.

*Vasyl Stefanyk Precarpathian National University, Ivano-Frankivsk, Ukraine*

Modern technologies play a crucial role in the development of society and Ukraine as a member of the European and world community cannot ignore this process. Science and its achievements for technological-information civilization are the main economic and reproductive factors. However, only new technologies and materials can solve the key problems of mankind, among which the main focus is on energy security. It is time to search and implementation of renewable energy sources and to develop new ways for energy accumulation.

These problems are widely investigated today in Ukraine, particularly in Vasyl Stefanyk Precarpathian National University. Scientific and educational centre "Nanomaterials in the generation and energy storage devices", which is supported by the Government of Ukraine and CRDF / USAID, was formed to consolidate the efforts of individual research groups. Activities of the Centre in the field of applied materials are connected with obtaining nanostructured materials, which physical and chemical properties have been modified for use in devices of energy generation and accumulation. In particular, the work on the formation of cathode compositions for lithium power sources based on nanodispersed oxides, hydroxides, sulphide, fluoride and phosphate metal, spinel structures is carried out. The whole technological chain from synthesis of material and to the construction of the model power source has been realizing through comprehensive studies of the structure, morphology, electrical and optical properties of synthesized materials. Application of nanostructured materials allows to use effectively both surface and volume localization position of  $\text{Li}^+$  ions. Thus, there is a need to develop effective methods for obtaining functional materials with preset renewable structural and physical-chemical properties.

Thus comprehensive research of current formation reactions in the electrochemical system and study of all its components interaction have become very important. Key factors that will determine the features of the charge transport kinetics in nanostructured systems compared with bulk samples are such as the small diffusion length of carriers, the effective use of guest positions in the material structure and the absence of a long-run arrangement, leading to reduce the possibility of phase transformations. Great attention is paid to obtaining compounds with defective crystalline and close to amorphous structure and nanocomposites. It was found out that the structure of these cathode materials is more stable during the processes of  $\text{Li}^+$  ions intercalation-deintercalation at discharge-charge due to preventing of new phases formation and the electrode material destruction. High specific surface of material promote



course of heterogeneous intercalation-deintercalation reactions in kinetic mode that allows using such material in power sources with high rates of discharge.

Titanium and silicon dioxides ( $\text{SiO}_2$ ,  $\text{TiO}_2$ ) and composites on their base, oxides and hydroxides of magnesium ( $\text{MgO}$ ,  $\text{Mg}(\text{OH})_2$ ), amorphous  $\text{H}_2\text{TiO}_3$  and  $\text{Ti}(\text{OH})_4$ , iron oxides ( $\alpha\text{-Fe}_2\text{O}_3$ ,  $\gamma\text{-Fe}_2\text{O}_3$ ), tin oxides, iron and magnesium fluorides and their crystalline hydrates are investigated to search for cheap and environmentally safe cathode materials for LPS. The main advantage of the majority of these materials is their low cost, chemical stability and nontoxic. Obtained results about establish the kinetic characteristics of the process of lithium ions intercalation in the nanodispersed hydrated titanium dioxide is an important step toward finding ways to increase energy capacity of lithium power sources and realization the global research purpose – maximal increasing of specific energy performance of electrochemical energy devices and combination of superhigh energy density with highpower with the use of cheap, safe and technologically simple electrode materials.

The main emphasis is put on a comprehensive study of current formation reactions in the electrochemical system. The relationships between physical-chemical characteristics of oxide nanomaterials, conditions of their synthesis and kinetics of electrochemical intercalation of lithium ions process are studied. The optimal conditions for obtaining and modification of nanodispersed materials based on oxides of titanium, silicon, iron are determined that allows to achieve time- and temperature-stable values of specific capacity of lithium power sources primary elements based on them at 600-1000 mA·h / g. Composites of metal oxides / carbon and doped by polyvalent elements (V, Cr, Mn, Fe) titanium oxide are being researched. The influence of synthesis conditions on crystal and electronic structure, phase composition and morphology of nanostructured titanium oxides are being studied complexly.

Problems of cathode materials formations based on heterovalent substituted lithium-iron spinels have been investigated. High stability of spinel structure, the possibility of controlling the formation processes of both cation and anion vacancies and more controlling over the conductive and the dielectric properties of the material by choosing the doping elements and sintering regimes allow to form "frozen" nonequilibrium states in spinel, which alter the kinetics of processes on the surface dividing electrode material / electrolyte. They impede the exothermic processes between them and increase the stability of the electrode at high positive potentials. As a result, the stability characteristics at cycling are increasing, high-speed charge-discharge capabilities are improving and conditions for use of these structures as a cathode material for electrochemical power sources are opening. By modifying their properties we can achieve high values of charge-discharge characteristics. Researches in the field of magnetic nanomaterials are going on and new areas are starting to research such as development of photoelectrochemical energy converters based on dye-sensitized nanodispersed titanium oxide.

Great attention is paid to technological research in the field of nanoporous carbon materials and building on their basis the molecular energy storage - supercapacitors. Activate carbon obtained from raw vegetable and synthetic origin has been used for the production of supercapacitors. The activate carbon from plant material, which has ordered structure, is the most interesting from the scientific point of view. In this case, pore formation at heating is carried out using the bonded water in the original material, which ensures even pore volume distribution and structure of raw materials determines the high (up to 1000 m<sup>2</sup> / g) specific surface area value and the estimated pore size distribution. Using the synthesized activate carbon in the supercapacitors design allows reaching the values of specific capacity 100-110 F / g (for proton electrolyte) and 200-250 F / g (for aprotic electrolytes). Synthesized porous carbon carbon material is used in fundamental studies of the processes occurring at the interface electrode / electrolyte.

## Nanoparticle formation by pulsed laser ablation

Ostafiychuk B.K.<sup>1</sup>, Kotlyarchuk B.K.<sup>1</sup>, Popovych D.I.<sup>2</sup>, Serednytski A.S.<sup>1</sup>

<sup>1</sup>*Vasyl Stefanyk Precarpathian National University, Ivano-Frankivsk, Ukraine*

<sup>2</sup>*Institute of Applied Problems of Mechanics and Mathematics NASU, Lviv, Ukraine*

In this work we present the results of theoretical and experimental researches of reactive pulsed laser ablation (PLA) of metal target. A mathematical model for description of PLA of *Zn* target in oxygen ambient and formation thus nanodroplet fractions is developed. For model construction we used the non-stationary heat transfer equation taking into account the standard enthalpy of formation of *ZnO*. The effect of recoil pressure on the free part of the molten layer of target is described by the Laplace's equation. Modelling the movement of the liquid, taking into account advection on a target surface under the action of the recoil pressure, we use the Navier-Stokes equations. Profile of surface deformation of target after action the laser pulse is calculated, that enable describe character of drops formation from crater edges. The proposed mathematical model describes partial character of nanodrops formation immediately from the crater at synthesis of nanopowders [1].

Experimental researches of processes of PLA have enable to establish that size distribution is defined by duration of the laser pulse and its energy. At high intensity ( $E=3,2-7,8 \text{ J/cm}^2$ ) of laser pulse takes place formation: material of small fraction, because of processes of coagulation and coalescence of cluster in plume; thermally induced fraction of the large particles generated, obviously, ablation of drops directly with crater. Last fraction is characterised by more homogeneous nanostructure and has the regular spherical form. Identified more difficult dependence of distribution of particles quantity from their size and analysed the mechanism of nanogranules formation. Obtained and analysed both x-ray and energy-dispersive characteristics of the synthesized *ZnO* nanostructures. The carried out analysis to establish nonmonotonic of dependence of mass of the received particles from laser pulses frequency and energy. At frequencies ( $n \geq 7 \div 56$ ) total mass of produced particles reaches saturations in process of energy density increase of laser radiation, that is connected with interaction between serial laser pulses and the generated particles up to their partial or full evaporation. The analysis of dependence of mass of produced nanoparticles depending on laser pulses frequency for set energy has shown that optimum laser pulses frequency for effective generation of nanogranules takes place.

1. B.K.Kotlyarchuk, I.F.Myronyuk, D.I.Popovych, A.S.Serednytski. Synthesis of oxide nanopowder material and research of their luminescent properties // *Physics and chemistry of solid state*, – 2006. – V.7, №3. – P. 490-494.

## Surface engineering to enhance hydrophobic/hydrophilic properties of diamond films

Ostrovskaya L.Yu.<sup>1</sup>, Ralchenko V.G.<sup>2</sup>, Bolshakov A.P.<sup>2</sup>, Vlasov I.I.<sup>2</sup>,  
Kulakova I.I.<sup>3</sup>

<sup>1</sup>*Research Center for Studying Surface and Vacuum Properties, Moscow, Russia*

<sup>2</sup>*A.M.Prokhorov General Physics Institute RAS, Moscow, Russia*

<sup>3</sup>*Moscow State University, Moscow, Russia*

Polycrystalline diamond (PCD) films have many valuable properties - high hardness, high thermal conductivity, biocompatibility, chemical inertness, and can be produced by chemical vapor deposition (CVD) on large area. For many applications it is important to fabricate these films with wettability variable in a wide range, ideally from complete wetting to complete unwetting.

Here we present experimental data on wetting and interfacial interaction of diamond films with water, focusing primarily on effects of surface microstructuring (patterning) and surface functionalization. Polycrystalline and nanocrystalline diamond films with grain size ranged from 100  $\mu\text{m}$  to a few nanometers were grown in a microwave plasma on Si substrates. The samples have been characterized with Raman spectroscopy, AFM and SEM.

Effects on water contact angle ( $\theta$ ) of (i) two-dimensional periodical microstructures such as pyramids, holes, pillars; (ii) random nanopores; (iii) surface termination via oxidation, hydrogenation and fluorination have been studied. We have shown a possibility to prepare highly hydrophobic ( $\theta = 124^\circ$ ) and highly hydrophilic ( $\theta = 2-5^\circ$ ) diamond films by combining the surface nanostructuring of diamond with chemical treatment. This range of  $\theta$  variation significantly exceeds that for unstructuring single crystal diamond ( $\theta = 36 - 93^\circ$ ) [1]. The observed wetting behavior can be explained using the Wenzel or Cassie-Baxter models. In addition, the data on wetting of PCD with tin and glycerol will also be given.

The results obtained are important for engineering diamond materials with tailored wettability for a number of applications such as biomedicine, microfluidics and electrochemistry.

1. Ostrovskaya L.Yu., Ralchenko V.G., Bolshakov A.P., Saveliev A.V., Dzbanovsky N.N., Shmegeera S.V. Wettability of ultrananocrystalline diamond and graphite nanowalls films: a comparison with their single crystal analogs // Journal of Nanoscience and Nanotechnology. – 2009. – V.9, №6. – P. 3665-3671.

## **Change of the direction of radiation of heterolaser with quantum dots under the influence of acoustic wave**

Peleshchak R.M., Kuzyk O.V., Dan'kiv O.O., Uhryn Y.O. Kostiv A.M.

*Drohobych Ivan Franko state pedagogical university, Drohobych, Ukraine*

The InAs/GaAs semiconductor heterostructures with InAs quantum dots have a high quantum output of photoluminescence are a perspective material for near-infrared spectral region lasers constructing. Sources of infrared radiation, that can quickly readjust its frequency and direction of radiation, are important elements of high-resolution laser spectroscopy and optical communication systems [1, 2]. The elastic deformations of heterostructure material are an important factor, which influences on the spectral characteristics of heterolaser, particularly the direction of radiation.

A theory of modulation of a heterolaser's radiation direction on quantum dots under the influence of acoustic wave has been developed in this work.

Acoustic wave, which is the source of periodic non-homogeneous elastic deformation, leads to a periodical changes of components of the tensor of dielectric permeability of the heterostructure's material [3]. Thus, acoustic-optic interaction leads not only to change of refraction coefficient with time, but also to its non-homogeneous spatial distribution perpendicularly to the resonator. Therefore the direction of radiation of the heterolaser will be changing with time.

To determine the heterolaser's direction of radiation deviation angle there have been calculated components of tensor of deformation material of the quantum dot and matrix that undergo the influence of an acoustic wave.

It has been established, that the direction of radiation amplitude of the deviation angle depends on the acoustic wave frequency, length of resonator and sizes of quantum dots. The maximum deviation is observed at the moment of time when there is no shift of the radiation frequency.

1. Uchida N. and Niizeki N. // Proc. IEEE. – 1973. – V.61, №8. – P.1073-1092.
2. Suhre D., Taylor L., and Melamed N. // Opt. Eng. – 1992. – V.31, №10. – P. 2118-2123.
3. Kulakova L.A. // Appl. Optics. – 2009. – V.48. – P. 1128–1134.

## **Interdependent dissipative and conservative self-organization in self-assembly of low-dimensional 3D systems**

Perekrestov V.I.<sup>1</sup>, Kshnyakin V.S.<sup>2</sup>

<sup>1</sup>*Sumy State University, Sumy, Ukraine,*

<sup>2</sup>*Sumy State A.S.Makarenko Pedagogical University, Sumy, Ukraine*

The work presented deals with the self-assembly mechanisms of low-dimensional porous systems of Al, Ti, Cu, Ni, Si and C by means of interdependent dissipative and conservative self-organization. On the first stage of technological process dissipative self-organization of critically low steady-state supersaturations in the accumulative plasma-condensate systems (APCS) [1] takes place. The main physical principles of this self-organization are determined by self-consistent changes in nonlinearly interdependent temperature of the growth surface, supersaturation and depositing flux. When approaching the steady-state mode of APCS operation, a volume selected near the growth surface can be considered as a conservative system in first approximation. Meanwhile, the conservative self-assembly of low-dimensional 3D systems is determined by free energy minimization.

Three main problems are solved in the work. First, the mathematical model of self-organization of critically low steady-state supersaturations is considered. Second, the mathematical models are developed describing self-assembly of developed surfaces of amorphous Si condensate and highly porous Al structure. The models are based on field selectivity and Gibbs-Thomson effect which in total determine changes of the chemical potential difference in different places of the growth surface. And in the third place, the extensive experimental material is obtained that confirms the mathematical models developed. Structure and morphology of condensates were studied by scanning and transmission electron microscopy, high energy electron and X-ray diffraction as well.

Systematizing experimental and theoretical material, we conclude that

- a) formation of low-dimensional 3D systems is caused by spatially distributed selectivity of adatoms attaching to the active centres of the growth surface which appear and disappear during the whole technological process;
- b) habitus of crystals, being composite elements of low-dimensional 3D structures, are determined by extreme minimization of free energy.

1. V.I.Perekrestov, A.I.Olemskoi, Yu.O.Kosminska, A.A.Mokrenko // Phys. Lett. A. - 2009. - №373. – P. 3386.

## Numerical simulation of nanoplasmonic antireflection coatings for solar cells

Anders Pors<sup>1</sup>, Alexander V. Uskov<sup>1,2,3</sup>, Morten Willatzen<sup>1</sup>,  
Igor E. Protsenko<sup>2,3</sup>

<sup>1</sup>Mads Clausen Institute (MCI), University of Southern Denmark, Sønderborg, Denmark

<sup>2</sup>P. N. Lebedev Physical Institute, Moscow, Russia

<sup>3</sup>Plasmonics LTD, Moscow, Russia

Application of nanoplasmonics in photovoltaics attracts much attention at present [1-2]. The main idea behind *nanoplasmonic photovoltaics* is to use plasmonic nanoparticles as *nanoantennas* in order to improve coupling of incident light into solar cells.

We have modelled the input efficiency of photons into solar cells due to plasmonic nanoparticles. Fig.1 shows the spectrum of the efficiency for various densities of gold nanoparticles placed on silicon surface. At low nanoparticle densities, the efficiency grows linearly with the density. With increasing nanoparticle densities when collective effects in the nanoparticle ensemble become important, the efficiency reaches its maximum. This maximum can achieve values up to 95%.

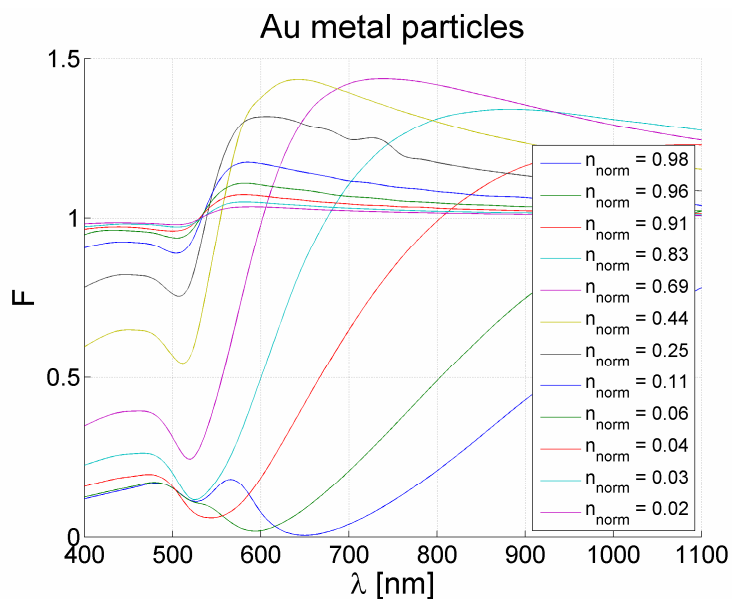


Fig. 1.

We have further modeled nanoplasmonic coatings with aluminum particles and found that aluminum provides superior characteristics as compared to gold for silicon solar cells. In actual fact, aluminum nanoplasmonic coatings can provide a solar cell performance improvement by factor 1.5–2.

1. Catchpole K.P. and Polman A. Plasmonic solar cells // Opt. Express. – 2008. – V.16, №26. – P. 21793-21800.
2. Atwater H.A., Polman A. Plasmonics for improvement photovoltaic devices // Nature Materials.–2010.–V. 9, № 3.– P. 205-213.

## **Strain deformation properties of film materials: the problem, achievements and prospects of investigations**

Protsenko I. Yu., Tyschenko K. V.

*Sumy State University, Sumy, Ukraine*

Generalized experimental and theoretical results on strain deformation effect in single and multilayered film materials. Analyzed known classical semiphenomenological and phenomenological theoretical models [1] that are not always satisfactory agreement with experimental results. Shown that better correspondent can be achieved by considering the deformation depends not only mean free path but also the specular parameter of the external surfaces of films and transmission coefficient of grain boundaries and interfaces.

The experimental results of strain deformation effect on range elastic and plastic deformation of single and multilayer films (see, for example, [2]) on substrates that are deformed elastically (the case of film systems based on Fe and Cr; Cu and Cr or Fe and Pd (Pt) on polystyrene (PI) were presented. The results of similar investigates on the example of film system Fe/a-Gd/PI, in which amorphous Gd film plastically deformed. It causes certain features of strain deformation effect, which analyzed in detail. It was concluded that a fundamental aspect of the problem of strain deformation effect might be related magnetodeformation effect because it can be similar to the effect of GMR. Applied aspect should be connected [3] to the research of heterogeneous film systems and nanotubes where are experiencing strain deformation coefficient order 10 or  $10^3$  units, respectively.

This work is done in frame of the theme № 0109U001387.

1. Дехтярук Л.В., Проценко І.Ю., Чорноус А.М. Транспортні розмірні ефекти у двошарових полікристалічних плівках // *Успехи физ. мет.* – 2007. – Т.8, №1. – С. 2-64.
2. Buryk I.P., Velykodnyi D.V., Odnodvoretz L.V., Protsenko I.E., Tkach E.P. Tensorresistive effect in thin metal films in the range of elastic and plastic strain // *Technical Physics.* – 2011. – V.56, №2. – P. 232-237.
3. Однодворець Л.В., Проценко С.І., Чорноус А.М., Проценко І.Ю. Ефект тензочутливості в металевих плівкових матеріалах // *Успехи физ. мет.* – 2007. – Т.8, №2. – С. 109-156.



## Physical processes in multilayer films and spin-valve structures

Protsenko S.I.

*Sumy State University, Sumy, Ukraine*

In work the possible physical processes which connected with the kinetics and dynamics of the motion electrons and phase transitions in multilayer film systems and the spin-valve structures based on nanodimension films of Co and Cu (Ag, Au) or Fe and Cr(Cu). Among these processes we included the processes of mutual diffusion of atoms, which cause the formation of solid solutions with unlimited (film systems based on Fe and Cr or Co and Cu) or limited solubility (systems based on Co and Ag(Au) or Fe and Cu) atoms, and processes of electron scattering on grain boundaries, interfaces and magnetic moments of Co grains or domains of solid solutions (see, for example, [1, 2]).

Based on the experimental results [3, 4] also analyzed the influence of longitudinal strain and magnetic field on strain deformation effect, magnetoresistance (MR) at three of its geometry measurement and giant magnetic resistance. The proposed phenomenological model of magnetodeformation effect [5], the essence of which is depending on the strain deformation coefficiente of magnetic field. This effect, as MR, may be anisotropic character. Shown that accounting depends parameters of carried (speculary parameter and coefficion transition at the grain boundaries and interfaces) to better correspondence experimental and calculated based on the results of the developed models.

Effective spin-valve structure [6] based on nanoscale films of Co, Cu (Au) and Cr has been proposed and investigated by method МОКЕ its magnetic characteristics.

1. Проценко С.І., Чешко І.В., Однодворець Л.В., Пазуха І.М. Структура, дифузійні процеси і магніторезистивні та електрофізичні властивості плівкових матеріалів: Монографія / За загальною ред. проф. Проценка І.Ю. – Суми: СумДУ, – 2008. – 197 с.
2. Проценко С.І., Чешко І.В., Великодний Д.В., Пазуха І.М., Однодворець Л.В., Проценко І.Ю., Синашенко О.В. Структурно-фазовий стан, стабільність інтерфейсів та електрофізичні властивості двошарових плівкових систем // Успехи физ. мет. – 2007.– Т.8, №4. – С. 247-278.
3. Сынашенко О.В., Ткач Е.П., Бурык И.П., Однодворец Л.В., Проценко С.И., Шумакова Н.И. Магниторезистивные свойства многослойных наноразмерных пленочных систем // ВАНТ. Серия: Вакуум, чистые материалы, сверхпроводники. – 2009. – №6, Вып.18. – С. 169–174.
4. Ткач О.П., Однодворець Л.В., Непійко С.О., Проценко С.І. Магніторезистивні властивості нанорозмірних плівкових систем на основі Fe і Pd. – 2009. – Т.7, №3. – С. 256–61.
5. Проценко С.І. Магнітодеформаційний ефект у тонких металевих плівках // Ж. нано- та електрон. фіз.- 2009. – Т.1, №2. – С. 7–10.
6. Cheshko I.V., Protsenko S.I., Odnodvoret L.V., Shifalovich P. Magneto-optical and magnetoresistivity properties of Co/Cu(Au)-based spin-valve structure // Tech. Phys. Lett. – 2009. – V.35, №10. – P. 903-905.

## Gas sensors on p-n junctions: problems and prospects

Ptashchenko O.O.<sup>1</sup>, Ptashchenko F.O.<sup>2</sup>

<sup>1</sup>*I.I. Mechnikov National University of Odessa, Odessa, Ukraine*

<sup>2</sup>*Odessa National Maritime Academy, Odessa, Ukraine*

The influence of ammonia, water and ethanol vapors on stationary  $I$ - $V$  characteristics and kinetics of surface currents in GaAs, GaP, GaAsP, AlGaAs, GaN, GaInN, and Si  $p$ - $n$  junctions was studied. A two-dimensional calculations of non-equilibrium processes in  $p$ - $n$  junctions due to adsorption of electrically-active molecules were performed.

It is established, that the gas sensors on  $p$ - $n$  junctions have significant advantages over sensors with polycrystalline structure, as well as sensors with Schottky barrier. Gas sensitivity of sensors on  $p$ - $n$  junctions is due to physical rather than chemical adsorption of molecules. An evidence of this is a small decay time of the signal (<100 s) after removal of the studied vapors from the container with the  $p$ - $n$  junction. Such sensors operate at room temperature and do not require special heating. On the surface current in  $p$ - $n$  junctions affect those molecules that are donors or acceptors in the semiconductor. Therefore, these sensors are selective, i.e. their sensitivity to different gases is different. Thus, the sensitivity of studied sensors on silicon  $p$ - $n$  junctions to ammonia vapors is 1000 times higher than to ethanol vapors and about 2000 times higher than to water vapors. The electronic mechanism of gas sensitivity causes a short response time of sensors and opens possibilities of its reduction. A high barrier for electrons and holes in the  $p$ - $n$  junction causes low background current, which leads to a high relative sensitivity of gas sensors. Modern  $p$ - $n$  junction technologies have a high reproducibility that enables to produce the sensors with fixed parameters.

Over the current range 10nA – 1mA the  $I$ - $V$  characteristics of the direct current of  $p$ - $n$  junctions, measured in dry air, can be described with the expression

$$I(V) = I_0 \exp(qV / n_i kT), \quad (1)$$

where  $I_0$  is a constant;  $q$  denotes the electron charge;  $k$  is the Boltzmann constant,  $T$  is temperature;  $n \approx 2$  is the ideality coefficient. Such  $I$ - $V$  characteristics are related to the recombination at deep levels in the depletion layer and at the surface. Adsorption of  $\text{NH}_3$  molecules significantly increased the direct and reverse currents.

For the calculations of non-equilibrium processes in  $p$ - $n$  junctions in the presence of donor gas was used a scheme, shown in Fig. 1. It is established that the threshold of the gas sensor sensitivity is defined by the equation

$$N_{it} = N_f + N_s + N_a - N_d^+, \quad (2)$$

where  $N_{it}$  is the threshold density of adsorbed ions;  $N_f$ ,  $N_s$ ,  $N_d^+$  and  $N_a$  are, accordingly, surface densities of fast and slow centers, ionized donors and acceptors in the surface depleted layer in  $p$  region. Relation (2) shows that the sensitivity threshold can be reduced by surface doping of the  $p-n$  structure with donors.

It is experimentally shown that surface doping with sulphur atoms strongly reduces the sensitivity threshold and increases the sensitivity of GaAs  $p-n$  junctions to ammonia and water vapors.

A negative sensitivity of silicon  $p-n$  junctions, i.e. a reduction of surface current in ammonia vapors is observed, which can be explained with presence of acceptor centers on the  $n$ -region surface.

Some specific mechanisms of the internal signal amplification are realized in sensors on  $p-n$  junctions.

The main drawback of sensors on  $p-n$  junctions is a slow signal drift during prolonged exposure to adsorbed vapors. The basic mechanism of the

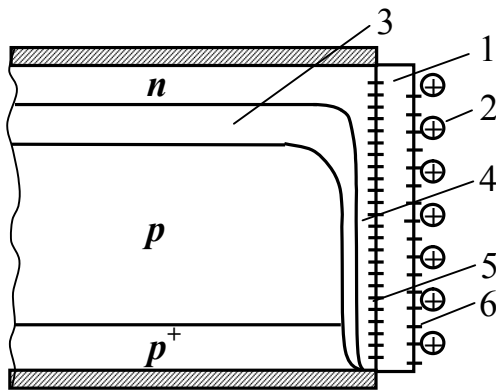


Fig. 1. Schematic of the  $p-n$  structure in a donor gas: 1 – oxide layer; 2 – ions; 3 – depletion layer; 4 – conductive channel; 5 – surface (fast) centers; 6 – centers on the oxide surface (slow centers).

surface current drift is recharging of slow centers, located on the outer oxide layer surface. It is experimentally shown that reducing of the oxide layer thickness, improving its structure and replacing of the oxide with another dielectric layer leads to an increase in sensitivity and reduces the signal drift.

Sensors on  $p-n$  junctions, especially of silicon, are technologically compatible with microelectronic amplifying elements. This allows fabricate gas sensors and amplifying elements in one technological cycle in a single crystal.

The effect of ammonia and water vapors is studied on forward and reverse emitter-collector, base-collector and emitter-base currents, as well on the kinetics of the corresponding currents in

silicon transistors. The gas sensitivity of transistors is found much higher than the sensitivity of single silicon  $p-n$  junctions. This effect is due to formation of a surface conductive channel, which shorts the base-collector junction. Such a channel in the emitter-base junction reduces the gas sensitivity at low bias voltages. The sensitivity of silicon transistors to ammonia vapors is much higher than to water vapors. The response time of transistor sensors at room temperature is  $\sim 100$ s.

## Formation of needle-like crystal inclusions SbSI in the bulk and film glassy matrix

Rubish V.M.<sup>1</sup>, Guranich O.G.<sup>1</sup>, Gorina O.V.<sup>1</sup>, Rigan M.Yu.<sup>1</sup>, Gera E.V.<sup>1</sup>,  
Guranich P.P.<sup>2</sup>, Azhniuk Yu.M.<sup>3</sup>, Gomonnai A.V.<sup>3</sup>

<sup>1</sup>*Uzhgorod Scientific-Technological Center of the Institute for  
Information Recording, NASU, Uzhgorod Ukraine*

<sup>2</sup>*Uzhgorod National University, Uzhgorod, Ukraine*

<sup>3</sup>*Institute of Electron Physics, NASU, Uzhgorod, Ukraine*

The present paper is devoted to investigation conditions of forming nano- and microsize crystal inclusions SbSI (SbSI (antimony sulphoiodide) – is a well-known ferroelectric-semiconductor) in the bulk and film glassy matrix on the basis of  $(As_2S_3)_{100-x}(SbSI)_x$  glasses.

$(As_2S_3)_{100-x}(SbSI)_x$  ( $x=55, 60, 70, 80, 90$ ) glasses were prepared by vacuum melting of the corresponding mixture of SbSI and  $As_2S_3$  components in quartz ampoules. The homogenization temperature and time were 800-850 K and 24 h, respectively. Cooling of melts was carried out in the air ( $x=55, 60, 70$ ) and into cold (273 K) water ( $x=80, 90$ ).

Thin films ( $d=1-2 \mu\text{m}$ ) were deposited by vacuum thermal evaporation of  $(As_2S_3)_{100-x}(SbSI)_x$  glasses from quasiclosed effusive cells on cool silica substrates. A uniform thickness of layers was provided by planetary rotation of substrates.

Raman spectra were investigated with the help of DFS-24 spectrometer on the  $\lambda=0,63 \mu\text{m}$ . Investigations of X-ray diffraction patterns of glassy, crystallized and crystalline materials were carried out on «ДРОН-3» X-ray apparatus ( $\lambda=1.5418 \text{ \AA}$ ).

It was established that in conditions of continuous heating in the region  $T_g-T_c$  (glass forming and crystallization temperature, respectively) or isothermal annealing in the same temperature region, formation needle-like nanocrystals SbSI in  $(As_2S_3)_{100-x}(SbSI)_x$  bulk and film glassy matrix occurs with their further growing. Reflexes coinciding with lines for polycrystal SbSI appear on X-ray diffraction patterns of crystallized glasses. Raman spectra of crystallized glasses contain sharp bands at 107-110, 138-140 and 316-320  $\text{cm}^{-1}$ . For polycrystalline SbSI, the maxima of these bands are at 108, 138 and 318  $\text{cm}^{-1}$ . The mechanism of formation of nanocrystals SbSI in glassy matrix is discussed.

It is shown that with annealing temperature and time raising, the intensity of bands in Raman spectra and reflexes on X-ray diffraction patterns is growing while their half-width is decreasing. It testifies to growing of sizes of crystalline inclusions on glassy matrix.

The investigation results of influence of electric field and laser irradiation on the sizes and orientation of needle-like crystal inclusions of SbSI in glassy matrix have been adduced.

## Epitaxial IV-VI quantum dots for mid-infrared devices

Schwarzl T.<sup>1</sup>, Eibelhuber M.<sup>1</sup>, Hochreiner A.<sup>1</sup>, Groiss H.<sup>1</sup>, Kolkovsky V.<sup>2</sup>,  
Karczewski G.<sup>2</sup>, Wojtowicz T.<sup>2</sup>, Heiss W.<sup>1</sup>, Springholz G.<sup>1</sup>

<sup>1</sup>*Institute of Semiconductor Physics, University of Linz, Austria*

<sup>2</sup>*Polish Academy of Sciences, Warszawa, Poland*

Lead salts have long been used for mid-infrared (MIR) light sources. In particular, the wide wavelength tunability of IV-VI lasers make them well suited for spectroscopy applications. The symmetric band structure and small non-radiative Auger recombination rates provide excellent perspectives for realization of long wavelength lasers with high operation temperatures. For optically pumped microdisk lasers with strong vertical and lateral optical confinement, we have recently demonstrated continuous-wave laser emission at 4.3  $\mu\text{m}$  wavelength up to temperatures as high as 0 °C [1]. This represents the highest cw operation temperature for all interband lasers in this wavelength region.

For further improvements, quantum dots (QDs) as active regions are highly desirable. However, conventional IV-VI Stranski-Krastanow QDs only exhibit weak luminescence due to strain-induced type-II band alignment [2]. As an alternative, we have developed a novel fabrication method for epitaxial PbTe QDs embedded in CdTe matrices [3]. CdTe and PbTe are practically lattice-matched but exhibit a different lattice structure. Therefore, these MBE grown dots are produced by phase separation rather than by lattice-mismatch strain. As shown by Fig. 1, the resulting QDs exhibit almost spherical shapes with abrupt interfaces as well as intense continuous-wave photoluminescence (PL) at room temperature [3, 4]. The emission wavelength of the dots can be tuned by adjusting the dot size, which can be achieved by either changing the amount of deposited PbTe [3, 4] or by varying the growth temperature.

In this work, the structural and optical properties [3, 4] of this unique QD system are described in detail and the first MIR devices are presented. In particular, we show cw QD light emitting diodes (LEDs) operating up to 300 K [5] as well as cw optically pumped QD lasing up to 200 K. For the latter, PbTe/CdTe microdisks were fabricated by photolithography and wet chemical etching. A SEM image of a single microdisk is shown in Fig. 2(d). The QD microdisks were optically pumped at 1064 nm below the CdTe band gap, resulting in cw laser emission at around 3.7  $\mu\text{m}$  wavelength up to temperatures as high as 200 K (Fig. 2(a)). The laser intensity at 200 K as a function of the pump power is depicted in Fig. 2(b) and exhibits a clear laser threshold. This not only represents the first QD laser emitting at wavelengths longer than 2  $\mu\text{m}$  but also further improvements in device structure and processing seem to make room temperature operation feasible.

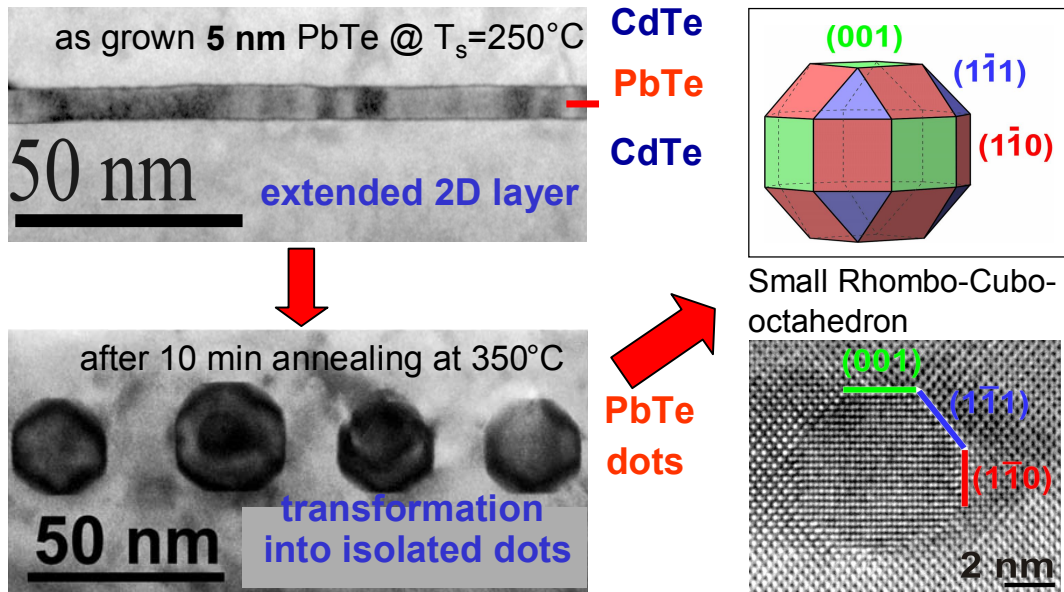
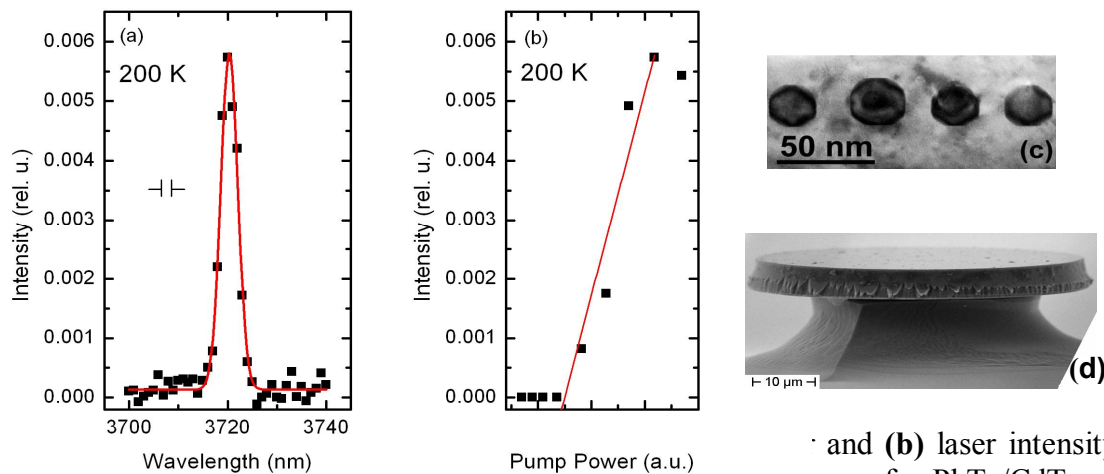


**Fig. 1: (left)** Cross-sectional TEM images illustrating the formation process of PbTe quantum dots in CdTe by phase separation and interface minimization. In our MBE growth scheme, a low-temperature grown 2D PbTe layer embedded in CdTe is subjected to post growth annealing, which transforms the layer into highly symmetric isolated PbTe dots without a connecting wetting layer. Thus, the formation of QDs is not driven by strain but by the immiscibility of layer materials. **(right)** The quantum dots show the shape of small rhombo-cubo-octahedrons with atomically sharp interfaces as proven by the high resolution TEM image.



and **(b)** laser intensity versus age of a PbTe/CdTe reference sample as in the active region. **(d)** SEM image of a typical CdTe microdisk structure with 40 μm diameter and a single active PbTe dot layer in the center of the CdTe waveguide. The undercut in the GaAs substrate is achieved by selective isotropic wet chemical etching and provides an effective mode confinement.

1. M.Eibelhuber et al. Appl. Phys. Lett. **97**, 061103 (2010)
2. M. Simma et al., Appl. Phys. Lett. **88**, 201105 (2006)
3. W. Heiss et al., Appl. Phys. Lett. **88**, 192109 (2006); H. Groiss, et al., APL **91**, 222106 (2007)
4. T. Schwarzl et al., Phys. Rev. B **78**, 165320 (2008)
5. Hochreiner et al., Appl. Phys. Lett. **98**, 021106 (2011)

## The influence of thickness of solid metallic nanofilm on its physico-chemical properties

Shirinyan A.S.<sup>1</sup>, Bilogorodskyy Y.S.<sup>2</sup>

<sup>1</sup>*Kiev Taras Shevchenko National University, Kiev, Ukraine*

<sup>2</sup>*Cherkasy B. Khmelnytsky National University, Cherkasy, Ukraine*

The behaviour of the thin films changes when their thickness becomes nanometric one [1]. The dependence of pair potentials of atomic interactions on the size of a nanosystem is substantiated for the case of thin films. In most experimental cases the lattice parameter can be presented as the function of the thickness of the film in the form:  $a(h) = a_{\infty}(1 + b/h)$ , where  $a_{\infty}$  – asymptotic value,  $b$  – the fitting parameter,  $h$  – the thickness. Such result allows one to write the size-dependent potential energy of atomic interaction. For example, for the fcc metals described due to Morse potentials one can write energy of interaction in the first coordination sphere in the following form:

$$\Phi(h) = D \left( \exp \left\{ -\frac{2\alpha \cdot a_{\infty}}{\sqrt{2}} \left( 1 - \frac{r_0\sqrt{2}}{a_{\infty}} + \frac{b}{h} \right) \right\} - 2 \exp \left\{ -\frac{2\alpha \cdot a_{\infty}}{\sqrt{2}} \left( 1 - \frac{r_0\sqrt{2}}{a_{\infty}} + \frac{b}{h} \right) \right\} \right).$$

Here  $D = |U(r_0)|$  and  $\alpha$  – the parameters of energy of dissociation and degree of anharmonicity, correspondingly;  $r_0$  – the equilibrium distance between two atoms.

We introduce the new methodology of nanophase diagram construction due to size-dependent pair potentials [2]. The formation of nanophases in thin films is considered on Bi-Sn system and the size dependence of transition temperatures and limit solubilities of the components are outlined.

Work is partially supported by the Ministry of Education and Science in the framework of the grant of Cabinet of Ministers of Ukraine for young scientists: award dated 11 October 2010.

1. Шірінян А.С., Макара В.А. Актуальні проблеми наноматеріалів і нанотехнологій // Наносистеми, наноматеріали, нанотехнології. – 2010. – Т.8. №. 2. – С. 223-269.
2. Ширинян А.С., Белогородский Ю.С. Построение фазовой диаграммы сплошных нанопленок Bi-Sn с помощью модели зависимости потенциалов атомного взаимодействия от размера системы // Металлофизика и Новейшие Технологии. – 2010. – Т. 32. №. 11. – С. 1493-1508.

## **Physics of thin films: theoretical basis of big science on nanomaterials**

Shpilevsky E.M.

*A.V. Luikov Heat and Mass Transfer Institute of NAS of Belarus, Minsk, Belarus*

Nanomaterials are the most rapidly growing and the most promising area of modern materials. The speech of R.F. Feynman (Nobel Laureate 1965), in 1959 with public lecture "There's a lot of whole at the bottom" is often considered at the day of birth of the science of nanomaterials. It is more correctly to regard J.J. Thomson (Nobel Laureate 1906) as the founder of study of nanomaterials, because in 1901 he first established the dependence of resistivity of metal films on their thickness [1].

The most important feature of nanostructures is the fact, that the size is of both the kinetic and thermodynamic parameter of the properties. Just in the thin films the size effects were found (both classical and quantum size effects). From the variety of nanostructures (zero-, one-, two-, three-dimensional) the thin films are the most studied. The accumulated theoretical and empirical luggage is impressive. The features of well-known physical effects (Hall, Gause, Seebeck, other galvanomagnetic, tenzoelectric, thermoelectric effects) were first discovered on the investigation of thin film samples. It should be emphasized that the matter is not in a priority. It is important, that the experience and findings of the world scientific community of last six decades will not be rejected.

The study of the properties of ferromagnetic films in the 20 – 30-th years led to the creation of magnetic recording media. Further studies of the properties of metal films led to the arising of the new branch of industry - microelectronics. The changing of the solubility limits and the melting points of metal films from their thickness have been found both theoretically and experimentally at the work of 50-60-th years. The dependence of the diffusion characteristics by the film thickness and the features of the generating and the growth of the phases were revealed in articles of 60-70-th years. It should be noted the significant contribution of Soviet scientists, especially of Moscow, Kharkov, Minsk, Novosibirsk scientific schools.

The effect of giant magnetoresistance (Nobel Prize 2007), which differs from the Gause effect by its value, sign and by the mechanism of dispersion of charge carriers, as well as the effect of the plasmon resonance absorption observed on the metal nonoparticles have been identified and studied in thin continuous and island films.

Vigorous impulse to the development of nanostructured materials was got after the discovery of carbon nanoparticles - fullerenes and carbon nanotubes. The metals, which are modified by carbon nanoparticles (fullerenes and carbon nanotubes) have a unique frequency dependence of electrical properties [2]. At



specific ratios of components fullerenes act not only as components of composite materials, but also as agents of chemical reactions to obtain new substances. For example, the compounds  $Me_xC_{60}$  for copper and tin are obtained[3].

The metals which are doped by fullerenes and carbon nanotubes exhibit the increasing strength and electrical resistance that is associated with nanoscale structures and the emergence of significant mechanical stresses and lattice distortions. For these materials the decrease in the friction coefficient and the increase durability are observed. Unusual properties have ceramics and ferromagnetic materials doped by fullerenes and carbon nanotubes [4].

New approaches in the development of nanomaterials have provided the studies of size effects, the processes of molecular self-organization in conjunction with chemical reactions, as well as the interactions in ensembles of nanoparticles. At the report the recent advances and problems in the investigations and production of nanostructured materials will be discussed.

At the title of the report the term "big science of nanomaterials", is used premeditatedly as a protest against the calked translation of foreign word "nanoscience". In Russian, "nanoscience" sounds like a very small science. Russian-language perception of "nanoscience" implies "nanoscientists", "nanoideis" and "nanoresults", which belong to "nanoscience". The term "nanoscience" should be considered as the Russian-speaking jargon and it is not correct to use such term among the educated people of the scientific community.

The range of applications of nanostructured materials is wide - this is the unique coatings (hardening, anticorrosion, antifriction, light protectional), optoelectronic devices (sensors, emitters, photodetectors, photoresisters, waveguides, heating elements), biomedical products (implants, containers for the targeted delivery of drugs in the body, molecular filters, membranes), medicines. Created nanomaterials allow now to put the question about the wide introduction their into practice.

1. Thomson J.J. On the theory of electrical conduction throught thin metallic films. Proc. Cambridge Pil. Soc. – 1901. – №11. – P. 120-122.
2. Shpilevsky M. É., Shpilevsky É. M., Stel'makh V. F. Fullerenes and fullerene-like structures: the basis for promising materials // Journal of Engineering Physics and Thermophysics. – 2001. – V.74. №6. – P. 1499-1508.
3. Baran L.V., Shpilevsky É. M., Okatova G.P. Phase composition and structure of films of Cu-C60, subjected to ion and thermal stresses. // Perspektivnyye materialy – 2004 – № 4 – P. 76-81 (in Rus).
4. Shpilevsky E.M., Zhdanok S.A., Schur D.V. Containing carbon nanoparticles materials in hydrogen energy // Hydrogen Materials Science and Chemistry of Carbon Nanostructures. II. Mathematics, Physics and Chemistry. NATO Science Series. Dordcht/Boston/London: Kluwer Academic Publishers, – 2010. – V.181. – P. 21-36.

## Photoelectric properties of metal-semi-insulating CdTe barrier structures

Sklyarchuk V. M., Sklyarchuk O.V., Rarenko I.M., Dremlyuzhenko S.G.

*Yuriy Fedkoivych Chernivtsi National University, Chernivtsi, Ukraine*

CdTe - a promising material for the detectors of X- and  $\gamma$ -radiation, which could be used without cryogenic cooling. The high atomic number ensures effective absorption of  $\gamma$ -rays, and due to the wide band gap (1,47-1,48 eV at room temperature) detector dark currents is small at high applied voltages, especially for the semi-insulating material, whose conductivity is close to the intrinsic. Using the Schottky barrier diode structure creates favorable conditions for the effective carrier collection. The width of the space-charge region is very important parameter for optimal use of the diode as a detector of X- and  $\gamma$ -radiation. This depletion layer, in which the electric field is localized, determines the efficiency and energy resolution of the detector. Traditional evaluation of the space-charge region thickness by capacity measurements is almost impossible in so high-resistance semiconductor. We study the photosensitivity spectrum of diode to evaluate the space charge region thickness

Ni-CdTe Schottky diodes were fabricated using high-resistance ( $4\cdot 6\cdot 10^9 \Omega\text{cm}$  at 297K) p-CdTe, produced by Acrorad Corporation, Japan. Both ohmic and Schottky contacts were deposited by vacuum evaporation of semitransparent thin (10-20 nm) Ni film on the crystal surface pre-treated by Ar ion etching. The reverse current was equal  $10^{-11}\text{-}10^{-12}$  A at  $V=1$  V and  $2\text{-}3\cdot 10^{-9}$  A at  $V=1000$  V; photoelectromotive force - 0,25-0,45 V. Investigated diodes exhibited photosensitivity under illumination from both the rectifying and ohmic contacts. It suggests the active region of detector is wide (with crystal thickness 0,5 mm and diffusion length for this semiconductor material 0.1 mm, space-charge region width is about 0.4 mm). Spectral dependence of the photoelectric quantum yields, calculated taking into account the distribution of electric field in the semiconductor bulk, diffusion and drift currents and surface recombination at both contacts, are in good agreement with experimental results.

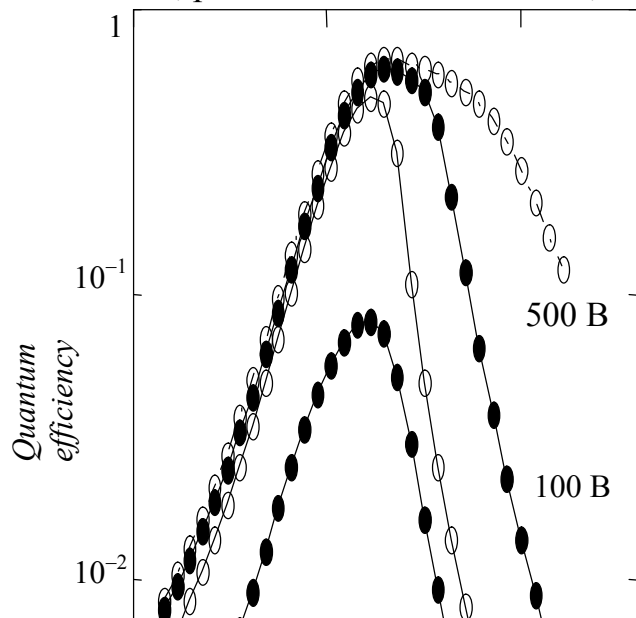
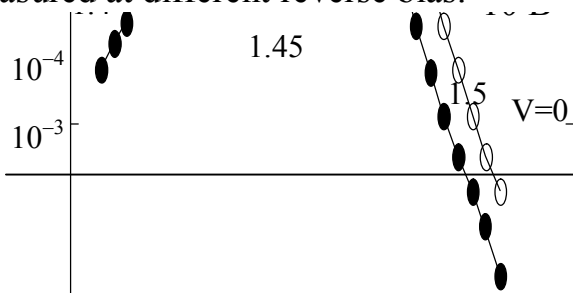


Fig.1. Spectral dependences of the photoelectric external quantum yield measured at different reverse bias.



## Quantum electron transport in ultra thin metal films.

Stasyuk Z.V., Bihun R.I.

*Ivan Franco Lviv national university, Lviv, Ukraine*

Thin layers of substance are basic elements of many devices of modern electronic techniques. The further development of electronics is impossible without microminiaturisation of electronic systems by nanotechnology, in particular, by techniques of electrically stable ultrathin-thickness covering formation. Properties of ultrathin slabs can essentially differ from properties concerning thick layers which are used in nowadays engineering. This difference first of all is caused by prevailing influence of the surface phenomena on ultrathin layer structure and electric parameters.

The current theoretical and experimental researches on electron charge transport in ultrathin (layer thickness are 2-12 nm) electrically continuous metal films (temperature coefficient of resistance  $\beta > 0$ ) under the condition of inequality realisation  $d < l$  were analysed and reviewed. Here  $d$  is the film thickness,  $l$  is the charge mean free path. The peculiarities of film structure are meant as crystal lattice parameters and the crystalline average linear sizes.

The fabrication of ultrathin electrically continuous metal film on dielectric substrate surface is a problem of considerable difficulty due to the action of surface tension forces. These phenomena lead to coagulation of metal particles. As a result there is some critical thickness layer  $d_c$  at which current starts to flows (percolation threshold is observed here). The technological features of film formation (the speed of material condensation, the substrate temperature at layer deposition, the modes of further heat treatment) defines the average of  $d_c$  as well as the properties of condensate material, in particular fusion temperature. Essential decrease  $d_c$  may be reached at epitaxial growth of metal film on the oriented substrate. The other effective way of  $d_c$  decrease is preliminary deposition of surfactant underlayers of superficially active substances of a subatom thickness on dielectric substrate with precluding coagulation of metal condensates. This technique allowed the formation of ultrathin conductive coverings. In particular, the Hall voltage investigation on 1-3 nm thickness chrome films deposited on surfactant germanium underlayer was performed in [1].

The electron transport phenomena are essentially influenced by electron scattering on film surface when the mean free path of electron becomes commensurable to the thickness of a metal film  $d$ . Thus the contribution of surface scattering in the total electron relaxation time is close to the contribution of bulk scattering. The thickness dependence of kinetic parameters of electrically continuous metal films is described within the framework of the classical and internal size effect theories [2].

With further reduction of metal layer thickness when the electron mean free path satisfies the condition  $d < l$ , the quasiballistic electron transport in a film (without changes of the power spectrum of electron in metal film) is presented. Thus charge carriers surface scattering in metal film becomes dominating. The

contribution of surface scattering has essentially influenced the macroscopic surface inhomogeneity because the mean linear grain sizes are commensurable to film thickness. The quasiballistic electron transport in metal films can be described by size dependencies of kinetic coefficients proposed in Namba theory and within the framework of polycrystalline layer heterogeneous cross section [2]. The treatment of experimental data by the mentioned theories allows the reliable calculation of the average amplitude of one-dimensional surface asperity  $h$ . The calculated values  $h$  well coordinate with experimental data of direct STM and AFM investigation.

When the film thickness does not exceed 5 - 8 nm the quantum effects which have influence on electron transport in film are possible. Existence of changes in the transport phenomena caused by dimensional quantization was predicted by I.M.Lifshitz and A.N.Kosevich [3]. Quantum size effects are most brightly displayed in semimetal films. The length of an electron de-Broglie wave length in these materials in 10 times exceeds interatomic distances and consequently the interference of electronic waves is influenced poorly by imperfections of film surface. In metal films the situation is essentially different as a de Broglie electron wave length is commensurable to interatomic distances. Therefore, to observe oscillation of the kinetic coefficients in thin metals layers it is necessary to provide high perfection surface structure. In the quantum electron transport range of films thickness the laws of residual conductivity size dependens  $\sigma_{res}=1/[\rho(d)-\rho_{\infty}]$  takes place. The theoretical expressions are most convenient for direct experimental comparison with theoretical data has been received by Fishman and Calecki [4]:

$$\sigma_{res} \sim d^2 \left\{ 1 - \frac{6}{(3n\pi^5)^{2/3}} \frac{1}{d} \right\},$$

where  $n$  - is the current carriers concentration,  $d$  - is the film thickness. This expression may be transformed to:  $\sigma_{res} \sim d^{\alpha}$ , where  $\alpha$  are changing from 2,1 (pure metals) to 6 (semiconductors).

Modern theoretical approaches of quantum size effect in kinetic phenomena of metal films are based on assumption that the metal sample electronic structure is the same as in bulk materials. Quantum size effect in metal film is a consequence of electron system size limitation along  $Z$  axis in thin film thickness direction. Calculation of the electron band structure of metal film by various theoretical approaches well known in literature shows major distinction in electron structure parameters computed data. Therefore, it is very difficult to establish the precise criteria of quantum size effect models application region.

1. Schroder K., Zhang L. // Phys. Stat. Sol. B. – 1994. – V.183. – P. k5-k8.
10. Стасюк З.В., Лопатинський А.І. // ФХТТ. – 2001. – Т.2, №4. – P. 521.
11. Лифшиц И.М., Косевич А.М. // Изв. АН СССР, сер.физ. – 1955. – Т.19, 395.
12. Calecki D., Fishman G. // Phys.Rev.Lett., – 1989. V. 62. – P. 1302-1305.

## Deposition, structural and optical properties of $\text{Cu}_7\text{GeS}_5\text{I}$ thin films

Studenyyak I. P.<sup>1</sup>, Miklosh N. Yu.<sup>1</sup>, Vorohta M.<sup>2</sup>, Matolin V.<sup>2</sup>,  
Cserhati C.<sup>3</sup>, Kökényesi S.<sup>3</sup>

<sup>1</sup>Uzhhorod National University, Uzhhorod, Ukraine

<sup>2</sup>Charles University, Prague, the Czech Republic

<sup>3</sup>University of Debrecen, Debrecen, Hungary

$\text{Cu}_7\text{GeS}_5\text{I}$  compounds belong to argyrodite family and are known as superionic conductors. They exhibit rather high electrical conductivity and low activation energy at room temperature. Therefore, they are promising materials for creation of solid state batteries on their base. At room temperature  $\text{Cu}_7\text{GeS}_5\text{I}$ -based solid solutions crystallize in the cubic symmetry (space group  $F\bar{4}3m$ ), no phase transitions were revealed in the temperature 77–370 K. Optical studies have shown that the absorption edge of  $\text{Cu}_7\text{GeS}_5\text{I}$  crystals exhibits an Urbach behaviour in a wide temperature range.

The amorphous films were deposited onto glass substrates by non-reactive radio frequency magnetron sputtering. The film growth rate was 3 nm/min, the film thickness was 1.265  $\mu\text{m}$ . The deposition was carried out at room temperature in Ar atmosphere. Optical transmission spectra  $T(\lambda)$  of  $\text{Cu}_7\text{GeS}_5\text{I}$  thin films were studied in the interval of temperatures 77–300 K by an MDR-3 grating monochromator. From the temperature studies of interference transmission spectra, the spectral dependences of absorption coefficient as well as dispersion dependences of refractive index were derived. The analysis of the experimental dispersive dependence of the refractive indices has shown to be well described by a known optical-refractometric relation. The linear increasing of refractive index with temperature in the interval 77–300 K is observed.

It is shown that the optical absorption edge spectra in the range of their exponential behaviour in amorphous  $\text{Cu}_7\text{GeS}_5\text{I}$  thin films, similarly to the single crystals, are described by Urbach rule. At  $T=300$  K, the optical pseudogap value  $E_g^*$  in  $\text{Cu}_7\text{GeS}_5\text{I}$  thin film equals 1.885 eV while in the single crystal it is 2.125 eV; the Urbach energy  $E_U$  in  $\text{Cu}_7\text{GeS}_5\text{I}$  thin film is 93.5 meV while in the single crystal it equals 35.0 meV.

The temperature behaviour of the Urbach absorption edge in  $\text{Cu}_7\text{GeS}_5\text{I}$  thin films is explained by electron-phonon interaction which is strong in amorphous films. The transition from bulk three-dimensional  $\text{Cu}_7\text{GeS}_5\text{I}$  crystals to two-dimensional film structures leads to the strengthening of the electron-phonon interaction. An essential characteristic of the absorption edge spectra of the thin films under investigation is a lengthy Urbach tail which results in the Urbach energy  $E_U$  being more than by an order of magnitude higher than in the crystal caused by growing influence of static structural disordering.

## Colloidal semiconductor quantum dots light-emitting devices

G.A. Sukach<sup>1</sup>, A.B. Bogoslovskaya<sup>2</sup>

<sup>1</sup>*National University of Life and Environmental Sciences of Ukraine, Ukraine*

<sup>2</sup>*V. Lashkaryov Institute of Semiconductor Physics NAS of Ukraine, Ukraine*

A number of startup companies around the globe continue to search more efficient and better color rendering luminescent materials for solid-state lighting. Today colloidal semiconductor quantum dots (QDs) attracted great scientific and technical interest from scientists as efficient, spectrally pure component of light-emitting devices owing to their unique size-dependent optical and electronic properties, based on quantum confinement effect of the electronic states. QDs with different sizes simultaneously emit light at different wavelength to achieve white emission.

The major advantages of LEDs based on QDs are the easy tuning of the saturated color emission across the visible-NIR range, high photoluminescence quantum yields and the high chemical and optical stability of the nanocrystal composites.

Among different method for the fabrication of stable white-LEDs comprising QDs, color-conversion WLEDs have been the most widely used. The use of QD for color conversion has several advantageous features, including strong optical absorption towards shorter wavelengths, spectral tunability, high quantum efficiency and photostability, relatively narrow and symmetric PL with high photobleaching thresholds, and reasonably small spectral overlap between absorption and emission. To date color-conversion WLEDs that integrate combinations of colloidal QDs as phosphors on InGaN LED chip/or an InGaN-GaN multiple-wavelength QWs LEDs have been successfully demonstrated.

The optical properties of QDs can be drastically improved by coating the light-emitting core with a monolayer or a few monolayers of a higher band gap material shell. White light generation may be controlled and tuned by multi-color quantum-dot-quantum-well emitters made of onion-like core/shell/shell heteronanocrystals integrated on InGaN/GaN LEDs.

The optical properties of the WLEDs such as the tristimulus coordinates, color temperature, and color rendering index may be adjusted by hybridizing QD of various single, dual, trio, and quadruple combinations on InGaN/GaN LEDs.

Novel classes of hybrid WLEDs based on polymer/QDs nanocomposites comprising a fluorescent polymer and nanoparticles have been realized. Hybrid organic - quantum dot QD-LEDs combine the color purity and durability of QDs with the efficiency, flexibility, and low processing cost of organic light-emitting devices.

The integration of colloidal QDs into LEDs has the potential for fabrication of stable high-quality white LEDs with high color rendering indices, as is required for future solid state lighting applications.

## **Transport properties of complicated resonance tunnel nanosystems**

Tkach M., Seti Ju., Voitsekhivska O.

*Chernivtsi National University, Chernivtsi, Ukraine*

The open complicated nanostructures, as resonance-transport systems are intensively used in functional devices (quantum cascade lasers, detectors and generators) with the precise physical characteristics. These devices operate due to the physical phenomena taking place in their active elements – complicated resonance tunnel structures with the flowing electronic currents, interacting with electromagnetic fields and different dissipative subsystems (phonons, impurities and so on).

The consistent theory explaining the transport properties of complicated resonance tunnel nanostructures is still absent due to the fact that such systems are the quantum-mechanical objects demanding taking into account many features of basic model that makes the establishment of the final theory the rather complicated process.

In the proposed paper the transport properties of two-, three- or four-barrier RTS are studied in the frames of the model of rectangular potentials and different effective masses of conductivity electrons.

Solving the complete Schrodinger equation there are studied and analysed the permeability coefficients for the resonance tunnel nanostructures and their conductivity depending on the geometric design. It is established the presence of optimal geometric configurations of active elements of quantum cascade lasers and quantum cascade detectors for the providing of maximum effectiveness of these devices operating.

1. C. Gmachl, F. Capasso, D.L. Sivco, A.Y. Cho. Recent progress in quantum cascade lasers and applications. // *Rep.Prog.Phys.* – 64. – P. 1533.
2. N. V. Tkach and Ju. A. Seti. Evolution of the Spectral Parameters of // Quasiparticles in an Open Symmetrical Three\_BARRIER Resonant Tunneling Nanostructure. *Phys. Sol. State.* - 2011. - 53. - P. 590.
3. N. V. Tkach and Ju. A. Seti. Optimization of the Configuration of a Symmetric Three Barrier Resonant Tunneling Structure as an Active Element of a Quantum Cascade Detector. *Semiconductors.*- 2011. – 45. – P. 376.

## Composite nickel-boron-nanodiamond coatings and there physical and mechanical properties

Tsybulskaya L.S., Gaevskaya T.V., Purovskaya O.G.

*Research Institute for Physical Chemical Problems of Belarusian State University,  
Minsk, Belarus*

Composite electrodeposited nickel-diamond-nanodiamond and nickel-boron-nanodiamond coatings are used for production of the frame diamond-containing disks for semiconductor chipping and for cutting of ultra-hard materials (policor, sapphire, corundum and others), as well as for production of faceting disks for grinding and polishing of diamond raw materials. Enhanced hardness and wear resistance, good durability and stability are the advantages of these composite materials. A novelty of the proposal consists in the replacement of nickel matrix with synthetic diamond power of different dispersion ( $0,5\div 40\ \mu\text{m}$ ) with nickel-boron, nickel-nanodiamond or nickel-boron-nanodiamond matrix. This replacement leads to the increase in microhardness and wear resistance of the composite coatings and in surface concentration of diamond power. We used morpholine-borane as a boron-containing compound and ultradisperse diamond (product of the detonating explosion) with a particle size of  $3\div 5\ \text{nm}$  and a specific surface area of  $200\div 450\ \text{m}^2/\text{g}$  as a nanodiamond. The composite coatings were electrodeposited onto steel, aluminum and Al alloys in a bath containing  $0,05\div 0,5\ \text{g/l}$  morpholine-borane and  $1\div 5\ \text{g/l}$  nanodiamonds in the galvanostatic regime with a current density ranging from  $0,5$  to  $5,0\ \text{A/dm}^2$ . The boron content in the composite coatings has been shown to increase from  $1$  to  $4,3\ \text{at.}\%$  with increasing the concentration of morpholine-borane, and to decrease by  $\approx 0,05\ \text{at.}\%$  with increasing the cathodic current density. The content of nanodiamonds in the coatings does not exceed  $4\div 5\ \text{at.}\%$ . Optimal conditions of the deposition are the following: the cathodic current density –  $2\div 2,5\ \text{A/dm}^2$ , the temperature –  $45\div 50\ ^\circ\text{C}$ , the concentration of nanodiamond in the bath –  $1\div 2\ \text{g/l}$  and the concentration of morpholine-borane –  $0,15\div 0,2\ \text{g/l}$ . Under these conditions the boron content in the composite coatings is  $1,7\div 2,5\ \text{at.}\%$  and the content of nanodiamonds –  $1,5\div 2,5\ \text{at.}\%$ . X-ray diffraction study showed that the incorporation of boron up to  $2,5\ \text{at.}\%$  leads to the decrease of the grain size from  $30$  to  $10\ \text{nm}$  and the lattice parameter of nickel from  $0,3524$  to  $0,3514\ \text{nm}$ . It was revealed that the simultaneous incorporation of boron and nanodiamonds in the nickel matrix in an optimal concentration leads to the increase in microhardness of the coatings from  $2,9$  (Ni) to  $6,5$  (Ni-B $_{2,5}$ ) and up to  $8,5\ \text{GPa}$  (Ni-B $_{2,5}$ -C $_2$ ), to the decrease of the wear intensity under dry sliding conditions from  $0,1$  (Ni) to  $0,04$  (Ni-B $_{2,5}$ ) and up to  $0,02\ \text{g/m}$  (Ni-B $_{2,5}$ -C $_2$ ). In addition, this is favourable to more uniform distribution of the synthetic diamond power in the surface layer and results in increasing its content in the coating up to  $80\text{-}90\ \%$ .



## IR spectroscopy investigation of polaritons in ZnO films located in a uniform magnetic field

Venger E.F.<sup>1</sup>, Ievtushenko A.I.<sup>2</sup>, Davidenko S.M.<sup>2</sup>,  
Melnychuk L.Yu.<sup>2</sup>, Melnychuk O.V.<sup>2</sup>

<sup>1</sup>*V. Lashkaryov Institute of Semiconductor Physics, NAS of Ukraine, Kyiv, Ukraine*

<sup>2</sup>*Mykola Gogol State Pedagogic University, Nizhyn, Ukraine*

We present the results of IR spectroscopy investigation of the properties of transparent highly textured and single-crystalline optically anisotropic ZnO films on “semi-infinite” 6H-SiC and Al<sub>2</sub>O<sub>3</sub> substrates. The spectra of attenuated total reflection (ATR) were taken, in the actual frequency regions for ZnO film (400–600 cm<sup>-1</sup>) and “semi-infinite” optically anisotropic 6H-SiC and Al<sub>2</sub>O<sub>3</sub> substrates (400–1200 cm<sup>-1</sup>), using a spectrophotometer ИКС-31 with an attachment ИПО-22.

A mathematical model has been developed, with additive and phenomenological contribution from oscillators to the permittivity of optically isotropic and anisotropic ZnO films on optically anisotropic 6H-SiC and Al<sub>2</sub>O<sub>3</sub> substrates. This made it possible to simulate ATR spectra taking into account the effect of a uniform magnetic field. It was shown that presence of anisotropy and interrelation between magnetoplasmons and low-frequency optical phonons leads to appearance of new properties of surface polaritons that differ essentially from those in cubic semiconductors, namely, appearance of new dispersion branches and their splitting in the high-frequency spectral region, anisotropy of damping coefficients, etc. A novel dispersion branch was found, for the first time, in the region of “residual rays” for a zinc oxide film on optically anisotropic doped 6H-SiC substrates. The limiting frequency of that branch increases monotonically. It was shown that appearance of that branch is owing to the effect of magnetic field on the film–substrate system.

We developed software for dispersion analysis of ATR spectra of the structures under investigation, with allowance made for variation of the quality of substrate surface processing. The results on electron concentration in heavily doped ZnO films and 6H-SiC substrates obtained with the Hall method agree well with those given by the dispersion analysis of the transmission and ATR spectra for ZnO films whose thickness is below 0.5 μm.

It was found that increase of both doping level in the ZnO film and strength of uniform magnetic field deform the ATR spectra of ZnO films on optically anisotropic 6H-SiC and Al<sub>2</sub>O<sub>3</sub> substrates in the region of “residual rays”. Based on the ATR study of the ZnO/6H-SiC structures, it was found that the zinc oxide films electron concentration  $n_0 = (0.3 \div 2.8) \times 10^{18} \text{ cm}^{-3}$ , charge carrier mobility  $\mu_L = 11 \div 80 \text{ cm}^2/(\text{V}\cdot\text{s})$  and conductivity  $\sigma_0 = 90 \div 225 \text{ }\Omega^{-1}\cdot\text{cm}^{-1}$ . These values agree with those obtained with other methods.

It is shown that IR spectroscopy diagnostics of anisotropic structures enables one to get the values of conductivity and charge carrier mobility in thin ZnO films.

## On mechanism of nanocluster growth

Vengrenovich R.D., Ivanskii B.V., Yarema S.V.

*Yurii Fed'kovich Chernivtsi National University, Chernivtsi, Ukraine*

The purpose of this study is to determine the mechanism of cluster growth in the Ostwald's ripening (OR) process by comparison of the mostly used in practice numerical characteristics, such as a mean radius, dispersion, root-mean-square deviation asymmetry coefficient, and excess computed for experimentally obtained histograms and theoretical curves for volume disperse systems.

The initial and central momentums of  $g(u)$  are given in the form:

$$\alpha_s(u) = \int_0^1 u^s g(u) du, \quad (1)$$

$$\mu_s(u) = \int_0^1 (u - \langle u \rangle)^s g(u) du. \quad (2)$$

Let us determine some important numerical characteristics of function  $g(u)$ , which are represented through its momentums (1) and (2). So, the area under the curve  $g(u)$ , being equal to the number of particles in the unite volume, is determined by the zero momentum  $\alpha_s(u)$ :

$$\alpha_0(u) = \int_0^1 g(u) du. \quad (3)$$

A mean relative radius is:

$$\langle u \rangle = \alpha_1(u) / \alpha_0(u) = \int_0^1 u g(u) du / \int_0^1 g(u) du. \quad (4)$$

Dispersion is:

$$D(u) = \langle u^2 \rangle - (\langle u \rangle)^2 = \mu_2(u) / \alpha_0(u). \quad (5)$$

Asymmetry coefficient is:

$$S(u) = \mu_3(u) / \alpha_0(u) \sigma(u)^3, \quad (6)$$

Excess is:

$$E(u) = \mu_4(u) / \alpha_0(u) \sigma(u)^4. \quad (7)$$

As a model mechanism of growth, we consider the case when particle growth in a matrix is realized through simultaneous action of the diffusion and the Wagner mechanisms of mass transfer. The size distribution function for this case is determined as:

$$g'_{J.C.-B.}(u) = u^2 (1-u)^{-B} (u + x^2 + x)^D \exp\left[\frac{C}{1-u}\right], \quad (8)$$

where  $B$ ,  $C$ ,  $D$  are known coefficients, and  $x$  is the share of the diffusion flow  $j_v$  in general flow  $j$ .

In Table 1 we represent the main numerical characteristics of the generalized distribution (8), computed following Eqs. (3)-(7).

Table 1.

	$\langle u \rangle$	$D(u)$	$\sigma(u)$	$S(u)$	$E(u)$
$x = 0$	0.444	0.025	0.157	-0.291	2.48
$x = 0,1$	0.486	0.023	0.151	-0.372	2.598
$x = 0,2$	0.516	0.022	0.149	-0.455	2.72
$x = 0,3$	0.543	0.022	0.148	-0.529	2.839
$x = 0,4$	0.566	0.022	0.148	-0.597	2.957
$x = 0,5$	0.586	0.022	0.147	-0.659	3.074
$x = 0,6$	0.605	0.021	0.146	-0.716	3.191
$x = 0,7$	0.622	0.021	0.146	-0.771	3.31
$x = 0,8$	0.638	0.021	0.145	-0.823	3.43
$x = 0,9$	0.653	0.021	0.144	-0.872	3.552
$x = 1$	0.667	0.021	0.143	-0.92	3.675

Fig. 1a shows a histogram of the size distribution function for nanoclusters of aluminum (*Al*) normalized to unity along the coordinates. Nanoclusters were obtained by annealing of amorphous alloy  $Al_{85}Ni_8Y_5Co_2$  for temperature  $T = 508K$  during 2.5 min.

In the same way we normalized a histogram shown in Fig. 1b. This histogram corresponds to the relative size distribution function of nanoclusters  $Al_3Sc$  obtained in the corresponding alloys *Al – Sc* with exposure of them during 1 hour for temperature  $T = 400^\circ C$ .

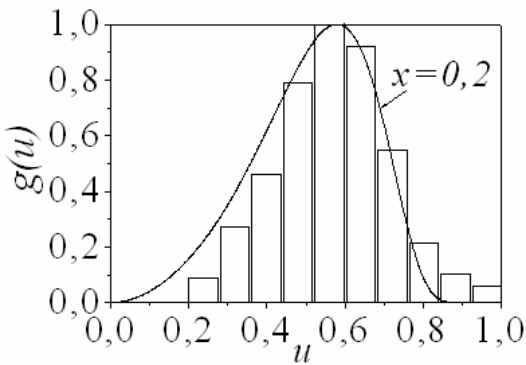


Fig. 1a

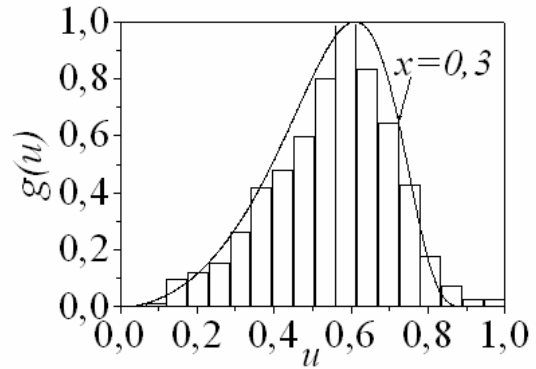


Fig. 1b

In Table 2 we represent the numerical characteristics of histograms shown in Figs. 1a and 1b, respectively. Computations were made following Eqs. (3) – (7), where integrals were replaced by the corresponding sums.

Table 2

	$\langle u \rangle$	$D(u)$	$\sigma(u)$	$S(u)$	$E(u)$
Fig. 1a	0.542	0.226	0.15	-0.459	2.873
Fig. 1b	0.545	0.022	0.148	-0.567	2.977

## **Control of layer thickness during laser spectral analysis of micron and submicron metal coatings**

Voropay E., Ermalitskaya K.

*Belarusian State University, Minsk, Belarus*

One of the most important requirements to the source of substance evaporation and atom spectra excitation is minimal constant layer thickness. Standard sources such as electric discharges even after very short time provide rather big (equal to a few millimeters) destruction of sample surface. Thickness of majority of functional and protective metal coatings of industry production is about few micrometers. To perform layer-by-layer quantitative analysis the thickness of each evaporated layer should be not more than one tenth of coating.

Nanosecond laser pulse with energy 100 mJ penetrates to 5 micrometer depth from the surface. To reduce layer thickness new method for changing laser energy density was suggested. In that case laser ray was focused in point situated at some distance  $f$  from the surface – fig. 1.

## Interfacial superconductivity of $A^{IV}B^{VI}$ semiconductor heterostructures

Yuzepovich O.I.<sup>1,2</sup>, Bengus S.V.<sup>1,2</sup>, Mikhailov M.Yu.<sup>1</sup>, Fogel N.Ya.<sup>3</sup>

<sup>1</sup>*B. Verkin Institute for Low Temperature Physics and Engineering, NAS of Ukraine, Kharkov, Ukraine;*

<sup>2</sup>*International Laboratory of High Magnetic Fields and Low Temperatures, Wroclaw, Poland*

<sup>3</sup>*Solid State Institute, Technion, Haifa, Israel*

In this report we discuss superconducting nanostructures with different topology which are self-organizing at the interfaces of IV–VI semiconductor heterostructures. They are epitaxially grown from two semiconductors with different periods of the crystal lattice. The “joining” of crystal lattices occurs through the formation of a periodic grid of misfit dislocations at the interface. The grid becomes conductive and superconductive at low temperatures [1-4] due to elastic stresses and zone inversions in semiconductors. The superconductivity of heterostructures is an unusual property since the individual semiconductors are not superconductors. The period of the grid varies from 3.3nm to 25nm, depending on the combination of semiconductors (for PbTe/PbS – 5.2nm) [2].

We have established a correlation between the structural and superconducting properties of bilayer heterostructures PbTe/PbS with different thicknesses of the semiconductor layers  $d$ . We have shown that bilayer heterostructures can be conditionally divided into 3 categories (Fig.1).

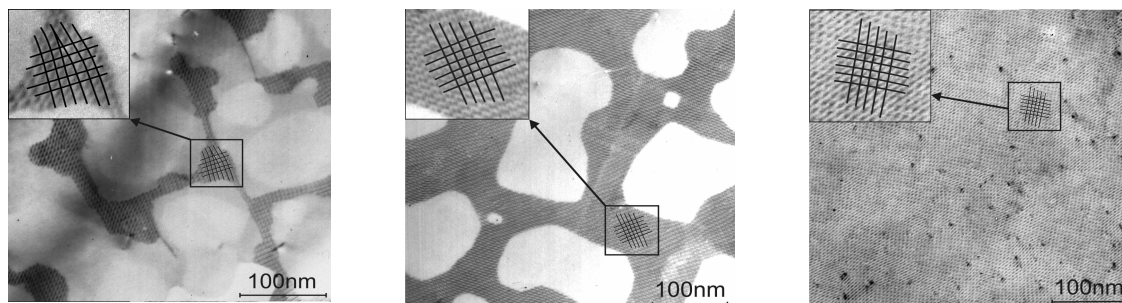


Fig.1. Electron microscope image of PbTe–PbS/KCl bilayer heterostructures with  $d_{\text{PbTe}}$  [nm]: 1 (a), 3 (b), and 30 (c). The thickness of the PbS layer is 40nm.

The first category is comprised of samples with a relatively perfect misfit dislocations grid covering the whole interface ( $d \geq 100\text{nm}$ ). They exhibit metallic type of conductivity in the normal state and demonstrate a complete transition to the superconducting state. The second category ( $40 > d > 80\text{nm}$ ) contains samples with discontinuous misfit dislocations grid and they may have semiconductive or metallic type conductivity, but in either case the superconductivity occurs at low temperatures. The third category ( $d < 40\text{nm}$ ) contains samples with an island grid of misfit dislocations, they demonstrate semiconductor-type conductivity and no superconducting transition [4]. Also substantial differences in the

behaviour of bilayer and multilayer heterostructures are found. The minimum thickness  $d$  at which superconductivity appears for bilayers is several times larger than for multilayers [4].

Here we present results of experimental studies of PbTe/PbS heterostructures with the different  $d$  in high magnetic fields.

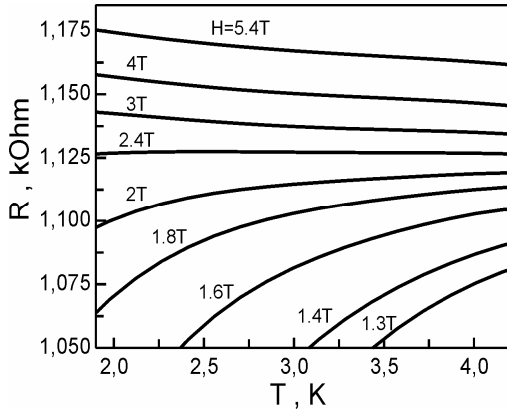


Fig.2.

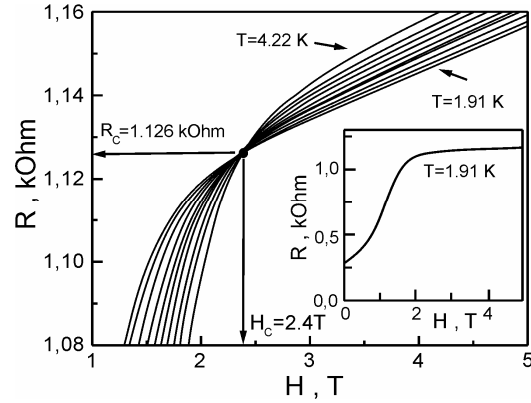


Fig.3.

We found that the presence of defects in superconducting interfacial nanonets (defects in dislocation grids) essentially influences on the possibility of realization of the superconductor-insulator transition (SIT). As follows from the TEM study [2], such defects are present in the PbTe/PbS with  $d < 80\text{nm}$ . All typical features of the SIT have been observed for the heterostructures with  $60\text{nm} < d < 80\text{nm}$ : the fan-like set of  $R(T)$  dependences with horizontal separatrix which separates superconducting and insulating states (Fig.2, PbTe/PbS  $d=75\text{nm}$ ), the crossing of  $R(H)$  curves in a single point (Fig.3, parallel magnetic field) and the negative magnetoresistance in high magnetic fields. For samples with  $d < 60\text{nm}$  (with more defect conducting interface) in the middle magnetic fields quasi-reentrant behavior is observed:  $R(T)$  have two extremums – minimum close to  $T_{conset}$  and maximum at lower temperatures after that the superconducting transition takes place. For this case  $R(H)$  are crossing but single point is not observed.

The SIT is not observed (above 1.6K) for heterostructures with more perfect nanonets ( $d > 100\text{nm}$ ) as well as for multilayers. The nature of the SIT in studied systems is most probably associated with the Josephson links breaking between superconducting islands. Additional experiments at lower temperatures are required for the detailed interpretation of the phenomenon. This work was supported by the grant of the Ukrainian National Nanoscience Program.

1. N.Ya. Fogel et al., Phys. Rev. Lett. **86**, 512 (2001).
2. N.Ya. Fogel et al. Phys.Rev. **B66**, 174513 (2002).
3. N.Ya. Fogel et al., Phys. Rev. **B73**, RC161306 (2006).
4. O.I. Yuzepovich et al., Low Temp. Phys. **34**, 985 (2008).

## **Crystal-chemistry dependence of the energetic redistribution of the valence electrons and experimental evaluation of changes of the band energy of materials due to their dispersion to nanosizes**

Zaulychnyy Ya.V.

*National Technical University of Ukraine "Kiev Polytechnic Institute" Engineering-physical faculty, Kyiv, Ukraine and Institute for Problems of Materials Science, National Academy of Sciences of Ukraine, Kyiv, Ukraine*

The ultra-soft X-ray spectroscopy method has been employed to study the crystal-chemistry dependence of the energetic redistribution of the valence electrons due to decreasing particle sizes of powders to nanosizes for the following materials: diamond, BN, TiC, TiN, TiO<sub>2</sub>, BaTiO<sub>3</sub>, SiO<sub>2</sub>, Al<sub>2</sub>O<sub>3</sub> and some their allotropic modifications.

It has been established [1,2] that the character of changes of energy of electrons involved in broken bonds, when their amount becomes comparative with the amount of atoms in the nanoparticle volume, depends upon: a) the degree of localization of the valence electrons near the atoms and bonds directions; b) relations of the density of covalent-bonding and nonbonding electronic states; c) the existence of bonds between anions; d) the degree of  $\pi$ -overlapping in carbon nanomaterials; e) the geometry and the basis of the nearest environment, kinds of atoms, lattice symmetry and the degree of ordering.

In the present work, it has been shown that, in nanocrystalline powders due to disappearing a split of the electronic levels and increasing their energy after breaking bonds, density of states decreases and the distribution of the covalent-bonding states becomes narrow. In this case, the density of occupied nonbonding orbitals increases. In disordered turbostrate h-BN, amorphous SiO<sub>2</sub> (aerosyl) and Al<sub>2</sub>O<sub>3</sub> the energy distribution of nonbonding electronic states narrows due to decreasing energy of the high-energy electrons because of relaxational recombination of bonds.

The technique of evaluation of changes of band energy  $E^{\text{nano}}/E^{\text{coarse}}$  based on findings of changes for parameters of X-ray emission bands derived for coarse and nanopowders has been proposed.

1. Zhurakovsky E.A. et al. // Dokl. Akad. Nauk SSSR. – 1985. – V. 248. – P. 1360, in Russian.
2. Zaulychnyy Ya.V. // Powder Met. Metal Ceram. –1999. V. 38, №387. – P. 493.

## Magnetic field dynamics of the photoluminescence bands of the semimagnetic quantum structures based on *ZnSe*

Zayachuk D.M.<sup>1</sup>, Slobodskyy T.<sup>2</sup>, Astakhov G.V.<sup>2,3</sup>, Slobodskyy A.<sup>4,5</sup>

<sup>1</sup>*Lviv Polytechnic National University, Lviv, Ukraine*

<sup>2</sup>*Physikalisches Institut der Universität Würzburg, Würzburg, Germany*

<sup>3</sup>*A. F. Physico-Technical Institute, Russian Academy of Sciences, St. Petersburg, Russia*

<sup>4</sup>*Light Technology Institute, Karlsruhe Institute of Technology (KIT), Karlsruhe, Germany*

<sup>5</sup>*Zentrum für Sonnenenergie- und Wasserstoff-Forschung Baden-Württemberg, Stuttgart, Germany*

Quantum heterostructures containing layers of diluted magnetic semiconductors (DMS) have been extensively studied during the last decades. The main focus has been made on both fundamental and practical applications, especially for different spin-electronic devices. Two typical approaches usually applied to the fabrication of DMS heterostructures are the heterostructures with a DMS layer as a quantum well (QW) or the heterostructures with DMS layers as quantum barriers. In the first case, both the free carriers and the 3d element ions are located in the same layer of a QW. This leads to a strong interaction between the free carriers and the localized 3d-electrons of ions, which intensifies the effects caused by the magnetic field. However, the presence of magnetic impurities in a QW stimulates spin relaxation processes. Hence, it is preferable to separate the carriers from the magnetic media. In this case, the exchange interaction between the free 2D carriers of nonmagnetic quantum well and the ions of magnetic impurities in the barrier is driven by penetration of the carrier wave function tails into the barrier.

In this paper we report the measurements of photoluminescence (PL) of the semimagnetic 150 nm  $Zn_{0.9}Be_{0.05}Mn_{0.05}Se$  /  $d$  nm  $Zn_{0.943}Be_{0.057}Se$  / 2.5 nm  $ZnSe$  / 30 nm  $Zn_{0.943}Be_{0.057}Se$  structures as a function of thickness  $d$  of the intermediate nonmagnetic barrier  $Zn_{0.943}Be_{0.057}Se$  between the  $Zn_{0.9}Be_{0.05}Mn_{0.05}Se$  semimagnetic barrier and  $ZnSe$  QW and magnetic field at the low temperature 1.2 K being based on our publications [1, 2]. The investigation of PL provides a great amount of useful information on the changes of the energy characteristics and physical properties of the structures under the effect of a magnetic field. At the same time, the interpretation of the results of PL measurements comes across a problem of fundamental character. The magnetic and non-magnetic layers of the semimagnetic quantum structures are subjected to different effects produced by an external magnetic field. As a result, the PL bands caused by different layers are often superimposed on one another. Therefore, quantitative analysis of the experimental PL spectra necessitates their preliminary decomposition into elementary constituents. Exactly here a problem emerges concerning the unambiguity of decomposition. Here we show that the method of averaging can be advantageously used in quantitative analysis of the mentioned above structures. It ensures a precision in determining the single component energy



sufficient for quantitative analysis. A precision of determination of both the band full width at half maximum and the intensity of the components is sufficient at least for qualitative analysis.

Using the method of averaging strong evidence has been obtained that the intermediate nonmagnetic barrier: (i) changes the energy of the PL bands in both the *ZnSe* QW and  $Zn_{0.9}Be_{0.05}Mn_{0.05}Se$  semimagnetic barrier layers; (ii) increases the total PL intensity of the structures; (iii) decreases the degree of circular polarization of the QW exciton emission in the structure; (iv) extinguishes the PL band caused by the indirect transitions in real space between the 2D conduction band of the *ZnSe* QW and both the *Mn* complex and the valence band of the  $Zn_{0.9}Be_{0.05}Mn_{0.05}Se$  layer. The obtained data enable us to conclude that the emission bands appearing in the semimagnetic  $Zn_{0.9}Be_{0.05}Mn_{0.05}Se$  barrier of the structures under study are formed in the contact layers strained by the immediate  $Zn_{0.943}Be_{0.057}Se$  or *ZnSe* layers. The shifts of the band gap as well as of the donor and acceptor levels under the effect of biaxial compression of the  $Zn_{0.9}Be_{0.05}Mn_{0.05}Se$  layer by the  $Zn_{0.943}Be_{0.057}Se$  layer are estimated.

There are two different rates  $(\chi N_0)_{1H}$  and  $(\chi N_0)_{1L}$  of the shift of the short wave bands of the PL spectra of the structure under study in a magnetic field caused by giant Zeeman splitting. The larger rate  $(\chi N_0)_{1H}$  is observed in the high magnetic fields and corresponds to the emission transition between *C* and *V* bands of the  $Zn_{0.9}Be_{0.05}Mn_{0.05}Se$  barrier. A smaller rate  $(\chi N_0)_{1L}$  is observed in low magnetic fields and corresponds to the emission transition between the  $Zn_{0.9}Be_{0.05}Mn_{0.05}Se$  conduction band and an energy level of the acceptor complex containing *Mn*. The intermediate nonmagnetic barrier  $Zn_{0.943}Be_{0.057}Se$  does not change the  $(\chi N_0)_{1H}$  value. At the same time, it decreases the  $(\chi N_0)_{1L}$  value by approximately 22 %. This supports the assumption that: (i) the deformation of the  $Zn_{0.9}Be_{0.05}Mn_{0.05}Se$  layers plays a key role in forming the *Mn* complexes; (ii) the 2D carriers of the *ZnSe* QW provide a substantial contribution to the formation of the exchange integral for the *Mn* ions as a component of the complex in strained layers. The  $Zn_{0.943}Be_{0.057}Se$  immediate barrier changes the effect of giant Zeeman splitting of the semimagnetic  $Zn_{0.9}Be_{0.05}Mn_{0.05}Se$  barrier energy levels on a move of the energy levels of *ZnSe* QW in a magnetic field and a polarization of the QW exciton emission.

1. Zayachuk D.M., Slobodskyy T., Astakhov G.V., Gould C., Schmidt G., Ossau W., and Molenkamp L.W., EPL – 2001. – **91**, – 67007.
2. Zayachuk D. M., Slobodskyy T., Astakhov G.V., Slobodskyy A., Gould C., Schmidt G., Ossau W., and Molenkamp L.W. // Phys. Rev. B – 2011. –**83**, – 085308.

## Regularities of optical properties of complex metal chalcogenides in crystalline, glass-like and thin-film states

Zinchenko V.F.

*A. V. Bogatsky Physico-Chemical Institute of NAS of Ukraine, Odesa, Ukraine*

General regularities of the change of short-wave limit ( $\lambda_1$ ) of the optical transparency interval of complex metal chalcogenides at the substitution for heavier analogue (metal or chalcogen) and at transition from crystalline (glassy) state to thin-film coating are established and discussed.

It has been shown that coatings of the rather small thickness (100-300 nm), obtained from complex chalcogenides are x-ray amorphous or mixed, crystalline amorphous. For most of them a sufficient gypsochromic shift of the value  $\lambda_1$  is observed. Vitriifying of the bulk samples verso versa results in bathochromic shift of  $\lambda_1$  (Table).

Table

Gypsochromic shift of the short-wave limit of transparency interval in thin-film coatings

Polycrystalline (glassy) sample		Thin-film coating	
Composition	$\lambda_1$ , nm	Structure	$\lambda_1$ , nm
ZnIn <sub>2</sub> S <sub>4</sub>	530	x-ray amorphous	490
ZnIn <sub>2</sub> Se <sub>4</sub>	730	x-ray amorphous	670
CdIn <sub>2</sub> S <sub>4</sub>	560	cryst.+x-ray amorphous	540
CdGa <sub>2</sub> Se <sub>4</sub>	650	cryst.+x-ray amorphous	510
MnIn <sub>2</sub> S <sub>4</sub>	560	cryst.+x-ray amorphous	450
EuGa <sub>2</sub> S <sub>4</sub>	520	x-ray amorphous	350
EuGa <sub>2</sub> Se <sub>4</sub>	520	x-ray amorphous	390
EuIn <sub>2</sub> S <sub>4</sub>	600	x-ray amorphous	430
EuIn <sub>2</sub> Se <sub>4</sub>	870	x-ray amorphous	590
TlSbS <sub>2</sub>	880	x-ray amorphous	700
Tl <sub>2</sub> GeS <sub>3</sub>	520 (640)	x-ray amorphous	460
Tl <sub>2</sub> Ge <sub>2</sub> S <sub>5</sub>	470 (650)	x-ray amorphous	550
Tl <sub>2</sub> GeSe <sub>3</sub>	800	x-ray amorphous	750
Tl <sub>2</sub> Ge <sub>2</sub> Se <sub>5</sub>	600 (840)	x-ray amorphous	680

The observed phenomena should be explained from the point of view of nano-sized structures which are formed at the rapid condensation of supersaturated vapour of chalcogenide on the substrate at the thermal evaporation in deep vacuum. The connection between the crystal symmetry, ability to form glasses and optical properties of the thin-film coatings is established.

**СЕКЦІЯ 1 (усні доповіді)  
ТЕХНОЛОГІЯ ТОНКИХ ПЛІВОК (МЕТАЛИ,  
НАПІВПРОВІДНИКИ, ДІЕЛЕКТРИКИ, ПРОВІДНІ  
ПОЛІМЕРИ) І МЕТОДИ ЇХ ДОСЛІДЖЕННЯ**

17-20 травня 2011 р.

**SESSION 1 (oral)  
THIN FILMS TECHNOLOGY (METALS,  
SEMICONDUCTORS, DIELECTRICS, CONDUCTIVE  
POLYMERS) AND THEIR RESEARCH METHODS**

May, 17-20, 2011

## Surface plasmon resonance techniques for in situ control of underpotential Te deposition on polycrystalline Au surface

Beketov G.V., Ushenin Yu.V., Rengevych O.V.

*Institute of Semiconductor Physics, Kiev, Ukraine*

The controlled deposition of single atomic layers lies at the core of the atomic layer epitaxy (ALE). A very promising approach to ALE technology is based on electrochemical methods (ECALE) utilizing the underpotential deposition (UPD) of the elements from solutions of their salts. This technique can be used for low-temperature synthesis of nanolayered semiconductors such as cadmium and zinc chalcogenides. One of key issues of the ECALE technology is development of the *in-situ* control techniques of the deposition process. One of successful methods for this purpose is based on the surface plasmon resonance spectroscopy (SPR) and related techniques, which were proved to be especially suited for probing of ultrathin surface coverages.

In this work regular SPR spectroscopy is compared with SPR measurements using reflectivities of both *p*- and *s*-components of the polarized light and the SPR ellipsometry. In the regular SPR, formation of the first Te monolayer under cathodic polarization (Fig.1) on a polycrystalline Au film manifested itself as a change of the resonant curve shape and position (Fig.2).

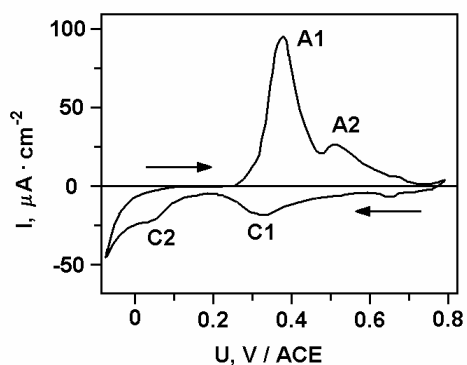


Fig. 1. Cyclic voltammogram of Te deposition on Au film. Peak C1 corresponds to UPD of Te.

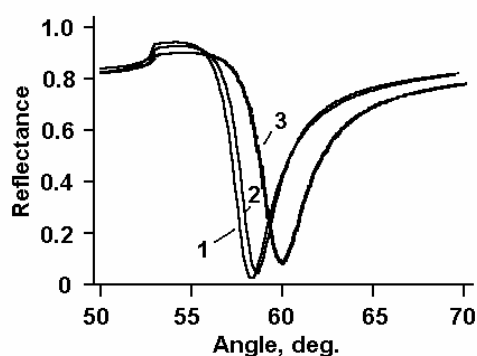


Fig. 2. SPR resonance on Au 40 nm polycrystalline film during Te electrochemical deposition. 1 – initial conditions, 2 – after peak C1, 3 – bulk deposition.

With the SPR ellipsometry, the phase shift between the *p*- and *s*-components of the incident light was also detected, resulting in a considerable gain in sensitivity. According to these observations, cathodic peak C1 (Fig.1) was attributed to UPD deposition of Te, while cathodic currents at more negative potentials corresponded to bulk polycrystalline deposition.

## Effect of microwave radiation on the properties of ohmic contacts to the $n^+ - n - n^+$ -GaN–Al<sub>2</sub>O<sub>3</sub> structures

Belyaev A.E.<sup>1</sup>, Boltovets N.S.<sup>2</sup>, Vitusevich S.A.<sup>1</sup>, Ivanov V.N.<sup>2</sup>, Konakova R.V.<sup>1</sup>, Lebedev A.A.<sup>3</sup>, Milenin V.V.<sup>1</sup>, Sveshnikov Yu.N.<sup>4</sup>, Sheremet V.N.<sup>1</sup>

<sup>1</sup>*V. Lashkaryov Institute of Semiconductor Physics, NAS of Ukraine, Kiev, Ukraine*

<sup>2</sup>*State Enterprise Research Institute “Orion”, Kiev, Ukraine*

<sup>3</sup>*Ioffe Physico-Technical Institute of RAS, Sankt-Peterburg, Russia*

<sup>4</sup>*Close Corporation “Elma-Malakhit”, Moscow, Zelenograd, Russia*

The importance of researches of ohmic contacts to GaN epitaxial layers is dictated by difficulties of making of heat-resistant reproducible low-resistance ohmic contacts to large-area gallium-nitride epitaxial structures intended for modern manufacturing technologies.

The  $n^+ - n - n^+$ -GaN–Al<sub>2</sub>O<sub>3</sub> heteroepitaxial structure, with dislocation density in GaN of  $\sim 10^8$  cm<sup>-2</sup>, was grown on an Al<sub>2</sub>O<sub>3</sub> substrate (thickness of  $\sim 400$  μm) using MOCVD technique. The layer parameters are as follows:  $n^+ \sim 10^{18}$  cm<sup>-3</sup>, thickness  $d_{n^+} \approx 0.8$  μm;  $n \sim 10^{17}$  cm<sup>-3</sup>,  $d_n \approx 1.5$  μm; the buffer layer  $n^+ \approx 10^{18}$  cm<sup>-3</sup>,  $d_{n^+} \approx 3$  μm. Metallization was deposited by magnetron sputtering of the layers Ti(50 nm)-Al(20 nm)-TiB<sub>x</sub>(100 nm)-Au(200 nm). Ohmic contacts were formed after thermal annealing at  $T = 900$  °C for 30 s in the nitrogen atmosphere. The contact structures were formed using photolithography. The upper estimate of contact resistivity  $\rho_c$  was performed using the radial TLM (Transition Line Method). Microwave treatment of the samples under investigation was made in free space with magnetron radiation (frequency of 2.45 GHz, emittance of 1.5 W/cm<sup>2</sup>) for 1-1000 s.

From our experimental results, it follows that the following three sections may be separated in the  $\ln(\Delta RT)$  vs  $q/kT$  curve for the initial sample, here  $\Delta R$  is the difference between the total resistances. The first one (77-170 K) is a section where  $\rho_c$  practically does not depend on temperature (tunneling mechanism). The second one (170-270 K) is an activation section, with activation energy of  $\sim 0.23$  eV (thermionic-field-emission mechanism). The third section (270-375 K) is characterized by growth of  $\rho_c$  with temperature (metallic conductivity). After microwave treatment for 60 s, the second section became shorter (160-180 K), with activation energy of  $\sim 0.28$  eV. The third section (180-375 K) was characterized by a weak temperature dependence of  $\rho_c$ . After microwave treatment for 1000 s, the tunneling mechanism of current transport was observed in the 77-154 K temperature range, and the thermionic-field-emission mechanism with activation energy of  $\sim 0.10$  eV was realized in the 140-175 K temperature range, while weak temperature dependence of the curve  $\ln(\Delta RT)$  vs  $q/kT$  was observed in the 175-375 K temperature range. After nine months of sample keeping at room temperature, the tunneling mechanism of current transport dominated over the whole temperature range used (77-375 K).

## Optical properties of a DC magnetron sputtered TiO<sub>2</sub> thin film

Brus V.V.

*Frantsevich Institute for Problems of Materials Science, NAS of Ukraine, Chernivtsi, Ukraine*

Titanium dioxide (TiO<sub>2</sub>) is one of the most promising materials among transparent, conductive oxides. TiO<sub>2</sub> thin films are intensively used in different optical and photoelectric devices due to their high transparency for visible light, large value of refractive index and controllable specific electric resistance. These properties enable TiO<sub>2</sub> thin films to be applied in antireflective coatings, optical filters, wide band gap “windows” for solar cells, etc. [1,2].

A number of techniques are used for TiO<sub>2</sub> thin films preparation, in particular, magnetron sputtering, electron-beam evaporation, spray pyrolysis etc..

Investigation of the structural, electrical and optical properties of TiO<sub>2</sub> thin films is very important for their efficient practical application.

This work deals with determining of optical properties of a TiO<sub>2</sub> thin film deposited by DC reactive magnetron sputtering technique by employing the envelope method [3, 4].

The titanium dioxide thin film deposition was carried out using a universal coating system Laybold – Heraeus L560 by DC reactive magnetron sputtering of a pure titanium target in a constant pressure atmosphere of argon and oxygen gas.

It is worth noting that any additional heating of the substrate wasn't applied. The equilibrium temperature of the substrate induced by the technological heat was 250°C.

During the deposition process, the partial pressures of argon and oxygen were equal to  $5 \cdot 10^{-3}$  and  $4 \cdot 10^{-4}$  mbar, respectively. Set up magnetron power was 250 W. The deposition process lasted for 20 minutes.

The transmission spectrum of the TiO<sub>2</sub> thin film was obtained by means of a CФ-2000 spectrophotometer. The experimental data were measured within the range of wavelength from 200 to 1100 nm with 1 nm step.

The transmission spectrum of the TiO<sub>2</sub> thin film possessed periodic picks and valleys caused by interference effects. The envelope method was applied to determine the thickness of the film  $d$  and main optical constants as functions of wavelength, in particular, the refractive index  $n(\lambda)$ , absorption coefficient  $\alpha(\lambda)$  and extinction coefficient  $k(\lambda)$ . The density of the thin film was calculated,  $\rho = 3.72 \text{ g/cm}^3$ .

The TiO<sub>2</sub> thin film was established to be an indirect band semiconductor with the band gap energy  $E_g = 3.15 \text{ eV}$ .

1. Diebold U. The surface science of titanium dioxide // Surface Science Reports. – 2003. – V. 43. – P. 53-229.
2. Soga T. Nanostructured Materials for Solar Energy Conversion // Elsevier, Amsterdam. – 2006. – P. 615.
3. Sanchez-Gonzalez J., Diaz-Parralejo A., Ortiz A.L. Determination of optical properties in nanostructured thin films using the Swanepoel method // Applied Surface Science. – 2006. – V. 252. – P. 6013-6017.
4. Gumus G., Ozkendir O.M., Kavak H., Ufuktepe Y. Structural and optical properties of zinc oxide thin films prepared by spray pyrolysis method // Journal of Optoelectronics and Advanced Materials. – 2006. – V. 8, № 1. – P. 299-303.

## Chemical etching of doped by IV<sup>th</sup> group impurities CdTe single crystals using (NH<sub>4</sub>)<sub>2</sub>Cr<sub>2</sub>O<sub>7</sub>–HCl aqueous solutions

Chukhnenko P.S.<sup>1</sup>, Tomashik Z.F.<sup>1</sup>, Ivanitska V.G.<sup>2</sup>, Tomashik V.M.<sup>1</sup>

<sup>1</sup>*V.E. Lashkaryov Institute of semiconductor Physics, Kyiv, Ukraine*

<sup>2</sup>*Yurriy Fedkovych Chernivtsi National University, Chernivtsi, Ukraine*

The nature and mechanism of the chemical dissolution of doped by IV<sup>th</sup> group elements (Ge, Sn, Pb) and undoped cadmium telluride single crystals in aqueous solutions of (NH<sub>4</sub>)<sub>2</sub>Cr<sub>2</sub>O<sub>7</sub> – HCl had been investigated. The surface condition after etching was studied using metallographic analyses.

Experiments were hold by using the method of rotated disk on the chemical-dynamical polishing equipment in the range of temperatures 285 – 306 K and the rate of disk rotation within the limits of  $\gamma = 46 - 123 \text{ min}^{-1}$ . The rate of crystals dissolution was determined by the time indicator with exactness  $\pm 0.5$  mkm using the crystals thickness difference before and after etching. Etchant mixtures were prepared using 38 % HCl, 26% solution of (NH<sub>4</sub>)<sub>2</sub>Cr<sub>2</sub>O<sub>7</sub>.

We defined the region of polishing solutions, which is within the limits of 70 – 95 vol.% (NH<sub>4</sub>)<sub>2</sub>Cr<sub>2</sub>O<sub>7</sub> in etching composition by the exploring of concentration range 40 – 95 vol.% (NH<sub>4</sub>)<sub>2</sub>Cr<sub>2</sub>O<sub>7</sub> in the binary etching mixture (NH<sub>4</sub>)<sub>2</sub>Cr<sub>2</sub>O<sub>7</sub> – HCl. The chemical etching rate of crystals in polishing range is 3.7 – 9.8 mkm/min. The crystal surfaces after etching have a metallic brilliance like a mirror. About unpolishing solutions the etching rate hold to 2.5 mkm/min, in so doing the state of crystal surfaces get worse up to the grey mat coating.

The highest quality surface was obtained with a solution of 70 vol.%(NH<sub>4</sub>)<sub>2</sub>Cr<sub>2</sub>O<sub>7</sub> – 30 vol.%HCl. It was defined that process of dissolution CdTe, CdTe(Ge), CdTe(Sn), CdTe(Pb) in this etchant is limited by the diffusion stages, because the apparent energy of activation is 13,2 – 16,5 kJ/mol. To support this information we got the linear dependence between: 1) the dissolution rate and the rate of disk rotation (in the range  $\gamma = 40 - 123 \text{ min}^{-1}$ ); 2) the dissolution rate and the temperature (in the range  $T = 285 - 305.5 \text{ K}$ ).

The etching rate changes upon stirring from 7.8 to 10.5 mkm/min for undoped CdTe and from 6.8 to 12.7 mkm/min for doped CdTe. The etching rate with stirring at 306 K is 12.5 mkm/min, which is about 1.5 times faster that one at 285 K. The dissolution rate of doped CdTe crystals changes in the next range: CdTe(Ge) > CdTe(Sn)  $\approx$  CdTe > CdTe(Pb).

The etchant system composed of (NH<sub>4</sub>)<sub>2</sub>Cr<sub>2</sub>O<sub>7</sub> – HCl aqueous solution provides the high quality of etched surfaces doped and undoped CdTe and this system is characterized by the low rate of etch up to 10 mkm/min, therefore it can be used for the finishing crystals and films polishing. Also the solutions of this system can become the base for the etching of semiconductors A<sup>II</sup>B<sup>VI</sup> type by the chemical-mechanical polishing.

## Double pulse laser quantitative layer-by-layer analysis of brass and bronze micron coatings

Ermalitskaya K.

*Belarusian State University, Minsk, Belarus*

Double pulse laser spectroscopy is method of quantitative analysis based on a evaporation of substance and an excitation of atomic spectra of elements by double laser pulse divided by microsecond interpulse delay. The main advantage of this method is small destruction of sample surface during analysis. All experiments were performed on laser double pulse spectrometer LSS-1 (production of the joint Belarusian-Japanese enterprise LOTIS), which enables a layer-by-layer analysis of coating without additional surface pretreatment.

The potentialities of the LSS-1 two-pulse laser spectrometer are demonstrated by the quantitative layer-by-layer analysis of brass and bronze coatings for steel wire, produced by the Belarusian metallurgic plant (Zhlobin, Belarus) and used in manufacturing of metal cord for tire production. Fig. 1 shows the element concentrations (copper Cu, tin Sn, zinc Zn, and iron Fe) as a function of the depth in coatings with a thickness of 2.5  $\mu\text{m}$  (brass-plated wire) and 1.5  $\mu\text{m}$  (bronze-plated wire). A bronze coating of flanged wire consists of copper Cu and tin Sn, and bronze coating consists of copper Cu and zinc Zn; the total content of the remaining elements being below tenths of a percent.

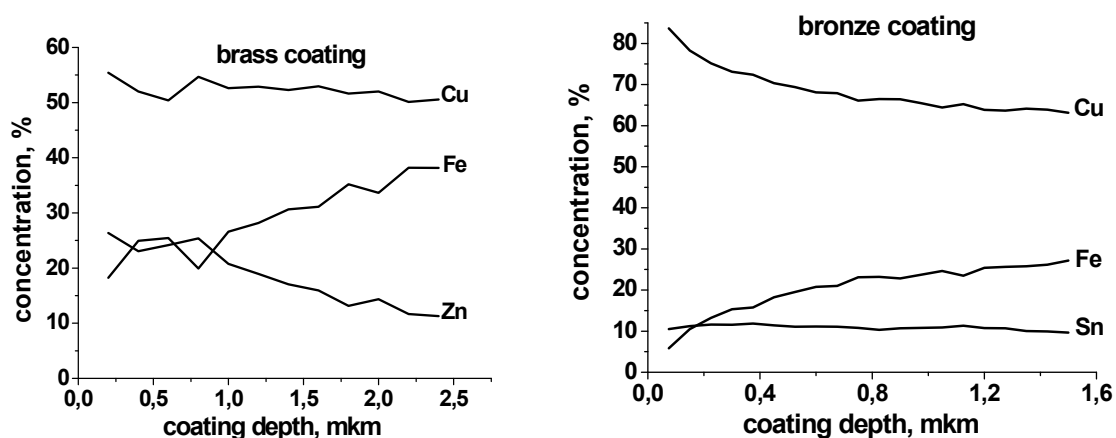


Fig. 1 Concentrations of the elements versus the depth of brass and bronze coatings for steel wire.

Growing concentrations of iron in depth of the coating point to the fact that in the coating Fe is present not as an accidental impurity but due to the surface irregularity of steel wire increasing with the depth. In the process of bronze or brass wire drawing to produce metal cord, size of irregularities on the surface of steel wire is decreased contributing to higher quality of the coatings and better mechanical characteristics.



## Detection of growth additives in YIG films by optical methods

Garpul O.Z., Solovko Y.T.

*Precarpathian National University named after V. Stefanyk, Ivano-Frankivsk, Ukraine*

The presence of growth defects in single crystal ferrite films leads to the violation of local charge neutrality and the distortion of their crystal lattice. Furthermore, because of technological factors, ions are always present in the films. Thus, their influence on properties iron garnets can be reduced only to a certain theoretical minimum [1].

The objective of our investigation is to identify these impurities, as well as establishing their depth distribution using optical methods such as X-ray photoelectron spectroscopy (XPS) optical spectrometry and optical microscopy. The samples under investigation were 4.28 mm thick single crystalline YIG films (with lattice constants of  $a_{pl}=12,3697\text{Å}$ ), grown by liquid phase epitaxy on (111) gadolinium-gallium garnet substrates ( $\text{Gd}_3\text{Ga}_5\text{O}_{12}$ ,  $a_{pd}=12,382\text{Å}$ ). The measurements were carried out using a Kratos Axis Ultra X-ray photoelectron spectrometer. IR absorption spectra in the range of  $400\text{-}4000\text{ cm}^{-1}$  were recorded at room temperature using an Thermo-Nicolet infrared Fourier spectrometer. Absorption spectra in the range  $10000\text{-}50000\text{ cm}^{-1}$  were recorded using a Percin-Elmer Lambda Bio-40 spectrophotometer. A MC 300X MET metallographic microscope was used to detect modification of surface properties of the films caused by impurities.

The presence of growth impurities in the films under investigations ( $\text{Pb}^{2+}$ ,  $\text{Pb}^{4+}$ ,  $\text{B}^+$ ,  $\text{Pt}^{4+}$ ,  $\text{Ir}^{4+}$  platinum and other) is caused by synthesis conditions (e.g. solvent type, choice of crucible, amount of supercooling, the nature post processing). XPS measurements have shown the presence of iridium ions in the films ( $\text{Ir}_{4f_{5/2}} - 62\text{eV}$ ,  $\text{Ir}_{4d_{5/2}} - 298\text{eV}$ ,  $\text{Ir}_{4p_{3/2}} - 494\text{eV}$ ), while  $\text{Pb}^{2+}$ ,  $\text{Pb}^{4+}$ ,  $\text{B}^+$  and  $\text{Pt}^{4+}$  ions have not been found. The measurement depth was  $\sim 30\text{Å}$ . Optical spectrometry also found no sign of lead ions throughout the entire film depth. The platinum ions were not detected in the recorded spectra due to complexity of their complexity of optical signature. Optical microscopy allows clear observations of  $\text{Ir}^{4+}$  inclusions (Fig. 1), which are significant enough to substantially distort anisotropic lattice structure of garnets.

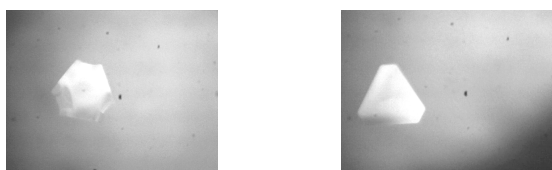


Fig. 1. The inclusion of iridium observed by microscope MC 300X MET.

In conclusion, our study demonstrates how the depth distribution of growth defects can be measured quantitatively using a combination of previously described measurement techniques. It is important to point out that no single technique is sufficient for this purpose. Instead the results from all techniques must be analyzed together. Thus, this investigation develops a methodology to monitor the distribution of growth defects in iron garnet films which is crucial for a number of practical applications.

1. Randoshkin V.V., Chervonenkis A.Ya. Applied mahnytoptyka. – M. Energoatomezdat. – 1990. – . 320p.

## Effect of heat treatment on infrared reflection, surface structure and chemical composition of PbTe films

Harbachova A.N.<sup>1</sup>, Malashkevich G.E.<sup>1</sup>, Freik D.M.<sup>2</sup>

<sup>1</sup>*B.I. Stepanov Institute of Physics of the NAS of Belarus, Minsk, Belarus*

<sup>2</sup>*Physical-chemical Institute at the Vasyl Stefanyk Precarpathian National University, Ivano-Frankivsk, Ukraine*

Narrow gap lead chalcogenide semiconductors and structures on their basis are promising for infrared applications, such as infrared photodetectors and injection lasers for terahertz range. In addition, these compounds attract a great attention due to their thermo-electric properties in middle region of temperatures (600-850 K).

In present work we investigated the effect of air heat treatment on surface microstructure, chemical composition and optical properties in middle IR-range of PbTe films. The films under investigation were prepared by means of precipitation from the gas – dynamical steam on glassy substrates and their thicknesses were about  $\sim 0.1 \mu\text{m}$ . These films were subjected to further annealing in the air at 300, 350 and 400°C. The investigation was carried out using LEO – 1420REM scanning electron microscope and «Nicolet Nexus» (USA) FTIR spectrometer.

It was found out that the heat treatment applied exerts strong effect on PbTe films IR reflection (Fig. 1) as well as their chemical composition and surface microstructure. Thus, the content of Pb relatively to total Pb+Te amount varies from 72.21 to 77.34% and from 67.73 to 76.23% for the films precipitated on substrates at temperatures 90°C (Fig. 1a) and 60°C (Fig. 1b), respectively. It's necessary to emphasize that the effect of treatment temperature on samples IR reflection and chemical composition is not linear and IR shift direction correlates with the relative amount of Te in the films. The reasons of discovered effect are discussed.

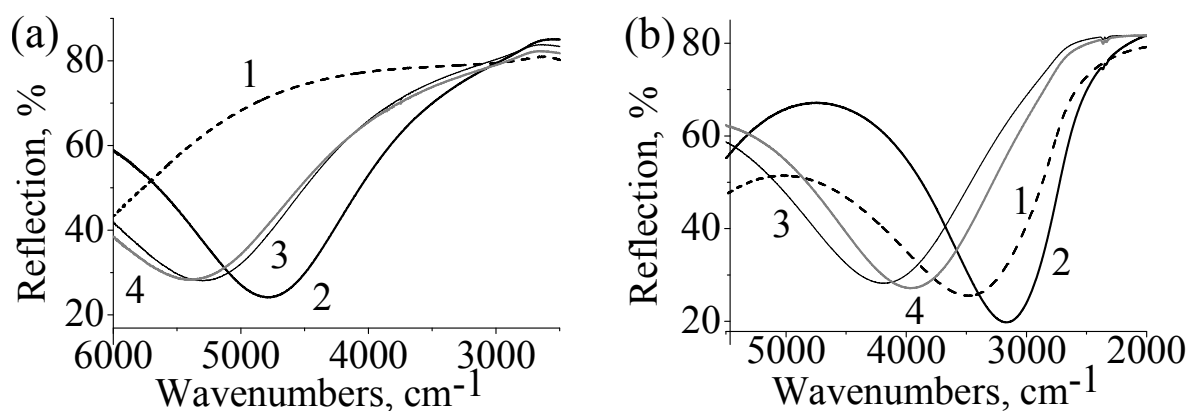


Fig. 1. Infrared reflection spectra of PbTe films before (1) and after annealing in the air at 300 (2), 350 (3) and 400°C (4).

## Nitrogen and aluminum doping of ZnO films by magnetron sputtering of Zn targets containing different amount of Al

Ievtushenko A.I.<sup>1</sup>, Lashkarev G.V.<sup>1</sup>, Lazorenko V.I.<sup>1</sup>, Khyzhun O.Y.<sup>1</sup>, Klochkov L.O.<sup>1</sup>, Bykov O.I.<sup>1</sup>, Tkach V.M.<sup>2</sup>, Kutsay O.M.<sup>2</sup>, Starik S.P.<sup>2</sup>

<sup>1</sup>Frantsevich Institute for Problems of Materials Science, NASU, Kyiv, Ukraine

<sup>2</sup>Bakul Institute for Superhard Materials, Kyiv, Ukraine

The ecological and economic benefits of zinc oxide (ZnO) which has physical properties similar to GaN makes it promising for devices optoelectronics, acoustooptics, photonics, etc. Therefore the last decade the investigation of ZnO attracts the attention of many researchers around the world: about 10 000 publications devoted to the study of this material are produced each year accordingly to Scopus search. The properties of ZnO strongly depend on the concentration of donor intrinsic defects which always exist in as-grown oxide. This leads to the problems of deposition high quality ZnO films, including of p-type ones doping, controlling of their characteristics, etc. So the important task of present ZnO materials science is the control of defect concentration in ZnO films by improvement of deposition and doping technologies as well as further treatment techniques.

Therefore to solve these problems, we carried out ZnO doping by donor impurity of aluminum and by acceptor impurity of nitrogen. To improve quality of ZnO films all ones were deposited by the layer by layer growth approach [1] in reactive magnetron sputtering using Zn, Zn:0.7 %Al or Zn:1.4 %Al targets. In order to minimize the doping effect on the quality of the ZnO films the doping was carried out *in-situ* at the growth of films.

In order to increase nitrogen solubility in ZnO and therefore reach higher compensation of donor: we increased nitrogen pressure in the working chamber as well as carried out Al-N codoping. ZnO:N films with different nitrogen concentrations were deposited on Si, SiN<sub>x</sub> and quartz substrates. The investigations of XRD, EDX, AFM, transmittance spectra, X-ray photoelectronic and Fourier transform infrared spectroscopy were carried out. The influence of different amount of nitrogen dopant on the structure, optical properties and morphology of ZnO:N films caused by changing defect concentration will be presented.

The increasing of the concentration of donor impurities in ZnO is a promising for development effective transparent conductive films on its basis. Therefore the high quality aluminum doped ZnO films were deposited on glass substrates. We report the influence of changing oxygen pressure on structural, morphological, electrical and optical properties of ZnO:Al films. Our investigations of ZnO:Al films deposited by magnetron technology will be discussed as well as the prospects of their applications.

1. A.I. Ievtushenko, V.A. Karpyna, V.I. Lazorenko, G.V. Lashkarev, et al. Thin Solid Films. – 2010. – V.518, №16. - P. 4529-4532.

## The channels of strain relaxation in InGaN/GaN and AlN/GaN multilayer structures

Kladko V.P., Kuchuk A.V., Safriuk N.V., Belyaev A.E.

*V. Lashkaryev Institute of Semiconductors Physic, National Academy of Science of Ukraine, Kyiv, Ukraine*

The strain relaxation mechanisms of heterostructures define their structure properties and possibility of implementation in devices. This is extremely important for III-nitride structures with hexagonal structure.

The influence of initial state of template, density of dislocation, thermal strain and density of cracks on strain level of SL's grown by MBE on different templates have been investigated (Fig.1). Structural perfection of the SL structures is strongly dependent on the initial strain state of template/buffer system. It was shown the role of dislocations and cracks in relaxation processes and explained the reason of their propagation [1, 2].

We find that for growth on AlN templates, the structure is crack-free with the excess of strain revealed by the formation of misfit dislocations. However, for growth on GaN templates, the higher initial strain in the SL layers leads to cracking of the film. In this case, though the material between the cracks is left with fewer dislocations. The role of thickness variations barrier/well on the strain level and of SL's system was established and discussed for the first time. It is important to point out that the above described changes in the thickness of the SL barriers and wells considerably affect the position of the GaN/AlN SL's electronic miniband [2].

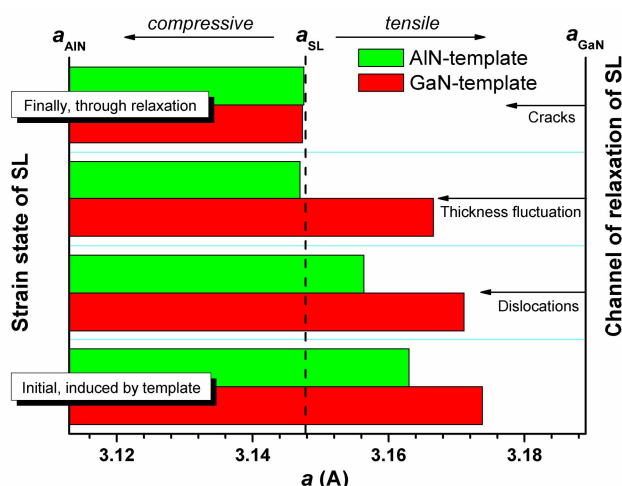


Figure 1. Variation of the in-plane lattice parameters of GaN/AlN SLs grown on GaN- and AlN-template. The lattice parameters of relaxed AlN ( $a_{\text{AlN}}$ ) and GaN ( $a_{\text{GaN}}$ ) are indicated by solid lines. The dashed line corresponds to in-plane lattice parameter ( $a_{\text{SL}}$ ) for completely relaxed symmetrical SL ( $t_{\text{GaN}} = t_{\text{AlN}} = 1.98 \text{ nm}$ ).

1. V. P. Kladko, A. V. Kuchuk, N. V. Safriuk, V. F. Machulin, A. E. Belyaev, H. Hardtdegen, S. A. Vitusievich. // Appl. Phys. Lett. –2009. – **95**. – 031907.
2. V.P. Kladko, A.V. Kuchuk, N.V. Safriuk, V.F. Machulin, P.M. Lytvyn, V.G. Raicheva, A.E. Belyaev, Yu.I. Mazur, E.A. DeCuir Jr, M.E. Ware, G.J. Salamo / J. Phys., D: Appl. Phys. – 2011. – **44**. – 025403.

## Application of diamond-like carbon films as antireflection coatings for thin film solar cells

Klyui N.I.<sup>1</sup>, Severinova I.D.<sup>1</sup>, Kolomzarov Yu.V.<sup>1</sup>, Khripunov G.S.<sup>2</sup>,  
Klyui A.N.<sup>3</sup>, Staschuk V.S.<sup>3</sup>

<sup>1</sup> V. Lashkarev Institute of Semiconductor Physics National Academy of Sciences of Ukraine, Kiev, Ukraine

<sup>2</sup> National Technical University "Kharkiv Polytechnic Institute", Kharkiv, Ukraine

<sup>3</sup> Taras Shevchenko Kyiv National University, Kiev, Ukraine

Thin film solar cells (SCs) based on CdS/CdTe, CIS or CIGS structures are widely used now in semiconductor solar power engineering. Sometimes, the SCs are created even on flexible substrates. Very important task in such technology is development of highly conductive and transparent continuous front contacts. Such contacts are used because of low diffusion length of non-equilibrium carriers for the semiconductor films. Very perspective material for the contact is Al-doped ZnO (AZO) films. Refractive index of the films is close to 2.0 and may reach 2.3 in dependence on deposition method. Therefore, rather significant reflection losses in the spectral region where the SCs are sensitive exist. For the first time, we propose to use diamond-like carbon (DLC) films with low refractive index as antireflection coatings for the thin film SCs. The DLC films were deposited by PE-CVD method on AZO-glass structures. The transparency spectra and optical properties of the AZO and DLC films were also studied. It has been shown that due to application of the DLC films transmittance of front AZO contacts may be substantially improved. In particular, in spectral region 430-850 nm (region of CdS/CdTe based SC photosensitivity) integral increasing of transmittance may exceeds 10% (fig. 1). As a result short circuit current and efficiency of thin film SCs may be also

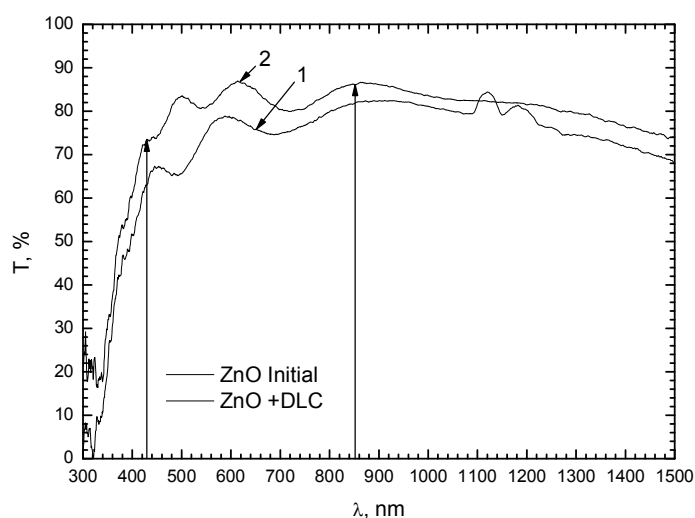


Fig. 1. Transparency of ZnO films (18 Ohm/sq): 1 – initial; 2 – covered by DLC film. Vertical arrows show region of photosensitivity for CdS/CdTe based SCs.

improved. The work was supported by Science and Technology Center in Ukraine (project #4301).

## Investigation of $p$ - $n$ junction temperature and thermal parameters of semiconductor devices

Kudryk Ya.Ya.

*V. Lashkaryov Institute of Semiconductor Physics, NAS of Ukraine, Kyiv, Ukraine*

The  $p$ - $n$  junction temperature dynamics was investigated for various semiconductor devices, in particular, p-i-n diodes and white LEDs. The specificity of studies of chip thermal resistance was shown for the devices under consideration. The results of investigations of pulsed  $I$ - $V$  curves of a white LED as function of heat sink temperature as well as  $p$ - $n$  junction temperature as function of time are presented in Fig. 1.

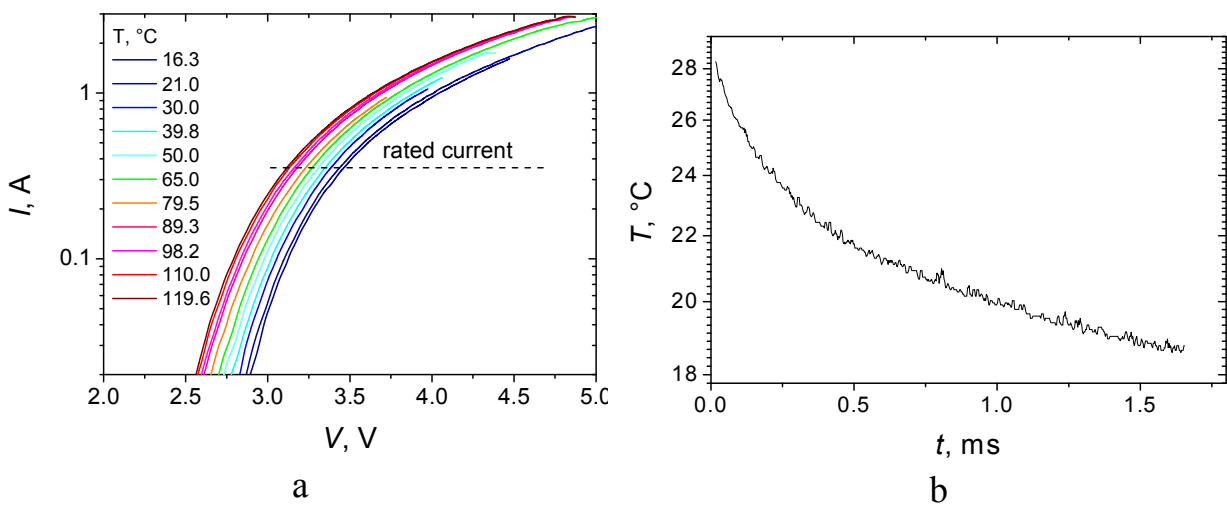


**Fig. 1.** Pulsed  $I$ - $V$  curves of a LUW\_W5AM Golden Dragon plus LED (rated current of 350 mA, pulse duration  $\tau = 10 \mu\text{s}$ ) in the 16–119 °C temperature range (a); kinetics of LED temperature relaxation (b).

To construct correctly a thermal model, one should determine the areas of thermal power release ( $p$ - $n$  junction, semiconductor bulk, ohmic contacts). A considerable part of power is dissipated at the series resistance (semiconductor and ohmic contacts) even at the rated current. The portion of energy dissipated in each of the areas may vary over a wide range, depending on the bias amplitude; thus, investigation of the  $p$ - $n$  junction temperature is possible at small biases only (Fig. 1a). At the same time, to heat the  $p$ - $n$  junction up to the maximal operating temperature, the currents much over the rated one are required. The thermal relaxation kinetics enables one to separate the thermal parameters of the semiconductor chip and package as well as to predict device failures.

## Present state of the art of amorphous carbon films

Kutsay O.M., Novikov M.V., Gontar O.G., Starik S.P., Gorohov V.Yu.,  
Garashchenko V.V., Tkach V.M.

*Institute for Superhard Materials of the National Academy of Science of Ukraine,  
Kyiv, Ukraine*

The historical beginning of the carbon films chronology starts from P. DeWilde, A. Thenard and C.R. Hebd publications in 1874. The authors have shown a hard film formation at an electrical discharge in hydrocarbon vapor. Now we classify such films as the hydrogenated amorphous carbon films enriched with oxygen. Thus today the carbon film celebrates 137-th anniversary. During long time the carbon films were regarding as the useless surface pollutions. For the first time their useful practical application was considered in the 60-th years of last century. The polymer-like amorphous carbon films have been used as the dielectric layers in electronic devices. It is important to note, that by the CVD technologies we always deposit hydrogenated carbon (a-C:H) film only. But initially for the PVD technology it is a hydrogen-free amorphous carbon (a-C) film producing. The first PVD a-C films were deposited and reported by S. Aisenberg and R. Chabot (USA) in 1971 by a carbon ion beam accelerated to a negatively biased substrate. They give designation “diamond-like” for the carbon film due to its properties that stack up to those of diamond: high hardness, high wear resistance, low friction coefficient, chemical inertness, high electrical resistivity and IR optical transparency. From this moment the interest to such films grows in a huge degree. The diamond-like properties of the films have stimulated a lot of research on their deposition and characterization, and on the development of possible applications. The special place in a carbon film family occupies a tetrahedral amorphous (ta-C) film with more than 80 % of tetrahedral carbon bonds. In relation with above it is important to recollect I.I. Aksenov, et al. (Ukraine) pioneer work in 1978. For the first time they report about the tetrahedral carbon film deposition by the filtered cathodic vacuum arc (FCVA) plasma beams. Thus we can claim today that the properties of amorphous carbon films cover a wide range of values between those of diamond, graphite and hydrocarbon polymers.

By the own experience in carbon CVD and PVD coating technology [1-7] we critically analyze nowadays and possible future of amorphous carbon film practical applications.

1. Novikov N.V., Gontar A.G., Khandozhko S.I., et al. // *Diamond Rel. Mater.* **9** (2000) 792.
2. Romanko L.A., Gontar A.G., Kutsay A.M., et al. // *Diamond Rel. Mater.* **9** (2000) 801.
3. Kutsay O.M., Gontar A.G., Novikov N.V., et al. // *Diamond Rel. Mater.* **10** (2001) 1846.
4. Kutsay O., Bello I., Lifshitz, et al. // *Diamond Rel. Mater.* **12** (2003) 2051.
5. Luk W.Y., Kutsay O., Bello I., et al. // *Diamond Rel. Mater.* **13** (2004) 1427.
6. Kutsay O., Loginova O., Gontar A., et al. // *Diamond Rel. Mater.* **17** (2008) 1689.
7. Fodchuk I.M., Tkach V.M., Ralchenko V.G. et al. // *Diamond Rel. Mater.* **19** (2010) 409.

## Effect of thermal annealing on the electrical parameters of ohmic contacts to $n-n^+-n^{++}$ -InP

Novytskyi S.V.

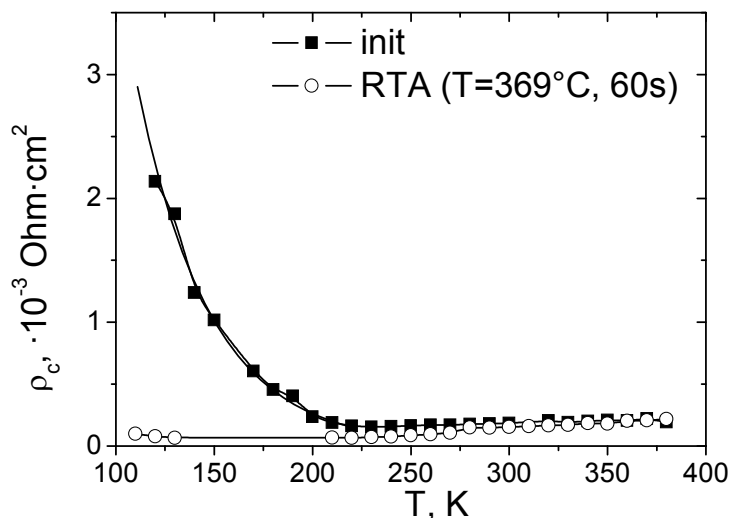
*V. Lashkaryov Institute of Semiconductor Physics, NAS of Ukraine, Kyiv, Ukraine*

It is known that InP practically is not exceeded by GaAs in bandgap and charge carrier mobility, while outperforming it in drift velocity and thermal conductivity. This makes InP promising for development of highly efficient short mm-wave Gunn diodes.

To take advantage of the merits of this material, it is necessary to develop reliable thermally stable ohmic and barrier contacts to InP. One of the ways for solution of this problem is application of multilayer contact structures with refractory metals and their compounds as diffusion barriers [1, 2].

We studied  $I$ - $V$  curves and temperature dependence of contact resistivity  $\rho_c$  in the 100–380 K range for Au(500Å)–Ge(500Å)–TiB<sub>2</sub>(1000Å)–Au(2000Å) ohmic contacts to InP, both before and after rapid thermal annealing (RTA) at a temperature of 369 °C for 60 s. The thickness of  $n-n^+$  epitaxial layers was  $d = 2 \mu\text{m}$ ; the dopant concentration in them was  $N_D = 9 \times 10^{15} \text{ cm}^{-3}$ .

For initial (before RTA) layer,  $\rho_c$  decreased as temperature grew from 120 K up to 220 K. This may be owing to the thermionic mechanism of current transport. In the 220–380 K temperature range,  $\rho_c$  did not vary considerably. This may indicate the field mechanism of current transport. For a sample subjected to RTA (369 °C, 60 s),  $\rho_c$  remained practically unchanged over the whole temperature range.



1. W.C. Huang Effect of Au overlayer on PtSi ohmic contacts with  $n$ -InP // Applied Surface Science 245. – 2005. – P.141-148.
2. O.A. Ageev, A.E. Belyaev, N.S. Boltovets, R.V. Konakova, V.V. Milenin, V.A. Pilipenko Interstitial Phases in Technology of Semiconductor Devices and VLSI (in Russian). – 2008. – P. 104-108.



## **Analysis of deformation and stress in silicon single – layer epitaxial structures**

Oksanich A.P., Petrenko V.K., Sedin Y.A.<sup>1</sup>

*Kremenchug Mikhail Ostrogradskiy National University,  
Kremenchug, Ukraine*

<sup>1</sup>*Krivoi Rog Institute of Kremenchug University of Economics, Information Technologies and Management, Krivoi Rog, Ukraine*

There is a tendency in the production of silicic single-layer epitaxial structures (SSES) to install the equipment with high efficiency with the diameter (100 – 200 mm). It leads to the additional requirements to the alteration of form, thermal stress, developed in the process of heating and as a result, the unacceptable large number of structural breach appear in the sort of accumulations, slip lines and other structural breaches.

The theoretical and practical results of the reseach of thermal field in spherically curved SSES which are on the surfase of hot pedestal are presented in this paper.

They think that SSES exexchange heat with pedestal through heat radiation. Heat exchange at the expense of conductance between SSES and surrounding gas is taken into account.

Calculated values of temperature show that the temperature depends on the radius of approximally parabolically. Besides the reseaches of averege in thickness of SSES temperature, in this paper such temperature distributions in thickness of SSES in assumption are examined. In each point the temperature is distrsbuted as a parabola of vertical applicate with the coefficient which depends on radial applicate. The equation of these coeficients are obtained.

The definite dependence of the SSES deformation from the temperature distribution by radius is defined. Radial gradient of the temperature which causes additional curve is taken into account.

Calculations of temperature distrsbution for a large size pedestal are given.

Heat exchange of radiation from the oufer surface of warmed-up pedestal and a compound radiation of compound exchange is taken into account.

It leads to the formation of complex shapes of lending and heighten values of inner tension.

## Method of undestroying control of remaining stresses in single – layer epitaxial structures

Oksanich A.P., Pritchyn S.E.

*Kremenchug Mikhail Ostrogradskiy National University, Kremenchug, Ukraine*

As it's generally known, the presence of internal stresses in silicon structures can considerably decrease the margin of mechanical safety of structure.

Solution of the internal stresses determination task, caused by the technological operations of single-layer epitaxial structures (SSES) making by a non-destructive method, allows to get additional data, characterizing trouble in the process of these operations while SS surface processing.

For the SSES round wafer the size of remaining stresses in the value can be defined as follows:

$$\sigma(\alpha) = \frac{E}{3b^2(1-\nu)} \left[ (h-a)^2 \frac{dW(\alpha)}{d\alpha} - 4(h-a)W(\alpha) + 2 \int_0^a W(\xi) d\xi \right], \quad (1)$$

where E is the module Jung;  $\nu$  – coefficient of Poisson; b - is a radius of wafer; h is a thickness of wafer;  $W(\alpha)$  – is a bend of wafer after a layer removing with thickness  $\alpha$ .

For the decision of task of non-destructive control of remaining tension in SSES we worked out a method, which computer is the basis of - controlled infrared polariscope realized in the automated complex offered by us [1]. The got results are presented on picture 1.

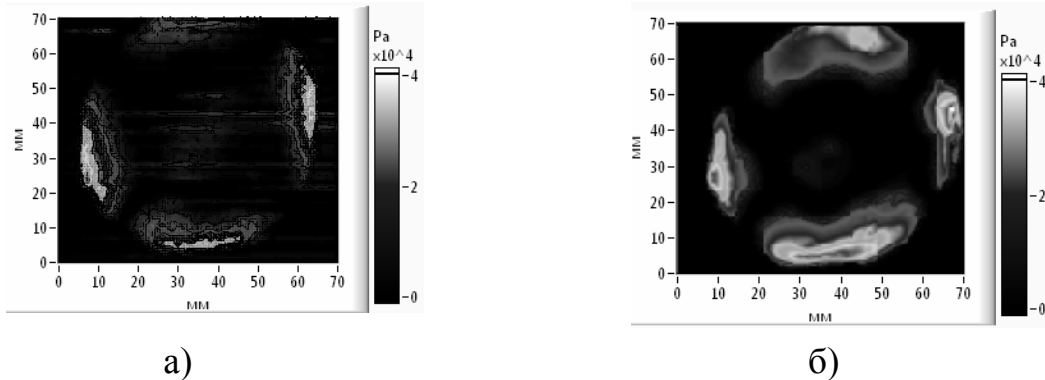


Fig. 1. Remaining tensions are in SSES: a) SSES with a legitimate value ( $>2,5 \times 10^4 \text{Pa}$ ), б) SSES with a border value ( $<3 \times 10^4 \text{Pa}$ ).

1. А.П.Оксанич. Автоматизированный комплекс для измерения внутренних напряжений в пластинах GaAs / Оксанич А.П., Притчин С.Э., Краскевич В.Е., Батареев В.В.// Складні системи і процеси. – Запоріжжя. – 2006. – № 2. – С. 40-50.

## Controlled elimination of thin layers from the surfaces of Bi and Sb chalcogenides by $(\text{NH}_4)_2\text{Cr}_2\text{O}_7$ –HBr solutions

Pavlovich I.I.<sup>1</sup>, Tomashik V.M.<sup>1</sup>, Tomashik Z.F.<sup>1</sup>, Stratiychuk I.B.<sup>1</sup>,  
Kravtsova A.S.<sup>1</sup>, Kopyl O.I.<sup>2</sup>

<sup>1</sup>*V. Lashkaryov Institute of Semiconductor Physics, National Academy of Sciences of Ukraine, Kyiv, Ukraine*

<sup>2</sup>*Institute of Thermoelectric, Department of Education and Science and National Academy of Ukraine, Chernivtsi, Ukraine*

In order to develop the methods of controlled elimination of thin layers from the surfaces of  $\text{Bi}_2\text{Te}_3$ ,  $p\text{-(Bi}_2\text{Te}_3)_{0,25}(\text{Sb}_2\text{Te}_3)_{0,72}(\text{Sb}_2\text{Se}_3)_{0,03}$  and  $n\text{-(Bi}_2\text{Te}_3)_{0,9}(\text{Sb}_2\text{Te}_3)_{0,05}(\text{Sb}_2\text{Se}_3)_{0,05}$ , using etching mixtures  $(\text{NH}_4)_2\text{Cr}_2\text{O}_7$ –HBr, we have studied the dependence of etching rate ( $v$ ) on the concentration of components, temperature, stirring rate of solutions ( $\gamma$ ) and ageing time of etchant. Crystalline samples  $\text{Bi}_2\text{Te}_3$ ,  $n\text{-(Bi}_2\text{Te}_3)_{0,9}(\text{Sb}_2\text{Te}_3)_{0,05}(\text{Sb}_2\text{Se}_3)_{0,05}$  and  $p\text{-(Bi}_2\text{Te}_3)_{0,25}(\text{Sb}_2\text{Te}_3)_{0,72}(\text{Sb}_2\text{Se}_3)_{0,03}$  were grown by vertical growth zone melting of the components.

The process of chemical etching of Bi and Sb chalcogenides plates was performed on the installation for the chemical-dynamic polishing (CDP) in the temperature range 283-303 K and  $\gamma = 36\text{-}120 \text{ min}^{-1}$ . The etchants were prepared using 48 % HBr and 23 %  $(\text{NH}_4)_2\text{Cr}_2\text{O}_7$ . The dissolution rate of crystals was measured by the difference of the sample thickness before and after etching using the watch indicator 1MYHP to within  $\pm 1$  micron. Thus, in etchant compositions of  $(\text{NH}_4)_2\text{Cr}_2\text{O}_7$ –HBr in the concentration range 20-95 vol. %  $(\text{NH}_4)_2\text{Cr}_2\text{O}_7$  the semiconductor etching rate varies within: for  $\text{Bi}_2\text{Te}_3$  – (0.3-1.5)  $\mu\text{m}/\text{min}$ , for  $n$ -type – (0.4-6.2)  $\mu\text{m}/\text{min}$  and  $p$ -type semiconductors – (0.3-1.5)  $\mu\text{m}/\text{min}$  respectively, and in all the mixtures polished surface was obtained.

We have found that the process of dissolution of these materials in the polishing etchants  $(\text{NH}_4)_2\text{Cr}_2\text{O}_7$  is limited by the diffusion stages, as the calculated apparent activation energy does not exceed  $E_a = 30 \text{ kJ/mol}$ . This is confirmed by the data obtained from the dependence  $v = f(\gamma)$ .

A series of etchants for the controlled elimination of thin layers from the single crystal surfaces and films of  $\text{Bi}_2\text{Te}_3$ ,  $p\text{-(Bi}_2\text{Te}_3)_{0,25}(\text{Sb}_2\text{Te}_3)_{0,72}(\text{Sb}_2\text{Se}_3)_{0,03}$  and  $n\text{-(Bi}_2\text{Te}_3)_{0,9}(\text{Sb}_2\text{Te}_3)_{0,05}(\text{Sb}_2\text{Se}_3)_{0,05}$  at CDP rates 0.3-6.2  $\mu\text{m}/\text{min}$  and high surface quality was developed based on compositions  $(\text{NH}_4)_2\text{Cr}_2\text{O}_7$ –HBr. This is confirmed by analysis of surface microstructure using the universal stage microscope ZEISS JENATECH INSPECTION with a digital camcorder with increasing from  $25\times$  to  $1600\times$ . The method of rinsing samples after etching was elaborated: after CDP the plates should be immediately washed by the 0.05 M solution of  $\text{Na}_2\text{S}_2\text{O}_3$  and 15 % NaOH, and then rinsed with plenty of distilled water and dried up in a stream of air.

## **Modeling of the defect structure of single crystal gadolinium gallium garnet, using statistical dynamic scattering theory**

Pylypiv V.M.<sup>1</sup>, Kyslovskyy Ye.M.<sup>2</sup>, Vladimirova T.P.<sup>2</sup>, Olikhovskii S.I.<sup>2</sup>, Garpul O.Z.<sup>1</sup>

<sup>1</sup>*V. Stefanyk Prekarpathian National University, Ivano-Frankivsk, Ukraine*

<sup>2</sup>*G.V. Kurdyumov Institute for Metal Physics of NASU, Kyiv, Ukraine*

These findings lead to the conclusion that a new diagnostic method of the defect structure of real crystals with complex basis has been developed. This method allows conducting precise quantitative measurements of deformations and defects in implanted layers of garnet films, which are widely used in magnetic and magneto-optical devices.

In this work, we established a theoretical basis for the modern crystallography of real crystals with a complex basis, which takes into account the presence of various structural defects and enables us to describe in a self-consistent manner the coherent and diffuse components of diffraction patterns of imperfect crystals within the framework of statistical diffraction [1].

The complex structural factors and the Fourier components of polarizability of perfect gadolinium gallium garnet Gd<sub>3</sub>Ga<sub>5</sub>O<sub>12</sub> (GGG) crystals have been calculated for a set of reflexes and the two characteristic x-ray wavelengths. In addition, the relationships between these parameters as well as coherent diffractive components of x-ray spectra and the concentration of anti-structural defects and vacancies have been investigated.

Quantitative characteristics of the defect structure in GGG single crystals have been determined from the analysis of the measured spectra for two reflexes based on statistical dynamic theory of diffraction in imperfect crystals [2].

Optical and electron spectroscopy was used to demonstrate that garnet crystals grown by liquid phase epitaxy possess a number of various growth defects, such as inclusions, pores, dislocation loops and their complexes. This qualitative conclusion is further complemented with quantitative diagnosis of essential micro defects using a high resolution X-ray diffractometry. In this technique the average size and concentration of microdefects is computed from the analysis of the diffraction reflection curves (DRC).

1. Massa W. Crystal structure determination // Second edition, Berlin, Springer. – 2004. – P. 210.
2. Datsenko L.I., Molodkin V.M., Osinovskii M.E.: Dynamical scattering of X-rays by real crystals // Nauk. Dumka, Kiev. – 1998.

## Studying of hot wall epitaxy technological parameters and current mechanism investigation of II-VI thin film heterostructures

Semikina T.V.<sup>1</sup>, Yaroshenko M. V.<sup>1</sup>, Bobrenko Yu.N.<sup>1</sup>,  
Paszkowicz W.<sup>2</sup>, Minikayev R.<sup>2</sup>, Komashchenko V.N.<sup>1</sup>

<sup>1</sup>*V.E. Lashkaryov Institute of Semiconductor Physics, National Academy of Sciences of Ukraine, Kiev, Ukraine*

<sup>2</sup>*Institute of physics Polish Academy of Science, Warsaw, Poland*

Thin film materials II-VI, namely CdSe, CdS, ZnSe, ZnS and other are used for creation of different types of solar cells (CdS/CdTe, CuIn(Ga)S(Se)), information record devices, irradiation sensors. The development of electronics component base on materials II-VI is possible under complex studying materials properties in dependence on technological regimes of preparation. Information about mechanisms of current transport in thin film heterostructures is important for development of high speed diodes, transistors for terahertz range and etc. The presented results concern the issue of regulation of crystalline structures and film thickness due to altering of some technological parameters, and studying of current transport mechanism from current-voltage characteristics (I-V) of heterostructures based on film CdS, CdSe, ZnS.

The affects of temperature of chamber, substrate and evaporating temperature of powder in the cell on crystalline structure of CdS and CdSe films are studied by XRD methods and optical microscopy. The substrate temperature and type of substrate materials do not show the influence on the crystalline grain size of grown films that is new result which could be explained on the base of hypothesis of hot adatoms [1]. The dependence between grain size and temperature of evaporator of powder in the cell has the straight correlation before the critical temperature value when the re-evaporation process begins.

The heterostructures Mo-CdSe-ZnS-Cu<sub>x</sub>S that work as ultraviolet sensor [2] are deposited and their electrical properties are investigated. The calculation of parameters is made from dark I-V characteristics measured in temperature range from -50 °C to 30 °C. We obtained that forward current has the exponential dependence on voltage, weak temperature dependence, and constant  $d(\ln I)/dU$  at temperature altering, linear correlation between  $\ln I$  and  $T$ . Such properties are typical for tunneling – recombination mechanism of charge carriers in sheath range near of interface. The reverse current of heterostructures shows the absence of saturation current, current power dependence on applied voltage. The reverse current temperature dependence is under exponential low. Consequently, the process of thermal generation of charge is not the determinative in charge transfer.

The hot wall epitaxy technology is studied concerning the deposition of films and heterostructure based on II-VI materials. On the base of XRD measurements it is obtained that the textured films grow with preferable hexagonal phase. The observed micro crystallites consist of nanoblocks

(nanograins) and their sizes do not correlated with altering technological parameters. The main technological parameters affect on size of growing microcrystallites but do not change the preferable grow phase. The I-V analyses show that the main mechanism of charge transport is tunneling process. The predominance of tunneling in charge transfer mechanism makes a forecast that heterostructures based on materials II-VI (CdSe, CdS, ZnSe, ZnS) could be used for development of tunneling and resonance tunneling diodes and transistors for terahertz range.

1. Chopra K.L. Electrical phenomena in thin film. – Ed. ‘Mir’, M., 1972. – 432 p.
2. Bobrenko Yu.N., Yaroshenko N.V., Sheremetova H.I., Semikina T.V., Atdayev B.S. UV photodetectors based on thin films of ZnS // TKYeA. – 2009. – V. 83, №5. – P. 29-31.

## The effect of the isovalent doping with cadmium on the microstructure and UV cathodoluminescence of the ZnO films

Shtepliuk I.I.<sup>1</sup>, Lashkarev G.V.<sup>1</sup>, Khyzhun O.Y.<sup>1</sup>, Kowalski B.<sup>2</sup>, Reszka A.<sup>2</sup>, Lazorenko V.Y.<sup>1</sup>, Timofeeva I.I.<sup>1</sup>, Khomyak V.V.<sup>3</sup>

<sup>1</sup> I. Frantsevich Institute for Problems of Material Science, NASU, Kiev, Ukraine

<sup>2</sup> Institute of Physics PAS, Warsaw, Poland

<sup>3</sup> Yu. Fedkovych Chernivtsi National University, Chernivtsi, Ukraine

Among compounds belonging to the A<sup>II</sup>B<sup>VI</sup> group, ZnO is one of the most attractive functional material for semiconductor optoelectronic devices operating in blue and ultraviolet regions of the optical range. Due to its outstanding electronic properties and a variety of point defects, zinc oxide exhibits an extremely rich luminescence spectrum [1]. In this respect, the most important technological task is deposition of the ZnO films that display efficient luminescence in the desired spectral region, especially in the ultra-violet spectral range. One of the possible ways for a solution of this problem should be doping of the ZnO with isovalent impurities [2]. In our work it is shown that the isovalent impurity of the cadmium leads to a substantial improvement of the structural and optical properties of the zinc oxide film.

Table 1

The parameters of microstructure of the un-doped and ZnO: Cd films

Sample	Diffracton angle $2\theta_{(002)}$ , deg	FWHM, deg	Lattice period $c$ , nm (XRD)	Biaxial stress $\sigma$ , GPa	Grain size $D$ , nm	Dislocation density $\delta \cdot 10^{15}$ , m <sup>-2</sup>
ZnO (A)	34.54	0.74	0.518	1.33	11	8.2
0.4%Cd-doped ZnO (B)	34.51	0.35	0.5201	0.34	24	1.7

We have deposited the Cd-doped ZnO textured (002) films by the RF multistage reactive magnetron sputtering method. It was found that even small concentration of cadmium (0.4%) affects significantly on the luminescent properties of the films. The possible mechanisms of the influence of the isovalent impurity (cadmium) on the luminescent properties are discussed.

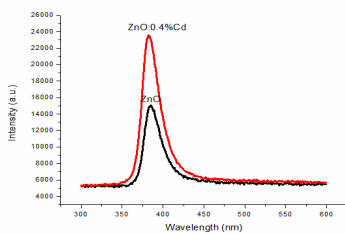


Fig. 1. CL spectra for samples A, B doped ZnO (a).

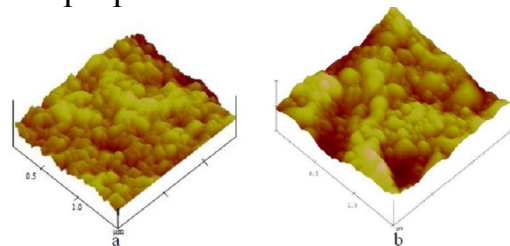


Fig. 2. AFM images of the un- and 0.4%Cd-doped ZnO (b) films.

- Ozgur U., Alivov Ya. I., Liu C., Teke A., Reshchikov M. A., Doan S., Avrutin V., Cho S-J and Morkoc H. // Appl. Phys. – 2005.– V.98. – P.041301.
- Fistul V.I. Atoms of doping impurities in semiconductors. // Fizmatlit Publ.: Moscow. – 2004.

## **Investigation of features of thin-films by electron-probe microanalysis and Auger-electron spectroscopy**

Slusar T.V.<sup>1</sup>, Legkova G.V.<sup>1</sup>, Ponomarev S.S.<sup>2</sup>, Sobolev V.B.<sup>3</sup>,  
Grebenshchikov D.V.<sup>1</sup>, Sushchenko O.N.<sup>1</sup>

<sup>1</sup>*National Aviation University, Kiev, Ukraine*

<sup>2</sup>*CJSC "Proton-21", Kiev, Ukraine*

<sup>3</sup>*Technology Center of NAS of Ukraine, Kiev, Ukraine*

Investigation into Co<sub>2</sub>CrGa thin-films has been performed by methods of different locality: electron-probe microanalysis - EPMA (microanalyzer JXA-8200) and Auger-electron spectroscopy - AES (JAMP-9500F JEOL, Japan), in order to compare characteristics of the thin-films, to analyse applicability of the methods, as well as to estimate influence of production method on characteristics of thin-films.

The longitudinal locality of EPMA ( $\sim 10^{-6}$  m) exceeds thickness of thin-films ( $10^{-7}$ - $10^{-8}$  m). Therefore composition of the thin-films has been determined by Philiber-Tixier and Reuter methods that take into account capture of substrate by the probe.

Results of analysis of the same thin-films by two methods definitely established difference between composition of the films and the initial bulk sample. It points out that technology of thin-film formation should be changed.

Results of EPMA have shown influence of thickness of thin-film deposited by material of the same composition in identical conditions. Research of the thin-films by AES has shown regular change of their composition in the longitudinal section (in depth). It evidences instability of the processes occurring during substance evaporation, and also explains the reason for differences between results of AES analysis and depth-averaged data obtained by EPMA.

It has been discovered that linear dependence of EPMA results of thin-films on the probe accelerating voltage. Along with other inappropriate factors, it indicates necessity to improve the correction method of thin-films composition, determined by EPMA.

### Conclusions

1. Deposition of thin-films by the flash-method cannot reproduce the original composition of evaporated material, and provide even change of the composition in the longitudinal section.

2. EPMA along with Philiber-Tixier and Reuter correction program can be used for research of thin-films, although it requires further improvement.

3. Optimal characteristics of thin-films is their average composition (EPMA) and gradient of composition change (AES).



## The electronic densities of states in PbTe crystal doped with Eu

Syrotyuk S.V., Shved V.M.

National University Lviv Polytechnic, Lviv, Ukraine

The semiconductors doped with d- and f-elements have attracted much attention, because they can be used in the new electronic devices and in spintronics. The electronic, optical and magnetic properties are changed due to dopants. The PbTe crystals are used in infrared techniques and in thermoelectric devices [1]. Here the electronic densities of states and magnetic properties in PbTe crystal doped with Eu have been evaluated within the Green's function method [2]. The obtained results are shown on Fig. 1. Spin  $\uparrow$  – up,  $\downarrow$  – dn, total density of states – tot, partial densities of states – s, p, d, f.

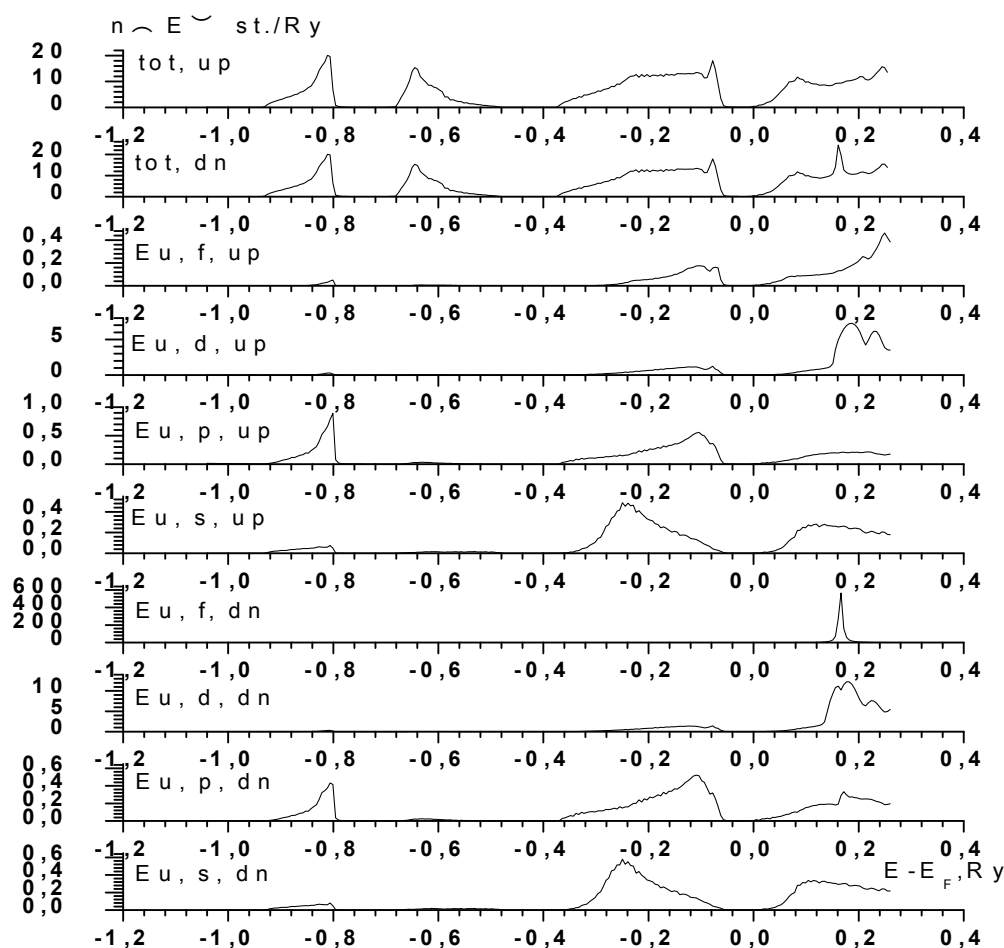


Fig. 1. Densities of states in the PbTe crystal doped with Eu (3%).

1. Шперун В.М., Фреїк Д.М., Запхляк З.Ш. Термоелектрика телуриду свинцю та його аналогів. – Івано-Франківськ: Плай. - 2000. – 250 с.
2. H. Akai, Phys. Rev. Lett. – 1998. – V.81. – P. 3002.

## Investigation of the electrical characteristics of ohmic contacts to Si- and SiC-based thin-film structures

Vinogradov A.O.<sup>1</sup>, Lichman K.A.<sup>2</sup>, Sheremet V.N.<sup>3</sup>

<sup>1</sup>*Ivan Franko Zhytomyr State University, Zhytomyr, Ukraine*

<sup>2</sup>*State Enterprise Research Institute “Orion”, Kyiv, Ukraine*

<sup>3</sup>*V. Lashkaryov Institute of Semiconductor Physics, NAS of Ukraine, Kyiv, Ukraine*

We studied  $I$ – $V$  curves and contact resistivity  $\rho_c$  of the Au–Ti–Pd– $n^+$ – $n$ –Si and Au–Ni– $n^+$ – $n$ –SiC ohmic contacts.

The metallization layers were obtained using magnetron sputtering of metals onto the  $n^+$ – $n$ –Si and  $n^+$ – $n$ –SiC substrates heated up to 100 °C. The thickness of each of metal films as well as  $n^+$ –Si and  $n^+$ –SiC layers did not exceed 100 nm. The dopant concentration in the  $n^+$ –layer was  $\sim 10^{20}$  cm<sup>–3</sup> while that in  $n^+$ –SiC was  $\sim 2 \times 10^{19}$  cm<sup>–3</sup>. The ohmic contacts were formed using thermal annealing at  $T = 400$  °C for Si and 1000 °C for SiC structures.

The  $I$ – $V$  curves measured in the 77–400 K temperature range were linear for both types of contacts. The contact resistivity of ohmic contacts to  $n^+$ – $n$ –Si ( $n^+$ – $n$ –SiC) was  $\sim 1.82 \times 10^{-5}$   $\Omega \cdot \text{cm}^2$  ( $\sim 10^{-4}$   $\Omega \cdot \text{cm}^2$ ).

An analysis of  $\rho_c(T)$  enabled us to determine the current transport mechanism in ohmic contacts to silicon and silicon carbide device structures under consideration. The features of current transport in the contact structures of both types are discussed.

## Structure of the polyaniline films on the amorphous metallic alloy $\text{Al}_{87}\text{Ni}_8\text{Y}_5$

Yatsyshyn M.M.<sup>1</sup>, Boychyshyn L.M.<sup>1</sup>, Demchyna I.I.<sup>1</sup>, Pandyak N.L.<sup>2</sup>

<sup>1</sup>*Ivan Franko National University of L'viv, L'viv, Ukraine*

<sup>2</sup>*National Forestry Engineering University of Ukraine, L'viv, Ukraine*

The conventional electrode materials for the electrochemical oxidation of the aniline (An) to polyaniline (PAn) are polycrystalline metals (Au, Pt, Al, Fe, Ni, Pb, Ti), nonmetallics (graphite, glass carbon) and metal's oxides (indium-tin-oxide ITO). The difference between noble and base metals consists in the absent or presence of the native formed oxide films on their surface. It is accepted as a fact that the polymerization processes are similar on the different electrodes, however the mechanisms of the macromolecules nucleation and structure of produced polyaniline films has essential distinctions [1].

The character of the voltammograms for the potentiodynamic regime during aniline oxidation or for the PAn redox transitions is identical practically on the metallic electrodes [2]. However, it was shown by us that these processes on the surface of the amorphous metallic alloy  $\text{Al}_{87}\text{Ni}_8\text{Y}_5$  differ from one on the conventional electrodes. The form of the wave of aniline oxidation and potentiodynamic curves for the redox transitions of PAn become similar to processes on the conventional electrodes only after the activation of the surface of  $\text{Al}_{87}\text{Ni}_8\text{Y}_5$ -electrode.

The structure of the produced PAn films, which has been studied by the infrared spectroscopy (spectrophotometer Specord M80), X-ray diffraction method (diffractometer DRON 3, Cu  $K\alpha$  radiation) and analysis of images of scanning electron microscope (PEMMA-102-02), differs for contact and outer sides of electrode. The greater quantity of polyaniline deposits on the contact side of electrode that good correlates with higher reactivity of this side (in comparison with outer side) in other electrochemical processes. The film formed on the contact side of electrode is granular, while on the outer side – even, homogeneous practically. The size of polymer grains, formed on the contact electrode side. is  $\sim 1-2 \mu\text{m}$ .

1. Biallozor S., Kupniewska A. Conducting polymers electrodeposited on active metals // *Synth. Met.* – 2005. – V. 155. – P. 443-449.
2. Yatsyshyn M.N., Boychyshyn L.M., Demchyna I.I., Nosenko V.K. Electrochemical oxidation of aniline on the surface of thr amorphous metallic alloy  $\text{Al}_{87}\text{Ni}_8\text{Y}_5$  // *Russ. J. Electrochem.* – 2011. (in press).

**СЕКЦІЯ 1 (стендові доповіді)  
ТЕХНОЛОГІЯ ТОНКИХ ПЛІВОК (МЕТАЛИ,  
НАПІВПРОВІДНИКИ, ДІЕЛЕКТРИКИ, ПРОВІДНІ  
ПОЛІМЕРИ) І МЕТОДИ ЇХ ДОСЛІДЖЕННЯ**

19 травня 2011 р.

**SESSION 1 (poster)  
THIN FILMS TECHNOLOGY (METALS,  
SEMICONDUCTORS, DIELECTRICS, CONDUCTIVE  
POLYMERS) AND THEIR RESEARCH METHODS**

May, 19, 2011

## Ferromagnetism in Co-doped ZnO films: micro-Raman and magnetic studies

Avramenko K.<sup>1</sup>, Strelchuk V.<sup>1</sup>, Bryksa V.<sup>1</sup>, Lytvyn P.<sup>1</sup>, Morhain C.<sup>2</sup>,  
 Deparis C.<sup>2</sup>, Tronc P.<sup>3</sup>, Pashchenko V.<sup>4</sup>, Bludov O.<sup>4</sup>

<sup>1</sup>V. Lashkaryov Institute of Semiconductor Physics NAS of Ukraine, Kyiv, Ukraine

<sup>2</sup>Centre de Recherches sur l'Heteroepitaxie et ses Applications, CNRS, Valbonne, France

<sup>3</sup>Centre National de la Recherche Scientifique, Ecole Supérieure de Physique et de Chimie Industrielles de la Ville de Paris, Paris, France

<sup>4</sup>B. Verkin Institute for Low Temperature Physics and Engineering NAS of Ukraine, Kharkov, Ukraine

In this work, we have studied magnetic, structural, optical and electronic properties of undoped, 5% and 15%Co doped ZnO films grown by molecular beam epitaxy on the sapphire substrates. We provide experimental evidence for important role of electrons which rise ferromagnetism properties up to room temperature.

From magnetization maps and SQUID measurements ferromagnetic

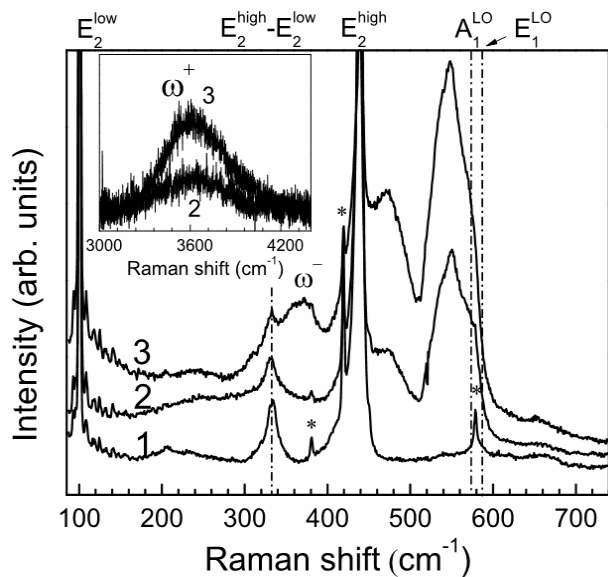


Fig.1. The micro-Raman spectra for the undoped (1), 5%Co (2) and 15%Co (3) doped ZnO films. The sapphire modes show by asterisks.  $E_{exc} = 2.54$  eV.  $T = 300$ K.

behavior of  $Zn_{1-x}Co_xO$  films is clearly put into evidence. In the micro-Raman spectra of (0001)  $Zn_{1-x}Co_xO$  films we detected  $E_2^{low}$ ,  $E_2^{high}-E_2^{low}$ ,  $E_2^{high}$  phonon modes at 101, 333, 437  $cm^{-1}$ , respectively (Fig. 1). The  $\omega^-$  and  $\omega^+$  (see insert on Fig. 1) longitudinal-optical-phonon-plasmon coupled modes (LOPCMs) are also detected at  $\sim 342$ ,  $\sim 368$   $cm^{-1}$  and at  $\sim 3400$ ,  $\sim 3500$   $cm^{-1}$  for 5% and 15%Co doped ZnO films, respectively. From modeling the  $\omega^-$  LOPCMs bands we obtained the temperature dependence of the electron mobility for both samples. The charge mobility achieve 98 and 130  $cm^2/Vs$  at  $T = 300$  K for the  $Zn_{1-x}Co_xO$  films with  $x = 5\%$  and  $x = 15\%$ , respectively.

It was clearly showed that for the  $Zn_{1-x}Co_xO$  films with high magnetization the value of the carrier mobility is also higher. This result could indicate that the ferromagnetism of the  $Zn_{1-x}Co_xO$  films is related with free charge carriers which mediate room-temperature ferromagnetism in the  $Zn_{1-x}Co_xO$  films.

## Analysis of electron microscope images of amorphous films

Bobik M.Yu.

*Uzhgorod national university, Uzhhorod, Ukraine*

In our work the theory of transmission electron microscopy images of amorphous materials and nanosystem of complex chemical composition is developed taking into account as amplitude so diffraction contribution to the contrast. It is showed that three electron scattering components within the range of objective lens aperture diaphragm are responsible for forming contrast of electron microscopy images of such objects: elastic non-coherent, elastic coherent and inelastic background. Variations of electron microscopy images intensity due to elastic non-coherent scattering are determined by distributing of atomic density, changes of chemical composition and deviation of geometrical thickness of local areas of the tested specimen. The contribution of elastic coherent scattering to the contrast of images is conditioned by differences of structural factors of different local areas, and contribution of inelastic background – by the differences of intensity of such background.

In practical usage of the actual number are most common cases. 1. EM image of amorphous object of clearance is uniform when the contrast between different areas is not exceeding a few percent. Structure parameters such amorphous matrix defined direct image analysis. 2. Also a clear contours shown unlimited heterogeneity matrix statistically randomly distributed on the image plane. The study of such images requires the deployment of three components of contrast: geometric thickness, chemical composition and atomic density of local areas. The first contribution is determined by additional studies of surface topography standard methods of scanning electron microscopy or atomic force microscopy. Variation of chemical composition in different parts of heterogeneity can be identified by methods of local X-ray microanalysis. If they are larger than measurement error, it should be for local areas with different chemical composition of standard tables of atomic electron scattering factors. Then the contribution to the contrast of the image changes the chemical

composition will be determined by the difference of integrals  $\int_0^{\alpha} \sum_{i=1}^N F_i^2(s) ds$  for

the various elements of the image. Once you've deleted a total contrast EM images above identified two deposits, receive a third component of contrast caused by differences in average atomic density of local areas of the object. 3. The facility has clearly highlighted included that correspond to features in the form of phase separation in amorphous matrix. 4. The most complex case corresponds to the object in the matrix which combines all the above types of heterogeneity.

## Research of the contrast of the micro electronic images of the amorphous tapes

Bobyk M.Y., Svatyuk O.Y.

*Uzhgorod National University, Uzhgorod, Ukraine*

Nowadays micro electronic research allows to measure a number of important structural parameters of thin-films in a short time frame. But in most cases it relates to the study of the crystalline objects. In the case of amorphous tapes quantitative micro electronic methods are developed far less. Currently, very few theoretical as well as experimental works are dedicated to the analysis of these aspects. But most of all it relates to the research of the amorphous tapes of a compound chemical composition.

In order to solve such a task one should give clear physical definition of the important quantifier which is the contrast between different local areas of image. It is also worth to specify the difference between such metrology parameters as a coefficient of contrast of the photographic material as well as the local contrast of certain optical display –  $K$ . Coefficient of contrast is a tangent of the angle slope of the straight line of the correspondent curve of the specific photo material. While analyzing micro electronic images different scholars give different definitions to the notion of “contrast”. The basis of this concept is the size of intensity of the sounding electronic bunch. However, it is quite difficult to measure this quantifier experimentally.

Therefore, we offer a strict determination of the size of contrast of the corresponding micro electronic images. With this aim the analogical value of the contrast in classic optics is used:

$$K = \frac{B_{\max} - B_{\min}}{B_{\max} + B_{\min}},$$

whereas  $B_{\max}$  і  $B_{\min}$  are maximal and minimum luminosity of the object by a light ray. Such definition of the “contrast” notion can be also used in the field of analytical electronic microscopy. In this case the size of «luminosity» of local areas of the recording environment as well as the intensity of the micro electronic image of the electronic bunch  $I$  in these areas is the  $B$  parameter. Therefore, a contrast between two micro electronic images will be the  $K$  quantifier, which can be calculated in the following way:

$$K = \frac{|I_1 - I_2|}{I_1 + I_2},$$

whereas  $I_1$  та  $I_2$  – are the quantifiers of the electronic bunches` intensity which form the image of two local areas of the so called “EM image”. The correlation received can be directly applied for the numerical micro electronic analysis of images registered as a digital file with the help of imaging plates.

For the images registered on photographic plates one should use the quantifier of their darkening –  $D$ . It is worth taking the following aspects into

consideration: 1. In the area of small darkening ( $D < 0,3$ ) a direct proportion between  $D$  and intensity  $I$  exists. 2. In the area of darkening  $D$  rating from 0,3 to 2 the quantifier of darkening is proportional to  $\log(I)$ . 3. In the area of darkening  $D > 2$  the quantitative analysis of the micro electronic images on the photographic plates becomes incorrect. Therefore, depending from the quantifier of the darkening of photo materials one should use different mathematical approaches for the calculation of “contrast”.

Using the aforementioned theoretical correlations we received mathematical equations for the calculation of contrast of the micro electronic images formed due to different mechanisms of the electrons` dispersion: resilient coherent, resilient non-coherent and non-resilient ones.



## **Effects of smoothed factor in radial distribution functions method for amorphous films**

Borkach E.I., Ryaboschuk M.M.

*Uzhgorod national university, Uzhhorod, Ukraine*

Radial distribution function (RDF) method requires knowledge of structure factor of amorphous materials within the scattering vector  $s$  changes from zero to infinity. Experimentally this condition is almost impossible to provide because the precision diffraction pattern recorded in a limited range of changes from  $s \sim 7 \text{ nm}^{-1}$  to  $\sim 200 \text{ nm}^{-1}$ . Truncating of diffraction pattern intensity for small and for large  $s$  leads to the emergence of RDF fake items are called effects of breakage.

At first glance, the effects of breakage can be neglected because the intensity of coherent scattering becomes very small at large  $s$ . But the situation is complicated by the fact that the Fourier transform expression is not interference function  $i(s)$ , but product  $si(s)$ . For this product oscillations at large  $s$  is not reduced and are approximately constant.

The above behavior of the  $si(s)$  functions indicate a significant effect of integration limits in Fourier transform on the parameters RDF. The main method of reducing such effects is the introduction of  $\exp(-bs^2)$  smoothed parameter in Fourier transform expression. It provides a sharp decrease in the amplitude of oscillations of functions  $si_k(s)$  and thus eliminates signs on truncating effects RDF. But this procedure is equivalent to the introduction in real atomic net additional artificial disordering and therefore received adjusted again do not correspond to real atomic structure of amorphous networks studied object. Moreover, such treatment conducts to two negative consequences:

1. The smoothed factor is entered in the integrand of transformation of Fourier and that is why got RDF is not "clean", as is from mathematical convergence of interference function and this factor.

2. The smoothed factor changes the form of structural factor of amorphous substance substantially, that is why RDF turns out not from real experimental, but from some corrected interference function.

Therefore application of the smoothed factors in the experimental method of ФРРА substantially diminishes authenticity and exactness of quantitative analysis of short order parameters of amorphous materials.

## Features thermostimulated luminescence of aluminum oxide films

Burlak G.M., Vilinskaya L.N.

*The Odessa State Academy of Building and Architecture. Odessa, Ukraine.*

In [1] the presence of a series of thermostimulated luminescence (TSL) maxima, thermostimulated exoelectronic emission (TSEE) are shown for aluminum metal-oxide films which adsorbed only water or water vapours was observed.. It was interest to study the spectra of the TSL of aluminum oxide films in aqueous solutions of different compounds.

In this work samples which were films on aluminum foil of the technical cleanliness, received by an electrochemical method in a water solution of sorrel acids [3] were investigated. Curves TSL were measured on the plant consisting of the lightproof box, the filter absorbing IR-radiation, photoelectronic multiplier, small currents measuring device, copper-constantan thermocouples, recorder. Heating speed was maintained constant and was 0,3 K/c.

We have established, that owing to processing aluminum metal-oxide in water solutions of some inorganic compounds additional TSL bands appear and peaks, which existed earlier, quench. Chemical processing was carried out by boiling in KCl, NaCl 0,1 N water solutions.

Only the centers, responsible for TSL in this temperature interval, are not deactivated by sodium ions which were contained in all compounds we used. The maximum at 560 K is observed in all samples, therefore it, obviously, is connected with dissociative water adsorption which also was available in all cases.

The observed catalytic activity increase develop in the fact that after processing in sodium chloride for effective lightsum storage it is necessary for a sample not hours, and minutes. It can be explained by the fact that chlorine ions in a small amount increase catalytic activity of aluminum metal-oxide surface.

1. Vilinskaya L.N., Burlak G.M. Sensors on the basis of aluminum metal-oxide films // Photoelectronics. – 2009. – №18. – P. 92-94.

## **During the growth of nanoscale structures snTe on mica muscovite**

Chaviak I.I.

*Vasyl Stefanyk Precarpathian National University, Ivano-Frankivsk, Ukraine*

Thin films of semiconductor materials used in micro-and optoelectronics. The only commercially justified diode laser with wavelength  $\lambda \approx 20\mu\text{m}$  was established on the basis of compounds IV-VI [1]. Thin films of chalcogenides of tin have found use in multi-lines and the entire matrix of active elements [2-4].

Nanocrystalline structure of SnTe obtained by evaporation in open vacuum advance material synthesized material. Precipitation pair performed on muscovite mica. Note that the experiments conducted at a temperature of evaporation material spelling  $T_e = 700^\circ\text{C}$  substrate temperature  $T_s = (150-250)^\circ\text{C}$  and deposition time  $\tau = 2, 10, 15$  min., which determined the thickness of condensate. These nanostructures were investigated by methods of atomic force microscopy.

Analysis of results of AFM studies indicate that important technological factors that determine the growth mechanism SnTe nanocrystals on the substrate during deposition method of evaporation in open evaporation, their topology and dimensions are temperature evaporation material  $T_e$  and deposition (substrate) systems  $T_s$ , as well as the mass itself and condensate (a deposition time  $\tau$ ).

Change in  $T_s$  causes displacement deposition time intervals, resulting in growth trends. There is a growing size of crystals of cubic forms correct. Also revealed two temperatures to  $200^\circ\text{C}$  and after  $200^\circ\text{C}$ , which cause growth of crystals with subsequent reduction.

A common feature of selected technological factors of growing nanostructures is the formation of three-dimensional embryo. This dominant structure in the form of triangular pyramidal structures with a predominance of vertical or lateral growth depending on the growing technological factors.

1. T. Beyer, M. Tacke // Appl. Phys. Lett., – 1998, – T. **73**, – 1191.
2. L.G. Wang, P. Kratzer, M. Sheffler, N. Moll // Phys. Rev. Lett., – 1999. – 82. – P. 4042-4045.
3. D.M. Freik, A.P. Shpak, I.I. Chaviak, Yu.A. Kynutskyy // Nanosystems, nanomaterials, nanotechnology, – 2009. – T. 4, №4. – P. 1089-1111.

## Phase Transformations and Mechanisms of Synthesis for Compounds of $\text{Ag}_8\text{XSe}_6$ ( $\text{X} = \text{Si}, \text{Ge}, \text{Sn}$ ) Argyrodite Family.

Chekeylo M.V., Ukrainets V.O., Ukrainets N.A., Voytovich Ya.M.

*Lviv Polytechnic National University, Lviv, Ukraine*

Phase transformations (PT) and chemical reactions (CR) which accompany heating of stoichiometrically composed charge material for the synthesis of  $\text{Ag}_8\text{XSe}_6$  ( $\text{X} = \text{Si}, \text{Ge}, \text{Sn}$ ) argyrodite family compounds have been investigated. To identify of PT and CR charge materials of elementary selenium and those of binary composition of Ag-Se, Si-Se, Ge-Se, Sn-Se, which are used for synthesis of the binary chalcogenides  $\text{Ag}_2\text{Se}$ ,  $\text{SiSe}_2$ ,  $\text{GeSe}_2$ ,  $\text{SnSe}_2$ , which are of similar to argyrodites composition, have been investigated. As an example, the obtained by means of differential thermal analysis(DTA) method thermograms (by heating) of Ag-Si-Se(a), Ag-Se(b), Si-Se(c), Se(d) are given in Figure.

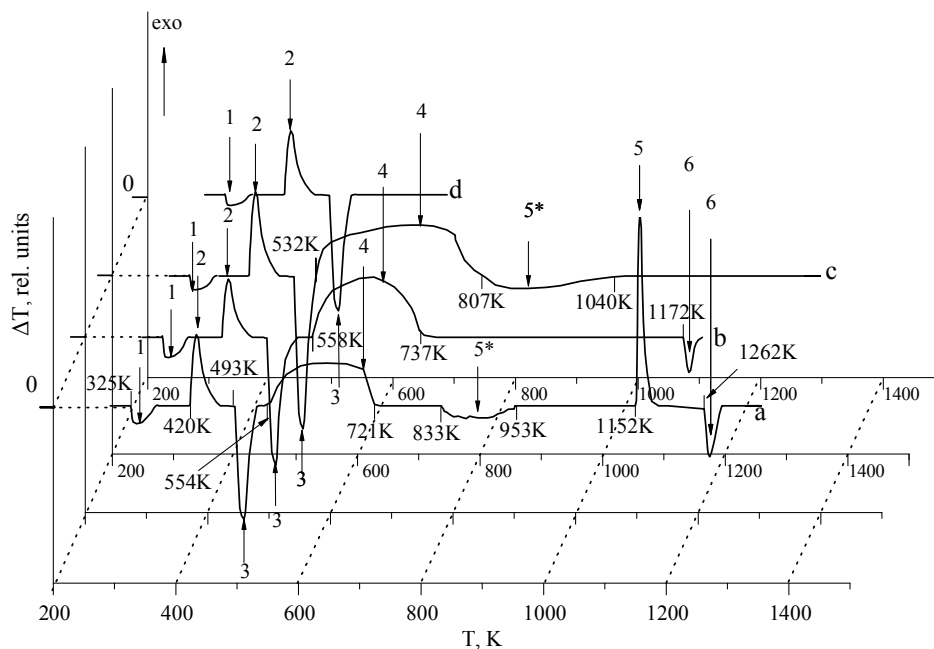


Figure.

The main types of PT and CR have been identified. The temperature ranges of proceeding CR and the temperatures of PT, as well as the value of enthalpy of the formation of  $\text{Ag}_8\text{XSe}_6$  ( $\text{X} = \text{Si}, \text{Ge}, \text{Sn}$ ) argyrodite family compounds have been determined. It is found that the synthesis of the  $\text{Ag}_8\text{SiSe}_6$ ,  $\text{Ag}_8\text{GeSe}_6$ ,  $\text{Ag}_8\text{SnSe}_6$  in all the cases proceeds from previously formed in triple charge material corresponding couples of binary components:  $\text{Ag}_2\text{Se}$ ,  $\text{SiSe}_2$ ;  $\text{Ag}_2\text{Se}$ ,  $\text{GeSe}_2$ ;  $\text{Ag}_2\text{Se}$ ,  $\text{SnSe}_2$ .

Physicochemical principles of the technology of  $\text{Ag}_8\text{XSe}_6$  ( $\text{X} = \text{Si}, \text{Ge}, \text{Sn}$ ) argyrodites synthesis have been developed.

## Research into injection structure formation of a thin electrode strip composite layer

Denysenko O.I.<sup>1</sup>, Tsotsko V.I.<sup>2</sup>

<sup>1</sup>*National Metallurgical Academy of Ukraine, Dnipropetrovsk, Ukraine*

<sup>2</sup>*Dnipropetrovsk State Agrarian University, Dnipropetrovsk, Ukraine*

Synthesis of a composite layer of a thin strip electrode of a secondary lithium source of current with utilization of injection technology [1] includes transportation of a portion of electrochemically active powder [2] by gas flow to the supersonic nozzle, acceleration of grains of powder, which are a part of the two-phase jet, in the nozzle and their impact deceleration on the strip. Microparticles accelerated to supersonic speeds when colliding into the substrate are embedded into it forming a composite structure.

We examined the dynamics of the temperature field and regularities of structure formation of the electrode matrix metal (aluminum) in the contact zones with oxide microparticles embedded into it by impact deceleration, conditions of melt and dissipative structures formation on the thin strip electrode under the energy influence of the two-phase jet [3] and shielding interaction of the near-surface layer of those microparticles which, after their collision with the electrode surface, have not left the coverage of the fast two-phase jet yet, with the oxide particles accelerated by this jet. We experimentally observed transformations of dispersivity of oxide grains of powder during injection syntheses of the composite layer of both thin strip electrode and composite microparticles synthesized in counter two-phase jets for the purpose of their further injection into the strip electrode near-surface layer instead of oxide grains of powder. We studied electrochemical effect of the lithium-manganese spinel embedded into aluminum for its surface densities within a range of 0.1 – 3.0 mg/cm<sup>2</sup>.

1. Denysenko O.I. Hardware-software complex for injection synthesis of composite functional materials // East European Journal of High Technologies, Edition – Kharkiv, 2010. – 3/1 (45). – P. 44-48.
2. Kotsyubynsky V.O., Chelyadyn V.L., Moklyak V.V., Ostafiychuk K.B., Nagirna N.I., Kolkovsky P.I., Grubyak A.B. Oxide electrode materials for lithium power sources // Physics and chemistry of solid state. – 2010. – V.11, №2. – P. 484-492.
3. Denysenko O.I., Tsotsko V.I., Spiridonova I.M., Peleshenko B.I. Formation of thin tape temperature field under effect of two-phase jet dispersed phase on tape surface // Physics and chemistry of solid state. – 2008. – V.9, №4. – P. 901-904.

## **Influence of dispersion of polysilicon on low-temperature conductivity in SOI structures**

Druzhynin A.O.<sup>1,2</sup>, Kogut I.T.<sup>3</sup>, Khoverko Yu.M.<sup>1,2</sup>, Koretskii R.M.<sup>1</sup>,

<sup>1</sup>*National Lviv Polytechnic University, Lviv, Ukraine*

<sup>2</sup>*International Laboratory of Low Temperatures and High Magnetic Fields, Wroclaw, Poland*

<sup>3</sup>*Precarpathian university named after V.Stephanyk, Iv-Frankivsk, Ukraine*

Nowadays polysilicon-on-insulator structures (SOI-structures) are widely used for manufacturing of different microelectronic sensors. Laser recrystallization of active elements of microelectronic sensors enables them to effectively improving the electrical properties. Because of the influence of laser recrystallization on polycrystalline material would be advisable to investigate the dispersion of polysilicon in SOI-structures. One of the known methods is the impedance analysis of the material.

Essentially, the impedance analysis method is that the studied sample is excited by a small sinusoidal signal is measured while it caused alarm at the exit. These measurements were carried out in the frequency range  $10^{-2}$ – $10^6$  Hz. Diagram of experimental data serves as the dependence  $Z''(Z')$ , where  $Z''$  – imagine resistance value and  $Z'$  real resistance, or in other words impedance hodograph. On the basis of experimental data frequency dependence  $Z''$  and  $Z'$  the building of equivalent electric circuits for analyzing the structure of the samples was carried out.

For our investigation SOI-structures with polysilicon resistors before and after recrystallization served as test samples. The impedance analysis was applied to boron doped polysilicon layers with carrier concentration  $3,9 \times 10^{19}$   $\text{cm}^{-3}$  before recrystallization and  $1,7 \times 10^{20}$   $\text{cm}^{-3}$  after recrystallization in temperature range 77–300K.

Results of experimental studies of obtained hodographs of recrystallized samples allow to conclude about increasing its homogeneity in comparison with nonrecrystallized samples so long as the hodograph curve is a semicircle. For homogeneous samples the impedance curve is a semicircle with diameter centered on the  $Z'$  axis and corresponds to a parallel RC circuit. Elements of the equivalent circuit R and C can be compared with the resistance and capacity of the sample and to compare the structure parameters before and after recrystallization.

Thereby the use of this method allows separating and identifying contributions of various microstructured elements in the conductivity of samples in othe words qualitatively and quantitatively describe grain size and grain boundaries contributions in the conductivity of the material what could be used in applications as well as in fundamental research.

## SPM force spectroscopy for testing adhesion and mechanical properties at nanolevel

Dyachyns'ka O.M.<sup>1</sup>, Lytvyn P.M.<sup>1</sup>, Trunov M.L.<sup>2</sup>, Aleksyeyeva T.A.<sup>3</sup>, Prokopenko I.V.<sup>1</sup>

<sup>1</sup>*V. Lashkaryov Institute of Semiconductor Physics, Kyiv, Ukraine*

<sup>2</sup>*Uzhgorod National University, Uzhgorod, Ukraine*

<sup>3</sup>*G. Kurdyumov Institute for Metal Physics, Kyiv, Ukraine*

The scanning probe microscopy (SPM) techniques are widely used for a surface nanoscale characterization. While 3D topography analysis is dominated applications of atomic force microscopy methods (partial realization of SPM), the physics of probe-sample interactions and quantitative analyses of adhesive and mechanical properties have become of increasing interest in recent years. Practical applications of force spectroscopy measurements are ranged from single molecular interactions [1] to nanotribology and nanomechanics of advanced materials [2,3].

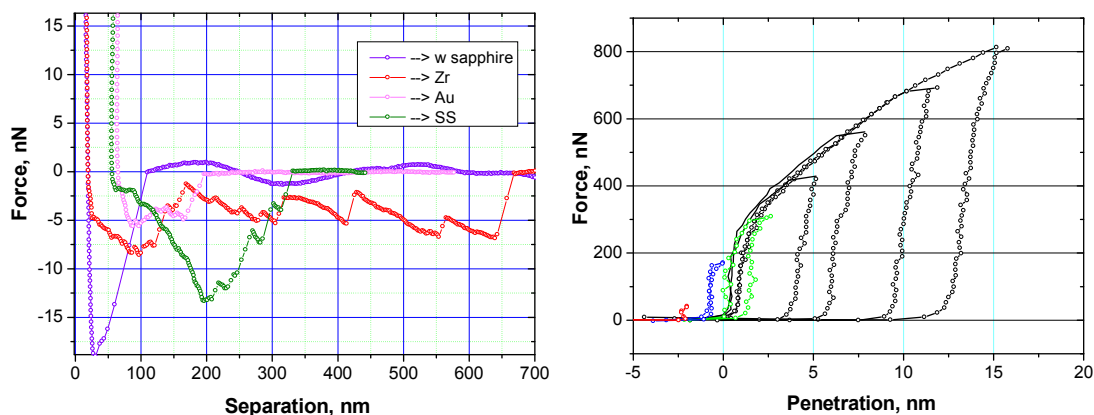


Fig. 1. Probe-sample interaction force curves in liquid buffer (a) and deformation curves of amorphous AsSe thin film (b). Some curves are horizontally shifted for better visualization.

The report presents a spatial application of bioadhesion force spectroscopy for biomaterials characterization as well nanomechanical measurements of photoplastic effects in thin films. These applications realize cases of small and extremely large probe-surface interaction forces and illustrate peculiarities of force-distance (force-penetration) data collection and analysis.

It is shown that proper measurements protocols and adequate data analysis provide reliable information concerning biophysical and mechanical properties of materials under nanocontact.

1. Handbook of Molecular Spectroscopy // A. Noy. – Springer: Livermore, 2008.
2. Testing of Materials and Devices // F. Yang, J. Li. – Springer Science + Business Media, LLC, 2008.
3. Nanotribology and Nanomechanics. An Introduction // B. Bhushan. – Springer-Verlag Berlin Heidelberg, 2008.

## **Diagnostics of nanoscale roughened surface by AFM spectroscopy of capillary forces**

Efremov A.A., Lytvyn P.M., Prokopenko I.V.

*V. Lashkaryov Institute for Semiconductor Physics of the NAS of Ukraine, Kyiv, Ukraine*

Quantitative measurements of capillary forces between atomic force microscope (AFM) probe and nanoobject make it possible to obtain data on local wetting, and consequently the surface energy with a spatial local resolution in order of the diameter of capillary bridge (10-20 nm). Controlled capillary interaction at the nanoscale reveals a number of new potential diagnostic and technological capabilities. Besides AFM can operate in different environments, providing simultaneously surface topography and force spectroscopy data with subnanometer and picoNewton resolution, respectively. In this paper, basing on AFM technique, authors make an attempt to develop a new theoretical and experimental approach for application of capillary forces (CF) as a unique diagnostic tool for roughened real surface, with a strongly correlated relief. Just for this case a successful use of CF-diagnostics is rather problematic because here different factors influence on CF in a similar manner. Firstly we selected the most reliable and at the same time rather simple theoretical models [1] describing liquid nanomeniscus geometry and forces occurring between (AFM) tip and a real surface. Then a special strategy of the experiment was developed. More sharp tip ( $R=10$  nm) was used before for a detailed surface topography. After this we applied more blunt-pointed ( $R=30$  nm) tip – for spatially agreed CF-measurements both in air and liquid. This technique was applied for diamond, and DLC films, subjected by different plasma treatments. Detailed statistical information about the surface, in particular a map for probe single and multiple touchdowns allow us to forecast most of characteristic tip-asperity configurations where meniscus should be formed and calculate their dynamic characteristics. The approach is quite different to existing ones [2] when a real roughened surface is replaced by a model stochastic field with 1-2 random harmonics only. The calculated and measured force distributions proved to be in a good accordance with each other. This fact open the door to further development of CF-spectroscopy diagnostic capabilities, especially for surface energy mapping, use of a liquid nanomeniscus in nanolithography, as well as application of CF for manipulations with nanoobjects of different nature on arbitrary complicated real surface.

1. Butt H-J and Kappl M., Normal capillary forces // *Advances in Colloid and Interface Science* . – 2009. – v.**146**, – P. 48-60.
2. Rabinovich Ya.I., Adler J. J., Esayanur M.S., et al Capillary forces between surfaces with nanoscale roughness // *Advances in Colloid and Interface Science*. – 2002. – v.**96**, – P. 213-230.



## How to improve TSD method for studying relaxation processes in dielectric films

Fedosov S. N. and Sergeeva A. E.

*Odessa National Academy of Food Technologies, Odessa, Ukraine*

Thermally stimulated depolarization current (TSDC) measurement with the linear increase of temperature is one of the powerful methods for identifying relaxation processes in dielectric films. However, the most commonly used mode with two short-circuited electrodes attached to the sample has a serious drawback. It is known that the intrinsic resistance of the current source  $r$  must be much larger than the input resistance  $R$  of the ammeter ( $r \gg R$ ), otherwise reading of the meter does not correspond to the real value of the current. In the TSDC method,  $R$  is constant, while  $r$  decreases with time and temperature. Thus, even if the condition  $r(T) \gg R$  is initially met, it might be destroyed at high temperatures, and the current shown by the meter becomes larger than the real depolarization current. Moreover, stray currents will not be limited any more by the resistance of the sample  $r$ , so the meter will show continuously increasing current, while the real current goes to zero at the end of the depolarization experiment.

To avoid the complications, we propose to connect in series with the sample an additional resistor  $R' \gg r(T)$  in the low temperature range of the measurement, but  $R' \ll r(T)$  at high temperatures. If the conditions are met, the TSDC will not be distorted at either temperature.

TSDC experiments on PVDF-PZT films formed during 0.5 h at 100 °C and  $E = 12$  MV/m with  $R' = 220$  MΩ periodically switched on and shorted have shown that current is the same in the low temperature part with and without  $R'$ . In the high temperature part the current with  $R'$  becomes much more relief than without  $R'$  with relaxation peaks clearly distinguishable. There is an important feature of the suggested mode. By periodic switching on and shortening the resistor  $R'$  one can obtain two TSDC curves, from which the temperature dependence of the intrinsic specific conductivity  $g(T)$  can be easily obtained.

$$g(T) = \frac{d}{A} \frac{I(T) - I'(T)}{[I'(T) \cdot (R + R') - I(T) \cdot R]} \quad (1)$$

where  $I(T)$  is the TSDC without  $R'$ ,  $I'(T)$  the current with  $R'$ ,  $d$  the sample thickness,  $A$  the surface area of the sample. The calculated temperature dependence of conductivity shows a typical exponential behavior.

Thus, the suggested modification increases informativity of the TSDC method allowing characterizing relaxation processes at high temperature and obtaining the temperature dependence of the specific conductivity.

## Poling of NLO polymer films in corona during their solidification

Fedosov S.N., Sergeeva A.E., Revenyuk T.A.

*Odessa National Academy of Food Technologies, Odessa, Ukraine*

One of the important directions in modern optoelectronics is application of polymer films as non-linear optical (NLO) frequency converters. Optical nonlinearity in such films is caused by polar molecules attached to the main chain of the polymer. Although the nonlinear optical susceptibility of NLO polymers is lower than that in inorganic crystals, polymers have advantages due to their high optical transparency, chemical resistance and excellent mechanical properties.

Effective poling of non-linear optical (NLO) polymer films, i.e. aligning the dipoles in one preferential direction, is usually performed at temperatures exceeding the glass transition temperature  $T_g$  of the polymer. However, some films decompose before  $T_g$  is reached. In a novel method we propose for poling NLO polymers, high mobility of the polymer matrix and chains necessary for alignment of the dipoles is provided by artificial lowering of the  $T_g$ .

The samples are poled in a corona discharge while they are still in a viscous state, or even during their spinning from solution. Thus, the solidification occurs in the electric field provided by the corona ions. The method was tested at the methylmetacrylate and 4-(methacryloyloxypropoxy)-4'-nitrostilbene copolymer having  $T_g$  of about 70 °C in the solid state. Cyclopentanol was used as a solvent.

We modified a photoresist spin coater by insulating the chuck, connecting the electrometer to measure the poling current, and placing a specially designed corona triode over the spin coater. Microscopic glass slides with evaporated aluminum electrodes were used as substrates. Films of the NLO polymer of about 20  $\mu\text{m}$  thickness were spun from solution. Kinetics of the solidification at room temperature was measured by monitoring the electric conductivity and the weight of the samples. After initial sharp decrease of both parameters due to evaporation of the solvent, the steady-state condition of the solidification was reached in about 1 h under a negative corona applied during all this time. In some samples we observed remarkable decrease of the poling current in 50-60 min indicating that poling is completed. Measurements of the pyrocoefficient and the thermally stimulated depolarization (TSD) current were performed in order to evaluate efficiency of poling.

It was found that the position of the  $T_g$  peak depended on the storage time of the poled samples gradually increasing from 54 to 68 °C. Relatively high values of the pyrocoefficient of about 2 C/m<sup>2</sup>K were observed clearly indicating that the side-chain dipoles were properly aligned during poling. The method can be recommended for poling other NLO polymers with the relatively high  $T_g$ .

## Low-temperature preparation of CuInSe<sub>2</sub> thin films with annealing in two-step vacuum-arc discharge

Grigorov S.N.<sup>1</sup>, Taran A.V.<sup>1</sup>, Timoshenko A.I.<sup>2</sup>

<sup>1</sup>National Technical University (KPI), Kharkov, Ukraine,

<sup>2</sup>Institute of Plasma Physics, KIPT, Kharkov, Ukraine

Ternary semiconductor compounds based on CuInSe<sub>2</sub> ( $\alpha$ -CIS) are of great interest for the production of solar cells and other optoelectronic devices [1]. Their utilization in such areas places more stringent requirements upon the structure of the obtained ternary compounds. Traditionally, the synthesis of large-crystalline CuInSe<sub>2</sub> semiconductor films takes place at rather high substrate temperatures (600-650°C). In recent years, due to production of solar cells on flexible polyamide substrates, a demand arose for the development of preparation methods of  $\alpha$ -CIS films having a perfect structure at relatively low substrate temperatures (< 450°C) [2].

In the article, three-component Cu-In-Se thin films of variable composition were obtained using the Vekshinsky technique on glass-ceramic, on (001) KCl crystals and KCl with a thin ( $\leq 5$  nm) PbS sublayer placed on a lengthy substrate at 400°C. There were revealed the CuSe<sub>2</sub> +  $\alpha$ -CIS,  $\alpha$ -CIS, ( $\alpha + \beta$ )-CIS,  $\beta$ -CIS, ( $\beta + \gamma$ )-CIS + In<sub>4</sub>Se<sub>3</sub> phase areas corresponding to the Cu<sub>2</sub>Se-In<sub>2</sub>Se<sub>3</sub> pseudo-binary section of the ternary Cu-In-Se phase diagram.

It was found that  $\alpha$ -CIS, ( $\alpha + \beta$ )-CIS, and  $\beta$ -CIS films on the KCl surface are texturized. Epitaxial films have grown on the surface of PbS sublayer.

By means of electron microscopy the defect structure of  $\alpha$ -CIS, ( $\alpha + \beta$ )-CIS,  $\beta$ -CIS films was studied. It was found that these grains have modulated structure containing lamellas with microtwins along the (112) planes. In addition, in  $\beta$ -CIS films the antiphase boundaries oriented along the (100), (010) planes and stacking faults along the (001) planes were found. Such defects explained as a shift in the (001)  $\beta$ -CIS plane by a vector  $R = \frac{1}{2} [110]$ , which preserves Se sublattice undisturbed, but causes the transition of Cu atoms into In sites.

The additional annealing of the ( $\alpha + \beta$ )-CIS films, obtained by the Vekshinsky technique on glass-ceramic, in two-step vacuum-arc plasma discharge at 550°C provided  $\beta$ -CIS  $\rightarrow$   $\alpha$ -CIS phase transition with the formation of homogeneous large-crystalline  $\alpha$ -CIS phase. But the modulated structure of  $\alpha$ -CIS grains is still preserved.

1. Rockett A., Birkmire H. Thin film photovoltaics // J. Appl. Phys. Rev. – 1991. – **70**. – P. 336-345.
2. Tiwari A.N., Krejci M., Haug F-J., Zogg H. 12.8% Efficiency Cu(In,Ga)Se<sub>2</sub> solar cell on a flexible polymer sheet // Progress in Photovoltaics: Research and Applications. – 1999. – **7**. – P. 118-127.

## **Interaction of CdTe and Cd<sub>1-x</sub>Zn<sub>x</sub>Te and Cd<sub>x</sub>Hg<sub>1-x</sub>Te solid solutions with HNO<sub>3</sub>–HI–tartaric acid system solutions**

Gvozdiyevskiy Y.Y.<sup>1</sup>, Tomashik V.M.<sup>2</sup>, Tomashik Z.F.<sup>2</sup>, Seritsan M.V.<sup>1</sup>,  
Denysyuk R.O.<sup>1</sup>

<sup>1</sup>*Ivan Franko Zhytomyr State University, Zhytomyr, Ukraine.*

<sup>2</sup>*V.Y. Lashkaryov Institute for Semiconductor Physics of NAS of Ukraine, Kyiv, Ukraine.*

Single crystals of the CdTe and Cd<sub>1-x</sub>Zn<sub>x</sub>Te solid solutions are most widely used in the production of photoreceivers, sensitive in IR region, ionizing radiation detectors and solar cell elements. At the production of the electronic devices it is important to have high quality surfaces of semiconductor materials and films. For processing of the semiconductor surfaces chemical-dynamic and chemical-mechanical etching is most often used.

In this work the investigation of the kinetic dependences of the CdTe, Cd<sub>0,2</sub>Hg<sub>0,8</sub>Te, Cd<sub>0,96</sub>Zn<sub>0,04</sub>Te and Cd<sub>0,9</sub>Zn<sub>0,1</sub>Te semiconductor materials chemical-dynamic etching by the aqueous HNO<sub>3</sub>–HI–tartaric acid solutions has been accomplished. The method of rotating disc was used for such investigations. To make etching solutions the 70 % HNO<sub>3</sub>, 55 % HI and 40 % tartaric acids were used. The etching process temperature was 293 K and rate of the disc rotation was equal to at 80 min<sup>-1</sup>. The samples surfaces were investigated with MPB – 2 (×24 ± 5 %) microscopes.

The dissolution rates of mention above semiconductor materials in the aqueous solutions of the HNO<sub>3</sub>–HI–tartaric acid system are within the intervals from 3.0 to 11.0 mkm/min and the polishing rates of these materials is 4.0-11.0 mkm/min. The increase of HI content in the etchant leads to the formation of round small pits on the semiconductor surfaces. Small quantity of tartaric acid leads to the improvement of plate's surface quality whereas at great concentrations grey films appear on the surface.

The decreasing of the etching rate of the CdTe single crystal by the aqueous solutions HNO<sub>3</sub>–HI–C<sub>4</sub>H<sub>6</sub>O<sub>6</sub> system is observed at its doping. Using the experimental data, obtained at the investigation of the temperature dependences of the chemical etching rate, it was shown that the dissolution of the CdTe and Cd<sub>1-x</sub>Zn<sub>x</sub>Te solid solutions is limited by the diffusion stages as the apparent activation energy is not higher that 9 kJ/mol.

The aqueous solutions HNO<sub>3</sub>–HI–C<sub>4</sub>H<sub>6</sub>O<sub>6</sub> can be used in CdTe, Cd<sub>0,2</sub>Hg<sub>0,8</sub>Te, Cd<sub>0,96</sub>Zn<sub>0,04</sub>Te and Cd<sub>0,9</sub>Zn<sub>0,1</sub>Te single crystals and films finishing polishing with surface roughness R<sub>z</sub> = 0,03 ≤ 0,05 mkm. After etching the samples should be well washed with 0.5 M Na<sub>2</sub>S<sub>2</sub>O<sub>3</sub> solution and then with large quantity of distilled water followed by the drying in the air stream.

## Determination of conductivity of thin metal films using eddy current method

Handetsky V.S., Tonkoshkur Yu.A.

*Dnepropetrovsk National University, Dnepropetrovsk, Ukraine*

As one of the main controlled parameters of the films used by their specific electrical conductivity. Monitoring this parameter usually carried out contact methods. Given the high conductivity of thin (up to several tens of nanometers) films [1], promising for the measurement and monitoring of this parameter is the use of contactless methods, in particular, the method of eddy currents. This method is based on an analysis of changes in active and reactive resistance of the coil sensor, exciting eddy currents in the test object.

In this paper we analyze the sensitivity of the method as applied to film objects. For the basic formulas are made by the active resistance of the coil sensor was accepted expression [2]

$$R_{\text{BH}} = 0.5\pi\omega\mu_0RW^2I_1(\alpha, \beta, \zeta) \quad (1)$$

$$\text{where } I_1(\alpha, \beta, \zeta) = \beta^2 \int_0^{\infty} J_1^2(x)^2 e^{-\alpha x} \phi(x) dx ;$$

$$\phi(x) = \frac{(x-m) \cdot e^{-2\zeta \cdot m} - 2xe^{-\zeta \cdot m} (x \cdot \cos(\zeta \cdot n) - n \cdot \sin(\zeta \cdot n)) + x(x+m)}{m^2(m-x) \cdot e^{-2\zeta \cdot m} - 2n^2e^{-\zeta \cdot m} \cdot (2n \cdot x \cdot \sin(\zeta \cdot n) + (n^2 - x^2) \cos(\zeta \cdot n)) + m^2(x+m)^2}$$

$$n = \frac{1}{\sqrt{2}} \sqrt{x^4 + \beta^4 - x^2}, \quad m = \frac{1}{\sqrt{2}} \sqrt{x^4 + \beta^4 + x^2}; \quad \alpha = 2h/R; \quad \beta = R\sqrt{\omega\sigma\mu_0}; \quad \zeta = 2d/R; \quad \omega = 2\pi f;$$

$f$  – frequency current in the coil;  $\mu_0$  – magnetic constant;  $W$  – number of turns of the sensor;  $J_1$  – Bessel function;  $R$  – radius of the coil;  $h$  – the distance between the coil and a conductive film;  $\sigma$  и  $d$  – electrical conductivity of the film material and its thickness.

Numerical analysis (1) at very low values  $\xi$  ( $\xi < 0,001$ ) make possible to establish the range of applicability of this method for measuring the conductivity of the films. In particular, we show that for films. with  $d = 0,05 \mu\text{m}$  and  $f = 250 \dots 300 \text{ MHz}$ ;  $R = 1 \text{ mm}$ ;  $h = 200 \mu\text{m}$  possible to fix the conductivity of the film with at least  $1 \text{ Om}^{-1}\text{sm}^{-1}$ .

1. Antonets I.V., Kotov L.N., Nekipelov S.V. Features of the nanostructure and electrical conductivity of thin films of various metals // Technical Physics. – 2004. – T. 74, №3. – P. 24 - 27.
2. Sobolev V.S., Shkarlet Yu.N. Overhead and on-screen gauges.– Novosibirsk: Science. - 1967. – 143 p.

## Features of the properties for photodetectors with vertical integration based on ZnO

Ievtushenko A.I.<sup>1</sup>, Lazorenko V.I.<sup>1</sup>, Horvath Zs.J.<sup>2,3</sup>, Lashkarev G.V.<sup>1</sup>,  
Dusheyko M.G.<sup>4</sup>, Baturin V.A.<sup>5</sup>, Karpenko A.Y.<sup>5</sup>

<sup>1</sup>Frantsevich Institute for Problems of Materials Science, NASU, Kyiv, Ukraine

<sup>2</sup>Research Institute for Technical Physics and Materials Science, Budapest, Hungary

<sup>3</sup>Obuda University, Budapest, Hungary

<sup>4</sup>National Technical University of Ukraine “KPI”, Kyiv, Ukraine

<sup>5</sup>Institute of Applied Physics, Sumy, Ukraine

ZnO is a wide-band ( $E_g \approx 3.37$  eV) direct-gap material which attracts a great attention to the development of the photodetectors for near-ultraviolet range. It is an electronic analog of GaN, but ZnO have economic and ecological benefits in comparison with GaN. There are many papers devoted to the formation detectors of a planar configuration [1]. One of the promising directions of microelectronics is the development and study of devices with a vertical structure. The reason is that in this vertical configuration of electrodes the interelectrode distance can be easily reduced without using expensive lithography processes. Therefore, the purpose of this report is devoted to the study of technological aspects for the deposition of ZnO films as well as the investigation of the photoelectrical properties of structures with vertical configuration of the electrodes.

Early we reported the positive role of nitrogen in ZnO for UV detectors [2]. Therefore, the undoped and nitrogen doped ZnO films with different concentrations of the nitrogen were deposited by magnetron sputtering on n-Si and ITO/glass substrates. Structural and optical properties of the films were examined by XRD, EDX and optical measurements. Aluminum as ohmic contact to Si and Ni as Schottky contact to ZnO were deposited by electron beam evaporation with thickness control. Ni/ZnO/n-Si/Al and Ni/ZnO/ITO layered structure of photodetectors were obtained. Current-voltage curves of photodiodes were studied in dark and under visible and UV irradiations using Keithley-236 Source Measure Unit. Features of the current-voltage characteristics and leakage current mechanisms are discussed. It was found an increase of photosensitivity with increasing nitrogen concentration in nitrogen doped ZnO films for all types of vertical structures. The maximum enhancement of reverse current under UV irradiation was two orders of value. The influence of deposition technology of ZnO films on the photoelectrical properties of detectors as well as the effect of nitrogen incorporation will be presented. Prospects for the application of ZnO photodetectors with vertical integration and requirements for their design will be discussed.

1. K. Liu, M. Sakurai, M. Aono *Sensors*. – 2010. – V.10. - PP.8604-8634.
2. A.I. Ievtushenko, G.V. Lashkarev, V.I. Lazorenko, et al. *J. Phys. Stat. Sol. (a)*. – 2010. – V.207, №7. - PP. 1746–1750.

## Auger-spectroscopic investigation of SnO<sub>2</sub> films with different thickness

Il'chenko V.V., Telega V.M., Lushkin O.E., Kovalenko V.S.

*Taras Shevchenko National University of Kyiv, Kyiv, Ukraine*

Nowadays SnO<sub>2</sub> films are widely used as active materials for gas sensors. One of the problems which appear during the technological manufacturing of such sensors is a stehiometry disorder in evaporated films.

In this work alloyed and unalloyed with nickel SnO<sub>2</sub> films with different thicknesses were investigated. Films were obtained using the magnetron nonreactive sputtering of thick stehiometric tin oxide on molybdenum pad. Investigation of film's element composition was carried out using the electronic Auger-spectroscopy method. In order to obtain the element's distribution profile along the film's thickness, the ion sputtering method was used. The measure of SnO<sub>2</sub> film's stehiometry was the relation of Auger-peaks amplitudes of tin and oxygen [1].

Analysis of total Auger spectra shows that the relation between Sn and O Auger-peaks' amplitudes absolute values along film's thickness remains almost constant. Its' increase on the first minutes of sputtering is related both with the peculiarities of electron beams' interaction with film, and with

the peculiarities of films' near-surface composition, which can be depended on the type of absorbed gases. It was also found out that the relation between Sn and O Auger-peaks' amplitudes absolute values increases with the decreasing of sputtered films' thickness. Analysis of Sn and O Auger-peaks amplitudes relation's changes

during the ion sputtering (Fig.1) allows making the additional conclusions about the obtaining opportunity of stehiometric tin oxide films using the method of nonreactive magnetron sputtering.

1. V.V Ilchenko, V.Kovalenko, Kobzistyy M.V., Lushkin O.E., Telega V.M.. «Research of impaction ion beam ob surface composition of tin oxide». X International young scientists' conference on applied physics. Kyiv 2010, p. 98-99.

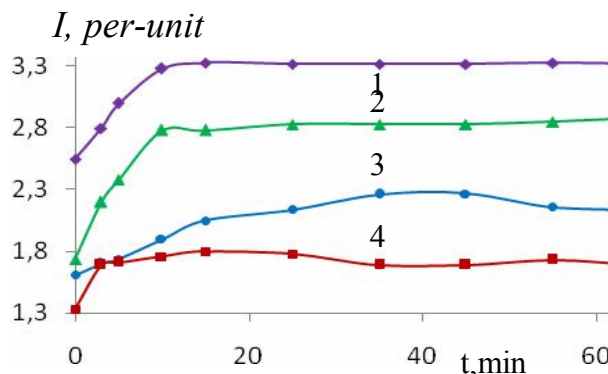


Fig. 1. Dependence of Sn/O Auger-peaks amplitudes relation with sputtering time: 1) Mo-SnO<sub>2</sub> (d<sub>SnO<sub>2</sub></sub>=20 nm); 2) Mo-SnO<sub>2</sub>+0,5%Ni (d<sub>SnO<sub>2</sub></sub>=20 nm); 3) Mo-SnO<sub>2</sub>+1%Ni (d<sub>SnO<sub>2</sub></sub>=1,8 μm); 4) thick layer of SnO<sub>2</sub> (d<sub>SnO<sub>2</sub></sub>=2 mm), where d – is the thickness of SnO<sub>2</sub>.

## **Lacks of radial distribution functions method in electron diffraction of amorphous films and nanosystems**

Ivanitsky V.P., Sabov V.I.

*Uzhgorod national university, Uzhgorod, Ukraine*

Electronic diffraction – actually unique direct method of research of structure of atomic networks for amorphous thin films and disordered nanosystems. Radial distribution functions (RDF) methods are based on use of Fourier integrated transformation. This method was used in x-ray researches and transferred in electron diffraction formally. Many essential features of electronic diffraction on amorphous nanosize samples haven't been considered. Therefore a number of lacks of method RDF application for nanosize systems, is analysed in detail.

1. In physical aspect the discreteness of a structure of substance within a near and intermediate order is ignored. In method RDF this discrete structure is described by continuous functions of atomic density which not always accordingly describe real atomic networks.

2. In methodological aspect aren't taken into consideration nano sizes of samples and of elements of their microstructure and diffractograms registration features. One of conditions of method RDF applicability is enough big size of a site of the investigated sample which is exposed to an irradiation. Besides, Fourier transformation demands, that intensity diffractogram has been given in infinite limits of electron scattering vectors. Actually, this area is limited by a range 5-200 nanometers<sup>-1</sup>.

3. In experimental aspect not always the appropriate attention is given to insufficient accuracy of diffraction pattern registration and to background from not elastic scattering. Modern devices of electronic research are equipped by filters for not elastic electrons and by systems of registration on the basis of imaging plates. But even such newest decisions provide accuracy of registration of coherent scattering intensity on peripheral sites of diffraction patterns only at level of 8-10 %. Besides, they not completely delete not coherent background from diffraction pattern. That is the problem of an exception of the given background remains unresolved and today.

4. In mathematical aspect it is specificity of mathematical procedure of Fourier transformation. It can be precisely spent only for the continuous differentiated functions. Radial distribution functions often don't satisfy to this condition, especially in the field of the first coordination peak.

5. Received RDF demands the corresponding analysis and calculation of shot order parameters of atomic network: coordination spheres radiuses, coordination numbers and dispersions of interatomic distances distribution. Procedure of definition of all these sizes from RDF remains ambiguous and brings additional errors in the received results.



## Applicability of radial diffraction functions method for amorphous thin films

Ivanytska G.M., Rubish V.M.

*Uzhgorod national university, Uzhgorod, Ukraine*

Radial distribution function method for amorphous thin films can be used at implementation of few conditions. One of them is determined by the form of that part of the investigated samples, which is exposed by electron beam. In electron diffraction she has a cylindrical form. His height is equal to the thickness of the investigated sample  $d$ , and the diameter  $D$  is equal to the electron beam diameter. In this cylindrical area it follows to distinguish two different subareas: external  $\Gamma$  and internal base  $B$ . External subarea embraces the external layers of all cylindrical area. A thickness of these layers must be approximately equal to the correlation radius  $R_K$  of atomic networks topological structural arrangement. The size of this radius for amorphous materials is equal to  $\sim 1$  nm. All other part of the cylindrical area will now behave to internal subarea  $B$ .

Physical basis of selection of these two subareas is their different role at forming of diffraction patterns. All atoms of internal subarea participate in forming of diffraction picture without any limitations. Atoms of external subarea are under various conditions. Than nearer there is an atom to border of cylindrical area, than the less will be his contribution to the general diffraction picture. We found the relation  $\gamma$  of atoms that are in subareas  $\Gamma$  and  $B$ :

$$\gamma = \frac{V_{\Gamma}}{V_B} = \frac{D^2 d}{(D - 2R_K)^2 (d - 2R_K)} - 1,$$

$V_{\Gamma}$  and  $V_B$  are volumes of corresponding subareas. It is possible to accept  $D = 10-40 \mu\text{m}$ , and  $d = 10-100 \text{ nm}$ . Then, taking into account, that  $D \gg R_K$ , can write:

$$\gamma = \frac{R_K}{(d - 2R_K)}.$$

As ensues from the got expression,  $\gamma$  is determined actually by thickness of investigated amorphous film, as a correlations radius of atomic networks short and intermediate order of most amorphous materials can be considered near to 1 nm. An analysis shows that within the limits of typical electron diffraction experiment error on a general diffraction picture it is possible a 4-5 per cents by influence of subarea  $\Gamma$  atoms it is possible to scorn, if the investigated film thickness exceeds 20-30 nm. Thus, by the radial distribution functions method the reliable quantitative parameters of atomic network short and intermediate order can be got only for amorphous films with a thickness anymore 30 nm.

## Molecular dynamics method for calculation of the metal film deposition

Keeprich V.I., Kornich G.V.

*Zaporizhzhya National Technical University, Zaporizhzhya, Ukraine*

A lot of complex thin-film systems with various properties are used in the majority of modern technologies of the micro- and nanoelectronics. There are many mathematical methods allowing carry out calculations and the relevant modeling of parameters for film systems creation and also their future properties. The method of the molecular dynamics (MD) is selected among these methods. By this method it is possible to explore behavior of separate particles of the system as well as groups of particles, and also to lead calculation with related parameters.

In the executed research the molecular-dynamic calculations of the coefficients required for modeling of metal thin film deposition has done. In the process of MD-modeling semiempirical potential of MEAM (the modified method of the embedded atom) for fcc lattice has been used.

$$E = \sum_i \left[ F(\bar{\rho}_i) + \frac{1}{2} \sum_{j(\neq i)} \phi(R_{ij}) \right],$$

where  $F$  – embedded function,  $\bar{\rho}_i$  – background electron density,  $\phi(R_{ij})$  – pair interaction between  $i$  and  $j$  atoms on the  $R_{ij}$  distance.

The potential can be used to obtain a high precision of calculation for the many physical properties, such as bulk modulus, defect formation and other important technological parameters.

During research MD calculations of interatomic jumps statistic and film deposition parameters were lead. These parameters are the sputtering and attachment coefficients at the different values of particles energy, which bombard substrate. Comparison of received values with other model calculations (SUSPRE, SRIM) and empirical data has shown deviation of results no more than 5%, which confirms the reliability of the given method.

Received by MD calculations coefficients have been used for computer experiments in the range of similar to diffusive models, in which evolution of various system of mass transfer on the substrate while the deposition of uniform and preferred-orientation films was investigated.

"Hybrid" modeling – MD for calculation parameters and continual model for examination of evolution of system, – allows to use advantages of both approaches – high physical precision of the data of first method and high velocity of calculations of second.

## To the birefringency's measuring of the uniaxial nanofilm

Kiryanov A.P.<sup>1,2</sup>, Kachurin Yu.Yu.<sup>2</sup>, Shapkarin I.P.<sup>3</sup>

<sup>1</sup>Scientific&Technological Center for Inique Instrumentation of RAS, Moscow, Russia;

<sup>2</sup>National Research University "MSTU named N.E. Bauman"; Moscow, Russia;

<sup>3</sup>Moscow State University of Disign&Technologies, Moscow, Russia

The birefringency's measuring of the nanofilm by means of a laser ellipso-meter fulfilled as the Michelson interferometer is shown. As known it's base of a Fourier-transform spectroscopy [1]. We placed linear polarizer prisms before and after beam-splitter. The entrance prism devides the He-Ne-laser's beam in two it's parts with transverse x- and y-polarizations. They are detected by detectors as interferograms  $I_{(x,y)(n,e)}(\Delta l)$  – functions of the optical path difference  $\Delta l$  for light beams in the interferometer's shoulders, and they relate to beams with linear (x- or y-) polarizations reflected by a nanofilm (n) or etalon (e). Its signals are processing by a computer.

The signals formulas are bulky. But our matter eases by next acts, namely:

- the condtion's selection for beam-splitter:  $E_{ox}t_x = E_{oy}t_y(\circ)$ ;  $\varphi_{tx} = \varphi_{ty} = 0(\circ)$

where  $E_{o(x,y)}t_{(x,y)}$  and  $\varphi_{(tx,ty)}$  – amplitudes of the electric vector of the laser beam before a beam-splitter, the module and phase of the complex amplitude transmission  $t_{(x,y)}^*$  of the beam-splitter for the beam with a linear x- or y-polarization;

- reduction of the signal  $I_{(x,y)n}(\Delta l)$  for nanofilm (n) by the signal  $I_{(x,y)e}(\Delta l)$  for etalon mirror (e):  $i_{(x,y)n}(\Delta l) = I_{(x,y)n}(\Delta l) / I_{(x,y)e}(\Delta l)$  (1)

- the difference  $\Delta i(\Delta l)$  reduced signals (1) is given by next relation:

$$\Delta i(\Delta l) = [R_{\xi} \sin(k\Delta l - \varphi_{\xi}) - R_{\eta} \sin(k\Delta l - \varphi_{\eta})] \cos 2\alpha \quad (2)$$

where  $R_{(\xi,\eta)}$  and  $\varphi_{(\xi,\eta)}$  – the module and phase of the complex amplitude reflection coefficient  $R_{(\xi,\eta)}^*$  of the light components with linear  $\xi$ - or  $\eta$ -polarization for nanofilm's material;  $k$  – the module of a wave vector;  $\alpha$  – the angle between axes  $\xi$  and  $x$  for the own linear polarization of the beam-splitter and nanofilm.

The formula (2) permits to fix the axis  $\xi$  along the axis  $x$  for a beam-splitter. Reduced film signal  $i_{(x,y)n}(\Delta l)$  for the beam with linear  $\xi||x$ - (or  $\eta||y$ -) polari-zation is given as:  $i_{(x,y)n}(\Delta l) = R_{(\xi,\eta)} \sin(k\Delta l - \varphi_{(\xi,\eta)})$  (3)

The complex Fourier transformation  $\mathfrak{T}^{-1}\{i_{(x,y)n}(\Delta l)\}$  gives the full set of the nanofilm's parameters  $(R_{\xi}, R_{\eta}, \varphi_{\xi}, \varphi_{\eta})$  [2] and the solution of the reverse task of a holoellipsometry [2] gives the birefringency and thickness of nanofilms.

1. Bell W.J. Introduce into the Fourier-spectroscopy / V., 1975.
2. Kiryanov A.P. In situ holoellipsometry: principles and applications // M., 2003.

## **Techological peculiarities of nanocomposite $\text{SiO}_x$ and $\text{SiO}_2(\text{Si})$ films obtaining by LP CVD method**

Kizjak A., Evtukh A., Pedchenko Yu.

*V. Lashkaryov Institute of Semiconductor Physics, Kiev, Ukraine*

Nanocomposite  $\text{SiO}_x$  и  $\text{SiO}_2(\text{Si})$  films are promising for some interesting applications among them nonvolatile memory, single electron transistors and resonant tunneling structures. The development of suitable technology is very important task. It was necessary to investigate the influence of technological regimes on nanocomposite films properties.

The main aim of this work was to develop the technology and investigate of structural properties of the nanocomposite  $\text{SiO}_x$  and  $\text{SiO}_2(\text{Si})$  films, obtained by low pressure chemical vapor deposition (LP CVD) method.

During LPCVD deposition the silicon enriched  $\text{SiO}_x$  films were obtained at two temperatures  $T = 680^\circ\text{C}$  and  $780^\circ\text{C}$ . As a variable parameters were total pressure of gas mixture ( $\text{SiH}_4:\text{N}_2\text{O}$ ) in the range of 0.75 - 1 Torr and partial pressure of silane ( $\text{SiH}_4$ ) (0.23 – 0.62 Torr).

The thickness and refractive index of the films were determined with ellipsometry method ( $\lambda = 632.8 \text{ nm}$ ). AFM NanoScope IIIa was used for study of film surface topology in regime of periodic contact of silicon probe with nominal curvature radius of 10 nm. TEM was also used to reveal silicon nanocrystals. IR-spectra of the films were measured by Furrier spectrometry Spectrum BX-II. All above mentioned parameters and, additionally, current-voltage and capacity-voltage curves were measured as before and after annealing in nitrogen at  $T=1100^\circ\text{C}$  during an hour.

As a result of performed investigations the technological process of  $\text{SiO}_x$  film with determined parameters obtaining for formation of nanocomposite  $\text{SiO}_2(\text{Si})$  films after following thermal annealing has been developed.

## Electrodeposition of thin film precursors for CIS based solar cells

Kopach G.I.<sup>1</sup>, Klochko N.P.<sup>1</sup>, Volkova N.D.<sup>2</sup>, Lyubov V.M.<sup>1</sup>, Momotenko O.V.<sup>1</sup>, Kopach A.V.<sup>1</sup>, Kharchenko M.M.<sup>1</sup>, Novikov V.O.<sup>1</sup>

<sup>1</sup>*National Technical University "Kharkiv Polytechnic Institute", Kharkiv, Ukraine*

<sup>2</sup>*National Aerospace University "Kharkiv Aviation Institute", Kharkiv, Ukraine*

CuInSe<sub>2</sub> (CIS) based thin film solar cells produced from electroplated precursors show record efficiencies of over 11%. In addition, electrodeposition comprises a high potential of cost reduction due to more efficient material consumption and lower investment costs as compared to production techniques involving high vacuum technology. In the production process, the elements copper, indium and selenium are simultaneously or stepwise deposited by electroplating on top of a molybdenum-coated substrate. However, the one-step electrodeposition process on which the CIS film is potentiostatically grown by co-deposition of Cu, In and Se simultaneously have been met difficulties concerning the control of the sample composition. To our opinion, stepwise electrodeposition of thin film precursors is more promising approach for CIS based solar cells, so, this work is devoted to the investigation of structure and physical properties of different electroplated Cu-In-Se compositions in order to obtain the optimized combinations.

Electrochemical deposition of copper, indium and selenium was carried out at room temperature in two electrode cells in simple aqueous electrolytes without organic additives. X-ray diffraction studies of the electrodeposited film structure were carried out using a diffractometer DRON-4 with Bragg-Brentano focussing in cobalt anode radiation. Precision determination of lattice constants of the electrodeposited layers was carried out by Nelson-Riley method. Investigation of the film preferred orientation was performed by analysis of the diffraction maxima and by calculating of the texture parameter. Determination of crystallites size for the studied films was carried out by Williamson-Hall formula. Surface morphology of the electrodeposited layers were studied using scanning electron microscope REM-100V by registration of secondary and reflected electrons at accelerating voltage 30 kV.

Analysis of crystal structure, surface morphology and physical-mechanical properties of the electrodeposited films and film compositions has revealed that only possible sequence of CIS precursor components in terms of optimization of above characteristics is Cu – In – Se. Particularly, the formation of InCu and Cu<sub>2</sub>In intermetallic compounds during electrodeposition of In onto Cu promotes improvement of the interlayer adhesion, In<sub>2</sub>Se<sub>3</sub> phase formed during electrodeposition of Se onto In has comparatively perfect structure, while immediate contact of Cu and Se is undesirable because of generation of Cu<sub>2</sub>Se crystal phase with heavy strained structure.

## **Regularities of porous copper and aluminium micro and nanostructures formation under conditions of quasi-equilibrium steady-state condensation**

Kornyushchenko A.S.

*Sumy State University, Sumy, Ukraine*

Due to the wide use of high porous materials as membranes, in fuel cells, sensors, catalysts and other devices the technologies of their formation attract great interest. Previously we have established technology of porous metal micro and nanostructures formation using self-organized ion sputtering devices. The carried out experiments have shown that regularities of structure formation of weakly volatile substances using self-organized systems are completely different from formation of polycrystalline obtained during deposition of high saturated vapors. It is shown, that while depositing weak supersaturated vapor flows mechanism of nucleation and structure formation doesn't obey equilibrium thermodynamics and is described by kinetic of atom-by-atom condensate formation only on active centers of growth surface. Relatively small concentration of such centers lead to high discreteness of their chemical building energy spectrum. Thus, we can introduce critical energy of chemical bonds  $E_c$ , below which atom-by-atom condensate formation becomes improbable.

Proximity of plasma-condensate system to equilibrium provide selective regime of condensation, when adatoms are bound only into active centers of growth surface forming micro and nanostructures with different architecture. Analysis of experimental data has shown that changing of technological conditions of condensation such as working gas pressure and discharge power following structure formation mechanisms are observed:

- tangential growth of weakly bound with each other crystals;
- normal growth of crystals having atomically rough surface;
- preferential growth of crystals in different crystallographic directions;
- condensation under conditions of field selectivity.

But what technological conditions correspond to one or other mechanism of structure formation have not been determined yet. Thus, aim of this work consists in systematization of structural forms of obtained metal condensates under different technological conditions and building structural forms diagram on the example of copper and aluminium.

1. V.I. Perekrestov, A.I. Olemskoi, A.S. Kornyushchenko, Yu.A. Kosminskaya, Self-Organization of Plasma–Condensate Quasi-Equilibrium Systems// *Physics of the Solid State*. – 2009. – V.51, №5. – P. 1060-1068.
2. V.I. Perekrestov, A.S. Kornyushchenko, Yu.A. Kosminskaya, Selective Processes that Proceed during Formation of Aluminum Layers near the Phase Equilibrium in a Plasma–Condensate System// *Technical Physics*. – 2008. – V.53, №10. – P. 1364-1372.

## Investigation of the photoluminescence spectra and crystal structure of epitaxial ZnO layers grow by the vapor phase epitaxy on GaAs (100) substrates

Kovalenko O.V., Ogol V.O., Polozov K.Yu.

*Dnipropetrovsk National University of name Olesya Gonchara, Dnipropetrovsk, Ukraine*

The wide-gap semiconductor ZnO is a suitable material for various optoelectronic devices operating in the visible part of the spectrum. Formation of extremely pure films of  $A_2B_6$  compounds with sharp boundaries makes it possible to synthesize superlattices, which are finding applications in laser technology and in various photoelectric devices. Single-crystal ZnO films are grown mainly by the molecular beam (MBE) and vapor phase epitaxy (VPE), method using metal-organic compounds, and powder or elemental sources. The most advanced MBE method makes it possible to synthesize high-purity epitaxial films with specified parameters over a large surface layer. The relatively inexpensive VPE technology characterized by low growth temperatures ( $T = 150 - 350$  °C), big temperature gradient ( $200 - 250$  °C/cm) is a competitive method for the synthesis of epitaxial structures.

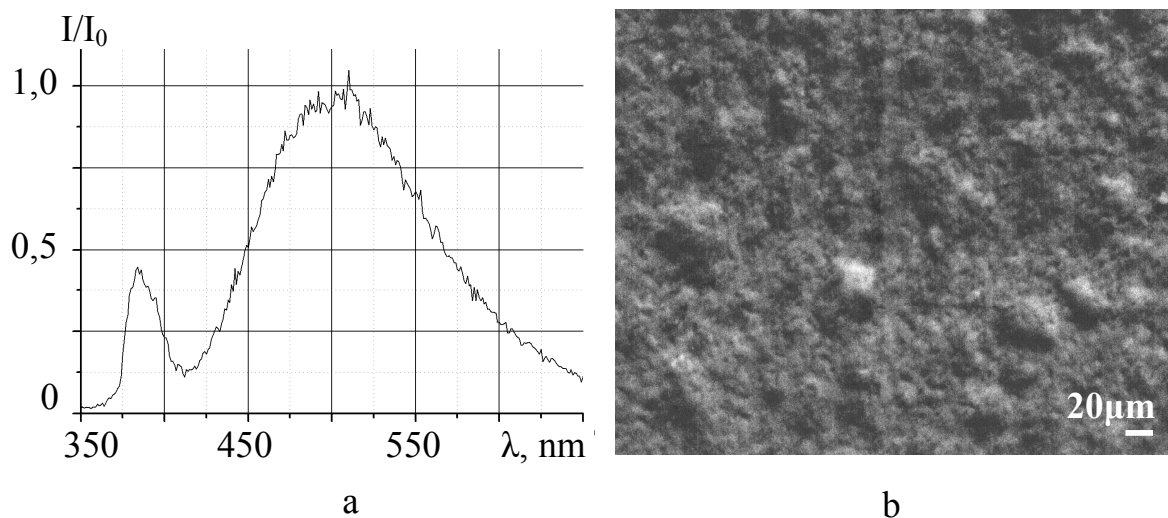


Fig. 1. Photoluminescence spectra (a) at  $T=300\text{K}$  and the form of the surface of polycrystalline ZnO epitaxial film (b) on GaAs(100) substrate.

Using of VPE technology ZnO layers of three types: polycrystalline, sharply textured and single-crystalline have been grown on GaAs(100) substrate. Photoluminescence spectra, form of the surface (Fig. 1), X-ray diffraction pictures and others physical properties of this samples have been studied.

## Structural characteristics of II-VI diluted magnetic semiconductor films

Kurbatov D.<sup>1</sup>, Kshnyakina S.<sup>1</sup>, Opanasyuk A.<sup>1</sup>, Danilchenko S.<sup>2</sup>

<sup>1</sup>Sumy State University, Sumy, Ukraine;

<sup>2</sup>Applied Physics Institute NAS of Ukraine, Sumy, Ukraine

Manganese-doped  $A_{2(1-x)}Mn_xB_6$  diluted magnetic semiconductors (DMS) have recently attracted a great deal of attention as a new class of semiconductors, as they exhibit an interesting combination of magnetism and semiconductivity [1], which are essential for future generation spintronics device applications [2]. For example, the  $Zn_{1-x}Mn_xS$  films are currently of great interest owing to their pronounced photoluminescence, magnetic and magneto-optical properties (giant Zeeman splitting and giant Faraday rotations). The  $A_{2(1-x)}Mn_xB_6$  DMS give the possibility of “tuning” the lattice constant and band parameters by varying the composition of the material.

$Zn_{1-x}Mn_xS$  films were deposited by the CSVS method [3] on ultrasonically cleaned glass substrates from stoichiometric  $Zn_{1-x}Mn_xS$  powder under different growth conditions: constant evaporation temperature  $T_e = 1273$  K, various substrate temperature  $T_s = 373 - 823$  K.

Structural investigations of the films were performed with X-ray diffractometer DRON 4-07 with  $CuK_\alpha$  radiation over the range  $20^\circ \leq 2\theta \leq 80^\circ$  (where  $2\theta$  is the Bragg angle) at room temperature. Diffraction patterns obtained under study were normalized to the intensity of (111) peak of the cubic phase. Phase analysis was done by comparison of interline distances and relative intensities from the investigated samples and references according to Joint Committee on Powder Diffraction Standards (JCPDS) [4].

Results of these studies enabled to determine dependence of the main structural film parameters, such as: texture, surface roughness, lattice parameters, grain and X-ray scattering domain sizes, microstrain on the growth conditions.

1. Galazka R.R., Nagata S., Keesom P.H. Paramagnetic-spin-glass-antiferromagnetic phase transitions in  $Cd_{1-x}Mn_xTe$  from specific heat and magnetic susceptibility measurements // *Phys. Rev. B.* – 1980. – V. 22. – P. 3344.
2. Awschalom D.D. et. al. Magnetoelectronics: Teaching magnets new tricks // *Nature.* – 2000. – V. 408. – P. 923.
3. Kurbatov D., Opanasyuk A., Khlyap H. Substrate temperature effect on the microstructural and optical properties of ZnS thin films obtained by close-spaced vacuum sublimation // *Phys. Status Solidi A.* – 2009. – V. 206 (7). – P. 1549.
4. Selected powder diffraction data for education straining (Search manual and data cards). Published by the International Centre for diffraction data. USA. – 1988. - P. 432.



## **Fabrication, morphology and structure of polycrystalline CdTe layers**

Kurilo I.V., Ilchuk H.A., Lukashuk S.V., Rudyi I.O., Ukrainets V.O.,  
Chekaylo M.V.

*National University 'Lvivs'ka Politekhnika', Lviv, Ukraine*

CdTe is well known as one of the most promising polycrystalline materials for the solar cells production. Operational characteristics of such devices depend on the cell elements' heterogeneity and are connected with structure and morphology of polycrystalline layers. Thereby it has attracted a great deal of attention for morphology, structure and composition poly-CdTe layers investigations.

Poly-CdTe layers were prepared using deposition in quasi-closed volume technique to the amorphous substrates of glass (C50-1 brand) and glass with layer ITO. The temperatures of substrate and source were 350 and 650 °C respectively. Changes of the distance between source and substrate, the composition and pressure of the vapor phase, the temperature of sources give an ability to control the speed of growth.

Polycrystalline layers with chaotically oriented crystallites were obtained regardless of deposition and cooling conditions. The layers with thickness 0.76–38.52 μm were obtained by change of deposition time. The significant part of crystallites is faceted by hexatetrahedron, rhombic dodecahedron, and trigontetrahedron forms and another part of crystallites is shapeless.

CdTe crystals and layers are inclined to the tendency of twinning through the small value of energy packing defect. It is revealed accretion twins, twins within the limits of one grain, polysynthetic twins and twins with several not parallel planes of twinning. Surplus of the one component enhances the twinning probability. The excess of Te was found out in all investigated sample layers.

The average grain size depends on deposition temperature, vapor phase composition, crystallization speed and substrate type. It grows with increase of layers thickness.

Elementary composition of the layers and homogeneity of the crystallites were investigated using wavelength-dispersive X-ray spectroscopy (WDS) in JEOL JXA-8200 equipment. Amount of Te in crystallites exceeds an amount of Cd as the result of the different partial pressures of metal and chalcogen. The concentration of Te in the crystallites center and grain boundaries differs by 0.073 % and it is in the range of the analysis accuracy.

Calculations of the mechanical stresses, caused by the thermal expansion coefficients difference, for the boundary layer–substrate were done. The stress value for the boundary layer–ITO is considerably larger than for pair a layer–glass ( $11.18 \times 10^7$  and  $0.21 \times 10^7$  Pa respectively).

## Experimental observation and theoretical analysis of multi-phonon excitations in textured ZnO films

Lashkarev G.V.<sup>1</sup>, Yaremko A.M.<sup>2</sup>, Karpyna V.A.<sup>1</sup>,  
Strelchuk V.V.<sup>2</sup>, Kolomys O.F.<sup>2</sup>

<sup>1</sup>*I.N.Frantsevich Institute for Problems of Material Science, Kyiv, Ukraine*

<sup>2</sup>*V.E.Lashkarev Institute for Semiconductor Physics, Kyiv, Ukraine*

ZnO is a direct bandgap semiconductor ( $E_g = 3.37\text{eV}$  at RT) which has got much attention due to its ability to generate ultraviolet (UV) radiation. A large binding energy of excitons ( $\sim 60\text{ meV}$ ) favors to excitonic transitions at room and higher temperatures. Besides ZnO has a strong enough constant of electron-phonon interaction (EPI) what promotes 8-9 phonon replicas observed in Raman spectrum of this crystal. In the series of papers the phonon replicas in ZnO were revealed in PL and Raman investigations but without theoretical consideration.

ZnO textured films of high structural perfectness were deposited by radio frequency reactive magnetron sputtering on sapphire (0001) substrate using layer-by-layer growth mode [1]. The resonant Raman scattering (RS) is a powerful method for the investigation of elementary excitations in crystals. Raman measurements were carried out in backscattering geometry ( $z(x,x)\bar{z}$ ) at room temperature using Horiba Jobin Yvon T64000 system. Multi-phonon structure of RS spectra can be explained in the frames of theoretical approach developed in [2]. Fig.1 shows experimental RS spectrum and theoretical result.

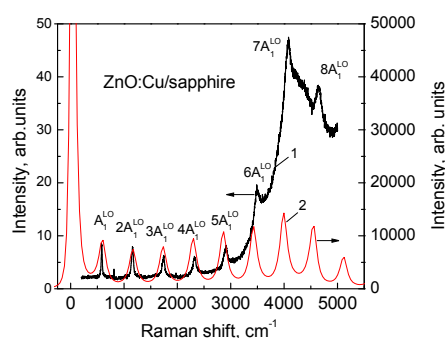


Fig. 1. Comparison of experimental RS spectra (curve 1) of ZnO:Cu film with calculated one (curve 2).

It is seen that positions of maxima of experimental spectrum are well enough described by theoretical dependences. In particular, we can see that number of maxima is eight, which is practically the same as for bulk crystal [3]. The numerical calculations show also that character of spectrum, i.e. the number of maxima and distribution of intensity different line is very sensitive to constant of EPI. The theoretical analysis allowed to determine the following main parameters describing LO phonons in RS: energy  $\Omega_{LO} = 72\text{ meV}$ ; constant of EPI  $\delta\chi^{0,1} = 0.2\text{ eV}$ ; damping constant  $\gamma = 10\text{ meV}$ .

1. Ievtushenko A.I., Karpyna V.A., Lazorenko V.I., et.al., *Thin Solid Films*. – 2010. – V.518. – P. 4529.
2. Yaremko A.M., Dzhagan V.M., Yukhymchuk V.O., et.al. // *J. Mol. Struct.* – 2010. – V.976. – P. 205.
3. Scott J.F. // *Phys. Rev. B*. – 1970. – V.2. – P. 1209.

## **Conditions for forming amorphous thin-films of the GaSb – Sn system**

Lutsyk N.Yu.

*Ivan Franko National University of L'viv, Physical Faculty, Chair of Physics of Metals*

Films of the GaSb-Sn system with the thickness near 500Å were prepared using method of a flash vacuum evaporation. Glass, ceramic and spallings NaCl monocrystals were served as substrates. Structure, substructure, concentration areas of existence of metastable solid solutions and an amorphous state and kinetics of structural transformations depending on technological conditions of evaporation of thin films of system GaSb-Sn were studied by methods of electronography and transmission electron microscopy. Equilibrium of system GaSb-Sn in a massive state is featured by the diagram of the eutectic type. The temperature of a substrate supported in a precipitation process of films has dominant effect on structure formation of explored films. Films precipitated on substrates at room temperature were amorphous up to 60% of Sn atom concentration. Two-phase polycrystalline films ( $\beta$ -Sn and GaSb) are formed at higher concentrations of Sn. With the increase of temperature of a substrate there is a forming the nonuniform amorphous films. Amorphous films at heat crystallized, but phases of a solid solution it is not observed. Initial crystallization phases are crystal grains  $\beta$ -Sn. The growth of crystallite sizes of  $\beta$ -Sn takes place with the temperature increase. A speed of continuous heating has essential influence on the density and sizes of metallic crystallites of  $\beta$ -Sn formed in the amorphous semiconductor matrix based on GaSb. With the further increase of temperature of substrates on the isotropic substrates, polycrystalline films of a metastable solid solution of substitution are formed for the concentration up to 20% of Sn<sub>2</sub>, and on spallings NaCl monocrystals textured and epitaxial films are formed.

## **Atomic force microscopy 3D metrology for assessment surface topography**

Lytvyn O.S., Lytvyn P.M., Korchovyι A.A., Litvin Yu.M., Prokopenko I.V.

*V. Lashkaryov Institute of Semiconductor Physics, NAS of Ukraine, Kyiv, Ukraine*

Much effort devoted to development of micro- and nanotechnology (MNT) devices and materials. Transfer of technology from the research stage, through production, out to the commercial marketplace reveals some areas of metrology where more research is needed than is carried out at the moment. Also, metrology does not just allow control of production but can allow legal, ethical and safety issues to be settled in a quantitative and informative manner. The analytical results and surveys in Europe and the USA clearly indicate that standardization is the major issue that is hampering commercial success of the MNT industry [1].

Whilst nanotechnology is the science and technology of structures varying in size from around 0.1 nm to 100 nm, nanometrology does not only cover this size range. It relates to measurements with accuracies or uncertainties in this and smaller size range. For these purposes the scanning probe microscopes are ideal candidates for measurements of dimensions and various physical and chemical properties. However, for these relatively new instruments, standardized calibration procedures still need to be developed.

The use of AFM's for practical traceable characterization of functional surfaces is preconditional on calibration of piezo scanners as well as practical consideration of the tip's interaction with the representative surfaces. At the same time the new set of surface characterization parameters based on area (or 3D) statistical functions is developed. The functional relationships between traditional 2D surface parameters and a range of the newly developed 3D parameters need to be established.

These and related issues of practical AFM metrological assistance of MNT as well as Ukrainian standardization procedures are proposed for discussion.

1. Fundamental Principles of Engineering Nanometrology (Micro and Nano Technologies). R.K. Leach, Elsevier Inc. – 2010. – 320 p.

## **Electrophysical properties of AlN obtained by high-frequency reactive magnetron sputtering**

Boyko V.G.<sup>1</sup>, Zayats M.S.<sup>1</sup>, Zayats S.M.<sup>1</sup>, Lozinskii V.B.<sup>1</sup>,  
Makarov A.V.<sup>1</sup>, V.I. Gorbulik<sup>2</sup>

<sup>1</sup>*V.E. Lashkarev Institute of Semiconductor Physics of National Academy of Sciences of Ukraine, Kyiv, Ukraine,*

<sup>2</sup>*Kharkiv National Technical University “KhPI”, Chernivtsi faculty*

Reason of study of nitride aluminum is associated with intensive using of wide-gap semiconductors for the creation of modern electronic devices [1]. AlN films were obtained by high-frequency (13.56 MHz) reactive magnetron sputtering of aluminum target in a gas mixture of Ar i N<sub>2</sub> (ratio1:3,5) at modernized industrial setup “Cathode 1M” [2]. Before AlN film deposition the substrate ion cleaning and heating to 250 - 300 °C temperature were carried out. Deposition rate was about 3 nm/min. the capacitor structures Al/AlN/Al on glass substrate were made to study the electrophysical parameters of films.

About 40 capacitor structures of area (S) 16,31 mm<sup>2</sup> and 20.54 mm<sup>2</sup> were made. Capacitance (C) and tangent of dielectric losses (tg δ) were measured using universal LCR meter E1-7 at the frequency of 1000 Hz. Dielectric constant (ε) of AlN film was obtained from the determined capacitance value.

Specific charge per unit area (Q<sub>pr</sub>), which was funded at the time of its dielectric breakdown, was evaluated from the formula  $Q_{pr}=C_{sc} * U_b$  where C<sub>sc</sub> - specific capacitance per unit area of obtained films.

These films had a dense amorphous structure with the composition close to stoichiometric. It was foud that the breakdown electric field intensity has reached on the best samples  $1.3 \times 10^6$  V/cm<sup>2</sup>, permittivity: static - 9, tangent of dielectric losses - 0,03-0,008, specific capacity of 15.4 nF/cm<sup>2</sup>.

The magnitude Q<sub>pr</sub> also is called quality factor of dielectric layer and determines its quality in the structure. Analysis of the results shows that the greatest value of this parameter reached 1.617 μC/cm<sup>2</sup>, which corresponds to the films with average quality that can be used practically, e.g. in thin-film electronics devices.

1. Schroeter Yu.G., Rebane Y.T., Zykov V.A., Sidorov V.G. Widegap semiconductors /under the editorship of V. Ilyina and A.Ya. Schick - Saint-Petersburg, Nauka – 2001 – 128 p. (in Russian).
2. Installation of magnetron sputtering, “Cathode-1M” Datasheet DLZHM 3,270,005 TO – 1986, 121 p. (in Russian).

## Properties of thin photosensitive polymer films obtained by spin-coating technique

Meshalkin A.<sup>1</sup>, Andries A.<sup>1</sup>, Achimova E.<sup>1</sup>, Bets L.<sup>1</sup>, Kryskov Ts.<sup>2</sup>, Optasyuk S.<sup>2</sup>

<sup>1</sup>*Institute of Applied Physics of Academy of Sciences of Moldova, Chisinau, Moldova*

<sup>2</sup>*Kamianets-Podilsky National University, Kamianets-Podilsky, Ukraine*

Nowadays polymers play a critical role in the advancement of the microelectronics and optoelectronic industry. They serve as photoresists in microlithography and as insulating dielectric materials in chips, displays, interconnects, and photonic devices [1, 2]. This paper deals with the study of spin coating processes for the deposition of polyepoxypropylcarbazole (PEPC) thin films sensitized with iodoform. Spin coating is currently the predominant technique employed to produce uniform thin films of photosensitive organic. Different concentration of polymer solution are proposed in order to obtain thin films with variable thickness (from 150 nm to 1000 nm) by spin coating technique.

Operation conditions for polymer solution deposited on 5 cm diameter optical glass substrate (BK7) was as follows: 2 cm<sup>2</sup> of liquid dispensed on the disk at rest, subsequently accelerated in about 10 s to 3000 rpm and spun for 20 s. The broad range of thicknesses can be covered by using polymer solution with increasing solids content or for a given solution by changing the final spin speed.

It was shown that by raising the polymer concentration from 2.5 to 12.5%, the final film thickness increase from 160 to 960 nm at a spin speed of 3000 rpm. Experimental results obtained by different methods of thickness measurements were compared, evidencing a good fit and enabling to define the quasi-linear thickness dependence for obtaining of required polymer film thickness. The obtained dependence can be successfully extended to other photosensitive polymer films in order to obtain required thickness.

Good surface quality and uniformity of the films was confirmed by the appearance of interference fringes in the transmission spectra, evidencing a uniform thickness and a small scattering / absorption in the film. Swanepoel's envelope method was employed to evaluate the optical constants such as the refractive index by using the optical transmittance spectra. From the fringe pattern in the transmittance spectrum refractive index was found to decrease with the increase of wavelength for the polymer thin films under investigation. Value of refractive index of PEPC film in the transparent region was found to be 1.61.

1. Polymers for Electronic and Photonic Applications; Wong, C. P., Ed.; Academic Press: San Diego, CA. – 1993.
2. Garrou, P. In Thin Film Technology Handbook; Elshabini-Riad, A., Barlow, F., Eds.; McGraw-Hill: New York. – 1997. – Chapter 9.

## Effect of radiation defects on properties of films and nanostructures based on ZnO

Myroniuk D.V., Lashkarev G.V., Lazorenko V.Y., Karpyna V.A.

*I. Frantsevich Institute for Problems of Material Science, NASU, Kiev, Ukraine*

Zinc oxide (ZnO) is a promising material for many applications, including piezoelectric transducers and optical devices. Recently, ZnO attracted interest as a material for ultraviolet (UV) and blue-light-emitting devices because of its wide band gap of 3.37 eV and large exciton binding energy of 60 meV. The large band gap of ZnO is suitable for the fabrication of UV emitters, blue and green LEDs, detectors of UV radiation, cathodoluminophors, transparent electrodes, transparent thin film transistors, acoustoelectric and acoustooptic devices, gas sensors etc.

For space applications, nuclear researches, extraction uranium ores and their treatment, devices have to operate in harsh radiation conditions involving high energy particles. An important point for applications is that the material should be as radiation resistant as possible in order for it reliable operating during extended periods. Presently, the main wide-band-gap materials for space applications include the III-V nitrides, SiC, and diamond. Whereas the effect of high-energy electron irradiation has been reported for ZnO[1], GaN [2], and SiC [3], no data are yet available regarding the irradiation of ZnO by heavy particles such as protons and  $\alpha$ -particles, as was reported for GaN. In particular, to our knowledge, data pertaining to radiation-induced deep level defects in ZnO are not available.

To optimize the use of ZnO devices it is essential to obtain basic physical understanding of its properties. Currently, we are interested in the problem of stabilizing properties of zinc oxide, associated with native point defects (zinc and oxygen vacancies, zinc interstitial, etc). This problem is closely related to the interaction of ZnO with high energy particles ( $\alpha$ -particles, protons, neutrons, etc). Their interaction with lattice leads to a generation of intrinsic defects similar to native thermodynamic equilibrium defects when growing thin films by different methods.

The types of defects generated by radiation, the processes of annealing and methods for their characterization are considered. The impact of radiation on properties of ZnO and other wide band gap semiconductors (GaN, SiC) are compared.

1. Look D.C., Reynolds D.C., Hemsley J.W., Jones R.L., and Sizelove J.R., Appl. Phys. Lett. – 1999. -№75. – P. 811.
2. Fang Z-Q., Look D.C., Kim W., Fan Z., Botchkarev A. and Morkoc H., Appl. Phys. Lett. – 1998. – V. 72. – P. 2277.
3. Hallen A., Henry A., Pellegrino P., Svensson B.G. and Abert D., Mater. Sci. Eng., B 61. – 1999. – P. 378.

## Preparation of chromium dioxide thin films by hydrothermal synthesis

Mytsyuk B.M., Nevdacha V.V., Pogorily A.M.

*Institute of Magnetism of NAS of Ukraine, Kyiv, Ukraine*

The ferromagnetic chromium dioxide ( $\text{CrO}_2$ ) is the technologically important metal oxide as a perspective material of spintronics devices.. Theoretical [1] and experimental [2] studies have confirmed that  $\text{CrO}_2$  is a half-metallic material with a nearly 100% spin polarization in the conduction band. That is, the majority electrons have density of the states, while, the minority ones have an energy gap at the Fermi surface. Accordingly,  $\text{CrO}_2$  would be expected to be suitable for spintronic devices. Chromium dioxide has to be synthesized under high pressure and high temperature because it is a metastable phase in the Cr-O system. Epitaxial thin films of  $\text{CrO}_2$  were prepared by chemical vapor deposition (CVD) [3,4] in a two-zone furnace or decomposition  $\text{CrO}_3$  in a pressure vessel [5].  $\text{CrO}_2$  was grown from a  $\text{CrO}_2\text{Cl}_2$ ,  $\text{Cr}_8\text{O}_{21}$  and  $\text{CrO}_3$  precursors. We tried hydrothermal methods for synthesis of  $\text{CrO}_2$  thin films. At the synthesis of the films the results of our researches for optimization of synthesis conditions of chromium dioxide powders were taken into account [6]. Chromium trioxide ( $\text{CrO}_3$ ) was used as precursor. The substrate used for epitaxial growth of  $\text{CrO}_2$  was the rutile form of  $\text{TiO}_2$  (100), which is isostructural with  $\text{CrO}_2$  ( $a=b=4.594$  Å and 4.420 Å,  $c=2.958$  Å and 2.916 Å for  $\text{TiO}_2$  and  $\text{CrO}_2$  respectively). Different physical and chemical factors on the hydrothermal synthesis of  $\text{CrO}_2$  were studied. Also, the effect of synthesis time on phase composition was obtained. The synthesis was performed in high pressure autoclaves with the swept volume about 12 cm<sup>3</sup>. The reactionary mixtures  $\text{CrO}_3$  with  $\text{H}_2\text{O}$  were prepared up to 15% of water. Experiment was carried out at a temperature 300...400 °C and partial pressure of oxygen and steams of water about 100 atm and about 150 atm respectively. X-ray analysis and electron microscopy researches of reaction products were performed. It turned out, that films of  $\text{CrO}_2$  were synthesized in all experiments.

1. K. Schwarz // J. Phys. F. – 1986. – V. 16. – P. L211-L215.
2. R.J. Soulen Jr., J.M. Byers, M.S. Osofsky, B. Nadgorny, T. Ambrose, S.F. Cheng, P.R. Broussard, C.T. Tanaka, J. Nowak, J.S. Moodera, A. Barry, and J.M.D. Coey // Science. – 1998. – V. 282. – P. 85–88.
3. S. Ishibashi, T. Namikawa, and M. Satou // Jap. J. Appl. Phys. – 1978. – V 17. – P. 249.
4. S. Ishibashi, T. Namikawa, and M. Satou // Mat. Res. Bull. – 1979. – V 14. – P. 51.
5. R.C. DeVries // Mat. Res. Bull. – 1966. – V. 1. – P. 83.
6. Ostapenko H.T., Mytsyuk B.M., Huz N.V., Kuts V.A., Mineral. J. – 2008. – V.30, №7. – P. 75-79.



## Mobility in semiinsulating GaAs doped compensating oxygen and chromium impurities

Novosyadly S.P., Voznyak Yu.V., Sorokhtey T.R.

*Vasyl Stefanyk Precarpathian National University, Ivano-Frankivsk, Ukraine*

In the case of mixed conductivity and Hall coefficient of conductivity can be represented by expressions (1) and (2). Where  $R_n=r_n/e_n$ ;  $R_p=r_p/e_p$ ;  $\sigma_n=e\mu_n n$ ;  $\sigma_p=e\mu_p p$ ;  $B$  - value of magnetic induction. These equations use a connection via expr. (3).

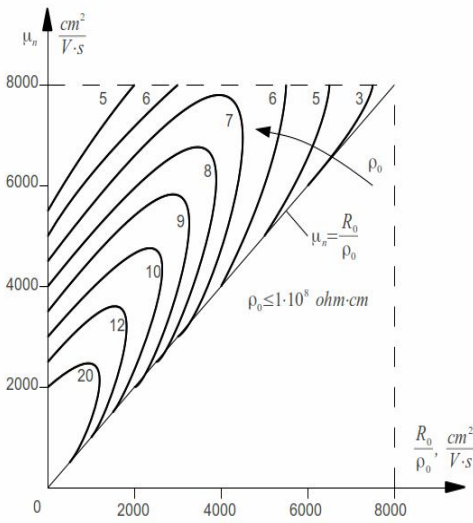


Fig. 1. dependence  $\mu_n=f(R_0/\rho_0)$ .

$$R = \frac{R_n \sigma_n^2 + R_p \sigma_p^2 + R_n R_p \sigma_n^2 \sigma_p^2 (R_n + R_p) B^2}{(\sigma_n + \sigma_p)^2 + \sigma_n^2 \sigma_p^2 (R_n + R_p) 2B^2}; \quad (1)$$

$$\sigma = \frac{(\sigma_n + \sigma_p)^2 + \sigma_n^2 \sigma_p^2 (R_n + R_p)^2 B^2}{\sigma_n (1 + R_n^2 \sigma_p^2 B^2) + \sigma_p (1 + R_p^2 \sigma_n^2 B^2)}; \quad (2)$$

$$1/B^2 + \mu_n^2 = S_{\rho,m} \rho_0 / \Delta\rho = S_{R,m} R_0 / (R_0 - R); \quad (3)$$

$$\sigma_{(n,p)} = \sigma_{(n,p)0} (1 - q\sigma_{(n,p)} \mu_{(n,p)}^2 B^2) \quad (4)$$

$$R_{(n,p)} = R_{(n,p)0} (1 - qR_{(n,p)} \mu_{(n,p)}^2 B^2)$$

$$S_{p,s} = \frac{bc}{1+bc} q\sigma_n \mu_n^2 + \frac{1}{1+bc} q\sigma_p \mu_p^2$$

$$S_{R,s} = \frac{b^2c}{b^2c-1} qR_n \mu_n^2 - \frac{1}{b^2c-1} qR_p \mu_p^2 + \quad (5)$$

$$+ \frac{2bc(bc+1)}{(b^2c-1)(bc+1)} (q\sigma_n \mu_n^2 - q\sigma_p \mu_p^2)$$

Where  $S_{R,m} = \mu_n^2 c(1+b)^2(1-c)/(b^2c-1)(1+bc)^2$ ,  $S_{\rho,m} = \mu_n^2 c(1+b)^2/b(1+bc)^2$ ,  $c=n/p$ ,  $b=\mu_n/\mu_p$ .

From equation (3) it is obvious that  $S_{\rho,m}$  and  $S_{R,m}$  express the inclinations  $1/B^2$  of  $\rho_0/\Delta\rho$  and  $1/B^2$  of  $R_0/(R_0-r)$ . Index "0" refers to zero magnetic field, Hall-factor taken equal to 1. For the monopolar conductivity in addition to equations. (1) and (2) use the following ratio (4). For  $\sigma$  such in this approximation  $S_p=S_{p,m}+S_{p,s}$  and  $S_R=S_{R,m}+S_{R,s}$  in (5). To calculate the monogram used value  $n_i^2 = np$ ,  $\mu_p^{-1} = 9 \cdot 10^{-4} + B\mu_n^{-1}$  and the Hall-factor value  $r_n=r_p=1$ . Study established the value of resistance were the following samples doped with Cr (from  $6 \cdot 10^7$  to  $1,7 \cdot 10^9$  ohm·cm), while the low resistance of undoped from  $3 \cdot 10^7$  to  $3 \cdot 10^8$  ohm·cm and  $n_i$  in the  $(1 \div 15) 10^6 \text{ cm}^{-3}$  for resistance was doped with oxygen within  $2 \cdot 10^7$  to  $2 \cdot 10^9$  ohm·cm. Then designed monogram relationship  $\mu_n=f(R_0/\rho_0)$  for GaAs, doped chromium becomes submitted in Fig. 1.

1. Insulating compound  $A^{III}B^V$  ed. JW Rice, trans. from English. Ed. MG Milvidenko – M.: Metallurgy, 1994. – 251 p.
2. Novosyadly S.P. Physical and technological bases of submicron VLSI – Ivano-Frankivsk: Simyk, 2003. 351 p.

## Physical and technological aspects of forming structures of gallium arsenide technology logic to selectively doped field-effect transistor (SDFT)

Novosyadly S.P., Voznyak Yu.V., Sorokhtey T.R., Daniluk O.V., Fryk O.B.

*Prekarpathian national university about Vasyl Stefanyk, Ivano-Frankivsk, Ukraine*

In the ring oscillator, which formed on them, made a switch at 10 ps at 300 K and 6 ps at 77 K and frequency divider SDFT to work on input frequencies to 10 GHz. They also created a storage device with an arbitrary sample volume 4K and 16K. In SDFT used importance of mobility and drift velocity of two-dimensional electron gas (2D), which is formed at the boundary between two semiconductor materials (highly doped AlGaAs and undoped GaAs superlattice as the layer structure). Figure 1 provided direct and inverted AlGaAs-GaAs structure with a locking pin and band diagram, which became the model of charge.

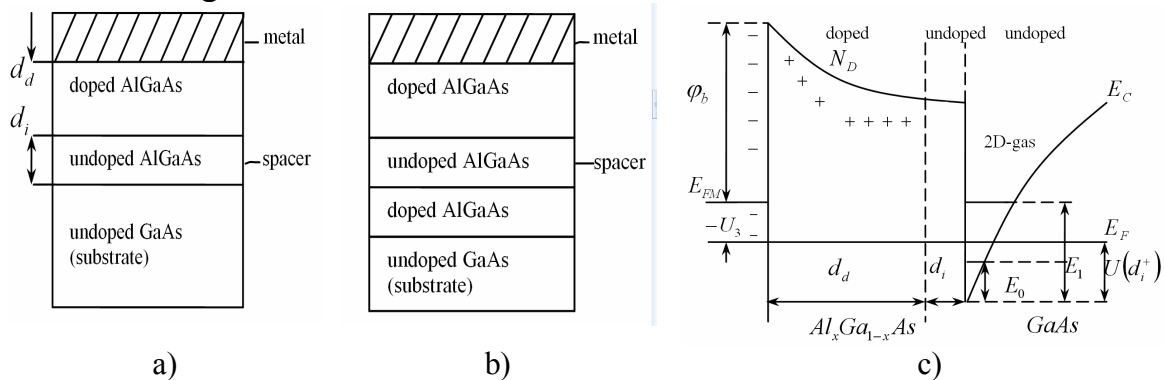


Fig 1. Direct a); inverse b); AlGaAs-GaAs structures with locking pin c) Band diagram of structure AlGaAs-GaAs (negative voltage on gate fully impoverishes AlGaAs layer and 2D-electron gas).

Under this model were determined current-voltage and capacitance-voltage characteristics normally open and normally closed SDFT, which became the basis of logic, which was conducted in the simulation program UM-SPICE. Estimation of time spent switching of the inverter, because of the charge and discharge the input capacitance. This defined capacity, which at the time uses inverter switching. To build a high-speed GaAs logic circuits to be used as a key SDFT digital circuitry. The use of silicon substrates with epitaxial layers of gallium arsenide (superlattices).

1. Новосядлий С.П. Суб- і наномікронна технологія структур ВІС. Івано-Франківськ // Місто НВ – 2010 – 456с.
2. Cirillo N.C., Jr Shur M.S., Vold P., Abrokwhah J.U., Tufte O.N. Realization of n-channel and p-channel high-mobility (AlGa)As/GaAs heterostructure insulating gate FETs on a planar water surface // IEEE Electron Dev. Lett.-1985 EDL-6(12) p.645-647.

## Temperature dependence of the dielectric characteristics of thin polymer films deposited in vacuum

Polishchuk S. G., Zadorozhniy V. G., Kobrin V.L.

*Odessa National Academy of Food Technologies, Odessa, Ukraine*

Properties of polymer films deposited by the vacuum evaporation depend on the deposition parameters, of which the most important one is the temperature. Studies of the temperature dependence of dielectric properties of thin polymer films deposited by evaporation in a vacuum were conducted over a wide temperature range. It was found that the dielectric loss tangent decreases with increasing temperature in the range of 280...373 K for films of nonpolar polytetrafluoroethylene (PTFE) and polyethylene (PE) polymers. This decrease was due to evaporation of adsorbed water vapors and separation of hydroxyl groups, which were the centers of the moisture sorption. With further increase of the temperature, the dielectric loss tangent slightly increases, so that its value at the temperature of 423 K does not exceed 0,0015. We believe that the reason of this increase is the contribution of higher molecular fractions. For films subjected to the heat treatment in a vacuum, the dielectric constant and dielectric loss tangent increase slightly at 323 K (their values do not exceed 1,9 and 0,0008, correspondingly). This is associated with re-evaporation of low molecular weight fractions, as well as removal of oxygen-containing groups and decrease in concentration of polar double bonds.

For polycarbonate (PC) films, the temperature dependences of the dielectric permittivity and the dielectric loss tangent are different due to the low-temperature  $\gamma$  - relaxation at about 223 K and the segmental mobility ( $\alpha$  - relaxation) leading to the maximum of the dielectric losses.

It was found that in the case of films produced without initiating the secondary polymerization during the deposition, the maximum at the curve ( $\gamma$  - relaxation) is shifted by 10 K to the region of low temperatures, as compared with the same peak in the case of films produced by using the electron-beam initiation of polymerization during their deposition with the surface power density of about 50 W/cm<sup>2</sup>.

Initiation of the secondary polymerization of macromolecule fragments deposited on the substrate during the film formation with their subsequent heat treatment results in decrease of the dielectric loss tangent and the dielectric permittivity of the films.

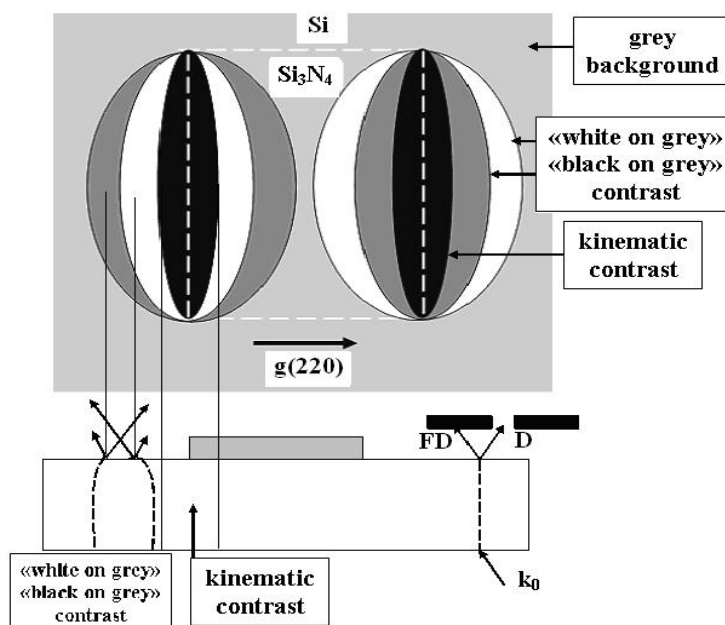
## Silicon nitride film-edge induced strain distribution in silicon crystal substrate

Prykhodko A.V.

*Zaporizhzhya National University, Zaporizhzhya, Ukraine*

Silicon substrates with thin dielectric films are in elastic bending deformation state. After a lithography mechanical stresses in substrate are redistributed because the film to become not continuous.

Two models which present film-edge induced strain or stress distributions in substrate are known. It is the concentrated force model for a film island with definite sizes [1] and the distributed force model for a semi-infinite film with one straight line boundary [2]. Experimental testing of these models till now are not carried out.



Thin film-edge induced substrate strain distribution may be observed by X-ray transmission topography. The X-ray topography diagram of 200 microns thickness silicon  $\{100\}$  substrate with a 0,5 microns silicon nitride film island under condition  $\mu \times t \approx 1$  is presented on figure. There are an inversions of X-ray diffraction contrast from «black on grey» to «white on grey» because the bending direction of atomic planes varies. The  $\{110\}$  planes bending distribution at silicon nitride film edge has been counted by concentrated force model [1] and compared to contrast area sizes on topogram. The qualitative adequacy of concentrated force model and experimental results has been established only, while a contrast area extents on the topogram are more that counted by simulation near five times.

1. Seiichi Isomae // J.Appl. Phys.– 1981.–V. 52, №4. – P. 2782-2791.
2. Hu S.M.// J.Appl. Phys.– 1979.–V 50, №7.– P. 4661-4666.

## Distribution of polarization in corona poled P(VDF-TFE) films

Sergeeva A.E., Fedosov S.N.

*Odessa National Academy of Food Technologies, Odessa, Ukraine*

Ferroelectric polymer films are usually corona poled to obtain a high residual polarization responsible for piezo- and pyroelectricity of the films. The present study was performed to reveal origin of polarization non-uniformity in corona poled P(VDF-TFE) copolymer films and to find its relation to the space charge.

Uniaxially stretched 20  $\mu\text{m}$ -thick ferroelectric films of 95/5 P(VDF-TFE) were electroded from one side and negatively charged in a corona triode at either constant current (CC), or constant voltage (CV) modes at 20 and 85 °C under the poling field from 55 to 110 MV/m. In some experiments, two sandwiched films were poled and then studied separately. Polarization profiles were measured by the piezoelectrically induced pressure step (PPS) method with resolution of 2 nm.

It has been found that polarization was non-uniformly distributed with a peak near a positive grounded electrode in CC poled films independently on the poling temperature. The polarized zone was not directly attached to the positive electrode, but was separated from the latter by a thin transition zone. In the CV poled films, polarization was non-uniform at near-coercive poling field, but it was rather high and uniform in case of high poling fields. From two sandwiched films poled in medium field, only the lower one was almost uniformly poled, while the upper film subjected to corona remained completely unpoled. At high field, the upper film was non-uniformly poled with very low magnitude of polarization.

It is clear from our results that injection of negative charges plays a dominant role in creation of the polarization non-uniformity. Charges are injected from the virtual electrode formed by corona ions adsorbed at the surface. Injected charges are trapped near the surface in case of high poling fields giving rise to almost uniform distribution of polarization. At low fields in the CV mode and during CC corona poling, conditions are favorable for penetration of the injected charge deep in the volume. The injected negative charge distorts uniformity of the poling field and that of residual polarization. Positive charges are either not injected, or trapped near the surface.

In order to obtain uniformly distributed polarization in corona poled P(VDF-TFE), we suggest that 1) CC poling must not be used, 2) field during the first poling must be at least two times higher than the coercive value, 3) moderate poling field can be applied, but in this case, the sample must be covered by additional film which will absorb injected charges and prevent them from causing non-uniformity of polarization in the main sample. We believe that the recommendations are applicable to other ferroelectric polymer films.

## **Anomalous stability of the surface potential in corona-charged PVDF films**

Sergeeva A.E., Revenyuk T.A. and Fedosov S.N.

*Odessa National Academy of Food Technologies, Odessa, Ukraine*

An attempt has been made in the present work to combine advantages of two methods of studying processes of charge storage and polarization in polymer films, namely, examining the surface potential decay under open-circuit conditions and application a constant-current corona charging. Polyvinylidene fluoride (PVDF) films were charged in a corona triode by rectangular current pulses. As a result, a correlation of surface potential stability with the electrical conductivity, controlled in its turn by the value of polarization, has been revealed.

The study was performed on metalized from one side 25- $\mu\text{m}$  thick PVDF films composed of amorphous and crystalline phases. The free surface was treated by a negative corona discharge generated by a pointed W electrode. A constant charging current of 80  $\mu\text{A}/\text{m}$  was maintained for 300 s by means of a feedback circuit. The partial decay of the surface potential was observed for another 300 s after switching off the corona discharge. Charging-discharging cycles were repeated until voltage at the sample became equal to the grid potential (3 kV).

The whole electrization process was thus divided into several stages each containing a period of voltage steep rise under a constant charging current and a period of voltage decay at intervals between adjacent current pulses. The voltage was automatically measured by Kelvin's method and continuously recorded.

The anomalous increase of the surface potential stability was observed during the charging. To analyze the potential-time dependence, we assumed a two-layer structure and substituted the real sample with the equivalent circuit consisting of two resistors and two capacitors. The problem was reduced to calculation of the transient responses of the circuit to step current application and to its removal.

It appeared that  $R_1$  remains constant while  $R_2$  increases from cycle to cycle. Additional experiments revealed that the first layer corresponded to the diffusive capacitance due to space charge over the sample surface that was dissolved after termination of the charging. It was concluded that the anomalous surface potential stability was caused by a decrease in conductivity, which in its turn was influenced by the balance between the delocalized (free) charge carriers (intrinsic and injected in the bulk) and the trapped charges.

The phenomenon can be explained assuming that additional deep trapping accompanies the build-up of polarization. New traps are most likely located at the crystallite boundaries due to the large-scale potential fluctuations caused by alignment of permanent dipoles in the crystallites. This state is apparently stable, since the trapped space charges compensate the local depolarization field.

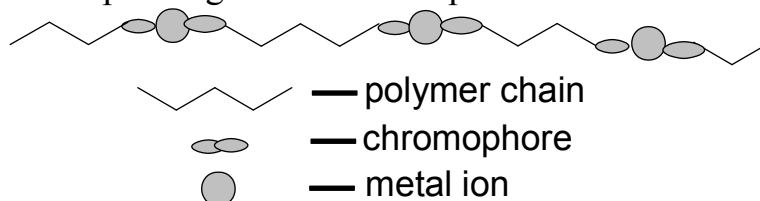
## The influence of the structure of polycomplexes with cobalt on their electro-optical properties

Sinyugina A.T., Savchenko I.A., Studzinskij S.L., Kolendo O.Yu.

*Kiev National Taras Shevchenko University, Kiev, Ukraine*

Azobenzene-containing polymers received more and more attentions in this decade for their potential applications in many fields, such as optical data storage, nonlinear optical materials, holographic memories [1-3].

We report on the development and characterization of new metal-containing polymers with azo chromophores and metal ions in the main chain. In previous work was investigated the formation of holographic diffraction gratings for similar compounds [4]. The aim of this work was the synthesis of new polycomplexes with cobalt and the investigation of optical and electrical properties of them depending on the chromophore structure.



The mechanism of electro-optical effect in samples, which previously were illuminated by linear polarized light, is connected with appearance and accumulation of photo induced dipole moments of azo groups isomers. We found that the polycomplexes with cobalt have a positive and negative sign of  $\delta I_E$ , that is depending from the structure of the azo chromophores.

1. Mubarak A., El-Sonbati A.Z., Ahmed S. Supramolecular structural and spectral perspectives of novel ruthenium (III) azodye complexes. // *J. of Coordinat. Chem.* – 2007. – V. 60, №17. – P. 1877-1890.
2. Li Lin, Ze Feng, Qianli Yu, et al. Self-assembly and photoresponsive behavior of amphiphilic diblock copolymers containing azobenzene moieties. // *Mol. Cryst. Liq. Cryst.* – 2009. – V. 508. – P. 214-225.
3. Hinghai Yu, Zhengsheng Fu, Honggang An, and et al. Synthesis and characterization of photochromic copolymer grafting azoaromatic cromospheres on pullulan. // *Internat. J. of Polym. Mater.* – 2011.– V. 60. – P. 40-50.
4. Davidenko N.A., Savchenko I.A., Davidenko I.I., Popenaka A.N., Shumelyuk A.N., and Bedarev V.A. Hologram recording and the electro-optic effect in azobenzene derivative polymers and azobenzene derivative-cobalt polycomplexes // *Technical Physics.* – 2007. – V.52, №4. – P. 451-455.

## **Influence of technological factors in the method of hot-wall on the process of thin films of CdTe**

Sokolov O.L., Potyak V.Yu

*Vasyl Stefanyk Precarpathian National University, Ivano-Frankivsk, Ukraine*

Thin films based on cadmium telluride are widely used in various fields of semiconductor instrumentation: detectors for producing infrared radiation, solar cells, also as protective coatings for semiconductor structures, such as infrared radiation detectors based on  $Hg_{1-x}Cd_xTe$ . In recent years, considerable interest CdTe films due to the possibility of building on the basis of quantum dots for spin and quantum information systems with a characteristic spin relaxation time of 100 ps [1].

This paper presents the results of investigation of the condensation of cadmium telluride on the substrate mica-muscovite under different technological parameters (temperature substrate, temperature evaporator, time deposition).

CdTe films obtained by hot-wall [2] at  $10^{-2}$  Pa vacuum. As the substrates used mica-muscovite. The temperature of deposition (substrate) varied within  $T_s = (100-350)$  °C. Temperature evaporator of the synthesized compounds CdTe advance variation within the  $T_e = (400-500)$  °C. Wall temperature maintained at 50 °C higher temperature evaporator. Thickness of condensate asked the time of deposition.

The main feature of hot-wall method is growing films to as close as possible to equilibrium. Such conditions are provided quasi-locked space in which the condensate is derived, and the selection of three temperature settings ( $T_w$ ,  $T_e$ ,  $T_s$ ) providing a constant temperature gradient of grows reactor. The value of these parameters were selected and optimized to experimental data.

Dependences of the condensation rate of technological parameters are set pattern: with increasing substrate temperature  $T_s$  at constant temperature evaporator  $T_e$  condensation rate decreases, with increasing temperature evaporator  $T_e$  with constant substrate temperature  $T_s$  condensation rate increases.

In the studied range of technological parameters of film thickness was obtained 0,10-20,0 microns. The regularities of structural formation tapes CdTe films investigated changing technological factors.

1. Tomashik V.M., Bylevych E.O., Tomashik V.N. Interaction with soluble cadmium telluride systems  $HNO_3$ -HCl (HBr) - tartaric acid // Condensed matter and interface boundaries, – 2002. – T.3, №33. – P. 237-241.
2. Freik D.M., Galuschak M.A., Mezhylovska L.Yo. . Physics and Technology semiconductor films. High School, Lviv, 152 p. (1988).



## Subphthalocyanine based multilayer photovoltaic cells

Pakhomov G.L., Travkin V.V.

*Institute for Physics of Microstructures of the Russian Academy of Sciences,  
Nizhny Novgorod, Russian Federation*

As known, introduction of subphthalocyanine SubPcBCl instead of conventional phthalocyanine complexes in multilayer organic photovoltaic cells (OPVC) results in significant increase of their power conversion efficiency ( $\eta$ ) [1]. Most typically, such OPVC consist of a planar SubPcBCl/fullerene heterojunction with additional ultrathin buffer layers adjacent to electrodes, all deposited sequentially on transparent substrate. Buffer layers may further exciton blocking, injection of charge carriers or minimize unwanted chemical reactions at the electrodes.

Earlier [2], we studied Schottky barrier cells based on SubPcBCl with particular interest in elucidating the role of top metallic cathode. In this report we describe fabrication of multilayer OPVC having initial configuration of glass/ITO/SubPcBCl/C60/Al type. At first, subphthalocyanine layer was doped by small aromatic molecules with strong electron accepting properties (e.g., chloranil) using surface diffusion method. Conductivity and photovoltaic parameters of these cells were measured in inert atmosphere and then compared with reference samples and literature. Secondly, OPVC with SubPcBCl layer doped with another convex-shaped phthalocyanine molecule, PcVO by co-sublimation method were manufactured and tested.

Finally, the cells were equipped with ultrathin bottom buffer layer deposited over the anode, ITO and top buffer layer inserted beneath the cathode, Al. Tris(8-hydroxyquinolato)aluminum (AlQ3) and vanadyl naphthalocyanine NcVO serve as buffer layer materials. It was found that the buffer layer material and its thickness may tune the output parameters of OPVC in a broad range, including both the short circuit current and open circuit voltage.

The effect of dopant on specific conductivity of SubPcBCl layer and characteristics of resulting OPVC is discussed. Mutual diffusion of components should be taken into account there.

1. G. Bottari, G. de la Torre, D.M. Guldi, T. Torres “Covalent and Noncovalent Phthalocyanine-Carbon Nanostructure Systems: Synthesis, Photoinduced Electron Transfer, and Application to Molecular Photovoltaics” *Chem. Rev.* – 2010. – №110. P.6768–6816.
2. G.L. Pakhomov, V.V. Travkin, A.Yu. Bogdanova, T.-F. Guo “Photovoltaic properties Schottky barrier cells utilizing subphthalocyanine layer” *Journal of Porphyrins and Phthalocyanines* 12. – 2008. – P.1182 – 1186.

## Forming a thin layer of composite metal band in the periodic energy action

Tsotsko V.I.<sup>1</sup>, Denysenko O.I.<sup>2</sup>

<sup>1</sup>*Dnipropetrovsk State Agrarian University, Dnipropetrovsk, Ukraine*

<sup>2</sup>*National Metallurgical Academy of Ukraine, Dnipropetrovsk, Ukraine*

In the current technology of thin-layer materials and coating materials using controlled energy localized effect on the surface of the material. To increase the efficiency of applying highly intensive energy flows that create the surface of the material limit for a solid state temperature, which can approach and exceed the melting point.

One way of surfacing, based on the principle of pulse surface treatment of the product particles of powdered material is gas-dynamic spraying method in which the grip of the functional particle basis is achieved by plastic deformation and heating components interacting at impact. Promising option for the specified process is to form a composite coating by injection of dispersed phase supersonic jet.

The practical interest in connection with the technological ease of synthesis of metal-composite electrode structures injector method is the possibility of applying a thin metal strip that moves relative to the current two-phase jet on it [1].

Experimental study of two-phase flow – the flow of solid particles of functionally active substance (dispersed phase MnO<sub>2</sub> or LiMn<sub>2</sub>O<sub>4</sub>) and air flow - on the surface of metal (aluminum tape thickness ~ 50 microns) has shown to achieve reliable coupling with the metal particles during their immersion in the metal at least half of their average diameter (200-400 nm). This minimal growth temperature ("temperature pedestal") to limit the maximum penetration of particles surface functionally active agent in aluminum tape is estimated to order of magnitude lower relative to the melting temperature metal tape.

Application of the principle of pulse surface film using a pulsed supersonic jet of dispersed phase or maintainer of the energy flow, which changes periodically, leading to the formation of unsteady temperature field depth attenuation which varies depending on the frequencies.

Analytical methods and numerical simulation on the example of course one-dimensional homogeneous model, the correlation between the depth of effective heating of the basic frequency bands and energy flow, acting on the metal surface.

The nature of damping the amplitude of the temperature field  $A(x)$  with distance from the surface of periodic energy in the metal's with reasonable accuracy can be described by the formula

$$A = A_0 e^{-\delta x}$$

where  $A_0$  – amplitude of temperature fluctuations on the surface film,  $\delta$  – coefficient of damping, depending on the frequency of the surface energy and coefficient of thermal metal.

1. Denysenko O.I., Tsotsko V.I., Spiridonova I.M., Peleshenko B.I. Formation of thin tape temperature field under effect of two-phase jet dispersed phase on tape surface // Physics and chemistry of solid state. – 2008. – V.9, №4. – P. 901-904.

## Structure and properties of electrochemically deposited Zn-Ni alloy coatings

Tsybul'skaya L.S., Purov'skaya O.G., Poznyak S.K., Gaev'skaya T.V.

*Research Institute for Physical chemical Problems of Belarusian State University,  
Minsk, Belarus*

Alloying of electrolytic zinc coatings with metals of the iron subgroup enhances substantially the duration of their protective action because these alloys, being anodic with respect to steel in an aggressive medium, demonstrate higher corrosion stability as compared with zinc. This effect is most strongly expressed in the case of Zn-Ni alloys containing 9-14 at.% Ni (Zn-Ni<sub>9÷14</sub>).

The aim of this work was to prepare the coatings of the above composition and to study their structure, morphology and corrosion stability in a chloride-containing medium (3,5 % NaCl solution).

Alkaline polyligand electrolyte was used for electrodeposition of the Zn-Ni coatings containing 9÷14 at.% Ni. The concentration of Zn(II) salt in the electrolyte remained constant (0,12 mol/l), whereas the concentration of Ni(II) salt was varied from 0,025 to 0,049 mol/l at a constant molar Ni(II)-to-ligand ratio (ligands - aminoacetic acid and triethanolamine): **1** – 0,025:0,46:0,09; **2** – 0,035:0,65:0,12; **3** – 0,049:0,9:0,17. The cathodic current density ranged from 0,5 to 5 A/дм<sup>2</sup>, the concentration of saccharine – from 2 to 10 g/l and the concentration of sulfanilic acid – from 0,1 to 0,5 g/l.

X-ray diffraction study showed that the Zn-Ni coatings with 9÷14 at.% Ni consist of the only  $\gamma$ -phase (Ni<sub>5</sub>Zn<sub>21</sub> intermetalloid), and the intensity of the  $\gamma$ -phase peaks increases as the Ni concentration grows. Scanning electron microscopy images of the coating surface testify that the Zn coating has smooth surface with a fine-grained structure, while a nodular morphology with pronounced micro- and nano-relief is characteristic of the surface of the Zn-Ni alloys.

Corrosion studies performed using electrochemical impedance spectroscopy showed that the corrosion stability of the coatings in neutral chloride-containing medium grows with increasing the Ni content in the alloy: the charge transfer resistance, calculated using appropriate equivalent schemes, after 500 hours of keeping the samples in 3,5 % NaCl solution is 0,5 kOhm·cm<sup>2</sup> for Zn, 2,5 kOhm·cm<sup>2</sup> – for Zn-Ni<sub>9</sub>, 3,5 kOhm·cm<sup>2</sup> – for Zn-Ni<sub>11</sub> и 7,2 kOhm·cm<sup>2</sup> for Zn-Ni<sub>14</sub>. Corrosion dissolution of the coatings at the initial stages seems to result in the destruction of the alloy with preferable dissolution of zinc from surface layers and in the formation of loose corrosion products with complex oxide-hydroxide composition. Enrichment of the coating surface with nickel owing to the zinc leaching gradually leads to the increase in corrosion stability of the Zn-Ni coatings.

## **Modification of surface morphology of the metalphthalocyanine films by laser irradiation**

Turiev A.M., Butkhuzi T.G. ,Ramonova A.G., Magkoev T.T., Tsidaeva N.I.

*The state University of North Ossetia, Vladikavkaz, Russia*

During the study of fragmentation of films of manganese phthalocyanine under the influence of laser radiation was found out the dependence of the spectral composition of the particles from the multiplicity of exposure [1]. Evidently, an irreversible changes of the surface condition take place in this process, that leads to the changes of the values of absorption and reflection coefficients. In this connection, the study was to investigate possible changes in the morphology of the surface irradiated by a laser pulse. In this study, using AFM, the films of copper and manganese phthalocyanines, vacuum-deposited on the surface of gallium arsenide were investigated. The film thickness was controlled by the resonance method at the time of deposition. The quality of the films was evaluated by comparing the IR absorption spectra of the films and the original powder. As a radiation source was used neodymium laser with photon energy 2.34 eV and 1.17 eV. Found that the effect of laser radiation leads to an irreversible change in surface topography. If the wavelength of the incident radiation falls in the region of intrinsic absorption, the reconstruction of the surface takes place and it is observed as leveling of surface in the AFM pictures, contained in the report. Irradiation in the area of transparency leads to heating of the substrate and annealing of the film occurs from the substrate, and, as shown in the AFM images, contained in the report, in the case of thin films the roughness of the surface is increasing. It is shown that the variation of laser wavelength changes the surface morphology of the exposed part of the films. Comparative analysis of topographic measurements of surface areas of the films before and after exposure of radiation with a wavelength  $\lambda_1$  shows, that, starting with some threshold, power density polymerization of the film takes place. The polymerization process is accompanied by an intense desorption of molecular fragments. Small part of their leaves the surface in the clusters, the rest are involved in the formation of the polymer films

Work performed on equipment of Center for Collective Use «Physics and technology of nanostructures» of the State University of North Ossetia.

1. Butkhuzi T.G. Turiev A.M., Magkoev T.T., Ziminov A.V. Investigation of the fragmentation of the peripherally substituted copper phthalocyanine films. Proceedings of AMS-2010.St.Petersburg, July, 2010.

## **A synthesis and study of the rhenium-containing nanoparticles in polyethylene matrix**

Yurkov G.Yu.<sup>1</sup>, Fionov A.S.<sup>1,2</sup>

<sup>1</sup>*A.A. Baikov Institute of Metallurgy and Materials Science, Moscow, Russia*

<sup>2</sup>*V.A. Kotelnikov Institute of Radio Engineering and Electronics, Moscow, Russia*

Development of nanoparticles-based composites is very high-perspective, first of all, because of a recently developed wide variety of sizes, forms, compositions and structures of nanoparticles produced by chemical methods. It allows to predict and vary physical properties of nanoparticles before using them as building blocks for nanomaterials.

Usage of Re-containing compounds rides on the rhenium refractoriness, high boiling temperature, mechanical strength and chemical inertness towards some gases. It makes rhenium nanoparticles to be a very attractive material for electronics and electrical engineering. Also rhenium-containing compounds are widely-used catalysts for ethylene and oil hydrogenation. So a goal of the present work is a development of synthetic procedure and study of composition for the composite nanomaterials consisting of rhenium-containing nanoparticles localized in matrix of low-density polyethylene. It will allow constructing of new catalysts, electrodynamically and optically active nanomaterials.

Rhenium-containing composites were obtained by thermodestruction of different rhenium complexes. The composites were characterized by TEM, EDS, XRD and EXAFS. Results of EDS analysis and transmission electronic microscopy of composites indicates a presence of rhenium-containing nanoparticles in composites. Composition of nanoparticles and their local atomic structure were studied by EXAFS spectroscopy. It was shown that Re-containing nanoparticles are  $15.0 \pm 0.3$  nm in size and consist of Re,  $\text{Re}_2\text{O}_7$ ,  $\text{ReO}_3$ ,  $\text{ReO}_2$ .

Also dependence of permittivity and propagation factor of microwaves on content of rhenium-containing nanoparticles localized in the volume of low-density polyethylene matrix was investigated. The correlations of permittivity and attenuation of microwave with composition of Re-containing nanoparticles were determined.

This work was partially supported by the Russian Foundation for Basic Research (grant nos. 11-07-00278-a, 11-08-00015-a).

## Crystallinity of deposited in vacuum thin polymer films studied by methods of differential thermal and thermogravimetric analysis

Zadorozhnyi V.G., Polishchuk S.G., Kobrin V.L.

Odessa National Academy of Food Technologies, Odessa, Ukraine

The crystallinity of thin film of hetero-polymers produced by evaporation and condensation in a vacuum has been studied by methods of differential thermal analysis (DTA) and thermogravimetric (TGA) analysis.

It has been found that the melting enthalpy of the films ( $\Delta H_m$ ), as well as the crystallinity of the films does not depend on the evaporation method and is determined by the condensation rate ( $V_c$ ) and the substrate temperature ( $T_c$ ) during condensation of vapors. It appeared that the surface treatment in glow discharge before deposition of films reduces  $\Delta H_m$ . At the same time, with increasing  $V_c$  and decreasing  $T_c$  the melting enthalpy increases. This leads to formation of the no equilibrium stressed structure. Irradiation of the condensed fragments by UV-radiation, or by electrons, or by a high - frequency discharge causes significant amorphization of the film.

The kinetic parameters were determined by the TGA method using the decomposition curve of the polymers. Results are presented in Table 1.

Table 1

Parameters of the rate equations of mass loss of films at different ways of initiation of polymerization

Material; method	mode $T_k, K; E, \text{эВ};$ $j, \text{mA/cm}^2$	$T_i,$ K	$\omega_i,$ kg	$(d\omega/dT)_i,$ mg/K	$E_a,$ kcal/mol
Teflon-4; thermal	$T_k=303$	700	80	- 2,5	31,5
	$T_k=423$	700	80	- 5,0	54,0
	$T_k=515 + \text{annealing}$	710	80	- 5,3	57,8
Teflon-4, electron-beam	$E=700; j=0,1$	660	100	-3,8	34
	$E=600; j=0,2 + \text{annealing}$	670	80	-6,0	61
Teflon-3; thermal, electron-beam	$T_k=232$	630	75	-4,4	51
	$T_k=423$	645	75	-4,4	51
	$E=250; j=0,15$	650	75,3	-4,3	48
Polystyrene; electron-beam	$E=200; j=0,15$	655	80	-7,2	68
Polyethylene, thermal, electron-beam	$T_k=276$ $E=600; j=0,1$	623	70	-5,3	52

$T_i$  – temperature at the inflection point;  $\omega_i$  – mass at the inflection point;  $(d\omega/dT)_i$  – the slope at the inflection point;  $E_a$  – activation energy.

## **Permolecular structure of heterogeneous-chain thin polymer films deposited in vacuum**

Zadorozhniy V.G., Polishchuk S.G., Kobrin V.L.

*Odessa National Academy of Food Technologies, Odessa, Ukraine*

Electron microscopic studies of the permolecular structure of the films have shown that during the electron beam decomposition of polytetrafluoroethylene (PTFE), polihlorotriftoretilena (PHTFE), polyethylene terephthalate (PET), polypropylene (PP), and polyethylene (PE) amorphous films are obtained (rings are seen at the electron-diffraction patterns). In the case of PTFE film, the structure depends on the evaporation rate ( $V_c$ ), and on the condensation temperature ( $T_c$ ). At the temperature of  $T=700$  K the, the films are composed of thin fibers, i.e. the fibrils having different width. The gaps between ribbons are also different: their boundaries become blurred at high magnifications, as well as unevenly etched. Increasing the temperature  $T$  and the evaporation rate  $V_c$  leads to the formation of spherulitic and dendritic structures. Annealing of the PHTFE and PET films in the temperature range of 500...600 K does not lead to appearance of the crystalline phase. In the case of PTFE and PE films, their permolecular structure changes markedly, so that the spherulites of different dimensions are formed.

Quite different results were obtained during the thermal decomposition and evaporation of polymers from iron ( $Fe$ ), tungsten ( $W$ ) and molybdenum ( $Mo$ ) evaporators. In the films there are permolecular formations of different types. The diffraction of electrons in the films leads to appearance of a large number of rings that is very unusual for polymers. This is related to evaporation of of  $Fe$ ,  $W$ , and  $Mo$  oxides at the evaporation temperature range of 700...1500 K and condensation of them on a substrate. As the result, they reinforce the film and cause appearance of the diffraction pattern.

Thus, it is shown that in studying the morphology of polymer films deposited in vacuum, it is necessary to consider not only decomposition of the polymeric materials, but also the material, of which an evaporator is made.

## Methods for determining the parameters of thermoelectric semiconductors

Zapukhlyak R.I.<sup>1</sup>, Terletskiy A.I.<sup>1</sup>, Tkachuk A.I.<sup>2</sup>

<sup>1</sup>*Vasyl Stefanyk Precarpathian National University, Ivano-Frankivsk, Ukraine*

<sup>2</sup>*Ivano-Frankivsk National University of Oil and Gas, Ivano-Frankivsk, Ukraine*

Taking measurements various techniques of thermoelectric parameters (including heat) solids, which generally can be divided into stationary and dynamic, realized in the respective measuring cells [1].

In particular, the authors [2] proposed measuring cell, which controls the flow of heat through the sample and measuring the temperature difference at the ends of the sample. This cell has a number of shortcomings that reduce the accuracy measurement of thermal conductivity coefficient ( $\chi$ ) and the relevant electrical parameters of a sample: the coefficient of thermopower ( $\alpha$ ) and conductivity ( $\sigma$ ).

These shortcomings include the following:

1. The temperature at the upper end of the sample is given by an internal heater, the temperature outside (guard) is automatically maintained equal to the internal temperature to eliminate heat transfer between the heaters. Due to the large thermal inertia heaters and peculiar to each thermostat hysteresis phenomenon, the effective maintenance of equal temperatures heaters with high precision is a complex task. This leads to undesirable heat transfer between heaters and an additional uncontrolled heat flow through the sample.

2. The flow of heat from the inner part of the heater goes in parallel pattern by loose insulation between sample and the security screen. However, the thermal conductivity depends on the power loose compaction of the material that can not be controlled.

3. To measure the electrical parameters provides individual contacts, while the temperature at the ends of the sample is controlled by separate thermocouples, which inserted into bore in the sample holes. This means that the sample leaves at least 8 leaders, each of which gives its contribution to the overall balance of heat flow through the sample.

We in [3] proposed method of stationary thermoelectric parameters of semiconductor materials, which largely devoid of deficiencies noted above. To implement this method here proposed measuring cell, which in a single experiment enables to get information on the full range of thermoelectric characteristics.

1. Д.М. Фреїк, Р.Я. Михайльонка, В.М. Кланічка. Методи вимірювання теплопровідності напівпровідникових матеріалів // Фізика і хімія твердого тіла. –2004. –Т. 5, –№ 1. С. 173-191.
2. Семенюк В.А., В.А. Бевз, А.В. Гармашов. Физическая электроника. – Львов, 1990. –№40. –С. 18-22.
3. Д.М. Фреїк, М.О. Галушак, А.І. Терлецький, Р.І. Запукхляк, Н.І. Дикун, А.І. Ткачук. Стаціонарні методи визначення термоелектричних параметрів напівпровідникових матеріалів // Методи та прилади контролю якості. –2010. –№25. –С. 92-96.



## The method of radiowave non-destructive monitoring of film protective coatings and low-temperature device for its application

Zharkov I.<sup>1</sup>, Korotash I.<sup>2</sup>, Rudenko E.<sup>2</sup>, Safronov V.<sup>1</sup>, Khodunov V.<sup>1</sup>

<sup>1</sup> *Institute of Physics of NAS of Ukraine;*

<sup>2</sup> *Institute of metal physics of NAS of Ukraine*

The development nanotechnologies and their broad usage in an industry requires creation of effect of methods of monitoring and diagnostics of parameters of nanostructured materials and multilayer structures as in engineering process and manufacture, and in service, and also creation of the relevant inventory for embodying these procedures [1], one of which is the radiowave way of non-destructive monitoring [2].

In this work is offered method of monitoring, in which microwave radiator and antenna, vacuum-tight VHFconnectors, the coaxial cables, delivering a probing signals and deducing out an information signal on a receiver recorder or the remedy of information processing, are disposed in the capable to move on three coordinates above an investigated surface low-temperature device, providing operation of instrumentation at temperature 77 K, minimising thermal noises of instrumentation and rising the relation "signal / noise", and device for monitoring and fixing of distance up to an investigated surface is supplied with the stop unit of driving of a stepper, bound on an electro circuit with a source of a power supply of an engine, and also signal sensor of a level of liquid cryoagent in a tank of the device for maintaining temperature of cooled instrumentation on a constant level, and the scanning is carried out the device on three coordinates through express inventory with three platforms transposed through steppers and kinematicly bound with them of screw pairs, servings for transformation of rotary movement in translational, thus in two horizontal orthogonally related migrations of the platform are shaded slide on rollers on two steams of collateral cylindrical guides through one screw pair, and at vertical migration the platform is shaded slide through two screw pairs, kinematicly by bound belt drive. The scanning is carried out under the given program.

1. Колл. авт., Система неразрушающего контроля. Виды (методы) и технология неразрушающего контроля. Справочное пособие. Сер. 28. выпуск 4. – М.: Государственное унитарное предприятие «Научно-технический центр по безопасности и промышленности Гостехнадзора России». – 2003. – С. 97
2. Ермолов И.Н., Останин Ю.Я., Методы и средства неразрушающего контроля качества. – М.: Высшая школа. – 1988. – С. 368

**СЕКЦІЯ 2 (усні)  
НАНОТЕХНОЛОГІЇ, НАНОМАТЕРІАЛИ І КВАНТОВО-  
РОЗМІРНІ СТРУКТУРИ**

19 травня 2011 р.

**SESSION 2 (oral)  
NANOTECHNOLOGIES AND NANOMATERIALS,  
QUANTUM-SIZE STRUCTURES**

May, 19, 2011

## Nanocomposites based on polytetrafluoroethylene with different modification hierarchy

Antanovich N.A.<sup>1</sup>, Kravchenko V.I.<sup>2</sup>, Gorbatsевич G.N.<sup>3</sup>, Struk V.A.<sup>3</sup>,  
Voropaev V.V.<sup>3</sup>.

<sup>1</sup> *Soligorsk Institute of Resource Saving Problems with Pilot Production, Soligorsk, Belarus*

<sup>2</sup> *The JSC "Belkard" education-methodological centre "Promagromash", Grodno, Belarus*

<sup>3</sup> *Yanka Kupala State University of Grodno, Grodno, Belarus*

In the nomenclature of polymer engineering materials special place occupy fluorine-containing composites obtained by modifying the PTFE by components of different composition, structure, dispersion and the mechanism of action. With rapidly increasing consumption amount fluorine-containing composites at units with extreme operating condition a substantiated methodology for their generation and processing of products do not exist, that did not allows to achieve the optimum effect of their application in various branches of engineering and chemical industries, including the production of compressed and liquefied gases [1].

The methodological approaches to the formation of nanocomposite materials based on polytetrafluoroethylene based on taking into account a structural hierarchy are considered. To improve the parameters of deformation-strength and tribological characteristics of PTFE suggested the use of fluorine-containing polymer-oligomer modifier with the size of individual particles less than 1 micron. Due to the presence of a nanosized polymer core in modifying particles is formed supramolecular structure with a high degree of ordering. Oligomeric polymolecular fraction of modifier improves the mobility of macromolecules and reduces the level of residual stresses in the composite.

Application of polymer-oligomer fluorine-containing modifier improves to increase the indicators of deformation-strength characteristics and wear resistance of polytetrafluoroethylene and expanding the range of its application in sealing devices and vacuum technology.

For manufacture of reinforced composites with enhanced strength and wear-resistance for friction units with extreme operation conditions has developed a technology of modifying on the interface level of structural hierarchy. Set level of interfacial interaction at the interface between the matrix and carbon fiber filler in these composites is ensured by the use of fluorine-containing finishes or mechano-chemical processes which lead to increased adsorption interaction of components. Optimized at different levels of structural hierarchy fluorine-containing nanocomposites are used for the manufacture of products of tribological and sealing purposes.

1. Auchynnikau Y.V., Struk, V.A., Gubanov, V.A. Thin films of fluorine-containing oligomers: the basics of synthesis, properties and applications. – Grodno, Grodno State Agrarian University, 2007. 326 pp.

## **Nanocomposite and nanophase coatings based on fluorine-containing components**

Auchynnikau Y.V.<sup>1</sup>, Kravchenko V.I.<sup>2</sup>, Struk A.V.<sup>2</sup>, Antanovich N.A.<sup>3</sup>,  
Andrikevich V.V.<sup>1</sup>.

<sup>1</sup> *Yanka Kupala State University of Grodno, Grodno, Belarus*

<sup>2</sup> *The JSC “Belkard” education-methodological centre “Promagromash”, Grodno, Belarus*

<sup>3</sup> *Soligorsk Institute of Resource Saving Problems with Pilot Production, Soligorsk, Belarus*

Thin-film coatings based on fluorine-containing components are widely used as finishing, water-repellent, antiwear, running-in [1]. The effectiveness of such coatings depends not only on the composition of components, but also the prevailing character of the structural hierarchy. When applying thin-film functional coatings from dilute solutions of fluorine-containing copolymers with molecular weight up to 2 thousands units on solid substrates, forming the adsorption type structure with pronounced structure imperfection. Under the influence of the mosaic force field of metal surface is formed a thin coating with different levels of structural orientation of the macromolecules with respect to the substrate and the degree of local areas ordering. Due to be structure formation at different hierarchical levels formed film has a sufficiently high load capacity, reduces the activity of the surface during interaction with the environment and retains the ability to alternating transfer at dynamic contact of the elements of a static or dynamic systems. The structural parameters of thin-film fluorine-containing coatings on nanophase and the interface level can be adjusted by changing the composition, structure and number of functional groups in the macromolecule, the number of treatments, energy (heat or ionizing) the impact of a set intensity. To improve the parameters of the fluorine-containing coatings service characteristics useful introduction to their composition of nanodimension modifiers of different composition and structure possessed uncompensated charge. With such modification is an implemented nanophase structure caused by the ordering of oligomeric macromolecules under the action of the nanoparticle force field. This maintains the required level of adsorption interaction at the interface of the coating with the solid substrate. Introduction to oligomeric matrix nanosized polymer-oligomeric fluorine-containing modifier allows to optimize the structure of the coating on three hierarchical levels - interphase, nanophase, supramolecular. Due to this a thin-film coatings maintain high hydrophobic properties while increasing the load capacity and durability. Developed compositions of nanocomposite and nanophase fluorine-containing coatings are effective for use in precision friction units, including operated under reverse the motion.

1. Auchynnikau Y.V., Struk, V.A., Gubanov, V.A. Thin films of fluorine-containing oligomers: the basics of synthesis, properties and applications. – Grodno, Grodno State Agrarian University, 2007. 326 pp.

## Hydrogen-induced effects in nano-crystalline GaSe and InSe layers

Balitskii O.A.

*Ivan Franko National University, Lviv, Ukraine*

Hydrogen has influenced on mechanical characteristics (increased their anisotropy) of gallium and indium monoselenides. Due to intensive intercalation between layers of crystals hydrogen exists in a molecular state, placed in the translation-ordered position. After definite concentration of hydrogen it is the possibility of penetration to matrix layer of crystals by hydrogen ions.

The complex investigations respect to establishment of physical features of forming of hydrogen localized states in the van der Waals gap of Ga(In)Se layered films were carried out. The temperature diapason of Ga(In)Se hydrogen intercalated structure existence was determined. The topology and micro-local features of hydrogen dissolved structure of Ga(In)Se nanofilms formation were established using method of TEM analyses and changing the anisotropy of their kinetic parameters. The process of hydrogen adsorption by layered thin films and crystals has accompanied by changing of adsorption band position in InSe and GaSe due to the increasing of intercalation level. After the increasing of hydrogen concentration ( $x > 2$ ) it is observed the dissociation of  $H_2$  molecules and introducing the ions to the matrix layers. Proton saturation can be described by reaction:  $Ga(In)Se + x H^+ + x e^- = H_x Ga(In)Se$ .

Changing the hydrogen concentration (in the diapason from  $x = 0$  to  $x = 2,5$ ) leads to nonlinear increasing of unit cell parameter  $c$  and can be described by dependence  $c(x) \sim th(x)$ . For GaSe unit cell parameter  $c$  has increased from  $1,589 \text{ nm}$  ( $x=0$ ) to  $1,594 \text{ nm}$  ( $x=2,5$ ), and further increasing of hydrogen concentration caused the increasing of unit cell parameter  $c$  only to  $1,596 \text{ nm}$ . In such case has formed the “nanoballs”, which limited by linear sizes of crystallites, which can reversed adsorb and desorbs the hydrogen. During the intercalation of crystals it has observed the increasing of unit cell parameter  $a$  (from  $0,375 \text{ nm}$  to  $0,377 \text{ nm}$ ), which certified the partial introduction of hydrogen to matrix layer.

From the gaseous hydrogen with pressure up to 10 MPa these type of crystals can adsorb up to 400 *wppm* (and the main quantity has introduced to the van der Waals gap and forms the “nanoballs” with a several *nm* thickness). The increasing of temperature leads to the desorption for the first of diffusive active hydrogen.

## **Exciton stokes shift in the quantum dot with degenerated band spectrum**

Bilysn'kyi I.V., Shevchuk I.S.

*Ivan Franko Drohobych State Pedagogical University, Drohobych, Ukraine*

Recently quantum dot (QD) systems have been intensively studied due to their interesting electron, hole, exciton properties and perspective application in electronic and optoelectronic devices. Since QD's demonstrate unique optical size-dependent properties, they are of particular interest in biological and biomedical studies. In these systems electron, hole and exciton states are influenced by a strong 3-D quasiparticle localization effect arising from the difference between band-gap values of the materials. Localization of charged particles (electrons, holes, and excitons) in QD's leads to a considerable enhancement of the interaction between particles. The electron-phonon interaction in QD's differs from that in the bulk material. It increases when the system dimensionality is reduced, the number of polarization oscillation branches interacting with electrons (holes) rises. There exist confined and interface (surface) optical phonons. The interaction of an electron with optical phonons cannot be neglected. At the interface the interaction of an electron with surface optical phonons can be compared with that of longitudinal optical phonons. In QD's made of high-degree ionicity materials, a strong electron-phonon interaction leads to the appearance of polaron states. Polaron states are observed in a significant change of electron and hole energy quantizing in a QD.

In the effective mass approximation in spherical nanocrystals with cubic crystalline lattice the energy and the wave function of the first quantum-sized electron level being two-fold degenerated with respect of a spin projection and the first quantum-sized hole level being four-fold degenerated with respect of its total angular momentum projection. The exciton ground state  $(1S_{3/2}1S_e)$  is eight-fold degenerated are determined.

The splitting of an eight-fold exciton state due to the electron-hole exchange interaction in a five-fold degenerated optically passive state with the total angular momentum 2 and a three-fold degenerated optically active state with the total angular momentum 1 is calculated.

Resonant Stokes shift caused by exciton level splitting due to the electron-hole exchange interaction as well as by exciton-phonon interaction is investigated.

## Possibilities of Kikuchi diffraction in researches of multilayer nanoscaled systems

Borcha M.<sup>1</sup>, Balovsyak S.<sup>1</sup>, Garabazhiv Ya.<sup>1</sup>, Fodchuk I.<sup>1</sup>, Tkach V.<sup>2</sup>.

<sup>1</sup> *Yuriy Fed'kovich Chernivtsi National University, Chernivtsi, Ukraine*

<sup>2</sup> *V.N.Bakul Institute of Superhard Materials National academy of Science of Ukraine,  
Kyiv, Ukraine*

The elastically distorted regions arising in multilayer system interfaces and thin films influence on their electrophysical characteristics and depend on growth conditions. The possibility of detection of strain field distribution in thin films or interfaces in multilayer systems emerges due to electron backscatter diffraction that gives local image of single sample parts with sizes of some nanometres [1, 2].

In this report we present the researches of textured diamond films synthesized by CVD method at different manufacturing conditions, as well as interfaces of multilayer nanoscaled  $GaAs / Ga_{1-x}In_xAs / GaAs$  systems. Investigations were performed by electron backscatter diffraction in a scanning electron microscope «Zeiss» EVO- 50 using CCD detector.

Electron backscatter diffraction patterns consist of great number Kikuchi lines (bands) therefore to increase the precision of determination of lattice parameter changes with Kikuchi method the correlation method and corresponding software were used for accurate identification of coordinates of Kikuchi lines intersections on the patterns.

Theoretical and experimental researches of intensity distribution in multibeam diffraction regions (Kikuchi lines intersections) indicated their high sensitivity to weak structural changes. It gave possibility to specify the influence of process-dependent parameters on homogeneity and perfection of diamond films and diamond crystals. The transformations of intensity distribution in two- and multi-beam regions of electron diffraction associated with structural imperfection and growth technological parameters were established for diamond films. Strain field distributions in interfaces in multilayer heterosystems were determined and corresponding strain tensors were constructed.

1. Fodchuk I., Balovsyak S., Borcha M., Garabazhiv Ya., Tkach V. Determination of structural homogeneity of synthetic diamonds with analysis of intensity distribution of Kikuchi lines // *Semiconductor physics, quantum electronics and optoelectronics*. - 2010. - Vol. 13. - №.3. - P.51-58 (253-262).
2. R.R. Keller, A. Roshko, R.H. Geiss, K.A. Bertness, and T.P. Quinn. EBSD Measurement of Strains in GaAs due to Oxidation of Buried AlGaAs Layers // *Microelectronic Engineering*, V.75, Issue 1, 2004, P. 96-102.

## Dielectric relaxation in solid solutions (1-x) NiAl<sub>0,5</sub>Fe<sub>1,5</sub>O<sub>4</sub> – x BaTiO<sub>3</sub>

Bushkova V.S.

*Precarpathian national university after Vasyl Stefanyk, Ivano-Frankivsk, Ukraine*

Currently the particular attention is paid to the study of composite materials based on nickel-aluminum ferrites, as those are applicable for the development of advanced materials with controlled dielectric and magnetic parameters in wide limits. Hitherto the dielectric parameters of nickel-aluminum ferrites and of the composites based on them has been studied little in sufficiently wide frequency and temperature ranges. The enlargement of both frequency and temperature measurement ranges greatly increases the possibility of detecting the nature of the observed phenomena. This is because different physical mechanisms are usually characterized by specific combinations of frequency and temperature dependencies.

The aim of this research is the synthesis and the study by means of impedance spectroscopy of nanocomposites of the (1-x) NiAl<sub>0,5</sub>Fe<sub>1,5</sub>O<sub>4</sub> – x BaTiO<sub>3</sub> system, where x = 0, 0.12, 0.25, 0.50. As the ferrite component, the nickel-aluminum ferrite was used, which had been synthesized by sol-gel method involving auto-combustion. Barium titanate was selected as the ferroelectric phase and was synthesized with the help of ceramic technology. Nanocomposites were obtained by means of successive mixing of source components and pressing into briquettes. The briquettes had been fired at 1350°C for 1 hour in the open air.

X-ray structural analysis was performed on a Dron-3 machinery, according to which all samples were biphasic, they had phases of spinel and perovskite. The measurement of the total complex impedance was carried out on Autolab PGSTAT 12/FRA-2 spectrometer in the frequency range of 0,01 Hz - 100 kHz and in the temperature range of 293 - 673 K in pitches of 50 K. The actual and imaginary parts of permittivity, relaxation time, activation energy, loss tangent and conductivity were determined on the basis of experimental dependencies of the total complex impedance.

The study of dielectric properties obtained from the analysis of impedance-spectra at different temperatures allowed detecting the regularities of their changes depending on the frequency, temperature and composition. As a result of this analysis, the dielectric properties of solid solutions of the (1-x) NiAl<sub>0,5</sub>Fe<sub>1,5</sub>O<sub>4</sub> – x BaTiO<sub>3</sub> system were determined.



## Thermal analysis of nickel-aluminum ferrites

Bushkova V.S., Kopayev A.V.

*Prekarpathian national university after Vasyl Stefanyk, Ivano-Frankivsk, Ukraine*

For today ferrites are actual objects and perspective materials for different practical application. Nickel-aluminum ferrites differ from many other materials that they have a complex practically important electric, magnetic and mechanical properties. Ferrites of composition of  $\text{NiAl}_x\text{Fe}_{1-x}\text{O}_4$  is perspective in a SHF-technique and as a magnetic component in composite electro-magnetic materials. In the last few years in a SHF – technique is appeared a new task - synthesis of different substances with the particles of nanometer size. This task arose up in connection with progressive development of nanotechnologies, in which are used nanocrystalline materials, which have unique characteristics as compared to greater in size materials of the same chemical composition.

For the synthesis of ferromagnetic oxide materials a method of the sol-gel with participation of auto-combustion (SGA) was used, which provided high chemical homogeneity and activity of ferrite powders. As compared to ceramic technology, which is based on the mechanical mixing of oxides with the next annealing by means of high temperature, which promotes to the chemical reaction and to the formation of dense microstructure, a method of SGA is by the simple and simultaneously by the economic method of receipt of nanosize materials.

Thermal analysis was conducted using simultaneous thermal analyzer STA 449 F3 Jupiter in the mode of the linear heating with a speed of  $10^\circ\text{C}/\text{min}$  in the temperature range  $25 - 1000^\circ\text{C}$ , which resulted in the experimentally obtained curves of thermogravimetric (TG) and of differential thermal analysis (DTA). Change of mass at heating was determined with an accuracy of  $10^{-6}$  kg, the DTA signal noise was no less than 50 nV.

From the analysis of the DTA curve implies that in the investigated material for  $x = 0.5$  at  $T = 550^\circ\text{C}$  takes place conversion, which is associated with the removal of organic residues from nickel-aluminum sample. Moreover, the TG curve testifies to it, because in area of foregoing temperature there is a loss of mass of nickel-aluminum ferrit.

## Characterization of sputtered Ag-CeO<sub>x</sub> thin films

Chundak M., Veltruská K., Václavů M., Vorokhta M., Khalakhan I.,  
Matolínová I., Matolín V.

*Charles University in Prague, Prague, Czech Republic*

Ceria doped by suitable metal or mixed with other oxide is widely used in commercial catalytic processes – three way catalyst and fluid catalytic cracking, it has also a potential uses as an additive for combustion catalysis and processes in fuel cell technology. Several works describing catalytic properties of silver doped cerium oxide powders were published. These systems were used in different catalytic reactions – for example the higher activity during methane oxidation reaction or catalytic oxidation of CO was observed.

In our study we examined Ag-CeO<sub>x</sub> layers prepared by nonreactive radio-frequency magnetron sputtering on different substrates – on Si(001) substrate, multiwall carbon nanotubes deposited on gas diffusion layer (MWCNT/GDL), carbon nanotubes (chemical vapour deposited) deposited on gas diffusion layer (CNT(CVD)/GDL) and carbon foil (C- foil) using a composite CeO<sub>2</sub>-Ag target. Prepared systems were characterized by X-ray photoelectron spectroscopy (XPS) and by Hard X-ray photoelectron spectroscopy (HAXPES). HAXPES was used due to its capability for providing an insight into the bulk electronic structure of solids and the chemical composition of buried layers and interfaces lying at depths of several tens of nm. Samples were also studied by scanning electron microscopy (SEM). Hydrogen and methanol fuel cell activity measurements were performed using carbon diffusion layer of micropolymer membrane fuel cell covered by multi-wall carbon nanotubes with sputtered Ag-CeO<sub>x</sub> layer on the surface.

Different states of silver were resolved by HAXPES – Ag<sup>0</sup>, Ag<sup>+</sup> and Ag<sup>2+</sup>. It was found that creation of Ag<sup>+</sup> and Ag<sup>2+</sup> species is influenced by the substrate type and it is connected with the reduction of CeO<sub>2</sub> to Ce<sub>2</sub>O<sub>3</sub> – especially on carbon nanotubes.

## **Photoluminescence decay dynamics of silicon-based light-emitting nc-Si-SiO<sub>x</sub> structures**

Dan'ko V.A., Michailovska K.V., Indutnyi I.Z., Shepeliavyy P.E.

*V. Lashkarev Institute of Semiconductor Physics National Academy of Sciences of Ukraine, Kyiv, Ukraine*

Thin-film porous nc-Si-SiO<sub>x</sub> light-emitting structures containing Si nanoclusters (nc-Si) embedded in the SiO<sub>x</sub> matrix attract the attention of many researchers, because of their promising applications in advanced electronic and optoelectronic devices. We present results of time-resolved photoluminescence (PL) measurements as a function of the photon emission energy and the content of Si in such structures. Investigated samples were obtained by thermal evaporation of silicon monoxide in a vacuum and oblique deposition onto silicon substrate with following annealing of the porous SiO<sub>x</sub> films in vacuum chamber at 975<sup>0</sup> C. During such annealing the thermally stimulated formation of the nc-Si occurs in the SiO<sub>x</sub> columns thus forming nc-Si-SiO<sub>x</sub> structures. Annealed nc-Si-SiO<sub>x</sub> samples were treated in the HF vapor at 50<sup>0</sup> C. As a result of HF vapor treatment, considerable PL intensity growth and blueshift of PL peak position are observed. Time-resolved PL was investigated at room temperature under excitation of a pulsed nitrogen laser (337 nm). PL signal was analyzed by monochromator and was detected by a photomultiplier in conjunction with a pulse oscillograph. Time-resolution of our system was 0.5 μs.

In order to analyze the temporal behavior we have fitted the experimental date to a stretched-exponential decay function that is frequently used to describe dispersive processes in disordered systems with a distribution of relaxation times:

$$I(t) = I_0 \exp[-(t/\tau)^\beta],$$

where  $\tau$  – is the PL decay time and  $0 \leq \beta \leq 1$  is the dispersion exponent.

All investigated nc-Si-SiO<sub>x</sub> samples at spectral range from 1.4 to 2.0 eV exhibit a nonexponential PL decay which can be fitted well by the stretched exponential function. It is found that decay time  $\tau$  decreases smoothly from 30 to 9 μs with the increasing of PL photon energy from 1.5 to 2.0 eV, respectively. But the  $\tau$  depends relatively weak on silicon content in the samples (Si content was varied by changing of the deposition angle at deposition of the porous SiO<sub>x</sub> films). Decreasing of the  $\tau$  with the increasing of emission energy is consistent with the quantum confinement effect (e.g. size dependent phenomena), where smaller nc-Si with larger energy gaps are characterized by a shorter radiative lifetime and corresponding radiative recombination process take place within the individual nc-Si. The stretch fitting parameter  $\beta$  has been found equal to 0.76-0.85 in dependence on silicon content in nc-Si-SiO<sub>x</sub> structures. Moreover, the value of  $\beta$  is almost independent on the PL photon energy. This means that the dispersion parameter  $\beta$  may be attributed to exciton migration between a disordered system of interconnected nanocrystals, or associated with the larger scale characteristics of the matrix (SiO<sub>x</sub>).

## Structure and hardness of worn layer

Danylenko M.I.<sup>1</sup>, Chernega S.M.<sup>2</sup>, Mameka N.O.<sup>1</sup>, Velychko A.<sup>2</sup>

<sup>1</sup>*Institute for Problems of Materials Science, Kyiv, Ukraine*

<sup>2</sup>*National Technical University of Ukraine "Kyiv Polytechnic Institute", Kyiv, Ukraine*

Shear deformation is realized by methods of severe plastic deformations such as equal channel angular pressures (ECAP), twist extrusion (TE) et al. for producing nanostructures with unique high properties [1]. However, these methods can be used only for strengthening of "soft" one-component materials.

Methods of surface deformation processing realize shear deformation in surface layers and widely used for strengthening of complex-alloyed alloys and composites. The most detailed analysis of surface severe plastic deformations (SSPD) was done by K.Lu and co-workers who investigated the changes of structural state in SSPD-processed near-surface layers of steel articles [2]. Authors [3] studied the gradient nanostructure on "cross-section" samples of steel 65r after severe surface plastic deformation. They revealed the dissolution of cementite  $Fe_3C$  and carbon redistribution on cell boundaries during plastic deformation. The free carbon on cell boundaries suppresses the recovery processes. Cell size in surface layer is about 20-30 nm and hardness in near-surface layer is about 12 GPa.

Samples of steel 20 after wear have been studied. Initial structure consists of ferrite and perlite grains and microhardness is in range 3-6 GPa. Hardness of worn layer is presented on Fig. 1. Different level and depth of hardening of worn layer is presented on Fig.2.

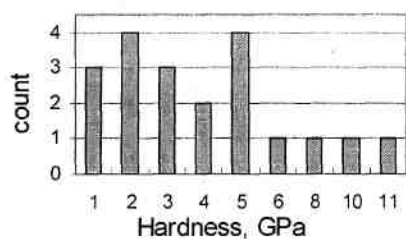


Fig. 1. Hardness of worn layer.

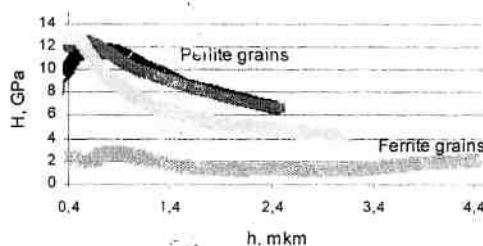


Fig. 2. Hardness vs indentation depth.

1. Segal V.M., Reznikov V.I., Kopylov V.I., *Procesy. Plasticheskogo Structuroobrazovania Metallov. Sci Eng. Minsk, –1994. – 23 lp (in Russian).*
2. Lu K., Zhahg H., Zhong Y., Fecht H.J. // *J.Mater. Res. – 1997. – 12, – 923.*
3. M.Danylenko, V. Gorban, Yu. Podrezov, S. Firstov, O. Rozenberg, S.Sheykin, Y. Yamabe-Mitarai, F.Morito // *Materials Science Forum Vols. – 2006. –P. 503-504, –787.*

## Enhancement of optical signals from molecules adsorbed on interface single wall carbon nanotube/gold

Dovbeshko G.I.<sup>1</sup>, Fesenko O.M.<sup>1</sup>, Gnatyuk O.P.<sup>1</sup>, Yakovkin K.I.<sup>1</sup>, Rynder A.D.<sup>2</sup>

<sup>1</sup>*Institute of Physics of National Academy of Sciences of Ukraine, Kyiv, Ukraine*

<sup>2</sup>*National University of Kyiv-Mohyla academy, Kiev, Ukraine*

It is well known an enhancement of optical processes near rough metal surface by a factor  $10^2 \dots 10^6$ , namely enhancement of Raman scattering (SERS), infrared absorption (SEIRA), metal enhanced fluorescence, second harmonics generation [1]. The aim of the present report was experimental observation of enhancement of vibration modes intensity of the molecules adsorbed on the surface of single wall carbon nanotubes (SWCNT) and then deposited on the gold support. This effect is similar to SERS and SEIRA.

The FTIR spectra of Poly A, Adenine and Thymine molecules adsorbed on the SWCNT were investigated. A Bruker IFS-66 instrument with a reflection attachment (the incidence angle of  $16.5^\circ$ ) was used for the registration of IR spectra in the reflectance mode in the  $400\text{-}7000\text{ cm}^{-1}$  region. The SERS experiment was done using a Via Raman Microscope (Renishaw) instrument with laser excitation at 785 nm with power of 0.3-60-mW. In this experiment we used the Klarite support.

The SEIRA application for the study of biomolecule/nanotube gives a possibility to increase a sensitivity of IR spectroscopy by 3–10 times and enhance the absorbance of biological molecules adsorbed on the nanotube surface located on the rough gold surface [2]. The characterization of Poly-A adsorbed on the separated nanotubes was probed and enhanced with a conventional Klarite SERS support. The factor of enhancement in SERS experiments on the Klarite support was equal to  $10^4\text{--}10^6$  [3] for different vibrations of poly-A on nanotubes. We have registered a signal from both the 1-2 nanotubes and the Poly-A adsorbed on these separated nanotubes. Possible mechanism of the enhancement is discussed.

**Acknowledgement.** We thank to Dr. Larisa Darchuk and Dr. Alessandro Damin for SERS measurements.

1. Kosobukin V.A. Effect of enhancement of external electric field near metal surface and its manifestation in spectroscopy // *Surface, Physics, Chemistry, Mechanics*. – 1983. – Vol. 12. – P.5-20.
2. Dovbeshko G.I., Fesenko O.M., Yakovkin K.I., Bertarione S., Damin A., Scarano D., Zecchina A., Obraztsova E. The Poly-A Interaction and Interfaces with Carbon Nanotubes // *Mol. Cryst. Liq. Cryst.*, – 2008. – Vol. 496, – P. 170-185.
3. Dovbeshko G.I., Fesenko O.M., Gnatyuk O.P., Shtogun Ya, Woods L., Bertarione S., Damin A., Scarano D., Zecchina A. Carbon Nanotubes. – India.: In-Tech., – 2010. – P. 697-719.

## Structural changes in iron-yttrium garnet implanted by nitrogen ions

Fodchuk I.M.<sup>1</sup>, Kazemirskiy T.A.<sup>1</sup>, Zaplitnyy R.A.<sup>1</sup>, Gutsuliak I.I.<sup>1</sup>,  
 Pietsch U.<sup>2</sup>, Davydok A.V.<sup>2</sup>, Pashniak N.V.<sup>2</sup>,  
 Bonchyk O.Y.<sup>3</sup>, Savitskiy G.V.<sup>3</sup>, Syvorotka I.I.<sup>4</sup>, Yaremiy I.P.<sup>5</sup>

<sup>1</sup>*Yuriy Fedkovych Chernivtsi National University, Chernivtsi, Ukraine*

<sup>2</sup>*University Siegen, 57068, Siegen, Germany*

<sup>3</sup>*Institute for Applied Problems of Mechanics and Mathematics of NASU, Lviv, Ukraine*

<sup>4</sup>*Scientific Research Company "Carat", Lviv, Ukraine*

<sup>5</sup>*Vasyl Stefanyk Precarpathian National University, Ivano-Frankivsk, Ukraine*

Experimental and theoretical aspects of ion implantation modification of the crystal structure of iron-yttrium garnet films by nitrogen ions were studied by methods of X-ray diffractometry. Relevance of research is due to the fact that introduction of impurities into the ferrite-garnet cells gives the ability to manage its magnetic parameters in a fairly wide range and to predict their behavior during operation of device structures based on them.

The possible types of defect models, which describe the growth and formed during implantation defective system, are analyzed and investigated in this paper. Selection of defect structure of the samples involved the presence of different types of growth and generated as a result of ion irradiation defects.

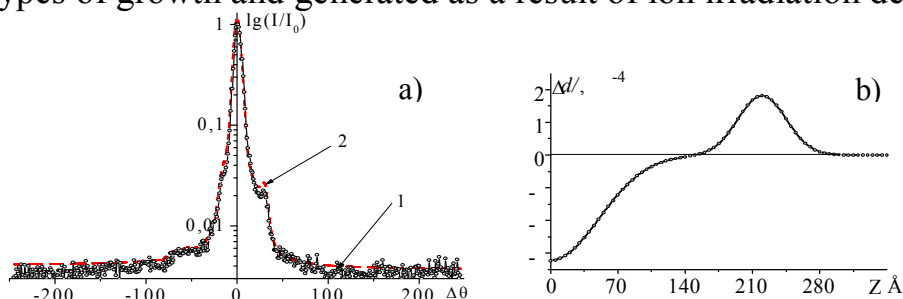


Fig. 1. a) Diffraction reflection curves.  $D=0,5 \cdot 10^{18} \text{ cm}^{-2}$ ,  $\text{Y}_{2,95}\text{La}_{0,05}\text{Fe}_5\text{O}_{12}$ ,  $\text{CuK}_\alpha$ -reflection (444), 1 – experimental curve, 2 – calculated; b) calculated profile of deformation in subsurface layers.

Simulation of diffraction reflection curves (Fig. 1), done with combined using a of Takagi-Topen equations solution and generalized theory of X-ray diffraction indicates the presence as dislocation loops of different sizes and cluster formation as well in an implanted structure (Table 1).

Table 1

Concentrations and sizes of defects, $\text{CuK}_\alpha$ -reflection (444)				
	dislocation loops	dislocation loops	disc-like clusters	spherical clusters
Size, Å	47	4500	20	1
Concentration, $\text{cm}^{-3}$	$2,7 \cdot 10^{15}$	$0,72 \cdot 10^9$	$4,5 \cdot 10^6$	$1 \cdot 10^{11}$

Good correlation of parameters of calculated and experimental diffraction reflection curves obtained by different methods of scanning and with various reflections, indicates the adequacy of the selected model of defective subsystem of resulting crystals.

## **Light emitting structures with silicon nanoclusters into the silica matrix**

Goltvyanskyi Ju., Khatsevich I., Melnik V., Nikirin V., Popov V., Oberemok O.  
*V. Lashkarev Institute of Semiconductor Physics National Academy of Sciences of Ukraine,  
 Kiev, Ukraine*

A light emitting structure with silicon nanoclusters (Si-nc) in SiO<sub>2</sub> matrix was realised in metal-oxide-semiconductor field-effect transistor (MOS FET). In such structure the Si-nc were built into a thin insulating layer of silica [1]. Possibility of injection electroluminescence (EL) is demonstrated for the used structures. The EL efficiency strongly correlates with photoluminescence properties of the nanoclusters in the SiO<sub>2</sub> matrix.

The light emitting structure creation consisted of the three stages:

- formation of the p<sup>+</sup>-type areas in n-Si wafer for MOS FET creation;
- deposition of dielectric layer with built-in nanoclusters;
- deposition of the ohmic and semitransparent field contacts.

For formation of dielectric layer with Si-nc the three-layered structure: SiO<sub>2</sub> (2 – 3 nm) / SiO<sub>1,5</sub> (10 - 20 nm) / SiO<sub>2</sub> (50 nm) was deposited. The structure annealing at the temperature of 1100 – 1150 °C (in Ar) provided formation of insulating silica layer with buried Si-nc.

The process of injection electroluminescence was realised by successive tunnelling of electrons and holes from a channel of MOS FET in Si-nc at the gate polarity changing. A negative voltage at the gate induces a formation of the p-type channel from which the holes tunnel to the nanoclusters. A positive voltage at the gate induces a tunnelling of the electrons from n-Si substrate to the nanoclusters. The recombination of electrons and holes in nanoclusters results in emitting of light, and a wave-length of this light depend on properties of Si-nc (mean size, energy state on the interface etc.).

Correlation of the formation condition of the layer with Si-nc (heat treatments, layer thickness, etc.) and light-emitting properties of the investigated structures was analysed.

1. R.J. Walters. Silicon Nanocrystals for Silicon Photonics: Thesis for the Degree of Doctor of Philosophy / Robert Joseph Walters. – California Institute of Technology, Pasadena, California. - 2007.– 155 p.

## Catalytic and adsorption properties of porous silicon with metallic and metal-oxide nano-inclusions

Gorbanyuk T.I.<sup>1</sup>, Litovchenko V.G.<sup>1</sup>, Mysakovych T.S.<sup>2</sup>,  
Solntsev V.S.<sup>1</sup>, Stasyuk I.V.<sup>2</sup>

<sup>1</sup>V. Lashkaryov Institute of Semiconductor Physics of NAS Ukraine, Kiev, Ukraine

<sup>2</sup>Institute for Condensed Matter Physics, Nat. Acad. of Sci. of Ukraine, Lviv, Ukraine

This work presents the results of theoretical and experimental studies of semiconductor structures based on porous silicon with embedded nanoclusters of catalytic (palladium), noncatalytic and metal-oxide (CuO<sub>x</sub>). The charge transport in slightly thermo oxidized porous silicon (Si<sub>por</sub>) in dependence of metal cluster (Pd, Cu, W, Al) depth distribution in porous silicon layer have been carried out by means of I(V) and C(V) characteristics, Auger electron spectroscopy, SEM and AFM microscopes

It was also found nanoporous silicon doped by Cu and/or CuO<sub>x</sub> demonstrates the enhanced adsorbative effects in the semiconductor-layered structures. In this case the using of thin catalytic composite metal/Si<sub>por</sub> films with d- and sp- metals (Cu, Pd, W) leads to the enhanced adsorption activity and stability to oxidation and ageing process (Table 1). The physical mechanism has been proposed for explain the observed phenomena. A model based on the combination of hopping and tunneling mechanisms of charge transfer have been proposed.

Density functional theory calculations have been used to investigate the adsorption of copper atoms on the H-passivated Si(001) surface. The surface is modeled using the cluster approximation. The possible sites for the copper adsorption are revealed and the adsorption energy is calculated. The bond lengths and Mulliken population analysis are reported for all considered sites of adsorption. We have also investigated the adsorption of oxygen on the Cu-Si cluster. In general, we have shown that copper can adsorb strongly on the H-terminated silicon surface and that the adsorption energy is dependent on the local bonding environment. Generally, Si surface loses charge.

Table 1  
The comparison of adsorption parameters (ultrahigh vacuum and real conditions)

Pd		Cu/Pd		
Pd-MIS (response, mV)	Pd <sub>4</sub> /W, thermal desorption peak area	Cu/Pd – МДН (response, mV)	Cu/Pd <sub>2</sub> /W thermal desorption peak area	O <sub>2</sub> /Cu/Pd <sub>2</sub> /W TD peak area
	(%)		(%)	(%)
<b>400</b>	(β <sub>1</sub> peak) 33,29	<b>600</b>	(β <sub>1</sub> peak) 15,67	9,50
	(β <sub>2</sub> peak) 28,24		(β <sub>2</sub> peak) 63,00	21,22
	(β <sub>3</sub> peak) 38,47		(β <sub>3</sub> peak) 21,33	69,28
	(β <sub>1</sub> peak+β <sub>3</sub> peak) <b>66,71</b>		(β <sub>1</sub> peak +β <sub>3</sub> peak) <b>84,33</b>	<b>90,50</b>



## Fabrication technology of graphene films on dioxide silicon layer and their properties

Gordienko S.O., Rusavsky A.V., Vasin A.V., Litvin P.M., Yukhimchuk V.A.,  
Nazarov A.N., Lysenko V.S.

*Lashkaryov Institute of Semiconductor Physics, NAS of Ukraine, Kyiv, Ukraine*

The present paper describes a method of obtaining few-layer graphene sheets on a thermally grown  $\text{SiO}_2$ . Graphene on a silicon dioxide substrate has been recently fabricated by using plasma-enhanced chemical vapor deposition technique [1]. The method based on solid-state dissolution of an overlying stack of a silicon carbide and a nickel thin film.

In this work we used RF magnetron sputtering for deposition of Ni and amorphous SiC films on  $\text{SiO}_2/\text{Si}$  substrate (see inset in Fig. 1b). The graphene film is formed by rapid thermal annealing (RTA) of the samples. The samples are annealed at 800-1100°C for 30 s in ambient pressure and nitrogen environment. During this time both the silicon and the carbon of the a-SiC are dissolved in the nickel layer. Upon cooling, the carbon segregates to the  $\text{SiO}_2$  interface forming a graphene layer. By choosing a nickel layer much thicker than the SiC layer, the silicon from the SiC is only dissolved in nickel or forms substoichiometric silicides [1]. We chose a thin SiC layer (from 50 to 70 nm) and a 500 nm thick nickel film. After RTA we removed the silicon-nickel layer by a nitric acid. Detailed analysis of the fabricated samples was performed, including Raman spectroscopy, optical microscopy, atomic force microscopy (AFM) and Auger electron spectroscopy. Results of investigation revealed presence few-layer graphene on sample after 800°C, 30 s annealing. In Fig. 1 Raman spectroscopy indicated the D-peak around 1350  $\text{cm}^{-1}$ , the G-peak around 1575  $\text{cm}^{-1}$  (see Fig. 1a), and (b) the 2D-peak around 2695  $\text{cm}^{-1}$  for samples.

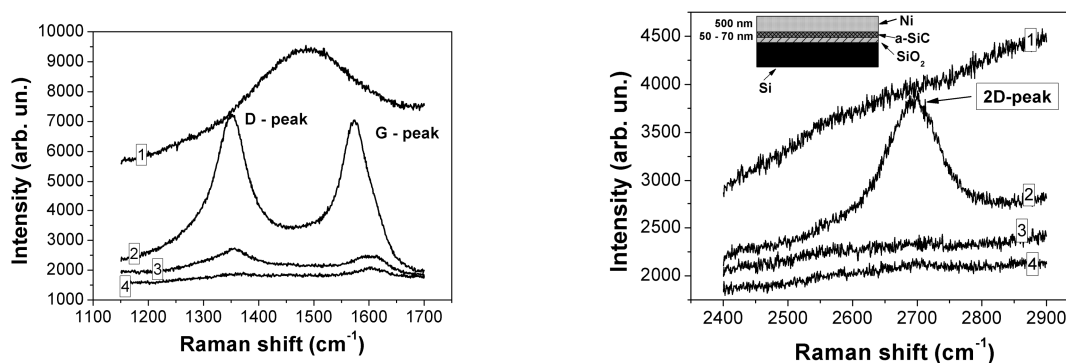


Fig. 1. Raman spectra excited at 457.9 nm for (a) first-order and (b) second-order scattering for different regimes of the RTA and thickness of the a-SiC film: 1 – 50 nm, no treatment, 2 – 50 nm, 800 °C, 3 – 70 nm, 1100°C, 4 – 50 nm, 1100°C.

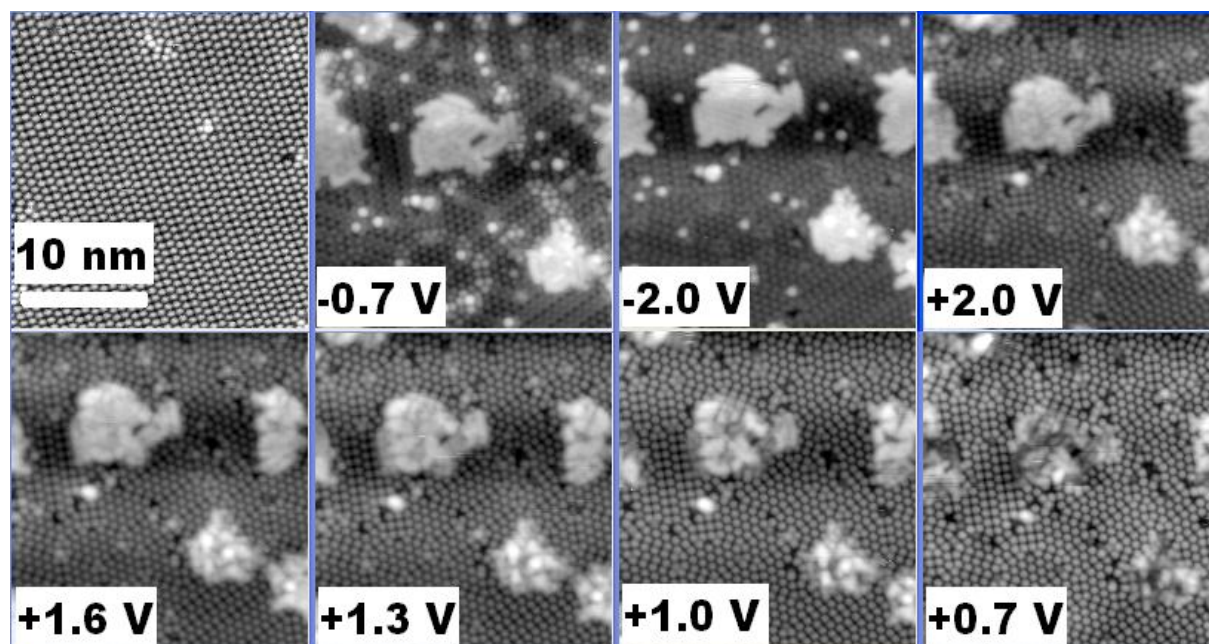
1. Hofrichter Jens et all. Synthesis of Graphene on Silicon Dioxide by a Solid Carbon Source // Nano Lett. – 2010 – V.10, – P. 36-42.

## Quantum size effect in submonolayer Bi films on Ge(111)

Goriachko A., Melnik P.V., Nakhodkin M.G.

*Taras Shevchenko National University of Kyiv, Kyiv, Ukraine*

Bismuth is attracting attention due to substantial difference between its semi-metallic bulk and metallic surfaces showing interesting spin-orbit effects. A continuous monolayer would represent the “ultimate” bismuth surface, which would require a substrate to be placed on. We present a detailed scanning tunneling microscopy (STM) investigation of ultrathin Bi films on Ge(111)-c(2×8) in the range up to 1.5 ML. Annealing the as-deposited Bi films at 450 K causes lateral redistribution of Bi due to surface diffusion: Densely packed two-dimensional Bi islands with no internal order are observed for deep-submonolayer coverages. The uncovered Ge substrate, which surrounds the islands becomes highly defective with numerous domain walls, antiphase boundaries, vacancies, etc.



STM images 25 nm × 25 nm in size: Upper left panel is the pure Ge(111)-c(2×8) substrate; Other panels show the same surface area with 0.25 ML Bi deposited at 300K and subsequently annealed at 450 K for 10 min. Indicated tunneling voltages were applied to the sample. Typical tunneling current in the constant current mode was ~0.3 nA.

In conclusion, atomically flat Bi islands show a clearly pronounced quantum size effect in empty electronic states, as proven by nonuniform local density of states distribution within each island's area observed in STM.

## Supramolecular assemblies with periodically modulated topology of the guest component and problem creating of electric generator and nanoscale structuring

Grygorchak I.I., Pokladok N.T., Ivaschyshyn F.O., Lukiyanets B.A., Bishchaniuk T.M.

National University Lviv Politechnik, Lviv, Ukraine

In spite of rapid development of nanoscience in general, and nanoelectronics and spintronics in particular, the problem of creating nanosource supply electrical power to nanoobjects is remaining unsolved. In this paper one proposes an approach to solve the problem. It is based on the phenomenons and effects observed in the formed intercalate supramolecular assemblies with the alternate semiconductor and molecular nanolayers. In particular, we irradiated by light with the fundamental edge absorption energy of GaSe  $\langle \text{FeCl}_3 \cdot 6\text{N}_2\text{O} \rangle$  nanostructures of VI and II stages, obtained in a magnetic field. It caused abnormal growth of photo-emf in the C-axis direction and formed photoelectret states with

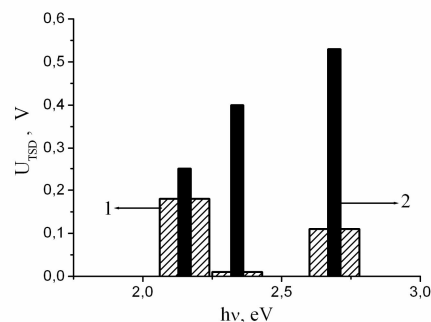


Fig. 1. Dependence of the photo-emf on energy of incident photons in nanostructures GaSe  $\langle \text{FeCl}_3 \cdot 6\text{N}_2\text{O} \rangle$  of VI (1) and II (2) stages, produced in a magnetic field.

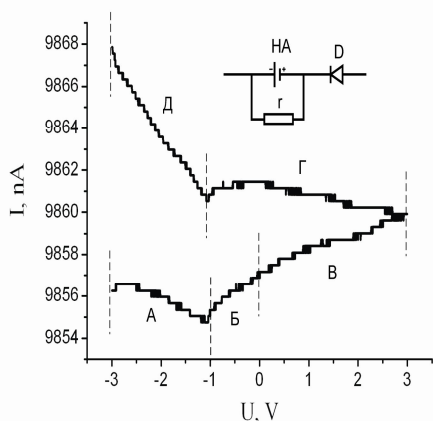


Fig. 2. Voltage-current characteristic of InSe  $\langle \text{RG} \rangle$ -nanostructure synthesized in electric field under simultaneous light illumination.

the low-temperature intervals of EMF-generations. The dependence of photo-emf on the incident photons energy is shown in Fig. 1.

Study of InSe  $\langle \text{RG} \rangle$  intercalate nanostructures (RG is a supramolecular content of rodamin) synthesized in the direct electric field under the simultaneous light irradiation, showed an unusual transformation of the voltage-current characteristic to the form shown in Fig. 2. Computer simulation allows us to construct the circuit diagram presented in inset of Fig. 2 with a nonlinear element HA as a nanoaccumulator. Nature of the thermally stimulated depolarization currents confirms this circuit diagram. Proposed in the paper physical model explains the results.

## Electrostatic potential and phonon modes in a multilayered quantum nanowells

Gryshchuk A.M, Gryshchuk V.V.<sup>1</sup>, Boiko I.<sup>2</sup>

<sup>1</sup> *Franco Zhitomir State University, Zhitomir, Ukraine*

<sup>2</sup> *Fedkovych Chernivtsi National University, Chernivtsi, Ukraine*

Last years experimentalists and theorists show the large interest to studying of the quantum nanowells [1], especially to the quantum cascade lasers, made on their basis. For this purpose to investigate physical properties of such systems, it is necessary to know time of a relaxation of carriers, a charge, linear and nonlinear optical properties, by the important factor which it should be considered is electron-phonon interaction. Therefore to have possibility to operate the cascade lasers, it is necessary to describe precisely optical and interface phonons modes, it takes Hamiltonian electron-phonon interaction on this system.

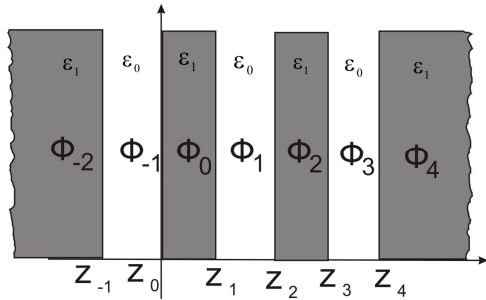


Fig. 1 Geometrical scheme of nanosystem.

Here we consider the nanoheterosystem consisting of five layers of flat nanowells  $\text{In}_{0.53}\text{Ga}_{0.47}\text{As}/\text{In}_{0.52}\text{Al}_{0.48}\text{As}$ . The system is placed into external medium  $\text{In}_{0.53}\text{Ga}_{0.47}\text{As}$ .

The dielectric function for any particular layer can be written as

$$\varepsilon_i(\omega) = \varepsilon_{i\infty} \frac{\omega^2 - \omega_{Li}^2}{\omega^2 - \omega_{Ti}^2}, \quad i = -2, -1, 0, 1, 2, 3, 4, \quad (1)$$

where  $\varepsilon_{i\infty}$  is high frequency dielectric constant of the  $i^{\text{th}}$  part of nanosystem,  $\omega_{Li}$  and  $\omega_{Ti}$  - are the frequencies of longitudinal and transversal optical phonons of its bulk analogue. As it follows from the dielectric continuum model the phonon spectrum for such a system is obtained by combining the electrostatic equations and getting the equation

$$\varepsilon_i(\omega)\Delta\Phi(z) = 0, \quad (2)$$

where  $\Phi(z)$  is the potential of phonon polarization field. The frequencies of phonons are determined by boundary conditions for polarization potential  $\Phi(z)$  and terms of electric displacement at  $z = z_i$ .

In working are considered the spectra of all types' phonons existing in a multilayered quantum nanowell. It is shown that there are confined optical (LO) and interface phonons of vibration in such nanosystem. The dependences of the phonons energy on the quantum layers and the Hamiltonian electron-phonon interaction are researched.

1. Tkach M.V. Electron-Phonon Interaction in Semiconductor Spherical Quantum Dot Embedded in a Semiconductor Medium (HgS/CdS) //, Phys Stat.Sol. – 2001. – V.225 – P. 331.

## Ultrafast carrier dynamics of silicon nanoparticles in fused silica

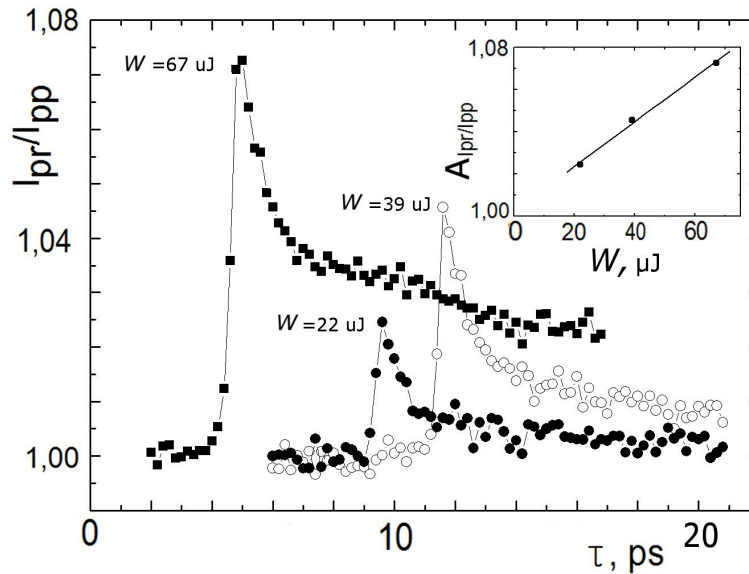
Kadan V.M.<sup>1</sup>, Blonskyi I.V.<sup>1</sup>, Indutnyi I.Z.<sup>2</sup>, Danko V.A.<sup>2</sup>, Korenyuk P.I.<sup>1</sup>

<sup>1</sup>*Institute of Physics NASU, Kyiv, Ukraine*

<sup>2</sup>*Institute of Semiconductor Physics NASU, Kyiv, Ukraine*

Ultrafast carrier dynamics of silicon nanoparticles in silica matrix has been studied under the femtosecond optical excitation. Amorphous SiO<sub>x</sub> films on the silica substrate are produced by nonstoichiometric vacuum evaporation with the silicon excess and annealed at 1100 K. Silicon nanocrystals are thus produced having about 4nm average diameter.

The nanostructured silica samples were excited with frequency doubled femtosecond laser pulses of 120 fs duration at 400 nm wavelength. This wavelength corresponds to the direct interband transitions, taking into account the quantum size effect. The transient absorption induced by the excitation pulses of different energies  $W$  is measured using the time-delayed white supercontinuum probing pulses.



The Figure shows the transient absorption  $I_{pr}/I_{pp}$  at 680 nm in the nanostructured samples versus the probe pulse delay  $\tau$  (from 0 to 21 ps) at different energies of the excitation pulse ( $W = 67; 39$ , and  $22 \mu\text{J}$ ). The amplitude of the transient absorption versus  $W$  is also shown in the insert.

The main result of the experiment is in the observation of the initial sharp rise of  $I_{pr}/I_{pp}$  and its subsequent two-stage decay, which is fast at small  $\tau$  and slower in the tens of picoseconds time range. Linear dependence of the amplitude of induced absorption  $A_{I_{pr}/I_{pp}}$  on  $W$  should also be noted.

Basing both on these and on a number of other experimental results, we propose a kinetic model for non-equilibrium electrons in Si-nanoparticles and analyze distinctive features of the electron Auger-scattering in the conditions of strong spatial limitation.

## Refractory nanocompositions for modifying of aluminum alloys

Kalinina N.E., Vilischuk Z.V.

*Dnepropetrovsk national university of the name Oles Gonchar, Dnepropetrovsk, Ukraine*

Demands of a complex of high mechanical properties and adaptability to manufacture are made to deformable aluminum alloys of systems Al-Zn-Mg-Cu and Al-Mg-Sc. In work high-strength aluminum alloys V93, V95, V96 and an average-strength alloy 01570 on the basis of widely used alloy AMg6 are studied.

High-strength aluminum alloys have low technological properties at the expense of allocation fragile phases on the basis of zinc, and alloys by system Al-Mg possess low properties of strength and don't give in to strengthening thermal processing.

The alloy 01570 is well welded, practically does not evince addiction to formation crystal flow in the time of welding and strength of the welded connections forms 0,9 – 1,0 from strength of the parent metal. The parent metal and welded connections, executed argonarc welding, do not evince the addiction to seasoned cracking.

At comparison of characteristics of alloys AMg6 and 01570 on a fluidity and durability limit, increase of the given characteristics for an alloy 01570 on 40 % and 20 % accordingly is observed. Plasticity of an alloy 01570 more low, than at AMg6, but is at high enough level.

The ordinary maintenance of the modifiers entered in fusion, makes some percent from weight of fusion. At industrial level delivery of the ordinary modifier (salts NaCl, NaF, KCl) are made by parties on 25 – 50 kg. The quantity entered nanomodifiers makes 0,01...0,1 % from weight fusion. Therefore it is economically expedient to use nanomodifiers instead of traditional in industrial scales.

Modifying by the nanodisperse refractory modifiers received by a plazmo-chemical method is offered with a purpose increases strength properties of multicomponent aluminum alloys. Criteria of modifiers are chosen: conformity of nuclear radiuses, a crystal lattice, temperature of fusion by components.

For alloys V93, V95, V96 the modifier – TiCN is offered. For an alloy as 01570 modifier served SiC  $\beta$  - updatings. Dispersion of refractory modifiers made to 100 nanometers. Additional hardening of an alloy 01570 is possible introduction disperse Sc.

## **SEM and AFM study of Pt-CeO<sub>2</sub> thin films prepared by magnetron sputtering for fuel cell applications**

Khalakhan I., Vorokhta M., Fiala R., Matolin V.

*Charles University in Prague, Prague, Czech Republic*

Simultaneous magnetron sputtering of Pt and cerium oxide provides oxide layers continuously doped with Pt atoms during the growth. Morphology of Pt doped cerium oxide catalyst films depends on many factors. Deposition on carbon nanotubes and flat carbon substrates leads to growth of solid solution films composed of nanorods oriented perpendicularly to the substrate surface forming highly porous structure. The films contain only cationic Pt<sup>2+</sup> and Pt<sup>4+</sup> and cerium oxide is partially reduced. The catalyst films reveal high catalytic activity as anode catalyst in proton exchange membrane fuel cells (PEMFC). The preparation of highly dispersed carbon nanotubes coated by sputtering make this method promising for large scale production of the PEMFC catalysts.

## Spatial local fluctuations of a quantum yield in InGaN/GaN structure

Kisseluk M.P.<sup>1</sup>, Vlasenko O.I.<sup>1</sup>, Lyashenko O.V.<sup>2</sup>

<sup>1</sup>*Institute of Semiconductor Physics of NASU, Kyiv, Ukraine*

<sup>2</sup>*Kyiv National University of Taras Shevchenko, Kyiv, Ukraine*

Acoustic emission (AE) method allows observing in materials, structures and devices on their bottom the beginning and dynamics of fast processes of degradation, fluctuation and a relaxation. Thus observations of a subject of inquiry are led in a real time irrespective of activity of external fields any (except ultrasonic) the nature and other methods of examinations used simultaneously.

In work the results of examination of fluctuations of a quantum yield in local areas InGaN/GaN light-emitting structures (LES) with one quantum hole are presented.

The previous examinations [1,2] LES by means of microscopy of a visible gamut have shown that intensity electroluminescence (EL) distribution on a visible surface of the active area at a direct current is nonuniform. Thus, recording of signals of an AE with sync in time was simultaneously spent. The analysis of the gained results has specified in correlation of signals of an AE and quantum yield fluctuation in separate areas that us contacts a relaxation of mechanical and thermo-mechanical stresses. At the same time with quantum yield fluctuations, degradation processes are fixed also.

Earlier the collective of authors had been presented results of experiment on studying of distribution of EL-intensity on a surface light-emitting structures with a quantum hole, but considering that radiation is generated in narrow enough epitaxial stratum, examination distribution of the EL to a stratum edge, orthogonal surfaces of the active area has been conducted. For this purpose on a LED it was shaped (additional grinding and polishing) a platform.

A joint use of AE-methods and an optical microscopy allows displaying processes of degradation and fluctuation in a real time. Experiment conducting AE radiants (defect formation field) thus allow to detect and identify, to size up a size of these local fields and their arrangement in at-blanket [1,2]. Correlation between fluctuation of quantity of quantum efficiency and AE signals is confirmed.

For a lateral edge light-emitting structures were observed fluctuations of intensity of the EL in a active area and an undercoat. The analysis of the gained effects has allowed to build model LES (LED) as matrixes of microdiodes with the various content of indium as a part of a solid solution of a quantum pit (active area).

It is necessary to score inhomogeneity of a current on a heterogeneous junction plane that leads to faster degradation of local field by most fluctuation indium because of a higher current density. Therefore, after failure of this section, there is a redistribution a current between other microdiodes to the subsequent failure of the following microdiode.

1. Lyashenko O.V., Veleshchuk V.P., Vlasenko O.I., Kisseluk M.P. //AIP Conference Proceedings. – 2009. – **1129**. – P. 395-398.
2. Veleschuk V.P., Lyashenko O.V., Vlasenko Z.K., Kisseluk M.P. // SPQEO. – 2010. – **13**, №1. – P. 79-83.



## Mechanical properties of ensembles of silicon nanowires grown on silicon substrate

Klimovskaya A.I.<sup>1</sup>, Shanina B.D.<sup>1</sup>, Lytvyn P.M.<sup>1</sup>, Kalashnyk Iu.Iu.<sup>1</sup>, Kamins T.I.<sup>2</sup>, Sharma S.<sup>2</sup>

<sup>1</sup>*Institute of Semiconductor Physics, National Academy of Sciences, Kyiv, Ukraine*

<sup>2</sup>*Quantum Science Research, Hewlett-Packard Laboratories, Palo Alto, CA, USA*

In the last few years, great attention has been paid on development of NEM devices due to a broad range of possible applications in metrology, communication and information technologies. Transit to this kind of devices allows improving the energy efficiency of microelectronic products. A central part of all NEM system is nano oscillator. A promising candidate on a role of the oscillators are nanowires grown on a substrate. Stability and long-term operation of these devices are evident to depend strongly on mechanical properties of oscillating electrode and mechanical strength of its fixed end(s). We carried out research of mechanical properties of dense ensembles of silicon nanowires grown on boron doped Si(100) substrates by using metal-catalyzed chemical vapor deposition. Some of these ensembles were doped with phosphorous during growth. Experiments have shown that growing of nanowires on a substrate results in a deformation of the substrate, and therefore deteriorate properties of this system.

A cross-sectional view and distribution of an induced current intensity are shown in Fig. 1. The most current, and consequently the most deformation, corresponds to an area of the substrate – nanowire interface. ESR-study have shown that a signal related to boron atoms doping the substrate is observed in all the samples. No boron signal in stress-free silicon is known to be observed due to a degeneracy of the valence band. Its appearance here suggests an uniaxial strain of the substrate that removes the degeneracy. A level of strength was found to depend on a temperature (Fig. 2) and on doping of nanowires by phosphorus. In the current research we have proposed how to minimize a deterioration of ensembles of silicon nanowires on a Si substrate.

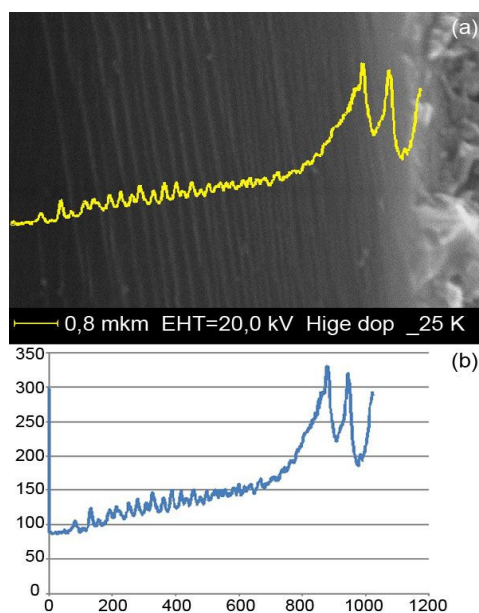


Fig. 1. SEM image (a) and distribution of intensity of a current in a cut of the sample (b).

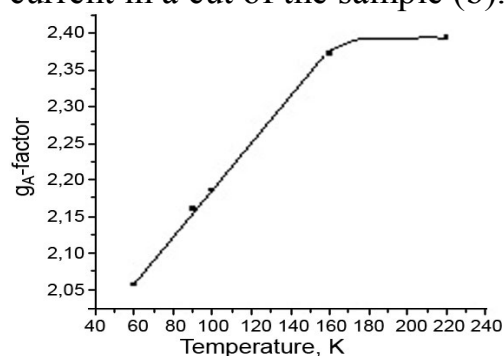


Fig. 2. Temperature dependence of the boron g-factor.

## **Self-organization of Cu and Ni nanosystems during quasi-equilibrium condensation at magnetron sputtering**

Kosminska Yu.O., Mokrenko A.A., Dyoshin V.B., Perekrestov R.V.

*Sumy State University, Sumy, Ukraine*

Aiming to produce the system of particles of identical form and sizes and possessing certain order in particle arrangement, it is rational to develop the approach of self-assembly of nanosystems at steady-state condensation of atoms onto a substrate in vicinity to thermodynamical equilibrium. At such approach minimization of the free energy is the driving force that can be observed during quantum dots formation by molecular-beam epitaxy. In order to obtain identical and isolated nanocrystals and eliminate layer-by-layer growth, we offer to use Volmer-Weber conditions but realized at quasi-equilibrium steady-state condensation. Thus, the aim of the present work is to reveal the forms and the mechanisms of structure formation of condensates on the example of copper and nickel under conditions of extremely low supersaturations.

By means of dc magnetron sputtering under conditions of low discharge powers (1.4÷7 W) and heightened substrate temperatures (620÷653 K) copper and nickel condensates were produced possessing indications of self-organized growth, porosity and fractality. The working gas (argon) pressure was 2.6÷10 Pa, argon being purified by titanium sputtering by two additional magnetrons to the value of residual chemically active gas pressure of  $7 \cdot 10^{-7} \div 10^{-8}$  Pa. KCl (001) fresh cleaved facets and glass were used as substrates. The condensate structure was studied on different stages of growth by means of scanning and transmission electron microscopy, and electron microdiffraction as well.

It was found that the growth form of condensates changes from highly textured polycrystalline films to 2D and 3D porous layers consisting of individual rounded clusters. The near-equilibrium nucleation of clusters occurs solely on active centres on substrates.

In case of increased density of primary clusters, being uniformly distributed over substrate surface, structure fragments growth is accompanied by mutual exchange of atoms that allows Ostwald ripening and, hence, self-organization of system of clusters, being equal in sizes.

In case of nonuniform distribution of primary clusters over substrate surface, fractal forms of condensates were observed on which the whisker system of diameter 30÷600 nm was formed after prolong condensation. Prevailing mechanism of fractal formation consists in homogeneous nucleation at splicing places of primary clusters in absence of usual coalescence.

## **Nanodimensionality criteria: physical justification and methodological calculations**

Liopo V.A., Avdejchik S.V., Struk V.A., Vorontsov A.S., Mihajlova L.V.,  
Eisymont Y.I.,\_Andrikevich V.V.

*Yanka Kupala Sate University of Grodno, Grodno, Belarus*

For analytical description of the structural features of polymeric nanocomposite materials is used the term "nanoparticle" which mean by the real object with dimensions not exceeding 100 nm. In this case the physical justification of the choice of the size criterion is not given, that does not allow for valid choice of nanodimension modifiers with different composition, structure and mechanism of the modifying action.

In view of classical concepts in quantum mechanics, the physics of condensed state and crystal physics analyzed the structure features, habitus and energy state of dispersed particles obtained by mechanical dispersion of semi-finished and condensation of atomic or molecular components. Based on different methodological approaches subject to Einstein's equations, the criterion of the Debye temperature, the uncertainty principle, Schrodinger equation, etc. is suggested an analytical expression for determining the dimensional boundary  $L_0$  of particle transition of the condensed medium from macro- to nanostate which is characterized by specific parameters of thermal physical and energy performance:  $L_0 = 230^{-1/2} \theta_D$ , where the  $\theta_D$  - Debye temperature [1].

This expression allows realizing estimates of various parameters of nanoparticles of various substances and chemical compounds and justifying technological modes of production and application. Analysis of the characteristics of the process of obtaining nanosized particles using the theory of point groups and closest packing enable to establish the most probable habitus due to crystal-chemical prehistory.

It is implemented physical justification of activity of nanoscale particles of different habitus caused by crystal-chemical structure of semi-finished product and the type of crystal lattice [1].

It is established the effect of the existence of uncompensated charge at the nanosized particles of different structure which promotes the formation of ordered quasi-crystalline structures in boundary layers and improves the performance of deformation-strength, tribological and protective properties of technical products of the functional polymer nanocomposites.

1. Avdejchik S.V. [and alt.] Introduction into Nanocomposite Engineering Materials Physics - Grodno, GSAU. – 2009.– 439p.

## Hierarchy levels of real objects nanostate: physical models in the analysis methodology

Liopo V.A., Sabutz A.V., Struk V.A., Avdejchik S.V., Sorokin V.G.

*Yanka Kupala Sate University of Grodno, Grodno, Belarus*

In the investigation of substances with isodesmic interatomic bonds are applicable models of spherical packings [1]. The simplest versions of such structures are metals that are used including as nanofillers in creating composite materials, such as polymer-based. To form a nanocrystal of the metal is possible in two ways: by dispersion of a large sample or the cultivation of nanoparticles from the melt, solution or vapor condensation. In this case a method of constructing sphere packings allows setting habit of nanoparticles of any size. The vast majority of metals are crystallized in three types of lattices: hexagonal closest packing (hcp), face-centered cubic (fcc) and body-centered cubic (bcc). The first two correspond to the closest spherical packing with the same coefficients compactness  $P=0.74$ . For the bcc packing  $P=0.68$ . At implementation the conditions of spherical packing around the central spherical atom all other atoms form a coordination spheres with certain radius ( $R$ ) and the number of atoms-balls in these spheres  $K(N)$  called the

coordination number. Value  $C = \sum_{n=1}^N K(n)$  determines the number of atoms in a

spherical cluster of coordination sphere with a radius  $R(N)$ . We analyzed the characteristics of the coordination spheres and spherical clusters to  $N=10000$  inclusive. Differences reticular spherical densities with the same radii of spherical particles and the number of atoms in them are established. The presence in the hcp lattice of the unit direction explains the absence of structures such as ...ABABCBCAC... with the possible exception for substances with cleavage. Research of habit of coordination spheres and the number of their constituent atoms showed that meeting conceptions that all particles smaller than 100 nm cover to nanoparticles are unacceptable. The atoms number within a sphere of radius  $R$ , that is  $N(R)$ , determined by the condition  $N = P \cdot (R/r)^3$ . If the atoms number in a particle is equal to 106, then  $R/r \approx 10^2$ , that is when  $r=1.4$ ,  $R=10$  nm.

Quantum-mechanical analysis of electrons and phonons behaviour shows that the size effects affecting the substance properties, that is defining the boundary between macro- and nanophases, with rare exceptions, do not exceed 20 nm. Studying the characteristics of the coordination spheres allow to suggest that the activity of metal nanocrystals is determined not only by their structural chemical properties, but also the reticular spherical density. This should be taken into account, for example, at using metal nanoparticles as modifiers of polymeric composite materials and at various heterogeneous systems creating.

1. Avdejchik S.V. [and alt.] Introduction into Nanocomposite Engineering Materials Physics - Grodno, GSAU. – 2009. – 439 p.

## **Influence of thermal treatments on light emitting properties of porous nanocomposite films nc-Si/SiO<sub>2</sub>**

Lisovskyy I.P., Litovchenko V.G., Voitovych M.V., Zlobin S.O.,  
Khatsevich I.M., Indutnyy I.Z., Shepelyavyi P.E.

*V. Lashkaryov Institute of Semiconductor Physics, National Academy of Sciences of Ukraine,  
Kiev, Ukraine*

The task to optimize luminescent properties of nc-Si/SiO<sub>2</sub> system remains currently important. An effective means to enhance the luminescence intensity is, in particular, annealing this system in the ambient of hydrogen, oxygen, nitrogen, and so on. Passivation of nc-Si inclusions surface with corresponding gas atoms leads to noticeable reduction of nonradiative recombination channel. In the case of porous nanocomposite films, which have a columnlike structure with high developed effective surface, influence of such a treatment should be substantially larger.

Porous nc-Si/SiO<sub>2</sub> systems were produced by high temperature treatment (975 °C, 15 min, vacuum) of porous SiO<sub>x</sub> ( $x \approx 1.78$ ) films obtained by the method of oblique (60°) deposition of thermally evaporated SiO particles in vacuum. The samples were annealed in vacuum ( $\sim 10^{-3}$  Pa) or in the ambient of air, argon, nitrogen or hydrogen within the temperature range of 100 – 550 °C. The spectra of IR-absorption and photoluminescence (PL) were measured.

Heat treatments considerably enhanced PL band ( $\sim 850$  nm) intensity and the efficiency of this effect depended on type of gas ambient – it was maximal (up to 30 times) for nitrogen atmosphere and minimal (up to  $\sim 5$  times) for inert (argon) or vacuum medium. It should be noted that in the latter case PL intensity has never been changed for solid SiO<sub>2</sub> films with imbedded Si nanocrystals.

PL band peak position practically did not change as well as maximum position of Si-O absorption band ( $\sim 1085$  cm<sup>-1</sup>). These facts mean that heat treatments did not alter number and size of silicon inclusions in the film. Hence, PL intensity enhancement is the most likely caused by structural transformations in oxide matrix near silicon nanocrystals surface. Two mechanisms, at least, may be involved. For the samples annealed in vacuum or in Ar atmosphere elevated temperatures (150 – 300 °C) lead to healing meta-stable defects (e. g. dangling bonds of silicon and oxygen) at ncSi – SiO<sub>2</sub> interface. In fact, this temperature interval is characteristic for radiation surface states annealing in planar Si – SiO<sub>2</sub> structures. Existing of such defects may be associated with oxide strained structure in porous film nanocolumns. If gas ambient is not inert passivation of more stable broken bonds of silicon and oxygen with corresponding gas molecules may additionally take place, reinforcing process of nonradiative recombination centers elimination.

## **Laser plasma techniques for nanoscale modified thin films production**

Luksha O.V.

*Uzhgorod national university, Uzhgorod, Ukraine*

The pulsed laser evaporation (PLE) is an effective technique for clusters and extraordinary crystalline and polyamorphic non-crystalline nanoscale modified thin films due to the creation of extreme condensation from powerful flows of matter. Electron-diffraction and electron-microscopy measurements were carried out on amorphous  $As_2Se_3$  films produced in all the three regimes of PLE. Analysis of the position of S and intensity I of the first sharp diffraction peak (FSDP) was carried out by diffractogrammes. Correlation size of middle range (MRO) is defined as  $D = 2\pi/s$ . By radial distribution function (RDF) analysis data we defined short range order (SRO) parameters of amorphous films structure. Besides MRO and SRO amorphous films parameters we investigated their change under heating and defined polyamorphous change temperature  $T_0$  and crystallization change temperature  $T_{cr}$ .

For the optimization process of  $As_2Se_3$  amorphous thin films deposition and definition of condensation parameters we investigated the main parameters of expanding laser plasma during each of all three regimes of PLE.

Thus characteristic structural peculiarity of deposited amorphous  $As_2Se_3$  films from laser plasma is: oscillation of correlation D size that corresponds to the cluster size in MRO model. SRO parameters peaks to possibility of obtaining by PLE technique of different types of nanoscale modified amorphous structures.

It should be mentioned that such variant of amorphous thin films structure is practically impossible to get by means of traditional methods of thermal vacuum evaporation and vapour condensation.

The results of structural investigations of amorphous  $As_2Se_3$  films under more detailed analysis corresponds to the data of laser plasma flow irradiation according to their mass, energetic and spatial distribution.

PLE technique let us carry out nanostructural modification of amorphous films both, within SRO range (0.1-0.3 nm) and MRO range (0.5-1.0 nm), where cluster structure is clearly seen.

For application field of particular importance are possible variations of nanostructure within SRO and MRO distances which are reached by means of PLE technique. Superphotosensitivity of amorphous chalcogenide films genetically connected with nanostructure change which is given by laser condensation conditions.

## Optical properties of modified silicon dioxide layers with Si-nanoclusters

Lukyanov A.N., Khatsevich I.M., Romanyuk B.M.,  
Yefanov V.S., Fomovskii F.V.

*V. Lashkarev Institute of Semiconductor Physics National Academy of Sciences of Ukraine,  
Kiev, Ukraine*

The structures with silicon nanoclusters (nc-Si) were obtained by implantation of  $\text{Si}^+$  ions with the energy  $E = 100$  keV and doses of  $5 \times 10^{16}$  and  $1 \times 10^{17} \text{ cm}^{-2}$  into a quartz substrate. Another method of nc-Si formation was thermal evaporation of  $\text{SiO}_x$  powder in vacuum onto quartz substrate to obtain non-stoichiometric  $\text{SiO}_x$  layer. For the formation of nc-Si all samples were subjected to high-temperature annealing (HTA) at  $1150^\circ\text{C}$  for 20 min in atmosphere of inert gas (Ar). To modify the properties of the light emitting structures of both types the structures were subjected to low-temperature annealing (LTA) at  $450^\circ\text{C}$  in air, and hydrogen plasma treatment. PL spectra were measured at room temperature under the excitation by AIG (473 nm) and HeCd (325 nm) lasers after HTA and the followed LTA, and also after hydrogen plasma treatment. Transmission spectra were measured in the range 200-1500 nm on the spectrophotometer Shimadzu UV-3600.

For structures with larger dose of implanted Si after HTA the PL band was shifted to long-wavelength region compared with the PL band of low-dose of implanted Si ( $\lambda_{\text{max}} \approx 570$  and  $\approx 470$  nm, respectively).

The intensity of PL bands of nc-Si formed by deposition  $\text{SiO}_x$  layer and HTA increases significantly after the next LTA. However, subsequent treatment of such modified structure of the nc-Si in hydrogen plasma leads to the reduction of PL intensity.

In accordance with the proposed mechanism, PL of nc-Si formed by low-dose of implanted Si ( $5 \times 10^{16} \text{ cm}^{-2}$ ) after HTA occurs by interband transitions in clusters with  $\lambda_{\text{max}} \approx 470$  nm, after followed LTA the  $\text{SiO}_x$  layers grow on the interfaces nc-Si/ $\text{SiO}_2$  and it allows irradiation through long-wavelength recombination centers in  $\text{SiO}_x$  ( $\lambda_{\text{max}} \approx 730$  nm). At that time high-dose of implanted Si ( $1 \times 10^{17} \text{ cm}^{-2}$ ) and HTA form stable recombination-active centers ( $\lambda_{\text{max}} = 570$  nm) in nc-Si without shifting PL band after LTA.

Peculiarities in transmittance spectra of the structures those appear near absorption edge were also explained.

## **Low frequency noise spectroscopy as a tool to study quantum-size structures**

Makoviychuk M.I.

*Yaroslavl Branch of the Institute of Physics and Technology of RAS, Yaroslavl, Russia*

The method of low frequency noise spectroscopy of structure-disordered semiconductors finds more and more broad application both in physical researches and in the analysis of different processes of micro- and nanotechnology. The practical realization of this method as a monitoring instrument of defect-impurity engineering for to solve the technological problems of silicon electronics are presented and discussed.

In presented activity the experimental results on analysis of flicker noise processes in disordered semiconductors on an example of designed production process of flicker noise gas sensor of a new generation are classified.

Studies concerned with the design of new approach for gas sensors based on ion-implanted silicon structures are analyzed. The influence of adsorbed molecules on the electronic state, electrical conductivity and flicker noise of the surface and inner interfaces in disordered silicon structures are discussed. The sensor properties of disordered silicon structures in the detection of various adsorbed molecules are described.

As they are grown and processed in microelectronics manufacturing, Si single crystals start to have different types of structural imperfection and impurity that may be detrimental to finished-device performance.

Defect/impurity flicker noise spectroscopy provides a rapid technique for investigating defect–impurity interaction and as such relates to defect/impurity engineering, which is concerned with reducing process-induced disturbances and impurity diffusion coefficients (in ion-implanted silicon) and with gettering metallic impurities. The above idea is implemented in a technology of new-generation flicker-noise gas sensors designed to be incorporated into microanalytical systems [1, 2].

1. Makoviychuk M.I. Flicker-noise gas sensors as basis elements of microanalytical systems. // Proceed. Int. Conf. “Micro- and nanoelectronics - 2007”. - Moscow: IPT RAS. –2007. – O1-22.
2. Makoviychuk M.I., Chapkevich A.L., Chapkevich A.A., Vinokurov V.A. Flicker-noise gas sensor. // Biomedical Engineering. – 2009. – V. 43, № 3. – P.109 - 113.



## **The electrization influence on molecular mobility of gold and silver nanocomposites based on polysaccharide arabinogalactan**

Nikolaeva M.N.<sup>1</sup>, Aleksandrova G.P.<sup>2</sup>

<sup>1</sup>*Institute of Macromolecular Compounds, Russian Academy of Sciences,  
S.-Petersburg, Russia*

<sup>2</sup>*A.E. Favorsky Institute of Chemistry, the Siberian Branch of the Russian Academy of  
Sciences, Irkutsk, Russia*

It is known that some areas of thin dielectric polymer films can be in highly conducting state when they are placed in the Metal-Polymer-Metal structures and when electric field is lower than a breakdown field  $E \ll E_c$  [1]. It had been assumed earlier [2] that the cause of the appearing of highly conducting channels in polymer films is its' electrization by the metal substrate while the conductivity of polymer films can be also influenced by the molecular mobility of polymers [2, 3]. The aim of this study is an attempt to determine whether there is a relationship between the electrization of polymer films and the molecular mobility of polymers as well.

We have observed proton spin-spin relaxation times ( $T_2$ ) dependence on polymer doping by silver and gold nanoparticles. Composites based on arabinogalactan with metals were formed as zero-valent metal particles with particle sizes of the metallic phase of several nanometers. Maximum conductive thickness values of the films deposited from their 2.5% solutions by spreading method are changing synchronously in an inverse way. There is a correlation obtained between the values of spin-spin relaxation in D<sub>2</sub>O solutions of larch arabinogalactan nanocomposites and the maximum conductive layer thickness of the films, deposited from their solutions. Thus, with the increase of  $T_2$  values and, consequently, the molecular mobility, increases the maximum thickness of the polymer film on which is still possible to register film resistance. Arabinogalactan structure differences in D<sub>2</sub>O and H<sub>2</sub>O influence on its macromolecular mobility and its films conductivity is also evaluated.

It's obvious that spin-spin relaxation of arabinogalactan composites with metal nanoparticles in water solutions is influenced by a lot of molecular processes but we suppose the one of them is electrization affecting both the conductivity and molecular mobility of arabinogalactan.

1. Arkhangorodskii V.M., et al. // JETP Lett. – 1990. – V.51. – P.67.
2. Ionov A.N., et al. // Polymer Sci.- Ser.A. – 2008. – V. 50. – P.174.
3. Nikolaeva M.N., et al. // 7th International Conference "Amorphous and microcrystalline semiconductors".-S.-Petersburg. – 2010. – P. 217.

## Features of X-wave diffraction image formation with clusters of edge dislocations

Novikov S.M., Struk A.Ya.

*Yuriy Fedkovych Chernivtsi National University, Chernivtsi, Ukraine*

Experimental diffractometry methods allow immediately obtain integral characteristics of crystal lattices distortions, but usually do not give an answer about the type of defects and their spatial orientation. This is especially true of areas with a high degree of heterogeneity, eg, boundaries of the film-substrate, where high concentration of dislocations, microdefects, dislocation loops leads to the formation of the defect complexes. Contribution to the total integrated intensity of these complexes is not synonymous and can lead to erroneous determination of type and concentration of defects. More sensitive to local distortions of crystal lattice are topographic techniques. Unequivocal interpretation of diffraction contrast is very difficult problem even for single defects, because many factors affect its formation [1, 2]. So topographic images modeling of defects complexes probably is one of the most effective methods for their identification by diffraction contrast.

The peculiarities of the diffraction images with complexes of perpendicular boundary dislocations, which form micro-cluster (with two, three or more dislocations) and low-angle dislocation boundaries (walls) are analyzed in this paper [3]. A number of complex diffraction effects for the wave fields generated by highly distorted crystal region along the lines of dislocations are observed during locations in the scattering plane of several perpendicular boundary dislocations. There are found various by intensity interference rescattering and reflection effects generated by "new" and existing wave fields on the thickness intensity distribution in case of presence in the same slip plane of boundary dislocations with parallel and antiparallel Burgers vectors (Fig. 1).

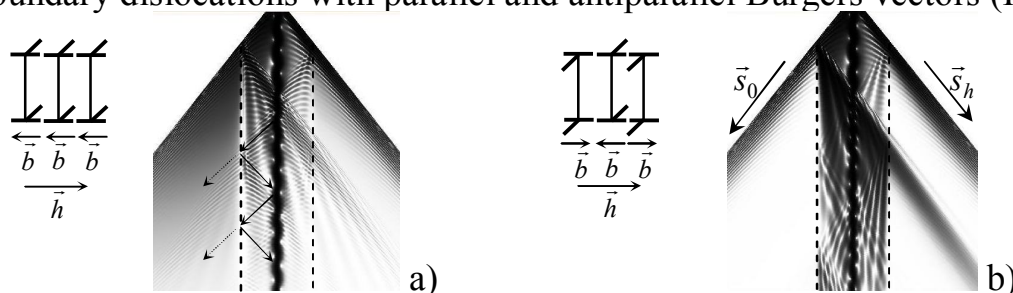


Fig. 1. There are shown central parts of the intensity distributions  $R_h(x, z)$  in the presence in crystal of Si dislocation cluster of three dislocations with same (a) and different (b) direction, with dislocation line perpendicular to the diffraction vector and located at a distance of 50  $\mu\text{m}$ .

1. Authier A., *Dynamical theory of X-ray diffraction* (Oxford Univer. Press: 2001).
2. Smirnova I.A., Suvorov E.V., Shulakov E.V., *FTT*, – 2007. – T.49, №6. – 1050.
3. Novikov S.M., Struk A.Ya., Fodchuk I.M., *Metallofiz. Noveishie Tekhnol*, –2010 – T.32, №9. – 1198.

## Properties of nanoscale magnetic materials obtained with cryochemical synthesis

Omelchenko S.A., Vorovsky V.Yu., Khmelenko O.V.,  
Gorban A.A., Kushnir N.A.

*O. Gonchar Dnepropetrovsk National University, Gagarin av., Dnepropetrovsk, Ukraine*

Cryochemical technology is one of the most promising for the creation of biocompatible magnetic nanomaterials, which can be used in medicine as magnetic carriers, delivering drugs to the desired location of the body, for the identification of cells with the subsequent health effects, to increase contrast magnetic resonance imaging. In this regard, particularly relevant is the study of the dependence of the structure and surface properties of nanoparticles on technological regimes cryochemical synthesis, and in particular, freeze-drying regimes cryogranules.

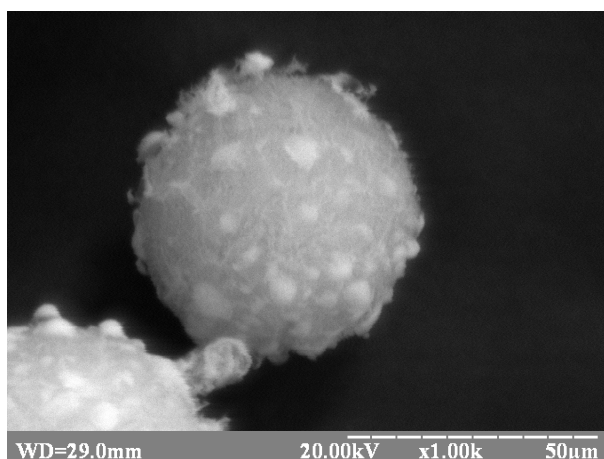


Fig. 1.

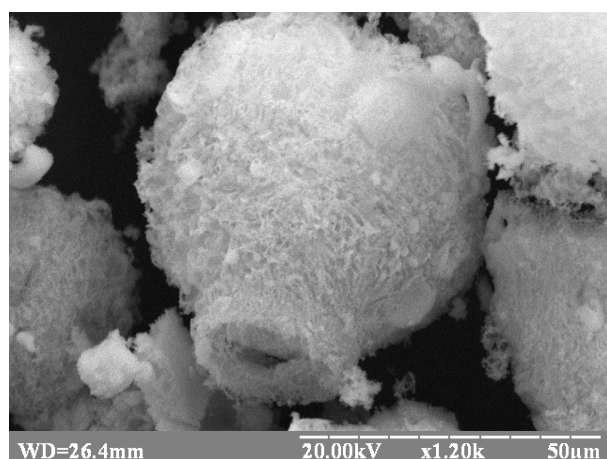


Fig. 2.

This is due to the fact that the results will create a magnetic nanomaterials with high surface area and high dispersion, which will improve functional ability of nanoparticles and quality products from nanoferrites. Biocompatible magnetic nano-materials will have higher efficiency in the delivery of drugs or identify of cells. The increase in the total area of the particles will also decrease the dose used to nano-medicine.

In this paper, drying cryogranules made on the designed and manufactured a laboratory apparatus for freeze-drying. The setup allows to perform drying in a wide range of temperatures (from  $-196^{\circ}\text{C}$  to  $+100^{\circ}\text{C}$ ) at pressures up to 10 Pa. On the example of a powder of nickel-zinc ferrite composition  $\text{Ni}_0, 5\text{Zn}_0, 5\text{Fe}_2\text{O}_4$  shown that drying at high intensity heat supply leads to a change in the surface structure of the dried cryogranules of plate-mesh to reticulo-

filamentous forms. (Fig. 1). Increase the intensity of heat supply leads to the formation of holes in the spherical surface on cryogranules annealing. (Fig. 2).

## Study of elemental composition and morphology of SiGe-nanoislands by Raman spectroscopy and high-resolution SEM with local Auger spectroscopy

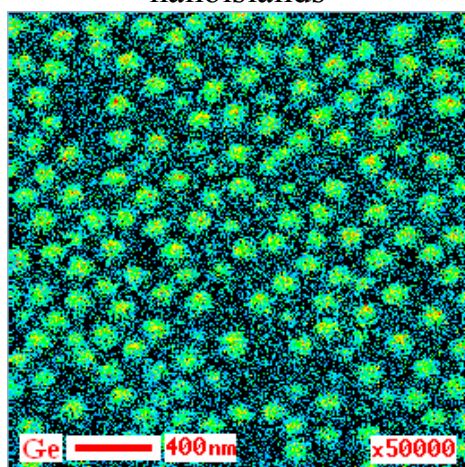
Ponomaryov S.S.,<sup>1</sup> Yukhymchuk V.O.<sup>1</sup>, Valakh M.Ya.<sup>1</sup>, Dzhagan V.M.<sup>1</sup>,  
Yaremko A.M.<sup>1</sup>, Krasil'nik Z.F.<sup>2</sup>, Novikov V.A.<sup>2</sup>

<sup>1</sup>*Institute of Semiconductor Physics, National Academy of Sciences of Ukraine, Kyiv, Ukraine*

<sup>2</sup>*Institute of Microstructure Physics, Russian Academy of Sciences, Nizhny Novgorod, Russia*

Application of self-induced growth mode according to Stranski-Krastanov model is one of the most promising ways of nanostructures formation, particularly, Ge epitaxy on Si substrate. Arrays of self-assembled Ge and SiGe nanoislands have been intensively investigated in the past decade due to their potential applications in near-IR optoelectronics and microwave devices and detectors. To fabricate high performance devices, it is necessary to know and control the electronic and optical properties of nanoislands. These physical properties critically depend on the following parameters: size, shape, surface density, homogeneity of distribution, mechanical stress and elemental composition of nanoislands.

Ge-Augur image of SiGe-nanoislands



The structures studied in this work were prepared by molecular beam epitaxy on a Si(001) substrate. The dual buffer layer was 200 nm thick Si-layer followed by Si<sub>0.9</sub>Ge<sub>0.1</sub>-layer of 10 nm in thickness. Then Ge with a nominal thickness of 8.8 ML was deposited onto the buffer layer at the substrate temperature of 700°C. The high-resolution (3 nm) SEM (HRSEM) coupled with Local (5÷8 nm) Auger Electron Spectroscopy (LAES) were used for a comprehensive study of the elemental composition and geometrical parameters of nanoislands. The Field Emission Auger Microprobe JAMP-9500F (JEOL,

Japan) equipped with Ar<sup>+</sup>-ion etching gun was used for a layer-by-layer analysis of the nanoislands in the growth direction. The high spatial resolution of LAES, capable of obtaining Si, Ge, C and O depth profiles of an individual nanoisland, was achieved by using the electronic correction of the probed spot drift. The results obtained from LAES for an individual island were compared with the data obtained by micro-Raman spectroscopy, averaged over both many nanoislands within the ensemble and over the height of the particular nanoisland. The average Si content in nanoislands obtained from Raman data is about 53 at. % is in good agreement with Si content obtained with LAES in the layer-by-layer analysis procedure.

## Influence of specular-diffuse reflection mechanism for charge carriers on high-frequency intraband conductivity of straight-line graphene ribbons

Ruvinskii B.M.<sup>1</sup>, Ruvinskii M.A.<sup>2</sup>

<sup>1</sup>*Ivano-Frankivsk National Technical University of Oil and Gas, Ivano-Frankivsk, Ukraine*

<sup>2</sup>*Vasyl Stefanyk Precarpathian National University, Ivano-Frankivsk, Ukraine*

Considerable number of works is devoted to the peculiar electronic properties of an infinite graphene as a two-dimensional massless Dirac fermion gas [1,2]. The aim of this work is the theoretical determination of intraband conductivity of limited graphene on the example of planar straight-line graphene ribbon(strip). Stipulated by the electrons transitions within the same zone intraband conductivity is dominant [2] at the frequencies of alternating electric field  $\omega < k_B T / \hbar$ , where  $k_B$  – Boltzmann constant,  $\hbar = h / 2\pi$ ,  $h$  – Planck constant,  $T$  – absolute temperature. For infinite graphene if the intraband conductivity prevails quantum consideration gives the same results as the quasi-classical kinetic equation. In case of the limited graphene quantum dimensional effects can be neglected if the typical linear sizes of the system exceed the average "thermal" de Broglie wavelength of current carriers. But if the linear size of the system is commensurable or less than the free path of current carriers, classical dimensional effects should be considered. In our work was calculated the dependence of integral intraband conductivity on the external field frequency, wire size and free length of electrons within different parameters' values of diffuse-specular mechanism for electrons scattering from the lateral wire borders. The calculations were conducted under boundary conditions using the Boltzmann kinetic equation, approximation of relaxation time  $\tau$  and linear response of charge carriers in alternating electric field  $\vec{E}$ . Received results show the importance of the classical size-effect. Thus, if  $\omega \ll 1/\tau$ , the real part of the intraband conductivity differs from zero. Diffuse scattering significantly reduces the value of the stationary and high-frequency conductivity in comparison with the infinite graphene [2]. Relative part growth of specular reflected current carriers leads to conductivity increase comparing to the pure diffuse scattering. The influence of boundary conditions takes place especially in the low-frequency region  $(\omega d / u) < 1$  when free path of charge carriers exceeds the width of the wire  $\ell > 2d$ . With large dimensionless electric field frequency  $\Omega = \omega d / u$  and with arbitrary value of specular reflection coefficient current phase lag from the voltage converges to  $\pi / 2$ , under this boundary condition conductivity becomes an imaginary value.

1. Geim A.K. and Novoselov K.S. // *Nature materials*, – 2007. – Т.6, P. 183-191
2. Фальковский Л.А. // *ЖЭТФ*. – 2008. – Т. 133, №3. – 663-669.

## Interband conductivity of straight-line graphene ribbon

Ruvinskii M.A.<sup>1</sup>, Ruvinskii B.M.<sup>2</sup>

<sup>1</sup> *Vasyl Stefanyk' Precarpathian National University, Ivano-Frankivsk, Ukraine;*

<sup>2</sup> *Ivano-Frankivsk National Technical University of Oil and Gas, Ivano-Frankivsk, Ukraine*

The problem of high-frequency interband conductivity of plane straight-line graphene wire has been solved with taking into account the classical dimensional effects of charge carriers from the lateral wire borders. The calculations has been fulfilled at arbitrary relations between the wire width and free path length of charge carriers (the wire length is much greater than its width). The homogeneous alternating electric field  $\vec{E}(t) = \vec{E}_0 \cdot \exp(-i\omega t)$  is directed along the graphene ribbon length. For the interband conductivity the influence of specular-diffuse mechanism of charge carriers reflection has been investigated in detail and has been revealed for the interband current in the cubic approximation on amplitude of the alternating electric field. The induced interband current  $I(t) = (G_0 U_0 + G_2 U_0^3 + \dots) \cdot \exp(-i\omega t)$  with the following odd corrections in point of voltage amplitude  $U_0$  on the wire ends. In case of the limited graphene the interband conductivity is dominant at the high frequencies of alternating electric field  $\omega > k_B T / \hbar$  as compared with the intraband conductivity.

Fig. 1 and 2 show the frequency dependence of real and imaginary parts of the interband integral conductivity at a sufficiently low temperature  $k_B T \ll \mu$  (in  $e^2 / 4\hbar$  units) at temperature  $T = 5\text{K}$ , carrier density  $n_0 = 10^{11} \text{sm}^{-2}$ , wire length  $L = 5 \cdot 10^{-3} \text{sm}$ , wire width  $2d = 5 \cdot 10^{-4} \text{sm}$ , amplitude of the alternating electric field  $E_0 = 200 \text{V/sm}$ , specularity coefficient: 1 –  $\alpha = 0.0$ , 2 –  $\alpha = 0.5$ , 3 –  $\alpha = 1.0$ , 4 – in the absence of electric field.

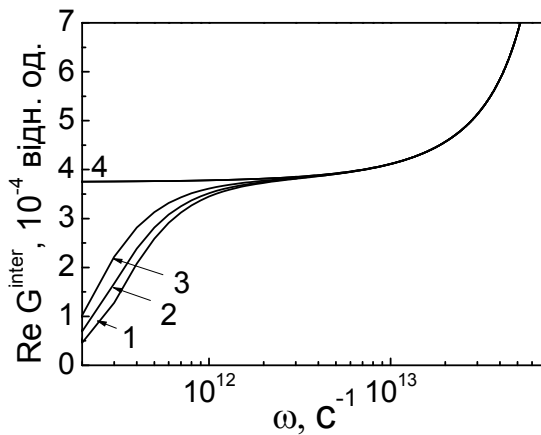


Fig 1

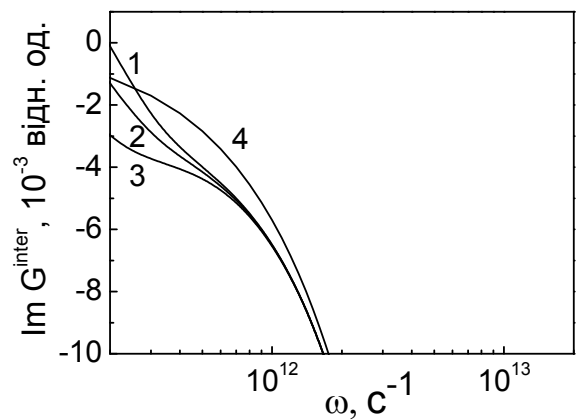


Fig 2

## Nanophase transitions in metal-polymeric composites

Ryskulov A.A.<sup>1</sup>, Struk A.V.<sup>2</sup>, Eisymont Y.I.<sup>3</sup>.

<sup>1</sup> *Tashkent Automobile and Road Institute, Tashkent, Uzbekistan,*

<sup>2</sup> *The JSC "Belkard" education-methodological centre "Promagromash", Grodno, Belarus,*

<sup>3</sup> *Yanka Kupala State University of Grodno, Grodno, Belarus*

The mechanism of multifunctional modifying effect of nanodimension particles and clusters metallic formations in metal-polymers based on the interaction of components at different hierarchical levels of structure: molecular, intermolecular, supramolecular and nanophase. The analysis of the modifying mechanisms of nanodispersed metallic components, obtained by thermolysis of organic precursors, high thermoplastic matrices is implemented. Modern methods of physico-chemical analysis established that the primary process of formation of metal-polymer nanocomposite is the adsorptive interaction of active centers of metal particles with the polymer macromolecule with the formation of spatial structure. These modifier nanoparticles can act as acceptors of free radicals, centers of spherulite structures and intermolecular physical "cross-linking" agents. During the exposure of metal-polymeric nanocomposite in operating conditions as a result of secondary processes leading adsorption bonds between the components are transformed into valence with the formation of high molecular metal-polymeric phase. It is realized nanophase transition "nanometal + polymer → highmolecular metal-containing compound", which is reversible that causes changes in the parameters of the nanocomposite structure under the influence of various operational factors and the corresponding transformation of its service characteristics. Inverse nanophase transitions are realized in metal-polymeric structures on the basis of mono- and mixtures matrixes that allow adjusting the parameters of deformation-strength and tribological characteristics in a wide range of values. In mixtures nanocomponents obtained by thermomechanical combination of matrix and alloying ingredients nanodisperse particles or metal clusters act as physical compatibilizer causes the increased compatibility of components and stabilization of their service characteristics. Thus, it is possible formation of metal-containing copolymer as a result of nanophase reversible transition. For manufacture of reinforced composites with enhanced strength and wear-resistance for friction units with extreme operation conditions has developed a technology of modifying on the interface level of structural hierarchy. Set level of interfacial interaction at the interface between the matrix and carbon fiber filler in these composites is ensured by the use of fluorine-containing finishes or mechano-chemical processes which lead to increased adsorption interaction of components. Optimized at different levels of structural hierarchy fluorine-containing nanocomposites are used for the manufacture of products of tribological and sealing purposes.

## Effect of quantum dot shape on the hole energy spectrum

Shakleina I.O., Sokolnyk O.A.

*Ivan Franko Drohobych State Pedagogical University, Drohobych, Lviv region, Ukraine*

The investigation of quantum dot (QD) structures is reported in a number of experimental works because they not only demonstrate interesting quantum-mechanical and optical phenomena but also show promise for their application in various fields of science and technology.

In the paper using the perturbation method (degenerated and non-degenerated) the effect of QD shape symmetry on hole energy level splitting.

Neglecting the corrugation of constant-energy surfaces in the k-space (spherical approximation), the Hamiltonian can be written

$$\mathbf{H} = \frac{1}{2} \left( \gamma_1 + \frac{5}{2} \gamma \right) \mathbf{p}^2 - \gamma (\vec{\mathbf{p}} \cdot \vec{\mathbf{J}})^2 + \Pi(\vec{r}). \quad (1)$$

The wave function, being a solution of the equation with Hamiltonian (1), is given as a product of eigen functions of the total momentum operator and radial functions

$$\psi_{f,M}(r, \theta, \varphi) = \sqrt{2f+1} \sum_{l=f-j}^{f+j} (-1)^{l-j+M} R_f^l(r) \sum_{m_l} \sum_{m_j} \begin{pmatrix} l & j & f \\ m_l & m_j & -M \end{pmatrix} Y_{lm}(\theta, \varphi) \chi_{m_j} \quad (2)$$

Different-shaped quantum dots under study (cubic, ellipsoidal, cylindrical and tetrahedral dots) were chosen under the condition of equal volumes and minimal value of deviation from spherical form which, in its turn determined a perturbation parameter.

First and second corrections to the ground and first excited states of a hole were found, the comparison of spectra of a simple and a complex band models was done.

The specific calculations were done in case of *GaSb/AlSb* structure. The QD radius dependence of the total correction of different states is obtained. It is shown that the QD form defines the number of split levels, the multipleness of degeneracy and the correction value. The range of quantum dot radii where perturbation theory works with respect to the geometry of considered shapes is determined.



## Size distribution function of disc-like clusters in heterosystems

Stasyk M.O., Ivanskii B.V., Moskalyuk A.V.

*Chernivtsi National University, Chernivtsi, Ukraine*

In last years, generalization of the Lifshitz-Slyozov-Wagner (LSW) theory for surface disperse systems (including, in part, island films) became of especial interest. Urgency of the problem grows now owing to development of nanotechnologies and forming semiconductor heterostructures with quantum dots.

Forming of heterostructures containing quantum dots of the specified density and homogeneity meets considerable experimental difficulties. However, the properties of such ready-to-wear structures may be modified in the process of the Ostwald's ripening (OR).

The theory of this phenomenon revealed by Ostwald [1] and referred now to its name was developed by Lifshitz and Slyozov, and Wagner [2, 3] (the LSW theory). Within the framework of this theory, the rate of growth of clusters, on the late stage of their ripening, is determined either by the volume diffusion coefficient  $D_v$  [2], or by the kinetic coefficient  $\beta$  at the interface of two phases [3]. Thus, two limiting cases (mechanisms), *viz.* diffusion and Wagner's, are considered in papers [2, 3], which are governed by the coefficients  $D_v$  and  $\beta$ , respectively.

We modify the LSW theory for study of disc-like quantum dots of radius  $r$  and constant height  $h$  (Fig. 1) growing under condition that the flow of a matter,  $j$ , consists of two parts, *viz.* diffusion,  $j_s$ , and Wagner,  $j_i$ , ones:

$$j = j_s + j_i \tag{1}$$

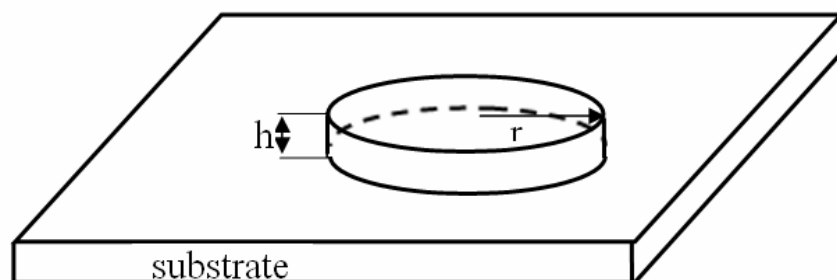


Fig.1. Disc-like  $r$ -radius cluster of constant height  $h$ .

Designating  $x = \frac{j_s}{j}$  and  $1 - x = \frac{j_i}{j}$  the shares of flow  $j_s$  and  $j_i$  in the general flow  $j$ , one obtains:

$$\frac{j_s}{j_i} = \frac{x}{1 - x} \tag{2}$$

Using Eq. (2), we find for such mechanism of cluster growth the following rate of growth:

$$\frac{dr}{dt} = \frac{A^*}{r^2} \left[ 1 + \left( \frac{1-x}{x} \right) \frac{r}{r_g} \right] \left( \frac{r}{r_k} - 1 \right), \quad (3)$$

where  $A^* = \frac{D_s C_\infty \sigma v_m^2}{hkT \ln l}$ ,  $D_s$  – surface diffusion coefficient,  $C_\infty$  – equilibrium concentration for temperature  $T$ ,  $\sigma$  – specific magnitude of surface energy,  $k$  – the Boltzmann's constant,  $l$  determines the distance from a cluster where mean concentration of adatoms,  $\langle C \rangle$ , takes place at a substrate, near some island of radius  $r$  ( $l=2,3$ ), while  $r_k$  and  $r_g$  are mean (critical) and maximal cluster sizes, respectively, and temporal dependences are:

$$r_g^3 = \frac{3}{2} A^* t, \quad (4)$$

$$r_k^3 = \frac{4}{9} A^* t. \quad (5)$$

Besides, we have computed the generalized relative size distribution function of clusters corresponding to two mechanisms of growth, i.e. Wagner and diffusion ones:

$$g'(u) = u^2 (1-u)^{-B} (u+x^2+x)^C \exp\left(\frac{D}{1-u}\right), \quad (6)$$

where:

$$B = \frac{2x^4 + 4x^3 + 10x^2 + 8x + 4}{a}, \quad (7)$$

$$C = -\frac{3x^4 + 6x^3 + 5x^2 + 2x + 1}{a}, \quad (8)$$

$$D = -\frac{2x^5 + 2x^4 - 4x^3 + 6}{a}, \quad (9)$$

$$a = x^4 + 2x^3 + 3x^2 + 2x + 1. \quad (10)$$

1. Ostwald W. Über die Vermeintliche Isometric des roten undgelben Quecksiberxyds und die Oberflachenspannung fester Korper // Zs. phys. Chem. – 1900. – V. 34. – H. 495-503.
2. Lifshits I.M., Slesov V.V. The kinetics of precipitation from supersaturated solid solution // J. Phys. Chem. Solids. – 1961.– V. 19, №1/2.– P. 35-50.
3. C. Wagner. Theorie der Alterung von Niderschlagen durch Umlösen (Ostwald Reifung) // Zs. Electrochem. – 1961. – V. 65. – N. 581-591.
4. R.D. Vengrenovich, B.V. Ivanskii and A.V. Moskalyuk. Ostwald ripening of nanoislands in semiconductor heterosystems and its influence on optical properties // Optoelectronics Review. – 2010. – V. 18, № 2. – P. 168.

## **Adjusting morphology and surface reduction of CeO<sub>2</sub>(111) thin films on Cu(111)**

Stetsovych O.<sup>1</sup>, Dvořák F.<sup>1</sup>, Steger M.<sup>2</sup>, Cherradi E.<sup>2</sup>, Matolínová I.<sup>1</sup>, Tsud N.<sup>1</sup>, Škoda M.<sup>1</sup>, Skála T.<sup>3</sup>, Mysliveček J.<sup>1</sup> and Matolín V.<sup>1</sup>

<sup>1</sup>*Charles University, Faculty of Mathematics and Physics, Praha, Czech Republic*

<sup>2</sup>*Heinrich-Heine-Universität, Institut für Experimentelle Physik der kondensierten Materie, Düsseldorf, Germany*

<sup>3</sup>*Sincrotrone Trieste SCpA, Basovizza-Trieste, Italy*

Adjustable morphology and degree of reduction represent desirable properties of model oxide substrates for heterogeneous catalysis. We investigate these properties in CeO<sub>2</sub> (ceria) thin films on Cu(111) using scanning tunneling microscopy and photoelectron spectroscopy. We identify growth mechanisms of ceria on Cu(111) — formation of incomplete oxide inter-facial layer and formation of three-dimensional ceria pyramids by stacking of monolayer-high islands. Using these mechanisms we control the coverage, the number of open monolayers, and the step density of ceria thin films on Cu(111). Annealing in vacuum allows us to control besides the morphology also the degree of ceria surface reduction. We find a correlation between surface reduction and morphological stability in annealed ceria layers. Oriented and stoichiometric thin films of ceria on Cu(111) can be prepared at temperatures as low as 150°C and 250°C. Both the morphology and the surface reduction of these films readily change with increasing temperature, which must be accounted for in considering temperature-programmed experiments with ceria on Cu (111).

## Influence of cluster configuration on the size distribution function

Vengrenovich R.D., Fuchila I.Ya., Stasyk M.O.

*Chernivtsi National University, Chernivtsi, Ukraine*

Low-dimension structures are among urgent and the most important subjects of modern physics of solid state. Importance of investigations in this field is connected both with novel physical problems and phenomena, and with the prospects of the development, on this base, of new quantum devices and systems with reach feasibilities for optoelectronics and nanoelectronics, information technologies of new generation, telecommunication means etc. Island films, in part, belong to such structures.

However, properties of an island film with specific size distribution function may change in the process of the Ostwald’s ripening (OR), that is the final (so-called ‘late’) stage of forming the new phase characterized by interaction between islands.

The first comprehensive theory of the OR with diffusion mechanism of mass transfer has been developed by Lifshitz and Slyozov. For the diffusion mechanism of mass transfer, atoms of dissolved matter reaching clusters through diffusion are entirely absorbed by clusters, so that the cluster growth is controlled by matrix diffusion and, in part, by the volume diffusion coefficient,  $D_v$ .

We have investigated the OR process in semiconductor heterostructures with quantum dots, when mass transfer is realized through surface diffusion, being controlled by the coefficient  $D_s$ . While the relative size distribution function depends on the form of clusters, we made our computations for of cone-like islands, cf. Fig. 1.

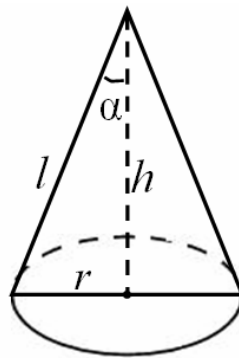


Fig. 1. Island (cluster) as an  $r$ -radius cone of height  $h$ .

The following size distribution function has been found for such mechanism of cluster growth:

$$g(u) = \frac{u^3 \exp\left(-\frac{1}{2(1-u)}\right) \exp\left(-\frac{\sqrt{2}}{12} \operatorname{arctg}\left(\frac{u+1}{\sqrt{2}}\right)\right)}{(1-u)^{19/6} (u^2 + 2u + 3)^{23/12}}, \quad (1)$$

where  $u = \frac{r}{r_g}$  is the relative size of clusters, and  $r_g$  is the maximal size of islands.

## **Carbon – supramolecular ansambles for caracitive accumulation and faraday generation of energy**

Venhryn B.Ya., Grygorchak I.I., Balaban O.V.

*Lviv Polytechnic National University, Lviv, Ukraine*

The problem on coupling of capacitive accumulation and Faraday generation of energy in one device has been solved in this work. It is reached by means of formation of active electrode as supramolecular complex C<18-Crown-6> in which the organic receptor is introduced in nano/mesopores of activated carbon. As such carbon we have used carbon, obtained by activated carbonization of fruit (apricot) stones and carbon, obtained by activated carbonization of wood.

Series of electrochemical measurement on determination of their specific characteristics and functional abilities was carried out with obtained materials. Electrochemical studies of activated carbon were carried out according to the three-electrode setup with chlorine–silver reference electrode. Impedance measurements were carried out over frequency range  $10^{-2}$ - $10^5$  Hz by means of “AUTOLAB PGSTAT-100” (ECO CHEMIE, Holland) measuring complex, attached with FRA-2 and GPES software. Cyclic voltammograms for electrochemical cells have been recorded with sweep voltage rate 0.01 V/s. “Charge-discharge” galvanostatic cycles have been formed by means of electronic galvanostatic device.

All measurements were taken at room temperature. Aqueous solution of KOH (7.6 m) was used as electrolyte.

In result it was shown that at anode polarization an organic receptor 18-Crown-6, introduced into activated carbon bonds the cations of K, decreasing in such way the active surface and hence - the specific capacitance. At positive values of potential it due to bounding with carbon matrix unblocks this matrix in respect to Faraday processes. The limiting process in symmetric system with electrodes on the base C<18-Crown-6> is the processes in negative region of potentials. The substitution of negative electrode in last system by zinc one leads to extension of positive region of polarization C<18-Crown-6> comparing with symmetric cell, resulting the occurrence of capacitive accumulation of energy at potentials from 0.4 to 1.24 V up to 154 F/g, whereas lower potentials the Faraday generation of energy with equivalent pseudocapitance  $\sim 10000$  F/g, corresponding to arc-like Nyquist plots.

**СЕКЦІЯ 2 (стендові доповіді)  
НАНОТЕХНОЛОГІЇ, НАНОМАТЕРІАЛИ І КВАНТОВО-  
РОЗМІРНІ СТРУКТУРИ**

20 травня 2011 р.

**SESSION 2 (poster)  
NANOTECHNOLOGIES AND NANOMATERIALS,  
QUANTUM-SIZE STRUCTURES**

May, 20, 2011

## Solubility of Silver in Glassy-like $\text{As}_2\text{Se}_3$ and Thermodynamic Properties of Glasses

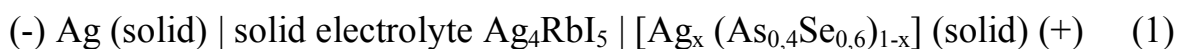
Babanly M.B., Veliyeva G.M., Mashadiyeva L.F., Shikhiyev Yu.M.

*Baku State University, Baku, Azerbaijan*

The chalcogenide glasses containing silver, possess semi-conductor, photo-electric, etc. properties, as well as high ionic ( $\text{Ag}^+$ ) conductivity and are perspective for using as solid electrolytes in solid-state sources of electric energy, displays etc. [1, 2].

In this work a possibility of application of EMF method with solid electrolyte  $\text{Ag}_4\text{RbI}_5$  for definition of area of glassformation in the Ag-As-Se system on  $\text{Ag-As}_{0,4}\text{Se}_{0,6}$  section and for studying of thermodynamic properties of glasses is considered. Earlier by this method had been studied thermodynamic properties of the pointed system in equilibrium – a crystalline state [3].

For carrying out of experiments a following concentration chains were constructed:



and their EMF were measured at 300 – 380 K temperatures range. Alloys- the right electrodes are prepared by fusing of elementary components of high degree of purity in vacuumed ( $\sim 10^{-2}$  Pa) quartz ampoules with the subsequent cooling on air.

From the results of EMF measurements of chains type (1) the concentration dependence of EMF at 300 K are constructed, according to which in the range of compositions  $0 < x < 0,4$  EMF is continuous function of composition and goes down with increasing of amount of silver in glasses. At compositions  $0,4 > x > 0,3$  EMF values remain almost constant. This fact confirms formation of homogeneous glasses in system  $\text{Ag-As}_{0,4}\text{Se}_{0,6}$  in the field of compositions  $0 < x < 0,4$ .

From the equations of temperature dependences of EMF partial thermodynamic functions of silver in alloys are calculated.

Thermodynamic functions of solubility of silver in glassy-like  $\text{As}_{0,4}\text{Se}_{0,6}$  are calculated by integration of the Gibbs-Duhem equation from which using corresponding data for glassy-like  $\text{As}_{0,4}\text{Se}_{0,6}$  standard integral thermodynamic functions of mixing of glasses are calculated. The comparative analysis of the received data with corresponding characteristics of the system Ag-As-Se in a crystalline state is carried out.

1. Popesku M.A. Non-crystalline Chalcogenides. Kluwer Acad. Publ., Niderland. – 2000. - 377p.
2. Balan V., Piarristeguy A., Ramonda M., Pradel A., Ribes M. // J. Optoelectron. Adv. Mater. – 2006. – V.8. – P. 2112-2116.
3. Babanly M.B., Mashadiyeva L.F., Veliyeva G.M., Imamaliyeva S.Z., Shikhiyev Yu.M. // Rus. J. Electrochem. – 2009 –V.45, No. 4. – P.399-404.

## Selective phase formation by the electrostatic template

Barabash M.Yu.<sup>1</sup>, Vlaykov G.G.<sup>2</sup>, Grynko D.A.<sup>1</sup>, Kunitsky Yu.A.<sup>1</sup>

<sup>1</sup>*Technical Center of NAS of Ukraine, Kiyv, Ukraine*

<sup>2</sup>*Institute of semiconductors physics of NAS of Ukraine, Kiyv, Ukraine*

Template is one of tools which allow to solve the problem of matter structuring in nano-scale via guided self-organization. Template is functional, space organized mikroinstrument for guiding physical and chemical self-organization processes of nanoobjects in space and in time through nearfield interaction on one surface.

Strong, spatially organized electrostatic field of template can influence the ballistic and diffusion transport of molecules and nanoparticles, absorption, nucleation, phase formation, surface chemical reactions, polarization, transport of charged carriers, energy of discrete levels, band energy diagram and processes symmetry, finally. Demonstrated facts of formation of heterogeneous surface sediment, which topology determined by template topology in conditions of condensation of polar or polarisable compounds (gold or organic dye molecules for example) on surface of electrostatic template [1].

Electrophotographic technique gives powerful tool for template programming by the use of optical field or charged particles beam. There are a few ways to prepare specified ordered topology of the electric field on the template surface. Surface modulated charge density on the surface of photoconductor film, volume bound modulated charge linked in the bulk of photoconductor film (electret template), the structure with the spatially modulated dielectric susceptibility are some of means. Photoelectret template formed by the capture of photogenerated charge carriers on deep traps of photoconductor film also. Heterogeneous localized volume charge can be generated when space modulated photocurrent flow through the film and charge carriers captured in deep traps. Since the photocurrent density determined by the intensity of optical field, it will caused the formation of spatially modulated localized charge programmed by light field. Experimental observation of spontaneous domain structure in photoelectrete templates can caused by strong local electric field in the dielectric thin film with localized regular distributed volume charge.

1. Vlaykov G.G. , Barabash M.Yu. , Zabolotny M.A. et.al. Template guided nanostructure synthesis // K. IMF NASU – 2010. – 230 p.



## Polarization phonons in wurtzite quantum well wire GaN/ZnO/GaN/ZnO/GaN

Boichuk V.I., Voronyak L.Ya., Voronyak Ya.M.

*Department of Theoretical Physics, Ivan Franko Drohobych State Pedagogical University  
Drohobych, Ukraine*

Wide possibilities of application of various nanoheterosystems in different fields of science and technology stimulate physicists to study their properties. In recent years wide-gap wurtzite semiconductor quantum heterostructures which consist of III-group nitrides attract much attention. In the paper in the dielectric continuum model the polarization potential is determined and the polarization phonon energy spectrum in the *GaN/ZnO/GaN* periodic quantum wire of wurtzite crystals placed in the *AlN* dielectric matrix is investigated. It is shown that in the *GaN/ZnO/GaN/ZnO/GaN* five-element quantum wire there arise

- four branches of confined phonons (quasitransverse та quasilongitudinal confined phonons in QW in *GaN* and *ZnO* cylindrical quantum dots);
- two branches of semiconfined phonons (quasitransverse and quasilongitudinal semiconfined phonons in *GaN* quantum semiwires);
- four branches of surface phonons (quasitransverse та quasilongitudinal side surface phonons at the boundary of the media *GaN/AlN*, *ZnO/AlN*);
- two branches of top surface phonons (quasitransverse and quasilongitudinal);
- two branches of exactly confined phonons (exactly confined phonons in *GaN* and *ZnO* cylindrical quantum dots).

The frequency ranges of all phonon branches are defined by the signs of permittivity tensor component of heterostructure materials. The dependence of phonon spectrum on structure size are investigated.

In the limit of large radii of quantum wires the obtained results show good agreement with the analogous results of two-dimensional structures.

## Secondary emission from synthetic opal infiltrated by colloidal gold and glycine

Boyko V.V.<sup>1</sup>, Dovbeshko G.I.<sup>1</sup>, Fesenko O.M.<sup>1</sup>, Gorelik V.S.<sup>2</sup>,  
Moiseyenko V.N.<sup>3</sup>, Sobolev V.B.<sup>4</sup>

<sup>1</sup> *Institute of Physics of National Academy of Sciences of Ukraine, Kyiv, Ukraine*

<sup>2</sup> *P.N. Lebedev Physics Institute Russian Academy of Sciences, Moscow, Russia*

<sup>3</sup> *Dnipropetrovsk National University, Dnipropetrovsk, Ukraine*

<sup>4</sup> *Technical Centre of NASU, Kyiv, Ukraine*

Photonic crystals (PC) is of great interest in device applications for optics, optoelectronics, sensors due to their potential in control of light emission and propagation. Forbidden and stop zones for light propagation are one of the characteristic features of PC that drastically affect the optical properties of PC as well as molecules inserted in the PC cavities. Our report is directed to study the secondary emission from synthetic opals fabricated from 230 nm silica globules infiltrated by colloidal gold and aqueous solution of glycine with excitations at 236, 253, 370 and 410 nm. The experiment was done by Perkin Elmer LS-55 fluorescence spectrometer with filters 290 nm, 390 nm and 430 nm.

Localization of stop zone of the initial PCs produced in Zelenograd (Russia) was found (from reflectance measurements at the angle of incidence 10°) in the region of 470-530 nm [1] with maximum at 505 nm. For infiltration we have used colloidal water solution (40 mg/l) of 10-20 nm gold nanoparticles and 1mg/ml water solution of  $\alpha$ -Gly powder (Sigma). Secondary emission from initial PC, PC after infiltration with colloidal gold,  $\alpha$ -Gly and colloidal gold with  $\alpha$ -Gly has been registered. The most drastic differences were observed in spectra for samples before and after infiltration with colloidal gold. The opal emission band in the region of 420-430 nm was suppressed by colloidal gold while a shoulder of the emission band near 500 nm was drastically increased. This intensity rise was found more prominent in the opal with colloidal gold and Gly. The last fact is connected with decrease of diffuse scattering with introduction of Gly molecules together with colloidal gold.

Thus, a swap of intensity of secondary emission from center of the luminescence band to the band side which corresponds to position of stop zone, have been registered. Confocal optical and electronic microscopy was applied for study of PC structure.

Acknowledgment: we thank Ukrainian-Russian project 4/10-24 “The glow of three-dimensional photonic crystals for optical and electrical excitation” for financial support.

1. Boyko V., Dovbeshko G., Fesenko O., Gorelik V., Moiseyenko V., Romanyuk V., Shvets T., Vodolazky P. New optical properties of synthetic opals infiltrated by DNA // *Mol.Cryst.Liq.Cryst.* – 2011. – Vol. 535, №1. – P. 30-41.

## Statistics of charge carriers in thin crystalline films

Budzhak Ya.S., Zub O.V.

*Lviv Polytechnic National University, Lviv, Ukraine*

It is known from the quantum mechanics that spatial quantization of energy spectrum of current carriers is observed in thin conductor crystalline films. That is why in the thin crystal structures there are the correlation dependence concentration of the current carriers  $n(d, \mu^*, T)$  on their thickness. In this work, using the results [1], where was shown that concentration of the current carriers  $n(d, \mu^*, T)$  of thin film crystal describes next general formula:

$$n(d, \mu^*, T) = \frac{x_0}{2d^3} \sum_{n=1}^{n_{\max}} \ln \left( \exp \left( \mu^* - \frac{\pi}{(1+p_0)^2 x_0} n^2 \right) + 1 \right), \quad (1)$$

Where entry are entered for the convenience of such designation:

$$x_0 = \frac{8\pi m d^2 k T}{h^2}, p_0 = \frac{h}{2\pi d} \sqrt{\frac{2}{mU}}, n_{\max} \approx \frac{1}{\pi p_0} + 1, \mu^* = \frac{\mu}{kT} - \text{a reduced chemical}$$

potential,  $k$  - Boltzmann's constant,  $m$  - the effective mass of charge carriers,  $h$  - Planck's constant,  $U$  - the depth of potential well.

To determine the absence of spatial quantization in thin crystalline films result the formula (1) as follows such form:

$$n(d, \mu^*, T) = n(\mu^*, T) \cdot \left[ 1 - \frac{1}{4d} \sqrt{\frac{h^2}{2mkT}} \cdot \frac{\ln(e^{\mu^*} + 1)}{F_{\frac{1}{2}}(\mu^*)} \right] \quad (2)$$

In these formulas  $n(d, \mu^*, T)$  - concentration of the current carriers with a parabolic dispersion law and chemical potential  $\mu^*$  in a massive crystal,  $F_{\frac{1}{2}}(\mu^*)$  - a famous integral of Fermi.

This analysis shows that spatial quantization of energy spectrum of charge carriers isn't observed if in the crystal thickness satisfies a condition:

$$d \gg \frac{1}{4} \sqrt{\frac{h^2}{2mkT}} \cdot \frac{\ln(e^{\mu^*} + 1)}{F_{\frac{1}{2}}(\mu^*)} \quad (3)$$

Therefore, that condition (3) for undegenerated or slightly degenerated electrons is described by (4) and (5) formulas:

$$d \gg \frac{1}{2} \sqrt{\frac{h^2}{2\pi mkT}} = \frac{1}{2} \cdot \lambda_D(T) \quad (4), \quad d \gg \frac{0.338}{\sqrt[3]{n}} = d_{cmam} \quad (5)$$

In these formulas  $\lambda_D(T)$  - the length of heat waves Debroylya,  $d_{cmam}$  - the average statistical distance between the charges carriers.

1. Budzhak Ya.S., Zub O.V. The thin crystalline films as a quantum size structure // Eastern-European journal of Enterprise Technologies. – 2010.– V. 2/5, №44. – P. 7-9.

## **Peculiarities of electroluminescence of CdTe nanocrystals incorporated into polymer films**

Budzulyak S.I., Ermakov V.M., Kalytchuk S.M., Korbutyak D.V.

*V.E. Lashkaryov Institute of Semiconductor Physics, National Academy of Sciences of Ukraine, Kyiv*

Hybrid polymer-quantum-dot light-emitting diodes (PQD-LED) fabricated from organic polymers and  $A_2B_6$  semiconductor nanocrystals combine main properties required for flat panel manufacturing including low weight, low power consumption, low turn-on voltage and acceptable compact size. Technology based on highly luminescent semiconductor nanocrystals can provide a significant improvement of color reproduction, increase of brightness and resolution compared to the existing thin-film flat displays technologies. However, processes that occur when a current passes through the polymer structure with quantum dots have not been studied sufficiently.

This work focused on the investigation of electroluminescence (EL) of CdTe nanocrystals incorporated into polydiallyldimethylammonium (PDDA) polymer film. The electroluminescence of the LED structure is detectable at approximately 4 V and its intensity increases with applied voltage with maximum at 9 V. Further voltage increase leads to decrease in intensity. EL emission spectrum at higher voltage shifts to longer wavelengths. It was established that shape of the current-voltage (I-V) curves is directly related to light emitting processes or their absence.

The EL spectra of investigated LED structures were compared with photoluminescence (PL) spectra for the same structures and PL spectra of CdTe nanocrystals in aqueous solutions. The marked redshift of EL from PL was observed. This redshift is a common phenomenon observed in CdTe nanoparticle LED structure [1] but there is still no reasonable explanation of its origin. In this paper, we consider a number of the redshift reasons and suggest a possible model for its explaining.

1. Schlamp M.C., Peng X., Alivisatos A.P. // J. Appl. Phys. – 1997 – V.82 – P. 5837.

## **Modeling of Spark Plasma Sintering Processes at Fabrication of Bulk Nanostructured Samples**

Bulat L.P., Nefedova I.A.

*St. Petersburg State University of Refrigeration and Food Engineering,  
St. Petersburg, Russia*

The spark plasma sintering (SPS) method is widely used in the technology of nanostructured materials for the creation of structures with a beforehand set properties. The method consists in the passing of impulses of the DC electric current through a powder from nanoparticles; thus the Joule heating on borders of nanoparticles and the corresponding sintering of the powder in a consolidated sample are realized. At the SPS process the borders between nanoparticles are warmed up very quickly to temperature up of the fusion of a given material.

In the present paper a method of simulation of the SPS processes by the finite-element scheme is offered by use of universal program system COMSOL Multiphysics. A thermoelectric based on bismuth telluride solid solution was applied as an initial material; the SPS method for fabrication of such nanostructured structure have started. The modeling of the temperature and the electric fields arising in the course of sintering at various modes of process is prepared. It is determined, that huge gradients of temperature are concentrated on the interfaces of nanoparticles; and the characteristic length of the temperature change becomes commensurable with the cooling length of the current carriers and phonons at a semiconductor. It leads to an occurrence of difficult superposition of the nonlinear and the nonlocal kinetic phenomena in the area of interfaces. The estimation of influence of these transport phenomena on technological features of the SPS process is prepared.

## Genesis of porous carbon surface due to thermal activation

Bydzulyak I.M., Rachiy B.I., Merena R.I., Mandzyuk V.I., Kuzyshyn M.M.

*Vasyl Stefanyk Precarpathian National University, Ivano-Frankivsk, Ukraine*

Porous carbon materials (PCM) got from phylogenous raw material own a high specific surface, considerable conductivity, fractal structure of pores, chemical stability to most electrolytes, that parallel to a cheapness and ecologically safe technology of receipt and utilization does them practically irreplaceable at the use as electrodes of supercapacitors. We explored the activated carbon got in a few stages, which consisted at carbonisation initial raw material in a reactor in the atmosphere of water steam at high pressure (~10 atm), chemical cleaning from mineral admixtures and ash in the concentrated hydrochloric acid, washing in the distilled water to neutral pH, washing in 30 % hydrochloric acid, and washing in the distilled water to neutral pH. However, the indicated operations do not provide the optimum pore size distribution. Therefore, the thermal activation of the material was realised for creation of additional porosity in the temperature interval of 573-873°C to open the internal porosity and formation of new pores. As a result, the change and development of carbon porous structure are observed: the size of pores is increased, there is a coalescence of two or a few pores in larger one, a part of micropores transforms in mesopores due to their growth, surface and volume of pores change, new pores appear. The increase of pore volume and surface area of material takes place as a result of burning of organic material and deleting of pitch. It is set, that the maximal specific capacity of electrochemical condensers is achieved at the use of the carbonized material prepared at 1100-1200°C with following thermal modification at a temperature of 640-680°C. Specific surface, total pore volume and pore size distribution of porous carbon materials were definite from the analysis of adsorption isotherms (table 1). The content of nanopores with 1,5-2,5 nm radius grows at the increase of thermal modification time. The experimental results testify that high temperature treatment can serve as an effective instrument of modification of carbon porosity.

Table 1

Structural-adsorption characteristics of carbon

Standard	Thermal treatment time, min	Specific surface, m <sup>2</sup> /g	Micropore surface, cm <sup>2</sup> /g	Total pore volume, cm <sup>3</sup> /g	Micropore volume, cm <sup>3</sup> /g
PCM	0	318	265	0,168	0,103
PCM1	90	681	616	0,332	0,247
PCM2	120	696	619	0,351	0,252
PCM3	150	725	655	0,362	0,266
PCM4	180	799	722	0,418	0,297

## Reception and determination of the refraction factor of nanodispersion particles of ammonium vanadite.

Chernenko I.M., Zaets A.P., Oleynik O.Y., Miroshnik S.A.

*Ukrainian state chemical-technological university, Dnepropetrovsk, Ukraine*

This work concerns the problem of obtaining properties of vanadium oxides with the phase transition semiconductor-metal. Oxides of this class are valuable materials for practical applications in electronics, optoelectronics and automatic control system. Currently, it is promising to obtain and use of nanoparticles of chemical products. The paper describes the results of the synthesis of precursors for the production of vanadium oxides, which serves as a nanodispersed vanadite ammonium  $\text{NH}_4\text{H}_3\text{V}_2\text{O}_6$ .

As a method for synthesizing ammonium vanadite used sol-gel technology. Getting  $\text{NH}_4\text{H}_3\text{V}_2\text{O}_6$  carried out in two stages. At the first stage created an aqueous solution of vanadium pentoxide  $\text{V}_2\text{O}_5$  in ethanoic acid  $\text{HOOC}-\text{COOH}$ . In this solution, the reaction occurs formation ethanoic-vanadium acid  $\text{H}_m[(\text{VO})_n(\text{C}_2\text{O}_4)_p]$ , in which the value of the stoichiometric coefficients  $m$ ,  $n$ ,  $p$  defined by the number of initial reagents. In the second stage was carried out the reaction of the obtained in the first stage acid with ammonium hydroxide. As a result of chemical reactions formed solution was identified as colloidal by ultramicroscopic method.

Isolated nanoparticle of colloid was identified by X-ray and chemical analysis as the product composition  $\text{NH}_4\text{H}_3\text{V}_2\text{O}_6$ . Physico-chemical properties of this substance little investigated. From the standpoint of knowledge about the properties of nano-dispersed environments is important to know the refractive index of ammonium vanadite, because this parameter determines the optical properties of matter and allows you to find optically nanoparticle size and concentration.

Refractive index was determined by the turbidity spectrum. For this purpose, the photoelectric colorimeter «КФК-2МП» and a spectrophotometer SPEKOL-11, allowing to determine the turbidity of the solution in the wavelength range 315-980 nm. Figure 1 shows a typical plot of turbidity  $\tau$  of the solution of the wavelength of light. According to Figure 1 for the environment observed functional dependence  $\tau \sim f(\lambda^{-4})$ , certificates of origin in her light scattering by the Rayleigh law.

From these relations, obtained at different concentrations ethanoic-vanadium acid and ammonium hydroxide was determined helper functions of relation turbidity on the ratio of the particle size to the wavelength of light and measure their refractive index. Using these functions built helper chart in a rectangular coordinate system. With the help of such diagrams measured refractive index of the nanoparticles vanadite ammonium and their concentration.

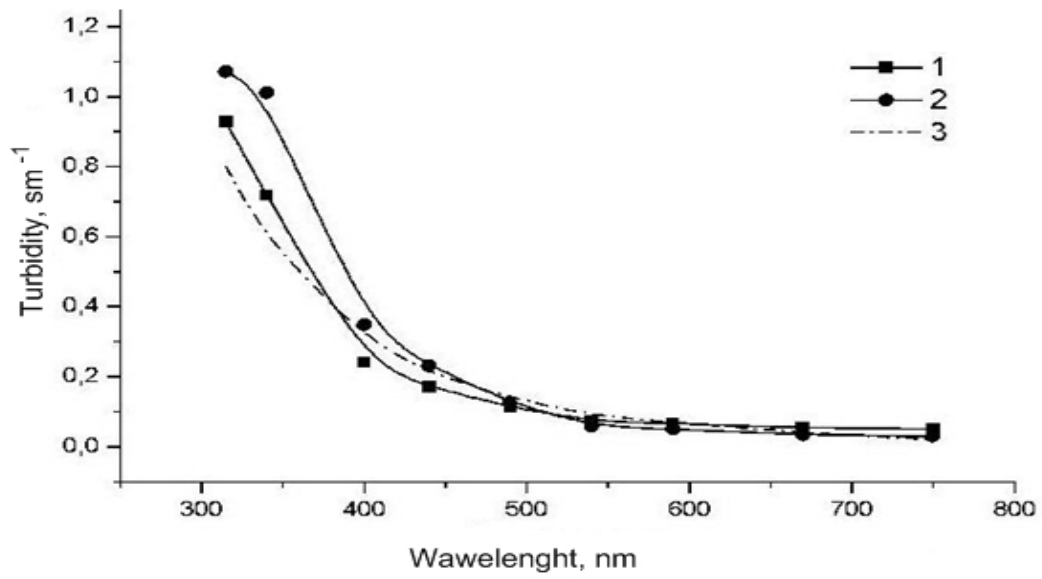


Fig. 1. The relation of turbidity on the wavelength of incident light for solutions containing ammonium hydroxide in the volume, ml: 1-1; 2-8; 3-calculated relation.



## Dynamic magnetic response of normal metal and superconductor ( $YBa_2Cu_3O_{7-x}$ ) thin films

Direglazov A.Yu., Kaminskiy G.G., Kasatkin A.L., Moskalyuk V.A.

*Institute of Metal Physics, NASU, KievUkraine*

Experimental studies of dynamic magnetic response in normal metal ( $Cu$ ) and high temperature superconductor  $YBa_2Cu_3O_{7-x}$  (YBCO) thin films were performed by use of  $ac$  susceptibility measurements within the frequency range  $f = 100\text{Hz} - 100\text{kHz}$  and temperature interval  $78 - 100\text{K}$  at two different amplitudes of applied  $ac$  magnetic field  $H_{ac}$ . These measurements revealed a rather strong frequency dependence of the complex  $ac$  magnetic susceptibility (both in normal metal and YBCO thin films), which is related to the  $ac$  conductivity of these films. To evaluate  $ac$  magnetic susceptibility and describe corresponding experimental data obtained in superconducting films, scenario of thermally assisted vortex dynamics or the critical state model are usually used. This approach seems to be favourable at large enough amplitudes of  $ac$  magnetic field. In this case all essential features of dynamic magnetic response (e.g., peak in  $\chi''(T, H_{ac})$  dependencies) emerge at low enough temperatures  $T < T_c$ , where such an approach seems to be applicable. Nevertheless, in our experiments small amplitudes of exciting  $ac$  magnetic field were used, and all essential features of dynamic response take place just in the vicinity of the critical temperature, where such an approach fails due to strong fluctuations of the order parameter. The obtained results are discussed in the framework of the nonlocal diffusion theory for electromagnetic field and induced current in a thin conducting plate, which is settled in applied perpendicular  $ac$  magnetic field and can be characterized by its nonlinear  $ac$  conductivity  $\sigma(\omega, T, H_{ac})$ .

1. Brandt E.H. // *Phys.Rev.* **B49**, 9024 (1994); **B55**, 14513 (1997).
2. Fisher D.S., Fisher M.P.A., Huse D.A. // *Phys.Rev. B* **43**, 130 (1991).
3. Nakielski G., Gorlitz D., Stodte C., Welters M., Kramer A., and Kotzler J. // *Phys.Rev.* **B55**, 6077 (1997).
4. Pan V.M., Pashitskii E.A., Ryabchenko S.M., Komashko V.A., Pan A.V., Dou S.X., Semenov A.V., Tretiachenko K.G., and Fedotov Yu.V. // *IEEE Trans. Appl. Supercond.* **13**, 3714 (2003).

## Investigation of Ga-In contacts to Si and Ge wires for sensor application

Druzhynin A.O.<sup>1,2</sup>, Khoverko Yu.M.<sup>1,2</sup>, Ostrovskii I.P.<sup>1</sup>, Nichkalo S.I.<sup>1</sup>, Nikolaeva A.A.<sup>3</sup>, Konopko L.A.<sup>3</sup>, Stich I.<sup>3</sup>

<sup>1</sup>Lviv Polytechnic National University, Lviv, Ukraine

<sup>2</sup>International Laboratory of Low Temperatures and High Magnetic Fields, Wroclaw, Poland

<sup>3</sup>Institute of Electronic Engineering and Industrial Technologies Academy of Science of Moldova, Kishinev, Moldova

Electrical properties of Si, Ge nanowires are hard to measure due to a problem of ohmic contact fabrication. The convenient method for contact creation is well-known welding of Pt or Au microwire. But this method is not appropriated for nanowires due to their strain because of large contacts.

The paper deals with making of Ga-In contacts to Si and Ge nanowires and studying their performances at temperature range 4,2-300 K. The wires were grown as by chemical vapour deposition method and by melting in glass.

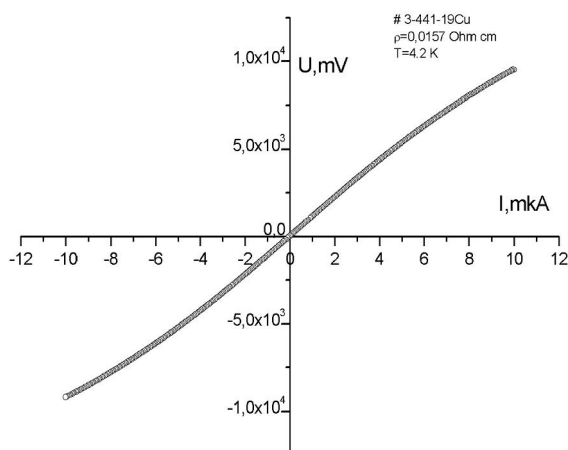


Fig.1. I-V characteristics of Si wires at 4,2 K.

free standing Si wires have diameters ranging from 5 to 50  $\mu\text{m}$ , while Ge nanowires in glass envelope have diameters about 100-200 nm. The I-V characteristics were ohmic in temperature range 77-300 K, while at low temperature a saturation was observed (see Fig.1), which is possibly explained by heating of electron gas.

The investigation of temperature dependencies of resistance for Si wires of various diameters has shown essential decrease of resistivity as the wire diameter decrease from 50 to 5  $\mu\text{m}$ . The obtained results allow to reach a metal-insulator transition (MIT) due to a change of the wire diameter. The studies of the wires in magnetic field up to 14 T have shown a substantial change of magnetoresistance at the dielectric side of MIT – magnetoresistance changes from +200% to -2 % depending on impurity concentration. For device in particular sensor application it is necessary to obtain the wires with minimal influence of magnetic field. Therefore the wires from metallic side of MIT are of great importance. So a choice of wire diameter allows us to obtain the wires with optimal performances for sensor design.

The investigation of temperature dependencies of resistance for Si wires of various diameters has shown essential decrease of resistivity as the wire diameter decrease from 50 to 5  $\mu\text{m}$ .

The work was partially supported by Ukrainian-Moldova Project M/111-2010.

## Effect of synthesis conditions on properties of nanocrystalline powders $ZrO_2$

Dudnik E.V.<sup>1</sup>, Lashneva V.V.<sup>1</sup>, Shevchenko A.V.<sup>1</sup>,  
Ruban A.K.<sup>1</sup>, Matveeva L.A.<sup>2</sup>

<sup>1</sup>Frantsevich Institute for Problems of Materials Science of NASU, Kiev, Ukraine;

<sup>2</sup>Institute of Semiconductors Physics NAS of Ukraine, Kiev, Ukraine

Hydrothermal methods are promising in producing of starting powders for designing of high-performance ceramics based on  $ZrO_2$ . The main advantages of the hydrothermal synthesis are in the homogeneity of the formation processes and growth of nucleuses through the mechanism of «dissolution - crystallization». These processes are realized at rather low temperatures and pressures. Thereof the homogeneous primary particles containing a small amount of structural defects are formed. Hydrothermal powders are freedom from "hard" agglomerates.

The purpose of this research is to investigate the properties variation of the nanocrystalline powder in the  $ZrO_2$ - $Y_2O_3$ - $CeO_2$ - $Al_2O_3$  system depending on the process of their producing.

Depending on the starting materials and the reacting medium pH hydrothermal synthesis of nanocrystalline powders based on  $ZrO_2$  included two types of chemical reactions. High-temperature hydrolysis under acid medium ( $pH < 2$ ) followed by mechano-chemical treatment of obtained M- $ZrO_2$  powders fall to the first type of reactions. The specific surface area of the nanocrystalline composite powders varied from 40  $m^2/g$  up to 85  $m^2/g$ . The blend of low-temperature cubic solid solution based on  $ZrO_2$  (F- $ZrO_2$ ) and monoclinic solid solution based on  $ZrO_2$  (M- $ZrO_2$ ) was formed in the produced powders. The powders are formed the high-concentrated stable suspensions under slip casting of aqueous slips. It will allow to receive the "regular" microstructures of moulds.

The second type of reactions is the hydrothermal decomposition of the hydroxides blend in an alkaline medium ( $pH > 9$ ). The specific surface area of the nanocrystalline composite powders varied from 120  $m^2/g$  up to 140. Low-temperature F- $ZrO_2$  is formed in the powders.

Powders were characterized of the developed interior porosity of agglomerates. These powders were used for producing of green bodies with uniaxial cold pressing followed by isostatic pressing. The castings and green bodies from hydrothermal powders were sintered in the narrow temperature range from 1250 to 1300 °C.

Various composites based on  $ZrO_2$  with bending strength between 600 and 1200 MPa as well as toughness ( $K_{Ic}$ ) between 5 and 18  $MPa \cdot m^{0,5}$  were produced.

## Insertion compounds of iodine and nano-graphite based on layered III-VI crystals

Duplavyy V.Y., Shevchyk V.V., Pyrlja M.M., Boledzyuk V.B.

*Chernivtsi Department of the I.M. Frantsevich Institute of Materials Science Problems of the National Academy of Sciences of Ukraine, Chernivtsi, Ukraine*

InSe and GaSe single crystals are characterized with a layered crystalline structure. The existence of Van der Waals gaps makes possible the formation of insertion compounds on the basis of layered crystals because of intercalation of foreign ions, molecules or atoms into interlayer spaces. There are a number of methods of intercalation into layered III-VI crystals. One of them is a direct exposure of an initial sample in a solution or vapour medium of an intercalant.

Iodine was intercalated into GaSe crystals in a closed glass ampoule placed into a furnace at a temperature of 40 °C. The exposure duration was from 1 to 7 weeks. The impedance across the layers was established to be increased insignificantly after the one week intercalation and then during the intercalation for 2 - 4 weeks the impedance continuously decreases to the value for the initial sample. The subsequent intercalation (for 5 weeks) causes a step-wise increase of the impedance by an order of magnitude in comparison to the initial sample. In addition, it was found the appearance of an electretic state in GaSe crystals intercalated for five weeks with a voltage  $U_e \approx 0.4$  V along the  $c$  axis.

Electrical properties of the insertion compounds of nano-graphite on the basis of layered InSe crystals were investigated, too. The intercalation was carried out by means of the exposure of InSe samples in an alcohol solution of nano-graphite during 2 - 4 months at 50 °C. The conductivity along the layers and free electron density were established to decrease with increasing the amount of inserted nano-dimensional graphite (longer exposure time) whereas the carrier mobility remains practically the same. The  $\sigma_{\perp c}(10^3/T)$  dependence shows that the conductivity decreases at increasing temperature from 80 to 200 K. The conductivity anisotropy  $\sigma_{\perp c}/\sigma_{\parallel c}$  was measured at 80 K for the initial InSe samples and those exposed in an alcohol solution of nano-dimensional graphite during 4 months. It was found that due to the intercalation this parameter decreased by two orders of magnitude because of the decrease of the conductivity along the layers.

## **Exciton spectrum renormalization due to the interaction with all types of phonons in open spherical QD**

Fartushynsky R.B., Voitsekhivska O.M., Shymanska Z.O.

*Chernivtsi National University, Chernivtsi, Ukraine*

General theory of electron-phonon interaction in closed complicated quantum dots is already established [1,2]. The frequencies of confined and interface vibrations are obtained and their quantization is performed. The theory of electron spectrum renormalization is developed in details only for the simplest closed quantum dots.

The theory of electron-phonon interaction in open quantum dots is absent at all because using the known quantum fields approaches it is impossible to make transition to the representation of second quantization at the electron wave functions for open system. This difficulty can be avoid observing the complicated nanosystem (well-barrier-well) placed into the external medium. The external well is to be so wide that the properties of closed system tendence to the respective open one. The exactness of approximation is controlled by relationship between the semiwidths of respective quasistationary bands in closed and open nanosystems.

Analytical and computer calculations are performed for the closed nanosystem HgS/CdS/HgS/CdS transiting into open nanosystem HgS/CdS/HgS when the thickness of the second well limits to infinity. The phonon spectrum is obtained within dielectric continuum model. Electron spectrum in closed spherical quantum dot is obtained within the effective mass approximation and rectangular potential wells model. In the framework of Green functions method it is performed the calculation of renormalized energies of electron and hole energy levels located near the resonance quasistationary states. There are calculated the partial contributions of all types of phonons into the shift of resonance level.

It was found that at the increasing of the external potential well width the magnitudes of the partial shifts of electron and hole energy levels due to the interaction with all types of phonons are decreasing, tending to the respective magnitudes for the open spherical quantum dot HgS/CdS/HgS in limit case.

This result gives the opportunity to study the electron- and hole-phonon interaction in open quantum dots, using for the theoretical calculations the wave functions and energy spectra of quasiparticles obtained for the respective closed systems for the limit case of infinitely deep external potential well.

1. Tkach M., Holovatsky V., Voitsekhivska O., Mykhalyova M., Fartushynsky R. Electron-phonon interaction in semiconductor spherical quantum dot embedded into semiconductor medium (HgS/CdS) // *Phys. Stat. Sol.* – 2001. – V. **225**, №2. – P. 331-342.
2. Holovatsky V., Mikhalyova M., Tkach M., Fartushinsky R. Ground electron state renormalization due to LO phonons in spherical nanoheterosystem HgS/CdS with arbitrary core size // *Third International School-Conference. Physical problem in material science of semiconductors. Chernivtsi, 7-11 September, 1999*, – P.198.

## **Synthesis of Silver nanoparticles block- and graft copolymers and inorganic polymer substances in water solutions**

Fedorchuk S.V., Zheltonozhskaya T.B., Kunitskaya L.R., Demchenko O.V.

*Kiev National Taras Shevchenko University, Kiev, Ukraine*

One of the actual aspects of the nanotechnology development is elaboration of the controlled synthesis methods of metal nanoparticles, which are active components of nanoscale electronics, photonics and sensorics. These nanoparticles are perspective for use in bioanalytical electrochemistry, biodiagnostics, biomedicine and others. However, high chemical activity of zero-valent silver can cause the unreversible aggregation of the nanoparticles that create the problem of their storage stability. To solve this problem, the development of nanoparticle synthesis methods in polymer matrices, which will provide the control of nanoparticle sizes and forms and their stabilization, is necessary. At the last time, amphiphilic block copolymers, which form micellar structures, are used to obtain the Ag-containing nanosystems. However in some cases (for example, at the use of silver nanoparticles in medicine and catalysis of chemical reactions) nanoparticles should be in the hydrophilic environment.

The aim of our work was to research the  $\text{Ag}^+$  reduction reactions from silver nitrate in polymer matrices of different chemical nature by using of borohydride. Hydrophilic block- and graft copolymers such as MEPEO-*b*-PAAm, PAAm-*b*-PEO-*b*-PAAm, PVA-*g*-PAAm which contained poly(ethylene oxide) and its monomethyl ether, polyvinyl alcohol and polyacrylamide, and also the grafted polymer inorganic substances  $\text{SiO}_2$ -*g*-PAAm were used as polymer matrices. The first types of the matrices forme the intramolecular polycomplexes, but the second one are able to form the polymer-colloid complexes. Both types of the matrices were used in order to obtain stable silver nanoparticles. It was shown that the block- and graft copolymers and the polymer inorganic substances are effective nanoreactors, which ensure, the chemical reduction of silver ions up to the nanoparticles with high rate and efficiency. It was observed that prolouged stabilization of silver nanoparticles in the water solutions can be achieved by varying of the chemical nature, molecular architecture, the negative charge density and a concentration of nanoreactor.

## About boride layer structure on the aluminium surface

Fedorenkova L.

*Dnepropetrovsk National University, Dnepropetrovsk, Ukraine*

Chemical, physical and mechanical properties of aluminium boride are like known material as boron carbide, silicon carbide, aluminium oxide. It form an unique material class combined physicochemical properties of heat-resisting crystals with typical amorphous semiconductor properties. Diffusion layer is formed on the aluminium surface as a result of treatment in electrolytic plasma. The layer has new qualitative characteristics in particular increased wear, corrosion and specific resistances.

The mechanism of boride layer with microcrystalline structure that formed on aluminium surface under specific condition of electrolytic plasma was investigated in this work.

It's shown the diffusion layer consists of aluminium borides with various modifications. There are high-boron compounds ( $\alpha$ -AlB<sub>12</sub>,  $\alpha$ -AlB<sub>10</sub>,  $\beta$  - AlB<sub>12</sub>, C<sub>4</sub>AlB<sub>24</sub>,  $\gamma$ -AlB<sub>12</sub>) and low-boron compounds (Al<sub>8</sub>B<sub>4</sub>C<sub>4</sub>, Al(BH<sub>4</sub>)<sub>3</sub>).

Boron atoms diffusion in metal under condition of treatment in electrolytic plasma has some peculiarities. Saturation operation can realize in several mass transfer mechanisms. This saturation process is characterized by surface local heating. The local temperature may be 10<sup>3</sup> - 10<sup>4</sup> K. Under the action such temperatures an ion implantation is realized and as a result a boron, hydrogen and aluminum atom mixtures are formed in metal without limitations determined by solubility and chemical activity.

Simultaneously with implantation the reaction diffusion of interstitial element in metal substantially along grain boundaries, dislocations as well as bulk of boundaries but a lesser degree takes place. Maximum boron penetration range in metal is 150  $\mu$ .

According to kinetic model of diffusion process in nonequilibrium conditions of the electrolytic plasma the diffusion layer has a "quasi"-structure of aluminium borides with various modifications on depth to 80  $\mu$  and nanocrystalline layer of aluminium borides formed on depth to 150 - 200  $\mu$ . This surface structure is unique as far as naturally fit in aluminum structure with integrity preserving.

So, structural changes occurred in the metal under electrolytic plasma action result to forming of aluminium borides structural analogs ("quasi"-structure) that determined a qualitative new properties of treated metal provided equipment reliability in extreme high temperature, aggressive environments, strong radiation fields and opened new perspectives for aluminium products use.

## Synthesis of Polycrystalline Yttrium Iron Garnet the Sol-Gel Method with the Subsequent Annealing

Fedoriv V.D., Yaremiy I.P., Stashko N.V.

*Vasyl Stefanyk PreCarpathian National University,  
Ivano-Frankivsk, Ukraine*

Yttrium Iron Garnet ( $Y_3Fe_5O_{12}$ ) is the most representative and well-known compound among the rare-earth garnets. In recent years, scientists' interest was focused on the research of the properties of garnet structures depending on the size of particles. Recently, polycrystalline YIG also found its application in magneto-optical recording media devices [1]. In this regard, alternative methods of synthesis of garnet structures that ensure weak-agglomerated homogeneous in size nanoparticles actively began to be developed and implemented.

Studied material was synthesized by the sol-gel method of autocombustion. As initial reagents there were used:  $Y(NO_3)_3 \cdot 6H_2O$ ,  $Fe(NO_3)_3 \cdot 9H_2O$  (nitrates crystalline hydrates of Y and Fe respectively),  $C_6H_8O_7 \cdot H_2O$  (citric acid) and  $NH_4OH$  (ammonia). Initial components for the formation of dispersed yttrium iron garnet were obtained by the method of deposition of colloidal solutions. The advantage of this method is that due to significant outgassing finely dispersed weak-agglomerated powder, in which metal oxides are mixed almost on molecular level, produce.

Synthesized by us material for production of polycrystalline  $Y_3Fe_5O_{12}$  was annealed at different temperatures. As a result of X-ray structure analysis the garnet structure formation has been observed at temperatures  $\geq 800$  °C. The garnet phase content is proportional to the size and temperature and it forms on the basis of accompanying phase  $\alpha$ - $Fe_2O_3$  and  $YFeO_3$ . Intensive formation of garnet structure begins at 900 °C. The processes that accompany the sintering of nanodisperse system determine the growth of coherent scattering areas size of garnet phase, which at annealing temperature 950 °C is 3500 Å. Simultaneously, a proportional reduction of the lattice constant of formed garnet phase is observed. Annealing at a temperature of 950 °C ensures that the lattice constant equal is 12,370 Å. Obtained results indicate about the expediency the used synthesis method utilization, because it allows for implement of less energy-intensive process.

*This work has been funded by the CDRF/USAID (UKX2 – 9200 – IF – 08) and the Ministry of Education and Science of Ukraine (M/130 – 2009).*

1. Guo X.Z., Ravi B.G., Devi P.S., Hanson J.C., Margolies J., Gambino R.J., Praise J.B., Sampath S. Synthesis of yttrium iron garnet (YIG) by citrate–nitrate gel combustion and precursor plasma spray processes // J. Mag. Mater. – 2005. – V.295. – P.145–154.



## Moire patterns of microscratches in silicon single crystals

Fodchuk I.M., Fesiv I.V., Novikov S.M. and Struk Ya.M.

*Yuriy Fedkovych Chernivtsi National University, Chernivtsi, Ukraine*

This paper presents the analysis of practical opportunities of X-ray LLL-interferometry for structural diagnostics of highly perfect silicon crystals.

Results of calculation of moiré patterns of deformation fields arising from microscratches under the effect of concentrated load on the plate of analyzer of silicon LLL-interferometer are presented. The (220) and (440) reflections of  $CuK_{\alpha}$ -radiation were used.

The moiré patterns were calculated with the use of eikonal two-wave approximation where diffraction vector is a function of spatial coordinates and serves as a slowly changing index of refraction [1]. Different model representations of scratches were considered, for example, in the form of one and more rows of certainly distributed concentrated forces, as well as dislocation clusters with different number of dislocations in the clusters.

The moiré patterns of microscratches arranged in parallel and perpendicular to diffraction vector are rather complicated and diverse. Arched different-period bands are observed with period increase on moving away from the microscratches [2].

On the whole, qualitative and quantitative agreement was obtained between the experimental and calculated topographic and moiré patterns in the field of strong deformations at a considerable distance from the scratch.

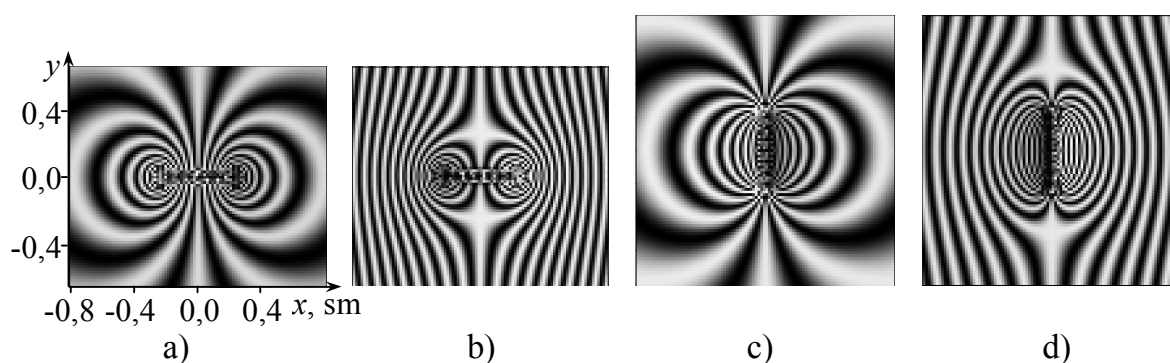


Fig. 1. The moiré patterns of 15 uniformly distributed concentrated forces without (a, c) and with phase moiré,  $\Lambda=1200 \mu\text{m}$  (b, d); forces arranged parallel (a, b) and perpendicular (c, d) to  $\vec{H}_{220}$  diffraction vector. Value of each local force is  $P_d=1$ , distance between forces is  $400 \mu\text{m}$ .

1. Fodchuk I.M., Raransky M.D. – *J. Phys. D: Applied Physics*. – 2003. – T. 36. – A55.
2. Raransky M.D., Shafranyk V.P., Fodchuk I.M. // *Metallofiz. Noveishie Tekhnol.* – 1985. – T.7, №5. – P. 63.

## Quantum-size effects in semiconductor structures

Freik D.M., Kharun L.T., Dobrovol'ska A.M., Kachmar A.

*Vasyl Stepanyk Precarpatian National University, Ivano-Frankivsk, Ukraine*

An electron subsystem changes its properties qualitatively when the size of that system in at least one direction becomes comparable to both the mean free path and the de Broglie wavelength of the carriers. In this case the electron movement in that direction becomes quantized and causes changes in the energy spectrum and properties. Theoretical predictions for an oscillatory behavior of the thickness dependences of the transport and thermodynamic properties due to the quantization of the energy spectrum in thin films and subsequent experimental evidence in Bi semimetallic layers stimulated an interest in looking for quantum size effects (QSEs) in thin films. A great number of works have been devoted to studying oscillations of the transport properties as a result of the QSE in thin films, but the objects of the majority of studies have been semimetal and metallic films. There are far fewer studies of the oscillatory behavior of the transport coefficients in semiconducting thin films. However, the probability of observing QSEs in semiconducting films is higher than in metallic layers since the Fermi energy  $\varepsilon_F$  in semiconductors can be rather low, whereas the Fermi wavelength  $\lambda_F$  is larger.

According to experimental data [1,2], thickness dependence of kinetic parameters of semiconductor nanostructures p-PbTe in polyamide – PM1/p-PbTe and p-SnTe on mica – STA/p-SnTe, explicit oscillatory behaviour. Naturally we assume that such behavior is due to size effects in quantum well, which created potential barriers, such as oxidative layer on the surface of nanocrystals p-PbTe, p-SnTe and polyamide PM1 or mica STA substrate, respectively. Model quantum well it is known [3], the simplest model potential of size-quantized film.

As evidenced by atomic force microscopy (AFM) [1,2], the analysis of thickness dependence of kinetic parameters of nanostructures, to consider the processes of self-organization. They determine the oscillation period  $\Delta d$ .

1. Остафійчук Б.К., Фреїк Д.М., Шпак А.П. Квантово-розмірні ефекти і осциляції кінетичних параметрів у напівпровідникових наноструктурах // Фізика і хімія твердого тіла. – 2010. – Т.11, №4. – С. 804-814.
2. Юрчишин І.К., Чав'як І.І., Лисюк Ю.В., Харун Л.Т. Розмірні ефекти термоелектричних параметрів у наноструктурах p-SnTe на слюді // Фізика і хімія твердого тіла. – 2010. – Т.11, №4. – С. 898-903.
3. Аскеров Б.М. Электронные явления переноса в полупроводниках. М. Наука. Гл.ред. физ.-мат. лит. –1985.– 320 с.

## Indium nanostructures formation on furrowed (100) surfaces of $\text{In}_4\text{Se}_3$ layered semiconductor crystals

Galiy P.V.<sup>1</sup>, Nenchuk T.M.<sup>1</sup>, Mazur P.<sup>2</sup>, Poplavskyy O.P.<sup>3</sup>, Buzhuk Ya.M.<sup>1</sup>

<sup>1</sup> Electronics Department, Ivan Franko Lviv National University, Lviv, Ukraine

<sup>2</sup> Institute of Experimental Physics, University of Wrocław, Wrocław, Poland

<sup>3</sup> Physicotechnical Faculty, Vasyl Stefanyk PreCarpatian National University, Ivano-Frankivs'k, Ukraine

The studies  $\text{In}_4\text{Se}_3$  layered semiconductor (100) cleavages with furrowed and chainlike surface structure in atomic scale that are stable and unreconstructed under the cleavage are of potential interest to have an anisotropy and low-conductive matrix/template for fabrication of surface-conductive self-assembled nanowires or nanostructures.

In order to characterize the  $\text{In}_4\text{Se}_3$  (100) cleavage surface structure after In deposition, we have performed an STM investigation. It's well-known, that direct correlation of the growth morphology with the electronic properties of the surface layers is a key to the understanding of underlying physics. In view of the still unclear electronic properties and the missing simultaneous structural and electronic investigation, we have studied the electronic structure of thin indium coatings grown on  $\text{In}_4\text{Se}_3$  (100) *in situ* cleavages as a function of the layer thickness of the deposited indium using spatially resolved scanning tunneling spectroscopy (STS). The last one allows us to probe both occupied and empty states, as well as real space and electronic properties simultaneously.

STM/STS data were obtained by a Omicron NanoTechnology STM/AFM System (Germany). The experiments were performed in UHV with base pressures better than  $1 \cdot 10^{-10}$  Torr. All STM/STS measurements were performed at room temperature. A clean  $\text{In}_4\text{Se}_3$  (100) surface was obtained by cleavage with stainless steel tip *in situ*. Indium was deposited with application of UHV thermal evaporator EFM-3 (Focus). The surfaces were thermo treated *in situ* after indium deposition at fixed temperatures up to 600 K.

When compared profiles, derived from STM, at low indium exposition (estimated up to 2 - 3 monolayers) to those of atomically clean surfaces the formation of In wires is obvious in the furrows along *c* direction. At high In exposition the surface is covered mainly with In - islands with flat terraces between them. In spite of such surface morphology the lattice parameters seems not to be significantly induced by In deposition. The indium modulation of the surface structure is visualized clearly but only after Fast Fourier Filtering of the STM images. The STS investigations give access to electronic properties of different surface areas while probing local density of states. STS spatially averaged normalized  $(dI/dV)/(I/V)$  versus sample bias *V* curves show the clear influence of In deposition on density of occupied states and less on empty states one.

## Photoinduced changes of transmittance in zirconia films stabilized with yttrium oxide

Gayvoronsky V.Ya.<sup>1</sup>, Brodyn M.S.<sup>1</sup>, Kopylovsky M.A.<sup>1</sup>, Rostotskiy A.I.<sup>1</sup>,  
Uklein A.V.<sup>1</sup>, Yatsyna V.O.<sup>1</sup>, Lubenets V.A.<sup>2</sup>, Konstantinova T.E.<sup>2</sup>

<sup>1</sup>*Institute of Physics NASU, Kiev, Ukraine*

<sup>2</sup>*Donetsk Institute for Physics and Engineering NASU, Donetsk, Ukraine*

Zirconium oxide is widely used in different technological and commercial applications from aviation to medicine. For technological applications tetragonal bulk phase of zirconia is needed, which is achieved with sintering of monoclinic one above 1100°C with admixture of aliovalent oxides. The dopants caused a formation of oxygen vacancies and drastically affect the structural, mechanical and dielectric properties of stabilized zirconia [1].

We applied nonlinear optical approach to study interaction of the CW laser beam with the trapped electron due to the strong localization of the electron density at the defect site. Its position relative to the valence band edge is about 2.3 – 2.5 eV for the reduced polycrystalline surfaces [1].

For preparation of investigated films the tape casting process was employed. As a base for the films nanopowders of the tetragonal phase of  $ZrO_2 - 3 \text{ mol } \% Y_2O_3$ , synthesized by joint deposition according to the chloride technology with the use of extreme forces at the step of formation of xerogel hydroxide, were used. Polyvinyl butyral was used as a binder for film preparation. The drying and sintering of the film were conducted in the multistep mode. There were three kinds of the films prepared for investigation, sintered at 1270C, 1350C and 1500C during 1 hour. The films thicknesses were 25 $\mu\text{m}$  for scattering properties study and 10 $\mu\text{m}$  for the nonlinear optical research.

We have applied CW radiation of the diode lasers at 405 nm and 1064 nm with energy quanta higher (3.06 eV) and lower (1.17 eV) the trapped electron level respectively. The technique to study photoinduced variation of the films transmittance versus the laser beam intensity is described in [2] with the proper account of optical scattering effects.

It was shown that with laser excitation at 405 nm all the films demonstrate photobleaching effect with typical saturation character. At tenth  $\text{mW}/\text{cm}^2$  laser intensity scale a reduction of the optical absorption is two times higher for the film (1500C) in comparison with others. For the near infrared laser excitation (1064 nm) the photodarkening effect takes place at laser intensities about 1 – 3  $\text{W}/\text{cm}^2$  – decrease of the films optical total transmittance of about 1.5% (1270C, 1350C) – 3 % (1500C). The observed effects can be explained with resonant single- and two-photon excitation of the trapped electron states.

1. M.V.Ganduglia-Pirovano, A.Hofmann, J.Sauer. // Surf. Sci. Rep. – 2007. – T.62. – P. 219.
2. V.Ya. Gayvoronsky, M.A. Kopylovsky et al. // Funct. Mat. – 2009. – T.16, №2, – P.136.

## Modeling of the vapour phase epitaxial at low temperatures growth of the III-V heteronanostructure layers by CVD-method

Guba S.K., Kurilo I.V., Petrovich R.Y.

*Lviv Polytechnic National University, Lviv, Ukraine*

The investigation and development of the methods creating hetero nanostructure layers on the basis of the  $A^{III}B^V$  compounds, which have quantized effects, are the actual problem of semiconductor electronics. The working temperature decrease at the isothermal regime of  $A^{III}B^V$  thin layers growth [1] is one of the basic tendencies of development of the hetero nanostructure growth technology in the chloride gas-phase systems. At present a great number of experimental and theoretical results obtained during the precipitation investigating  $A^{III}B^V$  layers in the wide range of temperatures and growth regimes are available [2]. There are many ways to describe the character of thermal mass transfer in reactors and the kinetics on the surface of substrates. But in the majority of studies the equilibrium character of chemical reactions of 3 and 5 group element sources was assumed a priori. This approach is correct only for the most of the regimes taking place in the “classical” temperature range of vapour phase epitaxial, but it’s unfit during the decrease in source temperatures, when the kinetics of chemical reactions becomes an essential factor. The nonequilibrium character of gas-phase formation makes the composition of the phase dependent on the reactor geometry, on gas-carrier field rates, on the source area and the temperature profile. Thermodynamically methods give us the possibility to obtain reliable data for the equilibrium composition of gas-phase and thermodynamical functions of compounds. But the question of the system kinetical parameters has not been studied yet and is very important in the zone of gas-phase formation. Gas-phase composition can be determined both by means of the experiment and the chemical equilibrium calculations [3].

The generalized methodology for kinetic modeling processes of gas phase formation and transport processes in chemical systems in the field of no nonequilibrium species as well as in the energy field is proposed. The probability methods of accounting the characteristics of energy- and mass-transport process based on the decision of Fokker – Plank common diffusion equation are used to solve this task. Therefore the final rates of particles transport are taken into account. The analytical expression of key density probability function is found as Green's function. It has allowed the system of the diffusion equations to be presented in an integrated form. The solution of the given equations for the concrete transport system and reactors allows the species real concentration as well as spacial-temporal dependencies in the volume of the reactor to be determined.

1. Губа С.К. Низкотемпературный изотермический метод хлоридной эпитаксии  $In_xGa_{1-x}As$  // Технология и конструирование в электронной аппаратуре. – 1998.– № 2. – С. 74-79.
2. Губа С.К., Петрович Р.Й. Кінетика низкотемпературного осадження з газової фази гетеронаноструктур  $In_{1-x}Ga_xAs/GaAs$  // Нові технології. – 2008.– Т.2, №20.– С. 230-235.
3. Guba S.K., Kurilo I.V. Gas-phase formation at the low-temperature isothermal growing of Bi-doped GaAs laers // Functional Materials. – 2001.– V.8, №2. – P. 234-239.

## Peculiarities of the structure of chemical bond of Cadmium

Gutsul I.V., Manyk O.M., Manyk T.O.

*Yuriy Fedkovych Chernivtsi National University, Chernivtsi, Ukraine*

Special demands to materials based on cadmium, used in nanostructures are required to current science and technology [1].

We need information of the technological properties this element taking into account the nature of chemical bond to create new materials with desired properties. Therefore, the purpose of this paper are the complex investigation of chemical bond formation of cadmium. The lattice parameters and the smallest interatomic distances we took into account to construct the molecular model of cadmium [2].

These results allowed to determine the spatial angles between the bond directions of cadmium and establish that chemical bonds are divided into five groups which corresponding interatomic distances:  $\varphi_1(R_{01}=2,979 \text{ \AA})$ ;  $\varphi_2(R_{1''1}=2,9845 \text{ \AA})$ ;  $\varphi_3(R_{01''}=2,9899 \text{ \AA})$ ;  $\varphi_4(R_{1'1}=3,3917 \text{ \AA})$ ;  $\varphi_5(R_{01'}=3,6912 \text{ \AA})$ .

The approximations of elastic bond were used to describe the elastic properties of cadmium [3]. This means that the fluctuations along the interatomic bonds are independent and are characterized by their elasticity coefficient  $f^{(\ell)}$  ( $1 \leq \ell \leq 5$ ), which are used to calculate the characteristic frequencies  $\omega_\ell$  and corresponding them characteristic temperatures  $T_\ell$  (numerical values are given in Table).

Numerical values of characteristic frequencies  $\omega_\ell$  and temperatures  $T_\ell$

$\varphi_\ell$	$\varphi_1$	$\varphi_2$	$\varphi_3$	$\varphi_4$	$\varphi_5$
$\omega_\ell, T_\ell$					
$\omega_\ell 10^{12}, \text{ Hz}$	42,26	34,5	23,19	18,99	16,43
$T_\ell, \text{ K}$	594	521,8	416	378	353

As the findings, polymorphic transformations in cadmium crystals occurs not only at 353 K but and at higher temperatures which leads to changes of chemical bond, crystal structure and hence of physical properties of cadmium and compounds based on it.

1. Ashcheulov A.A., Gutsul I.V., Manyk O.N., Manyk T.O., Marenkin S.F.. CdSb, ZnSb, and  $\text{Cd}_x\text{Zn}_{1-x}\text{Sb}$  low-symmetry crystals: Chemical bonding and technological aspects // *Inorganic Materials*. – 2010. – Vol. 46, No. 6. – P. 574-580.
2. Дриц Н.Е. Свойства элементов. М.: Металлургия, 1985.
3. Маник О.М. Багатофакторний підхід в теоретичному матеріалознавстві. Чернівці: Прут, 1999.

## **Charged impurities influence at energy spectrum and oscillator intensities of electron intra-band transitions in spherical quantum dot CdS/SiO<sub>2</sub>**

Holovatsky V., Frankiv I., Makhanets O.

*Chernivtsi National University, Chernivtsi, Ukraine*

The impurities play an important role in optical, electric and magnetic properties of semiconductors. The charged impurities inside of nanosystems can cardinally change the quasi-particles energy spectra. The presence of donor impurities in quantum dots (QD) or in the surrounding semiconductor medium causes the shift of electron localized energy states into the region of low energies and also changes the distribution of probability density of quasi-particle location in the nanosystem. Such changes essentially influence at the oscillator intensities of intra-band and inter-band transitions [1].

For the hydrogen-like impurity placed into the center of QD, the quantum mechanical problem of electron energies and wave functions obtaining within the one-band approximation is solved exactly. For the not central impurity, the exact solutions of Schrodinger equation do not exist, therefore one has to use different approximated methods.

In the paper it is performed the comparison of the energies and wave functions of ground and excited states of electron localized in QD CdS/SiO<sub>2</sub> with central donor impurity, obtained within the exact and approximated methods.

In the frames of variational method there are calculated the energies and wave functions of electron in QD with donor impurity in 1s, 1p, 2s and 2p states. It is investigated the influence of impurity location at the energy and probability distribution of electron location in nanosystem. The oscillator intensities of electron intra-band transitions are calculated and their dependences on donor position are investigated. It is proven the ability to use the perturbation theory for the calculation of the impact of donor impurity placed outside of QD at the energy spectrum of electron localized inside of QD.

At the base of the exact solution of Schrodinger equation for the electron bound in QD by central impurity, within the variational method, it is calculated the energy of electron ground state in QD with two donor impurities, one of which is in the central.

There are obtained the dependences of ground state energy and distribution of probability density of electron location in nanosystem on the position of impurities inside and outside of QD.

1. V. Holovatsky Oscillator strengths of electron quantum transitions in spherical nanosystems with donor impurity in the center. // *Physica E.* – 2009. – V.41. – P.1522-1526.

## **Optical properties of semiconductor materials with two-layer quantum dots**

Hols'kyi V.B., Kubay R.Yu.

*Department of Theoretical Physics, Ivan Franko Drohobych State Pedagogical University  
Drohobych, Ukraine*

Semiconductor materials with quantum dots (QD's) demonstrate different specific physical properties related to quantum-size effect and have wide application in opto- and nanoelectronic devices. In real structures where a nanocrystal consists of several dozens of monolayers one can hardly say that it has a regular shape. Therefore a rotation ellipsoid most closely describes a real QD shape. Since in [1] the tunnel microscopy shows that the shape of the InAs/GaAs QD is similar to ellipsoidal, these QD's attract much attention [2, 3]

In the paper the theory of charge energy spectrum in two-layer ellipsoidal QD's is developed. The parabolic band approximation is used to calculate electron and hole states. A two-layer nanocrystal of the form of prolate and oblate spheroids with two separation boundaries is considered. The stationary Schrödinger equation with the particle potential energy which is infinite at the interfaces of the heterostructure can be solved exactly. Using the found energy values and wave functions, quantum transition probabilities between the energy levels in the crystal are obtained.

The dependences of particle transition probabilities for different quantum numbers on the QD volume and the anisotropy degree of its form are obtained. The comparison of oblate and prolate spheroidal QD's is made.



## **X-ray emission study of aerosils nanonaprticles with high porous carbon materials interaction**

Zaulychnyy Ya.V.<sup>1</sup>, Ilkiv B.I.<sup>1</sup>, Foja O.O.<sup>1</sup>, Dymarchuk V.O.<sup>1</sup>, Zarko V.I.<sup>2</sup>

<sup>1</sup>*Frantsevich Institute for Problems of Materials Science of NASU, Kyiv, Ukraine;*

<sup>2</sup>*Chuiko Institute of Surface Chemistry of NASU, Kiev, Ukraine*

The study of carbon porous materials and nanosized oxides are topical due to their high surface activity. Porous carbon materials are widely used as high- performance sorption materials, catalyst carriers, membrane systems for filtration of either solution or gas [1, 2]. It is well known that electronic structure determines material properties. In this aspect electronic structure investigation of nanosized aerosils, high porous carbon materials and their composites are urgent.

Valent electron energy redistribution of nanosized SiO<sub>2</sub> and carbon after high frequency processing of A50 + C, A300 + C, A500 + C mixtures (50, 300, 500 is aerosil specific surface) were investigated by means of X-ray emission method.

Intensity decreasing of X-ray emission OK $\alpha$ -bands of A50, A300, A500 aerosils after SiO<sub>2</sub> + C synthesis is caused by decreasing of their size and as a result penetration of lager number of carbon atoms to porous.

Intensity of chemical bonds formation is proportional to aerosils specific surface.

Analysis of changes in valent electron energy distribution of both precursors testifies the formation of chemical bonds between carbon and SiO<sub>2</sub>.

Si-C-O chemical bonds form as a result of orbital overlapping of broken bonds of carbon and SiO<sub>2</sub> surface atoms. These bonds form as a result of nanoparticles penetration into carbon porous under high frequency vibration and high local temperature conditions.

1. Quinn D.F, Ragan S. Carbon suitable for medium pressure (6.9MPa) methane storage. // *Adsorp Sci Tech.* – 2000. – V. 18, № 6. – P. 515-527.
2. Frackowiak E., Beguin F. Carbon materials for the electrochemical storage of energy in capacitors. // *Carbon.* – 2001. – V. 39. – P. 937-950.

## **The effect of electrode material phase composition on specific energy characteristics of hybrid capacitors**

Ivanichok N.Y., Budzulyak I.M., Lisovskiy R.P., Yaremiy I.P.

*Vasyl Stefanyk Precarpathian National University, Ivano-Frankivsk, Ukraine*

The main requirements at selecting of electrode material for hybrid capacitor (HC) are high energy density, which would have been a constant for a long cycling, low toxicity, and low cost.

We have investigated the effect of technological parameters of  $\text{LiMn}_2\text{O}_4$  spinel and porous carbon material (PCM) on the HC parameters, which was formed from lithium  $\text{LiMn}_2\text{O}_4$  spinels as positive electrode and PCM as negative electrode in 1 M aqueous  $\text{Li}_2\text{SO}_4$  electrolyte. PCM was received by activation carbonization from vegetable raw materials with next heat treatment [1]. Synthesis of anode material on lithium manganese spinel base  $\text{Li}_{1+x}\text{Mn}_{2-x}\text{O}_4$  ( $0,1 \leq x \leq 0,5$ ) was carried out with manganese dioxide and lithium hydroxide at  $900^\circ\text{C}$  and subsequent sintering at  $1200^\circ\text{C}$ .

It is shown, that specific energy characteristics of HC depends on the obtaining temperature of spinel and lithium substitution degree. The maximum specific capacity is observed for HC with anode, containing 1,2 and 1,3 of lithium. The value of the specific capacity of electrochemical system with  $\text{Li}_{1,3}\text{Mn}_{1,7}\text{O}_4$  electrode (sintering temperature of  $900^\circ\text{C}$ ) is 20% higher compared with the material sintered finally at  $1200^\circ\text{C}$  temperature. To investigate the reasons of specific capacity changes X-ray analysis was carried out, which revealed that the samples with the substitution degree of 1,0 and 1,1 except lithium spinel phase also contain  $\text{Mn}_3\text{O}_4$  phase.  $\text{Li}_2\text{MnO}_3$  phase exists in samples with substitution degree of 1,3-1,5. At substitution degree increasing from 1,3 to 1,5 a quantity of  $\text{Li}_2\text{MnO}_3$  phase grows. It explains the deterioration of specific characteristics of the electrochemical system, because the  $\text{Mn}_3\text{O}_4$  and  $\text{Li}_2\text{MnO}_3$  phases don't participate in the charge accumulation. With the same reason, specific characteristics of HC synthesized about  $900^\circ\text{C}$  are greater in comparison with that with spinel obtained after the second sintering at  $1200^\circ\text{C}$  temperature.

Thus, it is shown that, selecting the composition of  $\text{Li}_{1+x}\text{Mn}_{2-x}\text{O}_4$  spinel used as an electrode material, one can form a HC, which exceeds in 3 times the energy density of symmetric capacitor produced on the PCM basis.

1. Patent № 88174. Ukraine МКІІ (2009) H01G 2/00, H01G 4/008. A method of nanoporous carbon obtaining for supercapacitor electrodes. I.I. Avramov, B.K. Ostafiychuk, I.F. Myronyuk et all. Claimed 06.03.2007. Published 25.09.2009. Bulletin № 18.

## Possibilities of coherent supercontinuum source for nanoscale systems characterization

Kachalova N.M.<sup>1</sup>, Voitsekhovich V.S.<sup>1</sup>, Khomenko V.V.<sup>1</sup>, R.V. Pilgun<sup>1</sup>,  
Yatsenko L.P.<sup>1</sup>

<sup>1</sup>*Institute of Physics National Academy of Science of Ukraine, Kyiv, Ukraine*

New types of optical waveguides, where achievements in optical technologies including methods and approaches of nonlinear optics of ultrashort pulses, optical micro-and nanostructures, physics of photonic crystals and nonlinear waveguide optics are combined, have played an increasingly important role in the creation of new compact and efficient fiber-optic systems for the generation of ultrashort laser pulses [1-3].

The universal supercontinuum source with a high density of spectral brightness and peak intensity is created. Source consists of photonic micro structured fiber of optimum length, pumped by a femtosecond Ti: Sapphire laser Mira Optima 900-F. Due to the large peak value of the intensity of input radiation (40 kW), we obtained supercontinuum with great peak density of the spectral intensity, approximately 300 mW/nm and the average power density of  $\sim 0.3$  mW/nm in spectral range from 530 to 1100 nm for signal level of at least 5 dB. Such a density peak power per nm allows ones the use of this source for the characterization of nanostructured systems.

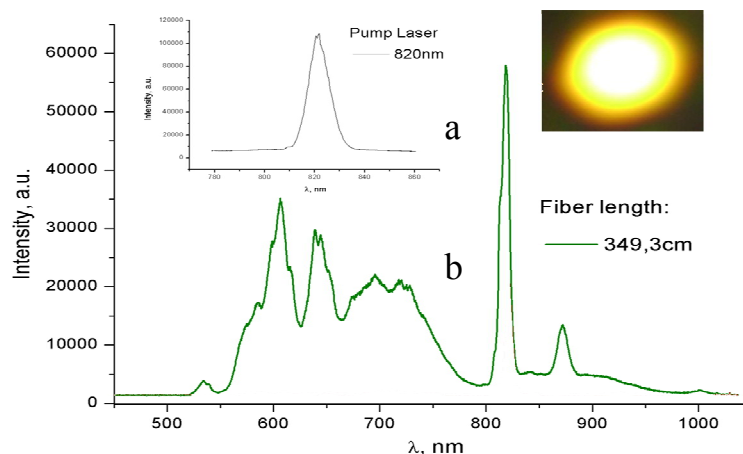


Fig. 1. a) Pump laser; b) supercontinuum spectrum; c) intensity density of an output field.

In this regard, it is interesting to use a our source of femtosecond supercontinuum in such applications:

- formation of fluorescent images with the required time resolution,
- non-contact analysis of the internal microstructure of inhomogeneous media using interferometric methods,
- characterization of nanoscale systems.

The use of such a broadband source provides significant advantages in comparison with a tunable laser, because it provides one-time opportunity characterization of nanosystems in a broad spectral range with a peak power of the order Tues.

1. Alfano R.R., Shapiro S.L. // *Phys.Rev. Lett.*, **24**, 584-587 (1970).
2. Ranka J.K., Windeler R.S., Stentz A.J. // *Opt.Lett.*, **25**, 25-27 (2000).
3. Желтиков А.М. *Микроструктурированные световоды в оптических технологиях* ФИЗМАТЛИТ, Москва. 2009.

## Photoluminescence of CdTe nanocrystals in colloidal solution and polymer matrix

Kalytchuk S. M.<sup>1</sup>, Korbutyak D. V.<sup>1</sup>, Khalavka Yu. B.<sup>2</sup>, Scherbak L. P.<sup>2</sup>

<sup>1</sup>*V. Lashkaryov Institute of Semiconductor Physics, National Academy  
of Sciences of Ukraine, Kyiv, Ukraine*

<sup>2</sup>*Yuriy Fedkovich Chernivtsi National University, Chernivtsi, Ukraine*

Light-emitting devices based on II-VI nanocrystals (NCs) are being extensively developed in many countries in recent years. Their emission wavelength can be changed due to the NCs size variation without changing their chemical composition. Substantial advantages of such devices compared to those already existing (based on p-n junctions) are their high stability and quantum efficiency of emission. We can assert now that light-emitting devices based on NCs will be not only an alternative to the conventional light-emitting diodes, but will have wide application prospects in novel developments of modern devices based on nanotechnologies: optical switches and amplifiers, laser diodes, white light-emitting diodes, photoelectric cells, single-electron transistors, solar elements, fluorescent markers for biological and medical investigations, etc.

Practical implementation of high light-emission characteristics of II-VI NCs into the production of optoelectronic devices requires a detailed study of their luminescence properties, which to a substantial degree depend on the technology of NC production.

The investigation of the photoluminescence (PL) spectra in a wide range of temperatures and excitation levels of II-VI NCs, prepared in various technological conditions, allows us, first, to optimize synthesis regimes for stable NCs and, second, to obtain an important information on the NC fundamental characteristics.

In this work, the techniques for CdTe NCs synthesis in a colloidal solution and their transfer into a polymeric matrix of poly(diallyldimethylammonium chloride) (PDDA) have been developed. Temperature dependences of the photoluminescence of CdTe NCs incorporated in a polymeric matrix have been investigated and analyzed in the temperature range from 5 to 300 K. A bimodal size distribution of CdTe NCs in PDDA has been established after their long-term storage at room temperature, which is manifested by existence of two bands (2.17 eV and 2.41 eV) in the PL spectra. Activation energies  $E_a = 150$  meV and  $E_a = 128$  meV of temperature quenching of these two PL bands of CdTe NCs incorporated in the PDDA polymeric matrix have been established. An excitonic mechanism of photoluminescence of CdTe NCs is established.

## Integrated T/RH thick-film sensor elements based on nanostructured spinel-type ceramics

Klym H.<sup>1,2</sup>, Hadzaman I.<sup>1,3</sup>, Shpotyuk O.<sup>1</sup>

<sup>1</sup>*Lviv Polytechnic National University, Lviv, Ukraine*

<sup>2</sup>*Scientific Research Company "Carat", Lviv, Ukraine*

<sup>3</sup>*Drohobych State Pedagogical University, Drohobych, Ukraine*

The problem of simultaneous temperature and relative humidity T/RH control consists in principally different sensitivities of monitored solid-state system to thermally- and moisture-activated environmentally-induced processes. Nanostructured spinel ceramics based on mixed transition-metal manganites and/or magnesium aluminates are known to be widely used for temperature measurement, in-rush current limiting, gas sensing, flow rate monitoring etc. But their sensing functionality is sufficiently restricted because of bulk performance allowing, as a rule, no more than one kind of application.

Thick-film performance of mixed spinel-type manganites restricted by  $\text{NiMn}_2\text{O}_4\text{-CuMn}_2\text{O}_4\text{-MnCo}_2\text{O}_4$  concentration triangle has a number of essential advantages, non-available for other ceramic composites. Within the above system, the fine-grained semiconductor materials possessing p<sup>+</sup>-type  $\text{Cu}_{0.1}\text{Ni}_{0.1}\text{Mn}_{1.2}\text{Co}_{1.6}\text{O}_4$  and p-type  $\text{Cu}_{0.1}\text{Ni}_{0.8}\text{Mn}_{1.9}\text{Co}_{0.2}\text{O}_4$  conductivity can be easily prepared. The multilayer thick-film structures involving semiconductor  $\text{NiMn}_2\text{O}_4\text{-CuMn}_2\text{O}_4\text{-MnCo}_2\text{O}_4$  and insulating (i-type)  $\text{MgAl}_2\text{O}_4$  spinels can be used as integrated T/RH sensors with extremely rich range of exploitation properties. The aim of this work is development of T/RH-sensitive thick-film structures for ecological environment control and monitoring.

The T-sensitive thick film p<sup>+</sup>-p structures based on spinel-type  $\text{NiMn}_2\text{O}_4\text{-CuMn}_2\text{O}_4\text{-MnCo}_2\text{O}_4$  ceramics possess good linear electrophysical characteristics in the region from 298 to 358 K. The values of B constants were 3615 K. The RH-sensitive i-type  $\text{MgAl}_2\text{O}_4$  thick films possess linear dependence of electrical resistance from RH without hysteresis in the range of RH ~ 40-99 %.

By using nanostructured spinel-type ceramics of mixed Mn-Co-Ni system with  $\text{RuO}_2$  additives, the T-sensitive elements prepared in thick-film performance attain additionally a better RH sensitivity. Despite improved long-term stability and good T-sensitive properties with character material B constant value, such thick-film elements possess only small RH sensitivity. This disadvantage occurred, because of relatively poor intrinsic pore topology proper to semiconducting mixed transition-metal manganite in contrast to insulating aluminates with the same spinel-type structure.

So, integrated T- and RH-sensitive thick-film elements based on nanostructured spinel-type ceramics can be used to produce T/RH-sensitive thick-film structures for ecological environment monitoring and control.

## Photocurrent features in MIS-structures with Si (CdTe) quantum dots

Korbutyak D. V. , Kryuchenko Yu. V. , Sachenko A. V. ,  
Budzulyak S. I. , Kalytchuk S. M.

*V. Lashkaryov Institute of Semiconductor Physics, National Academy  
of Sciences of Ukraine, Kyiv, Ukraine*

Understanding of photovoltaic properties of MIS-structures is based largely on the results of the study of current transport mechanisms. Many reviews and monographs are devoted to the analysis of  $I$ - $V$  dependencies under illumination and reversed bias conditions in traditional MIS-structures, while insufficient attention is paid to novel structures with nano-inclusions. In this work we report on the results of experimental and theoretical study of MIS-structures with silicon oxide films containing Si QDs as well as polymer films containing CdTe QDs.

The MIS-structures with Si QDs in silicon oxide films were formed by pulsed laser deposition (PLD) from a low-energy back flow of the erosion torch particles onto  $p$ -Si or  $n$ -Si substrate, placed in a target plane in vacuum chamber with the argon pressure of 10–15 Pa. The MIS-structures with CdTe QDs were formed by multistage layer-by-layer introduction of CdTe QDs from colloidal solutions into PVP polymer matrix. The oxide (polymer) film thicknesses were in the range of 50–500 nm.

$I$ - $V$  curves of the studied structures had a rectifying character and were asymmetric. In forward bias the current densities reached values of  $10^{-2}$ – $10^{-1}$  A/cm<sup>2</sup>, while in reverse bias in the dark no more than  $10^{-6}$ – $10^{-4}$  A/cm<sup>2</sup>. Multiplication factor on an average amounted to  $10^3$ – $10^4$ . Such a character of the  $I$ - $V$  curves is associated with the potential barrier arising at the interface between substrate and oxide (polymer) film with Si (CdTe) nanocrystals.

The results of  $I$ - $V$  curves analysis at the charge carrier accumulation regime are in accordance with the pattern of direct tunneling of charge carriers between NCs. Analysis of theoretically calculated  $I$ - $V$  curves under reverse bias and illumination indicates that at low values of reverse bias a regime of conductance inversion is realized, the photocurrent is growing rapidly, but it is smaller than that of photogeneration. At higher voltages in the nonequilibrium depletion regime a saturation of  $j_{ph}(U)$  dependence is achieved, and the through-flow current reaches the value of the photogeneration current. The photocurrent value strongly depends not only on the transparency coefficient of dielectric (oxide) film, but also the doping level of the semiconductor, flat band voltage and total recombination rate in the semiconductor.

## Nano formations and zone parameters of crystals (3HgS)<sub>1-x</sub>(In<sub>2</sub>S<sub>3</sub>)<sub>x</sub> (x = 0,5), doped by manganese

Koziarskyi I., Marianchuk P.

*Yuriy Fed'kovytsch Chernivtsi National University, Chernivtsi, Ukraine*

The crystals of solid solutions (3HgSe)<sub>1-x</sub>(In<sub>2</sub>S<sub>3</sub>)<sub>x</sub> (doped by manganese), were got by Bridgeman method.

Analysis of magnetic susceptibility ( $\chi$ ) was performed by Faraday method in the interval of T=77-300K and H=0,25-4 kOe. Samples (3HgSe)<sub>1-x</sub>(In<sub>2</sub>S<sub>3</sub>)<sub>x</sub> are diamagnetic, their magnetic susceptibility  $\chi_0 = -0,25 \cdot 10^{-6} \text{ cm}^3/\text{g}$  and does not depend on tension of the magnetic field (H) and temperature (T). Samples (3HgS)<sub>1-x</sub>(In<sub>2</sub>S<sub>3</sub>)<sub>x</sub> (doped by manganese) are paramagnetic and their magnetic susceptibility has a paramagnetic character.

Dependences  $\chi_{Mn}^{-1} = f(T)$  for the explored samples (3HgS)<sub>1-x</sub>(In<sub>2</sub>S<sub>3</sub>)<sub>x</sub>:<Mn> with temper of Mn ( $N_{Mn} < 0,5 \cdot 10^{20} \text{ cm}^{-3}$ ) are described by Curie law, at  $N_{Mn} = 0,68 \cdot 10^{20} \text{ cm}^{-3}$  - by Curie - Wase law with negative paramagnetic Curie temperature ( $\theta$ ). Value  $\theta < 0$  points that in the explored crystals the exchange interaction of antiferromagnetic characte between the atoms of Mn.

$$\chi_{Mn} = \frac{C}{T - \theta}; \quad (1)$$

$$C = \frac{xN_0 g^2 S(S+1)\mu_B^2}{3k_B M_0} = \frac{N_{Mn} \cdot \mu_{ef}^2}{3k_B \rho}; \quad (2)$$

Established that the peculiar properties of magnetic characteristics of (3HgS)<sub>1-x</sub>(In<sub>2</sub>S<sub>3</sub>)<sub>x</sub>:<Mn> crystals are stipulated by nano formations – clusters of multiple size where exchange (Mn-S-Mn) interaction take place. This exchange interaction is similar MnS faze because there obtained as a result of substitution atoms of Hg by atoms of Mn.

Extrapolation to zero averaged in the high-temperature dependencies  $\chi_{Mn}^{-1} = f(T)$ , which described by Curie - Wase law, gives value of  $\theta$  for each sample. This allows to get on the basis of the dependencies  $\chi_{Mn}^{-1} = f(T)$  and formula (1, 2), values of manganese concentrations ( $N_{Mn}$ ) for each sample. Increase (for the sample containing Mn -  $N_{Mn}$ ) effective magnetic moment of Mn atoms ( $\mu_{ef}$ ), with increasing temperature (set by the Curie-Weiss law (formula 1, 2) based on changes in slope of linear plots at  $T = T_s$ , the dependences  $\chi_{Mn}^{-1} = f(T)$ ), confirms that at  $T = T_s$  clusters conversion from "antiferromagnetic" in the paramagnetic state.

On the base of the optical research it was detect zone parameters of crystals (3HgS)<sub>1-x</sub>(In<sub>2</sub>S<sub>3</sub>)<sub>x</sub>: (x = 0,5;  $n = 5,7 \cdot 10^{19} \text{ cm}^{-3}$ ) have place a two type of direct optical transition: electrons transition from zone of heavy holes to the Fermi level ( $E_g^{op} = 0,56 \text{ eV}$ ) and – from zone of light holes to the Fermi level ( $E_g^{op} = 0,7 \text{ eV}$ ), for (3HgS)<sub>1-x</sub>(In<sub>2</sub>S<sub>3</sub>)<sub>x</sub>:< Mn > (x = 0,5;  $N_{Mn} = 0,47 \cdot 10^{20} \text{ cm}^{-3}$ ;  $n = 3,1 \cdot 10^{19} \text{ cm}^{-3}$ )  $E_g^{op} = 0,64 \text{ eV}$ .

## Surface topology of annealed and unannealed SnSe<sub>2</sub> crystals

Kudrynskyi Z.R.

*Frantsevich Institute of Material Science Problems, Chernivtsi Branch, National Academy of Sciences of Ukraine, Chernivtsi, Ukraine*

Atomic force microscopy (AFM) was used to investigate the surface properties of annealed and unannealed layered SnSe<sub>2</sub> crystals. The crystals were grown by chemical transport method, hence they were obtained as thin slices which were located in a random way in the ampoule and on its sidewalls. The maximum area of the slice made up ~1cm<sup>2</sup> and its thickness ranged between 5 and 100 μm. Such slices had specular surface and were not treated. The crystals were vacuum annealed at 400°C during 4 hours.

The three-dimensional AFM image of the uncleaved and unannealed surfaces of SnSe<sub>2</sub> crystal is composed of bright and dark spots. The shapes and the sizes of the spots are not in an orderly fashion. Such spots are up to the formation of crystal surface structure in the form of hollows and elevations, which defines roughness of the surface. Analysis of the surface cross cut shows that maximum values of the elevations and the hollows make up +6-8 nm and -11-15 nm, respectively. These values of the surface topology shows that they exceed interatomic distances by an order of magnitude.

The duration and the temperature of the annealing may affect the annealed surface topology significantly. These two factors of the annealing can be chosen arbitrarily. In this case the annealing was performed at 400°C during 4 hours.

The carried out investigations of the surface topology of annealed samples shows that during the annealing of the SnSe<sub>2</sub> crystals the smoothing of the curve occurs, which is up to the cross cut of the surface. As this takes place, the surface with bright and dark spots changes into the matt surface. The analysis of the surface cross cut relieves that the maximum values of the elevations and the hollows reduces to +4-5 nm and -3-4 nm, respectively. It means that the roughness of the surface improves twice as much. Therefore the long annealing favours rearrangement of the atomic structure of the crystal surface to the smoothing of mechanical surface tensions.

The performed AFM investigations of annealed and unannealed SnSe<sub>2</sub> crystal surfaces did not reveal the nanostructuring.

In conclusion, the obtained changes in SnSe<sub>2</sub> crystals surface topology during the annealing allow to assert that the annealing improves the surface properties to atomic roughness. Such results are important for the preparation of high quality semiconducting substrate, formed of these crystals, which are used to produce heterojunctions.



## Stokes shift in colloidal CdTe quantum dots

Kupchak I.M., Kalytchuk S.M., Korbutyak D.V.

*V. Lashkaryov Institute of Semiconductor Physics, National Academy of Sciences of Ukraine, Kyiv, Ukraine*

Colloidal nanocrystals (NCs) are currently of great interest for different opto- and nanoelectronic applications as well as for bio-labeling. Advanced wet chemical routes enabled producing of high-quality II-VI NCs with a narrow size distribution and a high fluorescence quantum yield at room temperature. It is generally accepted, that the luminescence of such NCs has an excitonic nature due to the size-dependence of luminescence pick position. However, photoluminescence (PL) spectra of CdTe NCs in the polymer matrixes exhibit large Stokes shift (red shift in energy of the lowest PL band maximum relatively to that of the lowest absorption band) around 600 meV, which is thousands times larger than corresponding values in the bulk CdTe. Currently, the explanations of such an effect are still a challenge.

In this contribution we calculate the Stokes shifts in the spherical CdTe NCs in the polymer matrices using multiband  $k \cdot p$  theory. The fine structure of the exciton has been calculated including Coulomb, short-range and long-range exchange interaction between electron and hole inside the NC and indirect interaction via interface polarization. To find the origin of this shift we examine an influence of NC size, potential barrier heights for electrons and holes at the interface and dielectric constant of the medium on the resonant component of the Stokes shift that is inherent even to a single CdTe quantum dot and arising purely due to singlet-triplet splitting of the lowest exciton state. We have found that these factors could increase the resonant Stokes shift by several orders of magnitude relatively bulk CdTe. Nevertheless, the calculated Stokes shifts remain much smaller than the observed experimental values.

Only taking into account the additional non-resonant contributions to the Stokes shift connected with the existence of the NC distribution over NC size (and, as a result – larger contribution of larger NCs into PL due to larger possibility of their excitation under high-energy laser irradiation) and phonon-assisted absorption and PL, we have achieved a satisfactory agreement between observed and calculated values of Stokes shift for colloidal CdTe NCs embedded layer-by-layer into polymer PDDA matrix.

## Influence of injection level and temperature on the quantum yield and radiation spectrum of power InGaN/GaN light-emitting diodes

Kysselyuk M.P.<sup>1</sup>, Vlasenko O.I.<sup>1</sup>, Myagchenko Yu.O.<sup>2</sup>,  
Sagan Ja.I.<sup>2</sup>, Lyashenko O.V.<sup>2</sup>, Veleschuk V.P.<sup>1</sup>

<sup>1</sup>*V. Lashkaryov Institute of Semiconductor Physics, NAS of Ukraine Kyiv, Ukraine*

<sup>2</sup>*Taras Shevchenko Kyiv National University, Kyiv, Ukraine*

Research of power light-emitting-diode (LED) structures due to purpose to study of the mechanisms of decreasing of electroluminescence, degradation and reasons of failure will allow improving technology of their formation and finding out the optimum conditions and modes of their exploitation. The manufacturers of LEDs above all things specify on dependence of the assured term of work from the current, as the last determines in particular a temperature condition the changes of which influence on character of dependence of radiation power of LED from current and distributing of energy in the radiation spectrum of LEDs.

The research of CVC and quantum yield (QY) of power LED (SUNSEON) allowed to analyze the mechanisms of electroluminescence and get high-quality and quantitative connection between the injection level and QY value, to find out the change of mechanisms of passage of current and to investigate losses related to recombination on the local states of heterojunction.

It is discovered that for some types of LED the polynomials coefficients, which are approximate the dependence of radiation power – current, depend on temperature, and also, that the absolute values of coefficients at the second degree substantially depend on power of probed LED.

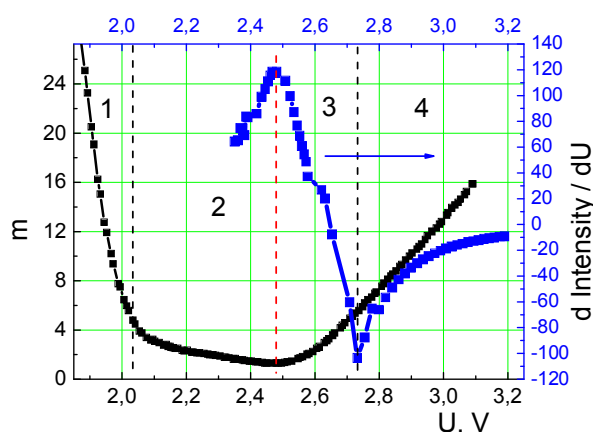


Fig. 1.

of current, 2 – generation-recombination, 3 – is growth of unideality factor and maximum of QY, 4 – linear growth of  $m$  (raise of injection) and slump of QY.

The registered changes in the LED radiation spectrums at different temperatures allow doing the quantitative estimations of subjective perception of the change of radiation color (recognition spectral sensitiveness of eye).

On fig. 1 is presented dependence of unideality factor  $m$  and derivative of QY on voltage. On this dependence it is possible to select 4 areas: 1 – prevails tunnel component

## Optical properties of a spherical quantum dot with a hydrogenic impurity

Leshko R.Ya., Turyans'ka L.M.

*Department of Theoretical Physics, Ivan Franko Drohobych State Pedagogical University  
Drohobych, Ukraine*

With the immensely rapid development of semiconductor nanotechnologies in the past ten years, it is possible to fabricate high precision quantum dots (QD's). But high precision does not guarantee by 100 % that there are not any defects. A QD can have an impurity. In this case the presence of an impurity is not desired. But on the other hand, the impurity can get into the system due to doping. In this case the impurity is needed in the QD. Therefore anyhow QD's can contain impurities.

The physical properties of the spherical QD such as the dipole transition, oscillator strength, and optical absorption coefficient can significantly depend on a presence of impurities in QD's.

In most works where the impurity is studied it is considered that an impurity is located in the centre of the QD. This assumption make it possible to get an exact solution of the Schrödinger equation for a spherical QD and to consider the polarization charges (PChs) which arise at the separation boundary [1 - 2].

In general, the impurity can be anywhere in the QD, even outside of it. In this case the Schrödinger equation does not have an exact solution. We use the linear variational method, analogous to [3], and the Ritz variational method to calculate the energy of a hydrogenic impurity. Also we take into account (neglect) the PChs to make the comparison in both cases. The first technique enables us to calculate the ground state and several excited states, such as S-, P-, D-states. The second method shows that the linear variational method is not so good for the ground state. But using the Ritz variational method to calculate excited states proves difficult. That is why we calculate only 1S and 1P states.

The absorption coefficients (ACs) associated with intersublevel transitions (1S-1P) induced by the polarized light can be calculated by using the compact density matrix approach, for which the total AC is given in [4]. Using this method we calculated the linear, third-order nonlinear ACs. It is shown that the total AC depends on both the quantum confinement and the position of the impurity in the QD. The PChs influence the AC but not so significantly.

1. Boichuk V.I., Bilynskyi I.V., Leshko R.Ya. // Ukr. J. Phys. – 2008. – V. 53. – P. 991.
2. Boichuk V.I., Bilynskyi I.V., Leshko R.Ya. // Cond. Matt. Phys. – 2008. – V. 11. – P. 653.
3. Zhu J.-L., Chen X. // Phys. Rev. B. – 1994. – V. 50. – P. 4497.
4. Vahdani M.R.K., Rezaei G. // Phys. Lett. A. – 2009. – V. 373. – P. 3079.

## Features of structure and properties of polymer electrolytes based on polyethylene oxide and anisometric nanofillers

Lysenkov E.A., Gomza Yu.P., Klepko V.V.

*Institute of Macromolecule Chemistry NAS of Ukraine, Kyiv, Ukraine*

The purpose of this work is to study the influence of the nature, the content and the topology of the form of anisometric nanofillers on the features of structure's forming, thermal properties and conductivity of model systems based on polyethylene oxide (PEO). Methods of dielectric relaxation spectroscopy, differential scanning calorimetry and wide angle x-ray scattering were used. As samples for investigation were used compositions of polyethylene oxide-1000,  $\text{LiClO}_4$  and nanofillers (MM, CNT, MM-CNT). It was shown, that introduction of anisometric nanofiller leads to the additional increasing of the part of the amorphous material of polymer matrix under act of the developed surface of the nanofiller. The use of nanofillers with an anisometric form leads to the substantial influence on the processes of the structure forming in polymer composites even at the maximum low concentrations of the nanofiller (0,3-0,5% for CNT). It was established, that at introduction of OMM in PEO-1000, as a result of the intercalation, PEO can form on each of internal surfaces monolayer of the substantially straightened fragments of polymer molecules, which leads to the increasing of the interlayer distance. The introduction of nanofillers in PEO, leads to the extreme change of thermophysical properties of these systems near the threshold of percolating. By the method of dielectric relaxation spectroscopy, it was established, that the relaxation processes and the levels of conductivity of the polymer electrolytes based on PEO substantially depend on the nature and content of the anisometric nanofillers. It is discovered that at the maximum concentration of the nanofiller (the threshold of percolating) the conductivity relaxation and the temperature dependence of the dc conductivity has extreme dependence on composition of polymer electrolytes based on PEO. Dc conductivity of the system increases with the increasing of the nanofiller content. The conductivity as a function of the temperature can be describe by Vogel-Tamman-Fulcher equation. It means that free volume mechanism is the main mechanism of charge transport. The main conclusion is that introduction of anisometric nanofillers into the PEO- $\text{LiClO}_4$  polymer electrolyte system leads to increase of amorphous part of the systems and to considerable increase of ionic conductivity.

## **Percolation properties of the system based on polypropylene glycol and carbon nanotubes**

Lysenkov E.A., Yakovlev Yu.V., Klepko V.V.

*Institute of Macromolecule Chemistry NAS of Ukraine, Kyiv, Ukraine*

The researches of the percolation properties of nanocomposites, filled by carbon nanotubes (CNT) have the important applied value and they are interesting from the fundamental point of view, as a process of the percolation clusters formation by anisometric nanofillers is not studied fully. It is known that distributing of charge carriers in the bulk and thermal motion of polar groups have a strong influence on the dielectric behaviour of the system. That's why, the research of the relaxation processes is the important approach to receipt the information about nature and types of molecular motions and distributing of nanofiller in the nanocomposite, which depends on its chemical composition, molecular structure, morphology, etc. In such cases, a fractal theory is irreplaceable for research of the difficult and irregular structure geometry, order and disorder in the real systems, and also receipt, as a result of analysis, information about their behaviour. For description the percolation behaviour of nanocomposites a fractal theory and the scaling approach are used. They give the picture of processes of structure's forming which take a place at formation of the continuous cluster. Therefore the purpose of this work were research of percolation properties of nanocomposites based on polypropylene glycol (PPG) and CNT and analysis of them, using a percolation theory and the scaling approach.

In the result of the research, the percolation properties of nanocomposites based on PPG and CNT were investigated and they were analysed, using a percolation theory and the scaling approach. It was established, that the investigated nanocomposites have a fractal structure. In the result of the researches of conductivity, the percolating threshold was certain for these nanocomposites, which is equal 0,45 %. Using the scaling approach the critical index  $t$  was certain  $t = 1,43 \pm 0,07$ , that testifies to formation of three-dimensional spatial percolation network from the clusters of carbon nanotubes and considerable aggregation of CNT after preparation of the samples. It was established, the value of percolating threshold, which was got from the impedancemetric data was confirmed by the microscopic researches. It was shawn, that a continuous cluster of carbon nanotubes was appear where the concentration of nanotubes equal 0,5 %. It was established, that the processes of charge transfer in the nanocomposites are described well within the framework of the model of the intercluster polarization. It testifies to the considerable deposit of intervals between percolating clusters in the conductivity of the system.

## Topology and growth mechanisms of lead telluride nanostructures

Lytvyn P.M.<sup>2</sup>, Lishchynskyy I.M.<sup>1</sup>, Bachuk V.V.<sup>1</sup>, Wojcik V.<sup>3</sup>

<sup>1</sup>*Vasyl Stefanyk PreCarpathian National University, Ivano-Frankivsk, Ukraine*

<sup>2</sup>V.Ye. Laskaryov Institute for Semiconductor Physics of National Academy of Sciences of Ukraine, Kyiv, Ukraine

<sup>3</sup>*Lublin University of Technology, Lublin, Poland*

Thin films of semiconductor materials used in micro-and optoelectronics. The only commercially justified diode laser with wavelength  $\lambda \approx 20\mu\text{m}$  was established on the basis of compounds IV-VI [1]. In addition, lead telluride - one of the promising thermoelectric materials for high temperatures (500-850) K [2]. Thin films of lead chalcogenides have found use in multi-lines of matrices and the entire active elements [3, 4].

Nanocrystalline structure of PbTe received evaporation in open vacuum advance synthetic material. Deposition carried out on a pair of fresh chips (111) crystals BaF<sub>2</sub> [5]. Note that the experiments conducted for various evaporation temperatures spelling  $T_e=(650-800)^\circ\text{C}$ , substrate temperature  $T_s=(50-250)^\circ\text{C}$  and deposition time  $\tau=15, 30$  and  $60$  min., Which determined the thickness of condensate. These nanostructures were investigated by means of atomic force microscopy.

Analysis of the results of AFM studies indicate that important technological factors that determine the mechanism of growth of PbTe nanocrystals on chips (111) BaF<sub>2</sub> deposition pairs in open vacuum, their topology and size is temperature evaporation  $T_e$  and deposition (substrate) systems, as well as the most mass of condensate (sedimentation time  $\tau$ ).

A common feature for selected technological factors of growing three-dimensional nanostructures is the formation of embryos by a mechanism Folmer-Weber. It is dominated by a pyramidal structure in triangular formation with a predominance of vertical or lateral growth, depending on the growing technological factors. Increasing temperature causes evaporation spelling significant increase in their size as in the vertical well and lateral directions. Average height of nanostructures varies from a few nanometers (3-4) nm at spelling  $T_e=650^\circ\text{C}$  for several dozen (40-60) nm at spelling  $T_s=800^\circ\text{C}$  provided stable substrate temperature ( $T_s=50^\circ\text{C}$ ) and deposition time ( $\tau = 30$  min). Similar results were obtained for other conditions  $\tau=15$  and  $60$  min.

1. Beyer T., Tacke M. // Appl. Phys. Lett. – 1998. – V.73. – 1191.
2. Shperun V.M., Freik D.M., Zapuhlyak R.I. Thermoelectricity lead telluride and its analogues. (Ivano-Frankovsk: Plai 2000).
3. Sizov F.F. // Foreign Overseas Electronics, 2:31 (1977)
4. Freik D.M., Galuschak M.A., Mezhylovska L.Yo. Physics and Technology semiconductors films. (Lviv: High School, 1988).
5. D.M. Freik, P.M. Lytvyn, I.I. Chaviak, I.M. Lishchynskyy, V.V. Bachuk, O.S. Krynytskyy, Growth processes of nanoscale structures and PbTe Oswald maturation. // Physics and Chemistry of Solids. – 2009. – V. 10, № 4.

## Electron spectrum in complicated hexagon semiconductor nanotubes

Makhanets O., Tsiupak N., Holovatsky V.

*Chernivtsi National University, Chernivtsi, Ukraine*

Recently, there have been appeared the papers of German scientists [1,2], observing the experimentally investigated luminescence spectra in arrays of complicated multi-shell semiconductor hexagon shape nanotubes. Such nanosystems are the basic elements of light radiating diodes, detectors, transistors and light transformers of new generation.

In the proposed paper, within the model of effective masses and rectangular potentials it is established the theory of electron energy spectra and wave functions in complicated hexagon semiconductor nanotube consisting of quantum wire (*GaAs*), surrounded by the thin shell-barrier (*AlAs*) and nanotube (*GaAs*) in the external medium (*AlAs*).

The effective masses  $\mu^{(e)}$  and potential energies  $U^{(e)}$  of electron in the plane perpendicular to the tube axis as functions of variables  $(\rho, \varphi)$ , have the hexagon symmetry. Therefore, the variables in the respective Schrodinger equation are not separated and, since, it can not be solved exactly. The approximated solution is found within Bethe variational method, introducing in the Hamiltonian the basic part in such a way that the magnitudes  $\mu^{(e)}$  and  $U^{(e)}$  are the functions of  $\rho$  variables only (in other words, replacing the hexagons by the circles of the respective radii). The energy difference arising due to the differences between the masses  $\mu^{(e)}(\rho, \varphi)$  and  $\mu^{(e)}(\rho)$  and potentials  $U^{(e)}(\rho, \varphi)$  and  $U^{(e)}(\rho)$  is taken into account in the Hamiltonian as perturbation. According to Bethe method, the radius of the smallest circle ( $\rho_0$ ) is used as variational parameter, over which it is performed the minimization of energy functional for the electron. As a result it is obtained the electron energy spectrum  $E_{n_\rho^e m^e}$  and wave functions  $|n_\rho^e m^e\rangle$  ( $n_\rho$  – radial,  $m$  – magnetic quantum numbers).

It is also investigated the dependence of electron energy spectrum on radius of inner wire, thicknesses of shell-barrier and nanotube.

1. A. Fontcuberta i Morral, D. Spirkoska, J. Arbiol, M. Heigoldt, J. R. Morante, G. Abstreiter Prismatic Quantum Heterostructures Synthesized on Molecular-Beam Epitaxy GaAs Nanowires // Small – 2008 – V.4, N. 7. – P. 899-903.
2. M. Heigoldt, J. Arbiol, D Spirkoska, J. M. Rebled, S. Conesa-Boj, G. Abstreiter, F. Peiro, J. R. Morantece, A. Fontcuberta i Morral Long range epitaxial growth of prismatic heterostructures on the facets of catalyst-free GaAs nanowires // J. Mater. Chem., – 2009 – V.19. – P. 840-848.

## Energetic spectrum of electron in infinitely deep oblate ellipsoidal quantum dot

Maronchuk I.I., Petrash A.N., Smirnov S.B.

*Sevastopol National University of Nuclear Energy and Industry, Sevastopol, Ukraine*

Quantum dots, with sizes ranging from a few hundreds to many thousands of atoms [1], are thought to have wide potential for future technology applications such as possible high effective multijunction sun elements in the form of quantum dots with intermediate zones. Geometry of such a quantum dots can differ from spherical due to influence of various factors. The best approximation for describing of these objects is an oblate ellipsoid of revolution.

In the proposed model the wall of the ellipsoid assumed to be opaque, and an electron can move freely in the bulk. The main distinction of our model from that of [2] is that we deal with a quantum well with geometry of the oblate ellipsoid of revolution, while authors of [2] have investigated a prolate ellipsoid. Decreasing the small ellipsoid semiaxis  $c$  along  $z$ -axis and increasing the big semiaxis  $a$  in such a way that the volume is constant we get a quantum film.

The problem is solved by transition to the oblate spheroidal coordinates

$$x = d\sqrt{(\xi^2 + 1)(1 - \eta^2)} \cos \varphi, \quad y = d\sqrt{(\xi^2 + 1)(1 - \eta^2)} \sin \varphi, \quad z = d\xi\eta$$

In the effective mass approximation the description of the electron motion in such a quantum well is reduced to the follow boundary problem:

$$\Delta \psi(\xi, \eta, \varphi) = -\frac{2Em^*}{\hbar^2} \psi(\xi, \eta, \varphi), \quad \psi|_{\xi=\xi_0} = 0.$$

The Schrödinger equation are factorized after the substitution [3]

$$\psi_{nlm}(\xi, \eta, \varphi) = R_{nlm}(p, i\xi) S_{lm}(p, \eta) e^{\pm im\varphi},$$

where  $p = kd / 2$ ,  $d = \sqrt{a^2 - c^2}$  – the distance between the ellipsoid focuses, and  $k = \sqrt{2m^* E} / \hbar$ . Due to rotational invariance  $m = 0, 1, 2, \dots$

Energetic spectrum of electron can be founded from the equation  $R_{nlm}(kd / 2, i\xi_0) = 0$ . To solve this equation numerically we applied the shooting method. In the thin film limit the values of the energy of the confined electrons can be computed analytically. We have established dependence of the optical transition energy on the system anisotropy.

1. Yoffe A.D. Semiconductor quantum dots and related systems: electronic, optical, luminescence and related properties of low dimensional systems // *Advances in Physics.* – 2001. – V.50, №1. – P. 1-208.
2. Cantele G., Ninno D., Iadonisi G. Confined states in ellipsoidal quantum dots // *J. Phys.: Condens. Matter.* – 2000. – V.12. – P. 9019-9036.
3. Li L.-W., Kang X.-K., Leong M.-S. Spheroidal Wave Functions in Electromagnetic Theory. – Wiley. – 2002. – 295 p.



## Transformations of microdefect structure of silicon crystals after high-energy electron irradiation

Molodkin V.B.<sup>1</sup>, Olikhovskii S.I.<sup>1</sup>, Kyslovskyy Ye.M.<sup>1</sup>, Vladimirova T.P.<sup>1</sup>,  
 Kochelab E.V.<sup>1</sup>, Reshetnyk O.V.<sup>1</sup>, Dovganyuk V.V.<sup>2</sup>, Fodchuk I.M.<sup>2</sup>,  
 Lytvynchuk T.V.<sup>2</sup>, Klad'ko V.P.<sup>3</sup> and Swiatek Z.<sup>4</sup>

<sup>1</sup>*G.V.Kurdyumov Institute for Metal Physics of NASU, Kyiv, Ukraine*

<sup>2</sup>*Yuriy Fedkovych Chernivtsi National University, Chernivtsi, Ukraine*

<sup>3</sup>*Lashkar'ov Institute of Semiconductor Physics of NASU, Kyiv, Ukraine*

<sup>4</sup>*Institute of Metallurgy and Materials Science, Polish Academy of Science, Krakow, Poland*

The quantitative characterization of complex microdefect structures in silicon crystals grown by Czochralski method and irradiated with various doses of high-energy electrons (18 MeV) has been performed by methods of the high-resolution X-ray diffractometry. Reciprocal space maps from the samples under investigation were measured by *PANalytical X'Pert Pro MRD XL* diffractometer for a symmetrical Si (333) reflection of  $\text{CuK}_{\alpha 1}$  radiation. Additionally, the diffraction profiles for (111) and (333) reflections were measured in  $\omega$ - and  $\omega$ - $2\theta$  scanning mode.

Dose dependencies of concentrations and average sizes of dislocation loops and concentrations of interstitial silicon atoms attached to them after irradiation have been determined on the base of characterization results obtained by using the formulas of the statistical dynamical theory of X-ray diffraction by imperfect crystals with randomly distributed microdefects of several types [1]. In the microdefect structure model used for the treatment of measurement results, the presence of two types of microdefects, namely, disc-shaped oxygen precipitates and circular dislocation loops, was supposed. When analyzing the measured diffraction profiles the contribution of thermal diffuse scattering and influence of instrumental function were taken into account.

The role of dominant microdefects in the formation of balances of primary and secondary irradiation defects and in the creation of residual distributions of electrically active centers and traps has been elucidated. The accounting for the interaction of point defects and microdefects has allowed for the more correct quantitative description of the results obtained by other methods in the investigation of the influence of high-energy particle irradiation on the defect-impurity structure of silicon single crystals.

1. Molodkin V.B., Olikhovskii S.I., Kislovskii E.N., Vladimirova T.P., Skakunova E.S., Seredenko R.F. and Sheludchenko B.V. // *Phys. Rev. B*, – 2008. – V. **78**. – 224109.

## Structure features of nanocrystalization in $\text{Fe}_{75}\text{Mo}_{2.5}\text{Mn}_{2.5}\text{Si}_6\text{B}_{14}$ amorphous alloy

Mudry S., Kulyk Yu.

*Faculty of Physics, Ivan Franko Lviv National University, Lviv, Ukraine*

It is known that amorphous and nanocrystalline materials possess by unique physical-chemical properties, which allow to use them in various areas of application. It was found that formation of  $\alpha$ -Fe nanocrystals in such amorphous materials as Finemet, Nanoperm and Hitperm is the reason of magnetic properties improving. Such nanocomposite systems are commonly formed at first stage of non-equilibrium crystallization and on that reason their thermodynamic state is far from equilibrium. Major physical-chemical properties in this state are most desired for application. Transition from this state to equilibrium one is accompanied by degradation of these improved properties, that motivates the importance of thermal stability studies.

In this work the method of X-ray diffraction at high temperatures was used in order to study the structure changes and nanocrystalization kinetics in  $\text{Fe}_{75}\text{Mo}_{2.5}\text{Mn}_{2.5}\text{Si}_6\text{B}_{14}$  amorphous alloy. Investigation was carried out in vacuum chamber within temperature range 293-873 K.

It was found that formation of initial  $\alpha$ -Fe(Si) nanocrystals from amorphous matrix occurs at  $T = 713$  K. Such parameters of nanocrystal structure as mean nanocrystal size, volume fraction and density were determined by means of integral analysis of intensity curves. It follows from experimental studies that within temperature range 713-768 K the effective size of nanocrystals is about 18 nm, depending slightly on temperature, whereas their volume fraction increases up to 40%. It should be noted also that nanocrystal density increases from  $10^{22} \text{ m}^{-3}$  at  $T = 713$  K up to  $10^{23} \text{ m}^{-3}$  at  $T = 763$  K, indicating the dominant contribution of nucleation processes into formation of nanocomposite system. Analyzing the parameters of crystal cell it was concluded that solubility of Si in  $\alpha$ -Fe(Si) nanocrystals increases with heating.

The deposition of rest amorphous phase and formation of  $\text{Fe}_3\text{B}$ -based metastable phase occur at heating up to  $T = 773$  K. The drastic increase of  $\alpha$ -Fe(Si) nanocrystal size up to  $\sim 45$  nm with their unchangeable volume fraction, is observed. The obtained results indicate that decomposition of rest amorphous phase reveals a polymorphous kind of decomposition. In order to explain the observed changes of nanocrystalline structure, the formation of diffusion regions at the nanocrystal-amorphous phase boundaries is supposed. These regions damp the nanograins growth process that results the formation of nanocomposite structure.

## Effect of laser irradiation on magnetic properties of amorphous alloy $\text{Fe}_{73.7}\text{Nb}_{2.4}\text{Cu}_{1.0}\text{Si}_{15.5}\text{B}_{7.4}$

Mudry S.I., Nykyruy Yu.S

*Ivan Franko Lviv National University, Physics of Metals Department, Lviv, Ukraine*

Characteristic feature of amorphous alloys, based on iron, is a unique combination of various properties, including magnetic, which makes them promising for practical use in the manufacture of magnetic elements with high service characteristics. The problems of predicting characteristics changes under various conditions of impact, and control of characteristics are of special interest. A laser irradiation seems to be promising to solve the problems.

Amorphous ribbon  $\text{Fe}_{73.7}\text{Nb}_{2.4}\text{Cu}_{1.0}\text{Si}_{15.5}\text{B}_{7.4}$ , obtained by rapid cooling from the melt, has been exposed to laser radiation of different power. Wavelength of laser radiation  $\lambda = 0,65 \mu\text{m}$ . Mode of laser operation - scanning the surface, density of pulses  $N \sim 2000\text{mm}^{-1}$ , pulse frequency  $f = 50 \text{ kHz}$ , a pulse duration  $\tau = 130\text{ns}$ . Irradiated samples were studied by X-ray analysis. The X-ray analysis has revealed, that amorphous ribbon crystallizes with the allocation phases  $\text{Fe}_3\text{Si}$ ,  $\text{Fe}_{23}\text{B}_6$ , and  $\text{Fe}_3\text{B}$  after irradiation with pulse energy  $E = 0.1971\text{mJ}$  and  $E = 0.245\text{mJ}$ . The ratio of phases and grain size depend on the pulse energy

Specific magnetic susceptibility of this material before and after irradiation has been measured by Faraday method. Based on experimental data we have determined the magnetization of unit volume of material  $J = \chi \times H$ , and magnetic permeability  $\mu = 1 + 4\pi\chi$ . Magnetic field  $H$  in the process of measurements was  $250\text{A/m}$ .

The temperature dependences of susceptibility  $\chi(T)$  for a full heating-cooling cycle within the range of  $300\text{-}1000\text{K}$  for amorphous and crystalline samples have been determined. The magnetic susceptibility decreases upon heating, which is typical for a ferromagnetic. The thermomagnetic curves  $\chi(T)$  characterize by a broad paramagnetic region ( $>150\text{K}$ ) for amorphous film, and irradiated film at pulse energy of  $0.197\text{mJ}$ . While for the film irradiated at  $E = 0.245\text{mJ}$ , magnetization monotonously decreases and reaches zero at temperature  $T \sim 1000\text{K}$ . Based on experimental data we have built dependence  $\chi^{-1}(T)$ , which allows determining paramagnetic Curie temperature.

## Structure of $\text{Cu}_6\text{PS}_5\text{I}$ nanoceramics under the influence of sintering conditions

Neimet Yu. Yu.<sup>1</sup>, Studenyak I. P.<sup>1</sup>, Kis-Varga M.<sup>2</sup>, Cserhati C.<sup>3</sup>, K ok enyesi S.<sup>3</sup>

<sup>1</sup>*Uzhhorod National University, Uzhhorod, Ukraine*

<sup>2</sup>*ATOMKI, Debrecen, Hungary*

<sup>3</sup>*University of Debrecen, Debrecen, Hungary*

$\text{Cu}_6\text{PS}_5\text{I}$  superionic conductor belongs to argyrodite family and is promising materials for creation of solid-state batteries, electrochemical and optical sensors on their base.

The nanocrystalline powders were obtained by ball milling the material in a stainless steel cylindrical vial with hardened steel balls. The average grain size were determined from the XRD patterns; for the material under investigation the average grain size was 53 nm. Pellets of 8 mm in diameter and 0.2 - 2 mm thick were pressed at 250 MPa and were placed in an evacuated ampoule of quartz glass. The ampoule was heated at a rate 100 K/h to the temperatures of 400 C, 500  C, 600  C and kept at this temperature during 24 h. Then the ampoule was cooled to room temperature.

Structural studies were performed using scanning electron microscopy (SEM) technique (Hitachi S-4300), the chemical composition is controlled by energy-dispersive X-ray spectroscopy (EDX) studies which enabled us to check the chemical composition in different points of the nanoceramic surface.

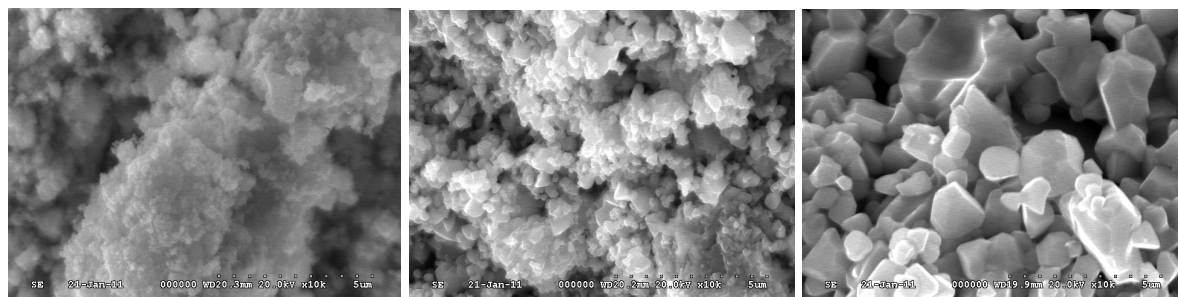


Fig. SEM-images of fractured surfaces on  $\text{Cu}_6\text{PS}_5\text{I}$  nanoceramic samples, prepared at different sintering temperatures (400 C, 500 C, 600 C respectively).

With sintering temperature increase the size of particles increases. Thus, at 400  C one can distinguish particles with a size of 50 nm (left image in Fig.). With further temperature increase the size of particles increases responsibly, becoming of micrometer size (at least 500 nm). Besides, tendency of particles increasing, ordering of a structure and decreasing of porosity is well seen. The structure in a 600  C sintered sample is more uniform but nevertheless there are some micrometer sized holes in it. A significant change of color with sintering temperature increase is observed (400  C sintered sample has brown color; 500  C sintered sample has orange color; 600  C sintered sample has red color).

## Polymer supramolecular structure contribution in conductive properties of polymer films

Nikolaeva M.<sup>1</sup>, Aleksandrova G.<sup>2</sup>, Martynenkov A.<sup>1</sup>

<sup>1</sup> *Institute of Macromolecular Compounds, Russian Academy of Sciences, S.-Petersburg, Russia*

<sup>2</sup> *A.E. Favorsky Institute of Chemistry, the Siberian Branch of the Russian Academy of Sciences Irkutsk, Russia*

The nature of electron transport through dielectric polymer films in the Metal-Polymer-Metal structures not evident until now. It is obtained [1] that dielectric polymer films of different chemical nature have different maximum conductive layer thickness (from hundreds of nanometers to several microns). So we took an attempt to find the reason contributing in maximum conductive layer thickness value for each polymer. For comparison of influence of polymer associative ability on conductive properties of polymer films maximum conductive layer thickness to average contour length of macromolecule ratios were estimated. These values demonstrate vicinity to one for polyimide and polysiloxaneimides having a low amount of interchain hydrogen bonds. At the same time maximum conductive layer thickness many times exceeds contour macromolecular lengths for arabinogalactan and polyamidine with the widespread system of hydrogen bonds. Average contour macromolecular lengths were estimated taking into account polymerization degrees and molecular masses of monomers. Ratios of maximum conductive layers thickness to length of linear macromolecules may be considered as suggestion of supramolecular structure influence on polymer films conductivity.

Maximum conductive layers thickness can change with change of solvent. For instance, it could become possible to observe difference in arabinogalactan conductive layer maximum thickness: 3 mkm for films deposited from D<sub>2</sub>O solutions and 8 mkm for H<sub>2</sub>O solutions. Similar dependences are observed also for polyamidine. Macromolecular associative ability obviously changes in deuterated water. So correlation between maximum conductive layers thickness of polymer films and polymer supramolecular structure due to intermolecular hydrogen bonds formation is observed.

1. Николаева М.Н. // Диссертация на соискание ученой степени канд. физ.-мат. наук – С.-Петербург: Физ.-Тех. ин-т им. А.Ф. Иоффе РАН, 2007.

## Peculiarities of planar self-ordering of SiGe nanoislands grown on strained Si<sub>1-x</sub>Ge<sub>x</sub> sublayers

Nikolenko A.S.<sup>1</sup>, Strelchuk V.V.<sup>1</sup>, Valakh M.Ya.<sup>1</sup>, Lytvyn P.M.<sup>1</sup>, Kladko V.P.<sup>1</sup>, Gudymenko O.Yo.<sup>1</sup>, Krasilnik Z.F.<sup>2</sup>, Lobanov D.N.<sup>2</sup>, Novikov A.V.<sup>2</sup>

<sup>1</sup>*V. Lashkaryov Institute of Semiconductor Physics, NAS of Ukraine, Kyiv, Ukraine*

<sup>2</sup>*Institute for Physics of Microstructures RAS, Nizhny Novgorod, Russia*

Structures under investigation were grown on Si (001) substrates by molecular-beam epitaxy at 700°C. Intermediate strained Si<sub>1-x</sub>Ge<sub>x</sub> sublayer with thickness of 10 nm and composition  $x = 0.22$  was grown on 100 nm thick Si buffer layer. Self-organized Ge islands were formed on the SiGe sublayer in Stranski-Krastanow growth mode by deposition of 9 and 11 monolayers (ML) of Ge.

Surface morphology of the investigated structures was studied by atomic-force microscopy (AFM) using Nanoscope IIIa. Raman spectra were measured using triple micro-Raman spectrometer Horiba Jobin-Yvon T-64000. X-ray diffraction study was carried out using high-resolution diffractometer PANalytical X'Pert PRO MRD.

It was shown that increase of deposited Ge volume from 9 to 11 ML leads to transition from bimodal size distribution of hut-clusters and pyramids to unimodal ensemble of dome-shaped islands. Also, the improvement of nanoislands ordering and considerable excess of total island volume above the volume of Ge deposited on Si<sub>1-x</sub>Ge<sub>x</sub> sublayer in 3.3 and 5 times were found [1].

From autocorrelation analysis of AFM scans the nanoislands were shown to be located in a specific orthogonal grid with lateral ordering in [010] and [-100] directions and strong correlation of short-range order up to four adjacent islands, which was especially pronounced in case of 10 ML of deposited Ge. From X-ray analysis it was shown that the origin of such ordering geometry is the small misorientation of the substrate in close to [-100] direction with corresponding components of 0.4 degree along [-1-10] direction and 0.3 degree in perpendicular [-110] direction [2].

Estimated from Raman spectra composition ( $x$ ) and deformations ( $\epsilon_{xx}$ ) were  $x = 0.32$  and  $\epsilon_{xx} = 0.001$  for islands, and  $x = 0.33$  and  $\epsilon_{xx} = -0.012$  for SiGe sublayer. From analysis of obtained data, the process of nanoislands growth was shown to be accompanied with strong uphill diffusion of Ge from SiGe sublayer into the nanoislands. This phenomenon is explained by Gorskii effect in presence of field of nonuniform elastic strains.

1. Valakh M.Ya., Lytvyn P.M., Nikolenko A.S., Strelchuk V.V., Krasilnik Z.F., Lobanov D.N. // Appl. Phys. Lett. – 2010. – V.96. – P. 141909.
2. Yefanov O., Kladko V., Gudymenko O., Strelchuk V., Mazur Yu., Zh. Wang, Salamo G. // Phys. Stat. Sol. (a). – 2006. – V.203. – P.154.

## **The perspectives of the development of the Si and GaAs of high-speed digital large integrated circuits**

Novosyadlii S.P., Kindrat T. P.

*Prekarpathian National University of Vasyl Stefanyk  
Ivano-Frankivsk, Ukraine*

The perspectives of the development of the transistor structures (TS) for the industrial production of competitive silicic and gallium arsenide-speed digital LSI - cell technology and design base of computer technology super - computer generation has a higher relevance in the modern electronics industry.

Improvements of Extra Large integrated circuits (VLSI) and Extra Large ultrafast integrated circuits (VZLSI) are based on the development of the new physical principles of device structures, technology projects and tracks production, structural and topological solutions components, pieces of circuitry, as well as modern methods of mathematical modeling-class and CAD-technological base element of silicic and gallium arsenide VLSI VZLSI (Novosyadlii S. P., 2003, 2010). The current disparity between the capabilities of organizations - manufacturers of highly productive and super - computers and the significant complexities of the realization of searching of the developments on new physical principles brought forward on the first place modern and perspective experimental and industrial examples of the developments VLSI VZLSI on the base of highly developed nanomicon and sub-technologies in gallium arsenide and silicon. Huge interest in the development of data can be, for the manufacture of super - computers in the U.S., Japan, Western Europe, which works very closely with semiconductor companies in the development of more rapid and more densely packed (gallium arsenide field and bipolar and MOS LSI-K) for the purpose of realization of flash, a high degree of integration as well as additional opportunity of increasing of the speed of operation through intensive cooling, including cryogenic treatment of liquid nitrogen (77K). For the realization of sub- and nanomicon VLSI VZLSI and at the present stage and in the nearest future will be used monosilicon and semi-insulating gallium arsenide, which has some outstanding advantages over silicon: high electron mobility and potential use of semi-insulating substrate, providing a high speed to the formed elements.

Gallium arsenide benefits of technology lie down in the increase of the high radiation resistance, wide temperature operating range from 77 K to 600 K and high system of the speed operation through the use of high mobility 2D electron gas in the lamellar structures. Gallium arsenide technology will take leading place for the formation of high-speed digital LSI provided technology, forming gallium arsenide structures on silicon substrates that will give a chance of sharply reducing of the cost of the substrate and structures and to move to larger diameters > 200 mm.

## Luminescent properties of low-dimensional ZnS obtained by self-propagating high-temperature synthesis

Optasyuk S.V.<sup>1</sup>, Zhuk A.G.<sup>2</sup>

<sup>1</sup> Ivan Ogienko Kamianets-Podilsky National University, Kamianets-Podilsk, Ukraine

<sup>2</sup> V.E. Lashkaryov Institute of Semiconductor Physic NAS Ukraine, Kiev, Ukraine

The photoluminescence spectra (PL) and photoluminescence excitation spectra (PLE) of ZnS doped with Cu, which was obtained by self-propagating high-temperature synthesis (SHS), were investigated.

We studied micron and submicron sized (low-dimensional) particles of ZnS:Cu. The PL and PLE spectra were obtained using the spectral complex SDL-2 at a temperature of 300K. PL was excited by radiation of a nitrogen laser LGI-21 ( $\lambda = 337,1$  nm).

Analysis of the PLE spectra shows that self excitation band ( $\lambda_{\max} \sim 339$  nm) dominates in the PLE spectrum for micron-sized particles, and also impurity excitation bands appear with  $\lambda_{\max} \sim 357$ ,  $\lambda_{\max} \sim 395$ ,  $\lambda_{\max} \sim 418$  nm, which strongly overlaps with each other. It is established that PLE spectrum of ZnS:Cu submicron sized particles differs significantly from the PLE spectrum of micron sized particles of ZnS:Cu.

For low-dimensional particles ZnS:Cu self excitation spectral band is shifted by 12 nm to shorter wavelengths to the 325 nm. The same behavior is observed for the impurity excitation band with a maximum at 357 nm, whose peak is shifted by 10 nm to shorter wavelengths in comparison with the micron sized ZnS:Cu. Shift of the self excitation band to shorter wavelengths indicates that in the studied low-dimensional particles quantum size effects appear, which means that the sizes of the particles do not exceed a few nanometers. Evaluation of sizes of the particles obtained by the SHS method shows that the average particle size is about 3 nm. Also, for low-dimensional ZnS:Cu particles, a shift of the PL spectrum to shorter wavelengths by 10 nm in comparison with the bulk material is observed.

Thus, using self-propagating high-temperature synthesis the nanosized ZnS:Cu was obtained. It is shown that for nanosized ZnS:Cu in the luminescence excitation spectrum, a shift of the self excitation band to shorter wavelengths is observed.



## Relaxation in Amorphous Phases and Initial Crystallization

Ovrutsky A.M., Prokhoda A.S., Taran E.A.

*The Dnepropetrovsk National University of O. Gonchara, Dnepropetrovck, Ukraine*

Relaxation phenomena and nucleation of crystallization centers have been studied by mean of molecular dynamics simulations for Al, Fe and some amorphous alloys ( $\text{Al}_{90}\text{Ni}_{10}$  and  $\text{Al}_{50}\text{Ni}_{50}$ ). The structure formation have been investigated by calculations of the local radial pair distribution functions. The energies of interatomic interaction averaged locally and also in the bulk of the amorphous phase are determined. Latencies of appearance of the first crystallization centre are found. It is researched how the size of the crystallization centre influences its structure and the local interaction energy. Formation of icosahedrons and their lifetimes have been studied also.

Procedures of modeling, which were applied, and interatomic potential, which were used, are described in our several works [1,2]. Visualization of the models and calculations of local radial pair distribution functions (LRPDF) were usually fulfilled with co-ordinates of atoms which were averaged on a time.

Identification of clusters in a non-crystalline phase was fulfilled as in Ref. [2]: calculations of the number of nearest neighbors and determination of bond-angles with nearest neighbors. Atoms having 12 nearest neighbors and 30 angles in  $60\pm 4^\circ$  were identified as centers of icosahedrons. Latencies  $\tau_n$  of appearances of the first crystallization centre (CC) have been determined from data about structural changes in the past after detecting of the well visible and growing CC with a lattice which responds to a structure of the certain crystal phase (as LRPDFs confirm that).

The small CC of Fe and Al have very imperfect and changeable structure. Initial ordering in the alloy  $\text{Al}_{90}\text{Ni}_{10}$  takes place in segments in the size  $>1$  nm in which there are no Ni-atoms. Apparently, the Ni-atoms, which are on boundary of a nucleus, hinder to magnification of its regularity. Therefore, the thermodynamic stimulus for growth of nucleus falls. It was found how averaged energy of atom interaction in the central part of CC changes with increase of its size.

The dependencies of numbers of cluster on time (icosahedrons and FCC-clusters) were determined. There are as well as single icosahedrons and the clusters consisting of several icosahedrons contacting among themselves. Contacts on vertexes with forming of stretched clusters take place more often. And we confirm the known opinion about stabilizing of the amorphous structure by icosahedrons. Average energies of atom interaction in clusters were determined for the models of pure aluminum and iron. With large degree of reliability it is found, that the energy of the icosahedron surrounding is less than for the FCC surrounding.

1. Ovrutsky A.M., Prokhoda A.S. // Crystallography Reports. – 2009. – V.54.– P. 631.
2. Ovrutsky A.M., Prokhoda A.S. // Journal of Crystal Growth. – 2011. – V.314. P. 258.

## Influence of Cr dopant on the properties of AsS glass

Paiuk O.<sup>1</sup>, Lishchynskyy I.<sup>2</sup>, Stronski A.<sup>1</sup>, Vlček M.<sup>3</sup>, Kryskov Ts.<sup>4</sup>,  
Oleksenko P.<sup>1</sup>

<sup>1</sup> *V.Lashkaryov Institute of semiconductor physics NAS of Ukraine, Kyiv, Ukraine*

<sup>2</sup> *Vasyl Stefanyk Precarpathian National University, Ivano-Frankivsk, Ukraine*

<sup>3</sup> *Faculty of Chemical Technology, University of Pardubice, Pardubice,  
Czech Republic*

<sup>4</sup> *Kamianets-Podilsky National University, Kamianets-Podilsky, Ukraine*

Nanostructured chalcogenide glasses are intensively investigated nowadays as perspective materials for a broad range of applications. This is due to their unique physical and optical properties. This report is concerned with studying of the effect of chromium dopant adding to arsenic sulfide glass on the structure and thermal properties by means of Raman spectroscopy and DSC calorimetry.

The glasses of composition As<sub>2</sub>S<sub>3</sub>, As<sub>2</sub>S<sub>3</sub>:Cr 0,5% and As<sub>2</sub>S<sub>3</sub>:Cr 0,75% were prepared by melt-quenching technique. DSC measurement was carried out by NETZSCH DSC 404 calorimeter. Heating rate was q= 10 K/min. From Table 1. one can see that doping with Cr concentration up to 0,75% weight doesn't substantially influence T<sub>g</sub> value. Room temperature Raman spectra were recorded using Fourier spectrophotometer Bruker IFS-55 Equinox with FRA-106 attachment. Nd-YAG laser (excitation wavelength - 1.06 μm).

Table 1

Glass transition temperature

Composition	T <sub>g</sub> , °C
As <sub>2</sub> S <sub>3</sub>	208,3
As <sub>2</sub> S <sub>3</sub> : Cr 0,5 %	204,9
As <sub>2</sub> S <sub>3</sub> : Cr 0,75 %	201,6

Introduction of Cr leads to the intensity increase of the main band at 346 cm<sup>-1</sup> which corresponds to antisymmetric As-(S)-As stretching vibrations in As(S)<sub>3/2</sub>-pyramids and 192, 227, 236, 365 cm<sup>-1</sup> bands, which correspond to the presence of As<sub>4</sub>S<sub>4</sub> nanophase. Intensity of 496 cm<sup>-1</sup> band, characteristic for the vibrations of S-S bonds is decreased with the Cr introduction. The difference spectra reveal the changes occurred in glass structure upon the variation of composition. From these spectra one can be seen that addition of Cr leads to intensity increasing of 150 cm<sup>-1</sup> band, which corresponds to vibrations of phase-decomposed S<sub>8</sub> rings and 317 cm<sup>-1</sup> band, which can be attributed to pyramidal structural AsS<sub>3</sub> units with additional sulfur atoms involved into (-S-S-) chains and join pyramidal fragments.

## Quasiparticle Energy States in Spherical Quantum Dot Superlattices

Pazyuk R.I., Ivakhiv N.F.

*Department of Theoretical Physics, Ivan Franko Drohobych State Pedagogical University  
Drohobych, Lviv region, Ukraine*

Nanoscale heterosystems of quantum dot (QD) arrays demonstrate interesting physical properties and are widely applied in solar cells, photodetectors, thermoelements.

Heterostructures of both chaotic and periodic QD location are used. In the first case the distances, as a rule, are larger than QD's themselves. Therefore from the point of view of theory the problem is reduced to study the properties of a single QD placed in a matrix. Heterostructures of ordered QD location are studied less.

In the paper the quasiparticle states in superlattices of spherical QD's are investigated. In the strong confinement regime subbarrier states of charged particles (electron/hole) are considered. The calculations were done in the case of the *GaAs/AlAs* system which is the system of periodically placed *GaAs* QD's in the *AlAs* environment.

In the superlattice the electron dispersion relations of not only the ground 1s-miniband but also first excited ones are obtained. In the superlattices of different geometries the dependences of electron 1s- and 1p-band widths on the QD radius of different dimensionality structures are studied. It is concluded from the comparison of dispersion relations of one- and two-dimensional superlattices that the lowest band width in the two-dimensional superlattice is larger than that of the one-dimensional superlattice.

The calculation of electron and hole energies of the *GaAs/AlAs* heterosystem shows that the  $E(\vec{k})$  spectrum consists of minibands with their extrema only in the centre or at the edges of each Brillouine miniband.

The electron (hole) energy spectrum genesis is studied changing the distance between QD's when the QD array transforms from 3-D superlattice in a combination of 2-D or 3-D superlattices.

The possibility of existence of electron-hole bound states – Frenkel type exciton states is shown. It is due to the fact that the lowest electron (hole) energy bands in QD superlattices are rather narrow for typical-sized QD's. It is mentioned that exciton band width is mainly determined by exchange interaction.

## Diffusion processes in ZnO nanopowders with oxygen absorption.

Popovych D.I., Onisimchuk V.V.

*Institute of Applied Problems of Mechanics and Mathematics NASU, Lviv, Ukraine*

In our research we have looked into the impact of oxygen diffusion on the photoluminescence outcome spectra and the formation of the surface oxide into ZnO nanoparticle. Nanopowders have been obtained while applying laser pulse reaction technology with further laser implantation of dopants. The investigation of nanogranules morphology by means of scanning electron microscopy (SEM) has proved that nanogranules tend to merge into conglomerates in cause of time. This can reduce diffusion processes intensity into interaction with gases due to contraction of effective surface.

The diffusion model of oxygen dispersion in ZnO nanopowder along with the related change in the luminescence of the material have been under study. In terms of oxygen dispersion depth following diffusion equation we have

$$\partial C(x,t) / \partial t = D_{ZnO} \partial^2 C(x,t) / \partial x^2$$

with the next extreme and initial conditions

$$C(\infty, t) = 0, C(x, 0) = 0,$$

$$-D_{ZnO} \frac{\partial C(x,t)}{\partial x} \Big|_{x=0} = -v_D C(0,t) + v N_{ZnO} + \tau^{-1} N_{ZnO}(0,t).$$

The last equation in this system is to determine the diffuse stream of atoms at the moment  $t$  with velocity  $v_D$  through the surface of ZnO nanopowder;  $N_{ZnO}(0,t)$ ,  $N_{ZnO}$  are the concentrations of the absorbed O-L atoms and absorption vacancies on nanopowder surface;  $v$  is absorption probability of O atoms;  $\tau$  is the average time diffusion bound. The diffusion coefficient is expressed as  $D = D_0 \exp(-E_a/kT)$  while the activation energy of O atoms of diffusion process for ZnO nanopowder equals  $E_a = 0,77 \text{ eB}$ . In case concentration rate closed to

saturation ( $t \rightarrow \infty$ ) the next formula is relevant  $C(0,t) = \frac{N}{\tau v_D} (1 - e^{-t/\tau} \operatorname{erfc} \sqrt{\frac{t}{\tau}})$ . The

revealed dependence of the photoluminescence intensity of ZnO nanopowders on the oxygen pressure rate correlates with the character of diffusive processes in ZnO nanopowder materials.

1. Kotlyarchuk B.K., Popovych D.I., Serednytski A.S., Zhyrovetsky V.M., Moisa M.I. Method of synthesis nanopowder materials and structures on their base. Patent of Ukraine № 11169 from 15.12.2005. bul. № 12.

## **Exciton energy dependence from the thickness of the semiconductor-based nanofilm**

Pugantseva O.V., Kramar V.M.

*Yu. Fed'kovych Chernivtsi National University, Chernivtsi, Ukraine*

The exciton effects are manifested significantly in the spectra of absorption, reflection, photoluminescence and photoconductivity of the flat semiconductor-based nanoheterostructures with quantum wells (QW) [1 - 3]. The dominance of no-phonon excitonic transition lines in the photoluminescence spectra [4] and the exciton energy dependence on the width of the QW, external fields and temperature are experimentally established [5].

Much experimental and theoretical works are devoted to the problem of researching of exciton states and their interaction with atomic vibrations in nanostructures with QW. In particular, in [6] was presented the analytical expressions for calculating the energy of the ground exciton state and exciton binding energy (BE) in the plane nanofilm (NF). These expressions have been obtained using the finite depth rectangular QW model. The electrostatic interaction images in heterojunctions planes have been neglected, but due to the significant differences in dielectric susceptibilities of well and barrier layers the images of electrostatic interaction must be considered.

This report presents the results of theoretical studying of influence of the quasiparticles interaction effects, with their electrostatic images, on value of BE and exciton transition energy in NF of various thicknesses. Specific calculations are performed by the examples of NFs, which are made on the basis of heterojunctions GaAs/Al<sub>0.3</sub>Ga<sub>0.7</sub>As, β-HgS/β-CdS and PbI<sub>2</sub>/polymethylacrylate. Heterojunctions are considered unstriated (in the first two nanosystems – due to the proximity of lattice parameters of the well and the barrier layers, in the latter – due to the peculiarities of layered semiconductor structures PbI<sub>2</sub>, which has flat surface in the direction of the layers growth). The later nanosystem, unlike the first two, is characterized by the infinitely deep QW and there is an essential difference between the dielectric susceptibilities on both sides of the heterojunction. The calculations results are well agreed with known experimental measurement data.

1. Avrutskii I.A., Litovchenko V.G. // *Sov. Phys. Stat. Sol.* – 1997. – V.31. – 875.
2. Jeon H.Ch., Kang T.W., Kim T.W. *et al.* // *J. Korean Phys. Soc.* – 2005. – 47, – 477.
3. Deveaud B., Kappei L., Berney J. *et al.* // *Chem. Phys.* – 2005. – V.318. – 104
4. Weisbuch C., Miller R.C., Dingle R. *et al.* // *Solid State Commun.* – 1981. – V.37. – 219.
5. Klochikhin A., Reznitsky A., Don B.D. *et al.* // *Phys. Rev. B* – 2004. – 69. – 085308.
6. Kramar V.M. // *Journal of Physical Studies.* – 2010. – V.14. – 1706

## Nanoporous thermostable polycyanurate-based film-forming materials

Starostenko O.M.<sup>1</sup>, Gusakova K.G.<sup>1</sup>, Grigoryeva O.P.<sup>1</sup>, Fainleib O.M.<sup>1</sup>,  
Sakhno V.I.<sup>2</sup>, Borzakovskiy A.E.<sup>2</sup>, Grande D.<sup>3</sup>

<sup>1</sup>*Institute of Macromolecular Chemistry of the NAS of Ukraine, Kyiv, Ukraine*

<sup>2</sup>*Institute of Nuclear Research of the NAS of Ukraine, Kyiv, Ukraine*

<sup>3</sup>*Institut de Chimie et des Matériaux Paris-Est, UMR 7182 CNRS – Université Paris XII - Val-de-Marne, Thiais, France*

Nanoporous polymer films are widely used in many branches of high-technology industry as membranes, adsorbents and filters for separation, depuration or microfiltration, as well as they can be used as low dielectric permittivity films for microelectronics. Numerous advanced technologies require a peculiar combination of properties for nanoporous polymer films, including high thermal stability, inertness, excellent resistance towards solvents and etching agents, etc. Polycyanurates (PCNs) represent a family of thermosetting cross-linked polymers that meet such requirements, in addition to their attractive intrinsic features, *i.e.* high glass transition temperatures ( $T_g > 250^\circ\text{C}$ ), low dielectric constants (2.5-3.2), inherent flame-retardancy, high adhesion to metals and composites. High reactivity of cyanate groups allows to get the variety of hybrid PCN-containing nanostructured materials with the improved complex of physico-mechanical properties.

In this study the ways of development of nanoporous cross-linked film-forming polycyanurates using radiation technology were developed. Thinfilms (~30-50  $\mu\text{m}$ ) based on PCN/poly- $\epsilon$ -caprolactone (CPL) and PCN/polyoxytetramethylene glycol (PTMG) were synthesized by *in situ* polycyclotrimerization in presence of 30 wt.% of PCL or PTMG at step heating from 150 to 210 $^\circ\text{C}$  during 9 hrs. Bombarding by  $\alpha$ -particles flux with energy of 27.2 MeV was carried out during 0.5-3.0 min using Cyclotron U-120. The etching of tracks appeared was carried out by alcohol solution of KON. Nanoporous structure with narrow pore size distribution and its geometrically regular shape was detected in samples studied using scanning electron microscopy and differential scanning calorimetric thermoporometry. It was established that the average pore diameter was  $\sim 30 \div 40$  nm and their maximal size didn't exceed 80 nm. The nanoporous samples showed stored physical-chemical properties (heat resistance, thermal, dielectric, etc.) as compared to the individual PCN film materials.

## Chemical bond and elastic properties of Selenium

Savchuk A.I., Manyk O.M., Bilynskyj-Slotylo V.R.

*Yuriy Fedkovych Chernivtsi National University, Chernivtsi, Ukraine*

Special demands to materials based on selenium, used for making nanostructures are required to current material science.

The purpose of this paper are the complex investigation of chemical bond formation of selenium. The power and energy parameters of chemical bonds are found to solve this problem. We took into account the availability of five the smallest interatomic distances to construct the molecular model of selenium.

These results allowed to establish that chemical bonds are divided into five groups which corresponding interatomic distances:  $\varphi_1(R_{01'})= 2,396 \text{ \AA}$ ;  $\varphi_2(R_{01})= 3,575 \text{ \AA}$ ;  $\varphi_3(R_{1'1})= 3,833 \text{ \AA}$ ;  $\varphi_4(R_{11})= 4,0945 \text{ \AA}$ ;  $\varphi_5(R_{01})= 4,363 \text{ \AA}$ , which confirms the double hexagonal densely packed structure of Se.

Grade elastic constants  $C_{ij}$  of selenium and anisotropy were conducted by the experimental data of Young's modulus, Poisson ratio, shear modulus and compressibility [1]. The relation of elastic constants becomes:

$$C_{33}:C_{11}:C_{12}:C_{13}:C_{44} = 5,51: 5,8: 3,76: 3,73: 1. \quad (1)$$

The approximations of elastic bond were used to describe the elastic properties of selenium [2]: the fluctuations along the interatomic bonds are independent and are characterized by their elasticity coefficient  $f^{(\ell)}$  ( $1 \leq \ell \leq 5$ ), which are used to calculate the characteristic frequencies  $\omega_\ell$  and corresponding them characteristic temperatures  $T_\ell$  (numerical values are given in Table).

Numerical values of characteristic frequencies  $\omega_\ell$  and temperatures  $T_\ell$

$\varphi_\ell$	$\varphi_1$	$\varphi_2$	$\varphi_3$	$\varphi_4$	$\varphi_5$
$\omega_\ell, T_\ell$					
$\omega_\ell 10^{12}, \text{ Hz}$	46,7	33,52	25,22	22,5	14,03
$T_\ell, \text{ K}$	490	475	465,7	462,6	453

The results reflect the fine structure of melting and crystallization and polymorphic transformations of selenium and leads to real possibility of choosing several technological solutions obtain new materials with desired properties.

1. Дриц Н.Е. Свойства элементов. М.: Металлургия, 1985.
2. Маник О.М. Багатофакторний підхід в теоретичному матеріалознавстві. Чернівці: Прут, 1999.

## A synthesis of quantum dots of CdTe stabilized by oxyethylenediphosphonic acid

Savchuk O.A.<sup>1</sup>, Trishchuk L.I.<sup>1</sup>, Tomashik V.M.<sup>1</sup>, Tomashik Z.F.<sup>1</sup>, Boruk S.D.<sup>2</sup>

<sup>1</sup>*V.Ye. Laskaryov Institute of Semiconductor Physics of NAS of Ukraine, Kyiv, Ukraine*

<sup>2</sup>*Yuriy Fedkovych Chernivtsi National University, Chernivtsi, Ukraine*

The modern methods of obtaining the CdTe nanocrystals (NC) are widely used in a number of fields of science and engineering because of a detection of quantum size effects. On the other hand, these techniques should resolve the problem of obtaining a lot of samples with sufficient control of their sizes and shapes in order to properties of NC will be not averaged due to heterogeneity of samples. The most widespread method of firmness control is using an adsorption modification of the NC surface. Usually, such modification changes the physical and chemical parameters of the system. As a rule the modifier adsorption decreases the surface energy. The latter facilitates a destruction of aggregates in the dispersed systems and prevents the formation of coagulation contacts between particles in the process of sedimentation.

Usually, modifiers of different type (polyvinyl alcohol, sodium polyphosphate, gelatin, thioglycolic acid, tio-glycerol, cysteine etc.) are applied in the process of the synthesis of CdTe NC. However, a problem is not solved due to majority of them are characterized a high level of toxicity. Thus, the main goal of present work is searching of nontoxic substances which should be characterized a capacity for stabilizing the CdTe NC.

In this work experimental study of synthesis of the CdTe NC stabilized by oxyethylenediphosphonic acid (OEDP) have been carried out. The synthesis was carried out by the use of ions of cadmium precipitated by ions of tellurium under an argon atmosphere in a three-necked flask equipped an electromagnetic mixer, thermometer, partitions and valves. H<sub>2</sub>Te electrochemical obtained in a galvanostatic cell was used as telluride ion source. The NC surface was stabilized by OEDP which was directly added in reactionary mixture in the process of synthesis. It was revealed that *pH* influences significantly on the process of synthesis of the CdTe NC. Fast aggregating occurs at high *pH*. In this case molecules of OEDP, associated by hydroxyl ions, lose a capacity of stabilizing NC. The best result is observed at *pH* = 2. It was established that the NC ageing process is quite sluggish and needs significant time under an anaerobic atmosphere or additional thermal treatment.

Advantage of the present method is application of nontoxic stabilizer of OEDP, simplified synthesis in comparison with methods using thiols and phosphorous-containing substances as stabilizers and also high stability of the CdTe NC systems.



## **Peculiarities of epoxy composites filled with high dispersed particles of titanium carbide**

Savchuk P., Kashitskiy V., Kyselyuk O.

*Lutsk National Technical University, Lutsk, Ukraine*

To get polymer composite protective films with high functional properties it is necessary to inject nano-sized (fine-dispersed) fillers.

While choosing fillers with the particles of optimum size it is necessary to take in consideration their ability to agglomeration in the final state, which increases with the increase of the specific surface of the filler, especially while using low viscous oligomers as a bond. Small gaps between particles prevent from penetrating polymer bond inside the units. As a result, during the solidifying the polymer, plugging of the units' particles of the filler takes place and causes the decrease of mechanical properties of the material.

The analysis of the granulometric composition of titanium carbide powder (product of mechanical and chemical synthesis) has shown that the size of the main fraction equals 10..30 mcm. The quantity of a larger size bunchings (100...500 mcm) decreases and mounts up to 10%.

So, it is inexpediently to form composite material with great division to the size of the particles because their moistening is full, and that descends interaction of the filler and matrix on the border of the phases division. For this reason the process of epoxy components formation with the utilization of external vectorial field is optimized in this work. It is a process of the ultrasonic treatment of the composition in a special bath.

At the same time the decrease of adhesive strength value is stated. It may be explained by the presence of amine low temperature hardener, that interacts actively with final groups of the epoxy component during ultrasonic treatment, that causes local formation of chemical bonds and the increase of residual stress (2.1...2.3 times).

During the ultrasonic treatment of the composition without the hardener the better stirring of the components on the microlevel takes place. It causes more even distribution of the components of material and effective transmitting of the stresses to all the particles of the composite via the border of the division matrix-filler.

As a result, under optimal volume of the filler 50 mass parts high values of adhesion (51 MPa), compressive strength (167 MPa) and low volume of residual stresses (0.3 MPa) are got by formation of surface layer with the controllable qualities. This surface layer consists of oriented macromolecules of the polymer situated on the surface of the filler particles.

## Growth of CdS and CdSe nanocrystal brushes from gas phase

Savulyak V.V., Gorlaty V.O., Solokha V.P., Zubarev R.A.,  
Galaktionov D.A., Fedoryak A.N., Grynko D.A.

*Institute of semiconductors physics of NAS of Ukraine, Kiev, Ukraine*

The artificial creation of quantum systems is a complex technological task, which is now solved by researchers. There are several alternative approaches that are based on the development of technologies of solid state semiconductor structures in nanometer-size range by means of lithography and their surface functionalization. But we can develop an alternative direction of synthesis of low-dimensional quantum systems by using controlled supramolecular self-organization in organic-inorganic systems [1]. Nanocrystals is just the type of objects to which this approach can be quite effective and will synthesize useful devices [1,2]. Arrays of nanocrystals can be used in optoelectronics, for creating effective solar cells, as well as for detecting biomolecules and nucleic acid sequences

Experimental growth of nanocrystal brushes was conducted on  $A_2B_6$  semiconductor's group (CdS, CdSe) from a gas phase using both Vapour-Liquid-Crystalline (VLC) and epitaxial mechanisms.

Obtained samples were analyzed by scanning electron microscopy using the devices JXA-8200 and JSM-1035 (JEOL). CdS whiskers grown with diameter 50-200nm and length of 0,3-30mkm, which gave ability to determine a list of growth parameters vs. growth conditions. In the series of experiments were obtained temperature dependencies of electrochemical potential, growth rate, diffusion length, nucleation speed and crystalization front speed of nanocrystals. Were studied the possibility to control nanocrystals diameter, length and shape by varying temperature and another growth parameters. Overall these results give ability to create vision of nanocrystal growth kinetics and suggest idea for details of nanocrystal growth from a gas phase.

1. Vlaykov G.G., Varabash M.Yu., Zabolotny M.A. et.al. Template guided nanostructure synthesis – К. IMF NASU, 2010. – 230 p.
2. Гринько Д.О., Федоряк О.М., Соболев В.Б., Носач О.В.. Газофазний синтез ниткоподібних нанокристалів CdS, Сборник научных трудов конференции “Физико-химические основы формирования и модификации микро- и наноструктур”, Харьков, Украина, 2009, сс. 306-309.

## Permeability coefficient for two-barrier resonance tunnel structure due to the electron-electron interaction

Seti Ju., Boyko I., Matijek V.

*Chernivtsi National University, Chernivtsi, Ukraine*

Recently, the growing interest to the semiconductor nanostructures is caused by the ability of their utilization in high frequency nano devices widely used in informational technologies, medicine, global monitoring of atmosphere, super fast calculations and many other spheres of mankind activity.

As a rule, the active elements of nano devices are the two-, three- or multi-layer resonance tunnel structures (RTS) [1], operating at the electron levels size quantization with the theory of spectral parameters developed in details. As for the accounting of electrons coupling processes and their influence at the electrons resonance tunneling the theory has been developed [2] within the approximated model of  $\delta$ -like potential barriers and unit electron effective mass using the rough simplifications. It is clear that the results obtained within this theory can present only the qualitative character.

Since, it is necessary to investigate the influence of electron-electron interaction at the permeability coefficient and the spectral parameters of electron quasi-stationary states obtained from it in the frames of the realistic model of rectangular potential barriers and different effective masses in the parts of two-barrier RTS. Therefore, it is solved the stationary Schrodinger equation

$$\left( -\frac{\hbar^2}{2} \frac{\partial}{\partial z} \frac{1}{m(z)} \frac{\partial}{\partial z} + U(z) + g |\Psi(z)|^2 \right) \Psi(z) = E \Psi(z), \quad (1)$$

where  $g |\Psi(z)|^2$  - describes the coupling between electrons in Hartree-Fock approximation.

The solution of non-linear equation (1) is obtained within the numeric Monte Carlo method or the direct iterations method or the iterations method with the approximated wave function square module.

The numeric calculations prove that all three methods give the close correlating results: the accounting of electron-electron interaction causes the shift of electron quasi-stationary states resonance energies into the high energetic region and the decrease of resonance widths does not changing the magnitude of permeability coefficient for the two-barrier RTS.

1. Gmachl C., Capasso F., Sivco D.L., Cho A.Y. // Rep.Prog.Phys., – 2001. – V.64. – 1533.
2. Elesin W.F. // JETP, – 2001. – V.92. – 710.

## Different states of water in nanoporous silicon layers

Shevchenko V.B., Korniyenko M.Ye., Makara V.A., Veblaya T.S.

*Kyiv Taras Shevchenko National University, Kyiv, Ukraine*

In our work we report the study of the different water states in PS samples subjected to various treatments by IR spectroscopy. The layers of nanoporous silicon (with the pore size of 2-5 nm) were obtained by electrochemical etching of 10 Ohm·cm p-type (100) Si wafers. As-prepared sample was studied as well as the samples subjected to different treatments at room temperature (such as exposition to aqueous vapour and immersion in distilled H<sub>2</sub>O) and vacuum annealing (10<sup>-2</sup> Pa) at 600 K. It was shown that the changes in the peak position and shape of OH stretching band during all treatments are observed. The position of this band varies between 2900 and 3550 cm<sup>-1</sup>, which is concerned with variation of the energy of hydrogen bonds and water states in PS.

A considerable long-wave shift of OH stretching band compared to the band of bulk water is observed for the initial samples (see Fig. 1). The low frequencies of OH absorption band can be due to the absorbed Si<sup>-σ</sup>...OH<sub>2</sub><sup>+σ</sup> complexes being, in turn, the sites for physisorption of water molecules. An increased acidity of surface site leads to strengthening the hydrogen bonds with surrounding water molecules and, correspondingly, to lowering of OH band frequency. Annealing at 600 K result in essential shift of OH stretching band maximum to higher frequencies (see Fig. 1). Vacuum annealing leads to water removal out of pores and partial desorption of hydrogen. As it is well known, water is adsorbed predominantly dissociatively onto the surface with great amount of unsaturated dangling bonds. This leads to formation of Si-OH species and subsequent physisorption of water on hydroxyls in the air.

Exposition to aqueous vapour and immersion in distilled H<sub>2</sub>O also cause to the short-wave shift of OH stretching band, which is assigned to decrease in HB energy.

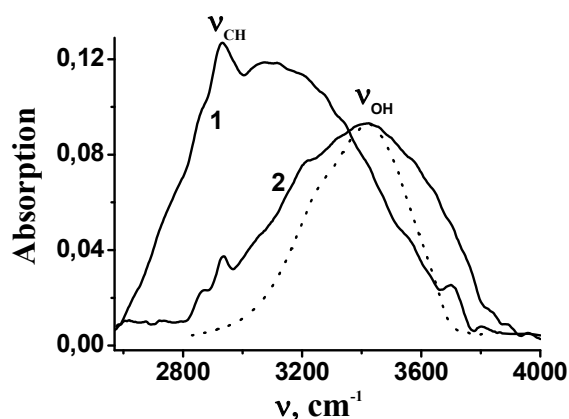


Fig. 1. IR absorption spectra of initial porous silicon sample (1) and the sample annealed at 600 K and exposed to the air for 3 hour (2). For comparison, IR absorption band of distilled water is shown by dotted line

## Surface modifications of amorphous chalcogenide functional materials

Shyplyak M.<sup>1</sup>, Makauz I.<sup>1</sup>, Pynzenyk V.<sup>1</sup>, Voynarovych I.<sup>1</sup>, Chereshnya V.<sup>1</sup>,  
Trunov M.<sup>1,2</sup>, Charnovich I.<sup>2</sup>, Kokenyesi S.<sup>1,2</sup>

<sup>1</sup>*Uzhgorod National University, Uzhgorod, Ukraine*

<sup>2</sup>*University of Debrecen, Debrecen, Hungary*

Investigations on the technology of bulk and thin layers of amorphous chalcogenide materials from As-S(Se) system for photonic applications were performed with aim to select photosensitive materials with best performance and establish the details of the mechanism of direct surface modifications at micro- and nanoscale dimensions. These modifications were made by laser irradiation (recording of microreliefs) and compared with surface relief formation by the e-beam. The influence of the polarization of the laser beam can be excluded this way and the basic role of the electron-hole excitation, charge carrier gradients in the surface relief formation processes can be extracted in more details. Examples of surface profiles created by e-beam recording presented in Fig. 1.

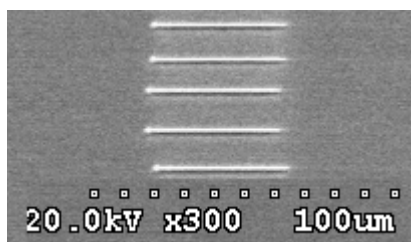


Fig.1. E-beam recorded lines on the surface of the As-Se layer.

Further development of the direct relief recording was made due to the creation of gold nanoparticle-thin chalcogenide layered structures [1], where plasmon-assisted processes occur under the resonance excitations. The results of plasmon-assisted local transformations gave us deeper insight to the mechanism of stimulated structural transformations in these types of functional materials. Applications for microlense-arrays and waveguide fabrication follow from these experimental results.

**Acknowledgement:** This work was supported by the Grant M/59-2009, as well as by the Intergovernmental Cooperation Grant, acknowledge the support of the TAMOP 4.2.1./B-09/1/KONV-2010-0007 project, which is co-financed by the European Union and European Social Fund.

1. Charnovych S., Kokenyesi S., Glodan Gy., Csik A. // Thin Solid Films, 2011, to be published.

## Morphology of gamma-neutron irradiated intrinsic oxide films of InSe

Sydor O.M.<sup>1</sup>, Sydor O.A.<sup>1</sup>, Dubinko V.I.<sup>2</sup>, Lytvyn O.S.<sup>3</sup>

<sup>1</sup> Chernivtsi Department of IPMS of NASU, Chernivtsy, Ukraine

<sup>2</sup> "Accelerator" R&D Complex at the NSC KIPT of NASU, Kharkiv, Ukraine

<sup>3</sup> Lashkarev Institute of Semiconductor Physics of NASU, Kyiv, Ukraine

A weak Van-der-Waals interaction between the layers of InSe gives a possibility to obtain easily atomically clean surfaces of splitted off samples. By means of a simple and low-cost method of thermal oxidation we have prepared on them high-grade intrinsic oxide films, which characterized with the maximum thickness of 0.35  $\mu\text{m}$  and a surface resistance about of 300  $\text{Ohm}/\square$ . The films have been subjected to irradiation by a mixed beam of neutrons with an energy 0 to 30 MeV and  $\gamma$ -quanta with an energy 8 to 35 MeV. The used fluences are:  $\Phi_1 = 1.2 \times 10^{14} \text{ n/cm}^2$  at a  $\gamma$ -quanta dose of  $7.3 \times 10^6 \text{ rad}$  and  $\Phi_2 = 1.2 \cdot 10^{15} \text{ n/cm}^2$  at a  $\gamma$ -quanta dose of  $7.3 \times 10^7 \text{ rad}$ . A homogeneous array of  $\text{In}_2\text{O}_3$  crystallites with individual sizes 25 – 30 nm covering the entire surface is typical for the initial sample (Fig. 1, *a*). For this surface the rms roughness is 2.03 nm, and the maximum height difference of the relief is 4.6 nm. The density of crystallites did not exceed the value of  $1 \times 10^{11} \text{ cm}^{-2}$ . After the irradiations with the  $\Phi_1$  and  $\Phi_2$  fluences the roughness decreases to about of 1.84 and 1.04 nm respectively. It means that smoothing the surface takes place, what can be related to its amorphization. Note that for the sample subjected to the maximum irradiation the formation a great quantity of narrow size distributed nanoformations with a height  $\sim 3 \text{ nm}$  and diameters of the basis to  $\sim 8 \text{ nm}$  occur on the entire oxide film surface (Fig. 1, *c*). Their density is  $2.4 \times 10^{11} \text{ cm}^{-2}$ . In our case radiation-induced defects can be related to oxygen vacancies.

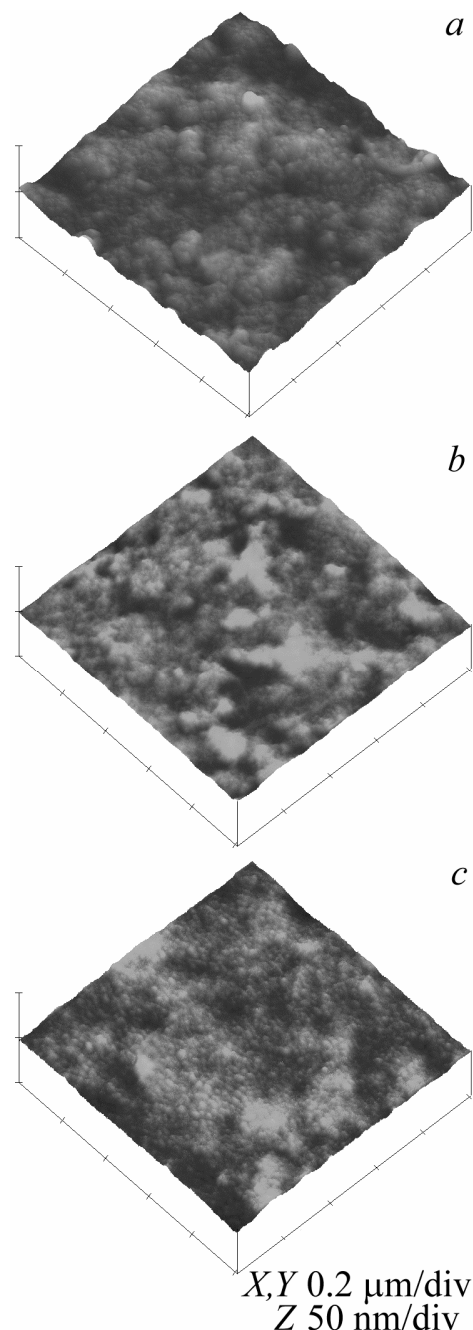


Fig. 1. AFM images ( $1 \times 1 \mu\text{m}$ ) of initial (*a*) and irradiated samples with  $\Phi_1$  (*b*) and  $\Phi_2$  (*c*) fluences.

## Synthesis and characterization of nanocrystalline $\text{LaFeO}_3$ by sol-gel auto-combustion method

Tafiychuk Y.M., Yaremiy I.P., Vylka I.Ja., Bushkova V.S.

*Vasyl Stefanyk Precarpathian National University, Ivano-Frankivsk, Ukraine*

Perovskites with a structural formula  $\text{ABO}_3$  where A is a rare earth element, B is 3d transition metals, have broad applications in advanced technologies such as catalysts, oxide fuel cell, chemical sensors, magnetic materials, electrode materials.  $\text{LaFeO}_3$  is very famous material thanks to its unique properties. Materials based on  $\text{LaFeO}_3$  at high temperatures have high electrical conductivity. Due to its magnetic properties, are widely used to store information, in nanoelektronics, as permanent magnets, etc.

The most common method of synthesis  $\text{LaFeO}_3$  is a solid-phase method. However, it requires significant energy costs. The latest time for receipt of materials became popular sol-gel technology.

One of the most promising methods for nanopowders production is the sol-gel auto-combustion method that allows you to synthesize mixture a specified stoichiometry, uniform throughout the volume. Compared with the solid-phase method, sol-gel auto-combustion method can reduce energy consumption on the synthesis and can increase uniformity of the material, so that formation perovskite phase occurs without supply heat from the outside, but thanks to internal thermal effects of chemical reactions that occur at the same time. At the same time, significantly the time of synthesis is reduced.

Synthesis perovskites by means of technology sol-gel auto-combustion occurs in the following stages: preparation of aqueous solutions of metal nitrates in their stoichiometric ratio, adding of the optimum amount of citric acid, bringing to pH 7 by adding 25% solution of  $\text{NH}_4\text{OH}$ , evaporation of the solution to the formation of sol and gel, drying of the gel at low temperatures to xerogel, controlling by the auto-combustion of xerogel to forming perovskite  $\text{LaFeO}_3$ .

X-ray diffraction XRD measurements were performed on DRON-3 using  $\text{Cu K}\alpha$  1.5406, radiation. The thermal decomposition process of the synthesized powder was investigated by simultaneous thermogravimetric and differential thermal analysis (TG-DTA) using STA 449 F3 Jupiter to 1200 °C with heating rate 10<sup>0</sup>/min. in static air and  $\text{Al}_2\text{O}_3$  as a reference.

## Obtaining homogeneous quantum-sized structures

Tkachuk A.I., Oleskiv R.B.

*Vasyl Stefanyk Precarpathian National University, Ivano-Frankivsk, Ukraine*

The problem of obtaining statistical homogeneous multicomponent functional nanosystems, deposited on amorphous, polycrystalline or crystalline substrates from the vapor phase by open evaporation in vacuum of mechanical mixture of multicomponent materials by hot wall or by molecular-beam epitaxy have not yet been fully resolved, because it's determined by the result of complexity condensation's control for such parameters as the density of steam, its composition and temperature, the indetermination for start and end of condensation.

When evaporation of a multicomponent mixture of materials, which are different in magnitude of partial vapor pressure, it's almost impossible mathematically to plan in advance the structure of vapor mixture, what is deposited on the substrate surface.

Developed and approved construction of small-scale and little energy intensive evaporator of mechanical mixture of multicomponent materials  $A^x B^y C^z \dots X^m$ , which have different discrete values of selective temperature evaporation.

For one cycle in the volume of the evaporator it is realized the complete evaporation process and synthesis of pre-planned mathematical model for thermodynamic equilibrium, considering all existing factors of evaporation materials multicomponent mechanical mixture and automatic emission in a vacuum chamber capacity of gas-dynamic flow within 0.6 seconds.

The thickness of deposited films on substrates of different nature is in direct dependence on mass of evaporated materials mixture, its composition is identical to composition of deposited vapor phase.

High emission speed of gasdynamic flow with high steam pressure from the evaporator's volume allows practically to minimize the contamination of deposited film on the substrate surface, which are discretely heated from 20 to 600°C, by residual gases of vacuum chamber and to obtain homogeneous nanostructures with a minimum number of growth structural defects, micro-tensions, packing defects, to realize selforganization of quantum structures.



## **Plasmachemical modification of adsorbents surface**

Trachevsky V.V., Kustovska A.D., Kosenko E.I.

*National Aviation University, Kyiv, Ukraine*

Nowadays the ways of possible using of adsorbents are various. In most processes the using of pure adsorbents is ineffective. A perceptible benefit from their using will be realized only when they are modified in accordance with a specific of their using. Thus, for the efficient use of adsorbents the modification of their surface by active functional groups can be perspective.

The traditional methods of ion exchange, percolation, coprecipitation, adsorption from gas phase, adsorption of metal vapor etc not always give the possibility to receive sorbents with expected operational characteristics.

The method of modification of adsorbent surface in low-temperature plasma is offered as an alternative to the traditional methods. The most perspective aspects of its use are concerned with the point that in according with the traditional processes in chemical technology the plasma processes do not need the using of liquid solutions (that means that they are potentially ecologically clear) and they are less energy-intensive.

The influence of low temperature plasma on the surface of adsorbent allows to change its contact properties (moistening, adhesion to the thin layers of metal, which are inflicted both by vacuum dispersion, and by other methods).

As a rule, improvement of adhesive conditions of adsorbents under act of low-temperature plasma is caused not only by cleaning of surface from the different sort of contaminations but also by formation of hydrophilic groups of different chemical nature, which provide high adhesive behaviors of the modified surfaces. Composition, structure and properties of such polar groups depends both on nature of adsorbent and on properties of plasma and nature of gas that creates plasma. If oxygen or air is used as working gas of plasma, then on the surface of the filler oxygen-containing arctic groups appear (carbonyl, alcoholic, esters, lactone etc). In the case of using of ammonia or his compounds with hydrogen on the surface groups containing nitrogen are created (amino-, amido- etc). As a result of polymerization of organic and element-organic compounds in plasma, on the surface of adsorbents the thin films of different chemical nature and composition appear. They are hydrophilic, hydrophobic or those which contain the atoms of metals.

Modification of surface of adsorbents was conducted by the developed method in a high-frequency electrodeless plasma charge on frequency of 13,56 MHz. The received results show that nanoparticles with diferent properties are created on the surface of adsorbent. This is proved by sufficient for statistically grounded conclusion number of researched patterns.

## Synthesis and investigations of gadolinium-gallium garnet nanomaterials

Tsvetkova O.<sup>1</sup>, Varvarenko S.<sup>2</sup>, Luchechko A.<sup>1</sup>, Kostyk L.<sup>1</sup>, Pavlyk B.<sup>1</sup>

<sup>1</sup>*Faculty of Electronics, Ivan Franko National University of Lviv, Lviv, Ukraine,*

<sup>2</sup>*Department of Organic Chemistry, Lviv Polytechnic National University, Lviv, Ukraine*

Much attention is paid to nanocrystalline materials, which are increasingly used in electronics, materials science and medicine. These materials exhibit special electrical, magnetic and optical properties as bulk single crystals by reducing their grain size. Therefore, production and investigation of nanocrystalline materials is an important step in creating appliances of a new generation.

The so-called soluble methods, including co-precipitation and Pechini ones were used to obtain  $Gd_3Ga_5O_{12}$  nanopowders, both nominal pure and doped by ions of rare earth elements ( $Tb^{3+}$ ). Thermal treatment of precursor at temperatures 850 and 950°C allowed to obtain nanopowders with a high degree of homogeneity and dispersion. Nanoceramics were received by compression of nanopowder with following annealing at 950°C. Nanofilms with different thicknesses and concentrations were made by application of organic resin mixed with nanopowders in necessary proportions to the sital or sapphire substrate.

X-ray studies of nanopowders, nanoceramics and nanofilms were carried out on diffractometer STOE STADI P ( $Cu K_{\alpha}$  - radiation). Phase analysis and crystallite size calculation were done using the package programs STOE STADI WinXPOW. Crystallite size estimated by using Scherrer formula was ~ 20-37 nm. The surface morphology was observed by atomic force microscope (AFM) Solver P47H-PRO. These nanoparticles had a distinctly cut form.

Synthesis results of nanopowders obtained by different methods have been compared. The effect of nanopowders dispersion, homogeneous and nanocrystalline grain size on the spectral-luminescent properties of  $Gd_3Ga_5O_{12}$  garnet, both nominally pure and activated by  $Tb^{3+}$  ions, are being discussed.

*X-ray studies were carried out in “Interfaculty scientific-educational laboratory of X-ray structure analysis” of Ivan Franko National University of Lviv.*

## Metastable nanostructures in the rapidly quenched iron alloys

Velikanova T.A., Karpets M.V.

Frantsevich Institute for Problems of Materials Science, NASU, Kyiv, Ukraine

The Fe–Cr–Mo–C system is the base for high-speed and die steels.

By High Temperature XRD-method ( $\text{CuK}\alpha$ , He atmosphere,  $V_{\text{heating}} \sim 50 \text{ K/min}$ ) the evolution of the phase composition of 64,9Fe19,6Mo14,5Cr1,0C (1 alloy) and 55,3Fe5,4Mo35,4Cr3,9C (2 alloy) (% at.) spinning ribbons ( $\sim 50 \mu\text{m}$  thick) have been studied from 293 K to liquidus with using of PowderCell 2.4<sup>1</sup> (Rietveld-analysis). Nanostructures on the base of the  $\pi$ -phase ( $cP20$ ,  $P4_132$ ,  $\beta$ -Mn) with coherence area  $\sim 50 \text{ nm}$  in the both alloys, and  $\chi$ -phase ( $cI58$ ,  $I43m$ ,  $\alpha$ -Mn) with coherence area  $\sim 20 \text{ nm}$  in the 2 alloy were observed at 293 K. It was shown that  $\pi$ -phase is metastable from 293 to 978 K and can be obtained in conditions of nonequilibrium crystallization in the both alloys only. The  $\chi$ -phase is stable from 1073 to 1473 K and forming in the solid state in the 1 alloy, and  $\chi$ -phase is metastable from 293 to  $\sim 900 \text{ K}$ , stable nearby 1173 K and forming in solid state in the 2 alloy. Crystal structure of identified phases is:  $\alpha$  ( $cI2$ ,  $Im\bar{3}m$ , W),  $\gamma$  ( $cF4$ ,  $Fm\bar{3}m$ , Cu),  $\eta$  ( $cF112$ ,  $Fd\bar{3}m$ ,  $\text{W}_3\text{Fe}_3\text{C}$ ), R ( $hR159$ ,  $R\bar{3}$ ,  $\text{Mo}_3\text{Cr}_2\text{Co}_5$ ),  $\text{Me}_{23}\text{C}_6$  ( $cF116$ ,  $Fm3m$ ,  $\text{Cr}_{23}\text{C}_6$ ).

Table

High Temperature XRD data for Fe–Mo–Cr–C spinning alloys

T, K	Alloy quantitative phase composition, % mass.	
	$\text{Fe}_{64,9}\text{Mo}_{19,6}\text{Cr}_{14,5}\text{C}_1$	$\text{Fe}_{55,3}\text{Mo}_{5,4}\text{Cr}_{35,4}\text{C}_{3,9}$
293	$50\pi + 9\alpha_1 + 32\alpha_2 + 9\text{R}$	$16\pi + 24\chi + 60\alpha$
773 (1 skan)	$41\pi + 25\alpha_1 + 24\alpha_2 + 10\text{R}$	–
773 (2 skan)	$31\pi + 38\alpha_1 + 20\alpha_2 + 11\text{R}$	–
873	$22\pi + 55\alpha_1 + 14\alpha_2 + 9\text{R}$	$22\pi + 18\chi + 60\alpha$
923	$14\pi + 77\alpha + 9\text{R}$	–
293 after 923	$93\alpha + 7\text{R}$	–
978	–	$14\pi_1 + 10\pi_2 + 60\alpha + 16\text{Me}_{23}\text{C}_6$
1073	$20\chi + 24\alpha + 48\gamma + 8\text{R}$	–
1173	–	$9\chi + 35\alpha + 24\text{Me}_{23}\text{C}_6 + 32\sigma$
1273	$45\chi + 2\alpha + 31\gamma + 22\eta$	–
1373	$46\chi + 7\alpha + 22\gamma + 25\eta$	$94\alpha + 6\text{Me}_{23}\text{C}_6$
1473	$55\chi + 27\alpha + 18\eta$	$100\alpha$
1523	$88\alpha + 12\eta$	$100\alpha + \text{L}$
1573	$38\alpha + 62\text{R} + \text{L}$	–
293 after 1573	$32\alpha + 68\text{R}$	$100\alpha$

<sup>1</sup> [ftp://ftp.bam.de/Powder\\_Cell/pcw23.exe](ftp://ftp.bam.de/Powder_Cell/pcw23.exe)

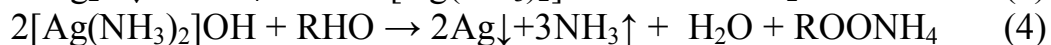
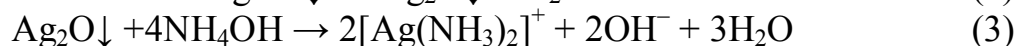
## Chemical Method of Preparing Colloidal Silver Liquid Composition

Voronych O.L., Kurta S.A.

*Vasyl Stefanyk' Precarpathian National University, Organic and analytical chemistry department, Ivano-Frankivsk, Ukraine*

Colloidal silver is a suspension of submicroscopic metallic silver particles in a colloidal base. Conventional fine silver particle colloidal dispersions are those in which fine particles of a noble metal such as silver have been dispersed in a low concentration of 10 % by weight at most and usually received by the electro-spark physical method in aqueous solution. Thus the development of chemical methods for obtaining of colloidal silver has practical interest.

Method based on chemical interaction of complex silver with reducing agent (e.g. glucose):



For preparing colloidal silver were used diluted solutions of silver nitrate, ammonia and reducer. Reaction proceeds in alkaline water medium. Completeness of reaction recovery of silver was controlled with the reaction with barium chloride solution which reacts with silver ion as described below [1]:



Colloidal silver prepared this manner had low stability and rapid agglomeration of particles occurs with the formation of larger aggregates. To stabilize suspension proposed to use hydrophilic protective colloids such as solutions of starch, carboxymethylcellulose, sugar, with the percentage of substances near 0.1-1 % [2–3]. Silver particles also can be precipitated on the filler surface such as silica or titanium dioxide.

It will be apparent that factors such as temperature and concentration of silver salt, ammonia and formalin and the the quantity and nature of the protective colloid would have significant influence on quality of the resulting colloidal silver and can be varied over a wide range.

1. Алексеев В.Н. Курс качественного химического полумикроанализа. М.: Химия. – 1973. – 584 с.
2. Pat. US 0264518 A1 C09K 3/00 Method for Preparing Liquid Colloidal Dispersion of Silver Particles and Silver Conductive Film / Kenji Kato, Masaya Yukinobu.– Nov. 23, 2006.
3. Pat. US 5187209 A61K 47/00; C08K 9/10; C12N 11/14 Colloidal Metal Dispersion, and a Colloidal Metal Complex / Hidefumi Hirai, Makoto Komiyama, Michitaka Otaki.–Feb. 16, 1993.

## Solig phase synthesis in amorphous chalcogenide multiulayers

Voynarovych I.<sup>1</sup>, Shiblyak M.<sup>1</sup>, Pynzenik V.<sup>1</sup>, Makauz I.<sup>1</sup>, Chereshnya V<sup>1</sup>,  
Kikineshi A.<sup>2</sup>

<sup>1</sup>*Uzhgorod National University, Uzhgorod, Ukraine*

<sup>2</sup>*Institute of Physics, University of Debrecen, Debrecen, Hungary*

Chalcogenide glasses, amorphous layers are rather widely investigated and applied in electronics due to the number of peculiar effects like optical and electrical memory, optical nonlinearity, transparency in infrared spectral region. Optically induced effects of darkening-bleaching, mass transports and change of the refractive index are promising for fabrication of integrated optical elements.

Bulk materials of the most known As(Ge)-S(Se,Te) systems can be obtained by the conventional liquid-phase method of direct syntesis from elemental components. Thin film of these materials usuly are prepared by thermal evaporation in vacuum, but decomposition of the original multicomponent glass changes of the parameters of lagers obtained at different temperature conditions may occure during the thermal evaporation . These can be eliminated in a number of nanomultilayers structures via solid phase syntesis during the interdiffusion of different adjacent layers prepared from different compositions (elemental or compound chalcogenides, metals or even dielectrics), which undergo heat- or light-, electric field treatments. New multicomponent phases with optimalsed parameters and laterally or vertically distributed structures can be obtained this way.

We have developed the technology of vapour phase deposition of thin film nanolayered, compositionally modulated structures, which consists of stacks 1-10 nm thick sub-layers ( from elemental Se, Te, binary As-(S,Se,Te) and some more complex chalcogenides, as well as Sb, Bi, Cu, Au metals and SiO<sub>x</sub> oxides, deposited on special glass, sapphire, silicon substrata.

They were used for investigations of change optical and electrical parameters (transmittance, refractive index, conductivity, permittivity), their change under the influences of laser irradiation, ion and e-beems, current pulses.

The main result of these stimulated solid state processes is the well localized change of optical and electrical parameters which in turn can be used for optical recording amplitude-phase relief and (in some cases) surface pattern formation.

*This work was supported by bilateral cooperation grant between Ukraine and Hungary M/59-2009.*

## **Energy states of electrons with position-dependent effective mass in the quantum nanoheterosystems**

Voznyak O.M., Voznyak O.O.

*Vasyl Stefanyk Precarpathian National University, Ivano-Frankivsk, Ukraine*

The study of semiconductor heterostructures, and more generally inhomogeneous crystals has given to extended discussion concerning using of the simple effective-mass model description for the dynamics of the electrons with the position-dependent mass in such systems.

When the systems with position-dependent mass are considering then except the purely applied importance, appear important general physical problems. They are related to the ordering of the coordinate and momentum operators in the Hamiltonian, and refining of boundary conditions on the border where the potential or mass are skipping.

Models, in which both mass and potential are piecewise continuous functions, have been investigated for various nanoheterosystems where the effective mass is a function of the coordinates. In this paper supersymmetric method for finding exact solutions of the basic and first excited states of the system, based on supersymmetric quantum mechanics, has been used for studying systems with effective mass of electrons depending on the coordinates. Under this approach, the technique of generating potentials with exact solutions for given position-dependent mass has been developed. It has been discovered, that the functions which express the dependence potential and mass of the particle coordinates are related each to other.

Using this technique we have been investigated, the energy states for systems with dependence of the effective mass on the coordinates expressed via power and hyperbolic functions. Considering the ground state in the case of constant potential, the conditions applied to the position-dependent mass to provide the bounded states existence, have been established. Fact, that the mass dependence on the position causes the existence of the bounded states in the case of motion in the constant potential, has been proved. Examples of exactly solvable potentials with position-dependent mass have been provided.

Conditions of the existence of exact solutions for the ground and first excited states have been considered. Examples of potential and position-dependend mass have been provided and exact solutions for the ground and first excited states have been found. Conditions under which bounded states exist have been determined. The cases providing existence of such states for motion in the constant potential have been investigated. It also has been provided examples of mass dependence on the coordinates for which was obtained solutions at constant potential.

## Crystal structure of epitaxial *Bi*-substituted ferrite-garnet films modified by double boron implantation

Yaremiy I.P., Tomyn U.O., Yaremiy S.I., Kravets V. I.

*Vasyl Stefanyk Precarpathion National University, Ivano-Frankivsk, Ukraine*

An important task that arises in the process of ion implantation is the creation of preassigned microstructure of surface layer. This task can be performed by the unmonochromatic or unmonoionic repeated implantation. To study the features of influence of the double implantation in comparison with monochromatic implantation, and the influence of the implantation succession on the strain profiles X-ray diffractometry investigation of Bi-substituted ferrite-garnet films implanted with  $B^+$  ions in mode  $E=150$  keV,  $D=1\cdot 10^{14}$   $\text{sm}^{-2}$  +  $E=60$  keV,  $D=7\cdot 10^{13}$   $\text{sm}^{-2}$  (series 1) and  $E=60$  keV,  $D=1\cdot 10^{14}$   $\text{sm}^{-2}$  +  $E=150$  keV,  $D=7\cdot 10^{13}$   $\text{sm}^{-2}$  (series 2) was conducted.

Investigation of the influence of double boron implantation on the crystal structure of superficial layers of epitaxial ferrite-garnet films showed that the results of their modifications depend on the sequence of implantation, and the strain profiles in the case of cumulative dose of  $\leq 2\cdot 10^{14}$   $\text{sm}^{-2}$  are monotonically decreasing.

Strain profiles deformation series 2 samples are shifted to the surface relative profiles series 1, which is connected with the destruction of the ordered crystal lattice structure by the preview of low implantation (60 keV) and thus with the distortion of channels, in which knocked matrix ions can move. The highest deformation in samples of series 1 in all cases is less than the highest deformation in samples of series 2.

To investigate influence of mechanical stress that exist in heterostructure on the strain profiles films with different degrees of mismatch of film and substrate lattice parameters in the plane of growth were studied. It was found that with the increasing of the mentioned mismatch in superficial layers of epitaxial ferrite-garnet films during ion implantation (regardless of the mode of implantation), the part of the strain profiles which characterizes the region of maximum nuclear energy loss shifts in the depth of the film. The thickness of disordered layer increases and the highest deformation reduces.

*This work was supported by the project UKX-9200-IF-08.*

## Determination of optimum parameters of the electrolyte-semiconductor during the creation of porous GaP

Yatsenko Yu.I.<sup>1</sup>, Kidalov V.V.<sup>1</sup>, Sukach G. A.<sup>2</sup>

<sup>1</sup> Berdyansk State Pedagogical University, Berdyansk, Ukraine,

<sup>2</sup> National University of Life and Environmental Sciences of Ukraine, Kiev, Ukraine

In this work we obtained of porous layers on single-crystal GaP by electrochemical etching in various acid solutions. Obtained current voltage characteristics of the etching process, and was established the value of pore formation for various acidic media.

For this experiment, we took samples of a single crystal of gallium phosphide doped with tellurium to a carrier concentration  $n = 1 \cdot 10^{17} \text{ cm}^{-3}$ . Etching was carried out on the plane (100). Parameters of the experiment is shown in table number 1.

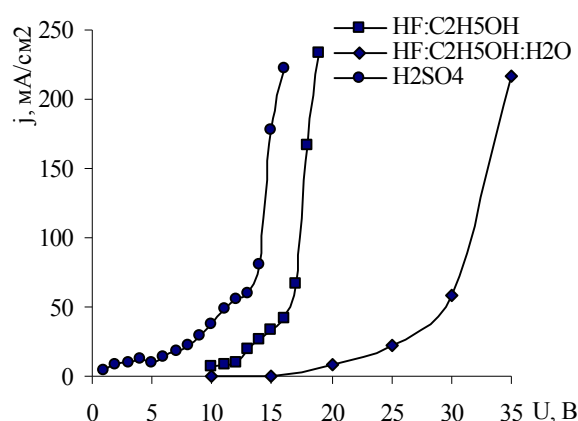
Table 1

Parameters of the experiment

Solution	Value substances	Time of digestion (min)
HF:C <sub>2</sub> H <sub>5</sub> OH	1:1	10
HF:C <sub>2</sub> H <sub>5</sub> OH:H <sub>2</sub> O	1:2:1	10
H <sub>2</sub> SO <sub>4</sub> :H <sub>2</sub> O	1:1	10

After creating a porous structure have been studied the chemical composition of the surface, and found that the percentage of impurities is about one percent. This indicates a high resistance to oxidation of GaP. [1]

Fig. 1 shows the current voltage characteristics of the etching process in various acidic media. Making the analysis of findings we can follow conclusions, which the voltage the beginning of the process of pore formation is 16-17 V for the solution of is HF: C<sub>2</sub>H<sub>5</sub>OH, 26-27V for the solution of is HF:C<sub>2</sub>H<sub>5</sub>OH:H<sub>2</sub>O, 13-14V for the solution of is H<sub>2</sub>SO<sub>4</sub>:H<sub>2</sub>O. If we increase the voltage to a value higher than the beginning of pore formation voltage then is activated growth of pores in a monocrystal volume.



1. Заварицкая Т.Н., Караванский В.А., Квит А.В., Мельник Н.Н. Исследования структуры пористого фосфида галлия // ФТП. – 1998, – Т. 32, №7. – С. 235-240.



## **Problems of metrology and standardization in nanotechnologies**

Zatirka O.I., Ilchenko V.V

*Taras Shevchenko Kiev University, Kiev, Ukraine*

Nanotechnologies standards of the leading countries in these fields are reviewed. Methods that verify the test subject is nanotechnology also were treated. Suitability of such methods using was proved. The analysis of standards correlation of different countries was performed.

Nanotechnologies are one of the most perspective and fast-developing branch of modern physics. That's why it is necessary to develop standards, which suggest criteria for physical parameters of subjects, which can be nanotechnology. It's necessary to assign modern and progressive branches of nanotechnologies, which must be standardized. The most precise equipment, which allows performing nanoscale (1nm to 100nm) measurements are AFMs, STMs and SEMs. Therefore standards for calibration this devices and standards for samples, which can be used in calibration was developed in USA [1]. Japan [2], Russia [3] and Germany [4] also developed similar standards. Besides, European Association of National Metrology Institutes exists [5]. It's necessary to understand which physical parameters influence the parameters of research class subjects and which experimental methods can be used for this subjects researching. Usually the special terminology base and methods should be developed for standard creation. The class of subjects for which this standard can be used should be determined too. The methods and recommended equipment must satisfy measurements accuracy rating and give determine information about belonging of developed subject to nanotechnology. Standards must control required confidence interval and deviations of measures and control ambient conditions during experimental procedure. Additionally, standard must contain measuring and calculating techniques for testing of developing subject.

1. ANSI Establishes. Nanotechnology Standards Panel, New York, August 5, 2004
2. [www.astm.org/Standards/E2490.htm](http://www.astm.org/Standards/E2490.htm)
3. <http://nicpv.ru/>
4. Wilkening, G., Koenders L. (eds.). Nanoscale Calibration Standards and Methods // Wiley-VCH. – 2005. – Weinheim, Germany.
5. [www.euramet.org](http://www.euramet.org)

ЗМІСТ

ПЛЕНАРНІ ДОПОВІДІ  
PLENARY SESSIONS

<b>Ahiska R., Ahiska G.</b> TEPAS Computer Controlled System for Measuring Parameters of Semiconductors in Real Thermoelectric Modules	9
<b>Aksimentyeva O., Opaynych I., Dyakonov V., Piechota S., Horbenko Yu., Szymchak H.</b> Ppolymer – magnet nanosystems	10
<b>Babanly M., Imamaliyeva S.Z., Yusibov Yu.A., Sadiqov F.M.</b> New ternary compounds $Tl_9LnTe_6$ type and variable composition phases on their base	11
<b>Baranskii P.I., Gaidar G.P.</b> Evolution of the Predictable Applications of Nanoobjects in the Field of Thermoelectricity	12
<b>Belyaev A.E., Boltovets N.S., Konakova R.V., Kudryk Ya.Ya., Milenin V.V.</b> Diffusion barriers in ohmic contacts to semiconductor device structures	13
<b>Berceshchuk M., Bojko M., Kryskov A., Kryskov Ts., Lyuba T., Rachkovsky O., Turnickyj V.</b> Strain-Resistance Effect in the Thin-Films of Cadmium and Germanium Tellurides. ( <i>V. Lashkaryov Institute of Semiconductor Physics, NAS of Ukraine, Kyiv, Ukraine; State Enterprise Research Institute "Orion", Kyiv, Ukraine</i> ). [179]	14
<b>Bercha D.M., Bondar V.M., Solonchuk L.S., Kharkhalis L.Yu., Shenderovskij V.A.</b> Non-Standard Dispersion Law for Charge Carriers in Highly Anisotropic and Layered Semi-Conductors and Related Effects	15
<b>Bilozertseva V.I., Khlyap H.M., Mamalui A.O., Dyakonenko N.L., Gaman D.O., Petrenko L.G.</b> Al-Bi-CVI thin films as gas sensors: structural, optical and electrical investigations	16
<b>Blonskyi I.V., Dmitruk I.M., Dmytruk A.M., Zubrillin N.G., Yeshchenko O.A., Kadan V.M., Korenyuk P.I., Pavlov I.A., Alexeenko A.A.</b> Induced Anisotropy Y of Surface Plasmon Optical Response in Spherical Noble Metal Nanoparticles in The Field of Powerful Femtosecond Pulses	18
<b>Bogach V.N., Dynich R.A., Zamkovets A.D., Ponyavina A.N.</b> Modification of absorption spectra of organic semiconductor thin films dopped with plasmonic nanoparticles	19
<b>Boichuk V.I., Bilyns'kyi I.V., Leshko R.Ya</b> Exciton and Impurity States in Quantum Dot Heterosystems	20
<b>Boltaev A.P., Bothe K., Kazaryan S.A., Krotova K.E., Pors A., Protsenko I.E., Pudonin F.A., Sherstnev I.A., Starodubtsev N.F., Uskov A.V., Willatzen M.</b> Metal Nano-Particles in the Applications for Photovoltaic, Light Emission and Microelectronic: Experiments and Theory	21
<b>Brodyn M., Volkov V., Lyakhovetsky V.</b> Nonlinear optical response and its dynamics of island gold films under femtosecond laser pulses excitation	23
<b>Budzhak Ya.S., Zub O.V.</b> Effect of Seebeck in thin crystalline films of Ge p-type conductivity	24
<b>Bulat L.P., Asach A.V., Nefedova I.A., Kozavkin D.O.</b> Accompanying Thermoelectric Phenomena at Operation of Micro- and Nanoelectronic Elements	25
<b>Davydyuk G.Y., Myronchuk G.L., Bozhko V.V.</b> Particularities of the formation and annealing of nano-size defect clusters in CdS single crystals irradiated with 1 MeV neutrons	26

<b>Dmitruk N.L., Korovin A.V., Malynych S.Z., Mamontova I.B.</b> Plasmonic Thin-Film Solar Cells With Enhanced Efficiency	26
<b>Druzhinin A.A., Maryamova I., Kutrakov A., Liakh-Kaguy N.</b> Silicon Whiskers for Sensor Electronics	29
<b>Freik D.M.</b> Quantum-size effects in nanostructures condensed matter	30
<b>Gasanzade S.G., Staryj S.V., Strikha M.V., Tetiorkin V.V., Shepelskii G.A.</b> Photosensitive MBE structures Cd <sub>x</sub> Hg <sub>1-x</sub> Te/CdTe/GaAs: determination of the parameters, finding of the unusual acceptor states	32
<b>Gayvoronsky V.Ya., Brodyn M.S., Kopylovsky M.A., Rostotskiy A.I., Yatsyna V.O., Golovan L.A., Tselikov G.I., Timoshenko V.Yu.</b> Effect of oxidation and porosity on nonlinear optical response of mesoporous silicon films	33
<b>Gotra Z.Yu.</b> Elements and optoelectronic devices based on organic materials	34
<b>Grigorchuk N.I., Tomchuk P.M.</b> Optoacoustical Effects in the Dielectric Media with a Metallic Nano-inclusions	35
<b>Grin'ko D.O., Barabash M.Yu, Kunitsky Yu.A., Vlaykov G.G.</b> Templates as instrument of nanotechnology	36
<b>Gurevich Yu.G.</b> Transport and recombination, new boundary conditions and perspectives	37
<b>Ivanitsky V.P., Sabov V.I.</b> Lacks of radial distribution functions method in electron diffraction of amorphous films and nanosystems	38
<b>Karachevtseva L., Kuchmii S., Lytvynenko O., Sizov F., Stronska O., Stroyuk A.</b> Electro-optical effects in 2D macroporous silicon structures with surface nanocrystals	39
<b>Kidalov V.V., Suchikova J.A., Konovalenko A.A., Sukach G.A.</b> Obtain and application of porous A <sup>3</sup> B <sup>5</sup> compounds	40
<b>Kiryanov A., Ali M.</b> IR Fourier-transform spectroholography of the light's scattering by twodimensional crystals	41
<b>Konstantinovich A.V., Konstantinovich I.A.</b> Oscillations in radiation spectrum of system of electrons moving in spiral in transparent medium	42
<b>Kopach G.I., Khrypunov G.S., Meriuts A.V., Deyneko N.V.</b> Influence of Back Contact on CdTe Thin Film Solar Cells Efficiency	43
<b>Korbutyak D.V., Kovalenko O.V.</b> Light-emitting properties of A <sup>2</sup> B <sup>6</sup> nanocrystals in colloidal solution and solid-state matrices	45
<b>Kovalenko A.V., Korbutyak D.V., Tishchenko V.V.</b> Using of Single Quantum Well Structures and Superlattices Based on The A <sub>2</sub> B <sub>6</sub> Compounds in a Modern Laser Systems	46
<b>Kovalyuk Z.D., Bakhtinov A.P., Vodop'yanov V.N., Netyaga V.V.</b> Spin-dependent tunneling in hybrid "ferromagnetic – layered semiconductor" AuNi - Ga <sub>2</sub> O <sub>3</sub> - p- GaSe heterostructures with carbon encapsulated Ni nanoparticles embedded in Ga <sub>2</sub> O <sub>3</sub>	48
<b>Lashkarev G.V., Karpyna V.A., Lazorenko V.I., Ievtushenko A.I., Khranovskyy V.D., Shteplyuk I.I., Demydyuk P.V., Myroniuk D.V., Yaremko A.M. and Yakimova R.</b> Films and Nanostructures for Optoelectronics Based on ZnO	49
<b>Lepikh Ya., Gordienko Yu., Druzhinin A., Evtukh A., Lenkov S.</b> Silicon nanowires, nanostructured and nanoporous silicon as materials for new generation sensors	51
<b>Litovchenko V.G., Strikha M.V.</b> The Modified Graphene – New Type of	52

Semiconductor Films	
<b>Lutsyk V.V.</b> Constitutional Diagrams with Kinematical and Minimal Surfaces for Heterogeneous Design	53
<b>Makhniy V.P., Khusnutdinov S.V.</b> Specific features of isovalent-substituted zinc oxide layers	54
<b>Malashkevich G.E., Khottchenkova T.G., Kouhar V.V., Sigaev V.N., Pestryakov E.V.</b> CeO <sub>2</sub> :Ln-containing nanostructures in oxide matrixes: spectroscopy, photophysics and technology	56
<b>Matveeva L.A., Neluba P.L., Venger E.F.</b> Technology and Physical Properties of the Heterosystems With C <sub>60</sub> Fullerenes	58
<b>Meglei D.</b> Some Properties of PbTe and Bi <sub>2</sub> Te <sub>3</sub> Crystals and Converters on Their Basis	60
<b>Myronyuk I.F., Gergel T.V., Danylenko M.I., Chelyadyn V.L.</b> Atomic Structure of Fumed Silica Nanoparticles	61
<b>Naidich Y.V., Gab I.I., Kostyuk B.D., Stetsyuk T.V., Dukarov S.V., Kryshchal A.P., Lytvin O.S.</b> Kinetics of dispergation and coagulation during annealing on air of silver nanofilms which were deposited onto oxide materials	63
<b>Ostafiychuk B.K.</b> Nanomaterials in accumulation and generation of energy devices	64
<b>Ostafiychuk B.K., Kotlyarchuk B.K., Popovych D.I., Serednytski A.S.</b> Nanoparticle formation by pulsed laser ablation	67
<b>Ostrovskaya L.Yu., Ralchenko V.G., Bolshakov A.P., Vlasov I.I., Kulakova I.I.</b> Surface engineering to enhance hydrophobic/hydrophilic properties of diamond films	68
<b>Peleshchak R.M., Kuzyk O.V., Dan'kiv O.O., Uhryn Y.O., Kostiv A.M.</b> Change of the direction of radiation of heterolaser with quantum dots under the influence of acoustic wave	69
<b>Perekrestov V.I., Kshnyakin V.S.</b> Interdependent dissipative and conservative self-organization in self-assembly of low-dimensional 3D systems	70
<b>Pors A., Uskov A.V., Willatzen M., Protsenko I.E.</b> Numerical Simulation of Nanoplasmonic Antireflection Coatings for Solar Cells	71
<b>Protsenko I.Yu., Tyschenko K.V.</b> Strain Deformation Properties of Film Materials: the Problem, Achievements and Prospects of Investigations	72
<b>Protsenko S.I.</b> Physical Processes in Multilayer Films and Spin-Valve Structures	73
<b>Ptashchenko O.O., Ptashchenko F.O.</b> Gas Sensors on p-n Junctions: Problems and Prospects	74
<b>Rubish V.M., Guranich O.G., Gorina O.V., Rigan M.Yu., Gera E.V., Guranich P.P., Azhniuk Yu.M., Gomonnai A.V.</b> Formation of needle-like crystal inclusions SbSI in the bulk and film glassy matrix	76
<b>Schwarzl T., Eibelhuber M., Hochreiner A., Groiss H., Kolkovsky V., Karczewski G., Wojtowicz T., Heiss W., Springholz G.</b> Epitaxial IV-VI quantum dots for mid-infrared devices	77
<b>Shirinyan A.S., Bilogorodskyy Y.S.</b> The influence of thickness of solid metallic nanofilm on its physico-chemical properties	79
<b>Shpilevsky E.M.</b> Physics of Thin Films: Theoretical Basis of Big Science on Nanomaterials	80
<b>Sklyarchuk V.M., Sklyarchuk O.V., Rarenko I.M., Dremlyuzhenko S.G.</b> Photoelectric properties of metal—semi-insulating CdTe barrier structures	82

<b>Stasyuk Z.V., Bihun R.I.</b> Quantum electron transport in ultra thin metal films	<b>83</b>
<b>Studenyak I.P., Miklosh N.Yu., Vorohta M., Matolin V., Cserhati C., Kőkényesi S.</b> Deposition, structural and optical properties of Cu <sub>7</sub> GeS <sub>5</sub> I thin films	<b>85</b>
<b>Sukach G.A., Bogoslovskaya A.B.</b> Colloidal semiconductor quantum dots light-emitting devices	<b>86</b>
<b>Tkach M., Seti Ju., Voitsekhivska O.</b> Transport properties of complicated resonance tunnel nanosystems	<b>87</b>
<b>Tsybulskaya L.S., Gaevskaya T.V., Purovskaya O.G.</b> Composite nickel-boron-nanodiamond coatings and there physical and mechanical properties	<b>88</b>
<b>Venger E.F., Ievtushenko A.I., Davidenko S.M., Melnichuk L.Yu., Melnichuk O.V.</b> IR spectroscopy investigation of polaritons in ZnO films located in a uniform magnetic field	<b>89</b>
<b>Vengrenovich R.D., Ivanskii B.V., Yarema S.V.</b> On mechanism of nanocluster growth	<b>90</b>
<b>Voropay E., Ermalitskaya K.</b> Control of layer thickness during laser spectral analysis of micron and submicron metal coatings	<b>92</b>
<b>Yuzepovich O.I., Bengus S.V., Mikhailov M.Yu., Fogel N.Ya.</b> Interfacial Superconductivity of A <sup>IV</sup> B <sup>VI</sup> Semiconductor Heterostructures	<b>93</b>
<b>Zaulychnyy Ya.V.</b> Crystal-chemistry dependence of the energetic redistribution of the valence electrons and experimental evaluation of changes of the band energy of materials due to their dispersion to nanosizes	<b>95</b>
<b>Zayachuk D.M., Slobodskyy T., Astakhov G.V., Slobodskyy A.</b> Magnetic field dynamics of the photoluminescence bands of the semimagnetic quantum structures based on <i>ZnSe</i>	<b>96</b>
<b>Zinchenko V.F.</b> Regularities of Optical Properties of Complex Metal Chalcogenides in Crystalline, Glass-Like and Thin-Film States	<b>98</b>

### Секція 1

**Технологія тонких плівок (метали, напівпровідники, діелектрики, провідні полімери) і методи їх дослідження**  
(усні доповіді)

### Session 1

**Thin films technology (metals, semiconductors, dielectrics, conductive polymers) and their research methods**  
(oral)

<b>Beketov G.V., Ushenin Yu.V., Rengevych O.V.</b> Surface plasmon resonance techniques for in situ control of underpotential Te deposition on polycrystalline Au surface	<b>100</b>
<b>Belyaev A.E., Boltovets N.S., Vitusevich S.A., Ivanov V.N., Konakova R.V., Lebedev A.A., Milenin V.V., Sveshnikov Yu.N., Sheremet V.N.</b> Effect of microwave radiation on the properties of ohmic contacts to the n <sup>+</sup> -n-n <sup>+</sup> -GaN–Al <sub>2</sub> O <sub>3</sub> structures	<b>101</b>
<b>Brus V.V.</b> Optical properties of a DC magnetron sputtered TiO <sub>2</sub> thin film	<b>102</b>
<b>Chukhnenko P.S., Tomashik Z.F., Ivanitska V.G., Tomashik V.M.</b> Chemical etching of doped by IV <sup>th</sup> group impurities CdTe single crystals using (NH <sub>4</sub> ) <sub>2</sub> Cr <sub>2</sub> O <sub>7</sub> –HCl aqueous solutions	<b>103</b>
<b>Ermalitskaya K.</b> Double pulse laser quantitative layer-by-layer analysis of brass	<b>104</b>

and bronze micron coatings	
<b>Garpul O.Z., Solovko Y.T.</b> Detection of growth impurities in the YIG films by optical methods	105
<b>Harbachova A.N., Malashkevich G.E., Freik D.M.</b> Effect of heat treatment on infrared reflection, surface structure and chemical composition of PbTe films	106
<b>Ievtushenko A.I., Lashkarev G.V., Lazorenko V.I., Khyzhun O.Y., Klochkov L.O., Bykov O.I., Tkach V.M., Kutsay O.M., Starik S.P.</b> Nitrogen and aluminum doping of ZnO films by magnetron sputtering of Zn targets containing different amount of Al	107
<b>Kladko V.P., Kuchuk A.V., Safriuk N.V., Belyaev A.E.</b> The channels of strain relaxation in InGaN/GaN and AlN/GaN multilayer structures	108
<b>Klyui N.I., Lukyanov A.N., Severinova I.D., Kolomzarov Yu.V., Khripunov G.S., Klyui A.N., Staschuk V.S.</b> Application of diamond-like carbon films as antireflection coatings for thin film solar cells	109
<b>Kudryk Ya.Ya.</b> Investigation of p-n junction temperature and thermal parameters of semiconductor devices	110
<b>Kutsay O.M., Novikov M.V., Gontar O.G., Starik S.P., Gorohov V.Yu., Garashchenko V.V., Tkach V.M.</b> Present state of the art of amorphous carbon films	111
<b>Novytskyi S.V.</b> Effect of thermal annealing on the electrical parameters of ohmic contacts to n-n <sup>+</sup> -n <sup>++</sup> -InP	112
<b>Oksanich A.P., Petrenko V.K., Sedin Y.A.</b> Analysis of deformation and stress in silicon single – layer epitaxial structures	113
<b>Oksanich A.P., Pritchyn S.E.</b> Method of undestroying control of remaining stresses in single – layer epitaxial structures	114
<b>Pavlovich I.I., Tomashik V.M., Tomashik Z.F., Stratiychuk I.B., Kravtsova A.S., Kopyl O.I.</b> Controlled elimination of thin layers from the surfaces of Bi and Sb chalcogenides by (NH <sub>4</sub> ) <sub>2</sub> Cr <sub>2</sub> O <sub>7</sub> -HBr solutions	115
<b>Pylypiv V.M., Vladimirova T.P., Kyslovskyy Ye.M., Olikhovskii S.I., Garpul O.Z.</b> Simulation of the defect structure of single crystal gadolinium gallium garnet, with the help of statistical dynamical theory of scattering	116
<b>Semikina T.V., Yaroshenko M.V., Bobrenko Yu.N., Paszkowicz W., Minikayev R., Komashchenko V.N., Sheremetova G.I.</b> Studying of hot wall epitaxy technological parameters and current mechanism investigation of II-VI thin film heterostructures	117
<b>Shtepliuk I.I., Lashkarev G.V., Khyzhun O.Yu., Kowalski B., Reszka A., Lazorenko V.Y., Timofeeva I.I., Khomyak V.V.</b> The effect of the isovalent doping with cadmium on the microstructure and UV cathodo-luminescence of the ZnO films	119
<b>Slusar T.V., Legkova G.V., Ponomarev S.S., Sobolev V.B., Grebenshchikov D.V., Sushchenko O.N.</b> Investigation of features of thin-films by electron-probe microanalysis and auger-electron spectroscopy	120
<b>Syrotyuk S.V., Shved V.M.</b> The electronic densities of states in PbTe crystal doped with Eu. ( <i>National University Lviv Polytechnic, Lviv, Ukraine</i> ). [164]	121
<b>Vinogradov A.O., Lichman K.A., Sheremet V.N.</b> Investigation of the electrical characteristics of ohmic contacts to Si- and SiC-based thin-film structures	122
<b>Yatsyshyn M.M., Boychyshyn L.M., Demchyna I.I., Pandyak N.L.</b> Structure of the polyaniline films on the amorphous metallic alloy Al <sub>87</sub> Ni <sub>8</sub> Y <sub>5</sub>	123

**Секція 1**

**Технологія тонких плівок (метали, напівпровідники, діелектрики, провідні полімери) і методи їх дослідження**  
(стендові доповіді)

**Session 1**

**Thin films technology (metals, semiconductors, dielectrics, conductive polymers) and their research methods**  
(poster)

<b>Avramenko K., Strelchuk V., Bryksa V., Lytvyn P., Morhain C., Deparis C., Tronc P., Pashchenko V., Bludov O.</b> Ferromagnetism in Co-doped ZnO films: micro-Raman and magnetic studies	125
<b>Bobik M.Yu.</b> Analysis of electron microscope images of amorphous films	126
<b>Bobyk M.Y., Svatyuk O.Y.</b> Research of the contrast of the micro electronic images of the amorphous tapes	127
<b>Borkach E.I., Ryaboschuk M.M.</b> Effects of smoothed factor in radial distribution functions method for amorphous films	129
<b>Burlak G.M., Vilinskaya L.N.</b> Features thermostimulated luminescence of aluminum oxide films	130
<b>Chaviak I.I.</b> The processes of growth of nanoscale structures SnTe on the mica substrate	131
<b>Chekaylo M.V., Ukrainets V.O., Ukrainets N.A., Voytovich Ya.M.</b> Phase Transformations and Mechanisms of Synthesis for Compounds of $Ag_8XSe_6$ (X = Si, Ge, Sn) Argyrodite Family	132
<b>Denysenko O.I., Tsotsko V.I.</b> Research into Injection Structure Formation of a Thin Electrode Strip Composite Layer Research into Injection Structure Formation of a Thin Electrode Strip Composite Layer	133
<b>Druzhynin A.O., Kogut I.T., Khoverko Yu.M., Koretskii R.M.</b> Influence of dispersion of polysilicon on low-temperature conductivity in SOI structures	134
<b>Dyachyn's'ka O.M., Lytvyn P.M., Trunov M.L., Aleksyeyeva T.A., Prokopenko I.V.</b> SPM force spectroscopy for testing adhesion and mechanical properties at nanolevel	135
<b>Efremov A.A., Lytvyn P.M., Prokopenko I.V.</b> Diagnostics of nanoscale roughened surface by AFM spectroscopy of capillary forces	136
<b>Fedosov S.N., Sergeeva A.E.</b> How to improve TSD method for studying relaxation processes in dielectric films	137
<b>Fedosov S.N., Sergeeva A.E., Revenyuk T.A.</b> Poling of NLO polymer films in corona during their solidification	138
<b>Grigorov S.N., Taran A.V., Timoshenko A.I.</b> Low-temperature preparation of $CuInSe_2$ thin films with annealing in two-step vacuum-arc discharge	139
<b>Gvozdiiyevskiy Y.Y., Tomashik V.M., Tomashik Z.F., Seritsan M.V., Denysyuk R.O.</b> Interaction of CdTe and $Cd_{1-x}Zn_xTe$ and $Cd_xHg_{1-x}Te$ solid solutions with $HNO_3$ -HI-tartaric acid system solutions	140
<b>Handetsky V.S., Tonkoshkur Yu.A.</b> Determination of conductivity of thin metal films using eddy current method	141
<b>Ievtushenko A.I., Lazorenko V.I., Horvath Zs.J., Lashkarev G.V., Dusheyko M.G., Baturin V.A., Karpenko A.Y.</b> Features of the properties for	142

photodetectors with vertical integration based on ZnO	
<b>Ilchenko V.V., Telega V.M., Lushkin O.E., Kovalenko V.S.</b> Auger-spectroscopic investigation of SnO <sub>2</sub> films with different thickness	143
<b>Ivanitsky V.P., Sabov V.I.</b> Lacks of radial distribution functions method in electron diffraction of amorphous films and nanosystems	144
<b>Ivanytska G.M., Rubish V.M.</b> Applicability of RDF method for amorphous thin films	145
<b>Keeprich V.I., Kornich G.V.</b> Molecular dynamics method for calculation of the metal film deposition	146
<b>Kiryanov A.P., Kachurin Yu.Yu., Shapkarin I.P.</b> To the birefringency's measuring of the uniaxial nanofilm	147
<b>Kizjak A., Evtukh A., Pedchenko Yu.</b> Technological peculiarities of nanocomposite SiO <sub>x</sub> and SiO <sub>2</sub> (Si) films obtaining by LP CVD method	148
<b>Kopach G.I., Klochko N.P., Volkova N.D., Lyubov V.M., Momotenko O.V., Kopach A.V., Kharchenko M.M., Novikov V.O.</b> Electrodeposition of thin film precursors for CIS based solar cells	149
<b>Kornyushchenko A.S.</b> Regularities of porous copper and aluminium micro and nanostructures formation under conditions of quasi-equilibrium steady-state condensation	150
<b>Kovalenko O.V., Ogol V.O., Polozov K.Yu.</b> Investigation of the photoluminescence spectra and crystal structure of epitaxial ZnO layers grow by the vapor phase epitaxy on GaAs(100) substrates	151
<b>Kurbatov D.I., Kshnyakina S.I., Opanasyuk A.S., Danilchenko S.M.</b> Structural characteristics of II-VI diluted magnetic semiconductor films	152
<b>Kurilo I.V., Ilchuk H.A., Lukashuk S.V., Rudyi I.O., Ukrainets V.O., Chekaylo M.V.</b> Fabrication, morphology and structure of polycrystalline CdTe layers	153
<b>Lashkarev G.V., Yaremko A.M., Karpyna V.A., Strelchuk V.V., Kolomys O.F.</b> Experimental observation and theoretical analysis of multi-phonon excitations in ZnO textured films	154
<b>Lutsyk N.Yu.</b> Conditions for forming amorphous thin films of the GaSb-Sn system	155
<b>Lytvyn O.S., Lytvyn P.M., Korchovyi A.A., Litvin Yu.M., Prokopenko I.V.</b> Atomic force microscopy 3D metrology for assessment surface topography	156
<b>Makarov A.V., Boyko V.G., Zayats M.S., Zayats S.M., Lozinskii V.B., Gorbulik V.I.</b> Electrophysical properties of AlN obtained by high-frequency reactive magnetron sputtering	157
<b>Meshalkin A., Andries A., Achimova E., Bets L., Kryskov Ts., Optasyuk S.</b> Properties of thin photosensitive polymer films obtained by spin-coating technique	158
<b>Myroniuk D.V., Lashkarev G.V., Lazorenko V.Y., Karpyna V.A.</b> Effect of radiation defects on properties of films and nanostructures based on ZnO	159
<b>Mytsyuk B.M., Nevdacha V.V., Pogorily A.M.</b> Preparation of chromium dioxide thin films by hydrothermal synthesis	160
<b>Novosyadly S., Voznyak Yu., Sorokhtey T.</b> Mobility in semi-insulating GaAs doped compensating oxygen and chromium impurities	161
<b>Novosyadly S.P., Voznyak Yu.V., Sorokhtey T.R., Daniluk O.V., Fryk O.B.</b> Physical and technological aspects of forming structures of gallium arsenide technology logic to selectively doped field-effect transistor (SDFT)	162



<b>Polishchuk S.G., Zadorozhniy V.G., Kobrin V.L.</b> Temperature dependence of the dielectric characteristics of thin polymer films deposited in vacuum	163
<b>Prykhodko A.V.</b> Silicon nitride film-edge induced strain distribution in silicon crystal substrate	164
<b>Sergeeva A.E., Fedosov S.N.</b> Distribution of polarization in corona poled P(VDF-TFE) films	165
<b>Sergeeva A.E., Revenyuk T.A., Fedosov S.N.</b> Anomalous stability of the surface potential in corona-charged PVDF films	166
<b>Sinyugina A.T., Savchenko I.A., Studzinskij S.L., Kolendo O.Yu.</b> The influence of the structure of polycomplexes with cobalt on their electro-optical properties	167
<b>Sokolov O.L., Potyak V.Yu.</b> Influence of technological factors in the method of hot-wall on the process of thin films of CdTe	168
<b>Travkin V.M., Pakhomov G.L.</b> Subphthalocynine based multilayer photovoltaic cells	169
<b>Tsotsko V.I., Denysenko O.I.</b> Forming a thin layer of composite metal band in the periodic energy action	170
<b>Tsybul'skaya L.S., Purovskaya O.G., Poznyak S.K., Gaevskaya T.V.</b> Structure and properties of electrochemically deposited Zn-Ni alloy coatings	171
<b>Turiev A.Y., Butkhuzi T.G., Ramonova A.G., Magkoev T.T., Nsideeva N.I.</b> Modification of surface morphology of the metalphthalocyanine films by laser irradiation	172
<b>Yurkov G.Yu., Fionov A.S.</b> A synthesis and study of the rhenium-containing nanoparticles in polyethylene matrix	173
<b>Zadorozhniy V.G., Polishchuk S.G., Kobrin V.L.</b> Crystallinity of deposited in vacuum thin polymer films studied by methods of differential thermal and thermogravimetric analysis	174
<b>Zadorozhniy V.G., Polishchuk S.G., Kobrin V.L.</b> Permolecular structure of heterogeneous-chain thin polymer films deposited in vacuum	175
<b>Zapukhlyak R.I., Terletskiy A.I., Tkachuk A.I.</b> Methods for determining the parameters of thermoelectric semiconductors	176
<b>Zharkov I., Korotash I., Rudenko E., Safronov V., Khodunov V.</b> The method of radiowave non-destructive monitoring of film protective coatings and low-temperature device for its application	177

## Секція 2

### Нанотехнології, наноматеріали і квантово-розмірні структури (усні доповіді)

## Session 2

### Nanotechnologies and nanomaterials, quantum-size structures (oral)

<b>Antanovich N.A., Kravchenko V.I., Gorbatshevich G.N., Struk V.A., Voropaev V.V.</b> Nanocomposites based on polytetrafluoroethylene with different modification hierarchy	179
<b>Auchynnikau Y.V., Kravchenko V.I., Struk A.V., Antanovich N.A., Andrikevich V.V.</b> Nanocomposite and nanophase coatings based on fluorine-	180

containing components	
<b>Balitskii O.A.</b> Hydrogen-induced effects in nano-crystalline GaSe and InSe layers	181
<b>Bilyns'kyi I.V., Shevchuk I.S.</b> Exciton stokes shift in the quantum dot with degenerated band spectrum	182
<b>Borcha M., Balovsyak S., Garabazhiv Ya., Fodchuk I., Tkach V.</b> Possibilities of Kikuchi diffraction in researches of multilayer nanoscaled systems	183
<b>Bushkova V.S.</b> Dielectric characteristics in solid solutions $(1-x) \text{NiAl}_{0,5}\text{Fe}_{1,5}\text{O}_4 - x \text{BaTiO}_3$	184
<b>Bushkova V.S., Kopayev A.V.</b> Thermal analysis of nickel-aluminum ferrits	185
<b>Chundak M., Veltruská K., Václavů M., Vorokhta M., Khalakhan I., Matolínová I., Matolín V.</b> Characterization of sputtered Ag-CeOx thin films	186
<b>Dan'ko V.A., Michailovska K.V., Indutnyi I.Z., Shepeliavyi P.E.</b> Photoluminescence decay dynamics of silicon-based light-emitting nc-Si-SiOx structures	187
<b>Danylenko M.I., Chernega S.M., Mameka N.O., Velychko A.</b> Structure and hardness of worn layer	188
<b>Dovbeshko G.I., Fesenko O.M., Gnatyuk O.P., Yakovkin K.I., Rynder A.D.</b> Enhancement of optical signals from molecules adsorbed on single wall carbon nanotubes	189
<b>Fodchuk I.M., Kazemirskiy T.A., Zaplitnyy R.A., Gutsuliak I.I., Pietsch U., Davydok A.V., Pashniak N.V., Bonchuk O.Y., Savitskiy G.V., Syvorotka I.I., Yaremiy I.P.</b> Structural changes in iron-yttrium garnet implanted by nitrogen ions	190
<b>Goltvyanskyi Ju., Khatsevich I., Melnik V., Nikirin V., Popov V., Oberemok O.</b> Light emitting structures with silicon nanoclusters into the silica matrix	191
<b>Gorbanyuk T.I., Litovchenko V.G., Solntsev V.S., Mysakovych T.S., Stasyuk I.V.</b> Catalytic and adsorption properties of porous silicon with metallic nanoinclusions	192
<b>Gordienko S.O., Rusavsky A.V., Vasin A.V., Litvin P.M., Yukhimchuk V.A., Nazarov A.N., Lysenko V.S.</b> Fabrication technology of graphene films on dioxide silicon layer and their properties	193
<b>Goriachko A., Melnik P.V., Nakhodkin M.G.</b> Quantum size effect in submonolayer Bi films on Ge(111)	194
<b>Grygorchak I.I., Pokladok N.T., Ivaschyshyn F.O., Lukiyanets B.A., Bishchaniuk T.M.</b> Supramolecular assemblies with periodically modulated topology of the guest component and problem creating of electric generator and nanoscale structurin	195
<b>Gryshchuk V.V., Boiko I.</b> Electrostatic potential and phonon modes in a multilayered quantum nanowells	196
<b>Kadan V.M., Blonskyi I.V., Indutnyi I.Z., Danko V.A., Korenyuk P.I.</b> Ultrafast carrier dynamics of silicon nanoparticles in fused silica	197
<b>Kalinina N.E., Vilischuk Z.V.</b> Refractory nanocompositions for modifying of aluminum alloys	198
<b>Khalakhan I., Vorokhta M., Fiala R., Matolin V.</b> SEM and AFM study of Pt-CeO <sub>2</sub> thin films prepared by magnetron sputtering for fuel cell applications	199
<b>Kisseluk M.P., Vlasenko O.I., Lyashenko O.V.</b> Spatial local fluctuations of a quantum yield in InGaN/GaN structure	200
<b>Klimovskaya A.I., Shanina B.D., Lytvyn P.M., Kalashnyk Iu.Iu., Kamins T.I.,</b>	201

<b>Sharma S.</b> Mechanical properties of ensembles of silicon nanowires grown on silicon substrate	
<b>Kosminska Yu.O., Mokrenko A.A., Dyoshin V.B., Perekrestov R.V.</b> Self-organization of Cu and Ni nanosystems during quasi-equilibrium condensation at magnetron sputtering	202
<b>Liopo V.A., Avdejchik S.V., Struk V.A., Vorontsov A.S., Mihajlova L.V., Eisymont Y.I., Andrikevich V.V.</b> Nanodimensionality criteria: physical justification and methodological calculations	203
<b>Liopo V.A., Sabutz A.V., Struk V.A., Avdejchik S.V., Sorokin V.G.</b> Hierarchy levels of real objects nanostate: physical models in the analysis methodology	204
<b>Lisovskyy I.P., Litovchenko V.G., Voitovych M.V., Zlobin S.O., Khatsevich I.M., Indutnyy I.Z., Shepelyavyi P.E.</b> Influence of thermal treatments on light emitting properties of porous nanocomposite films nc-Si/SiO <sub>2</sub>	205
<b>Luksha O.V.</b> Laser plasma techniques for nanoscale modified thin films production	206
<b>Lukyanov A.N., Khatsevich I.M., Romanyuk B.M., Yefanov V.S., Fomovskii F.V.</b> Optical properties of modified silicon dioxide layers with Si-nanoclusters	207
<b>Makoviychuk M.I.</b> Low frequency noise spectroscopy as a tool to study quantum-size structures	208
<b>Nikolaeva M., Aleksandrova G.</b> The electrization influence on molecular mobility of gold and silver nanocomposites based on polysaccharide arabinogalactan	209
<b>Novikov S.M., Struk A.Ya.</b> Features of X-wave diffraction image formation with clusters of edge dislocations	210
<b>Omelchenko S.A., Vorovsky V.Yu., Khmelenko O.V., Gorban A.A., Kushnir N.A.</b> Properties of nanoscale magnetic materials obtained with cryochemical synthesis	211
<b>Ponomaryov S.S., Yukhymchuk V.O., Valakh M.Ya., Dzhagan V.M., Yaremko A.M., Krasil'nik Z.F., Novikov V.A.</b> Study of elemental composition and morphology of SiGe-nanoislands by Raman spectroscopy and high-resolution SEM with local Auger spectroscopy	212
<b>Ruvinskii B.M., Ruvinskii M.A.</b> Influence of specular-difuse reflection mechanism for charge carriers on high-frequency intraband conductivity of straight-line graphene ribbons	213
<b>Ruvinskii M.A., Ruvinskii B.M.</b> Interband conductivity of straight-line graphene ribbon	214
<b>Ryskulov A.A., Struk A.V., Eisymont Y.I.</b> Nanophase transitions in metal-polymeric composites	215
<b>Shakleina I.O., Sokolnyk O.A.</b> Effect of quantum dot shape on the hole energy spectrum	216
<b>Stasyk M.O., Ivanskii B.V., Moskalyuk A.V.</b> Size distribution function of disc-like clusters in heterosystems	217
<b>Štetsovych O., Dvořák F., Steger M., Cherradi E., Matolínová I., Tsud N., Škoda M., Skála T., Mysliveček J., Matolín V.</b> Adjusting morphology and surface reduction of CeO <sub>2</sub> (111) thin films on Cu(111)	219
<b>Vengrenovich R.D., Fuchila I.Ya., Stasyk M.O.</b> Influence of cluster configuration on the size distribution function	220
<b>Venhryn B.Ya., Grygorchak I.I., Balaban O.V.</b> Carbon – supramolecular	221

ansambles for caracitive accumulation and faraday generation of energy

**Секція 2**

**Нанотехнології, наноматеріали і квантово-розмірні структури**

(стендові доповіді)

**Session 2**

**Nanotechnologies and nanomaterials, quantum-size structures**

(poster)

<b>Babanly M., Veliyeva G.M., Mashadiyeva L.F., Shikhiyev Yu.M.</b> Solubility of silver in glassy-like As <sub>2</sub> Se <sub>3</sub> and thermodynamic properties of glasses	223
<b>Barabash M.Yu., Vlaykov G.G., Grynko D.A., Kunitsky Yu.A.</b> Selective phase formation by the electrostatic template	224
<b>Boichuk V.I., Voronyak L.Ya., Voronyak Ya.M.</b> Polarization phonons in wurtzite quantum well wire GaN/ZnO/GaN/ZnO/GaN	225
<b>Boyko V.V., Gorelik V.S., Dovbeshko G.I., Moiseyenko V.N., Sobolev V.B., Fesenko O.M.</b> Secondary emission from synthetic opal infiltrated by colloidal gold and glycine	226
<b>Budzhak Ya.S., Zub O.V.</b> Statistics of charge carriers in thin crystalline films	227
<b>Budzulyak S.I., Ermakov V.M., Kalytchuk S.M., Korbutyak D.V.</b> Peculiarities of electroluminescence of CdTe nanocrystals incorporated into polymer films	228
<b>Bulat L.P., Nefedova I.A.</b> Modeling of Spark Plasma Sintering Processes at Fabrication of Bulk Nanostructured Samples	229
<b>Bydzulyak I.M., Rachiy B.I., Merena R.I., Mandzyuk V.I., Kuzyshyn M.M.</b> Genesis of porous carbon surface due to thermal activation	230
<b>Chernenko I.M., Zaets A.P., Olynyk O.Y., Miroshnik S.A.</b> Reception and determination of the refraction factor of nanodispersion particles of ammonium vanadite	231
<b>Direglazov A.Yu., Kaminskiy G.G., Kasatkin A.L., Moskalyuk V.A.</b> Dynamic magnetic response of normal metal and superconductor (YBa <sub>2</sub> Cu <sub>3</sub> O <sub>7-x</sub> ) thin films	233
<b>Druzhynin A.O., Khoverko Yu.M., Ostrovskii I.P., Nychkalo S.I., Nikolaeva A.A., Konopko L.A., Stich I.</b> Investigation of Ga-In contacts to Si and Ge wires for sensor application	234
<b>Dudnik E.V., Lashneva V.V., Shevchenko A.V., Ruban A.K., Matveeva L.A.</b> Effect of synthesis conditions on properties of nanocrystalline powders ZrO <sub>2</sub>	235
<b>Duplavyy V.Y., Shevchyk V.V., Pyrlja M.M., Boledzyuk V.B.</b> Insertion compounds of iodine and nano-graphite based on layered III-VI crystals	236
<b>Fartushynsky R.B., Voitsekhivska O.M., Shymanska Z.O.</b> Exciton spectrum renormalization due to the interaction with all types of phonons in open spherical QD	237
<b>Fedorchuk S.V., Zheltonozhskaya T.B., Kunitskaya L.R., Demchenko O.V.</b> Synthesis of Silver nanoparticles block- and graft copolymers and inorganic polymer substances in water solutions	238
<b>Fedorenkova L.</b> About boride layer structure on the aluminum surface	239
<b>Fedoriv V.D., Yaremiy I.P., Stashko N.V.</b> Synthesis of Polycrystalline Yttrium Iron Garnet the Sol-Gel Method with the Subsequent Annealing	240
<b>Fodchuk I.M., Fesiv I.V., Novikov S.M., Struk Ya.M.</b> Moire patterns of microscratches in silicon single crystals	241
<b>Freik D.M., Kharun L.T., Dobrovol'ska A.M., Kachmar A.</b> Quantum-size	242

effects in semiconductor structures

- Galiy P.V., Nenchuk T.M., Mazur P., Poplavskyy O.P., Buzhuk Ya.M.** Indium nanostructures formation on furrowed (100) surfaces of In<sub>4</sub>Se<sub>3</sub> layered semiconductor crystals 243
- Gayvoronsky V.Ya., Brodyn M.S., Kopylovsky M.A., Rostotskiy A.I. Uklein A.V., Yatsyna V.O., Konstantinova T.E., Lubenets V.A.** Photoinduced changes of transmittance in zirconia films stabilized with yttrium oxide 244
- Guba S.K., Kurilo I.V., Petrovich R.Y.** Modeling of the vapour phase epitaxial at low temperatures growth of the III-V hetero nanostructure layers by CVD-metod 245
- Gutsul I.V., Manyk O.M., Manyk T.O.** Peculiarities of the structure of chemical bond of cadmium 246
- Holovatsky V., Frankiv I., Makhanets O.** Charged impurities influence at energy spectrum and oscillator intensities of electron intra-band transitions in spherical quantum dot CdS/SiO<sub>2</sub> 247
- Hols'kyi V.B., Kubay R.Yu.** Optical properties of semiconductor materials with two-layer quantum dots 248
- Ilkiv B.B., Zaulychnyy Ya.V., Foja O.O., Dymarchuk V.O., Zarko V.I.** X-ray emission study of aerosils nanonaprticles with high porous carbon materials interaction 249
- Ivanichok N.Y., Budzulyak I.M., Lisovskiy R.P., Yaremiy I.P.** The effect of electrode material phase composition on specific energy characteristics of hybrid capacitors (*Vasyl Stephanyk Precarpatian National University*). [519] 250
- Kachalova N.M., Voitsekhovich V.S., Khomenko V.V., Pilgun R.V., Yatsenko L.P.** Possibilities of coherent supercontinuum source for nanoscale systems characterization 251
- Kalytchuk S.M., Korbutyak D.V., Khalavka Yu.B., Scherbak L.P.** Photoluminescence of CdTe nanocrystals in colloidal solution and polymer matrix 252
- Klym H., Hadzaman I., Shpotyuk O.** Integrated T/RH thick-film sensor elements based on nanostructured spinel-type ceramics 253
- Korbutyak D.V., Kryuchenko Yu.V., Sachenko A.V., Budzulyak S.I., Kalytchuk S.M.** Photocurrent features in MIS-structures with Si (CdTe) quantum dots 254
- Koziarskyi I., Marianchuk P.** Nano formations and zone parameters of crystals (3HgS)<sub>1-x</sub>(In<sub>2</sub>S<sub>3</sub>)<sub>x</sub> (x = 0,5), doped by manganese 255
- Kudrynskyi Z.R.** Surface topology of annealed and unannealed SnSe<sub>2</sub> crystals 256
- Kupchak I.M., Kalytchuk S.M., Korbutyak D.V.** Stokes shift in colloidal CdTe quantum dots 257
- Kysselyuk M.P., Vlasenko O.I., Myagchenko Yu.O., Sagan Ja.I., Lyashenko O.V., Veleschuk V.P.** Influence of injection level and temperature on the quantum yield and radiation spectrum of power InGaN/GaN light-emitting diodes 258
- Leshko R.Ya., Turyans'ka L.M.** Optical properties of a spherical quantum dot with a hydrogenic impurity 259
- Lysenkov E.A., Gomza Yu.P., Klepko V.V.** Features of structure and properties of polymer electrolytes based on polyethylene oxide and anisometric nanofillers 260
- Lysenkov E.A., Yakovlev Yu.V., Klepko V.V.** Percolation properties of the system based on polypropylene glycol and carbon nanotubes 261
- Lytvyn P.M., Lishchynskyy I.M., Bachuk V.V., Wojcik V.** Topology and 262

growth mechanisms nanostructures of lead telluride	
<b>Makhanets O., Tsiupak N., Holovatsky V.</b> Electron spectrum in complicated hexagon semiconductor nanotubes	263
<b>Maronchuk I.I., Petrash A.N., Smirnov S.B.</b> Energetic spectrum of electron in infinitely deep oblate ellipsoidal quantum dot	264
<b>Molodkin V.B., Olikhovskii S.I., Kyslovskyy Ye.M., Vladimirova T.P., Kochelab E.V., Reshetnyk O.V., Dovganyuk V.V., Fodchuk I.M., Lytvynchuk T.V., Klad'ko V.P., Swiatek Z.</b> Transformations of microdefect structure of silicon crystals after high-energy electron irradiation	265
<b>Mudry S., Kulyk Yu.</b> Structure features of nanocrystalization in Fe <sub>75</sub> Mo <sub>2.5</sub> Mn <sub>2.5</sub> Si <sub>6</sub> B <sub>14</sub> amorphous alloy	266
<b>Mudry S.I., Nykyruy Yu.S.</b> Effect of laser irradiation on magnetic properties of amorphous alloy Fe <sub>73.7</sub> Nb <sub>2.4</sub> Cu <sub>1.0</sub> Si <sub>15.5</sub> B <sub>7.4</sub>	267
<b>Neimet Yu.Yu., Studenyak I.P., Kis-Varga M., Cserhati C., Kökényesi S.</b> Structure of Cu <sub>6</sub> PS <sub>5</sub> I nanoceramics under the influence of sintering conditions	268
<b>Nikolaeva M., Aleksandrova G., Martynenkov A.</b> Polymer supramolecular structure influence on Metal/Polymer systems conductive properties	269
<b>Nikolenko A.S., Strelchuk V.V., Valakh M.Ya., Lytvyn P.M., Kladko V.P., Gudymenko O.Yo., Krasilnik Z.F., Lobanov D.N., Novikov A.V.</b> Peculiarities of planar self-ordering of SiGe nanoislands grown on strained Si <sub>1-x</sub> Ge <sub>x</sub> sublayers	270
<b>Novosyadliy S.P., Kindrat T.P.</b> The perspectives of the development of the Si and GaAs of high-speed digital large integrated circuits	271
<b>Optasyuk S.V., Zhuk A.G.</b> Luminescent properties of low-dimensional ZnS obtained by self-propagating high-temperature synthesis	272
<b>Ovrutsky A.M., Prokhoda A.S., Taran E.A.</b> Relaxation in Amorphous Phases and Initial Crystallization	273
<b>Paiuk O., Lishchynskyy I., Stronski A., Vlček M., Kryskov Ts., Oleksenko P.</b> Influence of Cr dopant on the structure of AsS glass	274
<b>Pazyuk R.I., Ivakhiv N.F.</b> Quasiparticle Energy States in Spherical Quantum Dot Superlattices	275
<b>Popovych D.I., Onisimchuk V.V.</b> Diffusion processes in ZnO nanopowders with oxygen absorption	276
<b>Pugantseva O.V., Kramar V.M.</b> Exciton energy dependence from the thickness of the semiconductor-based nanofilm	277
<b>Starostenko O.M.<sup>1</sup>, Gusakova K.G.<sup>1</sup>, Grigoryeva O.P.<sup>1</sup>, Fainleib O.M.<sup>1</sup>, Sakhno V.I., Borzakovskiy A.E., Grande D.</b> Nanoporous thermostable polycyanurate-based film-forming materials	278
<b>Savchuk A.I., Manyk O.M., Bilynskyy-Slotylo V.R.</b> Chemical bond and elastic properties of selenium	279
<b>Savchuk O.A., Trishchuk L.I., Tomashik V.M., Tomashik Z.F., Boruk S.D.</b> A synthesis of quantum dots of CdTe stabilized by oxyethylenediphosphonic acid	280
<b>Savchuk P.V., Kashitskiy V.P., Kyselyuk O.P.</b> Peculiarities of epoxy composites filled with high dispersed particles of titanium carbide	281
<b>Savulyak V.V., Gorlaty V.O., Solokha V.P., Zubarev R.A., Galaktionov D.A., Fedoryak A.N., Grynko D.A.</b> Growth of CdS and CdSe nanocrystal brushes from gas phase	282
<b>Seti Ju., Boyko I., Matijek V.</b> Permeability coefficient for two-barrier resonance tunnel structure due to the electron-electron interaction	283

<b>Shevchenko V.B., Korniyenko M.Ye., Makara V.A., Veblaya T.S.</b> Different states of water in nanoporous silicon layers	<b>284</b>
<b>Shplyak M., Makauz I., Pynzenyk V., Voynarovych I., Chereshnya V., Trunov M., Charnovich I., Kokenyesi S.</b> Surface modifications of amorphous chalcogenide functional materials	<b>285</b>
<b>Sydor O.M., Sydor O.A., Dubinko V.I., Lytvyn O.S.</b> Morphology of gamma-neutron irradiated intrinsic oxide films of InSe	<b>286</b>
<b>Tafiychuk Y.M., Yaremiy I.P., Vylka I.Ja., Bushkova V.S.</b> Synthesis and characterization of nanocrystalline LaFeO <sub>3</sub> by sol-gel auto-combustion method.	<b>287</b>
<b>Tkachuk A.I., Oleskiv R.B.</b> Receive of homogeneous quantum-size structures	<b>288</b>
<b>Trachevsky V.V., Kustovska A.D., Kosenko E.I.</b> Plasmachemical modification of adsorbents surface	<b>289</b>
<b>Tsvetkova O., Varvarenko S., Lucheckho A., Kostyk L., Pavlyk B.</b> Synthesis and investigations of gadolinium-gallium garnet nanomaterials	<b>290</b>
<b>Velikanova T.A., Karpets M.V.</b> Metastable nanostructures in the rapidly quenched iron alloys	<b>291</b>
<b>Voronych O.L., Kurta S.A.</b> Chemical Method of Preparing Colloidal Silver Liquid Composition	<b>292</b>
<b>Voynarovych I., Shplyak M., Pynzenik V., Makauz I., Chereshnya V., Kikineshi A.</b> Solig phase synthesis in amorphous chalcogenide multiulayers	<b>293</b>
<b>Voznyak O.M., Voznyak O.O.</b> Energy states of electrons with position-depedent effective mass in the quantum nanogeterosystems	<b>294</b>
<b>Yaremiy I.P., Tomyn U.O., Yaremiy S.I., Kravets V.I.</b> Crystal structure of epitaxial <i>Bi</i> -substituted ferrite-garnet films modified by double boron implantion	<b>295</b>
<b>Yatsenko Yu.I., Kidalov V.V., Sukach G.A.</b> Determination of optimum parameters of the electrolyte-semiconductor during the creation of porous GaP	<b>296</b>
<b>Zatirka O.I., Ilchenko V.V.</b> Problems of metrology and standardization in nanotechnologies	<b>297</b>

Наукове видання

**Фізика і технологія тонких плівок та наносистем**

**Матеріали  
XIII міжнародної конференції**

МКФТТПН-XIII

**Physics and Technology of Thin Films and Nanosystems**

**Materials  
of the XIII International Conference**

ІСРТТФН-XIII

Редактор *Дмитро Фреїк*

Технічний редактор *Богдан Дзундза*

Комп'ютерна верстка *Богдан Дзундза, Олександр Соколов, Віктор Борик,  
Лілія Туровська, Ігор Юрчишин, Любов Юрчишин,  
Андрій Ткачук, Лідія Харун*

Відповідальний за випуск *Олександр Соколов*

*Усі матеріали подані у авторській редакції*

Підписано до друку 22.04.2011.

Формат 60x84<sub>/16</sub>. Папір офсетн. Гарнітура “Таймс”.

Умовн. друк. арк. 17,34. Тираж 250.

Видавництво

Прикарпатського національного університету імені Василя Стефаника,  
вул. С. Бандери, 1, м. Івано-Франківськ, 76000.

Тел. 8(0342) 71-56-22.

E-mail: [vdvcit@pu.if.ua](mailto:vdvcit@pu.if.ua)

**Ф 83 Фізика і технологія тонких плівок та наносистем. Матеріали XIII Міжнародної конференції: У 2 т. – Т. 1. / За заг. ред. Заслуженого діяча науки і техніки України, д.х.н., проф. Фреїка Д.М. – Івано-Франківськ: Видавництво Прикарпатського національного університету імені Василя Стефаника, 2011. – 312 с.**